

Dissertation zur Erlangung des Doktorgrades  
der Fakultät für Chemie und Pharmazie  
der Ludwig-Maximilians-Universität München

**Structural and Ion-Pairing Effects on the  
Nucleophilic Reactivity of  
Carbanions and Organometallics**

Francisco Corral Bautista

aus

Ingolstadt

2014



## **Erklärung**

Diese Dissertation wurde im Sinne von § 7 der Promotionsordnung vom 28. November 2011 von Herrn Prof. Dr. Herbert Mayr betreut.

## **Eidesstattliche Versicherung**

Diese Dissertation wurde eigenständig und ohne unerlaubte Hilfe erarbeitet.

München, den

.....  
(Francisco Corral)

Dissertation eingereicht am                      24.06.2014

1. Gutachter    Prof. Dr. Herbert Mayr

2. Gutachter    Prof. Dr. Paul Knochel

Mündliche Prüfung am                              29.07.2014



Für meine Mutter



---

## Danksagung

Zu allererst möchte ich mich bei Prof. Dr. Herbert Mayr bedanken. Nicht nur für die Möglichkeit, diese Dissertation in seinem Arbeitskreis anfertigen zu können, sondern auch für den Freiraum bei der Gestaltung meines Forschungsbereiches, bin ich ihm zu großem Dank verpflichtet. Anerkennend möchte ich noch die Hilfs- und Diskussionsbereitschaft erwähnen, ohne die diese Arbeit nicht in dieser Form zustande gekommen wäre.

Bei Herrn Prof. Dr. Paul Knochel möchte ich mich ebenfalls für seine Diskussionsbereitschaft und Anregungen bedanken. Ebenfalls bedanke ich mich für die Zweitbegutachtung meiner Arbeit.

Den Mitgliedern des Prüfungsausschusses danke ich für ihre Teilnahmebereitschaft.

Für Anregungen und Kollaboration, möchte ich mich bei Lydia Klier und Roland Appel bedanken. Ebenfalls danke ich Martin Breugst für seine Hilfsbereitschaft zu Beginn meiner Arbeit.

Nathalie Hampel danke ich für ihre Unterstützung bei manchen Synthesen, sowie die Bereitstellung der Referenzelektrophile. Bei Hildegard Lipfert bedanke ich mich für ihr Organisationstalent und bei Brigitte Janker für ihre Hilfestellung bei sämtlichen technischen Fragen.

Bei Armin R. Ofial möchte ich mich für die schnelle und genaue Durchsicht meiner Publikationen bedanken. Für die zügige Durchsicht dieser Arbeit bedanke ich mich bei Dominik Allgäuer, Hans Laub und Johannes Ammer.

Bei meinen Arbeitskollegen möchte ich mich herzlich für die gute Zusammenarbeit bedanken. Ganz besonders bei Nathalie Hampel –ohne dich macht es nur halb so viel Spaß–, Katharina Böck „Schokorina“, Hans Laub –vor allem für unseren gemeinsamen Besuch bei der EuCheMS in Prag 2012–, Dominik Allgäuer, Johannes Ammer, Elija Wiedemann und Ángel Puente „Angelito“.

Den ehemaligen Mitgliedern des Olah-Labs, Tanja Kanzian, Roland Appel, Martin Breugst, Christoph Nolte, vor allem Sami Lakhdar –The President of the Olah-Lab– danke ich für die gute Arbeitsatmosphäre.

Bei meinen Freunden, die mich durch das Chemiestudium begleitet haben, Amelie Schreieck, Claudia Wilfer, Lydia Klier „den Mädchens“, Konstantin Sparrer, Jens Prescher und Anna Niedl bedanke ich mich herzlich. Ohne euch wäre es nicht so schön gewesen.

---

Bei meinem Vater und meinem Bruder möchte ich mich für ihre stetige Unterstützung während meines gesamten beruflichen Werdeganges bedanken. Ohne sie wäre ich nicht so weit gekommen.

Besonders bei meiner Mutter, die heute nicht mehr bei mir sein kann, die mich bei Allem unterstützt und mich immer ermutigt hat, bedanke ich mich von ganzem Herzen.



---

## Publications

### Quantification of the Nucleophilic Reactivities of Ethyl Arylacetate Anions

F. Corral Bautista, H. Mayr, *Eur. J. Org. Chem.* **2013**, 4255–4261.

### Quantification of Ion-Pairing Effects on the Nucleophilic Reactivities of Benzoyl- and Phenyl-Substituted Carbanions in Dimethylsulfoxide

F. Corral Bautista, R. Appel, J. S. Frickel, H. Mayr, *Chem. Eur. J.* **2014**, in press.

## Contributions to Conferences

### Nucleophilic Reactivities of Ethyl Arylacetate Anions

F. Corral Bautista, H. Mayr, 4<sup>th</sup> *EuCheMS Chemistry Congress*, Prague (Czech Republic) 2012.

### From Carbanions to Organometallic Compounds

F. Corral Bautista, H. Mayr, Workshop of the Sonderforschungsbereich 749, Wildbad Kreuth (Germany), 2013.

### From Carbanions to Organometallic Compounds: Quantification of Metal-Ion-Effects on Nucleophilic Reactivities

F. Corral Bautista, R. Appel, L. Klier, P. Knochel, H. Mayr, 5<sup>th</sup> *EuCheMS Chemistry Congress*, Istanbul (Turkey) 2014.

## Table of Contents

Chapter 0	Summary	1
Chapter 1	Introduction	14
Chapter 2	Quantification of the Nucleophilic Reactivities of Ethyl Arylacetate Anions	24
Chapter 3	Quantification of Ion-Pairing Effects on the Nucleophilic Reactivities of Benzoyl- and Phenyl-Substituted Carbanions in DMSO	66
Chapter 4	Quantification of the Nucleophilic Reactivities of Cyclic $\beta$ -Ketoesters	138
Chapter 5	From Carbanions to Organometallic Compounds: Quantification of Metal-Ion-Effects on Nucleophilic Reactivities	170
Chapter 6	Ambident Reactivity of Enolates in Polar Aprotic Solvents	231

## Chapter 0

### Summary

#### 1. General

Carbanions and metallorganic reagents belong to the most important intermediates in synthetic organic chemistry, allowing numerous types of transformations. Though their reactions have been studied thoroughly during the last decades, a systematic ordering of their reactivity in dependence of the structure or the nature of the carbon–metal bond (separated ions/ $\sigma$ -bonded organometallics) has not been achieved so far.

As previously shown, the linear-free energy relationship (1), where  $E$  is an electrophile-specific parameter, and  $N$  and  $s_N$  are nucleophile-specific parameters, can be applied to characterize the reactivities of nucleophiles and electrophiles. Eq. (1) is based on the reactions of  $\pi$ -,  $n$ -, and  $\sigma$ -nucleophiles with benzhydrylium ions, and structurally related Michael acceptors (reference electrophiles) covering a range of 40 orders of magnitude of reactivity, and therefore facilitates the comparison of reagents even when they do not have common reaction partners.

$$\lg k_2(20\text{ }^\circ\text{C}) = s_N(N + E) \quad (1)$$

In this thesis, Eq. (1) was applied to characterize the nucleophilic reactivity of carbanions with the goal to achieve a systematic ordering in dependence on their structure. Furthermore, the dependence of the reactivity on the counter ion as well as the transition from solvent-separated ions to organometallics with covalent metal–carbon bonds were studied using Eq. (1). The ambident reactivity of enolate ions was studied in the last part of this thesis. Thereby, the influence of the solvent on the alkylation reactions as well as on the reactivity of carbanions was analyzed kinetically.

#### 2. Quantification of the Nucleophilic Reactivities of Ethyl Arylacetate Anions

The second-order rate constants ( $k_2$ ) for the reactions of differently substituted ethyl arylacetate anions with quinone methides and diethyl benzylidenemalonates were determined in DMSO solution at 20 °C. The measured rate constants correlated linearly with the

electrophilicity parameters of the respective electrophile allowing us to derive their nucleophilicity parameters  $N$  and  $s_N$  (Figure 1).

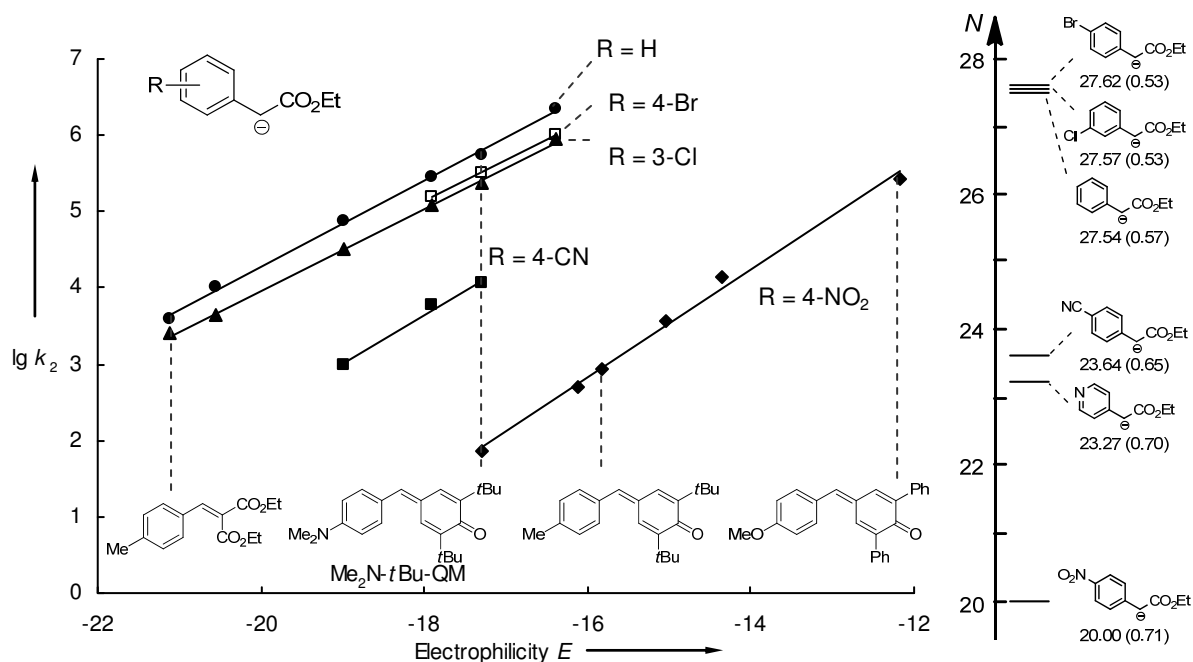


Figure 1: Left: Correlation of  $\lg k_2$  for the reactions of ethyl arylacetate anions with quinone methides and diethyl benzylidenemalonates with the electrophilicity parameters of the electrophiles. Right:  $N$  ( $s_N$ ) Parameters of the ethyl arylacetate anions.

The nucleophilic reactivities of the ethyl arylacetates cover a range of 4 orders of magnitude and are more reactive than analogously substituted benzyl anions as shown in Figure 2.

$k_{\text{rel}}(R = H)$	1.0			$6.5 \times 10^{-3}$	$1.0 \times 10^{-5}$	$1.6 \times 10^{-5}$
$k_{\text{rel}}(R = CN)$	1.0	$9.6 \times 10^{-1}$	$9.1 \times 10^{-2}$		$6.6 \times 10^{-5}$	$1.5 \times 10^{-5}$ [a]

Figure 2: Comparison of the relative second-order rate constants for the reactions of different benzyl anions with the  $\text{Me}_2\text{N}-t\text{Bu}$ -quinone methide (structure shown in Figure 1). The reactions of the ethyl arylacetates were set to unity. [a] Rate constant was calculated by Eq. (1).

The experimental and calculated [by Eq. (1)] rate constants for the reactions of the anion of ethyl 4-nitro-phenylacetate and different types of electrophiles, such as 1,2-diaza-1,3,-dienes or *trans*- $\beta$ -nitrostyrenes, were within a factor of three in a good agreement. As the ethyl arylacetate anions are highly reactive nucleophiles, they can be applied for the characterization of the reactivity of weak electrophiles.

### 3. Quantification of Ion-Pairing Effects on the Nucleophilic Reactivity of Benzoyl- and Phenyl-Substituted Carbanions in Dimethylsulfoxide

The kinetics of the reactions of acceptor substituted phenacyl and benzyl anions with benzhydrylium ions and structurally related Michael acceptors (reference electrophiles) were studied in DMSO solution at 20 °C. The influence of the counter ion on the kinetics was studied by varying the concentration of the metal cation in solution while the concentration of the nucleophile and the electrophile were kept constant. It was found that the structure of the carbanion has a considerable influence on the strength of the counter ion effects as shown for some representative examples in Figure 3.

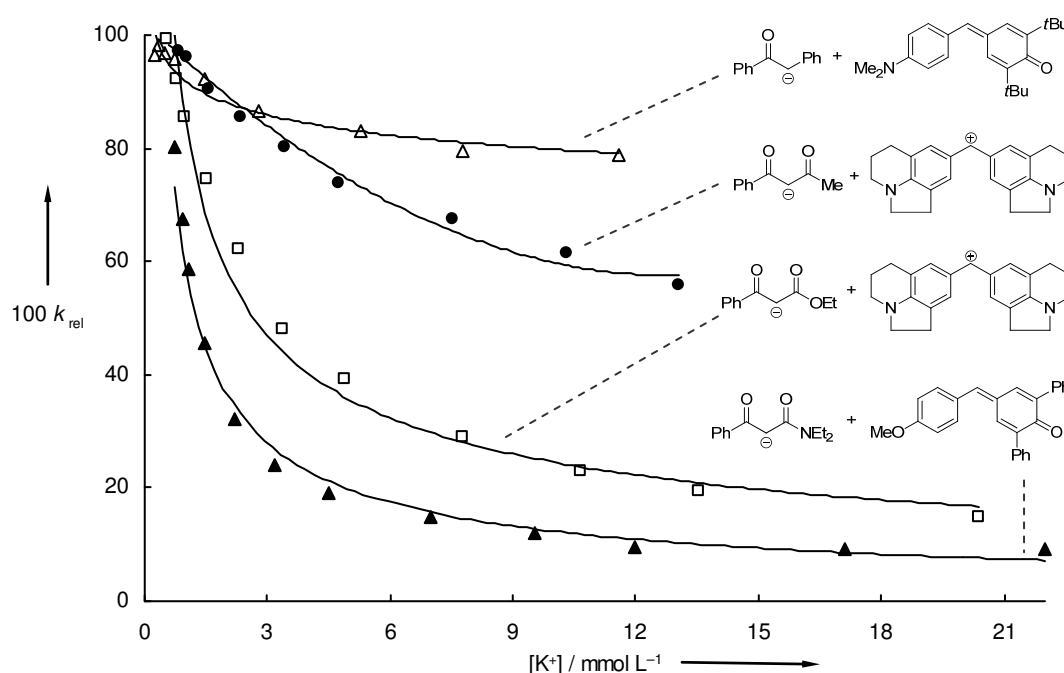


Figure 3: Plots of the relative first-order rate constants for the reactions of the anions derived from a monoketone, a  $\beta$ -diketone, a  $\beta$ -ketoester and a  $\beta$ -ketoamide ( $[\text{carbanion}] \approx 10^{-4} \text{ mol L}^{-1}$ ) with reference electrophiles ( $[\text{electrophile}] \approx 10^{-5} \text{ mol L}^{-1}$ ) versus the total concentration of potassium (varied by addition of  $\text{KBPh}_4$ ) in DMSO solution at 20 °C.

As all studied carbanions were derived from ketones, esters or  $\beta$ -dicarbonyls, counter ion effects were found in all experiments. However, while the reactivity of the anions of monoketones and monoesters decreased only to 60–80% of the reactivity of the free carbanions by increasing the potassium concentration to  $10 \text{ mmol L}^{-1}$ , the rate constants of the  $\beta$ -diketon-derived anions decrease to 40–60% of the original value and the reactivity of the anions of  $\beta$ -ketoesters or the  $\beta$ -ketoamide decreased even to 10–20% of the reactivity of the free carbanions.

Analogous experiments increasing the concentration of sodium (by addition of NaBPh<sub>4</sub>) or lithium (addition of LiBF<sub>4</sub> or LiCl) in the solution showed that the counter ion effect increases in the order potassium < sodium < lithium (Figure 4). Again, the anions derived from  $\beta$ -ketoesters showed the strongest counter ion effects.

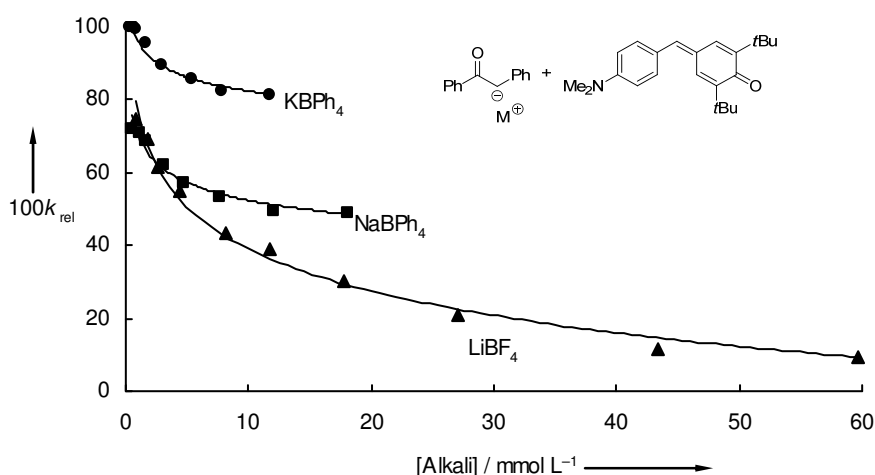


Figure 4: Plots of the relative first-order rate constants for the reactions of the anion of deoxybenzoin ([carbanion]  $\approx 10^{-4}$  mol L<sup>-1</sup>) with the Me<sub>2</sub>N-*t*Bu-quinone methide ([QM]  $\approx 10^{-5}$  mol L<sup>-1</sup>) versus the total concentration of alkali salt (varied by addition of KBPh<sub>4</sub>, NaBPh<sub>4</sub> or LiBF<sub>4</sub>) in DMSO solution at 20 °C.

Experiments as shown in Figures 3 and 4 and kinetic experiments in presence of 18-crown-6 revealed that, at concentrations  $\leq 10^{-3}$  mol L<sup>-1</sup>, the potassium salts behave as free carbanions in DMSO solution. Exceptions were the potassium salts derived from  $\beta$ -ketoesters or  $\beta$ -ketoamides, which already show interactions with potassium at  $10^{-4}$  mol L<sup>-1</sup>. By addition of 18-crown-6, we could also obtain the rate constants of the free carbanions in these cases.

The second-order rate constants of the reactions of the free carbanions with benzhydrylium ions and Michael acceptors correlated linearly with the electrophilicity parameters of the electrophiles (shown for some examples in Figure 5) and from these correlations, the nucleophilicity parameters  $N$  and  $s_N$  were determined (Figure 6).

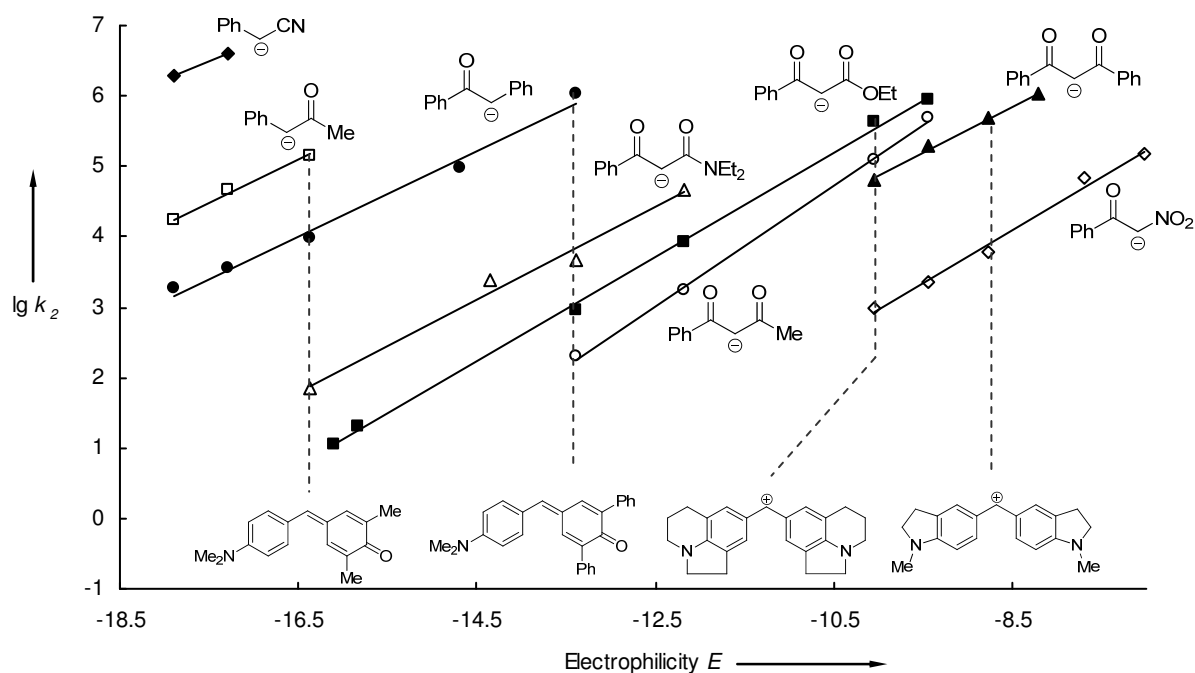


Figure 5: Correlation of  $\lg k_2$  for the reactions of benzoyl- and phenyl-substituted carbanions with benzhydrylium ions and Michael acceptors with the electrophilicity parameters of the electrophiles.

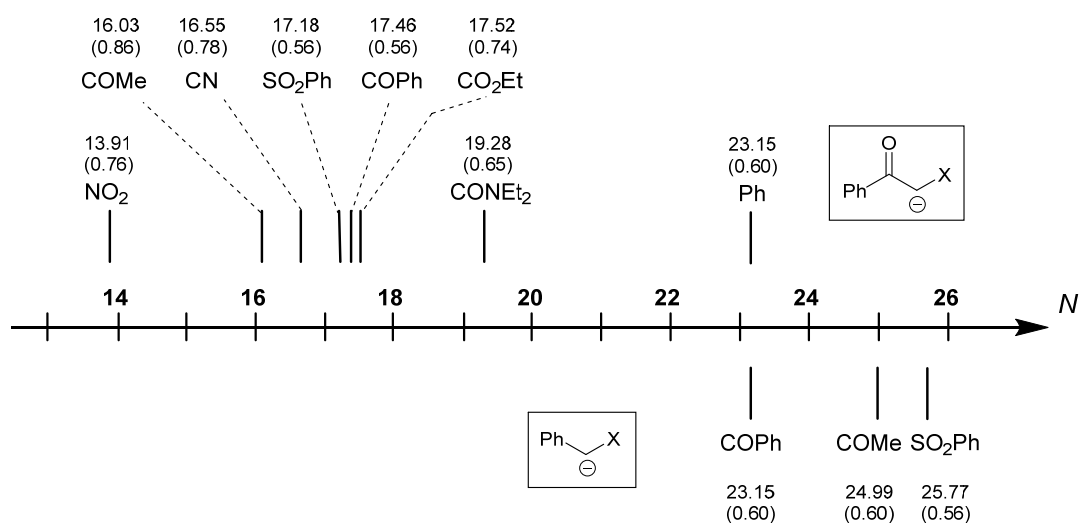


Figure 6: Nucleophilicity parameters  $N$  ( $s_N$ ) of the benzoyl-substituted carbanions (top) and phenyl-substituted carbanions (bottom).

As the phenyl-substituted carbanions are much more reactive than analogously substituted benzoyl carbanions, different reference systems had to be used when the reactivities in both series are compared (Figure 7). However, the illustration in Figure 7 reflects the saturation effect, as the differences in the relative reactivities are more pronounced for the phenyl-substituted carbanions than for the benzoyl-substituted carbanions.

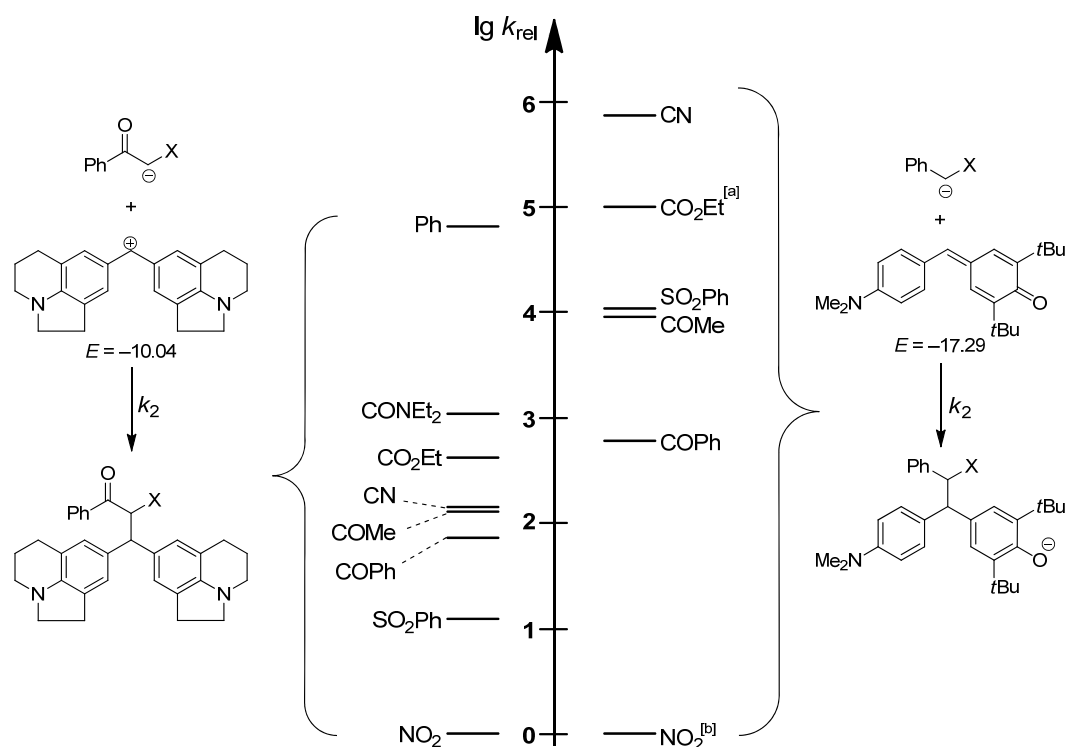


Figure 7: Relative rate constants for the reactions of the benzoyl-substituted carbanions with (lil)<sub>2</sub>CH<sup>+</sup> (left) and the phenyl-substituted carbanions with the NMe<sub>2</sub>-tBu-quinone methide in DMSO at 20 °C (right). Rate constants of the nitro-substituted carbanions were set to unity. [a] *Eur. J. Org. Chem.* **2013**, 4255–4261. [b] *J. Org. Chem.* **2004**, 69, 7565–7576.

Furthermore, Brønsted-plots showed once more that basicity is not a reliable parameter to predict relative reactivities of carbanions.

#### 4. Quantification of the Nucleophilic Reactivities of Cyclic $\beta$ -Ketoesters

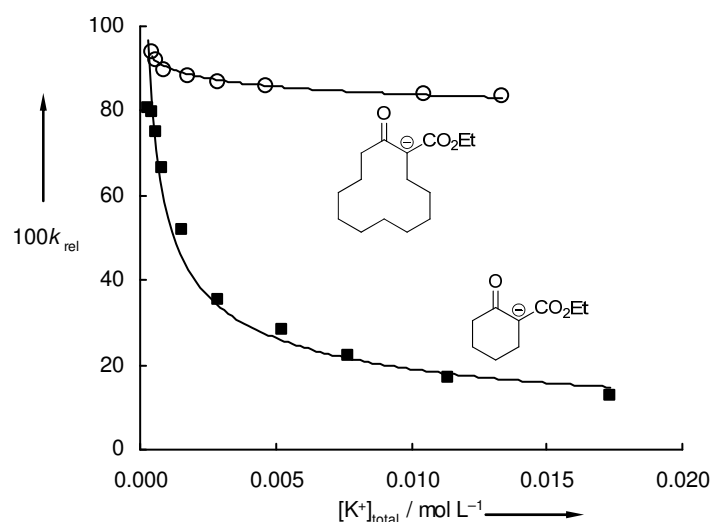
The rate constants for the reaction of the potassium salts of cyclic  $\beta$ -ketoesters with quinone methides (reference electrophiles) were determined in DMSO solution at 20 °C. Thereby, the ring-size of the  $\beta$ -ketoester was varied studying the 5–8- and the 12-membered rings. Like the anions derived from acyclic  $\beta$ -ketoesters, the studied potassium salts showed counter ion effects at low concentrations ( $10^{-4}$ – $10^{-3}$  mol L<sup>-1</sup>). However, it was found that the strength of the counter ion effect depends on the ring size. As shown in Table 1, the ratio between the second-order rate constants for the reactions of the anions of the cyclic  $\beta$ -ketoesters with the NMe<sub>2</sub>-Ph-quinone methide (for structure see Table 1) in presence of 18-crown-6 (free carbanions) and in absence of 18-crown-6 (potassium salts) decrease with increasing ring size.



Table 1: Second-order rate constants for the reaction of the anions of cyclic  $\beta$ -ketoesters with the NMe<sub>2</sub>-Ph-quinone methide in presence and in absence of 18-crown-6 (DMSO, 20 °C).

Ring Size	$k_2 / \text{L mol}^{-1} \text{s}^{-1}$		$k_2(\text{K}^+/\text{crown}) / k_2(\text{K}^+)$
	$\text{K}^+/\text{crown}$	$\text{K}^+$	
5	$1.69 \times 10^4$	$1.39 \times 10^4$	1.22
6	$1.33 \times 10^4$	$1.14 \times 10^4$	1.17
7	$1.09 \times 10^5$	$9.55 \times 10^4$	1.14
8	$9.38 \times 10^4$	$8.09 \times 10^4$	1.16
12	$3.09 \times 10^4$	$2.97 \times 10^4$	1.04

As shown in Figure 8, the relative rate constants of the reactions of the anions of the cyclic  $\beta$ -ketoesters with the NMe<sub>2</sub>-Ph-quinone methide at variable potassium concentrations (by addition of KBPh<sub>4</sub>) behave differently with respect to the ring size. While the reactivities of the 6-membered ring decrease to 10–15% of the reactivity of the free carbanion, the rate constants of the 12-membered ring remain at 80% with respect to the free carbanion at  $[\text{K}^+] \approx 10^{-2} \text{ mol L}^{-1}$ .

Figure 8: Plots of the relative first-order rate constants for the reactions of the anions of cyclic  $\beta$ -ketoesters ( $c \approx 10^{-4} \text{ mol L}^{-1}$ ) with the NMe<sub>2</sub>-Ph-quinone methide ( $c \approx 10^{-5} \text{ mol L}^{-1}$ ) versus the total concentration of potassium (varied by addition of KBPh<sub>4</sub>) in DMSO solution at 20 °C.

From kinetic experiments in the presence of 18-crown-6, the second-order rate constants for the reactions of the free carbanions of the cyclic  $\beta$ -ketoesters with quinone methides were determined in DMSO solution at 20 °C. The left part of Figure 9 shows two examples how the rate constants of these reactions vary with the ring size.

From linear correlations of the second-order rate constants of the reactions of the anions of the cyclic  $\beta$ -ketoesters with quinone methides with the electrophilicity parameters of the quinone methides, the nucleophilicity parameters  $N$  and  $s_N$  were derived (Figure 9, right). As shown in the right part of Figure 9, the sensitivities ( $s_N$ ) decrease with the ring size of the carbanions.

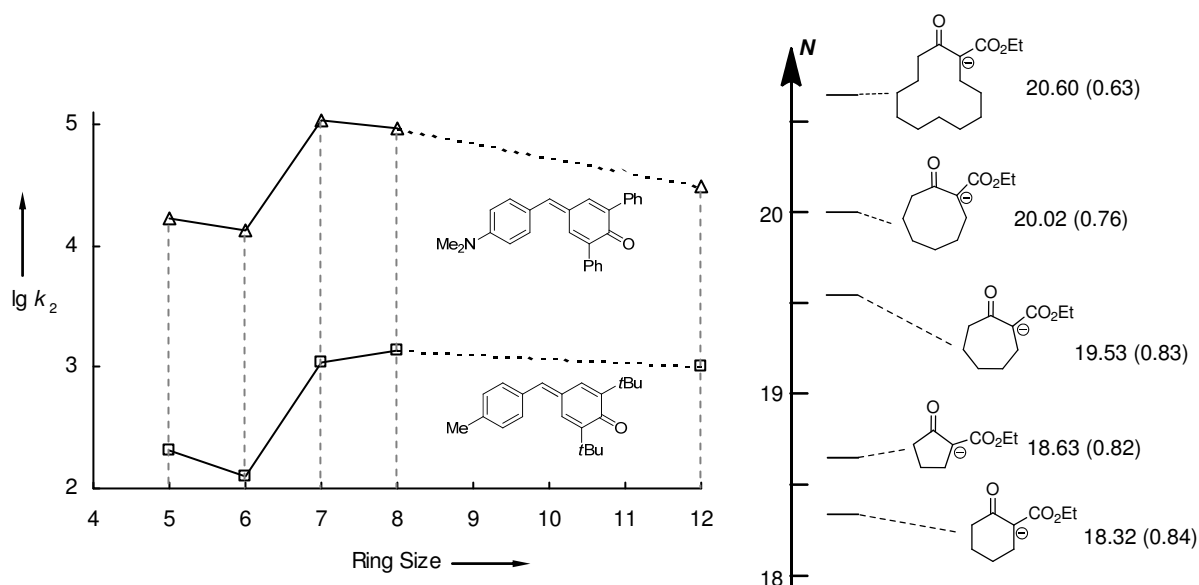


Figure 9: Left: Plots of the second-order rate constants for the reactions of the anions of the cyclic  $\beta$ -ketoesters with quinone methides versus their ring size. Right: nucleophilicity parameters,  $N$  ( $s_N$ ), of the free carbanions.

## 5. From Carbanions to Organometallic Compounds: Quantification of Metal-Ion-Effects on Nucleophilic Reactivities

The kinetics of the reactions of organometallic derivatives of cyclopentadiene, indene and fluorene with benzhydrylium ions and structurally related Michel acceptors (reference electrophiles) were studied in DMSO and  $\text{CH}_2\text{Cl}_2$  solution at 20 °C.

The kinetic experiments of the alkali metal derivatives (K, Na, Li) were performed in DMSO solution and show that the potassium salts of cyclopentadiene, indene and fluorene behave as free carbanions at concentrations of  $10^{-4}$ – $10^{-3}$  mol  $\text{L}^{-1}$  and that the reactivity of these alkali metal derivatives increase from cyclopentadiene  $\rightarrow$  indene  $\rightarrow$  fluorene due to benzoannulation. Furthermore, it was found that the counter ion effect increased in the same order as the reactivity: cyclopentadiene  $\rightarrow$  indene  $\rightarrow$  fluorene.

As the second-order rate constants of the reactions of the alkali derivatives with Michael acceptors correlated linearly with the  $E$ -parameters of the electrophiles, the nucleophilicity parameters  $N$  and  $s_N$  could be calculated according to Eq. (1) (Figure 10).

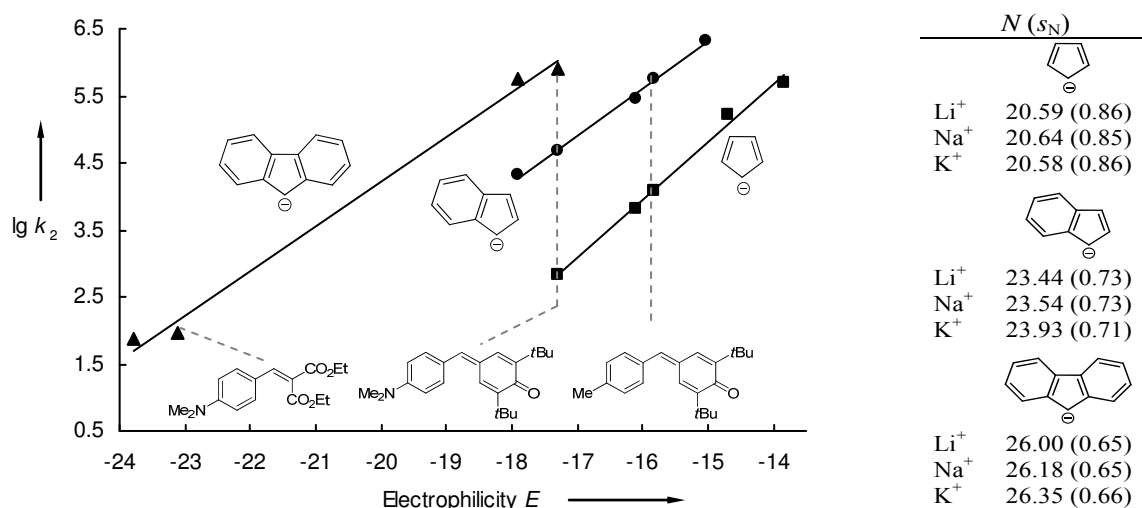
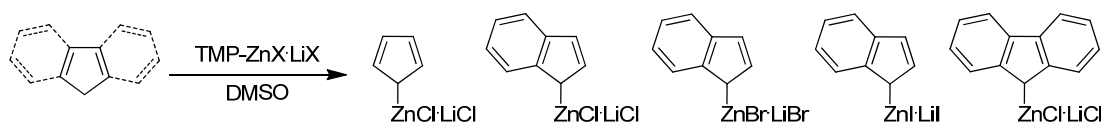


Figure 10: Left: Correlations of the second-order rate constants for the reactions of the potassium salts (free carbanions) of cyclopentadiene, indene and fluorene with Michael acceptors with their electrophilicity parameters. Right: nucleophilicity parameters  $N$  and  $s_N$  of the alkali derivatives of cyclopentadiene, indene and fluorene.

The zinc derivatives of cyclopentadiene, indene and fluorene were generated by treating the neutral compounds with TMP-bases as shown in Scheme 1.



Scheme 1: Generation of the zinc derivatives of cyclopentadiene, indene and fluorene. TMP = 2,2,6,6-tetramethylpiperidine.

The kinetics of the reactions of the organozinc reagents from Scheme 1 with benzhydrylium ions were performed in DMSO solution at 20 °C. These second-order rate constants correlated linearly with the electrophilicity parameters of the benzhydrylium ions allowing us to calculate the nucleophilicity parameters  $N$  and  $s_N$  of the organozinc derivatives (Figure 11).

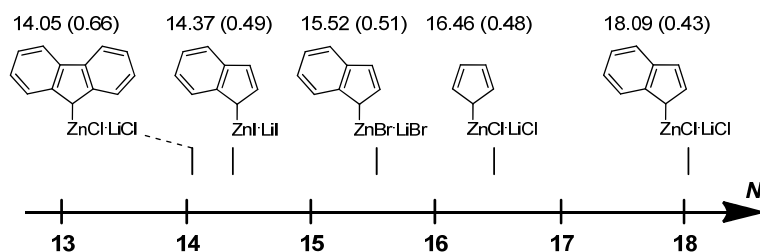
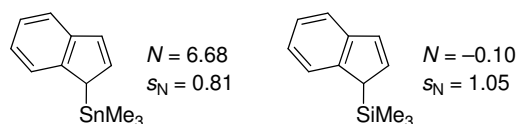


Figure 11: Nucleophilicity parameters,  $N$  ( $s_N$ ), of the zinc derivatives of cyclopentadiene, indene and fluorene.

Figure 11 shows how the reactivity of the organozinc derivatives of indene depend on the halide anion, being indenylzinc iodide the least reactive, while indenylzinc chloride is the most reactive nucleophile in this series. While the alkali derivatives of fluorene are considerably more reactive than the corresponding indenyl and cyclopentadienyl compounds, Figure 11 shows that the zinc derivative of fluorene is less reactive than the corresponding indenyl and cyclopentadienyl compounds. This reactivity ordering is explained by different reaction mechanisms: the zinc derivatives of cyclopentadiene and indene react with the benzhydrylium ions via a  $S_E2'$  mechanism whereas the zinc derivative of fluorene via a  $S_E2$  mechanism.

Kinetic experiments of the reactions of indenyl-zinc-reagents with benzhydrylium ions in presence of additives (LiCl, LiBr,  $Bu_4NCl$ ,  $MgCl_2$ ) showed that the nucleophilic reactivity increases with the concentration of the additives, which is explained by halide exchange and the formation of zincates. However, the magnitude of these effects depended on the organozinc reagent as well as on the additive.

The reactions of the tin and silicon derivatives of indene with benzhydrylium ions were studied kinetically in  $CH_2Cl_2$  solution at 20 °C. The second-order rate constants correlated linearly with the electrophilicities of the benzhydrylium ions. The nucleophilicity parameters of the organotin and organosilicon compounds were calculated according Eq. (1) from these correlations (Scheme 2).



Scheme 2: Nucleophilicity parameters  $N$  and  $s_N$  of the tin- and silicon-derivates of indene.

This work allowed us to investigate the changes in the reactivity of C-nucleophiles by metal-coordination as shown for indene in Figure 12. The nucleophilic reactivities of the different organometallic derivatives of indene cover a range of about 20 orders of magnitude.

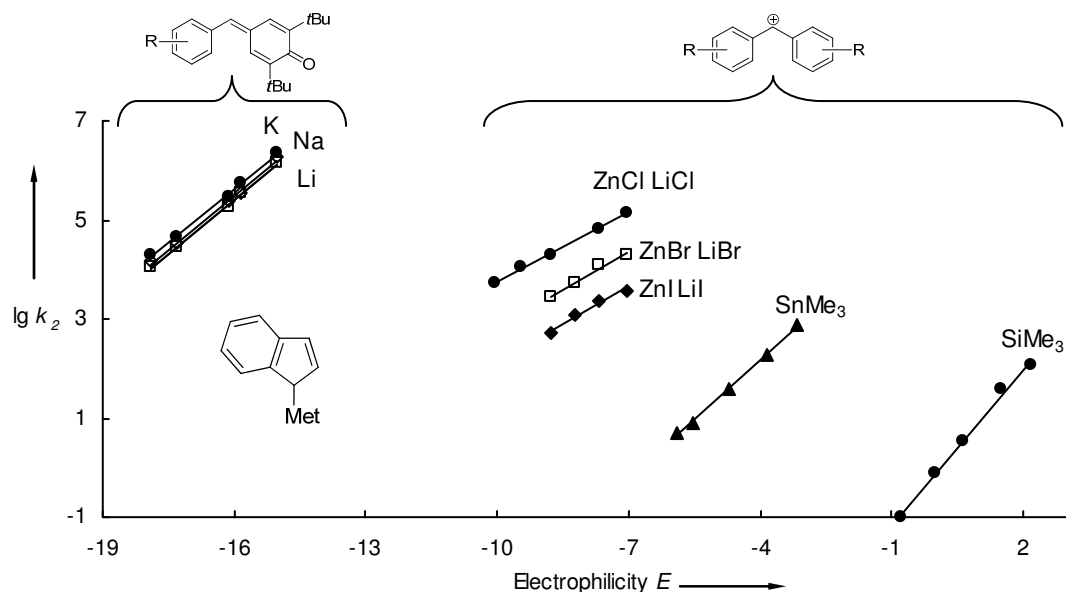
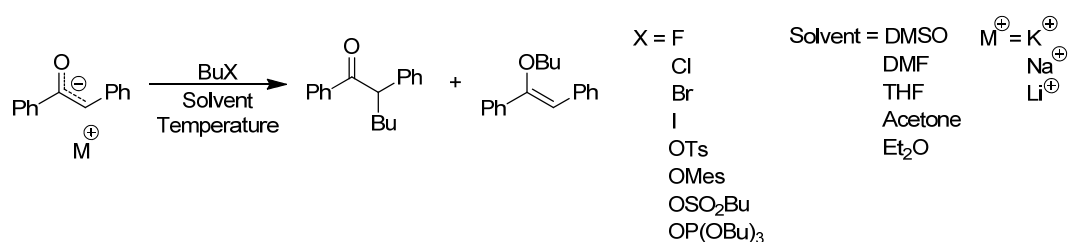


Figure 12: Correlation of the second-order rate constants for the reactions of different organometallic derivatives of indene with benzhydrylium ions and quinone methides with the electrophilicity parameters of the electrophiles.

## 6. Ambident Reactivity of Enolates in Polar Aprotic Solvents

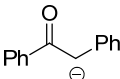
The ambident reactivities of enolate ions have been studied for decades concluding that their regioselectivity depends on the nature of the nucleophile and the electrophile, the solvent, the counter ion, temperature and concentration. In this work, we studied systematically the influence of these parameters on the alkylation reactions of the anion of deoxybenzoin (Scheme 3).



Scheme 3: Alkylation reaction of the anion of deoxybenzoin.

The synthetic experiments show that the oxygen-alkylation was favored when the solvent polarity increased. However, no linear relationships were found between the product ratios and various solvent polarity parameters ( $E_T^N$ , acceptor number, relative permittivity). Influenced by the solvent polarity, the amount of oxygen-alkylated product increased when the counter ion was better solvated ( $\text{Li} \rightarrow \text{Na} \rightarrow \text{K} \rightarrow \text{K/crown}$ ). Furthermore we found that the regioselectivity decreased with increasing temperature, and C-alkylation became more favored with decreasing concentrations.

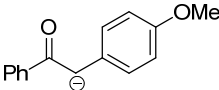
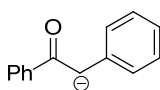
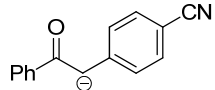
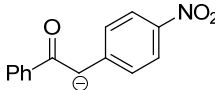
The reactions of the anion of deoxybenzoin with quinone methides (reference electrophiles) were studied kinetically in DMF, THF, and acetone solution at 20 °C. The obtained second-order rate constants for these reactions allowed us to calculate, according to Eq. (1), the nucleophilicities of the anion of deoxybenzoin in different solvents (Scheme 4).

	DMSO $N = 23.15$ $s_N = 0.60$	DMF $N = 26.69$ $s_N = 0.39$	THF $N = 24.36$ $s_N = 0.50$	Acetone $N = 21.94$ $s_N = 0.60$
---	-------------------------------------	------------------------------------	------------------------------------	--

Scheme 4: Nucleophilicity parameters of deoxybenzoin in different solvents.

The measured second-order rate constants for the reactions of the anion of deoxybenzoin with quinone methides did not correlate with different solvent parameters ( $E_T^N$ , acceptor number, relative permittivity). Moreover, the product ratios (C/O-alkylation) did not correlate with the nucleophilic reactivities in the respective solvent.

Introducing electron withdrawing groups in the anion of deoxybenzoin favored C-alkylation, while introducing electron demanding substituents favored O-alkylation. The nucleophilicity parameters of the anions of the substituted deoxybenzoins were derived from kinetic experiments of the carbanions with quinone methides in DMSO solution at 20 °C according to Eq. (1) (Scheme 5).

			
$N = 27.46$ $s_N = 0.41$	$N = 23.15$ $s_N = 0.60$	$N = 20.20$ $s_N = 0.70$	$N = 19.14$ $s_N = 0.64$

Scheme 5: Nucleophilicity parameters of the anions of substituted deoxybenzoins in DMSO.

The product ratios of the alkylation reactions of the anions of the substituted deoxybenzoins with butyl iodide and butyl tosylate correlated linearly with Hammett's  $\sigma_p^-$  parameters as well as with the nucleophilicities of the carbanions (Figure 13).

Kinetic studies of the reactions of deoxybenzoin with butylation agents were performed. However, the product ratios for the alkylations of the anion of deoxybenzoin with BuI in different solvents did not correlate with the second-order rate constants of these reactions. Analogously, no correlation was obtained when the product ratios of the alkylations of deoxybenzoin with different electrophiles (butyl halides, -tosylate) in THF were correlated with the second-order rate constants of these reactions.

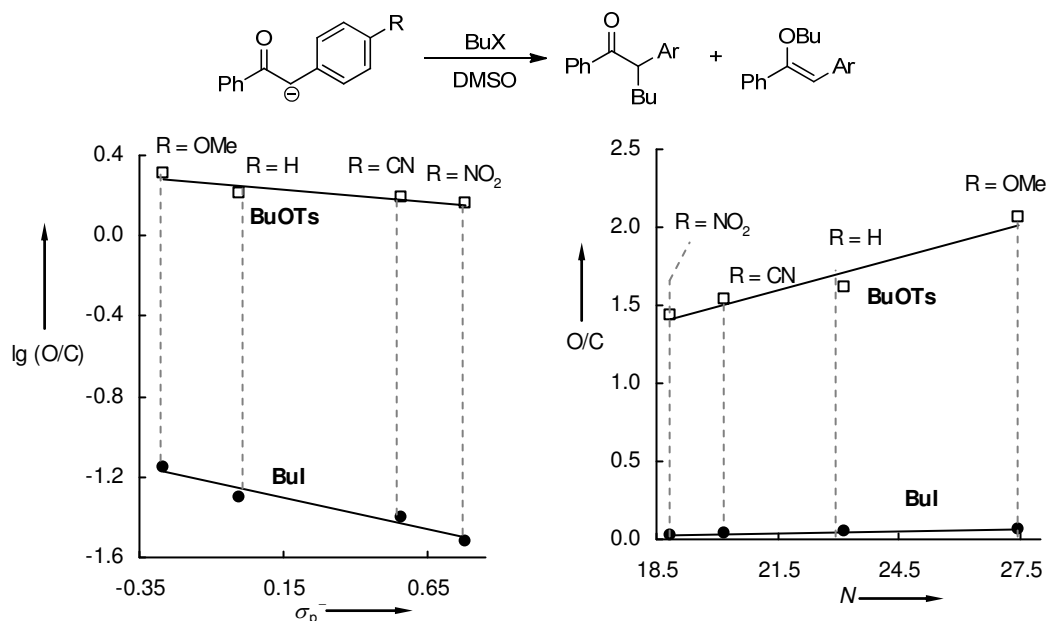


Figure 13: Correlation of the product ratios of the alkylations of the anions of substituted deoxybenzoins with butyl iodide and butyl tosylate in DMSO with  $\sigma_p^-$ -parameters (left) and the nucleophilicities of the carbanions in DMSO (right).

The data from the synthetic experiments and the kinetic measurements were compared with analogous experiments reported in the literature, which partly confirm and partly contradict the results of this work. Thus, it does not seem to be general rules which can predict the regioselectivity of enolate ions and each system has to be treated individually.

## Chapter 1

### Introduction

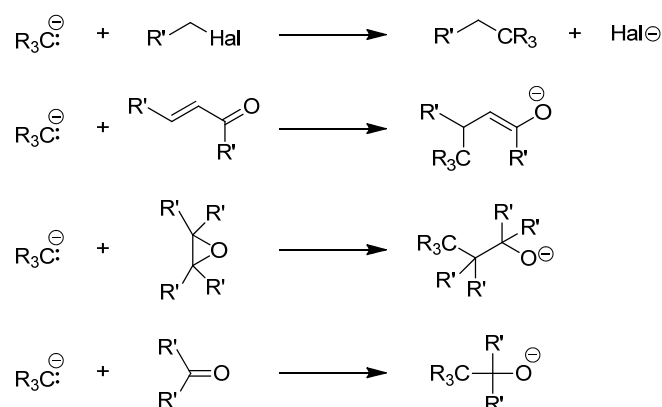
#### 1. General

Organometallic compounds generally contain a more or less polar carbon–metal bond.<sup>[1]</sup> Since Frankland's synthesis of diethyl zinc<sup>[2]</sup> and Grignard's synthesis of organo-magnesium compounds<sup>[3]</sup> in the middle of the nineteenth and in the early twentieth century, a wide range of organometallic compounds have been studied and numerous applications in synthetic chemistry have emerged from organometallic chemistry.<sup>[4,5]</sup> The formation of new carbon–carbon bonds is one of the central aims of organic chemistry, and organometallic compounds have been shown to be excellent nucleophiles for this approach as they can undergo practically unlimited transformations with all kinds of electrophiles.<sup>[4-6]</sup>

The reactivity of organometallic reagents depends strongly on the nature of the metal. Highly polarized carbon–metal bonds, such as in organo-lithium, organo-sodium or organo-magnesium compounds, are highly reactive, but often show low selectivity.<sup>[6a,7]</sup> Lower reactivity, associated with higher stability and remarkable tolerance towards functional groups is found when the carbon–metal bond becomes more covalent, as it is in organo-zinc reagents.<sup>[5,6d,e,8]</sup> Transition metals often enhance the reactivity of organometallic reactants without negative consequences for the selectivity.<sup>[9]</sup>

#### 1.1. Carbanion Chemistry

Carbanions belong to the most useful intermediates in synthetic organic chemistry which undergo numerous reactions as substitutions or additions as shown for some examples in Scheme 1.<sup>[10]</sup>



Scheme 1: Examples of reactions of carbanions with different electrophiles.



Depending on their structure, the stability and reactivity of carbanions reach from highly reactive intermediates with short live-times to carbanions which are even stable in aqueous solutions. One of the factors which affect the stability of carbanions is the hybridization of the carbanionic center. The increasing stabilization in the row  $sp^3$  to  $sp^2$  to  $sp$  hybridization<sup>[11]</sup> is demonstrated by the gas-phase acidities (heat of dissociation  $\Delta H^\circ$ ) for ethane ( $1759 \text{ kJ mol}^{-1}$ ), ethene ( $1714 \text{ kJ mol}^{-1}$ ) and ethyne ( $1582 \text{ kJ mol}^{-1}$ ).<sup>[12]</sup> A further factor which influences the stability and the reactivity, is the Hückel aromaticity. Comparison of the  $pK_a$  values in DMSO shows that the stability of the carbanions decreases from the cyclopentadienyl anion to the indenyl anion to the fluorenyl anion (Figure 1).<sup>[11,13]</sup>

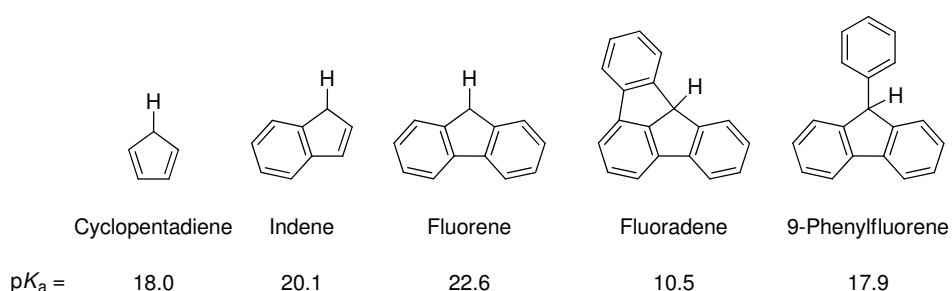


Figure 1: Cyclopentadiene and derivatives with their  $pK_a$  values in DMSO.<sup>[11,13]</sup> Figure adapted from ref.<sup>[11]</sup>

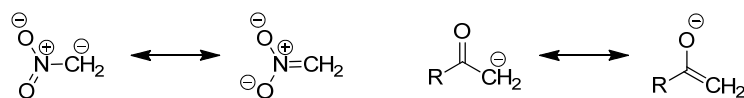
Another important factor contributing to the stability and reactivity of carbanions, is also shown in Figure 1: the substitution at the carbanionic center. Whereas the acidity decreases from cyclopentadiene to fluorene, 9-phenylfluorene has a similar  $pK_a$  value as cyclopentadiene and fluoradene is that acidic that its conjugated base is even stable in water.<sup>[11]</sup> The gas-phase acidities of methane, toluene, diphenylmethane, and triphenylmethane (Table 1),<sup>[14]</sup> show that the more highly substituted center is more likely to give up a proton, hence triphenylmethanide is the most stable carbanion in this series. As gas-phase acidities do not always describe the same situation as solution acidities,<sup>[14b]</sup> Table 1 also depicts the  $pK_a$  values in DMSO. However, not only the number of substituents (primary, secondary, tertiary carbanions), but the electron withdrawing ability of the groups adjacent to the anionic center influence the stability and the reactivity of a carbanion. As Table 1 shows, the gas-phase and solution acidities change by introducing electron withdrawing groups in methane, increasing the acidity in the series toluene  $\rightarrow$  acetonitrile  $\rightarrow$  acetone  $\rightarrow$  nitromethane.

Table 1: Gas-phase acidities of  $\alpha$ -substituted methanes.

	$\Delta H^\circ /$ <b><math>\text{kJ mol}^{-1}</math></b>	<b><math>\text{p}K_{\text{a}}</math></b> <b>(DMSO)</b>		$\Delta H^\circ /$ <b><math>\text{kJ mol}^{-1}</math></b>	<b><math>\text{p}K_{\text{a}}</math></b> <b>(DMSO)</b>
$\text{H}_3\text{C}-\text{H}$	1744 <sup>[a]</sup>	$\sim 56$ <sup>[b]</sup>	$\text{PhCH}_2-\text{H}$	1596 <sup>[a]</sup>	$\sim 43$ <sup>[b]</sup>
$\text{PhCH}_2-\text{H}$	1596 <sup>[a]</sup>	$\sim 43$ <sup>[b]</sup>	$\text{NCCH}_2-\text{H}$	1557 <sup>[c]</sup>	31.3 <sup>[d]</sup>
$\text{Ph}_2\text{CH}-\text{H}$	1526 <sup>[a]</sup>	32.3 <sup>[b]</sup>	$\text{CH}_3\text{COCH}_2-\text{H}$	1549 <sup>[c]</sup>	26.5 <sup>[b]</sup>
$\text{Ph}_3\text{C}-\text{H}$	1503 <sup>[a]</sup>	30.6 <sup>[d]</sup>	$\text{O}_2\text{NCH}_2-\text{H}$	1499 <sup>[c]</sup>	17.2 <sup>[d]</sup>

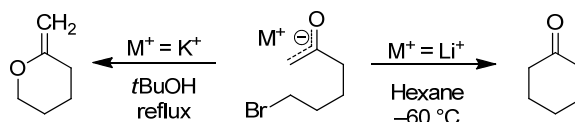
[a] From ref. <sup>[14]</sup> [b] From ref. <sup>[15]</sup> [c] From ref. <sup>[16]</sup> [d] From ref. <sup>[13a]</sup>

Especially when the negative charge of the carbanion is stabilized by resonance, as it is in nitromethane or in enolate ions (Scheme 2), remarkably stable carbanions can be obtained.



Scheme 2: Possible resonance structures of nitromethanide and of an enolate ion.

Such carbanions, in particular nitromethanides and enolate ions, can, due to the charge delocalization over more centers, attack possible electrophiles by different atoms (here carbon or oxygen); they are ambident nucleophiles.<sup>[17]</sup> The ambident reactivity of a ketone-derived enolate is shown in Scheme 3, where different conditions, such as counter ion, temperature and solvent lead to different reaction products.<sup>[18]</sup>

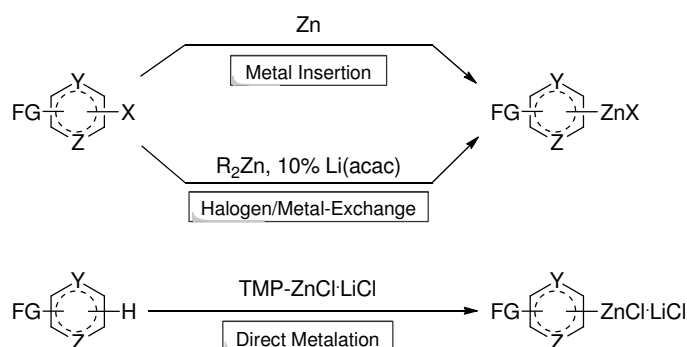
Scheme 3: Reactions of potassium 6-bromo-2-oxohexan-1-ide (left) and lithium 6-bromo-2-oxohexan-1-ide (right).<sup>[18]</sup>

However, the influence of counter ions, solvent, and temperature, which affect the ambident reactivity of enolates, have been studied for a variety of alkylation reactions of carbanions derived from ketones, esters,  $\beta$ -diketones,  $\beta$ -ketoesters and phenolates concluding that all these factors influence the regioselectivity of the alkylation reactions.<sup>[19]</sup> Furthermore, NMR experiments showed that the  $^1\text{H}$  and  $^{13}\text{C}$  chemical shifts of carbanions are affected by solvent, temperature and counter ion as well.<sup>[20]</sup> Lithium indenide in dimethyl ether, for example, undergoes a gradual conversion from contact ion pairs into solvent separated ion pairs by decreasing the temperature, as it was concluded from up field shifts of the resonances in  $^1\text{H}$  NMR experiments.<sup>[20a]</sup> The interactions of the carbanion and the counter ion, depending on the structure of the carbanion and the nature of the metal cation, can have consequences for

the configuration of the carbanion and/or lead to formation of dimers and aggregates having consequences to their reactivity.<sup>[21]</sup> Lithium enolates, for example, are known to form dimers and tetramers in ethereal solution, however, the reactive species in those solutions is the monomeric carbanion.<sup>[21g]</sup>

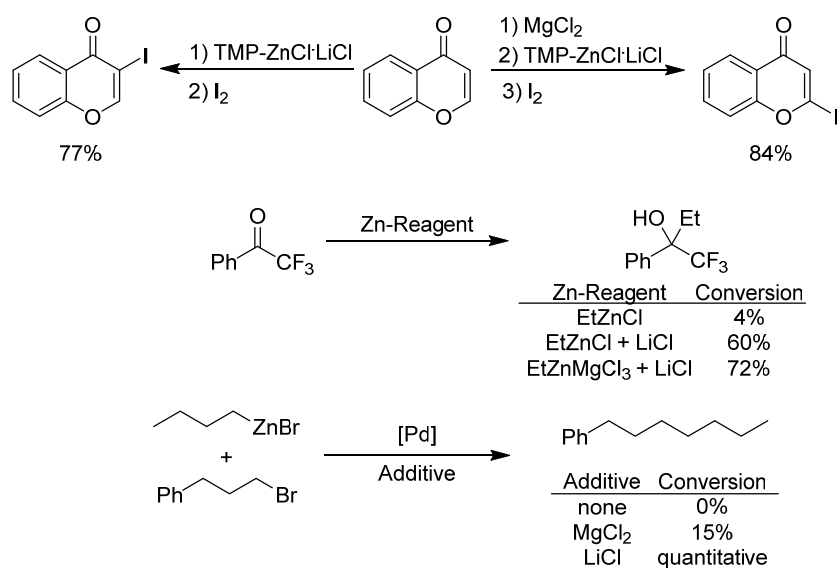
## 1.2. Organozinc Compounds

Organozinc reagents are characterized by polar  $\sigma$ -bonds between metal and carbon and consequently, their reactivity is more moderate than that of the corresponding organoalkali compounds. The low toxicity and price of zinc are not insignificant factors which promoted its applications in synthetic chemistry.<sup>[4,5,6d,e]</sup> As shown in Scheme 4, organozinc compounds are easily accessible by different routes as metal insertion in alkyl- and aryl-halides, by halogen/metal-exchange or by direct metallation using zinc-amine-bases.<sup>[6e]</sup>



Scheme 4: Different routes for the synthesis of organozinc reagents. Figure adapted from ref.<sup>[6e]</sup>

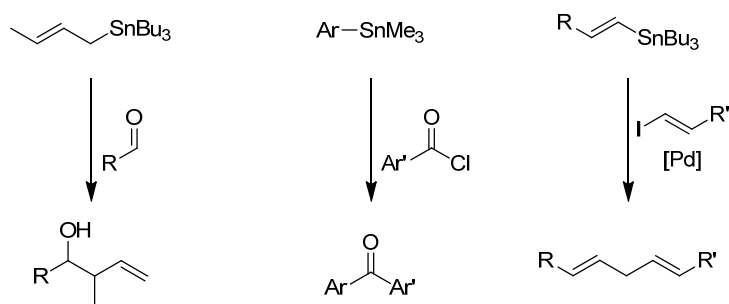
As mentioned above, organozinc reagents allow a wide range of transformations and reactions, however, additives such as lithium, magnesium, copper, etc., can influence their regioselectivity, enhance their nucleophilic reactivity or improve the yields in transition metal catalyzed reactions (Scheme 5).<sup>[4d,e,22]</sup>



Scheme 5: Transformations of organozinc reagents with different additives.

### 1.3. Organotin and Organosilicon Compounds

Organotin and organosilicon compounds are characterized by a even less polar carbon–metal bond, which makes them air and temperature stable.<sup>[1]</sup> Organotin reagents are versatile tools in organic synthesis including allylations or palladium catalyzed cross-couplings, such as the Stille-reaction (Scheme 6).<sup>[23]</sup>



Scheme 6: Examples for reactions of organotin reagents.

Organosilicon compounds are the most stable organometallic reagents, finding important industrial applications as in silicones and silanols.<sup>[24]</sup> Furthermore, silicon plays a significant role in synthetic chemistry as protecting-group for alcohols or as reagent in the Hosomi-Sakurai-,<sup>[25]</sup> Mukaiyama-aldol-reaction,<sup>[26]</sup> or the Peterson-olefination.<sup>[27]</sup>

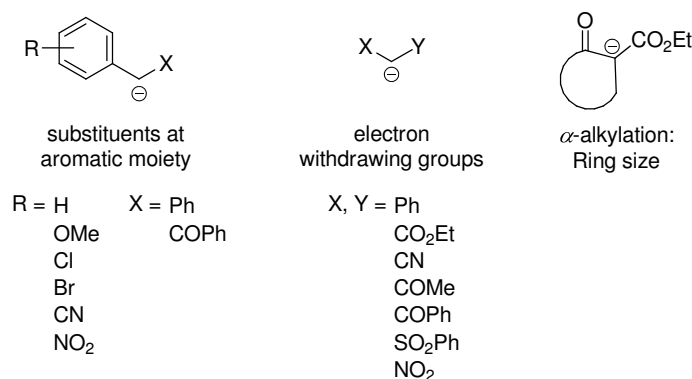
## 2. Objectives

As explained above, the structure of a carbanion is one of the principal factors influencing its stability and reactivity. However, the acidities ( $pK_a$  values) of their conjugate acids give only a rough idea about their reactivities.<sup>[28]</sup>

By application of the linear-free energy relationship (1),<sup>[29]</sup> where  $E$  is an electrophile-specific parameter, and  $N$  and  $s_N$  are nucleophile-specific parameters which are derived from the rates of the reactions of  $\pi$ -,  $n$ -, and  $\sigma$ -nucleophiles with benzhydrylium ions and structurally related Michael acceptors (reference electrophiles), a variety of reagents have previously been characterized.<sup>[30]</sup>

$$\lg k_2(20\text{ }^\circ\text{C}) = s_N(N + E) \quad (1)$$

This methodology allows the comparison of nucleophiles and electrophiles in a wide range of reactivity. Therefore, this method is applied for the characterization of the nucleophilic reactivities of carbanions of variable structure (Scheme 7). Thereby, the influence of  $\alpha$ - and remote substituents on the reactivity of carbanions is studied.



Scheme 7: General structures of carbanions studied in this thesis.

Kinetic experiments with carbanions in the presence of different counter ions as well as at high concentration of metal cations will show how the carbanion/metal ion interactions depend on the nature of the metal and the constitution of the carbanion.

The linear-free energy relationship (1) allows the characterization and comparison of nucleophiles and electrophiles towards their reactivity over a range of 40 orders of magnitude. Therefore the nucleophilic reactivities of free carbanions as well as organozinc, -tin and -silicon reagents can directly be compared.

The ambident reactivity of enolate ions is studied in the last part of this thesis. Thereby, the influences of solvent, counter ion, temperature and concentration on the regioselectivity, are

studied systematically. The effect of the solvent on the nucleophilic reactivity of carbanions is also analyzed in this part.

As parts of this thesis have already been published or will be submitted for publication, individual introductions will be given at the beginning of each chapter. In order to identify my contributions to multiauthor publications/chapters, the experiments which were not performed by me are marked in the respective Experimental Sections.

### 3. References

- [1] a) C. Elschenbroich, *Organometallchemie*, Teugner, Wiesbaden, **2008**; b) P. Powell, *Principles of Organometallic Chemistry*, Chapman and Hall, London, **1988**.
- [2] E. Frankland, *Liebigs Ann. Chem.* **1849**, 71, 171-213.
- [3] V. Grignard, *Compt. Rend. Acad. Sci. Paris* **1900**, 130, 1322-1324.
- [4] E.-I. Negishi, *Organometallics in Organic Synthesis*, Wiley-VCH, Weinheim, **1980**.
- [5] P. Knochel, *Handbook of Functionalized Organometallics*, Wiley-VCH, Weinheim, **2005**.
- [6] Selected Publications: a) I. Coldham, *J. Chem. Soc., Perkin Trans. 1* **1998**, 1343-1364; b) M. Schlosser, *Angew. Chem.* **2005**, 117, 380-398; *Angew. Chem. Int. Ed.* **2005**, 44, 376-393; c) R. E. Mulvey, F. Mongin, M. Uchiyama, Y. Kondo, *Angew. Chem.* **2007**, 119, 3876-3899; *Angew. Chem. Int. Ed.* **2007**, 46, 3802-3824; d) B. Haag, M. Mosrin, H. Ila, V. Malakhov, P. Knochel, *Angew. Chem.* **2011**, 123, 9968-9999; *Angew. Chem. Int. Ed.* **2011**, 50, 9794-9824; e) T. Klatt, J. T. Markiewicz, C. Sämann, P. Knochel, *J. Org. Chem.* **2014**, 79, 4253-4269.
- [7] G. Wu, M. Huang, *Chem. Rev.* **2006**, 106, 2596-2616.
- [8] a) S. Bernhardt, G. Manolikakes, T. Kunz, P. Knochel, *Angew. Chem.* **2011**, 123, 9372-9376; *Angew. Chem. Int. Ed.* **2011**, 50, 9205-9209; b) C. I. Stahakis, S. Bernhard, V. Quint, P. Knochel, *Angew. Chem.* **2012**, 124, 9563-9567; *Angew. Chem. Int. Ed.* **2012**, 51, 9428-9432.

- [9] a) L. Brandsma, S. F. Vasilevsky, H. D. Verkruijsse, *Application of Transition Metal Catalysts in Organic Synthesis*, Springer, Berlin, **1999**; b) E.-I. Negishi, *Handbook of Organopalladium Chemistry for Organic Synthesis*, Wiley-Interscience, New York, **2002**; c) N. Miyaura, A. Suzuki, *Chem. Rev.* **1995**, 95, 2457-2483.
- [10] a) R. B. Bates, C. A. Ogle, *Carbanion Chemistry*, Springer, Berlin, **1983**; b) L. Brandsma, *Preparative Polar Organometallic Chemistry 2*, Springer, Berlin, **1990**; c) V. Snieckus, *Advances in Carbanion Chemistry Vol. 1*, JAI Press, Greenwich, CT, **1992**; d) M. B. Smith, *March's Advanced Organic Chemistry*, 7<sup>th</sup> Ed., Wiley, Hoboken, **2013**, pp. 221-234.
- [11] E. Buncl, J. M. Dust, *Carbanion Chemistry*, Oxford, New York, **2003**.
- [12] a) C. H. de Puy, S. Gronert, S. E. Barlow, V. M. Bierbaum, R. Damrauer, *J. Am. Chem. Soc.* **1989**, 111, 1968-1973; b) K. M. Ervin, S. Gronert, S. E. Barlow, M. K. Gilles, A. G. Harrison, V. M. Bierbaum, C. H. de Puy, W. C. Lineberger, G. B. Ellison, *J. Am. Chem. Soc.* **1990**, 112- 5750-5759.
- [13] a) W. S. Matthews, J. E. Bares, J. E. Bartmes, F. G. Bordwell, F. J. Cornforth, G. E. Drucker, Z. Margolin, R. J. McCallum, G. J. McCollum, N. R. Vanier, *J. Am. Chem. Soc.* **1975**, 97, 7006-7014; b) F. G. Bordwell, G. E. Drucker, *J. Org. Chem.* **1980**, 45, 3325-3328; c) F. G. Bordwell, G. E. Drucker, H. E. Fried, *J. Org. Chem.* **1981**, 46, 632-635.
- [14] a) J. E. Bartmess, J. A. Scott, R. T. McIver Jr., *J. Am. Chem. Soc.* **1979**, 101, 6046-6056; R. W. Taft, F. G. Bordwell, *Acc. Chem. Res.* **1988**, 21, 463-469.
- [15] a) F. G. Bordwell, W. S. Matthews, N. R. Vanier, *J. Am. Chem. Soc.* **1975**, 97, 442-443; b) F. G. Bordwell, D. algrim, N. R. Vanier, *J. Org. Chem.* **1977**, 42, 1817-1819; c) F. G. Bordwell, *Acc. Chem. Res.* **1988**, 21, 456-463.
- [16] a) J. B. Cumming, T. F. Magnera, P. Kebarle, *Can. J. Chem.* **1977**, 55, 3474-3479; b) J. B. Cumming, P. Kebarle, *Can. J. Chem.* **1978**, 56, 1-9.
- [17] H. Mayr, M. Breugst, A. R. Ofial, *Angew. Chem.* **2011**, 123, 6598-6634; *Angew. Chem. Int. Ed.* **2011**, 50, 6470-6505, and references mentioned there.
- [18] H. O. House, W. V. Phillips, T. S. B. Sayer, C.-C. Yau, *J. Org. Chem.* **1978**, 43, 700-710.

- [19] Selected Publications: a) N. Kornblum, A. P. Lurie, *J. Am. Chem. Soc.* **1959**, *81*, 2705-2715; b) N. Kornblum, R. Seltzer, P. Haberfeld, *J. Am. Chem. Soc.* **1963**, *85*, 1148- c) G. Brieger, W. M. Pelletier, *Tetrahedron Lett.* **1965**, *40*, 3555-3558; d) W. J. Le Noble, H. F. Morris, *J. Org. Chem.* **1969**, *34*, 1969-1973; e) W. J. Le Noble, *Synthesis*, **1970**, 1-6; f) E. M. Arnett, V. M. de Palma, *J. Am. Chem. Soc.* **1977**, *99*, 5828-5829; g) R. Gompper, H.-U. Wagner, *Angew. Chem.* **1976**, *88*, 389-422; *Angew. Chem. Int. Ed. Engl.* **1976**, *15*, 321-333; h) R. Gompper, H.-U. Wagner, *Chem. Ber.* **1981**, *114*, 2866-2883.
- [20] a) J. van der Kooij, N. H. Velthorst, C. Maclean, *Chem. Phys. Lett.* **1972**, *12*, 596-598; b) D. H. O'Brien, C. R. Russell, A. J. Hart, *J. Am. Chem. Soc.* **1976**, *98*, 7427-7429; c) D. H. O'Brian, C. R. Russell, A. J. Hart, *J. Am. Chem. Soc.* **1979**, *101*, 633-639; d) R. N. Young, *Progress in NMR Spectroscopy*, **1979**, *12*, 261-286; f) H. Vogler, *J. Organomet. Chem.* **1985**, *293*, 131-137; g) H. Matsui, A. Yoshino, K. Takahasi, *Bull. Chem. Soc. Jpn.* **1994**, *67*, 363-367.
- [21] Selected Publications: a) H. E. Zaug, A. D. Schaefer, *J. Am. Chem. Soc.* **1965**, *87*, 1857-1866; b) M. Raban, E. A. Noe, G. Yamamoto, *J. Am. Chem. Soc.* **1977**, *99*, 6527-6531; c) M. Raban, D. P. Haritos, *J. Am. Chem. Soc.* **1979**, *101*, 5178-5182; d) S. M. Esakov, A. A. Petrov, B. A. Ershov, *J. Org. Chem. USSR (Engl. Trans.)* **1975**, *11*, 679-688; e) A. A. Petrov, S. M. Esakov, B. A. Ershov, *J. Org. Chem. USSR (Engl. Trans.)* **1976**, *12*, 774-778; f) A. Facchetti, A. Streitwieser, *J. Org. Chem.* **2004**, *69*, 8345-8355; g) A. Streitwieser, *J. Mol. Model.* **2006**, *12*, 673-680; h) A. L. Kurts, A. Macias, I. P. Beletskaya, O. A. Reutov, *Tetrahedron*, **1971**, *27*, 4759-4768; i) V. M. de Palma, E. M. Arnett, *J. Am. Chem. Soc.* **1978**, *100*, 3514-3525.
- [22] a) D. R. Armstrong, W. Clegg, P. García-Álvarez, A. R. Kennedy, M. D. McCall, L. Russo, E. Hevia, *Chem. Eur. J.* **2011**, *17*, 8333-8341; b) G. T. Achonduh, N. Hadei, C. Valente, S. Avola, C. J. O'Brien, M. G. Organ, *Chem. Commun.* **2010**, *46*, 4109-4111; c) L. Klier, T. Bresser, T. A. Nigst, K. Karaghiosoff, P. Knochel, *J. Am Chem. Soc.* **2012**, *134*, 13584-13587.
- [23] a) U. K. Roy, S. Roy, *Chem. Rev.* **2010**, *110*, 2472-2535; b) P. Espinet, A. M. Echavarren, *Angew. Chem.* **2004**, *116*, 4808-4839; *Angew. Chem. Int. Ed.* **2004**, *43*, 4704-4734; c) R. A. Rossi, *J. Organomet. Chem.* **2014**, *751*, 201-212; d) M. M. Heravi, E. Hashemi, F. Azimian, *Tetrahedron* **2014**, *70*, 7-21.



- [24] a) A. R. Bassindale, P. P. Gaspar, *Frontiers of Organosilicon Chemistry*, Royal Society of Chemistry, London, **1991**; b) B. Marciniec, J. Chojnowski, *Progress in Organosilicon Chemistry*, Gordon and Breach Publishers, Basel, **1995**; c) M. A. Brook, *Silicon in Organic, Organometallic, and Polymer Chemistry*, Wiley, New York, **2000**.
- [25] a) A. Hosomi, H. Sakurai, *J. Am. Chem. Soc.* **1977**, *99*, 1673-1675; b) L. Chabaud, P. J. Y. Landais, *Eur. J. Org. Chem.* **2004**, 3173-3199.
- [26] a) T. Mukaiyama, K. Narasaka, K. Banno, *Chem. Lett.* **1973**, 1011-1014; b) T. Mukaiyama, *Org. React.* **1982**, *28*, 203-311; c) T. Bach, *Angew. Chem.* **1994**, *106*, 433-435; *Angew. Chem. Int. Ed. Engl.* **1994**, *33*, 417-419; d) R. Mahrwald, *Chem. Rev.* **1999**, *99*, 1095-1120.
- [27] a) D. J. Peterson, *J. Org. Chem.* **1968**, *33*, 780-784; b) D. J. Ager, *Synthesis* **1984**, 384-398; c) D. J. Ager, *Org. React.* **1990**, *38*, 1-223.
- [28] a) T. Bug, H. Mayr, *J. Am. Chem. Soc.* **2003**, *125*, 12980-12986; b) T. Bug, T. Lemek, H. Mayr, *J. Org. Chem.* **2004**, *69*, 7565-7576; c) S. T. A. Berger, A. R. Ofial, H. Mayr, *J. Am. Chem. Soc.* **2007**, *129*, 9753-9761; d) F. Seeliger, H. Mayr, *Org. Biomol. Chem.* **2008**, *6*, 3052-3058; e) R. Appel, R. Loos, H. Mayr, *J. Am. Chem. Soc.* **2009**, *131*, 704-714; f) O. Kaumanns, R. Appel, T. Lemek, F. Seeliger, H. Mayr, *J. Org. Chem.* **2009**, *74*, 75-81.
- [29] H. Mayr, M. Patz, *Angew. Chem.* **1994**, *106*, 990-1010; *Angew. Chem. Int. Ed. Engl.* **1994**, *33*, 938-957.
- [30] Selected Publications: a) H. Mayr, T. Bug, M. F. Gotta, N. Hering, B. Irrgang, B. Janker, B. Kempf, R. Loos, A. R. Ofial, G. Remennikov, H. Schimmel, *J. Am. Chem. Soc.* **2001**, *123*, 9500-9512; b) R. Lucius, R. Loos, H. Mayr, *Angew. Chem.* **2002**, *114*, 97-102; *Angew. Chem. Int. Ed.* **2002**, *41*, 91-95; c) H. Mayr, B. Kempf, A. R. Ofial, *Acc. Chem. Res.* **2003**, *36*, 66-77; d) H. Mayr, A. R. Ofial, *Pure Appl. Chem.* **2005**, *77*, 1807-1821; e) D. Richter, N. Hampel, T. Singer, A. R. Ofial, H. Mayr, *Eur. J. Org. Chem.* **2009**, 3203-3211; f) H. Mayr, S. Lakhdar, B. Maji, A. R. Ofial, *Beilstein, J. Org. Chem.* **2012**, *8*, 1458-1478; f) For a comprehensive listing of nucleophilicity parameters  $N$ ,  $s_N$  and electrophilicity parameters  $E$ , see <http://www.cup.uni-muenchen.de/oc/mayr/DBintro.html>.

## Chapter 2

# Quantification of the Nucleophilic Reactivities of Ethyl Arylacetate Anions

Francisco Corral Bautista and Herbert Mayr

*Eur. J. Org. Chem.* **2013**, 4255–4261

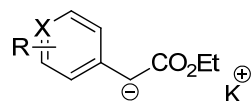
## 1. Introduction

The anions of ethyl arylacetates are frequently used as nucleophiles in Michael additions<sup>[1]</sup> and Claisen condensations.<sup>[2]</sup> Furthermore, they can easily be alkylated or added to carbonyl groups, imines, or acetylenes leading to a wide variety of products of biological and medicinal interest.<sup>[1d,3-5]</sup>

During the last decades, we have constructed a comprehensive nucleophilicity scale, which is based on reactions of  $\pi$ -,  $n$ -, and  $\sigma$ -nucleophiles with benzhydrylium ions, structurally related quinone methides, and diethyl benzylidenemalonates.<sup>[6-11]</sup> The second-order rate constants of these reactions have been described by Equation (1), where  $E$  is an electrophile-specific parameter, and  $N$  and  $s_N$  are nucleophile-specific parameters.<sup>[12]</sup>

$$\lg k_2 (20^\circ \text{C}) = s_N (N + E) \quad (1)$$

We now report on the kinetics of the reactions of the anions of ethyl arylacetates **1** (Scheme 1) with the reference electrophiles **2** and **3** (Table 1) in DMSO solution and use these data to include the anions **1a–f** in our nucleophilicity scale.<sup>[6f]</sup> Subsequently, we determine the rate constants for the reactions of the ethyl 4-nitrophenylacetate anion (**1e**) with different types of electrophiles and compare the results with the rate constants calculated by Equation (1).

	X	R	$\delta(\text{CH})^{[a]}$	$\lambda_{\text{max}}$
	<b>1a</b>	CH	H	3.40
	<b>1b</b>	CH	3-Cl	3.79
	<b>1c</b>	CH	4-Br	3.76
	<b>1d</b>	CH	4-CN	4.03
	<b>1e</b>	CH	4-NO <sub>2</sub>	4.62
	<b>1f</b>	N	H	3.80

Scheme 1: Anions of the ethyl arylacetates **1**, the <sup>1</sup>H NMR chemical shifts of the corresponding benzylic protons and  $\lambda_{\text{max}}$  (in nm) of the anions in DMSO solution. [a] <sup>1</sup>H NMR in [D<sub>6</sub>]-DMSO solution at 200 MHz. [b] Due to H-D-exchange with the solvent  $\delta(\mathbf{1a})$  was not observable.

Table 1: Quinone methides **2** and diethyl benzylidenemalonates **3** as reference electrophiles employed in this work.

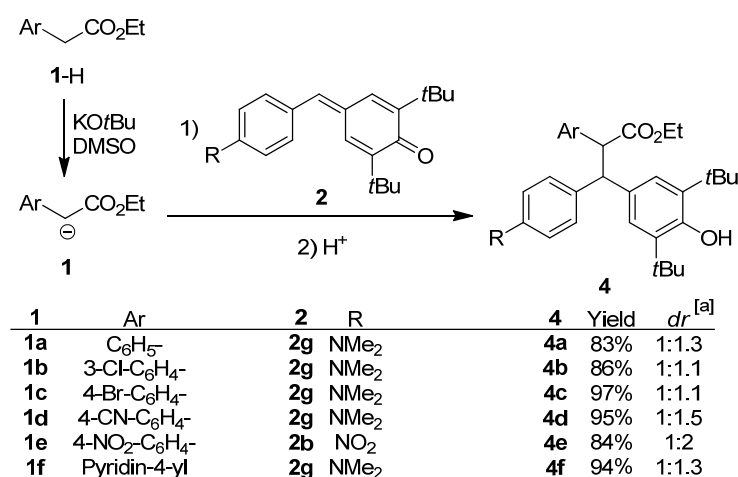
Electrophile	R <sup>1</sup>	R <sup>2</sup>		<i>E</i> [a]
	Ph	4-OMe	<b>2a</b>	-12.18
	<i>t</i> Bu	4-NO <sub>2</sub>	<b>2b</b>	-14.36
	<i>t</i> Bu	3-F	<b>2c</b>	-15.03
	<i>t</i> Bu	4-Me	<b>2d</b>	-15.83
	<i>t</i> Bu	4-OMe	<b>2e</b>	-16.11
	OMe	4-OMe	<b>2f</b>	-16.38
	<i>t</i> Bu	4-NMe <sub>2</sub>	<b>2g</b>	-17.29
			<b>2h</b>	-17.90
	R = 4-NO <sub>2</sub>		<b>3a</b> <sup>[b]</sup>	-17.67
	R = 3-Cl		<b>3b</b>	-18.98
	R = H		<b>3c</b>	-20.55
	R = 4-Me		<b>3d</b>	-21.11

[a] Electrophilicity parameters from refs.<sup>[6b,6e,13]</sup> [b] Used only for product studies.

## 2. Results and Discussion

### 2.1. Product Studies

Solutions of the anions **1** were generated by treatment of the esters **1-H** with potassium *tert*-butoxide (KO*t*Bu ~1.05 equiv.) in DMSO and combined with solutions of **2** in DMSO (with 5–10 % dichloromethane as cosolvent). After aqueous, acidic work-up, the crude reaction products **4** were purified by chromatography and characterized by NMR spectroscopy and mass spectrometry. In all cases, the products **4** were obtained in good to excellent yields as mixtures of two diastereoisomers (Scheme 2).



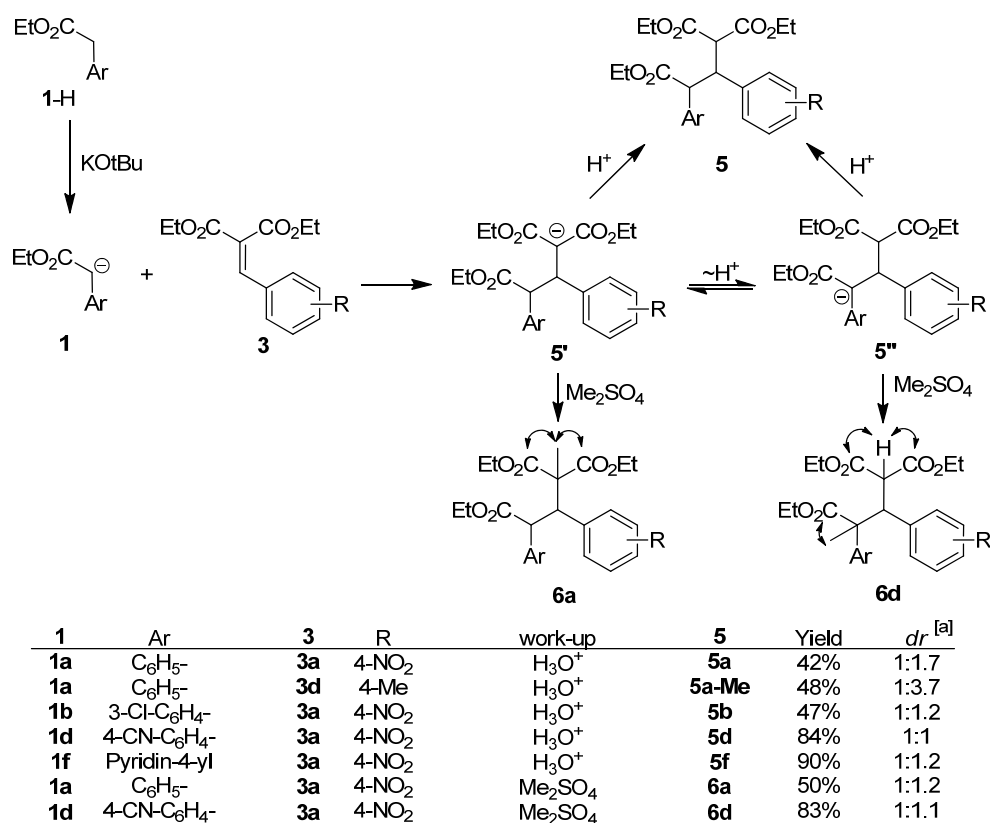
Scheme 2: Products of the reactions of the anions of ethyl arylacetates (**1**) with quinone methides **2** in DMSO at 20 °C. [a] Determined by <sup>1</sup>H NMR after purification by chromatography.

Only 14% of **5a** was obtained, when **1a** was combined with the benzyldienemalonate **3a** in DMSO even when 10 equiv. of **1a** were employed. Combinations of **1a** with less reactive electrophiles such as **3d**, gave complex product mixtures, from which the addition products **5** could not be separated. The adducts **5** could be isolated as the only products after acidic work-up, however, when the reactions were carried out in THF (Scheme 3). While the reactions of the unsubstituted anion **1a** and the *m*-chloro-substituted anion **1b** with **3a** gave around 45% of **5a** and **5b** respectively, almost quantitative yields of **5d** and **5f** were obtained from the reactions of the less reactive anions **1d** and **1f** with **3a**. Methylation of the initially formed anionic Michael adducts (**5'** and **5''**) yield different types of products, **6a** for Ar = Ph, and **6d** for Ar = 4-CN-C<sub>6</sub>H<sub>4</sub>. The HMBC-spectra of both diastereoisomers of **6a** show <sup>3</sup>J<sub>CH</sub> couplings of the methyl group to the two carbonyl carbons of the malonate group. On the other hand, the HMBC-spectra of both diastereoisomers of **6d** show <sup>3</sup>J<sub>CH</sub>-couplings from the Me-group to only one carboxyl-carbon and <sup>2</sup>J<sub>CH</sub>-couplings of the CH-group to the two carboxyl-carbons of the malonate group (Scheme 3). Though it is quite likely that the formation of **6a** and **6d** indicates that **1a** and **3a** yield an adduct with a malonate anion structure (**5'**), while **1d** and **3a** yield an ester-stabilized *p*-cyano-substituted benzyl anion (**5''**), this conclusion is not unequivocal because we do not know the relative rates of methylation and proton transfer.

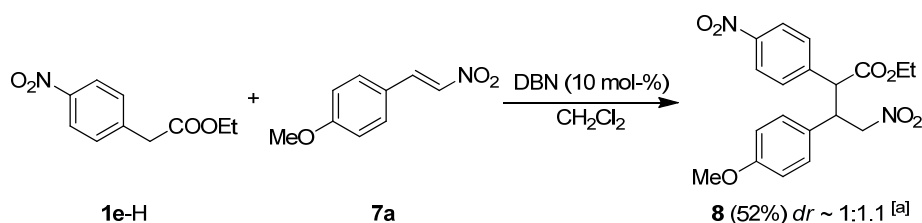
The reaction of ethyl 4-nitrophenylacetate (**1e-H**) with the *trans*-β-nitrostyrene **7a** catalyzed by 10 mol% of 1,5-diazabicyclo[4.3.0]non-5-ene (DBN) in dichloromethane gave 52% of **8** as a 1:1.1 mixture of two diastereoisomers (Scheme 4).

From the reaction of **1e** (generated from **1e-H** and KO<sup>*t*</sup>Bu) with the 1,2-diaza-1,3-diene **9a** in DMSO, **10** was obtained in 87% yield as a 1:1 mixture of diastereoisomers (Scheme 5).

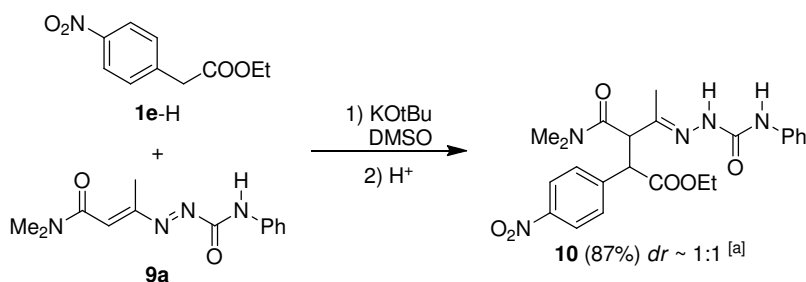
As the reactions of the anions **1** with the benzyldiene malononitrile **11** in DMSO are highly reversible, the addition products could not be isolated. However, when the CH acid **1e-H** was mixed with 1 equiv. of KO<sup>*t*</sup>Bu and 1 equiv. of **11** in [D<sub>6</sub>]-DMSO, the formation of the adduct **12** (as a mixture of two diastereoisomers) was observed by NMR spectroscopy (Scheme 6). Though not all <sup>1</sup>H NMR signals could be assigned to the reaction product **12**, the signals of the benzylic protons and carbons could unequivocally be assigned. With <sup>3</sup>J = 12 Hz, the vicinal coupling constant between the benzylic doublets is of similar magnitude as in the structurally analogous products **4** and **5**.



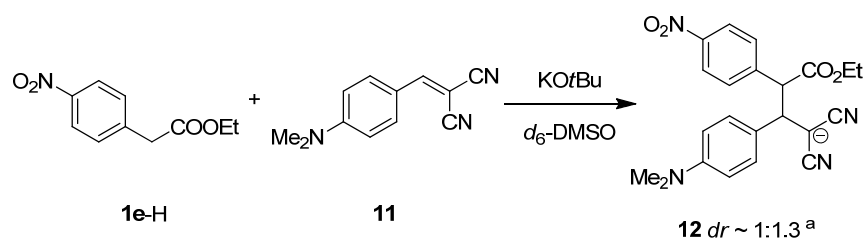
Scheme 3: Products of the reactions of the anions of ethyl arylacetates **1** with diethyl benzylidenemalonates **3** in THF at ambient temperature and HMBC correlations (double-headed arrows in formula of **6**). [a] Determined by <sup>1</sup>H NMR after purification by chromatography.



Scheme 4: Reaction of **1e-H** with the *trans*- $\beta$ -nitrostyrene **7a** with catalytic amounts of DBN in dichloromethane at 20 °C. [a] Determined by <sup>1</sup>H NMR-spectroscopy.



Scheme 5: Reaction of the anion **1e** with the 1,2-diaza-1,3-diene **9a** in DMSO at ambient temperature. [a] Determined by <sup>1</sup>H NMR-spectroscopy.

Scheme 6: Reaction of the anion **1e** with **11** in  $[\text{D}_6]$ -DMSO.

## 2.2. Kinetic Investigations

The reactions of the ethyl arylacetate anions **1a–f** with the electrophiles **2**, **3**, **7**, **9**, and **11** were performed in DMSO solution at 20 °C and monitored by UV-Vis spectroscopy at or close to the absorption maximum of one of the reagents (compare Table 2 and Experimental Section). Due to their low stability, the potassium salts of the ethyl arylacetates (**1a–f**)-K were not isolated, but were generated by deprotonation of the corresponding CH acids (**1a–f**)-H with KOtBu (typically 1.05 equiv.) in DMSO prior to the measurements. The complete deprotonation of the CH acids was demonstrated by combining solutions of (**1a–f**)-H with 1.05 equivalents of KOtBu in DMSO. After completion of the deprotonation, the concentration of the carbanions (determined by UV-Vis-spectroscopy) remained constant and did not even increase when 2–5 additional equiv. of KOtBu were subsequently added.

To simplify the evaluation of the kinetic experiments, one of the reactants, either the nucleophile or the electrophile, depending on their absorption spectra, was used in large excess ( $> 10$  equiv.). Thus, the concentrations of the major components remained almost constant throughout the reactions, and pseudo-first-order kinetics were obtained in all runs. The first-order rate constants  $k_{\text{obs}}$  were derived by least-squares fitting of the exponential function  $A_t = A_0 \exp(-k_{\text{obs}}t) + C$  to the time-dependent absorbances  $A_t$  of the minor component. Second-order rate constants were obtained as the slopes of plots of  $k_{\text{obs}}$  versus the concentrations of the compound used in excess (Figure 1).

For all reactions described in Tables 2 and 3, second-order rate constants were derived as the slopes of the linear plots of  $k_{\text{obs}}$  vs. the concentrations of the compounds used in excess.

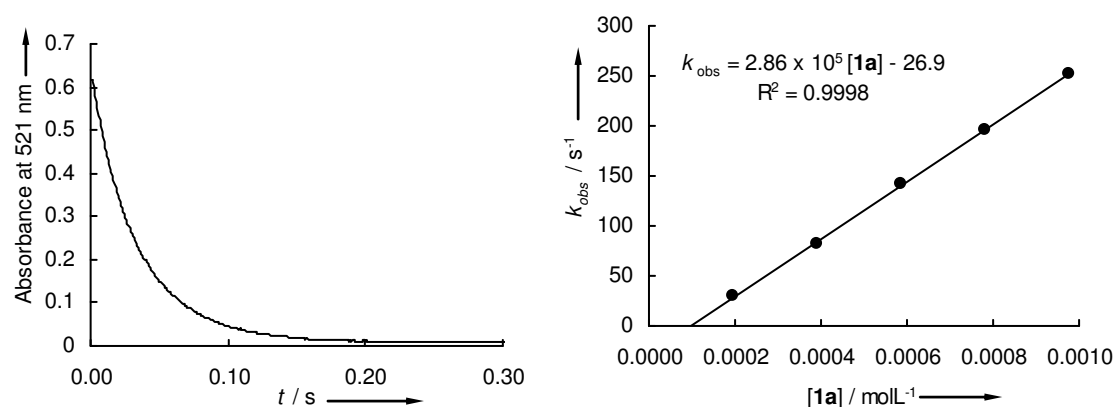
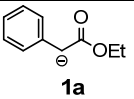
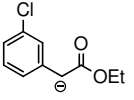
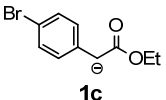
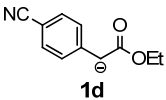
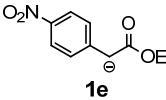
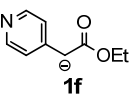


Figure 1: Plot of the absorbance  $A_t$  (521 nm) vs. time for the reaction of **1a** ( $1.77 \times 10^{-5} \text{ mol L}^{-1}$ ) with **2h** ( $1.95 \times 10^{-4} \text{ mol L}^{-1}$ ) in DMSO at 20 °C (left). Plot of the first-order rate constants  $k_{\text{obs}}$  vs. the concentration of **1a** (right).

Table 2: Second-order rate constants  $k_2$  for the reactions of the carbanions **1a–f** with the reference electrophiles **2** and **3** in DMSO at 20 °C.

Nucleophile	$N_{S_N}$	Electrophile	$k_2 / \text{L mol}^{-1} \text{s}^{-1}$	$\lambda / \text{nm}^{[a]}$	Excess of
 <b>1a</b>	27.54	<b>2f</b>	$2.21 \times 10^6$	407	<b>1a</b>
	0.57	<b>2g</b>	$5.51 \times 10^5$	486	<b>1a</b>
		<b>2h</b>	$2.86 \times 10^5$	521	<b>1a</b>
		<b>3b</b>	$7.43 \times 10^4$	340	<b>3b</b>
		<b>3c</b>	$1.00 \times 10^4$	340	<b>3c</b>
		<b>3d</b>	$3.91 \times 10^3$	345	<b>3d</b>
 <b>1b</b>	27.57	<b>2f</b>	$9.06 \times 10^5$	407	<b>1b</b>
	0.53	<b>2g</b>	$2.33 \times 10^5$	486	<b>1b</b>
		<b>2h</b>	$1.24 \times 10^5$	521	<b>1b</b>
		<b>3b</b>	$2.29 \times 10^4$	350	<b>3b</b>
		<b>3c</b>	$6.09 \times 10^3$	350	<b>3c</b>
		<b>3d</b>	$2.49 \times 10^3$	350	<b>3d</b>
 <b>1c</b>	27.62	<b>2f</b>	$9.89 \times 10^5$	407	<b>1c</b>
	0.53	<b>2g</b>	$3.21 \times 10^5$	486	<b>1c</b>
		<b>2h</b>	$1.53 \times 10^5$	521	<b>1c</b>
 <b>1d</b>	23.64	<b>2g</b>	$1.14 \times 10^4$	486	<b>1d</b>
	0.65	<b>2h</b>	$5.90 \times 10^3$	521	<b>1d</b>
		<b>3b</b>	$9.65 \times 10^2$	405	<b>3b</b>
 <b>1e</b>	20.00	<b>2a</b>	$2.63 \times 10^5$	422	<b>1e</b>
	0.71	<b>2b</b>	$1.35 \times 10^4$	374	<b>1e</b>
		<b>2c</b>	$3.68 \times 10^3$	354	<b>1e</b>
		<b>2d</b>	$8.80 \times 10^2$	371	<b>1e</b>
		<b>2e</b>	$4.90 \times 10^2$	393	<b>1e</b>
		<b>2g</b>	$7.21 \times 10^1$	450	<b>1e</b>
 <b>1f</b>	23.27	<b>2d</b>	$1.54 \times 10^5$	371	<b>1f</b>
	0.70	<b>2e</b>	$9.46 \times 10^4$	393	<b>1f</b>
		<b>2g</b>	$1.51 \times 10^4$	486	<b>1f</b>
		<b>2h</b>	$6.77 \times 10^3$	521	<b>1f</b>
		<b>3b</b>	$8.74 \times 10^2$	351	<b>3b</b>

[a] Monitored wavelength.

For all investigations in DMSO solution, the CH acids (**1a–f**)-H were deprotonated with KO<sup>t</sup>Bu leading to anions with potassium as counter ion: (**1a–f**)-K. It was found that the first-order rate constants  $k_{\text{obs}}$  obtained in the presence and in the absence of 18-crown-6 ether were on the same  $k_{\text{obs}}$  vs. concentration plots (see Experimental Section) indicating that the nature of the counterion does not play a role, i.e., that the determined rate constants reflect the reactivities of the free carbanions.

### 2.3. Correlation Analysis

Plots of  $\lg k_2$  for the reactions of the carbanions **1** with the reference electrophiles **2** and **3** against the electrophilicity parameters  $E$  were linear, as shown for some representative examples in Figure 2. As depicted in the Experimental Section, all reactions studied in this work followed analogous linear correlations, indicating that Equation (1) is applicable to these reactions. From the slopes of these correlations, the nucleophile-specific parameters  $s_N$  are derived, and the negative intercepts on the abscissa ( $\lg k_2 = 0$ ) correspond to the nucleophilicity parameters  $N$  (Table 2).

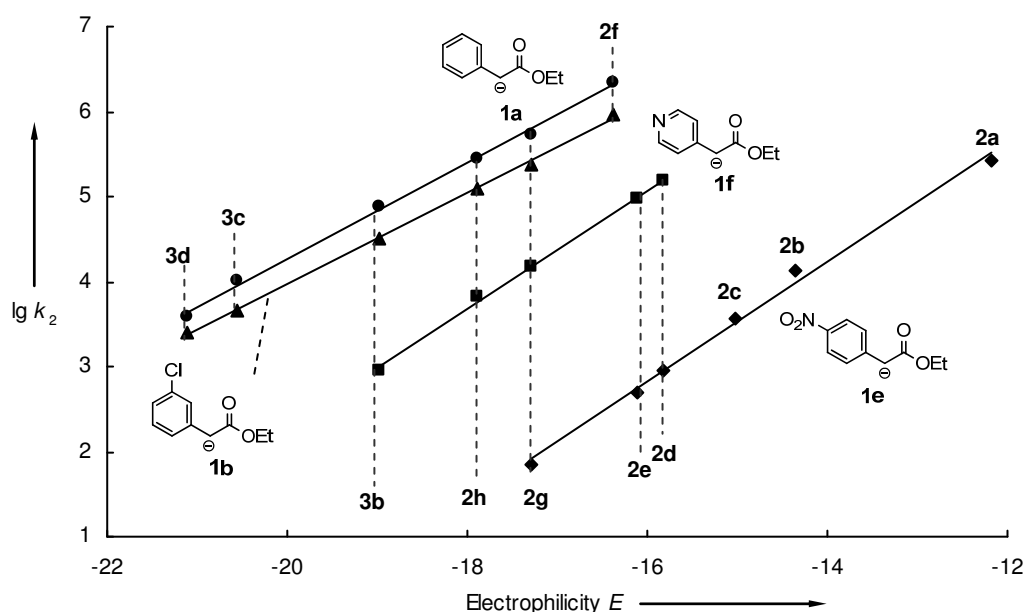


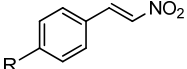
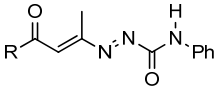
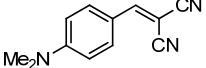
Figure 2: Correlation of the rate constants  $\lg k_2$  for the reactions of the nucleophiles **1** with the electrophiles **2** and **3** in DMSO with their electrophilicity parameters  $E$ .

In order to examine the applicability of the  $N$  and  $s_N$  parameters thus derived to predict rate constants for reactions with other classes of electrophiles, we investigated the rate constants for the reactions of the ethyl 4-nitro-phenylacetate anion (**1e**) with the *trans*- $\beta$ -nitrostyrenes



**7a,b**, the 1,2-diaza-1,3-dienes **9a,b**, and the benzyldiene malononitrile **11** in DMSO at 20 °C by the photometric method used above. Table 3 shows that in all cases the experimental rate constants agreed within a factor of 3 with those calculated by Equation (1), confirming the applicability of the reactivity parameters  $N$  and  $s_N$  reported in Table 2 for predicting rate constants with other types of electrophiles.

Table 3: Experimental and calculated [by Equation (1)] second-order rate constants for the reactions of ethyl 4-nitrophenylacetate anion (**1e**) with various electrophiles **7**, **9** and **11** in DMSO at 20 °C.

Electrophiles		$E$ [a]	$k_2^{\text{exp}} / \text{L mol}^{-1} \text{s}^{-1}$	$k_2^{\text{calc [b]}} / \text{L mol}^{-1} \text{s}^{-1}$	$k_2^{\text{exp}} / k_2^{\text{calc [b]}}$
	R = OMe <b>7a</b>	-14.70	$3.15 \times 10^3$	$5.79 \times 10^3$	0.54
	R = Br <b>7b</b>	-13.37	$1.66 \times 10^4$	$5.10 \times 10^4$	0.33
	R = NMe <sub>2</sub> <b>9a</b>	-15.38	$5.43 \times 10^3$	$1.91 \times 10^3$	2.8
	R = OEt <b>9b</b>	-13.28	$1.34 \times 10^5$	$5.90 \times 10^4$	2.3
	<b>11</b>	-13.30	$1.85 \times 10^4$	$5.71 \times 10^4$	0.32

[a] Electrophilicity parameters from refs.<sup>[14-16]</sup> [b] Calculated with Equation (1) from  $E$  in this Table and  $N$  and  $s_N$  from Table 2.

## 2.4. Structure-Reactivity Relationships

The narrow range of  $s_N$  for all nucleophiles listed in Table 2 ( $0.53 < s_N < 0.71$ ), which is illustrated by the almost parallel correlation lines in Figure 2, implies that the relative reactivities of these anions depend only slightly on the electrophilicities of the reaction partners. The reactivities towards the quinone methide **2g**, for which rate constants with all carbanions **1a–f** were determined, therefore reflect general structure-reactivity trends. The *m*-chloro- (**1b**) and *p*-bromo-substituted (**1c**) ethyl phenylacetate anions react approximately two-times more slowly with the electrophile **2g** than the unsubstituted ethyl phenylacetate anion (**1a**) indicating only a little stabilization of the negative charge by the halogen substituents. The anion of the *p*-cyano substituted ethyl arylacetate (**1d**), which is as reactive as the ethyl 2-(pyridin-4-yl)-acetate anion (**1f**), is more than one order of magnitude less reactive than the unsubstituted anion **1a**. The influence of the *p*-nitro-group is tremendous: **1e** is 7600 times less reactive than the unsubstituted anion **1a**.

As previously reported for the reactivities of other  $\alpha$ -acceptor substituted benzyl anions,<sup>[11d]</sup> only a poor correlation between nucleophilic reactivities of **1a–e** and Hammett's  $\sigma_p^-$  substituent constants<sup>[17]</sup> was observed (Figure 3). The downward curvature of the graph indicates that the conjugative interaction between the nitro group and the carbanionic reaction

center is much stronger than in the phenoxides which were employed for calibrating the  $\sigma_p^-$  values. Accordingly Kiyooka *et al.*<sup>[18]</sup> reported that the  $^1\text{H}$ - and  $^{13}\text{C}$ -chemical shifts of the anionic center of ethyl arylacetates and the corresponding infrared absorption maxima are affected more strongly by acceptor substituents in *p*-position than expected from the correlations with  $\sigma$  and  $\sigma_p^-$  parameters. Obviously, the nonlinearities of the Hammett correlations depicted in Figure 3 and reported by Kiyooka have the same origin, as Figure 4 shows a good linear correlation between the nucleophilic reactivities of the carbanions **1b–e** and their  $^1\text{H}$ -chemical shifts in DMSO solution

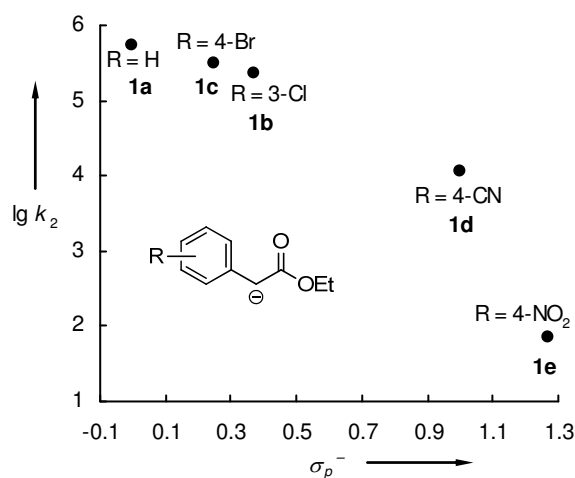


Figure 3: Correlation of the  $\lg k_2$  values for the reactions of **1a–e** with the quinone methide **2g** in DMSO at 20 °C with Hammett's substituent constants  $\sigma_p^-$ .

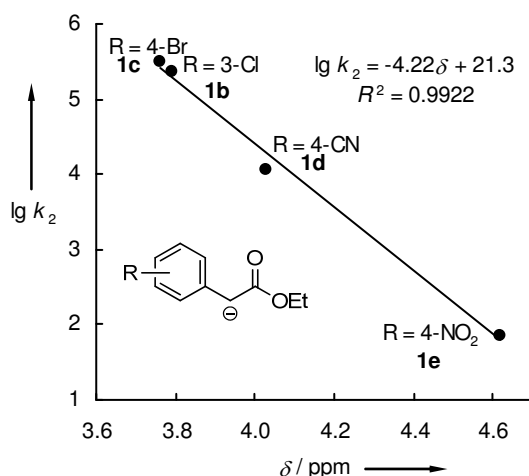


Figure 4: Correlation of the  $\lg k_2$  values for the reactions of **1b–e** with the quinone methide **2g** in DMSO at 20 °C vs. the  $^1\text{H}$ -chemical shifts (from Scheme 1) of the benzylic proton of the anions.

Scheme 7 shows how the reactivities of benzyl anions are affected by  $\alpha$ -acceptor substituents (reference quinone methide **2g**): the anion of ethyl phenylacetate has a similar nucleophilicity

as the anion of phenylacetonitrile. While the phenylsulfonyl group reduces the nucleophilic reactivity by one order of magnitude relative to ethoxycarbonyl, a benzoyl group reduces the reactivity by more than two orders of magnitude. Benzyl anions with an  $\alpha$ -nitro-group or an  $\alpha$ -trifluoromethylsulfonyl group, are five orders of magnitude less reactive.

	$k_{\text{rel}}(\text{R} = \text{H})$	$k_{\text{rel}}(\text{R} = \text{CN})$
	1.0	1.0
		$9.6 \times 10^{-1}$
		$9.1 \times 10^{-2}$
	$6.5 \times 10^{-3}$	
	$1.0 \times 10^{-5}$	$6.6 \times 10^{-5}$
	$1.6 \times 10^{-5}$	$1.5 \times 10^{-5}[\text{a}]$

Scheme 7: Comparison of the relative second-order rate constants for the reactions of different benzyl anions with the quinone methide **2g** in DMSO at 20 °C. Refs.<sup>[11b,d,e,f,19]</sup>. The rate constants for the reactions of the ethyl arylacetates with **2g** were set to unity. [a] Rate constant was calculated by Equation (1).

The Brønsted correlation in Figure 5 depicts that the nucleophilic reactivities of  $\alpha$ -acceptor substituted carbanions correlate only poorly with their Brønsted basicities in DMSO, indicating the important role of the intrinsic barriers.<sup>[20]</sup> It is obvious, however, that the  $\alpha$ -ethoxycarbonyl-substituted benzyanions are among the most nucleophilic as well as most basic carbanions of the series depicted in Figure 5.

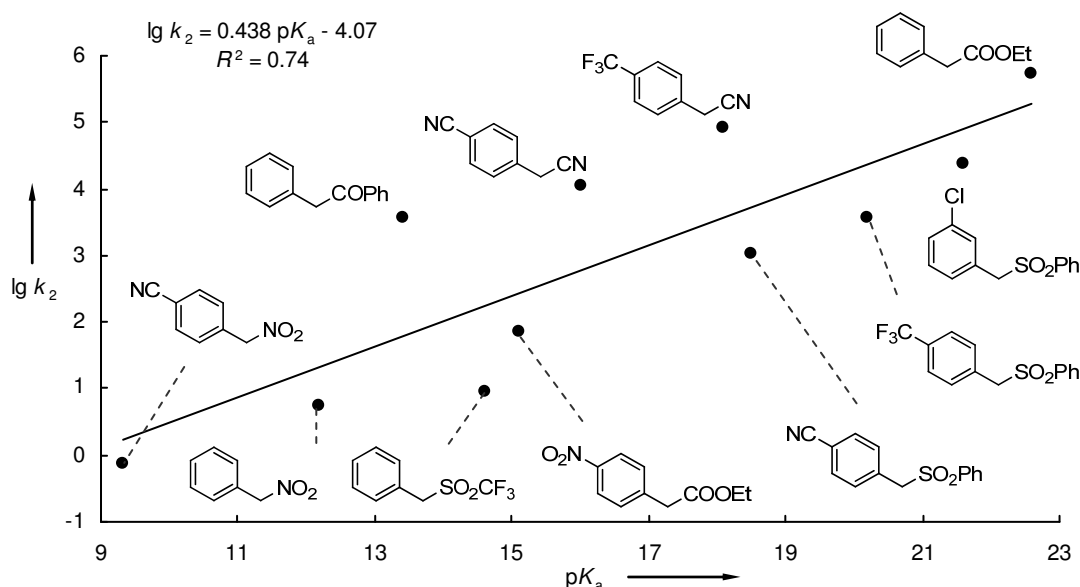


Figure 5: Correlation of  $\lg k_2$  for the reactions of the anions of the ethyl arylacetates **1a** and **1e** and other benzyl anions<sup>[11b,d,e,f,19]</sup> with the quinone methide **2g** in DMSO at 20 °C versus the  $pK_a$  values<sup>[21]</sup> of their conjugated acids.

### 3. Conclusions

The rate constants for the reactions of the anions of ethyl arylacetates with quinone methides and diethyl benzylidenemalonates in DMSO follow the linear free-energy relationship [Equation (1)] allowing us to include these compounds in our comprehensive nucleophilicity scale and compare their nucleophilicities with those of other nucleophiles. Variation of the substituents in the arene ring from X = H to X = 4-NO<sub>2</sub> decreases the reactivities by four orders of magnitude. Their nucleophilic reactivities are comparable to those of analogously substituted  $\alpha$ -cyano substituted benzyl anions, 10<sup>5</sup>-times higher than those of the corresponding  $\alpha$ -nitro- and  $\alpha$ -trifluoromethyl-substituted benzyl anions with the same substituents at the arene ring. The agreement of the experimental and calculated [by Equation (1)] rate constants for the reactions of **1e** with the electrophiles **7a,b**, **9a,b**, and **11** within an factor of three demonstrates the applicability of the *N* and *s<sub>N</sub>* parameters in Table 2 for predicting the rates of their reactions with various electrophiles. The ethyl arylacetate anions **1a–c** belong to the most reactive nucleophiles studied so far and, therefore, they should be applicable for deriving reactivity parameters of very weak electrophiles.

## 4. Experimental Section

### 4.1. General

#### Materials

Commercially available DMSO ( $\text{H}_2\text{O}$  content < 50 ppm) was used without further purification. The reference electrophiles used in this work were synthesized according to literature procedures.<sup>[6b,e,13]</sup> The ethyl arylacetates **1b**-H and **1d**-H were synthesized as described below. The ethyl arylacetates **1a**-H, **1c**-H, **1e**-H and **1f**-H were purchased from ABCR, Karlsruhe (Germany).

#### NMR spectroscopy

In the  $^1\text{H}$  and  $^{13}\text{C}$  NMR spectra chemical shifts are given in ppm and refer to tetramethylsilane ( $\delta_{\text{H}} = 0.00$ ,  $\delta_{\text{C}} = 0.0$ ),  $[\text{D}_6]\text{-DMSO}$  ( $\delta_{\text{H}} = 2.50$ ,  $\delta_{\text{C}} = 39.5$ ) or to  $\text{CDCl}_3$  ( $\delta_{\text{H}} = 7.26$ ,  $\delta_{\text{C}} = 77.0$ ),<sup>[22]</sup> as internal standards. The coupling constants are given in Hz. For reasons of simplicity, the  $^1\text{H}$ -NMR signals of AA'BB'-spin systems of *p*-disubstituted aromatic rings are treated as doublets. Signal assignments are based on additional COSY, gHSQC, and gHMBC experiments. Chemical shifts marked with (\*) refer to the minor isomer when the product was obtained as a mixture of two diastereomers.

#### Kinetics

As the reactions of colored quinone methides **2** with colorless nucleophiles **1** or of colored anions **1** with colorless diethyl benzylidenemalonates **3** yield colorless products (or products with a different absorption range than the reactants), the reactions could be followed by UV-Vis spectroscopy. As all reactions were fast ( $\tau_{1/2} < 10$  s), the kinetics were monitored using stopped-flow techniques. The temperature of all solutions was kept constant at  $20.0 \pm 0.1$  °C by using a circulating bath thermostat. In all runs the concentration of the colorless compound was at least 10 times higher than the concentration of the colored compound, resulting in pseudo-first-order kinetics with an exponential decay of the concentration of the minor compound. First-order rate constants  $k_{\text{obs}}$  were obtained by least-squares fitting of the exponential function  $A_t = A_0 \exp(-k_{\text{obs}}t) + C$  to the time-dependent absorbances. The second-order rate constants  $k_2$  were obtained from the slopes of the linear plots of  $k_{\text{obs}}$  against the concentration of the excess components.

## 4.2. Synthesis of the Ethyl Phenylacetates (1-H)

### 4.2.1. Ethyl 3-Chlorophenylacetate (1b-H)

3-Chlorophenylacetic acid (1.50 g, 8.79 mmol) was dissolved in 25 mL of ethanol with 4 droplets of sulfuric acid and heated to reflux for 12 h. After purification by flash chromatography, ethyl 3-chlorophenylacetate (**1b-H**) was obtained in 97 % (1.70 g, 8.56 mmol) yield.

<sup>1</sup>H NMR data is in agreement with the literature.<sup>[23]</sup>

### 4.2.2. Ethyl 4-Cyanophenylacetate (1d-H)<sup>[24]</sup>

Ethyl 4-bromophenylacetate (1.30 g, 5.34 mmol), sodium cyanide (316 mg, 6.45 mmol), potassium iodide (180 mg, 1.08 mmol), copper (I) iodide (106 mg, 0.557 mmol) and *N,N'*-dimethyl ethylenediamine (60  $\mu$ L) were mixed with 3 mL of toluene and heated under argon atmosphere for 21 h to 130 °C. The reaction was followed by GC/MS. After cooling, 20 mL aqueous ammonia (10 %) was added and the mixture was extracted (4 x 20 mL) with ethyl acetate. The combined organic layers were washed with brine and dried over sodium sulfate. After evaporation of the solvent, the crude product was purified by flash chromatography on silica with pentane/ethyl acetate as eluent. Ethyl 4-cyanophenylacetate (582 mg, 3.08 mmol, 58 %) was obtained as colorless solid.

Mp.: 93.2-93.8 °C. <sup>1</sup>H NMR data is in agreement with the literature.<sup>[24]</sup>

## 4.3. Reaction Products

### 4.3.1. Reactions of Ethyl Phenylacetates (1) with Quinone Methides (2)

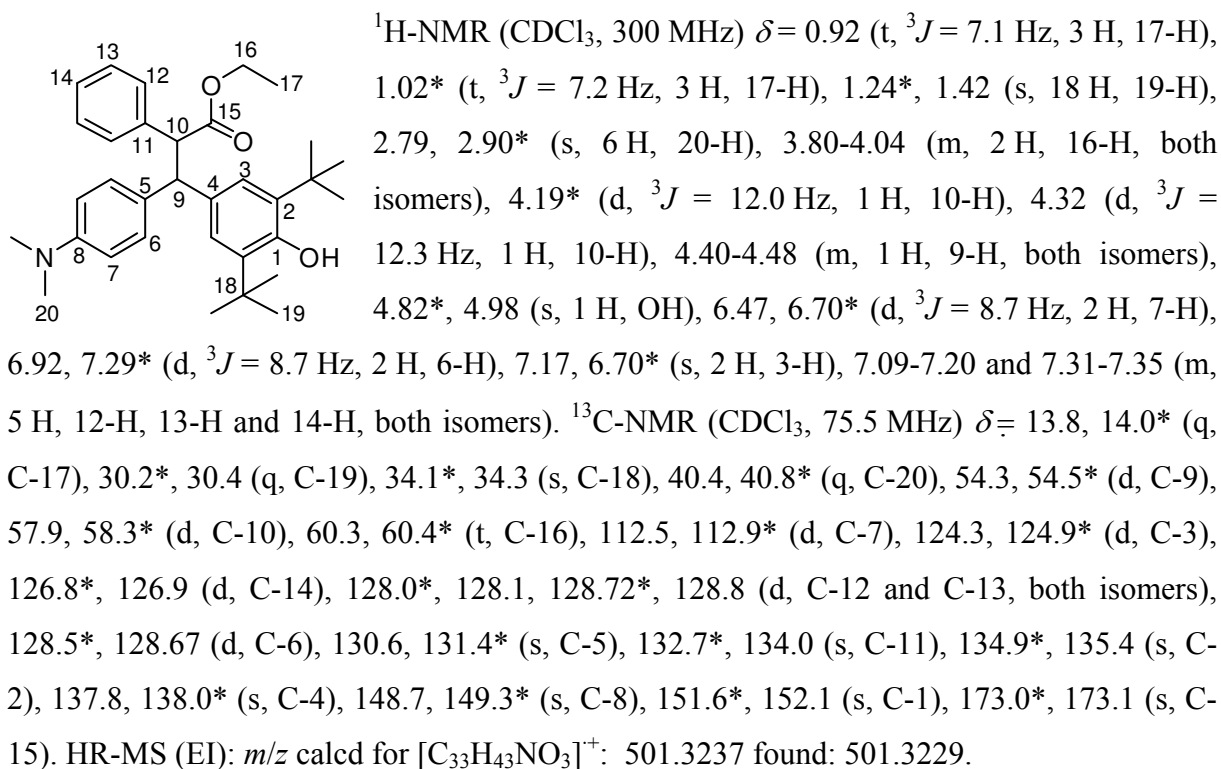
#### General Procedure 1 (GP1):

The anions **1** were generated by addition of the ethyl arylacetate **1-H** (50-70 mg, 1 equiv.) to a solution of KO<sup>*t*</sup>Bu (30-40 mg, 1.05 equiv.) in 5 mL of dry DMSO. Subsequently, a solution of the quinone methide **2** in DMSO (ca 5 mL with 5-10 % dichloromethane as cosolvent) was added. The mixture was stirred for 5 minutes before 0.5 % aqueous acetic acid (ca 50 mL) was added. The mixture was extracted with ethyl acetate (3 x 20 mL) and the combined organic phases were washed with brine (2 x 20 mL), dried over sodium sulfate and the

solvent was evaporated under reduced pressure. The crude reaction products were purified by column chromatography on silica (pentane/ethyl acetate) and subsequently characterized by NMR spectroscopy and mass spectrometry.

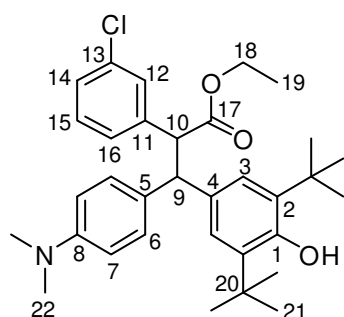
#### 4.3.1.1. Reaction of Ethyl Phenylacetate (**1a**) with the Quinone Methide **2g**

According to GP1, ethyl phenylacetate (**1a**-H, 50.1 mg, 0.305 mmol), KO<sup>t</sup>Bu (36.1 mg, 0.322 mmol), and **2g** (103 mg, 0.305 mmol) yielded ethyl 3-(3,5-di-tert-butyl-4-hydroxyphenyl)-3-(4-(dimethylamino)phenyl)-2-phenylpropanoate **4a** (127 mg, 0.253 mmol, 83 %, *dr* ~ 1:1.3) as colorless solid.



#### 4.3.1.2. Product of the Reaction of Ethyl 3-Chlorophenylacetate (**1b**) with the Quinone Methide **2g**

According to GP1, ethyl 3-chlorophenylacetate (**1b**-H, 59.6 mg, 0.300 mmol), KO<sup>t</sup>Bu (35.6 mg, 0.317 mmol), and **2g** (103 mg, 0.305 mmol) yielded ethyl 2-(3-chlorophenyl)-3-(3,5-di-tert-butyl-4-hydroxyphenyl)-3-(4-(dimethylamino)phenyl)propanoate **4b** (140 mg, 0.261 mmol, 86 %, *dr* ~ 1:1.1) as an orange oil.

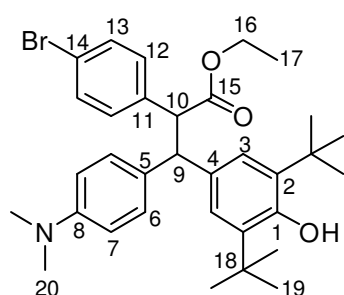


$^1\text{H-NMR}$  ( $\text{CDCl}_3$ , 600 MHz)  $\delta$  = 0.92, 1.03\* (t,  $^3J$  = 7.1 Hz, 3 H, 19-H), 1.26\*, 1.42 (s, 18 H, 21-H), 2.81, 2.90\* (s, 6 H, 22-H), 3.83-3.95 (m, 2 H, 18-H, both isomers), 4.17\* (d,  $^3J$  = 12.0 Hz, 1 H, 10-H), 4.29 (d,  $^3J$  = 12.2 Hz, 1 H, 10-H), 4.37\* (d,  $^3J$  = 12.0 Hz, 1 H, 9-H), 4.41 (d,  $^3J$  = 12.2 Hz, 1 H, 9-H), 4.86\*, 5.00 (s, 1 H, OH), 6.48 (d,  $^3J$  = 9.0 Hz, 2 H, 7-H), 6.68\*-6.71\* (m, 4 H, 3-H and 7-H), 6.92, 7.27\* (d,  $^3J$  = 9.0 Hz, 2 H, 6-H), 7.06-

7.11 and 7.16-7.19 (m, 14-H, 15-H and 16-H, both isomers), 7.15 (s, 2 H, 3-H), 7.39 (s, 1 H, 12-H).  $^{13}\text{C-NMR}$  ( $\text{CDCl}_3$ , 150 MHz)  $\delta$  = 13.8, 14.0\* (q, C-19), 30.2\*, 30.3 (q, C-21), 34.1\*, 34.3 (s, C-20), 40.6, 40.8\* (q, C-22), 54.3, 54.6\* (d, C-9), 57.6, 57.9\* (d, C-10), 60.6, 60.7\* (t, C-18), 112.6, 112.9\* (d, C-7), 124.2, 124.7\* (d, C-3), 128.4\*, 128.6 (d, C-6), 128.8 (d, C-12), 130.0, 130.8\* (s, C-5), 135.2\*, 135.4 (s, C-20), 148.9, 149.3\* (s, C-8), 151.8\*, 152.2 (s, C-1), 172.5\*, 172.6 (s, C-17), 126.7, 126.9, 127.16, 127.20, 129.0, 129.2, 129.3 (d, C-12\* and C-14, C-15, C-16, both isomers), 132.3, 133.6, 133.8, 133.9, 139.8, 140.4 (s, C-4, C-11, C-13, both isomers). HR-MS (EI):  $m/z$  calcd for  $[\text{C}_{33}\text{H}_{42}\text{ClNO}_3]^+$ : 535.2853 found: 535.2848.

#### 4.3.1.3. Reaction of Ethyl 4-Bromophenylacetate (1c) with the Quinone Methide 2g

According to GP1, ethyl 4-bromophenylacetate (**1c-H**, 74.2 mg, 0.305 mmol),  $\text{KO}^t\text{Bu}$  (35.7 mg, 0.318 mmol), and **2g** (99.8 mg, 0.296 mmol) yielded ethyl 2-(4-bromophenyl)-3-(3,5-di-tert-butyl-4-hydroxyphenyl)-3-(4-(dimethylamino)phenyl)propanoate **4c** (168 mg, 0.289 mmol, 97 %,  $dr \sim 1:1.1$ ) as an orange oil.



$^1\text{H-NMR}$  ( $\text{CDCl}_3$ , 300 MHz)  $\delta$  = 0.91, 1.02\* (t,  $^3J$  = 7.1 Hz, 3 H, 17-H), 1.26\*, 1.41 (s, 18 H, 19-H), 2.81, 2.90\* (s, 6 H, 20-H), 3.81-4.04 (m, 2 H, 16-H, both isomers), 4.15\* (d,  $^3J$  = 12.0 Hz, 1 H, 10-H), (4.26-4.42 (m, 2 H, 9-H, 10-H), 4.87\*, 4.99 (s, 1 H, OH), 6.48 (d,  $^3J$  = 8.7 Hz, 2 H, 7-H), 6.67-6.71\* (m, 4 H, 3-H, 7-H), 6.91 (d,  $^3J$  = 7.8 Hz, 2 H, 6-H), 7.05 (d,  $^3J$  = 8.7 Hz, 2 H, 13-

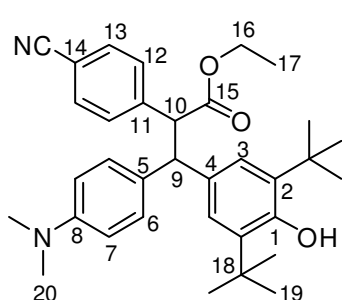
H), 7.14 (s, 2 H, 3-H), 7.20-7.32 (m, 8 H, 6\*-H, 12-H, 12\*-H).  $^{13}\text{C-NMR}$  ( $\text{CDCl}_3$ , 75.5 MHz)  $\delta$  = 13.8, 14.0\* (q, C-17), 30.2\*, 30.4 (q, C-19), 34.1\*, 34.3 (s, C-18), 40.6, 40.8\* (q, C-20), 54.3, 54.5\* (d, C-9), 57.9, 58.3\* (d, C-10), 60.3, 60.4\* (t, C-16), 112.5, 112.9\* (d, C-7), 124.3, 124.7\* (d, C-3), 126.8\*, 126.9 (d, C-6), 128.0, 128.1\* (d, C-13), 135.4, 135.4\* (s, C-2), 148.7, 149.3 (s, C-8), 151.6\*, 152.1 (s, C-1), 173.05\*, 173.09 (s, C-15), 128.5, 128.66,



128.71, 128.8 (C-5, C-12), 120.9, 121.0, 132.6, 134.0, 137.8, 138.0 (s, C-4, C-11, C-14). HR-MS (ESI):  $m/z$  calcd for  $C_{33}H_{43}BrNO_3^+$ : 580.2421 found: 580.2411.

#### 4.3.1.4. Reaction of Ethyl 4-Cyanophenylacetate (**1d**) with the Quinone Methide **2g**

According to GP1, ethyl 4-cyanophenylacetate (**1d**-H, 62.2 mg, 0.329 mmol), KO $t$ Bu (38.7 mg, 0.345 mmol), and **2g** (101 mg, 0.299 mmol) yielded ethyl 2-(4-cyanophenyl)-3-(3,5-di-tert-butyl-4-hydroxyphenyl)-3-(4-(dimethylamino)phenyl)propanoate **4d** (149 mg, 0.283 mmol, 95 %,  $dr \sim 1:1.5$ ) as orange crystals.

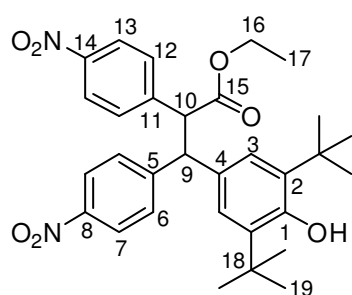


$^1H$ -NMR ( $CDCl_3$ , 300 MHz)  $\delta$  = 0.93, 1.02\* (t,  $^3J$  = 7.1 Hz, 3 H, 17-H), 1.41, 1.26\* (s, 18 H, 19-H), 2.81, 2.91\* (s, 6 H, 20-H), 3.83-4.02 (m, 2 H, 16-H, both isomers), 4.26-4.44 (m, 2 H, 9-H, 10-H, both isomers), 4.89\*, 5.02 (s, 1 H, OH), 6.47 (d,  $^3J$  = 8.7 Hz, 2 H, 7-H), 6.68\*-6.71\* (m, 4 H, 3-H, 7-H), 6.88 (d,  $^3J$  = 8.7 Hz, 2 H, 6-H), 7.15 (s, 2 H, 3-H), 7.25-7.34 (m, 4 H, 6\*-H, 12-H), 7.46 (d,  $^3J$  = 1.5 Hz, 2 H, 13-H).  $^{13}C$ -NMR ( $CDCl_3$ , 75.5 MHz)  $\delta$  = 12.8, 12.9\* (q, C-17), 29.2\*, 29.3 (q, C-19), 33.1\*, 33.3 (s, C-18), 39.5, 39.7\* (q, C-20), 53.6, 53.7\* (d, C-9), 57.0, 57.3\* (d, C-10), 59.8, 59.9\* (t, C-16), 109.7\*, 109.8 (s, C-14), 111.5, 111.8\* (d, C-7), 117.7\*, 117.8 (s, CN), 123.6\*, 123.1 (d, C-3), 127.3\*, 127.5 (d, C-6), 128.49\*, 128.55 (d, C-12), 129.1, 129.3\* (s, C-5), 130.7\*, 130.9 (d, C-13), 131.2, 132.1\* (s, C-4), 134.4\*, 134.6 (s, C-2), 142.3, 142.6 (s, C-11), 147.9, 148.4\* (s, C-8), 150.9\*, 151.3 (s, C-1), 171.0\*, 171.1 (s, C-15). HR-MS (EI):  $m/z$  calcd for  $[C_{34}H_{42}N_2O_3]^+$ : 526.3190 found: 526.3200.

#### 4.3.1.5. Reaction of Ethyl 4-Nitrophenylacetate (**1e**) with the Quinone Methide **2b**

According to GP1, ethyl 3-chlorophenylacetate (**1e**-H, 67.7 mg, 0.324 mmol), KO $t$ Bu (38.1 mg, 0.340 mmol), and **2g** (101 mg, 0.299 mmol) yielded ethyl 3-(3,5-di-tert-butyl-4-hydroxyphenyl)-2,3-bis(4-nitrophenyl)propanoate **4e** (137 mg, 0.250 mmol, 84 %,  $dr \sim 1:2$ ) as light yellow solid.

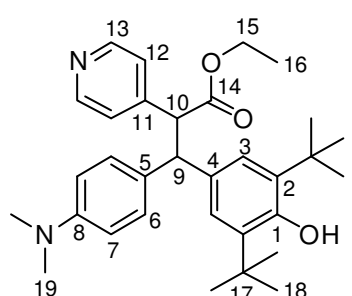
$^1H$ -NMR ( $CDCl_3$ , 300 MHz)  $\delta$  = 0.96, 1.02\* (t,  $^3J$  = 6.0 Hz, 3 H, 17-H), 1.22\*, 1.41 (s, 18 H, 19-H), 3.88-4.04 (m, 2 H, 16-H, both isomers), 4.40\*, 4.49 (d,  $^3J^*$  = 12.1 Hz,  $^3J$  = 12.3 Hz, 1 H, 9-H), 4.63\*, 4.71 (d,  $^3J^*$  = 12.1 Hz,  $^3J$  = 12.3 Hz, 10-H), 5.00\*, 5.14 (s, 1 H, OH), 6.64\*, 7.12 (s, 2 H, 3-H), 7.22, 7.36\* (d,  $^3J$  = 9.0 Hz, 2 H, 6-H), 7.51, 7.58\* (d,  $^3J$  = 9.0 Hz, 2 H, 12-



H), 7.93, 8.04\* (d,  $^3J = 9.0$  Hz, 2 H, 7-H), 8.05, 8.19\* (d,  $^3J = 9.0$  Hz, 2 H, 13-H).  $^{13}\text{C}$ -NMR ( $\text{CDCl}_3$ , 75.5 MHz)  $\delta = 14.0$ , 14.1\* (q, C-17), 30.3\*, 30.5 (q, C-19), 34.4\*, 34.6 (s, C-18), 55.1, 55.3\* (d, C-10), 57.0, 57.3\* (d, C-9), 61.6, 61.8\* (t, C-16), 123.6\* (d, C-7), 123.9-124.0 (m, C-4, C-4\*, C-7, C-13), 124.1\* (d, C-13), 124.4, 124.9\* (d, C-3), 129.0, 129.6\* (d, C-6), 128.8\* (d, C-12), 129.69-129.71 (m), 130.5, 130.9 (C-5, C-11, C-12), 136.4\*, 136.5 (s, C-2), 146.7, 147.0\* (s, C-8), 147.6, 147.5\* (s, C-14), 152.9\*, 153.3 (s, C-1), 171.3, 171.5\* (s, C-15). HR-MS (EI):  $m/z$  calcd for  $[\text{C}_{31}\text{H}_{36}\text{N}_2\text{O}_7]^+$ : 548.2517 found: 548.2519.

#### 4.3.1.6. Reaction of Ethyl Pyridine-4-acetate (1f) with the Quinone Methide 2g

According to GP1, ethyl pyridine-4-acetate (**1f**-H, 55.0 mg, 0.333 mmol),  $\text{KO}^t\text{Bu}$  (38.8 mg, 0.346 mmol), and **2g** (101 mg, 0.299 mmol) yielded ethyl 3-(3,5-di-tert-butyl-4-hydroxyphenyl)-3-(4-(dimethylamino)phenyl)-2-(pyridin-4-yl)propanoate **4f** (138 mg, 0.275 mmol, 94 %,  $dr \sim 1:1.3$ ) as an orange solid.



Major isomer: Mp.: 177.5-178.5 °C.  $^1\text{H}$ -NMR ( $\text{CDCl}_3$ , 300 MHz)  $\delta = 0.93$  (t,  $^3J = 7.1$  Hz, 3 H, 16-H), 1.42 (s, 18 H, 18-H), 2.80 (s, 6 H, 19-H), 3.83-3.95 (m, 2 H, 15-H), 4.31 (d,  $^3J = 12.2$  Hz, 1 H, 10-H), 4.42 ( $^3J = 12.2$  Hz, 1 H, 9-H), 5.06 (s, 1 H, OH), 6.47 (d,  $^3J = 8.7$  Hz, 2 H, 7-H), 6.91 (d,  $^3J = 8.7$  Hz, 2 H, 6-H), 7.15 (s, 2 H, 3-H), 7.26 (d,  $^3J = 6.3$  Hz, 2 H, 12-H), 8.41 (bs, 2 H, 13-H).  $^{13}\text{C}$ -NMR ( $\text{CDCl}_3$ , 75.5 MHz)  $\delta = 14.0$  (q, C-16), 30.5 (q, C-18), 34.5 (s, C-17), 40.7 (q, C-19), 54.4 (d, C-9), 57.9 (d, C-10), 61.0 (t, C-15), 112.7 (d, C-7), 124.2 (d, C-12), 124.3 (d, C-3), 128.8 (d, C-6), 129.6 (d, C-5), 133.4 (s, C-4), 135.8 (s, C-2), 147.1 (s, C-11), 149.7 (d, C-13), 149.2 (s, C-8), 152.5 (s, C-1), 172.1 (s, C-14). HR-MS (EI):  $m/z$  calcd for  $[\text{C}_{32}\text{H}_{42}\text{N}_2\text{O}_3]^+$ : 502.3190 found: 502.3185. Minor isomer: Mp.: 145.0-146.0 °C.  $^1\text{H}$ -NMR ( $\text{CDCl}_3$ , 300 MHz)  $\delta = 1.02$  (t,  $^3J = 7.1$  Hz, 3 H, 16-H), 1.26 (s, 18 H, 18-H), 2.91 (s, 6 H, 19-H), 3.88-3.94 (m, 2 H, 15-H), 4.22 (d,  $^3J = 12.2$  Hz, 1 H, 10-H), 4.40 ( $^3J = 12.2$  Hz, 1 H, 9-H), 4.91 (s, 1 H, OH), 6.70 (d,  $^3J = 8.7$  Hz, 2 H, 7-H), 7.27 (d,  $^3J = 8.7$  Hz, 2 H, 6-H), 6.73 (s, 2 H, 3-H), 7.14 (d,  $^3J = 6.3$  Hz, 2 H, 12-H), 8.38 (bs, 2 H, 13-H).  $^{13}\text{C}$ -NMR ( $\text{CDCl}_3$ , 75.5 MHz)  $\delta = 12.9$  (q, C-16), 29.2 (q, C-18), 33.1 (s, C-17), 39.7 (q, C-19), 53.4 (d, C-9), 56.8 (d, C-10), 59.9 (t, C-15), 111.8 (d, C-7), 123.0 (d, C-12), 123.6 (d, C-3), 127.3 (d, C-6), 129.4 (d, C-5), 130.8 (s,

C-4), 134.4 (s, C-2), 146.1 (s, C-11), 148.2 (d, C-13), 148.4 (s, C-8), 151.0 (s, C-1), 170.8 (s, C-14).

### 4.3.2. Reactions of Ethyl Phenylacetates **1** with Diethyl Benzylidenemalonates **3**

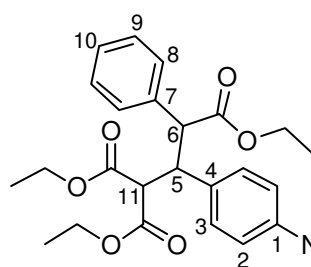
#### General Procedure 2 (GP2):

The anion **1** was generated *in situ* by addition of the ethyl arylacetate **1-H** (50-80 mg, 1 equiv.) to a solution of KO<sup>t</sup>Bu (40-60 mg, 1.05 equiv.) in 10 mL of dry THF. After 2 min., the diethyl benzylidenemalonate **3** was added. After stirring for 5 min. at room temperature, the mixture was poured to ca 50 mL of 0.5 % aqueous acetic acid. The mixture was extracted with diethyl ether (3 × 30 mL) and the combined organic layers were washed with brine (2 × 20 mL), dried over sodium sulphate, and the solvent was evaporated under reduced pressure. The crude reaction products were purified by column chromatography on silica (dichloromethane/methanol) and subsequently characterized by NMR spectroscopy and mass spectrometry.

#### 4.3.2.1. Reaction of Ethyl Phenylacetate (**1a**) with the Diethyl Benzylidenemalonate **3a** in DMSO

KO<sup>t</sup>Bu (403 mg, 3.59 mmol) was dissolved in dry DMSO. After adding ethyl phenylacetate (**1a-H**, 0.500 mL, 3.14 mmol) and stirring 2 min. at room temperature, the malonate **3a** (99.3 mg, 0.339 mmol) was added. 50 mL of 0.5 % aqueous acetic acid were added to the reaction mixture after 5 minutes. The mixture was extracted with ethyl acetate (3 × 30 mL), and the combined organic layers were washed with brine (2 × 20 mL), dried over sodium sulfate, and the solvent was removed by evaporation under reduced pressure. The crude product was purified by column chromatography on silica with ethyl acetate/pentane as eluent yielding triethyl 2-(4-nitrophenyl)-3-phenylpropane-1,1,3-tricarboxylate **5a** (20.7 mg, 45.2 μmol, 14 %, *dr* ~ 1: 1.5) as a light yellow oil.

<sup>1</sup>H-NMR (CDCl<sub>3</sub>, 400 MHz) δ = 0.93\* (t, <sup>3</sup>*J* = 7.2 Hz, 3 H, CH<sub>3</sub>), 1.06\* (t, <sup>3</sup>*J* = 7.2 Hz, 3 H, CH<sub>3</sub>), 1.07\* (t, <sup>3</sup>*J* = 7.2 Hz, 3 H, CH<sub>3</sub>), 1.09 (t, <sup>3</sup>*J* = 7.2 Hz, 3 H, CH<sub>3</sub>), 1.20 (t, <sup>3</sup>*J* = 7.2 Hz, 3 H, CH<sub>3</sub>), 1.23 (t, <sup>3</sup>*J* = 7.2 Hz, 3 H, CH<sub>3</sub>), 3.57\* (d, <sup>3</sup>*J* = 6.0 Hz, 1 H, 6-H), 3.80-4.21 (m, 11 H, CH<sub>2</sub> both isomers and 6-H from the main isomer), 4.23-4.29 and 4.37-4.42 (m, 4 H, 5-H and 11-H both isomers), 7.01-7.04 (m, 2 H, H<sub>arom</sub>), 7.12-7.04 (m, 3 H, H<sub>arom</sub>), 7.25, 7.66\* (d,



$^3J = 8.8$  Hz, 2 H, 3-H), 7.32\*-7.38\* (m, 3 H,  $H_{\text{arom}}$ ), 7.43\*-7.46\* (m, 2 H,  $H_{\text{arom}}$ ), 7.94, 8.15\* (d,  $^3J = 8.8$  Hz, 2 H, 2-H).  $^{13}\text{C}$ -NMR ( $\text{CDCl}_3$ , 100 MHz)  $\delta = 13.78$ , 13.82, 13.96, 14.0 (q,  $\text{CH}_3$  both isomers), 47.1, 47.6\* (d, C-5), 53.9, 54.0\* (d, C-6), 54.6, 55.1\* (d, C-11), 61.0, 61.36, 61.43, 61.61, 61.63, 61.9 (t,  $\text{CH}_2$  both isomers), 122.7, 123.0\* (d, C-2), 127.7, 128.4, 128.5, 128.95, 129.0 (d, C-8, C-9, C-10 both isomers), 130.7\*, 130.9 (d, C-3), 135.3\*, 135.4 (s, C-7), 145.4, 146.4 (s, C-4 both isomers), 146.7, 147.2\* (s, C-1), 167.3, 167.4, 167.73, 167.74, 171.5, 172.1 (s,  $\text{CO}_2$  both isomers). HR-MS (EI):  $m/z$  calcd for  $[\text{C}_{24}\text{H}_{27}\text{NO}_8]^{+}$ : 457.1731 found: 457.1732.

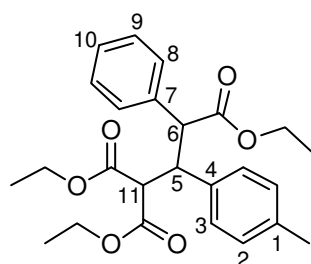
#### 4.3.2.2. Reaction of Ethyl Phenylacetate (1a) with the Diethyl Benzyldenemalonate 3a in THF

According to GP2, ethyl phenylacetate (**1a**-H, 56.2 mg, 0.342 mmol),  $\text{KO}^t\text{Bu}$  (39.4 mg, 0.351 mmol), and **3a** (100 mg, 0.341 mmol) yielded triethyl 2-(4-nitrophenyl)-3-phenylpropane-1,1,3-tricarboxylate **5a** (65.1 mg, 0.142 mmol, 42 %,  $dr \sim 1:1.7$ ) as a light yellow oil.

NMR data is consistent with 4.3.2.1. HR-MS (EI):  $m/z$  calcd for  $[\text{C}_{24}\text{H}_{27}\text{NO}_8]^{+}$ : 457.1731 found: 457.1733.

#### 4.3.2.3. Reaction of Ethyl Phenylacetate (1a) with the Diethyl Benzyldenemalonate 3d in THF

According to GP2, ethyl phenylacetate (**1a**-H, 258 mg, 1.57 mmol),  $\text{KO}^t\text{Bu}$  (181 mg, 1.61 mmol), and **3d** (105 mg, 0.400 mmol) yielded triethyl 3-phenyl-2-(p-tolyl)propane-1,1,3-tricarboxylate **5a-Me** (81.4 mg, 0.191 mmol, 48 %,  $dr \sim 1: 3.7$ ) as a colorless oil.

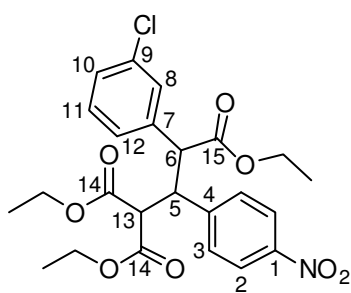


$^1\text{H}$ -NMR ( $\text{CDCl}_3$ , 300 MHz)  $\delta = 0.91^*$  (t,  $^3J = 7.1$  Hz, 3 H,  $\text{CH}_3$ ), 0.98-1.08\* (m, 6 H,  $2 \times \text{CH}_3$ ), 1.02 (t,  $^3J = 7.1$  Hz, 3 H,  $\text{CH}_3$ ), 1.20 (t,  $^3J = 7.2$  Hz, 3 H,  $\text{CH}_3$ ), 1.24 (t,  $^3J = 7.2$  Hz, 3 H,  $\text{CH}_3$ ), 2.18, 2.28\* (s, 3 H, 12-H), 3.54\* (d,  $^3J = 6.5$  Hz, 1 H, 6-H), 3.78-3.99 and 4.05-4.35 (m,  $\text{CH}_2$ , H-5, H-11 both isomers and H-6 main isomer), 6.85-6.92, 7.03-7.07, 7.10-7.15, 7.28-7.32, 7.47-7.50 (m,  $H_{\text{arom}}$  both isomers).  $^{13}\text{C}$ -NMR ( $\text{CDCl}_3$ , 75.5 MHz)  $\delta = 13.7$ , 13.98, 14.04 (q,  $\text{CH}_3$ , both isomers), 21.0, 21.1\* (q,

C-12), 47.0, 47.6\*, 52.2\*, 54.5, 55.7\*, 55.9 (d, C-5, C-6, C-11, both isomers), 60.6, 61.0, 61.1, 61.2, 61.6 (t, CH<sub>2</sub>, both isomers), 127.1, 128.0, 128.3, 128.56, 128.64, 129.2, 129.3, 129.47, 129.55 (d, C<sub>arom</sub>, both isomers), 134.3, 135.5\*, 136.1\*, 136.3 (s, C-4 and C-7), 136.4, 136.8\* (s, C-1), 168.1\*, 168.3, 167.68\*, 167.73, 172.0\*, 172.6 (s, CO<sub>2</sub>). HR-MS (EI): *m/z* calcd for [C<sub>25</sub>H<sub>30</sub>O<sub>6</sub>]<sup>+</sup>: 426.2037 found: 426.2040.

#### 4.3.2.4. Reaction of Ethyl 3-Chlorophenylacetate (1b) with the Diethyl Benzyldenemalonate 3a in THF

According to GP2, ethyl 3-chlorophenylacetate (**1b**-H, 72.4 mg, 0.364 mmol), KO<sup>t</sup>Bu (42.5 mg, 0.379 mmol), and **3a** (105 mg, 0.358 mmol) yielded triethyl 3-(3-chlorophenyl)-2-(4-nitrophenyl)propane-1,1,3-tricarboxylate **5b** (82.5 mg, 0.168 mmol, 47 %, *dr* ~ 1:1.2) as light yellow solid.



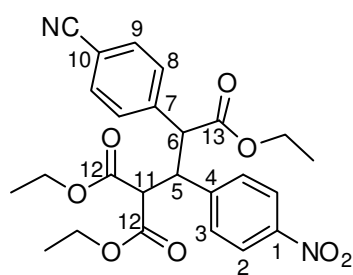
<sup>1</sup>H-NMR (CDCl<sub>3</sub>, 300 MHz)  $\delta$  = 0.95 (t, <sup>3</sup>*J* = 7.1 Hz, 3 H, CH<sub>3</sub>), 1.05-1.12 and 1.20-1.25 (m, CH<sub>3</sub>, both isomers), 3.55\* (d, <sup>3</sup>*J* = 6.3, 1 H, 6-H), 3.80-4.42 (m, CH<sub>2</sub>, 5-H both isomers, 6-H main isomer, 13-H both isomers), 7.04-7.14, 7.25-7.31, 7.44-7.45 (m, 8-H, 10-H, 11-H, 12-H, both isomers, 3-H main isomer), 7.65\* (d, <sup>3</sup>*J* = 8.7 Hz, 2 H, 3-H), 7.98, 8.15\* (d, <sup>3</sup>*J* = 9.0 Hz, 2 H, 2-H).

<sup>13</sup>C-NMR (CDCl<sub>3</sub>, 75.5 MHz)  $\delta$  = 13.8-14.0 (m, CH<sub>3</sub>), 47.0, 47.7\* (d, C-5), 53.6, 54.0, 54.2, 55.0 (d, C-6 and C-13, both isomers), 61.3, 61.60, 61.62, 61.7, 61.8, 62.0 (t, CH<sub>2</sub>, both isomers), 122.9, 123.1\* (d, C-2), 130.7\*, 127.1, 127.3, 128.0, 128.6, 129.0, 129.2, 129.7, 130.2 (d, C-8, C-10, C-11, C-12, both isomers), 130.7\*, 130.8 (d, C-3), 134.3, 134.8, 137.3, 137.5 (s, C-7, C-9, both isomers), 145.0, 146.0\* (s, C-4), 146.9, 147.3\* (s, C-1), 167.2, 167.5, 167.6 (s, C-14, both isomers), 171.0\*, 171.6 (s, C-15). HR-MS (EI): *m/z* calcd for [C<sub>24</sub>H<sub>26</sub>ClNO<sub>8</sub>]<sup>+</sup>: 491.1341 found: 491.1337.

#### 4.3.2.5. Reaction of Ethyl 4-Cyanophenylacetate (1d) with the Diethyl Benzyldenemalonate 3a in THF

According to GP2, ethyl 4-cyanophenylacetate (**4d**-H, 78.3 mg, 0.414 mmol), KO<sup>t</sup>Bu (48.8 mg, 0.435 mmol), and **3a** (100 mg, 0.341 mmol) yielded triethyl 3-(4-cyanophenyl)-2-

(4-nitrophenyl)propane-1,1,3-tricarboxylate **5d** (139 mg, 0.288 mmol, 84 %, *dr* ~ 1:1) as a light yellow solid.

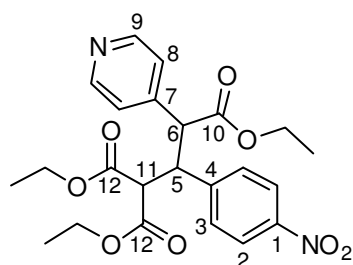


$^1\text{H-NMR}$  ( $\text{CDCl}_3$ , 300 MHz)  $\delta$  = 0.95 (t,  $^3J$  = 6.9 Hz, 3 H,  $\text{CH}_3$ ), 1.06 (t,  $^3J$  = 7.8 Hz, 3 H,  $\text{CH}_3$ ), 1.10 (t,  $^3J$  = 7.2 Hz, 3 H,  $\text{CH}_3$ ), 1.11 (t,  $^3J$  = 6.9 Hz, 3 H,  $\text{CH}_3$ ), 1.21 (t,  $^3J$  = 6.9 Hz, 3 H,  $\text{CH}_3$ ), 1.22 (t,  $^3J$  = 7.2 Hz, 3 H,  $\text{CH}_3$ ), 3.53 (d,  $^3J$  = 6.3 Hz, 1 H, 11-H), 3.85-4.26 (m, 14 H,  $\text{CH}_2$ , 6\*-H, 11\*-H), 4.36, 4.37 (s, 1 H, 5-H, both isomers), 5.53 (d,  $^3J$  = 11.1 Hz, 1 H, 6-H), 7.20 (d,  $^3J$  = 8.1 Hz, 2 H, 8-H), 7.27 (d,  $^3J$  = 8.7 Hz, 2 H, 3-H), 7.46 (d,  $^3J$  = 8.1 Hz, 2 H, 9-H), 7.57-7.68 (m, 6 H, 3-H, 8-H, 9-H), 7.98 (d,  $^3J$  = 8.7 Hz, 2 H, 2-H), 8.16 (d,  $^3J$  = 9.0 Hz, 2 H, 2-H).  $^{13}\text{C-NMR}$  ( $\text{CDCl}_3$ , 75.5 MHz)  $\delta$  = 13.7, 13.8, 13.9, 14.0 (q,  $\text{CH}_3$ ), 47.0 (d, C-5), 54.0 (d, C-11), 54.1 (d, C-5), 54.4 (d, C-6), 47.6, 55.0 (d, C-6 and C-11), 61.5, 61.7, 61.8, 61.86, 61.89, 62.1 (t,  $\text{CH}_2$ ), 111.9, 112.5 (s, C-10), 118.2, 118.3 (s, CN), 123.0, 123.2 (d, C-2), 129.8, 130.0 (d, C-9), 130.6, 130.7 (d, C-3), 132.3, 132.6 (d, C-8), 140.7, 141.0 (s, C-7), 144.6, 145.5 (s, C-4), 147.1, 147.4 (s, C-1), 167.0, 167.1, 167.4, 167.5 (s, C-12), 170.6, 171.1 (s, C-13). HR-MS (EI): *m/z* calcd for  $[\text{C}_{25}\text{H}_{26}\text{N}_2\text{O}_8]^+$ : 482.1684 found: 482.1692.

Due to *dr* = 1:1, the chemical shifts could not be assigned to the concerning isomer.

#### 4.3.2.6. Reaction of Ethyl Pyridine-4-acetate (**1f**) with the Diethyl Benzylidenemalonate **3a** in THF

According to GP2, ethyl pyridine-4-acetate (**1f**-H, 69.0  $\mu\text{L}$ , 0.421 mmol),  $\text{KO}^t\text{Bu}$  (50.6 mg, 0.451 mmol), and **3a** (98.9 mg, 0.337 mmol) yielded triethyl 2-(4-nitrophenyl)-3-(pyridin-4-yl)propane-1,1,3-tricarboxylate **5f** (139 mg, 0.303 mmol, 90 %, *dr* ~ 1:1.2) as a colorless oil.

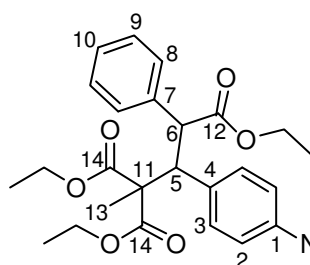


$^1\text{H-NMR}$  ( $\text{CDCl}_3$ , 600 MHz)  $\delta$  = 0.95-0.98 (m,  $\text{CH}_3$ ), 1.05-1.07 (m,  $\text{CH}_3$ ), 1.09-1.12 (m,  $\text{CH}_3$ ), 1.21-1.24 (m,  $\text{CH}_3$ ), 3.57\* (d,  $^3J$  = 6.6 Hz, 1 H, 11-H), 3.84-3.98 (m,  $\text{CH}_2$ , and 11-H major isomer), 4.02-4.07 and 4.11-4.20 (m,  $\text{CH}_2$ , both isomers), 4.23 (dd,  $^3J$  = 10.8 Hz,  $^4J$  = 6.0 Hz, 1 H, 5-H), 4.29\* (d,  $^3J$  = 10.2 Hz, 1 H, 6-H), 4.36\*-4.39\* (m, 1 H, 5-H), 4.45 (d,  $^3J$  = 10.8 Hz, 1 H, 6-H), 7.01\* (d,  $^3J$  = 6.0 Hz, 2 H, 8-H), 7.29\* (d,  $^3J$  = 7.2 Hz, 2 H, 3-H), 7.39-7.40 (m, 2 H, 8-H), 7.61 (d,  $^3J$  = 9.0 Hz, 2 H, 3-H), 7.97\*-7.99\* (m, 2 H, 2-H), 8.15-8.16 (m, 2 H, 2-H), 8.40-8.41\* (m, 2 H, 9-H), 8.62 (d,  $^3J$  = 4.4 Hz, 2 H, 9-H).  $^{13}\text{C-NMR}$  ( $\text{CDCl}_3$ , 150 MHz)  $\delta$  = 13.76,

13.78, 13.8, 13.9 (q, CH<sub>3</sub>), 46.7\*, 47.3 (d, C-5), 53.6\*, 53.9 (d, C-6), 54.0, 55.0\* (d, C-11), 61.5, 61.7, 61.8, 61.85, 61.88, 62.1 (t, CH<sub>2</sub>), 124.0\*, 124.1 (d, C-8), 123.0\*, 123.2 (d, C-2), 130.6, 130.7\* (d, C-3), 144.3, 144.5, 144.6 (s, C-4\*, C-7 both isomers), 145.5 (s, C-4), 147.0\*, 147.4 (s, C-1), 150.0\*, 150.4 (d, C-9), 167.0, 167.1\*, 167.4, 167.5\* (s, C-12), 170.4, 170.9\* (s, C-10). HR-MS (EI): *m/z* calcd for [C<sub>23</sub>H<sub>26</sub>N<sub>2</sub>O<sub>8</sub>]<sup>+</sup>: 458.1684 found: 458.1683.

#### 4.3.2.7. Reaction of Ethyl Phenylacetate (1a) with 3a and Subsequent Methylation

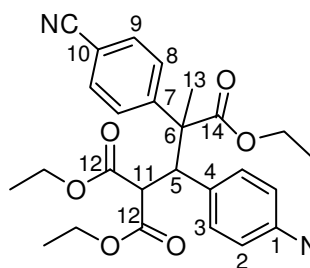
KOtBu (40.0 mg, 0.357 mmol) was dissolved in 5 mL of dry THF. After adding ethyl phenylacetate (1a-H, 54.0 μL, 0.339 mmol) and stirring 5 min at 0 °C, 3a (98.5 mg, 0.336 mmol) was added and the solution was stirred for further 5 min at 0 °C. Dimethyl sulfate (300 μL, 3.16 mmol) was added and stirred for 12 h at room temperature. The reaction mixture was extracted with diethyl ether (2 x 20 mL) after adding 30 mL of aqueous ammonia. The combined organic layers were washed with ammonia and brine and dried over sodium sulphate. The solvent was removed by evaporation under reduced pressure. After column chromatography on silica with dichloromethane/methanol as eluent, triethyl 2-(4-nitrophenyl)-1-phenylbutane-1,3,3-tricarboxylate 6a (79.8 mg, 0.169 mmol, 50 %, *dr* ~ 1:1.2) was obtained as a yellow oil.



<sup>1</sup>H-NMR (CDCl<sub>3</sub>, 300 MHz)  $\delta$  = 0.84 (t, <sup>3</sup>*J* = 7.1 Hz, 3 H, CH<sub>3</sub>), 1.05 (t, <sup>3</sup>*J* = 7.1 Hz, 3 H, CH<sub>3</sub>), 1.14 (t, <sup>3</sup>*J* = 7.2 Hz, 3 H, CH<sub>3</sub>), 1.15-1.28 (m, 3 x CH<sub>3</sub>, 13-H minor isomer), 1.50 (s, 3 H, 13-H), 3.53-3.94 and 4.05-4.19 (m, CH<sub>2</sub>, 5-H minor isomer, 6-H major isomer), 4.29 (d, <sup>3</sup>*J* = 11.7 Hz, 1 H, 5-H), 4.85\* (d, <sup>3</sup>*J* = 11.7 Hz, 1 H, 6-H), 6.99-7.09, 7.28-7.31, 7.55-7.58 (m, 8-H, 9-H, 10-H both isomers), 7.23, 7.63\* (d, <sup>3</sup>*J* = 9.0 Hz, 2 H, 3-H), 7.87, 8.15\* (d, <sup>3</sup>*J* = 9.0 Hz, 2 H, 2-H). <sup>13</sup>C-NMR (CDCl<sub>3</sub>, 75.5 MHz)  $\delta$  = 13.57, 13.64, 13.76, 13.80, 13.82, 13.9 (q, CH<sub>3</sub>), 20.3, 21.8\* (q, C-13), 52.5, 53.3\* (d, C-5), 52.8, 54.1\* (d, C-6), 57.6, 56.5\* (s, C-11), 60.7, 61.1, 61.4, 61.5, 61.70, 61.71 (t, CH<sub>2</sub>), 122.5, 123.0\* (d, C-2), 127.2, 128.0, 128.1, 128.2 (d, C-8, C-9, both isomers), 129.2, 130.1 (d, C-10, both isomers), 130.6\*, 130.9 (d, C-3), 135.1\*, 137.2 (s, C-7), 146.1, 147.08\* (s, C-4), 146.4, 147.11 (s, C-1), 170.1\*, 170.5\*, 170.7, 170.8 (s, C-14), 172.1\*, 172.9 (s, C-12). HR-MS (EI): *m/z* calcd for [C<sub>25</sub>H<sub>29</sub>NO<sub>8</sub>]<sup>+</sup>: 471.1888 found: 471.1897.

#### 4.3.2.8. Reaction of Ethyl 4-Cyanophenylacetate (**1d**) with **3a** and Subsequent Methylation

The reaction was performed as described under 3.2.7 from KO<sup>t</sup>Bu (40.2 mg, 0.358 mmol) ethyl 4-cyanophenylacetate (**1d**-H, 64.2 mg, 0.339 mmol), **3a** (99.3 mg, 0.339) and dimethyl sulfate (300  $\mu$ L, 3.16 mmol). Purification by column chromatography (silica with dichloromethane/methanol) yielded triethyl 3-(4-cyanophenyl)-2-(4-nitrophenyl)butane-1,1,3-tricarboxylate **6d** (140 mg, 0.282 mmol, 83 %, *dr* ~ 1:1.1) as a yellow oil.



<sup>1</sup>H-NMR (CDCl<sub>3</sub>, 300 MHz)  $\delta$  = 0.84 (t, <sup>3</sup>*J* = 7.1 Hz, 3 H, CH<sub>3</sub>), 1.01 (t, <sup>3</sup>*J* = 7.2 Hz, 3 H, CH<sub>3</sub>), 1.16-1.27 (m, 15 H, CH<sub>3</sub>), 1.18, 1.48 (s, 3 H, 13-H, both isomers), 3.46-3.82 and 3.90-4.24 (m, 13 H, CH<sub>2</sub>, 11-H minor isomer), 4.46 (d, <sup>3</sup>*J* = 10.3 Hz, 1 H, 11-H), 4.70, 5.02\* (d, <sup>3</sup>*J* = 10.3 Hz, 11.7\* Hz, 1 H, 5-H), 7.22-7.25 (m, 4 H, 3-H minor isomer and 8-H major isomer), 7.36 (d, <sup>3</sup>*J* = 8.4 Hz, 2 H, 9-H major isomer), 7.57-7.65 (m, 4 H, 3-H major isomer, 9-H minor isomer), 7.74\* (d, <sup>3</sup>*J* = 8.4 Hz, 2 H, 8-H), 7.91\*, 8.17 (d, <sup>3</sup>*J* = 9.0 Hz, 2 H, 2-H). <sup>13</sup>C-NMR (CDCl<sub>3</sub>, 75.5 MHz)  $\delta$  = 13.60, 13.64, 13.8-13.9 (q, CH<sub>3</sub>), 20.4, 22.7 (q, C-13, both isomers), 52.5, 53.5\* (d, C-11), 52.9, 54.2\* (d, C-5), 56.2, 57.5\* (s, C-6), 61.2, 61.67-61.69, 61.9, 62.0 (t, CH<sub>2</sub>), 111.3, 111.9\* (s, C-10), 118.2, 118.4 (s, CN), 122.9, 123.3 (d, C-2, both isomers), 130.0, 130.6 (d, C-3, both isomers), 131.1, 131.7 (d, C-8, both isomers), 132.0, 132.6 (d, C-9, both isomers), 140.7, 142.7 (s, C-7), 145.2, 146.1 (s, C-4), 146.8, 147.4\* (s, C-1), 170.63, 170.7, 171.3, 172.0 (s, C-12, both isomers), 170.56, 170.1 (C-14, both isomers). HR-MS (EI): *m/z* calcd for [C<sub>26</sub>H<sub>28</sub>N<sub>2</sub>O<sub>8</sub>]<sup>+</sup>: 496.1840 found: 496.1843.

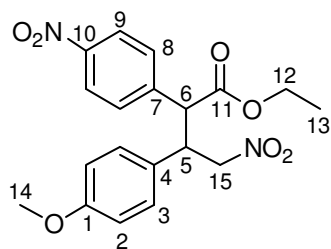
#### 4.3.3. Reactions of Ethyl 4-Nitrophenylacetate (**1e**-H) with Further Electrophiles

##### 4.3.3.1. Reaction of Ethyl 4-Nitrophenylacetate (**1e**-H) with the *trans*- $\beta$ -Nitrostyrene **7a**

Ethyl 4-nitrophenylacetate (**1e**-H, 130 mg, 0.621 mmol) and **7a** (103 mg, 0.575 mmol) were dissolved in dry dichloromethane (distilled from calcium chloride) in a dried Schlenk-flask, filled with argon. After the addition of 3 droplets of DBN, the reaction mixture was stirred at room temperature for 48 h. After evaporation of the solvent, the crude product was purified by flash chromatography on silica with ethyl acetate/pentane as eluent. Ethyl 3-(4-



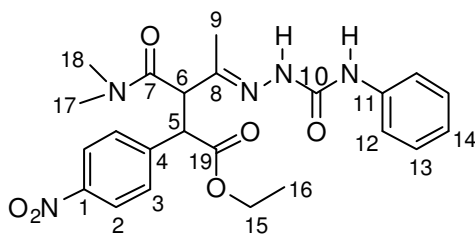
methoxyphenyl)-4-nitro-2-(4-nitrophenyl)butanoate **8** (116 mg, 0.299 mmol, 52 %, *dr* ~ 1:1.1) was obtained as yellow oil.



$^1\text{H-NMR}$  ( $\text{CDCl}_3$ , 300 MHz)  $\delta$  = 0.96, 1.23\* (t,  $^3J$  = 7.1 Hz, 3 H, 13-H), 3.69\*, 3.79 (s, 3 H, 14-H), 3.84-4.47 (m, 10 H, 5-H, 6-H and 12-H from both isomers and 15-H from the major isomer), 4.77\* (s, 1 H, 15-H), 4.80\* (s, 1 H, 15-H), 6.69\*, 6.92 (d,  $^3J$  = 8.7 Hz, 2 H, 2-H), 6.88\*, 7.22 (d,  $^3J$  = 8.7 Hz, 2 H, 3-H), 7.69, 7.32\* (d,  $^3J$  = 9.0 Hz, 2 H, 8-H), 8.03\*, 8.26 (d,  $^3J$  = 8.7 Hz, 2 H, 9-H).  $^{13}\text{C-NMR}$  ( $\text{CDCl}_3$ , 75.5 MHz)  $\delta$  = 13.8, 14.0\* (q, C-13), 46.4\*, 46.6 (d, C-5), 54.5\*, 55.06 (d, C-6), 55.12\*, 55.3 (q, C-14), 61.6, 62.1\* (t, C-12), 78.2, 78.6\* (t, C-15), 114.3\*, 114.4 (d, C-3), 123.7\*, 124.3 (d, C-9), 127.3\*, 128.1 (s, C-4), 129.0\*, 129.1 (d, C-2), 129.5\*, 129.6 (d, C-8), 142.6, 143.1\* (s, C-7), 147.3\*, 148.0 (s, C-10), 159.2\*, 159.6 (s, C-1), 170.2\*, 171.0 (s, C-11). HR-MS (EI): *m/z* calcd for  $[\text{C}_{19}\text{H}_{20}\text{N}_2\text{O}_7]^+$ : 388.1265 found: 388.1265.

#### 4.3.3.2. Reaction of Ethyl 4-Nitrophenylacetate (**1e-H**) with the 1,2-Diaza-1,3-Diene **9a**

Ethyl 4-nitrophenylacetate (**1e**, 56.6 mg, 0.271 mmol) was added to a solution of  $\text{KO}^t\text{Bu}$  (31.8 mg, 0.283 mmol) in 5 mL of dry DMSO. After 1 min. stirring, a solution of **9a** (66.0 mg, 0.254 mmol) in 5 mL of dry DMSO was added and stirred for 5 min at room temperature before 50 mL of aqueous acetic acid (0.5 %) were added to the reaction mixture. The mixture was extracted with ethyl acetate ( $3 \times 20$  mL). The combined organic layers were washed with brine and dried over sodium sulfate before the solvent was evaporated. The crude product was purified by column chromatography on silica with pentane/ethyl acetate (1:1) as eluent yielding (*E*)-ethyl 3-(dimethylcarbamoyl)-2-(4-nitrophenyl)-4-(2-(phenylcarbamoyl)-hydrazono)pentanoate **10** (103 mg, 0.219 mmol, 87 %, *dr* ~ 1:1) as colorless solid.

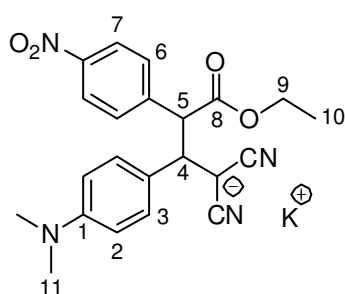


$^1\text{H-NMR}$  ( $\text{CDCl}_3$ , 600 MHz)  $\delta$  = 1.12\*, 1.17 (t,  $^3J$  = 6.9 Hz, 3 H, 16-H), 1.47\*, 1.78 (s, 3 H, 9-H), 2.72\*, 3.00 (s, 3 H, 17-H), 2.89\*, 3.15 (s, 3 H, 18-H), 4.04-4.21 (m, 2 H, 15-H, both isomers), 4.35, 4.46\* (d,  $^3J$  = 11.4 Hz, 1 H, 5-H), 4.52, 4.58\* (d,  $^3J$  = 11.4 Hz, 1 H, 6-H), 7.06-7.09 (m, 2 H, 14-H, both isomers), 7.28-7.33 (m, 4 H, 13-H, both isomers), 7.35, 7.56\* (d,  $^3J$  = 8.4 Hz, 2 H, 12-H), 7.46, 7.62\* (d,  $^3J$  = 8.4 Hz, 2 H, 3-H), 7.71, 8.29\* (s, 1 H,

NH), 8.15, 8.20\* (d,  $^3J = 8.4$  Hz, 2 H, 2-H), 8.96, 9.18\* (s, 1 H, NH).  $^{13}\text{C}$ -NMR ( $\text{CDCl}_3$ , 150 MHz)  $\delta = 13.5$ , 14.7\* (q, C-9), 13.9, 14.0\* (q, C-16), 35.6\*, 36.3 (q, C-17), 37.3, 37.8\* (q, C-18), 51.9, 52.0\* (d, C-5), 53.5\*, 54.9 (d, C-6), 61.8, 61.9\* (t, C-15), 119.26\*, 119.35 (d, C-12), 123.3\*, 123.6 (d, C-14), 123.7\*, 124.0 (d, C-2), 128.9\*, 129.1 (d, C-13), 129.4, 129.6\* (d, C-3), 137.5, 138.2 (s, C-11), 143.2\*, 143.3 (s, C-4), 144.8, 144.9\* (s, C-8), 147.5, 147.7\* (s, C-1), 153.3, 153.8\* (s, C-10), 168.0\*, 168.9 (s, C-7), 171.7, 171.6\* (s, C-19). HR-MS (EI):  $m/z$  calcd for  $[\text{C}_{23}\text{H}_{27}\text{N}_5\text{O}_6]^{+}$ : 469.1956 found: 469.11968.

#### 4.3.3.3. Reaction of Ethyl 4-Nitrophenylacetate (1e-H) with the Benzyldiene Malononitrile 11

Ethyl 4-nitrophenylacetate (**1e**, 20.1 mg, 96.1  $\mu\text{mol}$ ),  $\text{KO}^t\text{Bu}$  (11.2 mg, 99.8  $\mu\text{mol}$ ) and the benzyldiene malononitrile **11** (17.0 mg, 86.2  $\mu\text{mol}$ ) were mixed with 0.6 mL of  $[\text{D}_6]$ -DMSO in a NMR-tube under argon atmosphere. The formation of potassium 1,1-dicyano-2-(4-(dimethylamino)phenyl)-4-ethoxy-3-(4-nitrophenyl)-4-oxobutan-1-ide (**12**,  $dr \sim 1:1.3$ ) could be observed.



The following signals could be assigned:  $^1\text{H}$ -NMR ( $[\text{D}_6]$ -DMSO, 400 MHz)  $\delta = 2.74^*$ , 2.84 (s, 6 H, 11-H), 3.39 and 3.54 (d,  $^3J = 12.0$  Hz,  $^3J = 11.2$  Hz, respectively, 4-H, both isomers), 3.95 (d,  $^3J = 12.0$  Hz, 1 H, 5-H), 6.42\*, 6.64 (d,  $^3J = 8.6$  Hz, 2 H, 2-H), 6.88\*, 7.12 (d,  $^3J = 8.6$  Hz, 2 H, 3-H), 7.51\*, 7.73 (d,  $^3J = 8.7$  Hz, 2 H, 6-H), 7.97\*, 8.22 (d,  $^3J = 8.7$  Hz, 2 H, 7-H).  $^{13}\text{C}$ -NMR ( $d_6$ -DMSO, 100 MHz)  $\delta = 13.6$ , 14.0\* (q, C-10), 17.3, 18.2\* (s,  $\text{C}^-$ ), 40.2\*, 40.5 (q, C-11), 47.2\*, 47.3 (d, C-4), 57.3, 57.5\* (d, C-5), 60.0, 60.3\* (t, C-9), 112.0\*, 112.2 (d, C-2), 123.0\*, 123.1 (d, C-7), 127.3, 127.6\* (d, C-3), 129.8, 129.9\* (d, C-6), 148.3\*, 149.0 (s, C-1), 171.4, 171.7\* (s, C-8).

## 4.4. Deprotonation Experiments and UV-Vis Spectra

### 4.4.1. Deprotonation Experiments

The formation of the carbanions **1a–f** from their conjugate CH acids (**1a–f**)-H, were recorded by using diode array UV-Vis spectrometers. The temperature during all experiments was kept constant by using a circulating bath ( $20.0 \pm 0.02$  °C). Solutions of the CH acids (**1a–f**)-H in dry DMSO were added to a solution of KO<sup>t</sup>Bu (1.05 eq.) in dry DMSO respectively. After the equilibration of the absorption (30 to 40 s) the mixtures were treated subsequently with various equivalents of KO<sup>t</sup>Bu (dissolved in DMSO). In all cases a full deprotonation of the CH acid with one equivalent of base was monitored (Figure 6).

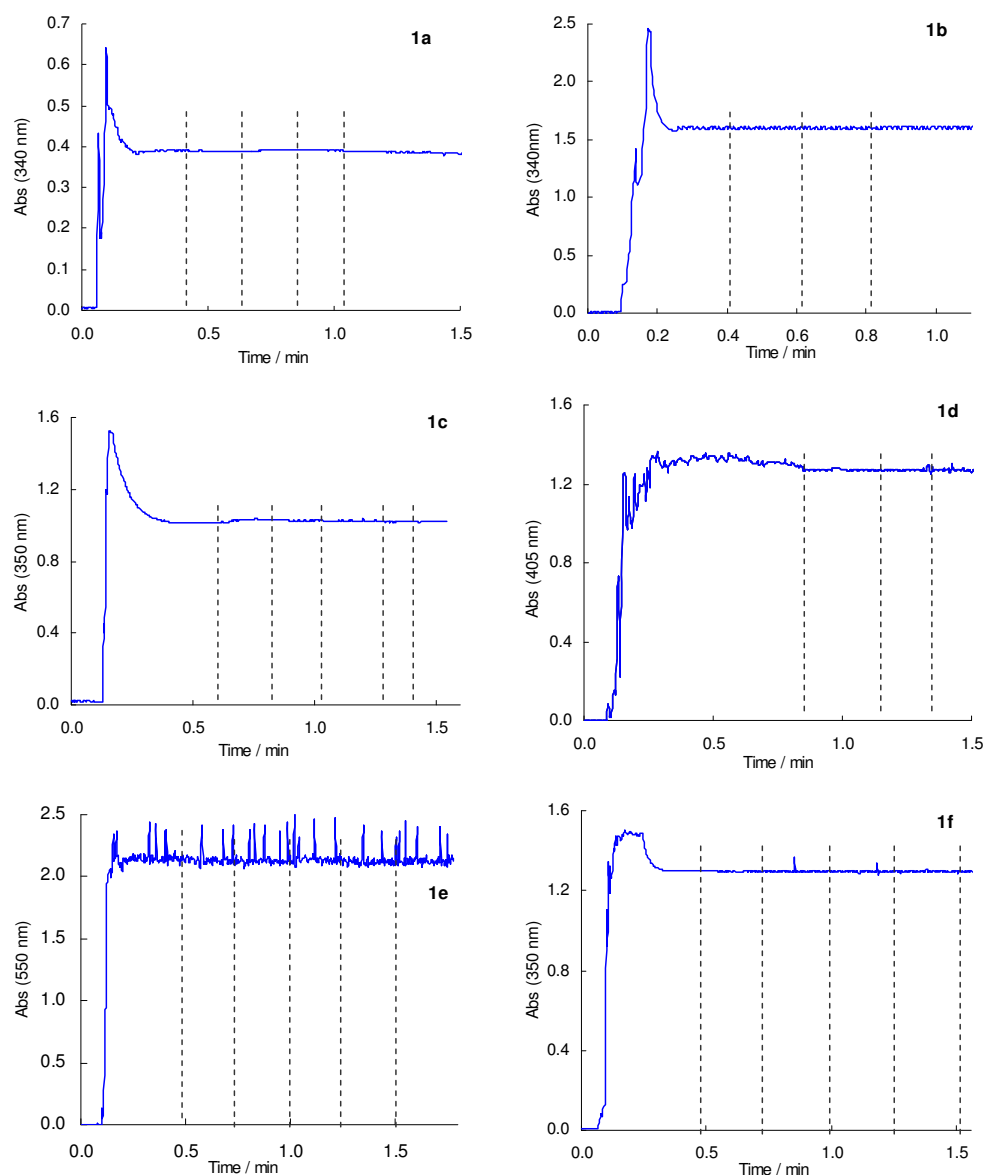


Figure 6: Formation of the Anions **1a–f** from the corresponding CH acids and KO<sup>t</sup>Bu in DMSO at 20 °C. Dashed lines mean an additional equivalent of KO<sup>t</sup>Bu.

### 4.4.1. UV-Vis Spectra

The UV-Vis Spectra of the anions **1a-f** were taken from the deprotonation experiments described above.

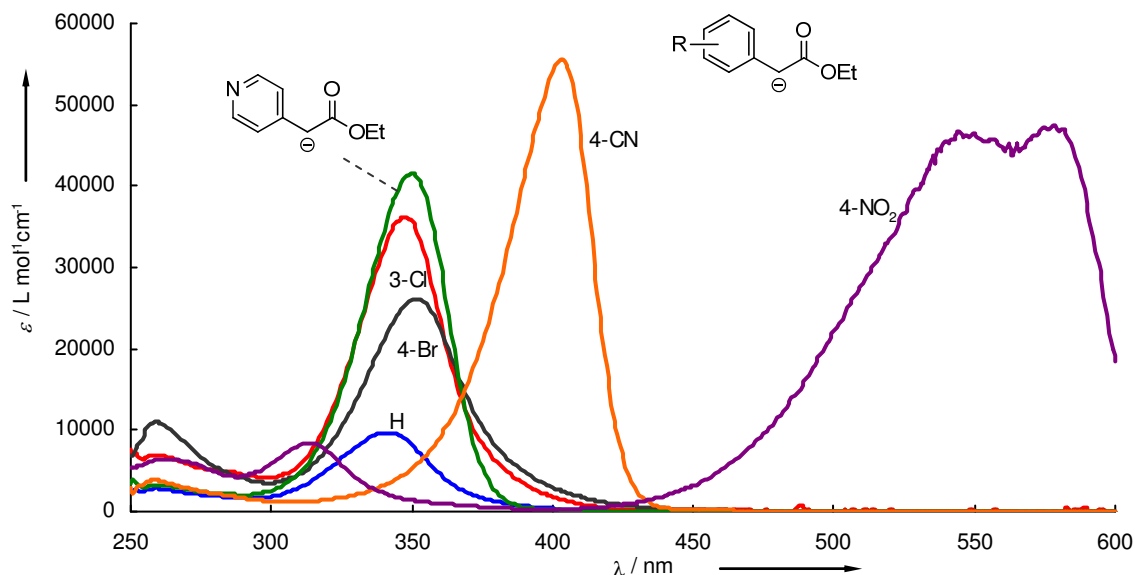


Figure 7: UV-VIS-Spectra of the Anions **1a-f** in DMSO.

## 4.5. Kinetic Experiments

### 4.5.1. Determination of the Nucleophilicity of Ethyl Phenylacetate Anions 1

#### 4.5.1.1. Reactions of the Potassium Salt of Ethyl Phenylacetate (**1a-K**)

Table 4: Kinetics of the reaction of **1a-K** (generated from **1a-H** by addition of 1.03 equivalents of KO<sup>t</sup>Bu) with **2f** (20 °C, stopped-flow, at 407 nm).

[ <b>2f</b> ] / mol L <sup>-1</sup>	[ <b>1a</b> ] / mol L <sup>-1</sup>	[ <b>1a</b> ]/[ <b>2f</b> ]	<i>k</i> <sub>obs</sub> / s <sup>-1</sup>
1.79 × 10 <sup>-5</sup>	1.40 × 10 <sup>-4</sup>	7.8	2.27 × 10 <sup>2</sup>
1.79 × 10 <sup>-5</sup>	1.58 × 10 <sup>-4</sup>	8.8	2.62 × 10 <sup>2</sup>
1.79 × 10 <sup>-5</sup>	1.93 × 10 <sup>-4</sup>	10.8	3.35 × 10 <sup>2</sup>
1.79 × 10 <sup>-5</sup>	2.10 × 10 <sup>-4</sup>	11.7	3.84 × 10 <sup>2</sup>

$$k_2 = 2.21 \times 10^6 \text{ L mol}^{-1} \text{ s}^{-1}$$

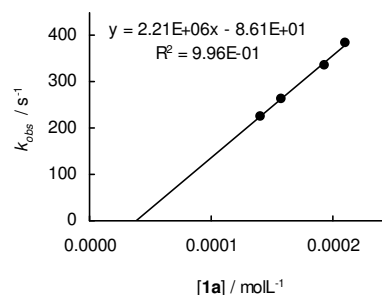
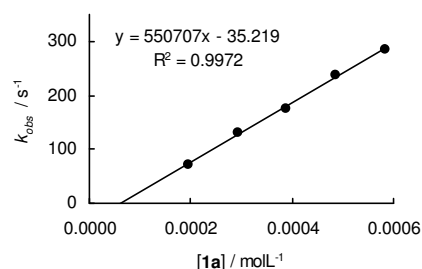


Table 5: Kinetics of the reaction of **1a**-K (generated from **1a**-H by addition of 1.04 equivalents of KO<sup>t</sup>Bu) with **2g** (20 °C, stopped-flow, at 486 nm).

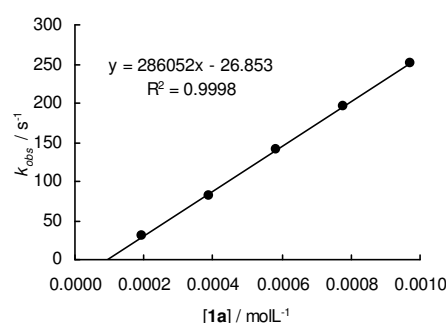
[ <b>2g</b> ] / mol L <sup>-1</sup>	[ <b>1a</b> ] / mol L <sup>-1</sup>	[18-crown-6] / mol L <sup>-1</sup>	[ <b>1a</b> ]/[ <b>2g</b> ]	$k_{\text{obs}}$ / s <sup>-1</sup>
$1.90 \times 10^{-5}$	$1.95 \times 10^{-4}$		10.3	$7.04 \times 10^1$
$1.90 \times 10^{-5}$	$2.92 \times 10^{-4}$	$3.18 \times 10^{-4}$	15.4	$1.30 \times 10^2$
$1.90 \times 10^{-5}$	$3.90 \times 10^{-4}$		20.6	$1.74 \times 10^2$
$1.90 \times 10^{-5}$	$4.87 \times 10^{-4}$	$5.30 \times 10^{-4}$	25.7	$2.38 \times 10^2$
$1.90 \times 10^{-5}$	$5.85 \times 10^{-4}$		30.8	$2.84 \times 10^2$

$$k_2 = 5.51 \times 10^5 \text{ L mol}^{-1} \text{ s}^{-1}$$

Table 6: Kinetics of the reaction of **1a**-K (generated from **1a**-H by addition of 1.04 equivalents of KO<sup>t</sup>Bu) with **2h** (20 °C, stopped-flow, at 521 nm).

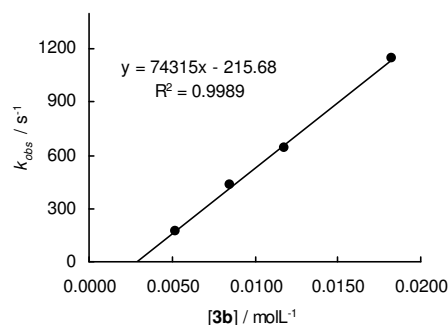
[ <b>2h</b> ] / mol L <sup>-1</sup>	[ <b>1a</b> ] / mol L <sup>-1</sup>	[18-crown-6] / mol L <sup>-1</sup>	[ <b>1a</b> ]/[ <b>2h</b> ]	$k_{\text{obs}}$ / s <sup>-1</sup>
$1.77 \times 10^{-5}$	$1.95 \times 10^{-4}$		11.0	$2.99 \times 10^1$
$1.77 \times 10^{-5}$	$3.90 \times 10^{-4}$	$4.24 \times 10^{-4}$	22.1	$8.25 \times 10^1$
$1.77 \times 10^{-5}$	$5.85 \times 10^{-4}$		33.1	$1.41 \times 10^2$
$1.77 \times 10^{-5}$	$7.80 \times 10^{-4}$	$8.48 \times 10^{-4}$	44.1	$1.97 \times 10^2$
$1.77 \times 10^{-5}$	$9.74 \times 10^{-4}$		55.2	$2.52 \times 10^2$

$$k_2 = 2.86 \times 10^5 \text{ L mol}^{-1} \text{ s}^{-1}$$

Table 7: Kinetics of the reaction of **1a**-K (generated from **1a**-H by addition of 1.04 equivalents of KO<sup>t</sup>Bu) with **3b** (20 °C, stopped-flow, at 340 nm).

[ <b>3b</b> ] / mol L <sup>-1</sup>	[ <b>1a</b> ] / mol L <sup>-1</sup>	[ <b>3b</b> ]/[ <b>1a</b> ]	$k_{\text{obs}}$ / s <sup>-1</sup>
$5.22 \times 10^{-3}$	$2.57 \times 10^{-4}$	19.5	$1.69 \times 10^2$
$8.48 \times 10^{-3}$	$2.57 \times 10^{-4}$	31.7	$4.30 \times 10^2$
$1.17 \times 10^{-2}$	$2.57 \times 10^{-4}$	43.9	$6.40 \times 10^2$
$1.83 \times 10^{-2}$	$2.57 \times 10^{-4}$	68.3	$1.15 \times 10^3$

$$k_2 = 7.43 \times 10^4 \text{ L mol}^{-1} \text{ s}^{-1}$$

Table 8: Kinetics of the reaction of **1a**-K (generated from **1a**-H by addition of 1.05 equivalents of KO<sup>t</sup>Bu) with **3c** (20 °C, stopped-flow, at 340 nm).

[ <b>3c</b> ] / mol L <sup>-1</sup>	[ <b>1a</b> ] / mol L <sup>-1</sup>	[18-crown-6] / mol L <sup>-1</sup>	[ <b>3c</b> ]/[ <b>1a</b> ]	$k_{\text{obs}}$ / s <sup>-1</sup>
$7.78 \times 10^{-4}$	$6.16 \times 10^{-5}$		12.6	$1.39 \times 10^1$
$1.56 \times 10^{-4}$	$6.16 \times 10^{-5}$	$6.73 \times 10^{-5}$	25.3	$2.35 \times 10^1$
$2.33 \times 10^{-3}$	$6.16 \times 10^{-5}$		37.9	$3.06 \times 10^1$
$3.11 \times 10^{-3}$	$6.16 \times 10^{-5}$	$6.73 \times 10^{-5}$	50.5	$3.89 \times 10^1$
$3.89 \times 10^{-3}$	$6.16 \times 10^{-5}$		63.1	$4.53 \times 10^1$

$$k_2 = 1.00 \times 10^4 \text{ L mol}^{-1} \text{ s}^{-1}$$

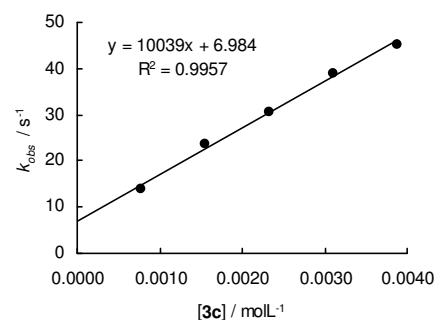
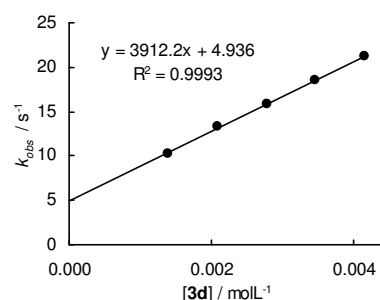


Table 9: Kinetics of the reaction of **1a**-K (generated from **1a**-H by addition of 1.02 equivalents of KO<sup>t</sup>Bu) with **3d** (20 °C, stopped-flow, at 345 nm).

[ <b>3d</b> ] / mol L <sup>-1</sup>	[ <b>1a</b> ] / mol L <sup>-1</sup>	[ <b>3d</b> ]/[ <b>1a</b> ]	$k_{\text{obs}}$ / s <sup>-1</sup>
$1.39 \times 10^{-3}$	$1.53 \times 10^{-4}$	9.1	$1.02 \times 10^1$
$2.09 \times 10^{-3}$	$1.53 \times 10^{-4}$	13.6	$1.33 \times 10^1$
$2.78 \times 10^{-3}$	$1.53 \times 10^{-4}$	18.1	$1.58 \times 10^1$
$3.48 \times 10^{-3}$	$1.53 \times 10^{-4}$	22.6	$1.85 \times 10^1$
$4.17 \times 10^{-3}$	$1.53 \times 10^{-4}$	27.2	$2.12 \times 10^1$

$$k_2 = 3.91 \times 10^3 \text{ L mol}^{-1} \text{ s}^{-1}$$

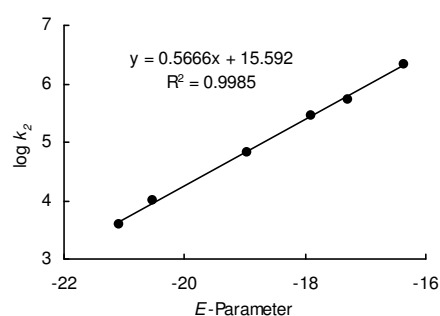


### Determination of Reactivity Parameters $N$ and $s_N$ for the Anion of Ethyl Phenylacetate (**1a**) in DMSO

Table 10: Rate Constants for the reactions of **1a** with different electrophiles (20 °C).

Electrophile	$E$	$k_2$ / L mol <sup>-1</sup> s <sup>-1</sup>	log $k_2$
<b>2f</b>	-16.38	$2.21 \times 10^6$	6.34
<b>2g</b>	-17.29	$5.51 \times 10^5$	5.74
<b>2h</b>	-17.90	$2.86 \times 10^5$	5.46
<b>3b</b>	-18.98	$7.43 \times 10^4$	4.87
<b>3c</b>	-20.55	$1.00 \times 10^4$	4.00
<b>3d</b>	-21.11	$3.91 \times 10^3$	3.59

$$N = 27.54, s_N = 0.57$$



#### 4.5.1.2. Reactions of the Potassium Salt of Ethyl 3-Chlorophenylacetate (**1b**-K)

Table 11: Kinetics of the reaction of **1b**-K (generated from **1b**-H by addition of 1.06 equivalents of KO<sup>t</sup>Bu) with **2f** (20 °C, stopped-flow, at 407 nm).

[ <b>2f</b> ] / mol L <sup>-1</sup>	[ <b>1b</b> ] / mol L <sup>-1</sup>	[ <b>1b</b> ]/[ <b>2f</b> ]	$k_{\text{obs}}$ / s <sup>-1</sup>
$1.38 \times 10^{-5}$	$1.35 \times 10^{-4}$	9.8	$8.57 \times 10^1$
$1.38 \times 10^{-5}$	$1.69 \times 10^{-4}$	12.2	$1.13 \times 10^2$
$1.38 \times 10^{-5}$	$1.84 \times 10^{-4}$	13.3	$1.32 \times 10^2$
$1.38 \times 10^{-5}$	$2.00 \times 10^{-4}$	14.5	$1.46 \times 10^2$
$1.38 \times 10^{-5}$	$2.15 \times 10^{-4}$	15.6	$1.56 \times 10^2$

$$k_2 = 9.06 \times 10^5 \text{ L mol}^{-1} \text{ s}^{-1}$$

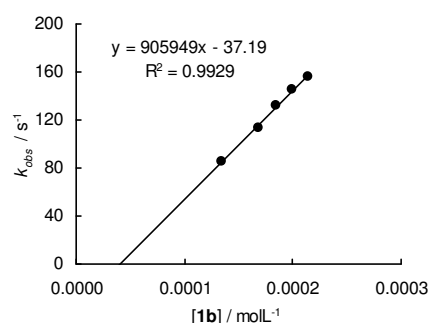
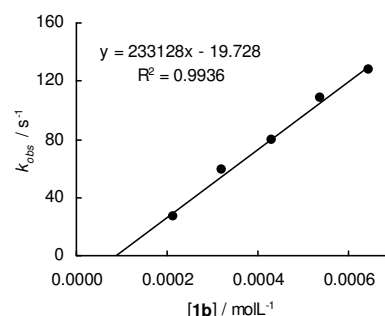


Table 12: Kinetics of the reaction of **1b**-K (generated from **1b**-H by addition of 1.02 equivalents of KO $t$ Bu) with **2g** (20 °C, stopped-flow, at 486 nm).

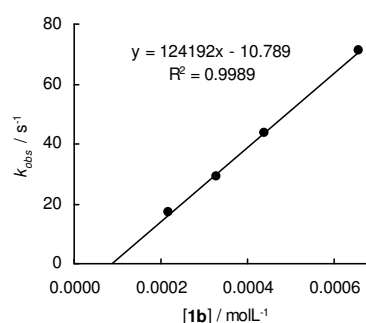
[ <b>2g</b> ] / mol L <sup>-1</sup>	[ <b>1b</b> ] / mol L <sup>-1</sup>	[ <b>1b</b> ]/[ <b>2g</b> ]	$k_{\text{obs}}$ / s <sup>-1</sup>
$1.88 \times 10^{-5}$	$2.15 \times 10^{-4}$	11.4	$2.70 \times 10^1$
$1.88 \times 10^{-5}$	$3.22 \times 10^{-4}$	17.1	$5.93 \times 10^1$
$1.88 \times 10^{-5}$	$4.29 \times 10^{-4}$	22.8	$7.97 \times 10^1$
$1.88 \times 10^{-5}$	$5.37 \times 10^{-4}$	28.5	$1.08 \times 10^2$
$1.88 \times 10^{-5}$	$6.44 \times 10^{-4}$	34.2	$1.28 \times 10^2$

$$k_2 = 2.33 \times 10^5 \text{ L mol}^{-1} \text{ s}^{-1}$$

Table 13: Kinetics of the reaction of **1b**-K (generated from **1b**-H by addition of 1.04 equivalents of KO $t$ Bu) with **2h** (20 °C, stopped-flow, at 521 nm).

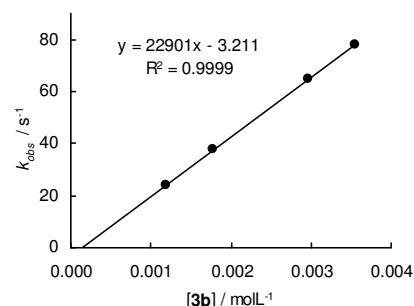
[ <b>2h</b> ] / mol L <sup>-1</sup>	[ <b>1b</b> ] / mol L <sup>-1</sup>	[18-crown-6] / mol L <sup>-1</sup>	[ <b>1b</b> ]/[ <b>2h</b> ]	$k_{\text{obs}}$ / s <sup>-1</sup>
$2.05 \times 10^{-5}$	$2.19 \times 10^{-4}$		10.7	$1.71 \times 10^1$
$2.05 \times 10^{-5}$	$3.28 \times 10^{-4}$	$3.56 \times 10^{-4}$	16.0	$2.89 \times 10^1$
$2.05 \times 10^{-5}$	$4.38 \times 10^{-4}$		21.3	$4.39 \times 10^1$
$2.05 \times 10^{-5}$	$6.57 \times 10^{-4}$		32.0	$7.09 \times 10^1$

$$k_2 = 1.24 \times 10^5 \text{ L mol}^{-1} \text{ s}^{-1}$$

Table 14: Kinetics of the reaction of **1b**-K (generated from **1b**-H by addition of 1.05 equivalents of KO $t$ Bu) with **3b** (20 °C, stopped-flow, at 350 nm).

[ <b>3b</b> ] / mol L <sup>-1</sup>	[ <b>1b</b> ] / mol L <sup>-1</sup>	[18-crown-6] / mol L <sup>-1</sup>	[ <b>3b</b> ]/[ <b>1b</b> ]	$k_{\text{obs}}$ / s <sup>-1</sup>
$1.19 \times 10^{-3}$	$1.24 \times 10^{-4}$		9.1	$2.38 \times 10^1$
$1.78 \times 10^{-3}$	$1.24 \times 10^{-4}$	$1.35 \times 10^{-4}$	13.7	$3.78 \times 10^1$
$2.97 \times 10^{-3}$	$1.24 \times 10^{-4}$	$1.35 \times 10^{-4}$	22.8	$6.48 \times 10^1$
$3.56 \times 10^{-3}$	$1.24 \times 10^{-4}$		28.7	$7.82 \times 10^1$

$$k_2 = 2.29 \times 10^4 \text{ L mol}^{-1} \text{ s}^{-1}$$

Table 15: Kinetics of the reaction of **1b**-K (generated from **1b**-H by addition of 1.04 equivalents of KO $t$ Bu) with **3c** (20 °C, stopped-flow, at 350 nm).

[ <b>3c</b> ] / mol L <sup>-1</sup>	[ <b>1b</b> ] / mol L <sup>-1</sup>	[18-crown-6] / mol L <sup>-1</sup>	[ <b>3c</b> ]/[ <b>1b</b> ]	$k_{\text{obs}}$ / s <sup>-1</sup>
$1.58 \times 10^{-3}$	$1.32 \times 10^{-4}$		11.9	6.78
$2.37 \times 10^{-3}$	$1.32 \times 10^{-4}$	$1.43 \times 10^{-4}$	17.9	$1.18 \times 10^1$
$3.15 \times 10^{-3}$	$1.32 \times 10^{-4}$		23.8	$1.62 \times 10^1$
$3.94 \times 10^{-3}$	$1.32 \times 10^{-4}$	$1.43 \times 10^{-4}$	29.8	$2.12 \times 10^1$
$4.73 \times 10^{-3}$	$1.32 \times 10^{-4}$		35.7	$2.61 \times 10^1$

$$k_2 = 6.09 \times 10^3 \text{ L mol}^{-1} \text{ s}^{-1}$$

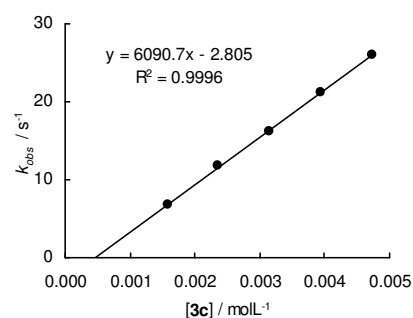
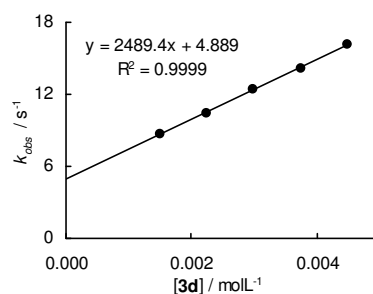


Table 16: Kinetics of the reaction of **1b**-K (generated from **1b**-H by addition of 1.06 equivalents of KOtBu) with **3d** (20 °C, stopped-flow, at 350 nm).

[ <b>3d</b> ] / mol L <sup>-1</sup>	[ <b>1b</b> ] / mol L <sup>-1</sup>	[ <b>3d</b> ]/[ <b>1b</b> ]	$k_{\text{obs}}$ / s <sup>-1</sup>
$1.50 \times 10^{-3}$	$1.01 \times 10^{-4}$	14.9	8.63
$2.25 \times 10^{-3}$	$1.01 \times 10^{-4}$	22.3	$1.04 \times 10^1$
$2.99 \times 10^{-3}$	$1.01 \times 10^{-4}$	29.7	$1.24 \times 10^1$
$3.74 \times 10^{-3}$	$1.01 \times 10^{-4}$	37.2	$1.42 \times 10^1$
$4.49 \times 10^{-3}$	$1.01 \times 10^{-4}$	44.6	$1.61 \times 10^1$

$$k_2 = 2.49 \times 10^3 \text{ L mol}^{-1} \text{ s}^{-1}$$

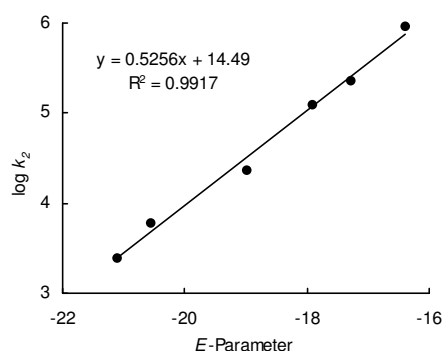


### Determination of Reactivity Parameters $N$ and $s_N$ for the Anion of Ethyl 3-Chloro-phenylacetate (**1b**) in DMSO

Table 17: Rate Constants for the reactions of **1b** with different electrophiles (20 °C).

Electrophile	$E$	$k_2$ / L mol <sup>-1</sup> s <sup>-1</sup>	$\log k_2$
<b>2f</b>	-16.38	$9.06 \times 10^5$	5.96
<b>2g</b>	-17.29	$2.33 \times 10^5$	5.37
<b>2h</b>	-17.90	$1.24 \times 10^5$	5.09
<b>3b</b>	-18.98	$2.29 \times 10^4$	4.36
<b>3c</b>	-20.55	$6.09 \times 10^3$	3.78
<b>3d</b>	-21.11	$2.49 \times 10^3$	3.40

$$N = 27.57, s_N = 0.53$$



#### 4.5.1.3. Reactions of the Potassium Salt of Ethyl 4-Bromophenylacetate (**1c**-K)

Table 18: Kinetics of the reaction of **1c**-K (generated from **1c**-H by addition of 1.06 equivalents of KOtBu) with **2f** (20 °C, stopped-flow, at 407 nm).

[ <b>2f</b> ] / mol L <sup>-1</sup>	[ <b>1c</b> ] / mol L <sup>-1</sup>	[ <b>1c</b> ]/[ <b>2f</b> ]	$k_{\text{obs}}$ / s <sup>-1</sup>
$2.24 \times 10^{-5}$	$2.41 \times 10^{-4}$	10.7	$1.32 \times 10^2$
$2.24 \times 10^{-5}$	$3.37 \times 10^{-4}$	15.0	$2.19 \times 10^2$
$2.24 \times 10^{-5}$	$4.33 \times 10^{-4}$	19.3	$3.00 \times 10^2$
$2.24 \times 10^{-5}$	$5.29 \times 10^{-4}$	23.6	$4.12 \times 10^2$
$2.24 \times 10^{-5}$	$6.26 \times 10^{-4}$	27.9	$5.11 \times 10^2$

$$k_2 = 9.89 \times 10^5 \text{ L mol}^{-1} \text{ s}^{-1}$$

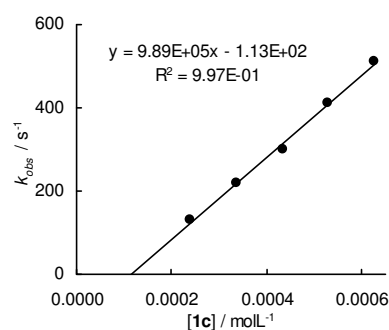
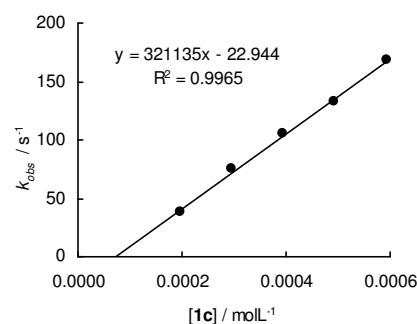




Table 19: Kinetics of the reaction of **1c**-K (generated from **1c**-H by addition of 1.04 equivalents of KOtBu) with **2g** (20 °C, stopped-flow, at 486 nm).

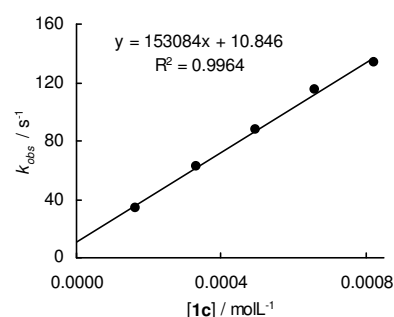
[ <b>2g</b> ] / mol L <sup>-1</sup>	[ <b>1c</b> ] / mol L <sup>-1</sup>	[ <b>1c</b> ]/[ <b>2g</b> ]	$k_{\text{obs}}$ / s <sup>-1</sup>
$1.88 \times 10^{-5}$	$1.97 \times 10^{-4}$	10.5	$3.77 \times 10^1$
$1.88 \times 10^{-5}$	$2.96 \times 10^{-4}$	15.7	$7.56 \times 10^1$
$1.88 \times 10^{-5}$	$3.95 \times 10^{-4}$	21.0	$1.06 \times 10^2$
$1.88 \times 10^{-5}$	$4.94 \times 10^{-4}$	26.2	$1.32 \times 10^2$
$1.88 \times 10^{-5}$	$5.92 \times 10^{-4}$	31.4	$1.68 \times 10^2$

$$k_2 = 3.21 \times 10^5 \text{ L mol}^{-1} \text{ s}^{-1}$$

Table 20: Kinetics of the reaction of **1c**-K (generated from **1c**-H by addition of 1.05 equivalents of KOtBu) with **2h** (20 °C, stopped-flow, at 521 nm).

[ <b>2h</b> ] / mol L <sup>-1</sup>	[ <b>1c</b> ] / mol L <sup>-1</sup>	[18-crown-6] / mol L <sup>-1</sup>	[ <b>1c</b> ]/[ <b>2h</b> ]	$k_{\text{obs}}$ / s <sup>-1</sup>
$1.69 \times 10^{-5}$	$1.65 \times 10^{-4}$		9.8	$3.42 \times 10^1$
$1.69 \times 10^{-5}$	$3.30 \times 10^{-4}$	$3.60 \times 10^{-4}$	19.5	$6.19 \times 10^1$
$1.69 \times 10^{-5}$	$4.95 \times 10^{-4}$		29.3	$8.80 \times 10^1$
$1.69 \times 10^{-5}$	$6.60 \times 10^{-4}$	$7.21 \times 10^{-4}$	39.1	$1.15 \times 10^2$
$1.69 \times 10^{-5}$	$8.25 \times 10^{-4}$		48.8	$1.34 \times 10^2$

$$k_2 = 1.53 \times 10^5 \text{ L mol}^{-1} \text{ s}^{-1}$$

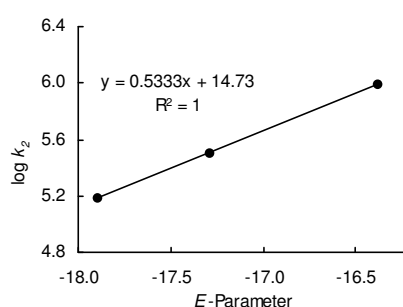


### Determination of Reactivity Parameters $N$ and $s_N$ for the Anion of Ethyl 4-Bromophenylacetate (**1c**) in DMSO

Table 21: Rate Constants for the reactions of **1c** with quinone methides (20 °C).

Electrophile	$E$	$k_2$ / L mol <sup>-1</sup> s <sup>-1</sup>	$\log k_2$
<b>2f</b>	-16.38	$9.89 \times 10^5$	6.00
<b>2g</b>	-17.29	$3.21 \times 10^5$	5.51
<b>2h</b>	-17.90	$1.53 \times 10^5$	5.18

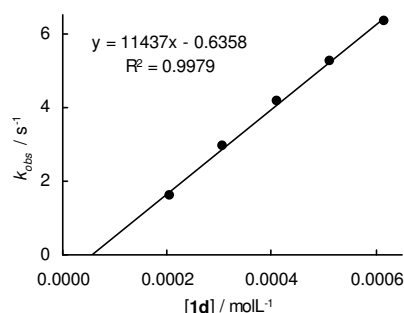
$$N = 27.62, s_N = 0.53$$



4.5.1.4. Reactions of the Potassium Salt of Ethyl 4-Cyanophenylacetate (**1d-K**)Table 22: Kinetics of the reaction of **1d-K** (generated from **1d-H** by addition of 1.04 equivalents of KO<sup>t</sup>Bu) with **2g** (20 °C, stopped-flow, at 486 nm).

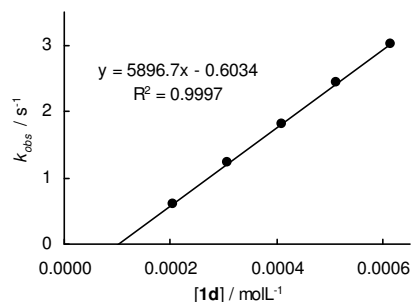
[ <b>2g</b> ] / mol L <sup>-1</sup>	[ <b>1d</b> ] / mol L <sup>-1</sup>	[18-crown-6] / mol L <sup>-1</sup>	[ <b>1d</b> ]/[ <b>2g</b> ]	$k_{\text{obs}}$ / s <sup>-1</sup>
$1.83 \times 10^{-5}$	$2.05 \times 10^{-4}$		11.2	1.61
$1.83 \times 10^{-5}$	$3.08 \times 10^{-4}$	$3.42 \times 10^{-4}$	16.9	2.95
$1.83 \times 10^{-5}$	$4.10 \times 10^{-4}$		22.5	4.14
$1.83 \times 10^{-5}$	$5.13 \times 10^{-4}$	$5.69 \times 10^{-4}$	28.1	5.25
$1.83 \times 10^{-5}$	$6.15 \times 10^{-4}$		33.7	6.32

$$k_2 = 1.14 \times 10^4 \text{ L mol}^{-1} \text{ s}^{-1}$$

Table 23: Kinetics of the reaction of **1d-K** (generated from **1d-H** by addition of 1.04 equivalents of KO<sup>t</sup>Bu) with **2h** (20 °C, stopped-flow, at 521 nm).

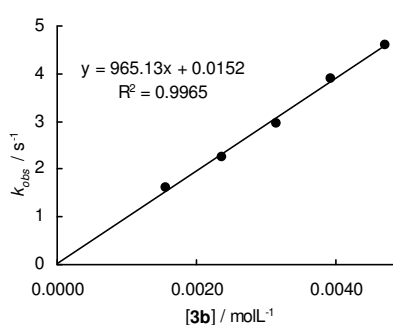
[ <b>2h</b> ] / mol L <sup>-1</sup>	[ <b>1d</b> ] / mol L <sup>-1</sup>	[18-crown-6] / mol L <sup>-1</sup>	[ <b>1d</b> ]/[ <b>2h</b> ]	$k_{\text{obs}}$ / s <sup>-1</sup>
$1.62 \times 10^{-5}$	$2.05 \times 10^{-4}$		12.7	$5.93 \times 10^{-1}$
$1.62 \times 10^{-5}$	$3.08 \times 10^{-4}$	$3.42 \times 10^{-4}$	19.0	1.23
$1.62 \times 10^{-5}$	$4.10 \times 10^{-4}$		25.4	1.80
$1.62 \times 10^{-5}$	$5.13 \times 10^{-4}$	$5.69 \times 10^{-4}$	31.7	2.43
$1.62 \times 10^{-5}$	$6.15 \times 10^{-4}$		38.0	3.02

$$k_2 = 5.90 \times 10^3 \text{ L mol}^{-1} \text{ s}^{-1}$$

Table 24: Kinetics of the reaction of **1d-K** (generated from **1d-H** by addition of 1.05 equivalents of KO<sup>t</sup>Bu) with **3b** (20 °C, stopped-flow, at 405 nm).

[ <b>3b</b> ] / mol L <sup>-1</sup>	[ <b>1d</b> ] / mol L <sup>-1</sup>	[ <b>3b</b> ]/[ <b>1d</b> ]	$k_{\text{obs}}$ / s <sup>-1</sup>
$1.58 \times 10^{-3}$	$7.72 \times 10^{-5}$	20.5	1.60
$2.37 \times 10^{-3}$	$7.72 \times 10^{-5}$	30.7	2.26
$3.16 \times 10^{-3}$	$7.72 \times 10^{-5}$	40.9	2.97
$3.95 \times 10^{-3}$	$7.72 \times 10^{-5}$	51.1	3.90
$4.73 \times 10^{-3}$	$7.72 \times 10^{-5}$	61.4	4.59

$$k_2 = 9.65 \times 10^2 \text{ L mol}^{-1} \text{ s}^{-1}$$

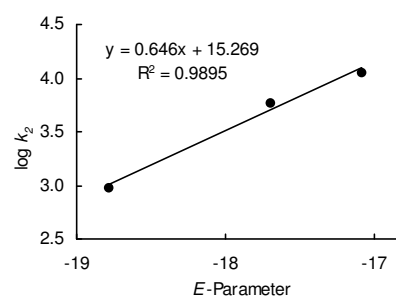


### Determination of Reactivity Parameters $N$ and $s_N$ for the Anion of Ethyl 3-Cyano-phenylacetate (**1d**) in DMSO

Table 25: Rate Constants for the reactions of **1d** with different electrophiles (20 °C).

Electrophile	$E$	$k_2 / \text{L mol}^{-1} \text{s}^{-1}$	$\log k_2$
<b>2g</b>	-17.29	$1.14 \times 10^4$	4.06
<b>2h</b>	-17.90	$5.90 \times 10^3$	3.77
<b>3b</b>	-18.98	$9.65 \times 10^2$	2.98

$$N = 23.64, s_N = 0.65$$

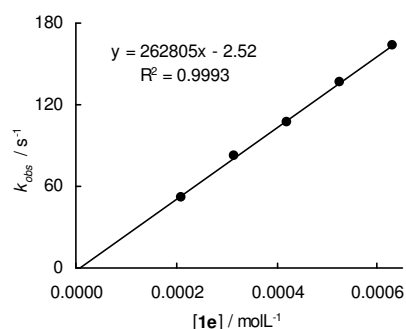


#### 4.5.1.5. Reactions of the Potassium Salt of Ethyl 4-Nitrophenylacetate (**1e-K**)

Table 26: Kinetics of the reaction of **1e-K** (generated from **1e-H** by addition of 1.04 equivalents of KOtBu) with **2a** (20 °C, stopped-flow, at 422 nm).

$[\mathbf{2a}] / \text{mol L}^{-1}$	$[\mathbf{1e}] / \text{mol L}^{-1}$	$[\text{18-crown-6}] / \text{mol L}^{-1}$	$[\mathbf{1e}]/[\mathbf{2a}]$	$k_{\text{obs}} / \text{s}^{-1}$
$1.54 \times 10^{-5}$	$2.11 \times 10^{-4}$		14.2	$5.18 \times 10^1$
$1.54 \times 10^{-5}$	$3.16 \times 10^{-4}$	$3.45 \times 10^{-4}$	21.3	$8.22 \times 10^1$
$1.54 \times 10^{-5}$	$4.22 \times 10^{-4}$		28.4	$1.08 \times 10^2$
$1.54 \times 10^{-5}$	$5.27 \times 10^{-4}$	$5.75 \times 10^{-4}$	35.5	$1.37 \times 10^2$
$1.54 \times 10^{-5}$	$6.32 \times 10^{-4}$		42.6	$1.63 \times 10^2$

$$k_2 = 2.63 \times 10^5 \text{ L mol}^{-1} \text{s}^{-1}$$

Table 27: Kinetics of the reaction of **1e-K** (generated from **1e-H** by addition of 1.05 equivalents of KOtBu) with **2b** (20 °C, stopped-flow, at 374 nm).

$[\mathbf{2b}] / \text{mol L}^{-1}$	$[\mathbf{1e}] / \text{mol L}^{-1}$	$[\text{18-crown-6}] / \text{mol L}^{-1}$	$[\mathbf{1e}]/[\mathbf{2b}]$	$k_{\text{obs}} / \text{s}^{-1}$
$2.12 \times 10^{-5}$	$2.72 \times 10^{-4}$		12.8	3.71
$2.12 \times 10^{-5}$	$4.07 \times 10^{-4}$	$4.42 \times 10^{-4}$	19.2	5.63
$2.12 \times 10^{-5}$	$6.79 \times 10^{-4}$	$7.36 \times 10^{-4}$	32.0	9.09
$2.12 \times 10^{-5}$	$8.15 \times 10^{-4}$		38.4	11.2

$$k_2 = 1.35 \times 10^4 \text{ L mol}^{-1} \text{s}^{-1}$$

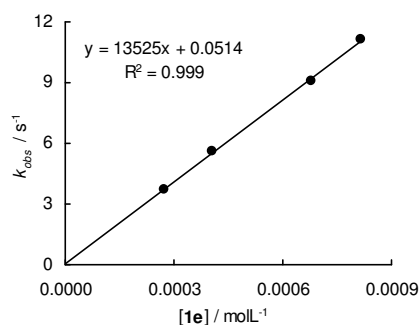
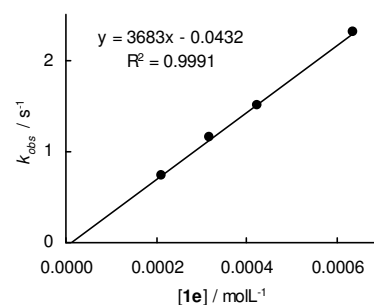


Table 28: Kinetics of the reaction of **1e**-K (generated from **1e**-H by addition of 1.05 equivalents of KOtBu) with **2c** (20 °C, stopped-flow, at 354 nm).

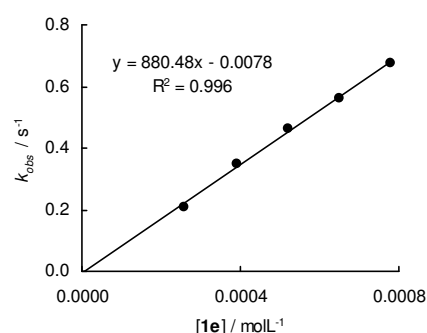
[ <b>2c</b> ] / mol L <sup>-1</sup>	[ <b>1e</b> ] / mol L <sup>-1</sup>	[18-crown-6] / mol L <sup>-1</sup>	[ <b>1e</b> ]/[ <b>2c</b> ]	$k_{\text{obs}}$ / s <sup>-1</sup>
$2.07 \times 10^{-5}$	$2.12 \times 10^{-4}$		10.2	$7.26 \times 10^{-1}$
$2.07 \times 10^{-5}$	$3.18 \times 10^{-4}$	$3.50 \times 10^{-4}$	15.3	1.15
$2.07 \times 10^{-5}$	$4.24 \times 10^{-4}$		20.4	1.50
$2.07 \times 10^{-5}$	$6.35 \times 10^{-4}$		30.6	2.30

$$k_2 = 3.68 \times 10^3 \text{ L mol}^{-1} \text{ s}^{-1}$$

Table 29: Kinetics of the reaction of **1e**-K (generated in from **1e**-H addition of 1.03 equivalents of KOtBu) with **2d** (20 °C, stopped-flow, at 371 nm).

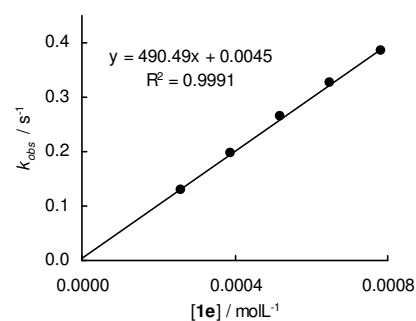
[ <b>2d</b> ] / mol L <sup>-1</sup>	[ <b>1e</b> ] / mol L <sup>-1</sup>	[18-crown-6] / mol L <sup>-1</sup>	[ <b>1e</b> ]/[ <b>2d</b> ]	$k_{\text{obs}}$ / s <sup>-1</sup>
$2.07 \times 10^{-5}$	$2.61 \times 10^{-4}$		12.6	$2.08 \times 10^{-1}$
$2.07 \times 10^{-5}$	$3.91 \times 10^{-4}$	$4.19 \times 10^{-4}$	18.8	$3.48 \times 10^{-1}$
$2.07 \times 10^{-5}$	$5.21 \times 10^{-4}$		25.1	$4.64 \times 10^{-1}$
$2.07 \times 10^{-5}$	$6.51 \times 10^{-4}$	$6.98 \times 10^{-4}$	31.4	$5.62 \times 10^{-1}$
$2.07 \times 10^{-5}$	$7.82 \times 10^{-4}$		37.7	$6.74 \times 10^{-1}$

$$k_2 = 8.80 \times 10^2 \text{ L mol}^{-1} \text{ s}^{-1}$$

Table 30: Kinetics of the reaction of **1e**-K (generated from **1e**-H by addition of 1.03 equivalents of KOtBu) with **2e** (20 °C, stopped-flow, at 393 nm).

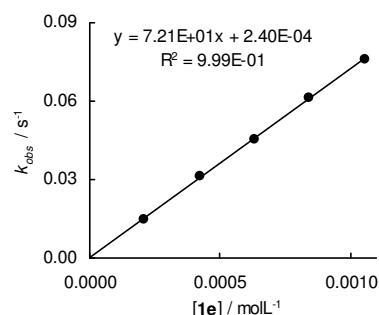
[ <b>2e</b> ] / mol L <sup>-1</sup>	[ <b>1e</b> ] / mol L <sup>-1</sup>	[18-crown-6] / mol L <sup>-1</sup>	[ <b>1e</b> ]/[ <b>2e</b> ]	$k_{\text{obs}}$ / s <sup>-1</sup>
$1.94 \times 10^{-5}$	$2.61 \times 10^{-4}$		13.4	$1.29 \times 10^{-1}$
$1.94 \times 10^{-5}$	$3.91 \times 10^{-4}$	$4.19 \times 10^{-4}$	20.1	$1.98 \times 10^{-1}$
$1.94 \times 10^{-5}$	$5.21 \times 10^{-4}$		26.8	$2.64 \times 10^{-1}$
$1.94 \times 10^{-5}$	$6.51 \times 10^{-4}$	$6.98 \times 10^{-4}$	33.5	$3.25 \times 10^{-1}$
$1.94 \times 10^{-5}$	$7.82 \times 10^{-4}$		40.3	$3.85 \times 10^{-1}$

$$k_2 = 4.90 \times 10^2 \text{ L mol}^{-1} \text{ s}^{-1}$$

Table 31: Kinetics of the reaction of **1e**-K (generated from **1e**-H by addition of 1.04 equivalents of KOtBu) with **2g** (20 °C, stopped-flow, at 450 nm).

[ <b>2g</b> ] / mol L <sup>-1</sup>	[ <b>1e</b> ] / mol L <sup>-1</sup>	[ <b>1e</b> ]/[ <b>2g</b> ]	$k_{\text{obs}}$ / s <sup>-1</sup>
$1.07 \times 10^{-5}$	$2.11 \times 10^{-4}$	19.8	$1.48 \times 10^{-2}$
$1.07 \times 10^{-5}$	$4.22 \times 10^{-4}$	39.5	$3.15 \times 10^{-2}$
$1.07 \times 10^{-5}$	$6.32 \times 10^{-4}$	59.3	$4.56 \times 10^{-2}$
$1.07 \times 10^{-5}$	$8.43 \times 10^{-4}$	79.1	$6.15 \times 10^{-2}$
$1.07 \times 10^{-5}$	$1.05 \times 10^{-3}$	98.8	$7.58 \times 10^{-2}$

$$k_2 = 7.21 \times 10^1 \text{ L mol}^{-1} \text{ s}^{-1}$$

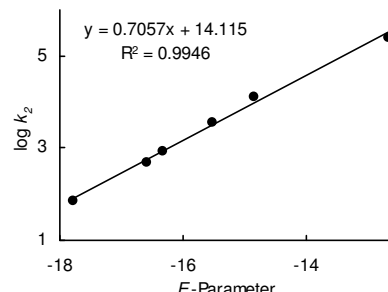


### Determination of Reactivity Parameters $N$ and $s_N$ for the Anion of Ethyl 4-Nitrophenylacetate (**1e**) in DMSO

Table 32: Rate Constants for the reactions of **1e** with quinone methides (20 °C).

Electrophile	$E$	$k_2 / \text{L mol}^{-1} \text{s}^{-1}$	$\log k_2$
<b>2a</b>	-12.18	$2.63 \times 10^5$	5.42
<b>2b</b>	-14.36	$1.35 \times 10^4$	4.13
<b>2c</b>	-15.03	$3.68 \times 10^3$	3.57
<b>2d</b>	-15.83	$8.80 \times 10^2$	2.94
<b>2e</b>	-16.11	$4.90 \times 10^2$	2.69
<b>2g</b>	-17.29	$7.21 \times 10^1$	1.86

$$N = 20.00, s_N = 0.71$$

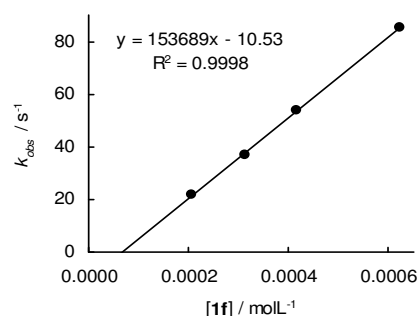


#### 4.5.1.6. Reactions of the Potassium Salt of Ethyl 2-(Pyridin-4-yl)-acetate (**1f-K**)

Table 33: Kinetics of the reaction of **1f-K** (generated from **1f-H** by addition of 1.04 equivalents of KO $t$ Bu) with **2d** (20 °C, stopped-flow, at 371 nm).

$[\mathbf{2d}] / \text{mol L}^{-1}$	$[\mathbf{1f}] / \text{mol L}^{-1}$	$[\text{18-crown-6}] / \text{mol L}^{-1}$	$[\mathbf{1f}]/[\mathbf{2d}]$	$k_{\text{obs}} / \text{s}^{-1}$
$2.01 \times 10^{-5}$	$2.08 \times 10^{-4}$		10.3	$2.15 \times 10^1$
$2.01 \times 10^{-5}$	$3.11 \times 10^{-4}$	$3.42 \times 10^{-4}$	15.5	$3.69 \times 10^1$
$2.01 \times 10^{-5}$	$4.15 \times 10^{-4}$		20.7	$5.37 \times 10^1$
$2.01 \times 10^{-5}$	$6.23 \times 10^{-4}$		31.0	$8.51 \times 10^1$

$$k_2 = 1.54 \times 10^5 \text{ L mol}^{-1} \text{s}^{-1}$$

Table 34: Kinetics of the reaction of **1f-K** (generated from **1f-H** by addition of 1.04 equivalents of KO $t$ Bu) with **2e** (20 °C, stopped-flow, at 393 nm).

$[\mathbf{2e}] / \text{mol L}^{-1}$	$[\mathbf{1f}] / \text{mol L}^{-1}$	$[\text{18-crown-6}] / \text{mol L}^{-1}$	$[\mathbf{1f}]/[\mathbf{2e}]$	$k_{\text{obs}} / \text{s}^{-1}$
$2.07 \times 10^{-5}$	$2.08 \times 10^{-4}$		10.0	$1.71 \times 10^1$
$2.07 \times 10^{-5}$	$3.11 \times 10^{-4}$	$3.42 \times 10^{-4}$	15.0	$2.69 \times 10^1$
$2.07 \times 10^{-5}$	$4.15 \times 10^{-4}$		20.1	$3.70 \times 10^1$
$2.07 \times 10^{-5}$	$5.19 \times 10^{-4}$	$5.69 \times 10^{-4}$	25.1	$4.63 \times 10^1$
$2.07 \times 10^{-5}$	$6.23 \times 10^{-4}$		30.1	$5.64 \times 10^1$

$$k_2 = 9.46 \times 10^4 \text{ L mol}^{-1} \text{s}^{-1}$$

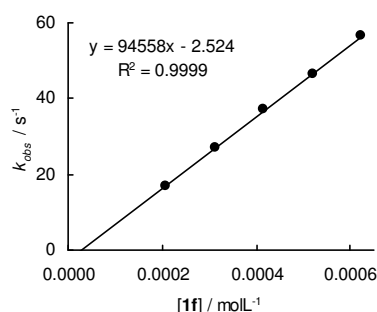
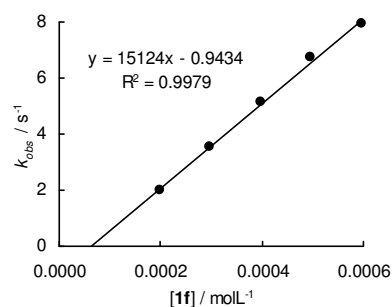


Table 35: Kinetics of the reaction of **1f**-K (generated from **1f**-H by addition of 1.05 equivalents of KO<sup>t</sup>Bu) with **2g** (20 °C, stopped-flow, at 486 nm).

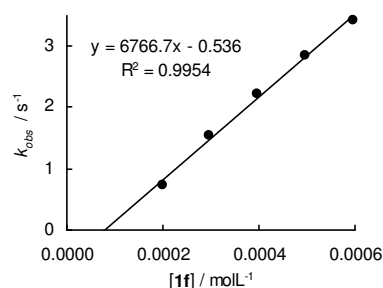
[ <b>2g</b> ] / mol L <sup>-1</sup>	[ <b>1f</b> ] / mol L <sup>-1</sup>	[ <b>1f</b> ]/[ <b>2g</b> ]	$k_{\text{obs}}$ / s <sup>-1</sup>
$1.87 \times 10^{-5}$	$1.99 \times 10^{-4}$	10.6	2.02
$1.87 \times 10^{-5}$	$2.98 \times 10^{-4}$	16.0	3.53
$1.87 \times 10^{-5}$	$3.97 \times 10^{-4}$	21.3	5.12
$1.87 \times 10^{-5}$	$4.96 \times 10^{-4}$	26.6	6.72
$1.87 \times 10^{-5}$	$5.96 \times 10^{-4}$	31.9	7.93

$$k_2 = 1.51 \times 10^4 \text{ L mol}^{-1} \text{ s}^{-1}$$

Table 36: Kinetics of the reaction of **1f**-K (generated from **1f**-H by addition of 1.05 equivalents of KO<sup>t</sup>Bu) with **2h** (20 °C, stopped-flow, at 521 nm).

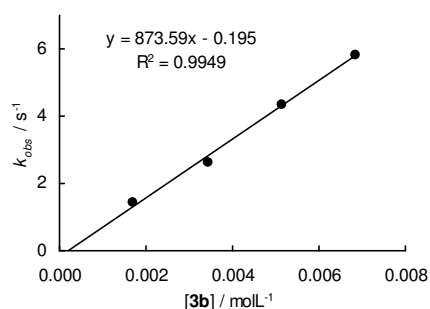
[ <b>2h</b> ] / mol L <sup>-1</sup>	[ <b>1f</b> ] / mol L <sup>-1</sup>	[ <b>1f</b> ]/[ <b>2h</b> ]	$k_{\text{obs}}$ / s <sup>-1</sup>
$1.66 \times 10^{-5}$	$1.99 \times 10^{-4}$	11.9	$7.26 \times 10^{-1}$
$1.66 \times 10^{-5}$	$2.98 \times 10^{-4}$	17.9	1.53
$1.66 \times 10^{-5}$	$3.97 \times 10^{-4}$	23.9	2.22
$1.66 \times 10^{-5}$	$4.96 \times 10^{-4}$	29.8	2.86
$1.66 \times 10^{-5}$	$5.96 \times 10^{-4}$	35.8	3.42

$$k_2 = 6.77 \times 10^3 \text{ L mol}^{-1} \text{ s}^{-1}$$

Table 37: Kinetics of the reaction of **1f**-K (generated from **1f**-H by addition of 1.05 equivalents of KO<sup>t</sup>Bu) with **3b** (20 °C, stopped-flow, at 351 nm).

[ <b>3b</b> ] / mol L <sup>-1</sup>	[ <b>1f</b> ] / mol L <sup>-1</sup>	[ <b>3b</b> ]/[ <b>1f</b> ]	$k_{\text{obs}}$ / s <sup>-1</sup>
$1.71 \times 10^{-3}$	$6.23 \times 10^{-5}$	27.5	1.42
$3.43 \times 10^{-3}$	$6.23 \times 10^{-5}$	55.1	2.60
$5.14 \times 10^{-3}$	$6.23 \times 10^{-5}$	82.6	4.35
$6.86 \times 10^{-3}$	$6.23 \times 10^{-5}$	101	5.83

$$k_2 = 8.74 \times 10^2 \text{ L mol}^{-1} \text{ s}^{-1}$$

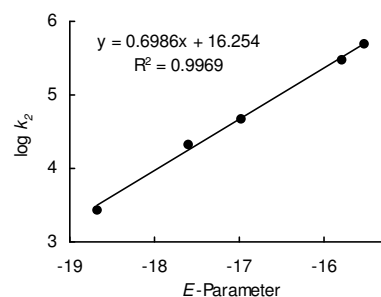


### Determination of Reactivity Parameters $N$ and $s_N$ for the Anion of Ethyl Pyridine-4-Acetate (**1f**) in DMSO

Table 38: Rate Constants for the reactions of **1f** with different electrophiles (20 °C).

Electrophile	$E$	$k_2 / \text{L mol}^{-1} \text{s}^{-1}$	$\log k_2$
<b>2d</b>	-15.83	$1.54 \times 10^5$	5.19
<b>2e</b>	-16.11	$9.46 \times 10^4$	4.98
<b>2g</b>	-17.29	$1.51 \times 10^4$	4.18
<b>2h</b>	-17.90	$6.77 \times 10^3$	3.83
<b>3b</b>	-18.98	$8.74 \times 10^2$	2.94

$$N = 23.27, s_N = 0.70$$



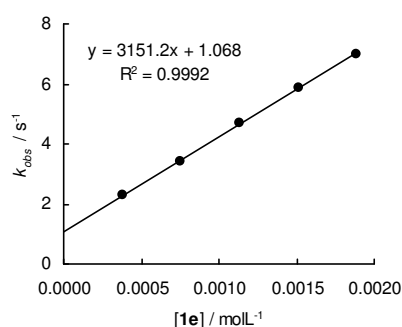
## 4.5.2. Reactions of Ethyl 4-Nitrophenylacetate Anion **1e** with Further Electrophiles

### 4.5.2.1. Reactions of **1e**-K with *trans*- $\beta$ -Nitrostyrenes **7**

Table 39: Kinetics of the reaction of **1e**-K (generated from **1e**-H by addition of 1.04 equivalents of KO $t$ Bu) with **7a** (20 °C, stopped-flow, at 363 nm).

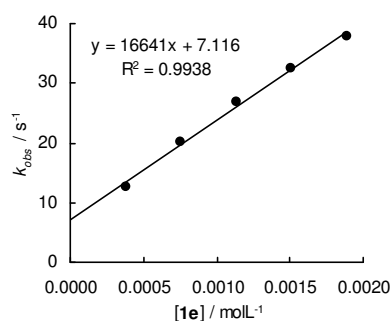
$[\mathbf{7a}] / \text{mol L}^{-1}$	$[\mathbf{1e}] / \text{mol L}^{-1}$	$[\mathbf{1e}]/[\mathbf{7a}]$	$k_{\text{obs}} / \text{s}^{-1}$
$3.29 \times 10^{-5}$	$3.78 \times 10^{-4}$	11.5	2.27
$3.29 \times 10^{-5}$	$7.55 \times 10^{-4}$	22.9	3.39
$3.29 \times 10^{-5}$	$1.13 \times 10^{-3}$	34.4	4.67
$3.29 \times 10^{-5}$	$1.51 \times 10^{-3}$	45.9	5.89
$3.29 \times 10^{-5}$	$1.89 \times 10^{-3}$	57.3	6.97

$$k_2 = 3.15 \times 10^3 \text{ L mol}^{-1} \text{s}^{-1}$$

Table 40: Kinetics of the reaction of **1e**-K (generated from **1e**-H by addition of 1.05 equivalents of KO $t$ Bu) with **7b** (20 °C, stopped-flow, at 340 nm).

$[\mathbf{7b}] / \text{mol L}^{-1}$	$[\mathbf{1e}] / \text{mol L}^{-1}$	$[\mathbf{1e}]/[\mathbf{7b}]$	$k_{\text{obs}} / \text{s}^{-1}$
$3.62 \times 10^{-5}$	$3.78 \times 10^{-4}$	10.4	$1.25 \times 10^1$
$3.62 \times 10^{-5}$	$7.55 \times 10^{-4}$	20.9	$2.02 \times 10^1$
$3.62 \times 10^{-5}$	$1.13 \times 10^{-3}$	31.3	$2.69 \times 10^1$
$3.62 \times 10^{-5}$	$1.51 \times 10^{-3}$	41.7	$3.24 \times 10^1$
$3.62 \times 10^{-5}$	$1.89 \times 10^{-3}$	52.1	$3.78 \times 10^1$

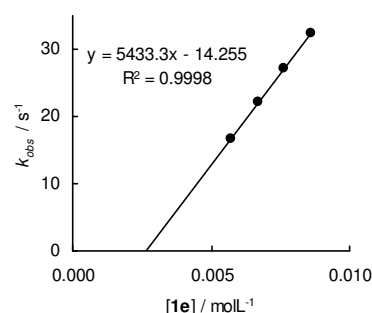
$$k_2 = 1.66 \times 10^4 \text{ L mol}^{-1} \text{s}^{-1}$$



4.5.2.2. Reactions of **1e-K** with 1,2-Diaza-1,3-Dienes **9**Table 41: Kinetics of the reaction of **1e-K** (generated from **1e-H** by addition of 1.03 equivalents of KO<sup>t</sup>Bu) with **9a** (20 °C, stopped-flow, at 390 nm).

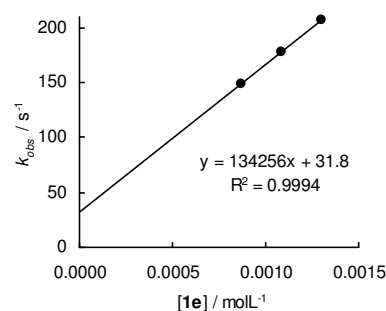
[ <b>9a</b> ] / mol L <sup>-1</sup>	[ <b>1e</b> ] / mol L <sup>-1</sup>	[ <b>1e</b> ]/[ <b>9a</b> ]	$k_{\text{obs}}$ / s <sup>-1</sup>
$4.98 \times 10^{-4}$	$5.72 \times 10^{-3}$	11.8	$1.68 \times 10^1$
$4.98 \times 10^{-4}$	$6.68 \times 10^{-3}$	13.8	$2.21 \times 10^1$
$4.98 \times 10^{-4}$	$7.63 \times 10^{-3}$	15.8	$2.73 \times 10^1$
$4.98 \times 10^{-4}$	$8.59 \times 10^{-3}$	17.7	$3.23 \times 10^1$

$$k_2 = 5.43 \times 10^3 \text{ L mol}^{-1} \text{ s}^{-1}$$

Table 42: Kinetics of the reaction of **1e-K** (generated from **1e-H** by addition of 1.04 equivalents of KO<sup>t</sup>Bu) with **9b** (20 °C, stopped-flow, at 390 nm).

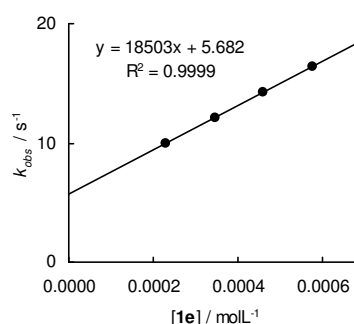
[ <b>9b</b> ] / mol L <sup>-1</sup>	[ <b>1e</b> ] / mol L <sup>-1</sup>	[ <b>1e</b> ]/[ <b>9b</b> ]	$k_{\text{obs}}$ / s <sup>-1</sup>
$8.30 \times 10^{-5}$	$8.70 \times 10^{-4}$	11.0	$1.48 \times 10^2$
$8.30 \times 10^{-5}$	$1.09 \times 10^{-3}$	13.7	$1.79 \times 10^2$
$8.30 \times 10^{-5}$	$1.30 \times 10^{-3}$	16.4	$2.07 \times 10^2$

$$k_2 = 1.34 \times 10^5 \text{ L mol}^{-1} \text{ s}^{-1}$$

4.5.2.3. Reactions of **1e-K** with 4-Dimethylamino-benzylidene malononitril **11**Table 43: Kinetics of the reaction of **1e-K** (generated from **1e-H** by addition of 1.06 equivalents of KO<sup>t</sup>Bu) with **11** (20 °C, stopped-flow, at 441 nm).

[ <b>11</b> ] / mol L <sup>-1</sup>	[ <b>1e</b> ] / mol L <sup>-1</sup>	[ <b>1e</b> ]/[ <b>11</b> ]	$k_{\text{obs}}$ / s <sup>-1</sup>
$2.11 \times 10^{-5}$	$2.31 \times 10^{-4}$	11.6	9.91
$2.11 \times 10^{-5}$	$3.46 \times 10^{-4}$	17.4	$1.21 \times 10^1$
$2.11 \times 10^{-5}$	$4.62 \times 10^{-4}$	23.2	$1.42 \times 10^1$
$2.11 \times 10^{-5}$	$5.77 \times 10^{-4}$	29.0	$1.64 \times 10^1$
$2.11 \times 10^{-5}$	$6.93 \times 10^{-4}$	34.9	$1.85 \times 10^1$

$$k_2 = 1.85 \times 10^4 \text{ L mol}^{-1} \text{ s}^{-1}$$





#### 4.6. $^1\text{H}$ NMR-Experiments

The determination of the chemical shifts of the benzylic proton of the anions of the ethyl arylacetates **1** were performed under argon atmosphere (glove-box) by mixing a solution of KOtBu (13-21 mg) dissolved in 0.3-0.4 mL of  $[\text{D}_6]$ -DMSO with the CH-acids **1-H** (18-35 mg) and subsequent dilution of the mixtures to 0.6 mL with  $[\text{D}_6]$ -DMSO (Table 41). The  $^1\text{H}$  NMR-spectra were acquired within 10 min. after mixing CH-acid and base using a 200 MHz NMR-spectrometer.

Table 44: Chemical shifts ( $\delta$  / ppm) of the benzylic protons of the potassium salts of the ethyl arylacetates **1** in  $[\text{D}_6]$ -DMSO (200 MHz, 20 °C).

<b>1</b>	<b>m(1-H) / mg</b>	<b>m(KOtBu) / mg</b>	<b><math>\delta_{\text{H}}</math> / ppm</b>
<b>1a</b>	24.5	18.1	- <sup>a</sup>
<b>1b</b>	35.2	21.1	3.79
<b>1c</b>	22.1	12.8	3.76
<b>1d</b>	23.0	15.1	4.03
<b>1e</b>	28.9	16.7	4.62
<b>1f</b>	17.8	13.3	3.80

a) Probably because of H-D-exchange with the solvent  $\delta(\mathbf{1a})$  was not observed.

#### 5. References

- [1] Selected examples for Michael additions using anions of ethyl arylacetates: a) E. D. Bergmann, D. Ginsburg, R. Pappo, *Organic Reactions*, Wiley, New York, **1959**, pp 179-555; b) W. Borsche, *Chem. Ber.* **1909**, 4496-4499; c) R. Connor, D. B. Andrews, *J. Am. Chem. Soc.* **1934**, 58, 2713-2716; d) R. Connor, W.M. R. McClellan, *J. Org. Chem.* **1939**, 3, 570-577; e) M. Kotake, T. Sakan, T. Miwa, *J. Am. Chem. Soc.* **1950**, 72, 5085-5087; f) D. Ivanov, G. Vassilev, I. Panayotov, *Synthesis* **1975**, 83-98; g) V. Dryanska, *Synth. Comm.* **1985**, 15, 899-906.
- [2] Selected examples for Claisen-type reactions using anions of ethyl arylacetates: a) C. R. Hauser, B. E. Hudson Jr., *Organic Reactions*, Wiley, New York, **1963**, pp 266-302; b) H. Scheibler, A. Emden, R. Neubner, *Chem. Ber.* **1930**, 1557-1562; c) N. C. Ross, R. Levine, *J. Org. Chem.* **1964**, 29, 2346-2350; d) H. N. Al-Jallo, F. H. Al-Hajjar, *J. Chem. Soc. (C)* **1970**, 2056-2058; e) G. H. Posner, E. M. Shulman-Roskes, *J. Org. Chem.* **1989**, 54, 3514-3515.
- [3] a) J. Sedgeworth, G. R. Proctor, *J. Chem. Soc., Perkin Trans. 1* **1985**, 2677-2687; b) D. F. Taber, K. K. You, A. L. Rheingold, *J. Am. Chem. Soc.* **1996**, 118, 547-556; c) J.

- Maeng, S. B. Kim, N. J. Lee, E. Choi, S.-Y. Jung, I. Hong, S.-H. Bae, J. T. Oh, B. Lim, J. W. Kim, C. J. Kang, S. Koo, *Chem. Eur. J.* **2010**, *16*, 7395-7399.
- [4] a) T. I. Bieber, R. Sites, Y. Chiang, *J. Org. Chem.* **1958**, *23*, 300-301; b) P. Langer, J. Wuckelt, M. Döring, *J. Org. Chem.* **2000**, *65*, 729-734.
- [5] R. Shankar, H. Shukla, U. S. Singh, V. Thakur, K. Hajela, *Synth. Commun.* **2011**, *41*, 2738-2746.
- [6] a) H. Mayr, T. Bug, M. F. Gotta, N. Hering, B. Irrgang, B. Janker, B. Kempf, R. Loos, A. R. Ofial, G. Remennikov, H. Schimmel, *J. Am. Chem. Soc.* **2001**, *123*, 9500-9512; b) R. Lucius, R. Loos, H. Mayr, *Angew. Chem.* **2002**, *114*, 97-102; *Angew. Chem. Int. Ed.* **2002**, *41*, 91-95; c) H. Mayr, B. Kempf, A. R. Ofial, *Acc. Chem. Res.* **2003**, *36*, 66-77; d) H. Mayr, A. R. Ofial, *Pure Appl. Chem.* **2005**, *77*, 1807-1821; e) D. Richter, N. Hampel, T. Singer, A. R. Ofial, H. Mayr, *Eur. J. Org. Chem.* **2009**, 3203-3211; f) For a comprehensive listing of nucleophilicity parameters  $N$ ,  $s_N$  and electrophilicity parameters  $E$ , see <http://www.cup.uni-muenchen.de/oc/mayr/DBintro.html>.
- [7] Reactivities of amines: a) F. Brotzel, Y. C. Chu, H. Mayr, *J. Org. Chem.* **2007**, *72*, 3679-3688; b) T. Kanzian, T. A. Nigst, A. Maier, S. Pichl, H. Mayr, *Eur. J. Org. Chem.* **2009**, 6379-6385.
- [8] Reactivities of solvents: S. Minegishi, S. Kobayashi, H. Mayr, *J. Am. Chem. Soc.* **2004**, *126*, 5174-5181.
- [9] Reactivities of ylides: a) R. Appel, R. Loos, H. Mayr, *J. Am. Chem. Soc.* **2009**, *131*, 704-714; b) R. Appel, N. Hartmann, H. Mayr, *J. Am. Chem. Soc.* **2010**, *132*, 17894-17900.
- [10] Reactivities of carbenes: B. Maji, M. Breugst, H. Mayr, *Angew. Chem.* **2011**, *123*, 7047-7052; *Angew. Chem. Int. Ed.* **2011**, *50*, 6915-6919.
- [11] Reactivities of carbanions: a) R. Loos, S. Kobayashi, H. Mayr, *J. Am. Chem. Soc.* **2003**, *125*, 14126-14132; b) T. Bug, T. Lemek, H. Mayr, *J. Org. Chem.* **2004**, *69*, 7565-7576; c) T. B. Phan, H. Mayr, *Eur. J. Org. Chem.* **2006**, 2530-2537; d) S. T. A. Berger, A. R. Ofial, H. Mayr, *J. Am. Chem. Soc.* **2007**, *129*, 9753-9761; e) F. Seeliger, H. Mayr, *Org. Biomol. Chem.* **2008**, *6*, 3052-3058; f) O. Kaumanns, R. Appel, T. Lemek, F. Seeliger, H. Mayr, *J. Org. Chem.* **2009**, *74*, 75-81.
- [12] H. Mayr, M. Patz, *Angew. Chem.* **1994**, *106*, 990-1010; *Angew. Chem. Int. Ed. Engl.* **1994**, *33*, 938-957.

- [13] O. Kaumanns, R. Lucius, H. Mayr, *Chem. Eur. J.* **2008**, *14*, 9675-9682.
- [14] I. Zenz, H. Mayr, *J. Org. Chem.* **2011**, *76*, 9370-9378.
- [15] T. Kanzian, S. Nicolini, L. De Crescentini, O. A. Attanasi, A. R. Ofial, H. Mayr, *Chem. Eur. J.* **2010**, *16*, 12008-12016.
- [16] T. Lemek, H. Mayr, *J. Org. Chem.* **2003**, *68*, 6880-6886.
- [17] C. Hansch, A. Leo, D. Hoekman, *Exploring QSAR – Hydrophobic, Electronic, and Steric Constants*, American Chemical Society, Washington, DC, **1995**; and references therein.
- [18] a) S.-I. Kiyooka, Y. Ueda, K. Suzuki, *Bull. Chem. Soc. Jpn.* **1980**, *53*, 1656-1660; b) S.-I. Kiyooka, K. Suzuki, *Bull. Chem. Soc. Jpn.* **1981**, *54*, 623-624.
- [19] Nucleophilicity of the anion of deoxybenzoin: compare Chapter 3 of this thesis.
- [20] a) R. A. Marcus, *J. Phys. Chem.* **1968**, *72*, 891-899; b) R. A. Marcus, *J. Am. Chem. Soc.* **1969**, *91*, 7224-7225; c) S. Hoz, H. Basch, J. L. Wolk, T. Hoz, E. Rozental, *J. Am. Chem. Soc.* **1999**, *121*, 7724-7725.
- [21] a) F. G. Bordwell, *Acc. Chem. Res.* **1988**, *21*, 456-463; b) É. S. Petrov, E. N. Tsvetkov, S. P. Mesyats, A. N. Shatenshtein, M. I. Kabachnik, *Izv. Akad. Nauk SSSR*, **1976**, 782-787; c) F. G. Bordwell, J.-P. Cheng, M. J. Bausch, J. E. Bares, *J. Phys. Org. Chem.* **1988**, *1*, 209-223; d) F. G. Bordwell, A. V. Satish, *J. Am. Chem. Soc.* **1994**, *116*, 8885-8889; e) J. R. Keeffe, J. Morey, C. A. Palmer, J. C. Lee, *J. Am. Chem. Soc.* **1979**, *101*, 1295-1297; f) R. Goumont, E. Kizilian, E. Buncel, F. Terrier, *Org. Biomol. Chem.* **2003**, *1*, 1741-1748; g) F. G. Bordwell, J. A. Harrelson Jr., *Can. J. Chem.* **1990**, *68*, 1714-1718; h) F. G. Bordwell, M. J. Bausch, *J. Am. Chem. Soc.* **1986**, *108*, 1979-1985; i) F. G. Bordwell, M. J. Bausch, J. C. Branca, J. A. Harrelson Jr., *J. Phys. Org. Chem.* **1988**, *1*, 225-241.
- [22] H. E. Gottlieb, V. Kotlyar, A. Nudelman, *J. Org. Chem.* **1997**, *62*, 7512-7515.
- [23] W.-B. Pan, F.-R. Chang, L.-M. Wei, M.-J. Wu, Y.-C. Wu, *Tetrahedron Lett.* **2003**, *44*, 331-334.
- [24] J. Zanon, A. Klapars, S. L. Buchwald, *J. Am. Chem. Soc.* **2003**, *125*, 2890-2891.

## Chapter 3

# Quantification of Ion-Pairing Effects on the Nucleophilic Reactivities of Benzoyl- and Phenyl-Substituted Carbanions in Dimethylsulfoxide

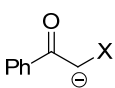
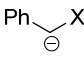
Francisco Corral Bautista, Roland Appel and Herbert Mayr

## 1. Introduction

Reactions of carbanions with alkyl halides, Michael acceptors, or carbonyl groups are among the most important methods for the formation of carbon-carbon bonds.<sup>[1]</sup> In previous work we have studied the nucleophilic reactivities of different types of carbanions<sup>[2]</sup> and found that  $pK_{\text{aH}}$  values are not a reliable measure for their relative reactivities.<sup>[2b,d,f,g]</sup> Since these investigations were mostly performed in DMSO solution at low ion concentrations, ion-pairing was neglected. We now examined the concentration range in which this assumption is justified and characterized the nucleophilic reactivities of the benzoyl-substituted carbanions **1** and the analogously substituted benzyl anions **2** (Scheme 1) by determining the rate constants of their reactions with the electrophiles shown in Table 1. The second-order rate constants are then analyzed by the linear free-energy relationship (1), where  $E$  is an electrophile-specific parameter, and  $N$  and  $s_N$  are solvent-dependent nucleophile-specific parameters.<sup>[3]</sup>

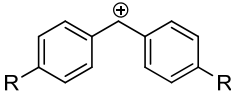
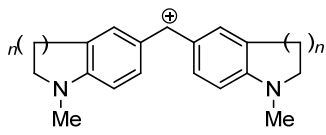
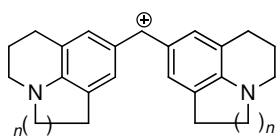
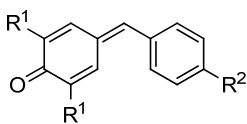
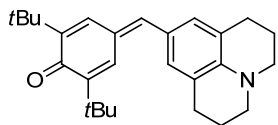
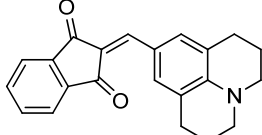
$$\lg k_2 (20\text{ }^\circ\text{C}) = s_N (N + E) \quad (1)$$

Relationships between structures and nucleophilic reactivities of the carbanions **1** and **2** are discussed.

					
<b>1-X</b>			<b>2-X</b>		
<b>1-X</b>	$\lambda_{\text{max}}$	$pK_{\text{aH}}$ <sup>[a]</sup>	<b>2-X</b>	$\lambda_{\text{max}}$	$pK_{\text{aH}}$ <sup>[a]</sup>
<b>1-Ph</b>	397	17.7			
<b>1-CONEt<sub>2</sub></b>	336				
<b>1-CO<sub>2</sub>Et</b>	327	15.5	<b>2-CO<sub>2</sub>Et</b> <sup>[b]</sup>	340 <sup>[c]</sup>	22.6
<b>1-CN</b>	328	10.2	<b>2-CN</b>	344	21.9
<b>1-COMe</b>	340	14.2	<b>2-COMe</b>	348	19.8
<b>1-COPh</b>	370	13.4	<b>2-COPh</b> <sup>[d]</sup>	397	17.7
<b>1-SO<sub>2</sub>Ph</b>	325	11.4	<b>2-SO<sub>2</sub>Ph</b>	310	23.4
<b>1-NO<sub>2</sub></b>	360	7.7	<b>2-NO<sub>2</sub></b> <sup>[b]</sup>		12.2

Scheme 1: Benzoyl-substituted carbanions **1-X** and benzyl anions **2-X** and their absorption maxima  $\lambda_{\text{max}}$  (in nm) in DMSO. [a]  $pK_{\text{aH}}$  in DMSO solution. From ref.<sup>[5]</sup> [b] The nucleophilic reactivities of the anions **2-CO<sub>2</sub>Et** and **2-NO<sub>2</sub>** were studied in previous work.<sup>[2b,2g]</sup> [c]  $\lambda_{\text{max}}$  from Ref.<sup>[2g]</sup> [d] **2-COPh** = **1-Ph**.

Table 1: Benzhydrylium ions **3a–f** and Michael acceptors **3g–p** employed as reference electrophiles in this study.

Electrophile			$E^{[a]}$	$\lambda_{\max}^{[b]}$	
	R = NMe <sub>2</sub>	<b>3a</b>	-7.02	613	
	R = N(CH <sub>2</sub> ) <sub>4</sub>	<b>3b</b>	-7.69	620	
	$n = 2$	<b>3c</b>	-8.22	618	
	$n = 1$	<b>3d</b>	-8.76	627	
	$n = 2$	<b>3e</b>	-9.45	635	
	$n = 1$	<b>3f</b>	-10.04	630	
	R <sup>1</sup> = Ph	R <sup>2</sup> = OMe	<b>3g</b>	-12.18	422
	R <sup>1</sup> = Ph	R <sup>2</sup> = NMe <sub>2</sub>	<b>3h</b>	-13.39	533
	R <sup>1</sup> = <i>t</i> Bu	R <sup>2</sup> = NO <sub>2</sub>	<b>3i</b>	-14.36	374
	R <sup>1</sup> = <i>t</i> Bu	R <sup>2</sup> = Me	<b>3j</b>	-15.83	371
	R <sup>1</sup> = <i>t</i> Bu	R <sup>2</sup> = OMe	<b>3k</b>	-16.11	393
	R <sup>1</sup> = OMe	R <sup>2</sup> = OMe	<b>3l</b>	-16.38	407
	R <sup>1</sup> = Me	R <sup>2</sup> = NMe <sub>2</sub>	<b>3m</b>	-16.36	490
	R <sup>1</sup> = <i>t</i> Bu	R <sup>2</sup> = NMe <sub>2</sub>	<b>3n</b>	-17.29	486
		<b>3o</b>	-17.90	521	
		<b>3p</b>	-14.68	520	

[a] Electrophilicity-parameters  $E$  were taken from ref. [3b,c,t,4]

[b] In nm in DMSO solution.

[a] Electrophilicity-parameters  $E$  were taken from ref. [3b,c,f,4] [b] In nm in DMSO solution.

## 2. Results and Discussion

### 2.1. Preparation of the Alkali Salts

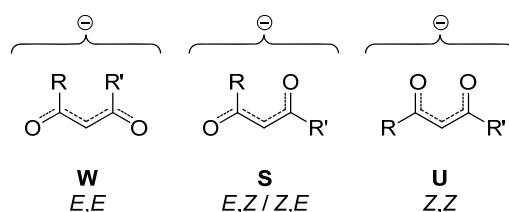
The alkali salts (**1-X**)-M were generated by treatment of the corresponding CH acids with alkali *tert*-butoxide (LiOtBu, NaOtBu, KOtBu) in ethanol and isolated after washing the precipitated salts with dry diethyl ether (Scheme 2).

The anions **1-X** show a single set of NMR signals in [D<sub>6</sub>]-DMSO solution, except for (**1-COMe**)-K, which shows two sets of broad signals in the ratio 1:1.3. For this anion four possible configurations have to be considered (Scheme 3).

$$\text{Ph}-\text{C}(=\text{O})-\text{CH}_2-\text{X} \xrightarrow[\text{EtOH}]{\text{MOtBu}} \text{Ph}-\text{C}(=\text{O})-\text{CH}^--\text{X} \text{M}^+ \quad (1-\text{X})-\text{M}$$

1-X	M	Yield	$\delta(\text{CH})$	$\delta(\text{C})$
1-Ph	K	-[a]	5.34	88.9
1-CONEt <sub>2</sub>	K	89%	5.05	78.6
1-CO <sub>2</sub> Et	K	66%	4.90	77.5
1-CO <sub>2</sub> Et	Na	67%	4.99	77.9
1-CO <sub>2</sub> Et	Li	78%	5.16	78.7
1-CN	K	77%	3.94	51.0
1-COMe	K	75%	5.28 / 5.55 <sup>[b]</sup>	93.3 / 96.3 <sup>[b]</sup>
1-COPh	K	79%	6.27	90.4
1-SO <sub>2</sub> Ph	K	86%	5.21	83.1
1-NO <sub>2</sub>	K	85%	7.23	109.1

Scheme 2: <sup>1</sup>H and <sup>13</sup>C NMR chemical shifts of the anionic centres of the alkali salts **1-X** ( $0.16 < c < 0.24 \text{ mmol L}^{-1}$ ) in [D<sub>6</sub>] DMSO. [a] Generated by treatment of the conjugate CH acid with KOtBu in DMSO solution. [b] Two isomers in solution (ratio 1:1.3).



Scheme 3: Possible configurations of  $\beta$ -dicarbonyl enolates.

Previous NMR investigations of the sodium salt of pentane-2,4-dione ( $\text{R} = \text{R}' = \text{CH}_3$  in Scheme 3) in methanol showed the presence of a mixture of the S- and U-configuration.<sup>[6]</sup> The absence of the W-configuration can be explained by the steric interaction between the coplanar R and R' groups. The U/S ratio increased when sodium iodide was added, due to the formation of the sodium complex of the bidentate U-configuration. Addition of more than one equivalent of 18-crown-6 led to the disappearance of the U-configuration, showing that the free enolate ion exists in the S-configuration exclusively; obviously, in the free carbanion the U-configuration is destabilized by the repulsive Coulomb interaction between the negatively charged oxygen atoms. Based on these investigations,<sup>[6,7]</sup> we assign the two sets of signals for **1-COMe** to the E,Z and Z,E configurations, the two nonidentical S-configurations of unsymmetrical  $\beta$ -dicarbonyl compounds.

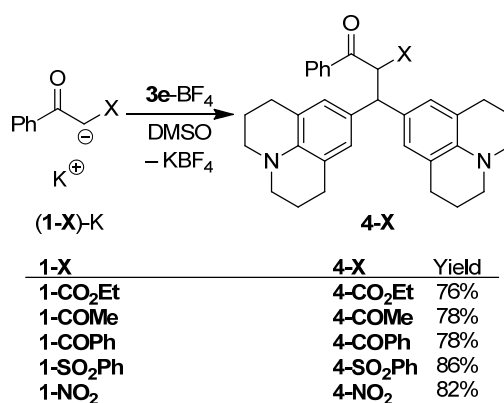
The increasing NMR shielding of the carbanionic carbon and the attached proton from  $\text{Li}^+$  to  $\text{Na}^+$  and  $\text{K}^+$  reflects the increasing electron density with increasing freedom of the carbanion **1-CO<sub>2</sub>Et** (Scheme 2).

Due to their low stability, the potassium salts of the anion of deoxybenzoin (**1-Ph**) and of the benzyl anions **2-CN**, **2-COMe** and **2-SO<sub>2</sub>Ph**, were not isolated in substance, but were generated by deprotonation of the corresponding CH acids with KOtBu or dimsyl potassium (typically 1.05 equiv.) in DMSO prior to combining them with the electrophiles. As the UV-

Vis absorbances of the carbanions **1-Ph**, **2-CN**, **2-COMe** and **2-SO<sub>2</sub>Ph** reached a limiting value when the corresponding CH acids are treated with 1.05 equiv. of base and did not increase further when additional 2-5 equiv. of base were added, one can conclude that 1.05 equiv. of base are sufficient for their complete deprotonation.

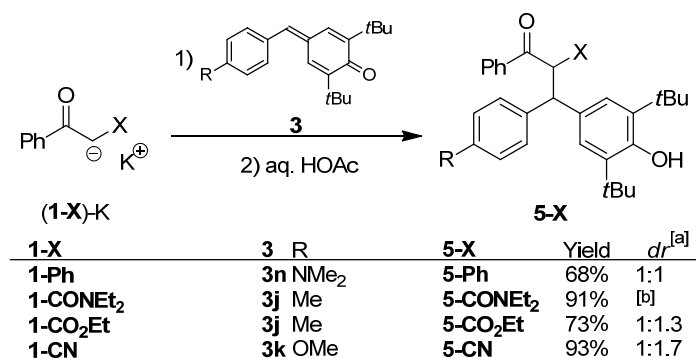
## 2.2 Product Studies

The benzhydrylium salt **3e**-BF<sub>4</sub> was added as a solid to equimolar solutions of the potassium salts (**1-X**)-K in DMSO. After decoloration of the blue solutions (typically within one to two minutes), water was added to precipitate the products **4-X**. After filtration, the crude products were recrystallized from ethanol or ethanol/CH<sub>2</sub>Cl<sub>2</sub> and characterized by NMR spectroscopy and mass spectrometry (Scheme 4).



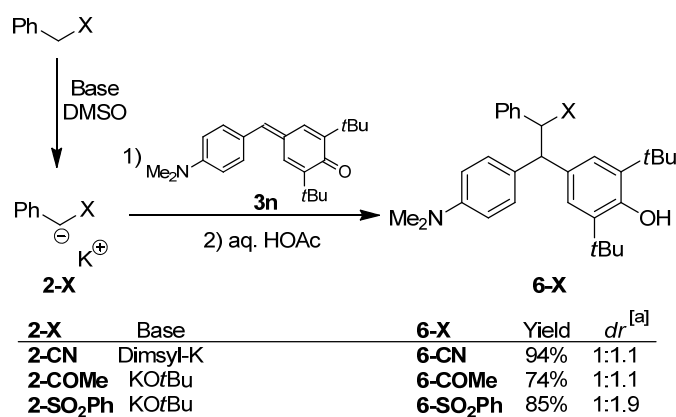
Scheme 4: Reaction of the potassium salts (**1-X**)-K with the benzhydrylium salt **3e**-BF<sub>4</sub> in DMSO.

Combination of solutions of the potassium salts (**1-X**)-K with solutions of the quinone methides **3j,k,n** in DMSO (with 5-10 % of dichloromethane as cosolvent) and workup with aqueous acetic acid yielded the crude reaction products **5-X** which were purified by chromatography and characterized by NMR spectroscopy and mass spectrometry. The most reactive carbanion **1-Ph** was not employed as a stable salt but was generated by deprotonation of deoxybenzoin with KO<sup>t</sup>Bu (~1.05 equiv.) in DMSO prior to adding the solution of the quinone methide **3n**. In all cases, the products **5-X** were obtained in good yields with low diastereoselectivity (Scheme 5).



Scheme 5: Reactions of the potassium salts (**1-X**)-K with the quinone methides **3** in DMSO. [a] Determined by <sup>1</sup>H NMR after purification by chromatography. [b] Could not be determined.

Solutions of the benzyl anions (**2-X**)-K in DMSO were obtained by treatment of the corresponding CH acids with 1.05 equiv. of dimsyl-K or KO<sup>t</sup>Bu. Addition of the quinone methide **3n**, followed by workup with aqueous acetic acid, gave the products **6-X** in good yields as mixtures of two diastereoisomers (Scheme 6).



Scheme 6: Reactions of the carbanions (**2-X**)-K with the quinone methide **3n** in DMSO at ambient temperature. [a] Determined by <sup>1</sup>H NMR spectroscopy after purification by chromatography.

### 2.3. Kinetic Investigations

The kinetics of the reactions of the carbanions **1-X** and **2-X** with the reference electrophiles **3** were studied in DMSO solution at 20 °C by monitoring the absorptions of the electrophiles with conventional or stopped-flow UV-Vis spectrometers. To simplify the evaluation of the kinetic experiments, the carbanions were used in large excess (> 10 equiv.). Thus, their concentrations remained almost constant throughout the reactions, and pseudo-first-order kinetics were obtained in all runs. The first-order rate constants  $k_{\text{obs}}$  were derived by least-squares fitting of the exponential function  $A_t = A_0 \exp(-k_{\text{obs}}t) + C$  to the time-dependent absorbances  $A_t$  of the electrophiles. Second-order rate constants (Tables 4 and 5) were



obtained as the slopes of linear correlations of  $k_{\text{obs}}$  with the concentrations of the nucleophiles (Figure 1).

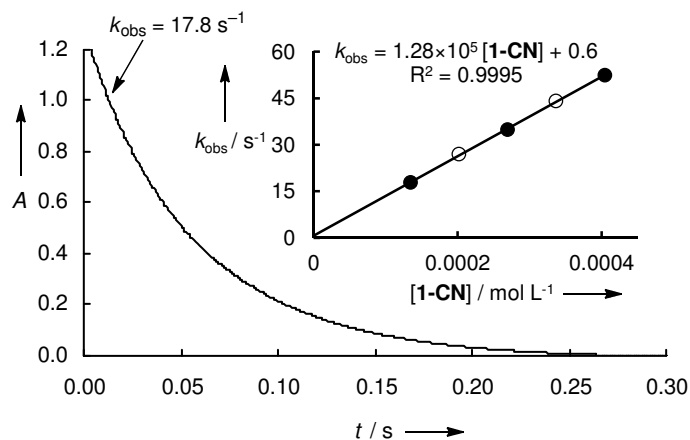


Figure 1: Decrease of the absorbance  $A$  (at 630 nm) during the reaction of  $(1\text{-CN})\text{-K}$  ( $1.35 \times 10^{-4} \text{ mol L}^{-1}$ ) with **3f** ( $1.71 \times 10^{-5} \text{ mol L}^{-1}$ ) in DMSO at 20 °C. Inset: Correlation of the first-order rate constants  $k_{\text{obs}}$  with the concentrations of  $(1\text{-CN})\text{-K}$ . Filled circles in absence, empty circles in presence of 2.4 equiv. of 18-crown-6.

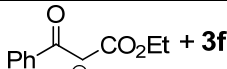
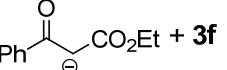
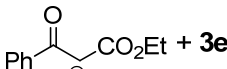
## 2.4. Counter Ion Effects

All carbanions **1-X** were obtained as alkali salts by treatment of ketones,  $\beta$ -diketones,  $\beta$ -ketoesters, and related compounds with alkali *tert*-butoxide. In order to examine how ion-pairing affects the kinetics of their reactions with electrophiles, we determined the first-order rate constants at constant concentrations of the carbanion salts ( $\approx 10^{-4} \text{ mol L}^{-1}$ ) and the electrophiles ( $\approx 10^{-5} \text{ mol L}^{-1}$ ) while variable concentrations ( $0 - 10^{-2} \text{ mol L}^{-1}$ ) of alkali salts (LiCl, LiBF<sub>4</sub>, NaBPh<sub>4</sub>, KBPh<sub>4</sub>, KOTf) were present (representative examples are shown in Table 2; detailed experimental data for further nucleophiles are in the Supporting Information). The measured rate constants were related to the second-order rate constants of the free carbanions ( $k_{\text{rel}} = 1$ ), which were taken from Tables 4 and 5 or from the quoted references. For comparison, we also studied the carbanions derived from the ester **2-CO<sub>2</sub>Et**, the  $\beta$ -diketones **7**, the diester **8-CO<sub>2</sub>Et** and the  $\beta$ -ketoester **8-COMe** (structures are shown in Figures 2–3). The observation that the addition of KOTf to solutions of **1-CO<sub>2</sub>Et** and **1-COMe** affects the kinetics in the same way as the addition of KBPh<sub>4</sub> (Table 2 and Supporting Information) indicates that the observed changes of the reaction rates are due to carbanion-potassium interactions and not due interactions of the BPh<sub>4</sub> anion with the electrophiles.

Table 2: First-order rate constants  $k_{\text{obs}}$  for the reactions of various carbanions with reference electrophiles in the presence of variable concentrations of alkali salts in DMSO at 20 °C.  $100 \cdot k_{\text{rel}}$  was calculated from the second-order rate constants of the free anions given in Table 4.

Reaction	M	Additive	[Alkali] <sup>+</sup> <sub>total</sub> / mol L <sup>-1</sup>	$k_{\text{obs}}$ / s <sup>-1</sup>	100· $k_{\text{rel}}$
$\text{Ph}-\overset{\text{O}}{\parallel}{\text{C}}-\text{CH}_2^--\text{Ph} + \mathbf{3n}$ (1-Ph)-M $c = 2.12 \times 10^{-4} \text{ mol L}^{-1}$	K			0.761 <sup>[a]</sup>	100
	K	KBPh <sub>4</sub>	$3.51 \times 10^{-4}$	0.748	98
	K	KBPh <sub>4</sub>	$4.80 \times 10^{-4}$	0.737	97
	K	KBPh <sub>4</sub>	$7.36 \times 10^{-4}$	0.729	96
	K	KBPh <sub>4</sub>	$1.48 \times 10^{-3}$	0.701	92
	K	KBPh <sub>4</sub>	$2.79 \times 10^{-3}$	0.658	86
	K	KBPh <sub>4</sub>	$5.27 \times 10^{-3}$	0.631	83
	K	KBPh <sub>4</sub>	$7.79 \times 10^{-3}$	0.604	79
$\text{Ph}-\overset{\text{O}}{\parallel}{\text{C}}-\text{CH}_2^--\text{Ph} + \mathbf{3n}$ (1-Ph)-M $c = 3.69 \times 10^{-4} \text{ mol L}^{-1}$	K			1.32 <sup>[a]</sup>	100
	Na	NaBPh <sub>4</sub>	$5.69 \times 10^{-4}$	0.950	71
	Na	NaBPh <sub>4</sub>	$1.11 \times 10^{-3}$	0.935	72
	Na	NaBPh <sub>4</sub>	$1.71 \times 10^{-3}$	0.909	69
	Na	NaBPh <sub>4</sub>	$3.09 \times 10^{-3}$	0.823	62
	Na	NaBPh <sub>4</sub>	$4.80 \times 10^{-3}$	0.757	57
	Na	NaBPh <sub>4</sub>	$7.74 \times 10^{-3}$	0.707	54
	Na	NaBPh <sub>4</sub>	$1.21 \times 10^{-2}$	0.652	49
$\text{Ph}-\overset{\text{O}}{\parallel}{\text{C}}-\text{CH}_2^--\text{Ph} + \mathbf{3n}$ (1-Ph)-M $c = 4.39 \times 10^{-4} \text{ mol L}^{-1}$	Na	NaBPh <sub>4</sub>	$1.82 \times 10^{-2}$	0.649	49
	K			1.58 <sup>[a]</sup>	100
	Li	none	$4.65 \times 10^{-4}$	1.18	75
	Li	LiBF <sub>4</sub>	$1.37 \times 10^{-3}$	1.10	69
	Li	LiBF <sub>4</sub>	$2.27 \times 10^{-3}$	0.976	62
	Li	LiBF <sub>4</sub>	$4.08 \times 10^{-3}$	0.871	55
	Li	LiBF <sub>4</sub>	$7.69 \times 10^{-3}$	0.688	44
	Li	LiBF <sub>4</sub>	$1.13 \times 10^{-2}$	0.616	39
	Li	LiBF <sub>4</sub>	$1.74 \times 10^{-2}$	0.480	30
	Li	LiBF <sub>4</sub>	$2.66 \times 10^{-2}$	0.333	21
$\text{Ph}-\overset{\text{O}}{\parallel}{\text{C}}-\text{CH}_2^--\text{Ph} + \mathbf{3n}$ (1-Ph)-M $c = 9.53 \times 10^{-4} \text{ mol L}^{-1}$	Li	LiBF <sub>4</sub>	$4.30 \times 10^{-2}$	0.178	11
	Li	LiBF <sub>4</sub>	$5.93 \times 10^{-2}$	0.145	9
	K			3.42 <sup>[a]</sup>	100
	Li	none	$1.01 \times 10^{-3}$	2.47	72
	Li	LiCl	$1.51 \times 10^{-3}$	2.52	74
	Li	LiCl	$2.01 \times 10^{-3}$	2.47	72
	Li	LiCl	$3.21 \times 10^{-3}$	2.18	64
	Li	LiCl	$6.05 \times 10^{-3}$	1.87	55
	Li	LiCl	$1.11 \times 10^{-2}$	1.43	42
	Li	LiCl	$2.12 \times 10^{-2}$	1.04	30
$\text{Ph}-\overset{\text{O}}{\parallel}{\text{C}}-\text{CH}_2^--\text{CO}_2\text{Et} + \mathbf{3f}$ (1-CO <sub>2</sub> Et)-M $c = 6.58 \times 10^{-4} \text{ mol L}^{-1}$	Li	LiCl	$3.46 \times 10^{-2}$	0.820	24
	Li	LiCl	$5.14 \times 10^{-2}$	0.706	21
	Li	LiCl	$7.65 \times 10^{-2}$	0.508	15
	K			282 <sup>[a]</sup>	100
	K	none	$6.58 \times 10^{-4}$	280	99.3
	K	KBPh <sub>4</sub>	$8.68 \times 10^{-4}$	260	92.2
	K	KBPh <sub>4</sub>	$1.08 \times 10^{-3}$	241	85.5
	K	KBPh <sub>4</sub>	$1.64 \times 10^{-3}$	210	74.5
	K	KBPh <sub>4</sub>	$2.41 \times 10^{-3}$	175	62.1
	K	KBPh <sub>4</sub>	$3.46 \times 10^{-3}$	136	48.2
	K	KBPh <sub>4</sub>	$5.00 \times 10^{-3}$	111	39.4
	K	KBPh <sub>4</sub>	$7.89 \times 10^{-3}$	82.1	29.1
	K	KBPh <sub>4</sub>	$1.08 \times 10^{-2}$	65.2	23.1
	K	KBPh <sub>4</sub>	$1.37 \times 10^{-2}$	55.0	19.5
	K	KBPh <sub>4</sub>	$2.08 \times 10^{-2}$	41.9	14.9

Table 2: Continuation.

Reaction	M	Additive	[Alkali <sup>+</sup> ] <sub>total</sub> / mol L <sup>-1</sup>	<i>k</i> <sub>obs</sub> / s <sup>-1</sup>	100· <i>k</i> <sub>rel</sub>
 + <b>3f</b> <b>(1-CO<sub>2</sub>Et)-M</b> <i>c</i> = 6.56 × 10 <sup>-4</sup> mol L <sup>-1</sup>	K			281 [a]	100
	K	none	6.56 × 10 <sup>-4</sup>	273	97.2
	K	KOTf	8.63 × 10 <sup>-4</sup>	236	84.0
	K	KOTf	1.07 × 10 <sup>-3</sup>	219	77.9
	K	KOTf	1.69 × 10 <sup>-3</sup>	178	63.3
	K	KOTf	3.15 × 10 <sup>-3</sup>	131	46.6
	K	KOTf	4.40 × 10 <sup>-3</sup>	107	38.1
	K	KOTf	6.32 × 10 <sup>-3</sup>	82.9	29.5
	K	KOTf	1.01 × 10 <sup>-2</sup>	61.0	21.7
	K	KOTf	1.39 × 10 <sup>-2</sup>	50.0	17.8
	K	KOTf	1.77 × 10 <sup>-2</sup>	43.1	15.3
 + <b>3f</b> <b>(1-CO<sub>2</sub>Et)-M</b> <i>c</i> = 5.34 × 10 <sup>-4</sup> mol L <sup>-1</sup>	K			229 [a]	100
	Na	NaBPh <sub>4</sub>	6.81 × 10 <sup>-4</sup>	114	49.8
	Na	NaBPh <sub>4</sub>	8.10 × 10 <sup>-4</sup>	95.0	41.5
	Na	NaBPh <sub>4</sub>	1.20 × 10 <sup>-3</sup>	64.3	28.1
	Na	NaBPh <sub>4</sub>	1.85 × 10 <sup>-3</sup>	41.9	18.3
	Na	NaBPh <sub>4</sub>	3.15 × 10 <sup>-3</sup>	26.9	11.7
	Na	NaBPh <sub>4</sub>	7.72 × 10 <sup>-3</sup>	23.4	10.2
	Na	NaBPh <sub>4</sub>	1.49 × 10 <sup>-2</sup>	15.7	6.9
	Na	NaBPh <sub>4</sub>	2.21 × 10 <sup>-2</sup>	11.8	5.2
	Na	NaBPh <sub>4</sub>	3.28 × 10 <sup>-2</sup>	11.0	4.8
	Na	NaBPh <sub>4</sub>			
 + <b>3e</b> <b>(1-CO<sub>2</sub>Et)-M</b> <i>c</i> = 6.48 × 10 <sup>-4</sup> mol L <sup>-1</sup>	K			580 [a]	100
	Li	LiCl	6.73 × 10 <sup>-4</sup>	58.1	10
	Li	LiCl	8.48 × 10 <sup>-4</sup>	33.5	5.8
	Li	LiCl	1.02 × 10 <sup>-3</sup>	28.7	4.9
	Li	LiCl	1.38 × 10 <sup>-3</sup>	24.7	4.3
	Li	LiCl	2.08 × 10 <sup>-3</sup>	18.0	3.1
	Li	LiCl	3.48 × 10 <sup>-3</sup>	11.7	2.0
	Li	LiCl	4.91 × 10 <sup>-3</sup>	9.56	1.6
	Li	LiCl	7.46 × 10 <sup>-3</sup>	7.04	1.2

[a] Calculated as  $k_{\text{obs}} = k_2 [\text{Nu}]$  from the second-order rate constants for the corresponding reactions the free anions (potassium salts or potassium salts in presence of 18-crown-6) given in Table 4.

In Figures 2–4, we plot the dependence of the relative rate constants  $k_{\text{obs}}$  for the reactions of various carbanions with reference electrophiles on the concentration of the potassium ions ( $[\text{K}^+]$ ), which was varied by addition of different amounts of KBPh<sub>4</sub>. Figure 2 shows that the reactivities of the anion of the monoketone **1-Ph** as well as that of the cyclic diketone **7b** (fixed W-configuration) were affected relatively little when up to 12 mmol L<sup>-1</sup> K<sup>+</sup> was added (80 and 73% of the reactivity of the free carbanion). In contrast the reactivities of the  $\beta$ -diketone-derived carbanions **1-COPh** and **7a** decreased noticeably with increasing potassium concentration, and reached a plateau at about 40% of the original value, probably due to a change from *E,Z* (S-shape) to *Z,Z* (U-shape) configurations which can interact more strongly with the potassium ions. The decrease of reactivity due to the addition of KBPh<sub>4</sub> is smaller for the  $\beta$ -diketone-derived anion **1-COMe**.

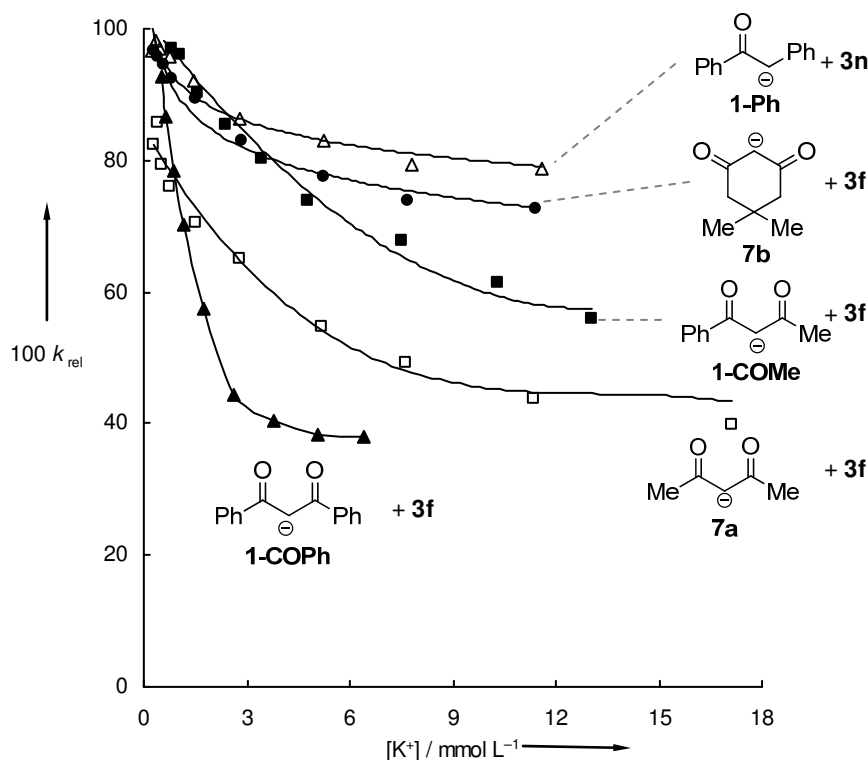


Figure 2: Plots of the relative first-order rate constants for the reactions of the anions derived from  $\beta$ -diketones and a monoketone with electrophiles versus the total concentration of potassium (varied by addition of  $\text{KBPh}_4$ ) in DMSO solution at 20 °C.

Figure 3 compares the reaction rates of monoester-,  $\beta$ -ketoester-, diester-, and  $\beta$ -ketoamido derived carbanions at variable concentrations of potassium ions. Like for the anion of the monoketone **1-Ph** (Figure 2), the reactivity of the monoester derived carbanion **2-CO<sub>2</sub>Et** depends only a slightly on the concentration of  $\text{K}^+$ . In contrast to the behaviour of the  $\beta$ -diketones in Figure 2, however, all anions from  $\beta$ -ketoesters and related compounds in Figure 3 show a significant decrease of reactivity with increasing potassium ion concentration, not only indicating that these carbanions interact with the counter ion  $\text{K}^+$  at lower concentrations (steeper decrease of  $k_{\text{obs}}$  shows higher equilibrium constants) but also that the coordination with potassium reduces the nucleophilic reactivities to a larger extent (lower level of the plateaus).

The rate constants for the mono-carbonyl substituted carbanions, which are plotted in Figure 4, depend less on the potassium ion concentration than those of the dicarbonyl substituted carbanions shown in Figures 2 and 3. While the reactivities of all diketones and ketoesters decrease to 60-20% of their original values (except the cyclic diketone **7b**) at a potassium concentration of  $[\text{K}^+] = 5 \text{ mmol L}^{-1}$ , the reactivity of the anion of benzoyl acetonitrile (**1-CN**) is the only one in Figure 4 which is affected significantly and is reduced to 60% at a  $5 \text{ mmol L}^{-1}$  concentration of potassium.

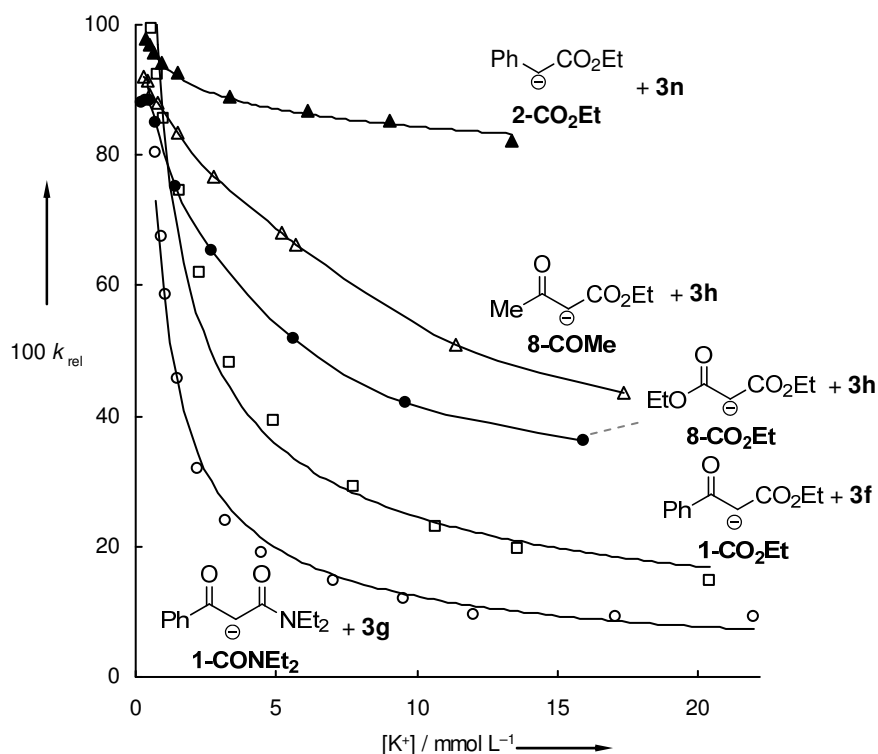


Figure 3: Plots of the relative first-order rate constants for the reactions of the anions of the ester **2-CO<sub>2</sub>Et**, the  $\beta$ -ketoesters **1-CONEt<sub>2</sub>**, **1-CO<sub>2</sub>Et**, **8-COMe** and the diester **8-CO<sub>2</sub>Et** with electrophiles versus the total concentration of potassium (varied by addition of  $\text{KBPh}_4$ ) in DMSO solution at 20 °C.

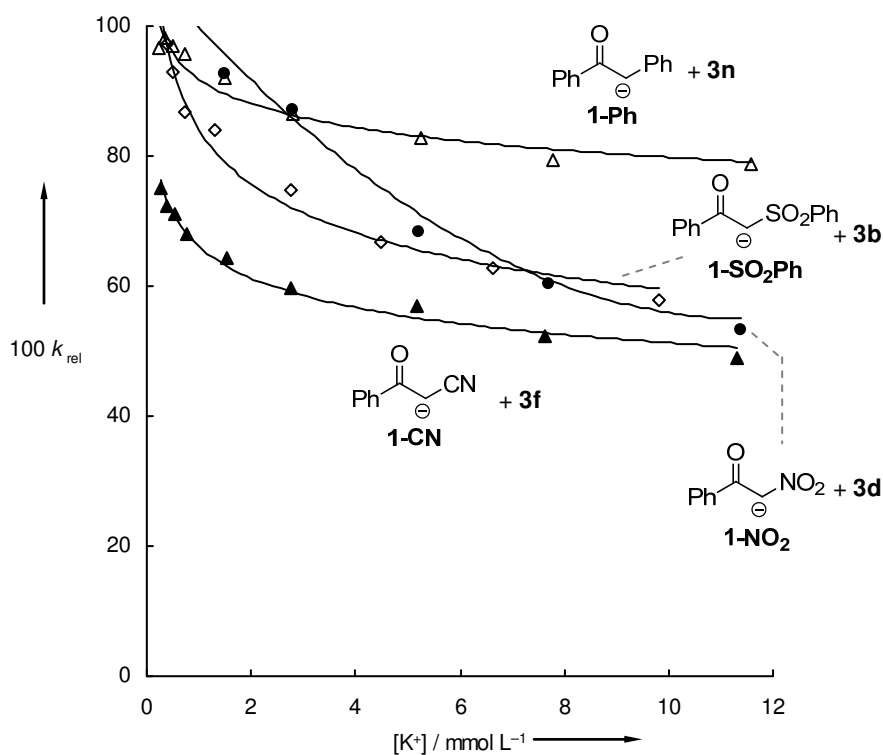


Figure 4: Plots of the relative first-order rate constants for the reactions of the anions of the ketones **1-Ph**, **1-CN**, **1-SO<sub>2</sub>Ph** and **1-NO<sub>2</sub>** with electrophiles versus the total concentration of potassium (varied by addition of  $\text{KBPh}_4$ ) in DMSO solution at 20 °C.

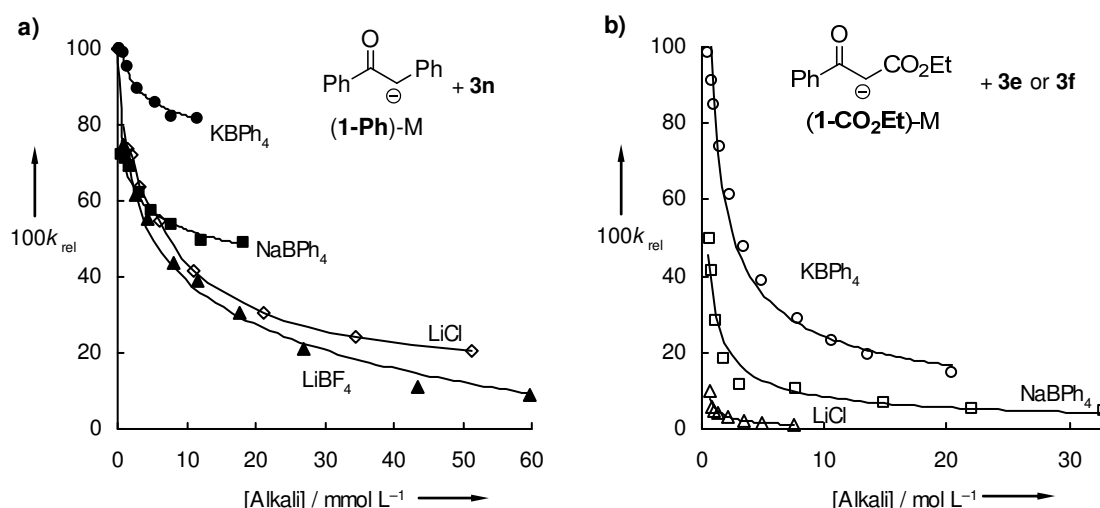
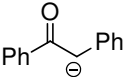
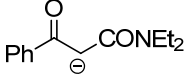
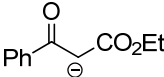


Figure 5: Plot of the relative first-order rate constants ( $100 \cdot k_{\text{rel}}$ ) for the reactions of a) **1-Ph** with **3n** and b) **1-CO₂Et** with **3e** ( $\text{Li}^+$ ) or **3f** ( $\text{Na}^+$  and  $\text{K}^+$ ) versus the total concentration of alkali metal ions in DMSO solution at 20 °C.

Figure 5 compares the influence of different alkali ions on the relative reactivities of **1-Ph** and **1-CO₂Et**. The reactivity of the anion of deoxybenzoin **1-Ph** is only slightly affected when the potassium concentration is increased (Figure 5a). When sodium is added, the reactivity decreases to 50% of the value of the free carbanion. Addition of lithium chloride or lithium tetrafluoroborate decreases the reactivities to 12% and 10% at  $[\text{Li}^+] \approx 50 \text{ mmol L}^{-1}$ , respectively, showing a subordinate effect of the anion of the lithium salt. Further increase of the  $\text{Li}^+$  concentration leads to a further decrease of reactivity without reaching a plateau at a 60–70  $\text{mmol L}^{-1}$  concentration. For the  $\beta$ -ketoester anion **1-CO₂Et** similar plots, but with more pronounced effects, were observed (Figure 5b). Addition of  $\text{KBPh}_4$  decreases the reactivity to 20% of the value of the free carbanion, while a plateau at about 5% of the initial reactivity of the free carbanion is reached with 20  $\text{mmol L}^{-1}$   $\text{NaBPh}_4$  and at 1–2% with 5  $\text{mmol L}^{-1}$   $\text{LiCl}$ .

Figures 2–4 illustrate that at concentrations  $\leq 1 \text{ mmol L}^{-1}$  in DMSO, counter-ion effects by  $\text{K}^+$  are negligible, which is confirmed by the observation that the measured pseudo-first-order rate constants for **(1,2)-K** in the presence and absence of 18-crown-6 fit the same  $k_{\text{obs}}$  versus  $[(1,2)\text{-K}]$  plots (example shown in Figure 1). Only in the reactions of the anions of the  $\beta$ -ketoamide **1-CONEt₂** and of the  $\beta$ -ketoester **1-CO₂Et**, which showed the strongest counter-ion effects in Figure 3, the addition of 18-crown-6 (18-c-6) increased the second-order rate constants by factors of 1.4 and 1.2, respectively (Table 3).

Table 3: Second-order rate constants  $k_2$  for the reaction of different alkali derivatives of **1-Ph**, **1-CONEt<sub>2</sub>** and **1-CO<sub>2</sub>Et** with the reference electrophiles **3** in DMSO at 20 °C.<sup>[a]</sup>

Anion	Electro- phile	Li <sup>+</sup>	$k_2 / \text{L mol}^{-1} \text{s}^{-1}$			$k_2(\text{K}^+/\text{crown})$ / $k_2(\text{K}^+)$
 <b>(1-Ph)-M</b>	<b>3h</b>	$9.12 \times 10^5$	$1.10 \times 10^6$	$1.05 \times 10^6$	[b]	
	<b>3p</b>	$7.83 \times 10^4$	$7.79 \times 10^4$	$9.68 \times 10^4$	[b]	
	<b>3m</b>	$8.89 \times 10^3$	$9.59 \times 10^3$	$9.88 \times 10^3$	[b]	
	<b>3n</b>	$2.74 \times 10^3$	$3.39 \times 10^3$	$3.59 \times 10^3$	[b]	
	<b>3o</b>	$1.66 \times 10^3$	$1.90 \times 10^3$	$1.83 \times 10^3$	[b]	
 <b>(1-CONEt<sub>2</sub>)-M</b>	<b>3g</b>			$3.26 \times 10^4$	$4.59 \times 10^4$	1.41
	<b>3h</b>			$3.43 \times 10^3$	$4.61 \times 10^3$	1.34
	<b>3i</b>			$1.69 \times 10^3$	$2.46 \times 10^3$	1.46
	<b>3l</b>			50.3	69.7	1.38
 <b>(1-CO<sub>2</sub>Et)-M</b>	<b>3e</b>	— <sup>[c]</sup>	$4.27 \times 10^5$	$8.14 \times 10^5$	$8.95 \times 10^5$	1.10
	<b>3f</b>		$1.84 \times 10^5$	$3.63 \times 10^5$	$4.28 \times 10^5$	1.18
	<b>3g</b>		$2.63 \times 10^3$	$7.18 \times 10^3$	$8.67 \times 10^3$	1.21
	<b>3h</b>		$2.45 \times 10^2$	$7.18 \times 10^2$	$8.92 \times 10^2$	1.24
	<b>3j</b>		5.64	17.2	19.9	1.16
	<b>3k</b>		3.67	8.84	11.5	1.30

[a] Derived from first-order rate constants determined at  $[\mathbf{1-X}] < 2.3 \times 10^{-3} \text{ mol L}^{-1}$ . [b] Rate constants in presence and in absence of 18-crown-6 are identical. [c]  $k_2$  could not be calculated because no linear correlation between pseudo-first-order rate constants and concentration (Figure 6).

Analogously, second-order-rate constants for the reactions of the sodium salts **(1-Ph)-Na** and **(1-CO<sub>2</sub>Et)-Na** with electrophiles could be derived because the corresponding pseudo-first-order rate constants correlated linearly with the concentrations of the carbanions at concentrations  $\leq 10^{-3} \text{ mol L}^{-1}$ . A linear relationship between the first-order rate constants and the concentrations of the carbanion was also found for the reactions of **(1-Ph)-Li** thus giving rise to the second-order rate constants listed in Table 3. Figure 6, on the other hand, reveals that the pseudo-first-order rate constants for the reactions of **(1-CO<sub>2</sub>Et)-Li** with **1e** do not increase linearly with the concentrations of the carbanion, probably because **(1-CO<sub>2</sub>Et)-Li** forms dimers or higher aggregates in solution, as previously reported for other lithium-enolates.<sup>[5,6b,e,f]</sup> As the equilibrium between monomer and aggregates shifts towards aggregation by increasing concentration, a nonlinear increase of  $k_{\text{obs}}$  with increasing  $[(\mathbf{1-CO_2Et})\text{-Li}]$  was observed.

The comparison of the second-order rate constants for the different alkali derivatives of **1-Ph**, **1-CO<sub>2</sub>Et** and **1-CONEt<sub>2</sub>** in Table 3 shows that the reactivity of the potassium salt of deoxybenzoin **(1-Ph)-K** corresponds to that of the free anion whereas **1-CO<sub>2</sub>Et** and **1-CONEt<sub>2</sub>** interact with  $\text{K}^+$ . While the sodium derivative of **1-Ph** is similarly reactive as the potassium compound, the corresponding lithium derivative reacts 0.7-0.9 times as fast as the free carbanion. In contrast, the second-order rate constants of the sodium derivative of **1-**

**CO<sub>2</sub>Et** are only 30-40% of those of the free carbanion, almost independent of the nature of the electrophile.

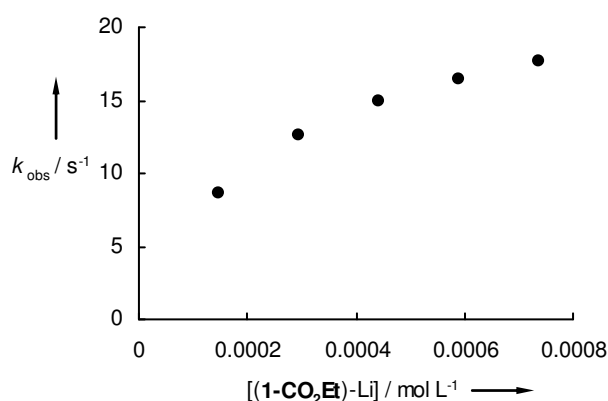


Figure 6: First-order rate constants for the reaction of **(1-CO<sub>2</sub>Et)-Li** with **1e** ( $1.35 \times 10^{-5}$  mol L<sup>-1</sup>, DMSO, 20 °C) and their correlation with the nucleophile concentration.

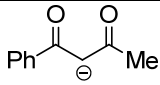
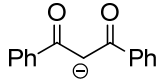
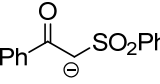
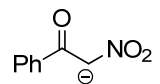
The second-order rate constants for the reactions of the free carbanions **1-X** and **2-X**, derived at concentrations  $\leq 10^{-3}$  mol L<sup>-1</sup> or in presence of 18-crown-6, with the reference electrophiles **3** in DMSO at 20 °C are summarized in Tables 4 and 5. In the following part, the reactivities of the free carbanions are discussed.

Table 4: Second-order rate constants  $k_2$  for the reactions of the carbanions **1** with the reference electrophiles **3** in DMSO at 20 °C.

<b>1-X</b>	$N^{[a]}$ ( $s_N$ )	Electro- phile	$k_2 /$ $L \text{ mol}^{-1} \text{ s}^{-1}$
$\text{Ph}-\text{C}(=\text{O})-\text{CH}_2^--\text{Ph}$ <b>1-Ph</b>	23.15 (0.60)	<b>3h</b>	$1.05 \times 10^6$
		<b>3p</b>	$9.68 \times 10^4$
		<b>3m</b>	$9.88 \times 10^3$
		<b>3n</b>	$3.59 \times 10^3$
		<b>3o</b>	$1.83 \times 10^3$
$\text{Ph}-\text{C}(=\text{O})-\text{CH}_2^--\text{C}(=\text{O})\text{NEt}_2$ <b>1-CONEt<sub>2</sub></b>	19.28 (0.65)	<b>3g</b>	$4.59 \times 10^4$
		<b>3h</b>	$4.61 \times 10^3$
		<b>3i</b>	$2.46 \times 10^3$
		<b>3l</b>	$6.97 \times 10^1$
$\text{Ph}-\text{C}(=\text{O})-\text{CH}_2^--\text{CO}_2\text{Et}$ <b>1-CO<sub>2</sub>Et</b>	17.52 (0.74)	<b>3e</b>	$8.95 \times 10^5$
		<b>3f</b>	$4.28 \times 10^5$
		<b>3g</b>	$8.67 \times 10^3$
		<b>3h</b>	$8.92 \times 10^2$
		<b>3j</b>	$1.99 \times 10^1$
		<b>3k</b>	$1.15 \times 10^1$
$\text{Ph}-\text{C}(=\text{O})-\text{CH}_2^--\text{CN}$ <b>1-CN</b>	16.55 (0.78)	<b>3e</b>	$3.21 \times 10^5$
		<b>3f</b>	$1.28 \times 10^5$
		<b>3g</b>	$3.65 \times 10^3$
		<b>3h</b>	$2.60 \times 10^2$
		<b>3j</b>	3.81
		<b>3k</b>	2.02

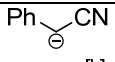
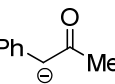
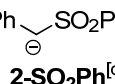


Table 4: continuation.

<b>1-X</b>	$N^{[a]}$ ( $s_N$ )	<b>Electro- phile</b>	$k_2 /$ $\text{L mol}^{-1} \text{s}^{-1}$
 <b>1-COMe</b>	16.03 (0.86)	<b>3e</b>	$4.79 \times 10^5$
		<b>3f</b>	$1.22 \times 10^5$
		<b>3g</b>	$1.77 \times 10^3$
		<b>3h</b>	$1.98 \times 10^2$
 <b>1-COPh</b>	17.46 (0.65)	<b>3c</b>	$1.06 \times 10^6$
		<b>3d</b>	$4.75 \times 10^5$
		<b>3e</b>	$1.95 \times 10^5$
		<b>3f</b>	$6.50 \times 10^4$
 <b>1-SO<sub>2</sub>Ph</b>	17.18 (0.56)	<b>3a</b>	$5.08 \times 10^5$
		<b>3b</b>	$2.27 \times 10^5$
		<b>3d</b>	$4.71 \times 10^4$
		<b>3e</b>	$2.14 \times 10^4$
		<b>3f</b>	$1.10 \times 10^4$
 <b>1-NO<sub>2</sub></b>	13.91 (0.76)	<b>3a</b>	$1.49 \times 10^5$
		<b>3b</b>	$6.83 \times 10^4$
		<b>3d</b>	$6.10 \times 10^3$
		<b>3e</b>	$2.33 \times 10^3$
		<b>3f</b>	$9.49 \times 10^2$

[a] Determination see below.

Table 5: Second-order rate constants  $k_2$  for the reactions of the carbanions **2** with the reference electrophiles **3** in DMSO at 20 °C.

<b>2-X</b>	$N^{[a]}$ ( $s_N$ )	<b>Electro- phile</b>	$k_2 /$ $\text{L mol}^{-1} \text{s}^{-1}$
 <b>2-CN<sup>[b]</sup></b>		<b>3n</b>	$3.89 \times 10^6$ <sup>[c]</sup>
		<b>3o</b>	$1.96 \times 10^6$ <sup>[c]</sup>
 <b>2-COMe<sup>[d]</sup></b>	24.99 (0.60)	<b>3m</b>	$1.44 \times 10^5$
		<b>3n</b>	$4.48 \times 10^4$
		<b>3o</b>	$1.69 \times 10^4$
 <b>2-SO<sub>2</sub>Ph<sup>[d]</sup></b>	25.77 (0.56)	<b>3m</b>	$1.95 \times 10^5$
		<b>3n</b>	$5.84 \times 10^4$
		<b>3o</b>	$2.66 \times 10^4$

[a] Determination see below. [b] Deprotonation with dimsyl potassium. [c] Approximate second-order rate constant obtained from a plot of [2-CN] vs  $k_{\text{obs}}$  that shows a large negative intercept. [d] Deprotonation with KO<sup>t</sup>Bu.

## 2.5. Correlation Analysis

Linear correlations were obtained for  $\lg k_2$  of the reactions of the carbanions **1** and **2** with the reference electrophiles **3** with their electrophilicity parameters  $E$ , as depicted for some representative examples in Figure 7. As documented in the Supporting Information, all reactions studied in this work followed analogous linear correlations, indicating that equation (1) is applicable to these reactions. From the slopes of these correlations, the nucleophile-specific parameters  $s_N$  were derived, and the negative intercepts on the abscissa ( $\lg k_2 = 0$ ) correspond to the nucleophilicity parameters  $N$  (Tables 4 and 5).

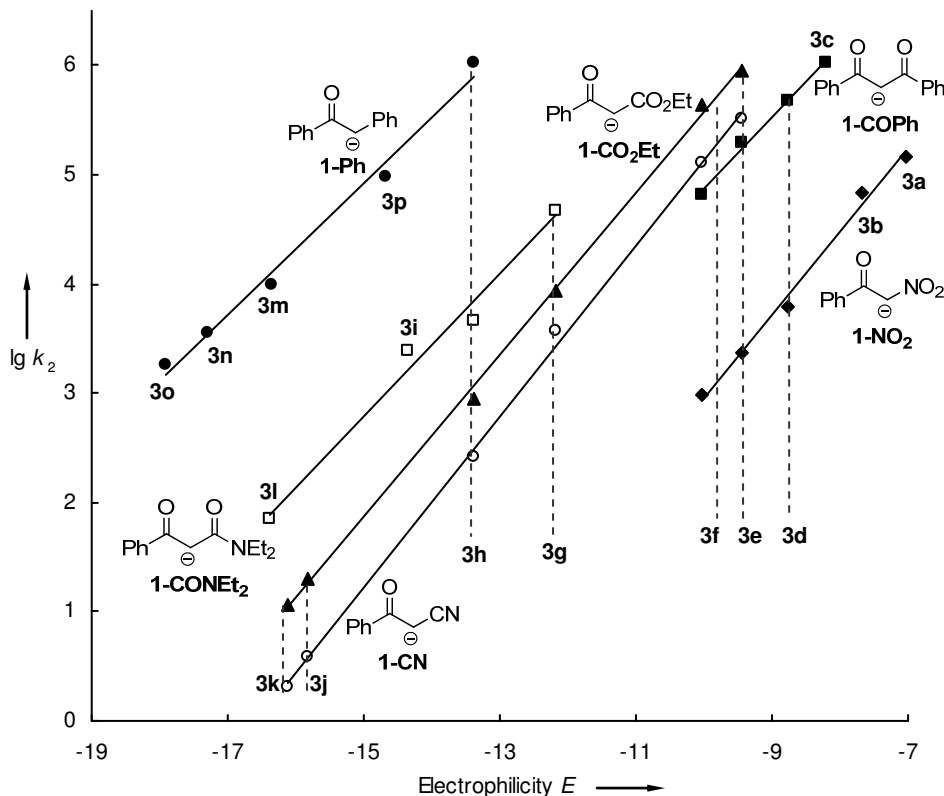


Figure 7: Correlation of the rate constants  $\lg k_2$  for the reactions of the nucleophiles **1** with the electrophiles **3** in DMSO with their electrophilicity parameters  $E$ .

## 2.6. Structure-Reactivity Relationships

Figure 8 compares the influence of the substituents  $X$  on the nucleophilicities of benzoyl- (**1-X**), ethoxycarbonyl- (**8-X**) and phenyl-substituted (**2-X**) carbanions. As the relative reactivities of these carbanions depend on the nucleophile-specific sensitivity  $s_N$ , Table 6 also reports relative reactivities within these reaction series towards a common electrophile. The following discussion shows that the qualitative conclusions drawn from Figure 8 ( $N$ -values) and Table 6 (relative rate constants) are identical.

In all three series, the nitro-substituted carbanions (**1-NO<sub>2</sub>**, **2-NO<sub>2</sub>**, **8-NO<sub>2</sub>**) are by far the least nucleophilic compounds while the phenyl substituted carbanions are the most reactive ones; the benzhydryl anion **2-Ph** has such a high nucleophilicity that it could not be measured with the methods employed in this work. Figure 8, furthermore, shows that all benzoylmethyl anions **1-X** are less reactive than analogously substituted ethoxycarbonylmethyl anions **8-X**, which are again less reactive than analogously substituted benzyl anions **2-X**. It is obvious that the substituent effects are not additive: while the cyano-substituted benzyl anion **2-CN** is significantly more reactive than all other acceptor substituted benzyl anions (Table 6), the cyano-substituted carbanions **1-CN** and **8-CN** are less reactive than their ester-substituted

counterparts **1-CO<sub>2</sub>Et** and **8-CO<sub>2</sub>Et**, respectively. Even when the highly reactive phenylacetone nitrile anion **2-CN** is disregarded, the much smaller substituent effects in the **1**- and **8**-series reflect the saturation effect, i.e., the reduced demand for delocalization of negative charge in benzoyl- (**1-X**) and ethoxycarbonyl (**8-X**) substituted carbanions compared to the benzyl anions **2-X**.

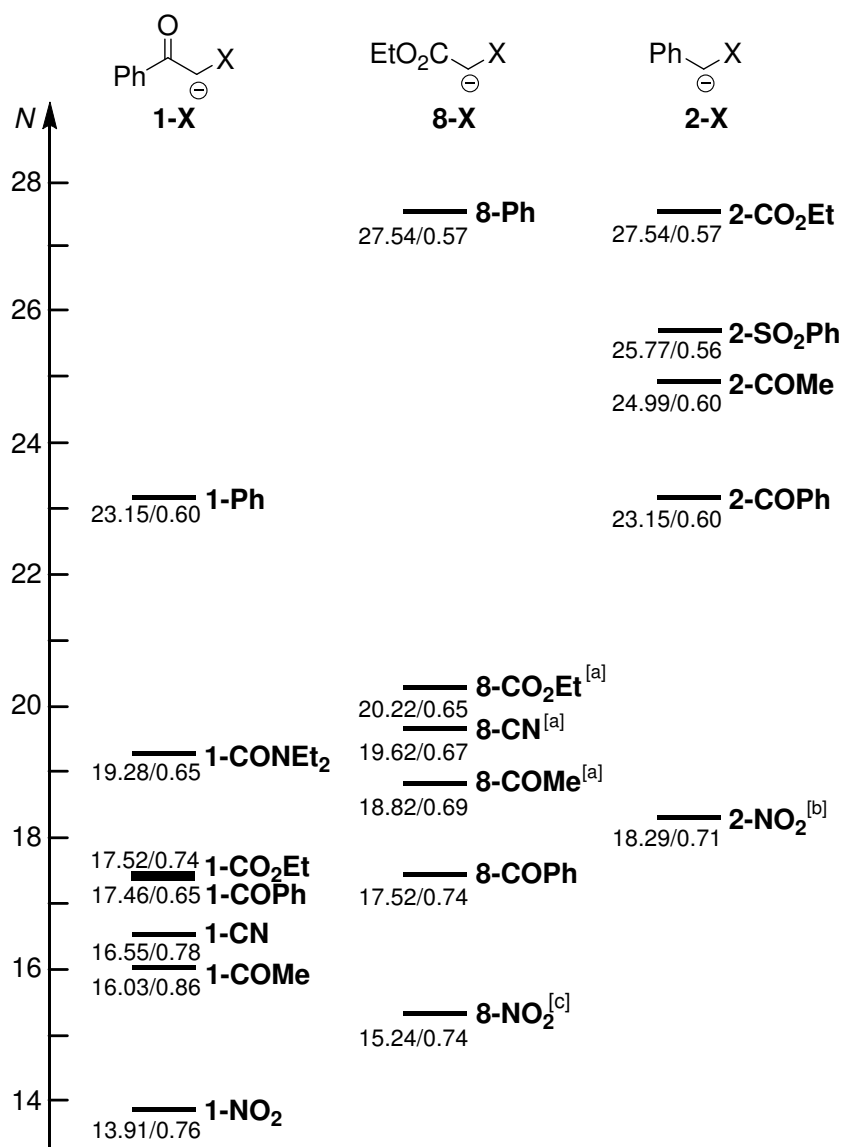
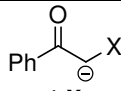
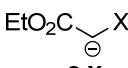
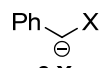


Figure 8: Structure-reactivity relationships for benzoyl substituted carbanions **1-X** (left), benzyl anions **2-X** (right) and ethoxycarbonyl substituted carbanions **8-X** (middle). [a] Ref.<sup>[3c]</sup> [b] Ref.<sup>[2b]</sup> [c] Ref.<sup>[8]</sup>

Table 6: Relative reaction rates of benzoylmethyl anions **1**, ethyl acetate anions **8** and benzyl anions **2** towards electrophiles.

			
<b>X</b>	<b>+ 3f</b>	<b>+ 3k</b>	<b>+ 3n</b>
Ph	$7.74 \times 10^4$ [a]	$1.44 \times 10^7$ [a,b]	
CONEt <sub>2</sub>	$1.04 \times 10^3$ [a]		
CO <sub>2</sub> Et	$4.51 \times 10^2$	$2.28 \times 10^3$ [c]	$9.95 \times 10^4$ [b]
CN	$1.35 \times 10^2$	$9.38 \times 10^2$ [c]	$7.02 \times 10^5$
COMe	$1.29 \times 10^2$	$3.52 \times 10^2$ [c]	$8.09 \times 10^3$
COPh	$6.85 \times 10^1$	$5.17 \times 10^1$	$6.48 \times 10^2$
SO <sub>2</sub> Ph	$1.16 \times 10^1$		$1.05 \times 10^4$
NO <sub>2</sub>	<b>1.0</b>	<b>1.0</b> [a,d]	<b>1.0</b> [c]

[a] Rate constants calculated by equation (1). [b] From ref. [2g] [c] From ref. [2a] [d] From ref. [8] [e] From ref. [2b]

A moderate, nonlinear correlation exists (Figure 9) between the reactivities of the benzyl anions **2-X** towards the quinone methide **3n** and the  $\pi$  electron densities ( $q_{CH}$ ) of the carbanionic center, which Pagani *et al.*<sup>[9]</sup> derived from the <sup>13</sup>C NMR shifts under consideration of the shielding effect. The behavior of the phenylsulfonyl group (**2-SO<sub>2</sub>Ph**) is peculiar. Though it concentrates slightly more electron density on the carbanionic center than the cyano-substituted anion, it is considerably less reactive than **2-CN** and has a similar nucleophilicity as the acetyl substituted benzyl anion **2-COMe**. Figures 17 and 18 in the Appendix illustrate that the second-order rate constants of the reactions of **1-X** and **2-X** with electrophiles do not correlate with the <sup>13</sup>C NMR shifts of the anionic centers.

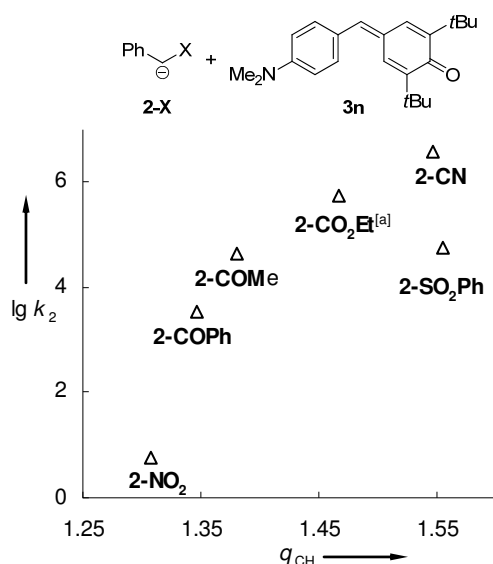


Figure 9: Correlation of  $\lg k_2$  for the reactions of the benzyl anions **2-X** with the quinone methide **3n** vs. the  $\pi$  electron densities  $q_{CH}$  of their carbanionic center.<sup>[9]</sup> [a] The  $q_{CH}$  value for the methyl ester is used for the ethyl ester **2-CO<sub>2</sub>Et**.

While Figure 10 shows a fair correlation of the nucleophilic reactivities of the benzoylmethyl anions **1-X** with Hammett's substituent constants  $\sigma_p^-$  of the substituents X, the corresponding correlation with  $\sigma_p$  is of lower quality (Figure 19, Appendix). In contrast, the nucleophilic reactivities of the analogously substituted benzyl anions **2-X** and ethyl acetate anions **8-X** neither correlate with  $\sigma_p^-$  nor with  $\sigma_p$  as illustrated in Figures 20 and 21 of the Appendix.

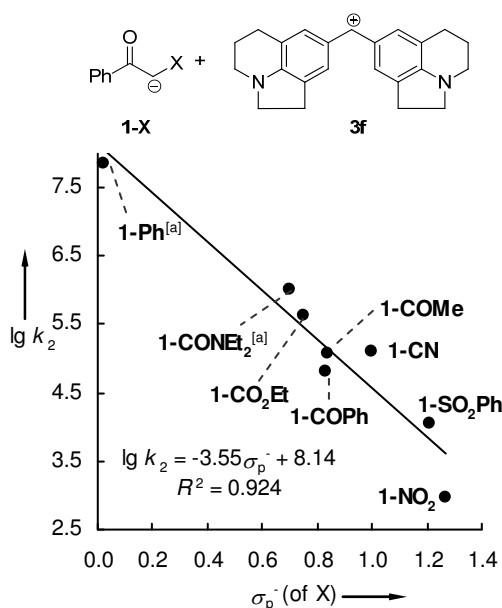


Figure 10: Plot of the rate constants for the reactions of the nucleophiles **1-X** with the electrophile **3f** vs. Hammett's  $\sigma_p^-$  substituent constants.<sup>[10]</sup> [a] Calculated with eq. (1).

Figure 11 shows a fair correlation of most nucleophilicity parameters  $N$  with the corresponding  $pK_{aH}$  values in DMSO,<sup>[5]</sup> from which several compounds deviate significantly. As different electrophiles had to be employed for determining the  $N$ -parameters for the phenacyl series **1-X** and the benzyl series **2-X**, one cannot construct a single Brønsted plot based on experimental rate constants for the carbanions of both series. However, when this correlation is split up in ordinary Brønsted plots, as depicted in Figure 12, correlations of moderate quality with Brønsted  $\alpha$ -values of 0.40 and 0.41 are obtained.

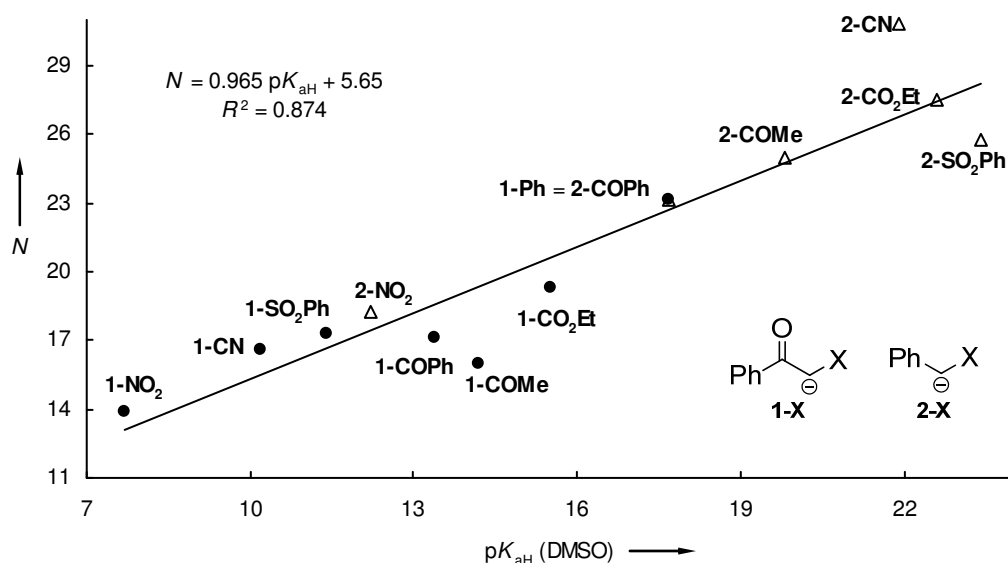


Figure 11: Correlation of the nucleophilicities  $N$  of the anions **1-X** and **2-X** with the  $pK_{aH}$  (DMSO) values.<sup>[5]</sup>

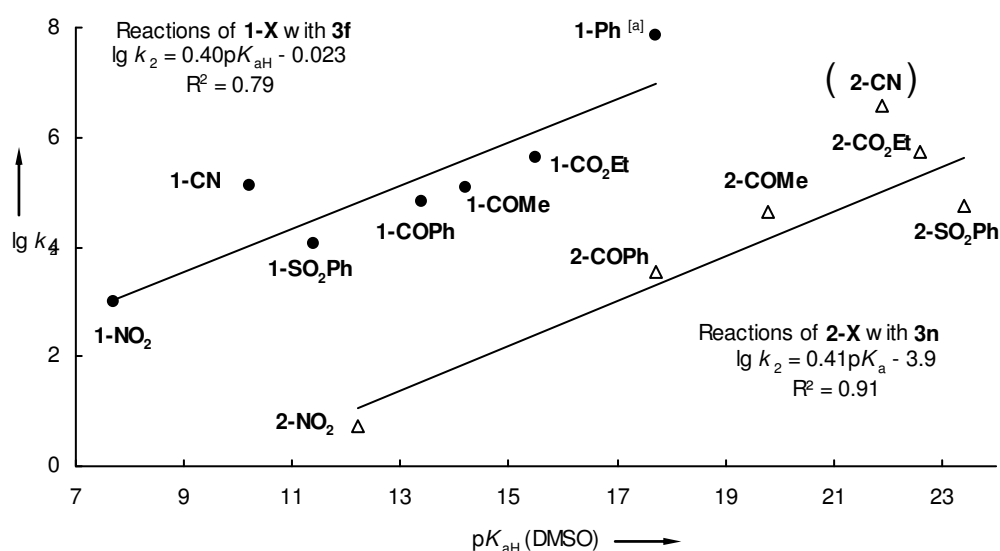


Figure 12: Brønsted plots of the second-order rate constants for the reactions of the anions **1-X** with **3f** and of the anions **2-X** with **3n** versus the  $pK_{aH}$  (DMSO) values.<sup>[5]</sup> [a] Calculated with eq. 1.

### 3. Conclusion

Stabilized carbanions have played a key-role as reference nucleophiles for the construction of our comprehensive reactivity scales,<sup>[3c,g]</sup> though the negligible role of ion-pairing has only been demonstrated in isolated cases.<sup>[2a,d-g,3c,11]</sup> The systematic investigation of the kinetics of the reactions of the potassium salts of **1**, **2**, **7** and **8** with benzhydrylium ions and quinone methides in this work showed that at carbanion concentrations  $\leq 10^{-3} \text{ mol L}^{-1}$  in DMSO, with only two exceptions, none of the reaction rates depend significantly on the concentration of

$K^+$ , which justifies to assign these rate constants to the reactivities of the free carbanions. At higher potassium ion concentration, different sensitivities of the reaction rates on variation of  $[K^+]$  were observed. At  $[K^+] \approx 10^{-2} \text{ mol L}^{-1}$ , for example, the reactivities of the monoketo- and monoester stabilized carbanions **1-Ph** and **2-CO<sub>2</sub>Et** decreased only slightly to about 80% of the value of the free carbanion, while the benzoyl-ester substituted carbanion **1-CO<sub>2</sub>Et** decreased to 20% and the benzoyl-amido substituted carbanion **1-CONEt<sub>2</sub>** to 10 % of the value of the free carbanion. In all other cases, the reactivities at  $[K^+] \approx 10^{-2} \text{ mol L}^{-1}$  were approximately 40-60% those of the free carbanions. Though  $Na^+$  and  $Li^+$  had a larger effect on the reactivities of the carbanions, the trends were analogous to those observed with  $K^+$ . Thus, in a  $0.01 \text{ mmol L}^{-1}$  solution of  $Li^+$ , the reactivity of **1-Ph** was 39% of that of the free carbanion, while the reactivity of **1-CO<sub>2</sub>Et** was only 1% of that of the free carbanion.

The reactivities of the free carbanions ( $\lg k_2$ ) correlate linearly with the electrophilicity parameters  $E$ , showing that equation (1) is applicable. Therefore it is possible to characterize the nucleophilic reactivities of the carbanions by the reactivity parameters  $N$  and  $s_N$ , to integrate these carbanions in our comprehensive nucleophilicity scale<sup>[31]</sup> and to predict potential electrophilic reaction partners. The reactivities correlate moderately with Bordwell's  $pK_{aH}$  values and show Brønsted plots with typical  $\alpha$ -values of 0.40 (carbanions **1-X**) and 0.45 (carbanions **2-X**). While the substituent effects are not additive, the reactivities of the anions **1** (PhCO-CH<sup>-</sup>-X), but not those of **2** (Ph-CH<sup>-</sup>-X), correlate linearly with Hammett's  $\sigma_p^-$  parameters. As the UV absorption maxima of the carbanions **1-X** and **2-X** are in the range of 300 to 400 nm, they can be used as reference nucleophiles for the rapid photometric determination of the reactivities of further synthetically important electrophiles.

## 4. Experimental Section

This chapter contains contributions from different authors. Experiments which were not performed by the author of this thesis are marked as follows: contributions from Roland Appel<sup>[RA]</sup>.

### 4.1. General

#### Materials

Commercially available DMSO ( $H_2O$  content < 50 ppm) was used without further purification. The reference electrophiles used in this work were synthesized according to literature procedures.<sup>[3b,c,f,4]</sup> The CH-acids were purchased as follows: (**1-Ph**)-H, (**1-COMe**)-

H were from Acros Belgium, (**1-CO<sub>2</sub>Et**)-H, (**1-COPh**)-H, (**2-CN**)-H from Merck Germany, (**2-SO<sub>2</sub>Ph**)-H from ABCR Germany, (**1-CN**)-H, (**1-NO<sub>2</sub>**)-H, (**2-COMe**)-H from Sigma-Aldrich Germany.

### NMR spectroscopy

In the <sup>1</sup>H and <sup>13</sup>C NMR spectra chemical shifts are given in ppm and refer to tetramethylsilane ( $\delta_{\text{H}} = 0.00$ ,  $\delta_{\text{C}} = 0.0$ ), [D<sub>6</sub>]-DMSO ( $\delta_{\text{H}} = 2.50$ ,  $\delta_{\text{C}} = 39.5$ ) or to CDCl<sub>3</sub> ( $\delta_{\text{H}} = 7.26$ ,  $\delta_{\text{C}} = 77.0$ ),<sup>[12]</sup> as internal standards. The coupling constants are given in Hz. For reasons of simplicity, the <sup>1</sup>H-NMR signals of AA'BB'-spin systems of *p*-disubstituted aromatic rings are described as doublets. Signal assignments are based on additional COSY, gHSQC, and gHMBC experiments. Chemical shifts marked with (\*) refer to the minor isomer when the product was obtained as a mixture of two diastereomers.

### Kinetics

As the reactions of colored electrophiles (benzhydrylium ions **3a–f** and Michael acceptors **3g–p**) with colorless nucleophiles **1** and **2** yield colorless products (or products with a different absorption range than the reactants), the reactions were followed by UV-Vis spectroscopy. Slow reactions ( $\tau_{1/2} > 10$  s) were determined by using conventional UV-Vis-spectrophotometers (diode array). Stopped-flow techniques were used for the investigation of rapid reactions ( $\tau_{1/2} < 10$  s). The temperature of all solutions was kept constant at  $20.0 \pm 0.1$  °C by using a circulating bath thermostat. In all runs the concentration of the nucleophiles was at least 10 times higher than the electrophile concentration, resulting in pseudo-first-order kinetics with an exponential decay of the electrophile concentration. First-order rate constants  $k_{\text{obs}}$  were obtained by least-squares fitting of the exponential function  $A_t = A_0 \exp(-k_{\text{obs}}t) + C$  to the time-dependent absorbances. The second-order rate constants  $k_2$  were obtained from the slopes of the linear plots of  $k_{\text{obs}}$  against the nucleophile concentration.

## 4.2. Synthesis of the Benzoylmethanes **1-H**

### 4.2.1. *N,N*-Diethyl-3-oxo-3-phenylpropanamide (**1-CONEt<sub>2</sub>**)-H

According to Hoffman et al.<sup>[3]</sup> ethyl 3-oxo-3-phenylpropanoate (5.55 g, 28.9 mmol) and diethylamine (3.50 g, 47.9 mmol) were heated to reflux in *o*-xylene (25 mL) for 4.5 h. After



removing the solvent and the excess of amine by distillation, the crude product was purified by column chromatography on silica with dichloromethane and methanol as eluent yielding 3.15 g (14.4 mmol, 50%) of *N,N*-diethyl-3-oxo-3-phenylpropanamide (**1-CONEt<sub>2</sub>**)-H as yellow oil.

<sup>1</sup>H NMR-chemical shifts are in agreement with the literature.<sup>[13]</sup>

#### 4.2.2. 1-Phenyl-2-(phenylsulfonyl)ethanone (**1-SO<sub>2</sub>Ph**)-H

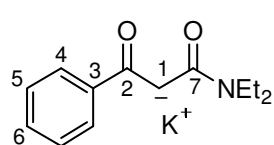
According to Suryakiran et al.<sup>[14]</sup> 2-chloro-1-phenylethanone (2.52 g, 16.3 mmol) and sodium benzenesulfinate (3.26 g, 19.9 mmol) were dissolved in of PEG-400 (150 mL) and stirred over night. The mixture was treated with water (200 mL) and extracted with ethyl acetate (2 x 40 mL). The combined organic layers were washed with brine (30 mL), dried over sodium sulphate, and the solvent was evaporated. After recrystallization from dichloromethane/pentane, 1-phenyl-2-(phenylsulfonyl)ethanone (**1-SO<sub>2</sub>Ph**)-H, (2.40 g, 9.22 mmol, 57 %) was obtained as colorless needles.

<sup>1</sup>H NMR-chemical shifts are in agreement with the literature.<sup>[14]</sup>

### 4.3. Synthesis of the Alkali-Salts 1-M

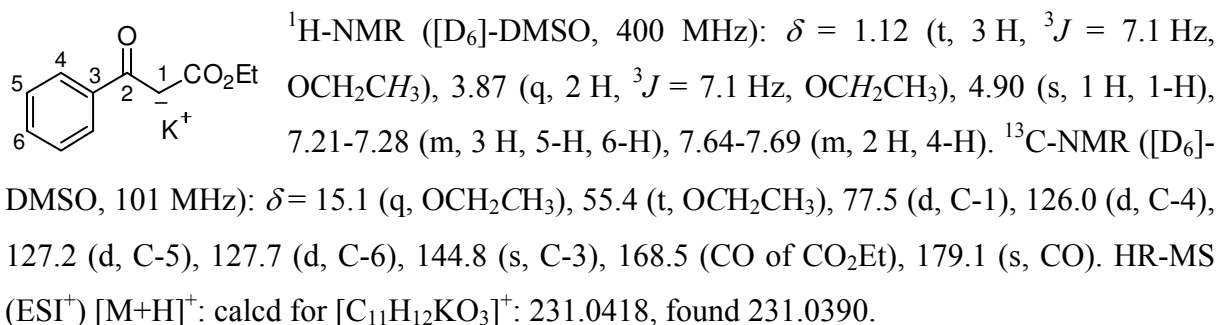
General procedure 1 (GP1): The CH-acid **1-H** (3-10 mmol, 1 equiv.) was added to a stirred solution of alkali *tert*-butoxide (LiOtBu, NaOtBu, KOtBu, 0.95-1 equiv.) in dry ethanol (15-20 mL) at 0 °C. After 10 min, the solvent was evaporated under reduced pressure and the remaining residue was washed with dry Et<sub>2</sub>O and/or dry *n*-pentane and filtrated under argon.

**4.3.1. Potassium 1-(diethylamino)-1,3-dioxo-3-phenylpropan-2-ide (**1-CONEt<sub>2</sub>**)-K** was obtained from *N,N*-diethyl-3-oxo-3-phenylpropanamide (**1-CONEt<sub>2</sub>**)-H, 989 mg, 4.51 mmol) and KOtBu (495 mg, 4.41 mmol) as a colorless solid (1.01 g, 3.92 mmol, 89 %).

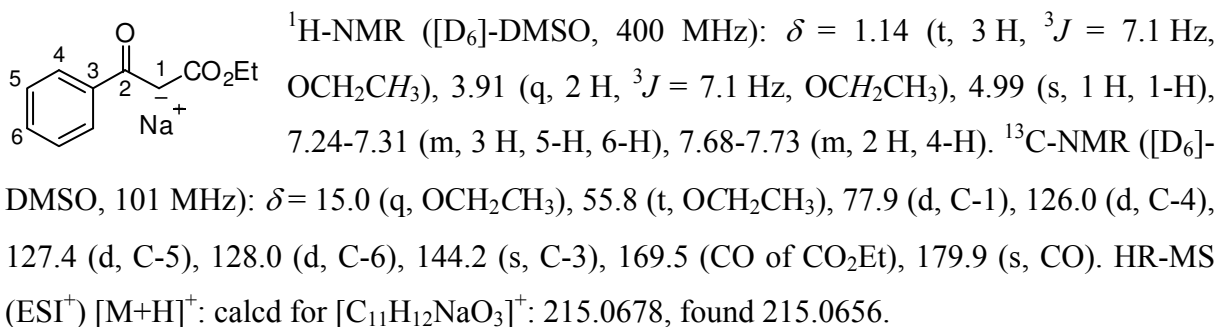


<sup>1</sup>H-NMR ([D<sub>6</sub>]-DMSO, 300 MHz):  $\delta$  = 1.06 (t, <sup>3</sup>*J* = 7.0 Hz, 6 H, NCH<sub>2</sub>CH<sub>3</sub>), 3.27 (q, <sup>3</sup>*J* = 7.0 Hz, 4 H, NCH<sub>2</sub>CH<sub>3</sub>), 5.05 (s, 1 H, 1-H), 7.16-7.27 (m, 3 H, 5-H, 6-H), 7.64-7.67 (m, 2 H, 4-H). <sup>13</sup>C-NMR ([D<sub>6</sub>]-DMSO, 75.5 MHz):  $\delta$  = 14.3 (q, NCH<sub>2</sub>CH<sub>3</sub>), 40.1 (t, NCH<sub>2</sub>CH<sub>3</sub>), 78.6 (d, C-1), 126.1 (d, C-4), 127.0 (d, C-6), 127.2 (d, C-5), 147.0 (s, C-3), 168.8 (s, CONEt<sub>2</sub>), 176.3 (s, CO).

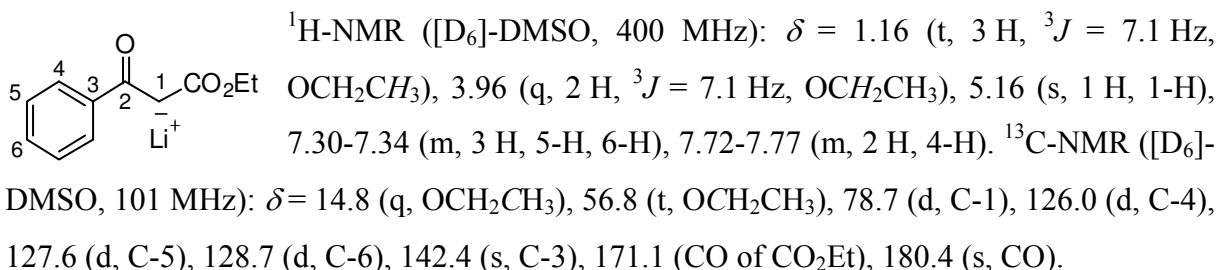
**4.3.2. Potassium 1-ethoxy-1,3-dioxo-3-phenylpropan-2-ide (1-CO<sub>2</sub>Et)-K<sup>[RA]</sup>** was obtained from ethyl benzoylacetate (2.00 g, 10.4 mmol) and KO<sup>t</sup>Bu (1.12 g, 9.98 mmol) as a colorless solid (1.51 g, 6.56 mmol, 66 %).



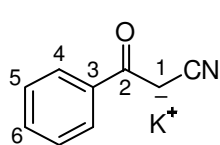
**4.3.3. Sodium 1-ethoxy-1,3-dioxo-3-phenylpropan-2-ide (1-CO<sub>2</sub>Et)-Na<sup>[RA]</sup>** was obtained from ethyl benzoylacetate (2.00 g, 10.4 mmol) and NaO<sup>t</sup>Bu (960 mg, 9.99 mmol) as a colorless solid (1.43 g, 6.68 mmol, 67 %).



**4.3.4. Lithium 1-ethoxy-1,3-dioxo-3-phenylpropan-2-ide (1-CO<sub>2</sub>Et)-Li<sup>[RA]</sup>** was obtained from ethyl benzoylacetate (2.00 g, 10.4 mmol) and LiO<sup>t</sup>Bu (800 mg, 9.99 mmol) as a colorless solid (1.54 g, 7.77 mmol, 78 %).

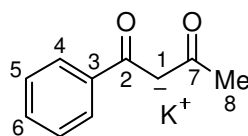


**4.3.5. Potassium 1-cyano-2-oxo-2-phenylethan-1-ide (1-CN)-K** was obtained from benzoylacetonitrile (500 mg, 3.44 mmol) and KO $t$ Bu (372 mg, 3.32 mmol) as a colorless solid (470 mg, 2.56 mmol, 77 %).



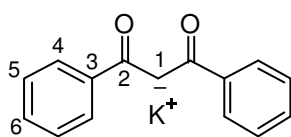
$^1\text{H-NMR}$  ( $[\text{D}_6]$ -DMSO, 400 MHz):  $\delta$  = 3.94 (s, 1 H, 1-H), 7.21-7.26 (m, 3 H, 5-H, 6-H), 7.58-7.63 (m, 2 H, 4-H).  $^{13}\text{C-NMR}$  ( $[\text{D}_6]$ -DMSO, 101 MHz):  $\delta$  = 51.0 (d, C-1), 125.5 (d, C-4), 127.2 (d, C-5), 127.7 (d, C-6), 127.8 (s, CN), 143.1 (s, C-3), 179.9 (s, CO).

**4.3.6. Potassium 1,3-dioxo-1-phenylbutan-2-ide (1-COMe)-K** was obtained from 1-phenylbutane-1,3-dione (750 mg, 4.62 mmol) and KO $t$ Bu (504 mg, 4.49 mmol) as a colorless solid (745 mg, 3.38 mmol, 75 %).



The solution of the anion **1-COMe** shows a mixture of *E* and *Z* conformers in a ratio of 1:1.3.  $^1\text{H-NMR}$  ( $[\text{D}_6]$ -DMSO, 400 MHz):  $\delta$  = 1.78, 2.21\* (s, 3 H, 8-H), 5.55, 5.28\* (s, 1 H, 1-H), 7.21-7.36 (m, 3 H, 5-H, 6-H), 7.68-7.73 (m, 2 H, 4-H).  $^{13}\text{C-NMR}$  ( $[\text{D}_6]$ -DMSO, 101 MHz):  $\delta$  = 29.8, 29.0\* (q, C-8), 93.3, 96.3\* (d, C-1), 126.3 (d, C-4), 127.4 (d, C-5), 128.1 (d, C-6), 144.5, 145.8\* (s, C-3), 179.4 (s, C-2), 187.1, 190.9 (s, C-7).

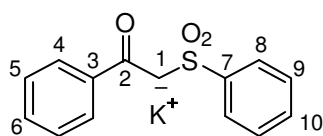
**4.3.7. Potassium 1,3-dioxo-1,3-diphenylpropan-2-ide (1-COPh)-K** was obtained from dibenzoylmethane (1.11 g, 4.95 mmol) and KO $t$ Bu (556 mg, 4.95 mmol) as a colorless solid (1.03 g, 3.93 mmol, 79 %).



$^1\text{H-NMR}$  ( $[\text{D}_6]$ -DMSO, 400 MHz):  $\delta$  = 6.27 (s, 1 H, 1-H), 7.32-7.36 (m, 6 H, 5-H, 6-H), 7.83-7.86 (m, 4 H, 4-H).  $^{13}\text{C-NMR}$  ( $[\text{D}_6]$ -DMSO, 101 MHz):  $\delta$  = 90.4 (d, C-1), 126.5 (d, C-4), 127.6 (d, C-5), 128.4 (d, C-6), 144.7 (s, C-3), 181.3 (s, CO).

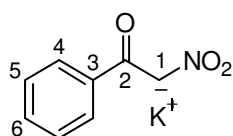
**4.3.8. Potassium 2-oxo-2-phenyl-1-(phenylsulfonyl)ethan-1-ide (1-SO $_2$ Ph)-K** was obtained from 1-phenyl-2-(phenylsulfonyl)ethanone (741 mg, 2.84 mmol) and KO $t$ Bu (308 mg, 2.75 mmol) as a colorless solid (705 mg, 2.36 mmol, 86 %).

$^1\text{H-NMR}$  ( $[\text{D}_6]$ -DMSO, 400 MHz):  $\delta$  = 5.21 (s, 1 H, 1-H), 7.24-7.28 (m, 3 H, 9-H, 10-H), 7.38-7.41 (m, 3 H, 5-H, 6-H), 7.63-7.65 (m, 2 H, 4-H), 7.94-7.97 (m, 2 H, 8-H).  $^{13}\text{C-NMR}$



([D<sub>6</sub>]-DMSO, 101 MHz):  $\delta$  = 83.1 (d, C-1), 125.5 (d, C-8), 126.0 (d, C-4), 127.4 (d, C-9), 127.7 (d, C-5), 128.4 (d, C-10), 129.7 (d, C-6), 142.6 (s, C-7), 148.6 (s, C-3), 175.6 (s, CO).

**4.3.9. Potassium 1-nitro-2-oxo-2-phenylethan-1-ide (1-NO<sub>2</sub>)-K** was obtained from 2-nitro-1-phenylethanone (1.28 g, 7.73 mmol) and KO<sup>t</sup>Bu (860 mg, 7.66 mmol) as a colorless solid (1.32 g, 6.49 mmol, 85 %).



<sup>1</sup>H-NMR ([D<sub>6</sub>]-DMSO, 300 MHz):  $\delta$  = 7.23 (s, 1 H, 1-H), 7.32-7.40 (m, 3 H, 5-H, 6-H), 7.66-7.70 (m, 2 H, 4-H). <sup>13</sup>C-NMR ([D<sub>6</sub>]-DMSO, 75.5 MHz):  $\delta$  = 109.1 (d, C-1), 126.3 (d, C-4), 127.9 (d, C-5), 130.0 (d, C-6), 141.7 (s, C-3), 176.3 (s, CO).

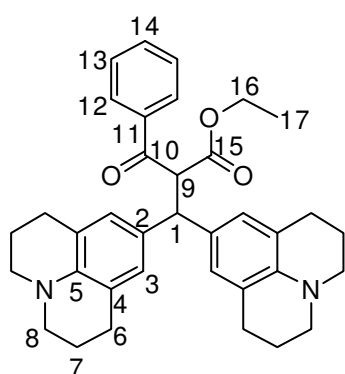
## 4.4. Reaction Products

### 4.4.1. Reaction Products of the Anions **1** with Benzhydrylium Tetrafluoroborate **3e-BF<sub>4</sub>**

General procedure 2 (GP2): The potassium-salt **1-X-K** (0.260-0.290 mmol) was dissolved in dry DMSO (10-15 mL) and the benzhydrylium tetrafluoroborate **3e-BF<sub>4</sub>** was added as a solid. After decoloration of the reaction mixture (approx. 1 to 2 min), water (20-25 mL) was added. The precipitated product was filtrated and recrystallized from ethanol/dichloromethane yielding the pure products **4**, which were subsequently characterized by NMR spectroscopy and mass spectrometry.

#### 4.4.1.1. Reaction of the Anion **1-CO<sub>2</sub>Et** with the Benzhydrylium Ion **3e**

According to GP2, the potassium salt (**1-CO<sub>2</sub>Et**)-K (63.4 mg, 0.275 mmol) and **3e-BF<sub>4</sub>** (120 mg, 0.270 mmol) yielded ethyl 2-benzoyl-3,3-bis(1,2,3,5,6,7-hexahydropyrido[3,2,1-ij]quinolin-9-yl)propanoate **4-CO<sub>2</sub>Et** (112 mg, 0.204 mmol, 76%) as yellow solid.

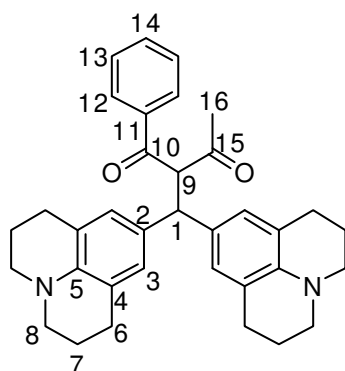


Decomposition at 139 °C. <sup>1</sup>H-NMR (CDCl<sub>3</sub>, 300 MHz):  $\delta$  = 1.01 (t, <sup>3</sup>*J* = 7.2 Hz, 3 H, 17-H), 1.78-1.87 (m, 4 H, 7-H), 1.88-1.97 (m, 4 H, 7-H), 2.44-2.64 (m, 4 H, 6-H), 2.71 (t, <sup>3</sup>*J* = 6.6 Hz, 4 H, 6-H), 2.96 (t, <sup>3</sup>*J* = 5.7 Hz, 4 H, 8-H), 3.05 (t, <sup>3</sup>*J* = 5.6 Hz, 4 H, 8-H), 3.95 (q, <sup>3</sup>*J* = 7.1 Hz, 2 H, 16-H), 4.61 (d, <sup>3</sup>*J* = 11.7 Hz, 1 H, 1-H), 5.22 (d, <sup>3</sup>*J* = 12.0 Hz, 1 H, 9-H), 6.56 (s, 2 H, 3-H), 6.72 (s,

2 H, 3-H), 7.38-7.44 (m, 2 H, 13-H), 7.49-7.56 (m, 1 H, 14-H), 7.94-7.99 (m, 2 H, 12-H).  $^{13}\text{C}$ -NMR ( $\text{CDCl}_3$ , 75.5 MHz):  $\delta$  = 13.8 (q, C-17), 22.1 and 22.2 (t, C-7), 27.5 and 27.7 (t, C-6), 49.7 (d, C-1), 49.9 and 50.8 (t, C-8), 59.8 (d, C-9), 61.1 (t, C-16), 121.4 (s, C-4), 126.1 and 126.4 (d, C-3), 128.3 (d, C-13), 128.6 (d, C-12), 129.7 and 129.9 (s, C-2), 132.9 (d, C-14), 137.4 (s, C-11), 141.2 and 141.5 (s, C-5), 168.2 (s, C-15), 194.0 (s, C-10). HR-MS (EI):  $m/z$  calcd for  $[\text{C}_{36}\text{H}_{40}\text{O}_3\text{N}_2]^+$  548.3033 found: 548.3020.

#### 4.4.1.2. Reaction of the Anion 1-COMe with the Benzhydrylium Ion 3e

According to GP2, the potassium salt (**1-COMe**)-K (63.4 mg, 0.288 mmol) and **3e**-BF<sub>4</sub> (127 mg, 0.286 mmol) yielded 2-(bis(1,2,3,5,6,7-hexahydropyrido[3,2,1-ij]quinolin-9-yl)methyl)-1,3-dione **4-COMe** (114 mg, 0.220 mmol, 78%) as yellow solid.

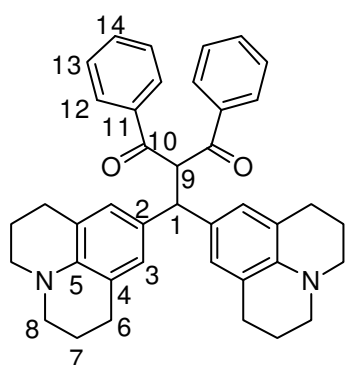


Decomposition at 135 °C.  $^1\text{H}$ -NMR ( $\text{CDCl}_3$ , 300 MHz):  $\delta$  = 1.77-1.85 (m, 4 H, 7-H), 1.88-1.96 (m, 4 H, 7-H), 2.06 (s, 3 H, 16-H), 2.45-2.63 (m, 4 H, 6-H), 2.70 (t,  $^3J$  = 6.5 Hz, 4 H, 6-H), 2.95 (t,  $^3J$  = 5.6 Hz, 4 H, 8-H), 3.06 (t,  $^3J$  = 5.6 Hz, 4 H, 8-H), 4.63 (d,  $^3J$  = 12.0 Hz, 1 H, 1-H), 5.43 (d,  $^3J$  = 12.0 Hz, 1 H, 9-H), 6.56 (s, 2 H, 3-H), 6.70 (s, 2 H, 3-H), 7.37-7.42 (m, 2 H, 13-H), 7.47-7.53 (m, 1 H, 14-H), 7.92-7.96 (m, 2 H, 12-H).  $^{13}\text{C}$ -NMR ( $\text{CDCl}_3$ , 75.5 MHz):  $\delta$  = 22.09 and 22.14 (t, C-7), 27.5, 27.6, 27.7 (2 x C-6 and C-15), 49.9 and 50.0 (t, C-8), 50.4 (d, C-1), 69.3 (d, C-9), 121.4 and 121.7 (s, C-4), 126.0 and 126.3 (d, C-3), 128.4 (d, C-12), 128.7 (d, C-13), 129.2 and 130.0 (s, C-2), 133.0 (d, C-14), 137.6 (s, C-11), 141.3 and 141.6 (s, C-5), 195.4 (s, C-10), 204.1 (s, C-15). HR-MS (EI):  $m/z$  calcd for  $[\text{C}_{35}\text{H}_{38}\text{O}_2\text{N}_2]^+$  518.2928 found: 518.2925.

#### 4.4.1.3. Reaction of the Anion 1-COPh with the Benzhydrylium Ion 3e

According to GP2, the potassium salt (**1-COPh**)-K (70.4 mg, 0.268 mmol) and **3e**-BF<sub>4</sub> (119 mg, 0.268 mmol) yielded 2-(bis(1,2,3,5,6,7-hexahydropyrido[3,2,1-ij]quinolin-9-yl)methyl)-1,3-diphenylpropane-1,3-dione **4-COPh** (121 mg, 0.208 mmol, 78%) as yellow solid.

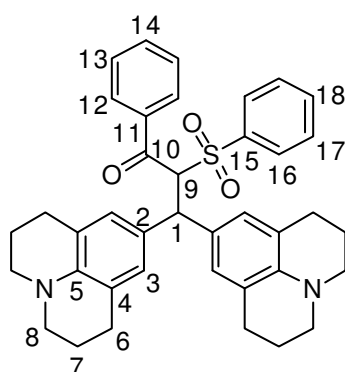
Decomposition at 186 °C.  $^1\text{H}$ -NMR ( $\text{CDCl}_3$ , 300 MHz):  $\delta$  = 1.79-1.872 (m, 8 H, 7-H), 2.47-2.63 (m, 8 H, 6-H), 2.92-3.00 (m, 2 H, 8-H), 4.85 (d,  $^3J$  = 11.5 Hz, 1 H, 1-H), 6.17 (d,  $^3J$  = 11.5 Hz, 1 H, 9-H), 6.57 (s, 4 H, 3-H), 7.31-7.36 (m, 2 H, 13-H), 7.42-7.47 (m, 1 H, 14-H),



7.83-7.86 (m, 2 H, 12-H) .  $^{13}\text{C}$ -NMR ( $\text{CDCl}_3$ , 75.5 MHz):  $\delta$  = 22.1 (t, C-7), 27.5 (t, C-6), 49.9 (t, C-8), 51.2 (d, C-1), 62.4 (d, C-9), 121.3 (s, C-4), 126.6 (d, C-3), 128.2 (d, C-13), 128.5 (d, C-12), 129.6 (s, C-2), 132.5 (d, C-14), 137.6 (s, C-11), 141.2 (s, C-5), 195.0 (s, C-10). HR-MS (EI):  $m/z$  calcd for  $[\text{C}_{40}\text{H}_{38}\text{O}_2\text{N}_2]^+$  578.2928 found: 578.2934.

#### 4.4.1.4. Reaction of the Anion 1-SO<sub>2</sub>Ph with the Benzhydrylium Ion 3e

According to GP2, the potassium salt (**1-SO<sub>2</sub>Ph**)-K (77.7 mg, 0.260 mmol) and **3e**-BF<sub>4</sub> (115 mg, 0.259 mmol) yielded 3,3-bis(1,2,3,5,6,7-hexahydropyrido[3,2,1-ij]quinolin-9-yl)-1-phenyl-2-(phenylsulfonyl)propan-1-one **4-SO<sub>2</sub>Ph** (137 mg, 0.222 mmol, 86%) as yellow solid.

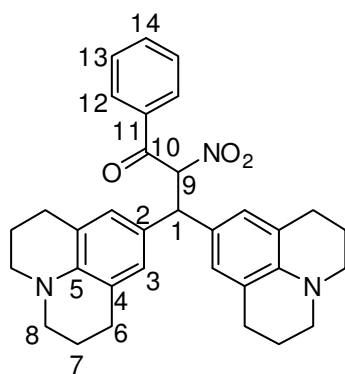


Decomposition at 153 °C.  $^1\text{H}$ -NMR ( $\text{CDCl}_3$ , 300 MHz):  $\delta$  = 1.66-1.79 (m, 4 H, 7-H), 1.82-1.92 (m, 4 H, 7-H), 2.26-2.65 (m, 8 H, 6-H), 2.90 (t,  $^3J$  = 5.7 Hz, 4 H, 8-H), 3.02 (t,  $^3J$  = 5.6 Hz, 4 H, 8-H), 4.48 (d,  $^3J$  = 11.7 Hz, 1 H, 1-H), 5.93 (d,  $^3J$  = 12.6 Hz, 1 H, 9-H), 6.41 (s, 2 H, 3-H), 6.48 (s, 2 H, 3-H), 7.27-7.35 (m, 2 H, H<sub>arom</sub>), 7.41-7.55 (m, 6 H, H<sub>arom</sub>), 7.86-7.89 (m, 2 H, 12-H) .  $^{13}\text{C}$ -NMR ( $\text{CDCl}_3$ , 75.5 MHz):  $\delta$  = 21.9 and 22.2 (t, C-7), 27.3 and 27.5 (t, C-6), 49.8 and 50.0 (t, C-8), 50.8 (d, C-1), 58.4 (d, C-9), 121.2 and 121.5 (s, C-4), 126.1 and 126.7 (d, C-3), 128.09, 128.14, 128.3, 128.5, 132.6, 132.7 (C-12, C-13, C-14, C-16, C-17, C-18), 126.9, 128.1, 140.1 (C-2, C-11, C-15), 192.7 (s, C-10). HR-MS (EI):  $m/z$  calcd for  $[\text{C}_{39}\text{H}_{40}\text{O}_3\text{N}_2\text{S}]^+$  616.2754 found: 616.1908.

#### 4.4.1.5. Reaction of the Anion 1-NO<sub>2</sub> with the Benzhydrylium Ion 3e

According to GP2, the potassium salt (**1-NO<sub>2</sub>**)-K (58.7 mg, 0.289 mmol) and **3e**-BF<sub>4</sub> (127 mg, 0.286 mmol) yielded 3,3-bis(1,2,3,5,6,7-hexahydropyrido[3,2,1-ij]quinolin-9-yl)-2-nitro-1-phenylpropan-1-one **4-NO<sub>2</sub>** (123 mg, 0.236 mmol, 82%) as yellow solid.

Decomposition at 174 °C.  $^1\text{H}$ -NMR ( $\text{CDCl}_3$ , 300 MHz):  $\delta$  = 1.74-1.82 (m, 4 H, 7-H), 1.89-1.97 (m, 4 H, 7-H), 2.39-2.58 (m, 4 H, 6-H), 2.72 (t,  $^3J$  = 6.6 Hz, 4 H, 6-H), 2.94 (t,  $^3J$  = 5.7 Hz, 4 H, 8-H), 3.08 (t,  $^3J$  = 5.7 Hz, 4 H, 8-H), 4.79 (d,  $^3J$  = 11.7 Hz, 1 H, 1-H), 6.48 (s, 2 H, 3-H), 6.75 (s, 2 H, 3-H), 6.83 (d,  $^3J$  = 11.7 Hz, 1 H, 9-H), 7.37-7.32 (m, 2 H, 13-H), 7.50-7.56



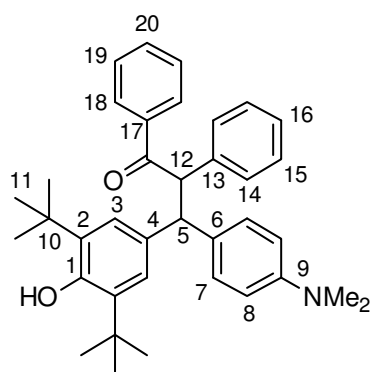
(m, 1 H, 14-H), 7.81-7.84 (m, 2 H, 12-H).  $^{13}\text{C}$ -NMR ( $\text{CDCl}_3$ , 75.5 MHz):  $\delta$  = 21.9 and 22.0 (t, C-7), 27.5 and 27.7 (t, C-6), 49.8 and 49.9 (t, C-8), 51.4 (d, C-1), 91.1 (d, C-9), 121.6 (s, C-4), 124.6 and 126.5 (s, C-2), 125.7 and 125.8 (d, C-3), 128.4 (d, C-13), 128.7 (d, C-12), 133.5 (d, C-14), 135.8 (s, C-11), 141.8 and 142.1 (s, C-5), 189.1 (s, C-10). HR-MS (EI):  $m/z$  calcd for  $[\text{C}_{33}\text{H}_{34}\text{O}_3\text{N}_3]^+$  520.2595 found: 520.2599.

#### 4.4.2. Reaction Products of the Anions **1** with Quinone Methides

**General procedure 3 (GP3):** The reactions of the carbanions **1-X** with the Michael acceptors **3j,k,n** were carried out either by dissolving the corresponding CH-acid **1-H** with a slight excess of  $\text{KO}^t\text{Bu}$  in dry DMSO (10 mL) or by directly dissolving the potassium salts (**1-X**)- $\text{K}^+$  in dry DMSO (10 mL). Subsequently, a solution of the quinone methide **3** in DMSO (ca 5 mL with 5-10 % dichloromethane as cosolvent) was added. The mixture was stirred for 5 min before 0.5 % aqueous acetic acid (ca 50 mL) was added. The mixture was extracted with ethyl acetate ( $3 \times 20$  mL), and the combined organic phases were washed with brine ( $2 \times 20$  mL), dried over sodium sulfate and the solvent was evaporated under reduced pressure. The crude reaction products were purified by column chromatography on silica (pentane/ethyl acetate) and subsequently characterized by NMR spectroscopy and mass spectrometry.

##### 4.4.2.1. Reaction of the Anion **1-Ph** with the Quinone Methide **3n**<sup>[RA]</sup>

According to GP3, 1,2-diphenylethanone (98.1 mg, 0.500 mmol),  $\text{KO}^t\text{Bu}$  (58.0 mg, 0.517 mmol), and **3n** (169 mg, 0.501 mmol) yielded 3-(3,5-di-*tert*-butyl-4-hydroxyphenyl)-3-(4-(dimethylamino)phenyl)-1,2-diphenylpropan-1-one **5-Ph** (181 mg, 339  $\mu\text{mol}$ , 68%, *dr* ~ 1:1) as orange solid.



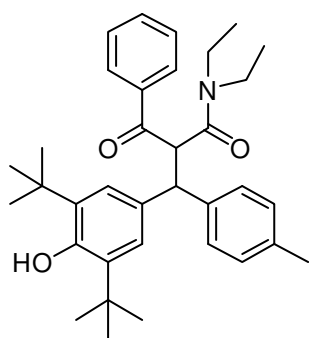
$^1\text{H}$ -NMR ( $\text{CDCl}_3$ , 599 MHz):  $\delta$  = 1.25 (s, 18 H, 11-H both isomers), 2.81, 2.85 (s, 6 H,  $\text{NMe}_2$ ), 4.70-4.73 (m, 1 H, 5-H), 4.84, 4.87 (s, 1 H, OH), 5.22, 5.39 (d,  $^3J$  = 11.5 Hz and 11.7 Hz, 1 H, 12-H), 6.48, 6.62 (d,  $^3J$  = 7.2 Hz and 6.6 Hz, 2 H, 8-H), 6.65, 7.01 (s, 2 H, 3-H), 6.88, 7.20 (d, 2 H,  $^3J$  = 8.7 Hz and 8.6 Hz, 7-H), 7.03-7.10 (m, 3 H, 14-H, 16-H), 7.14-7.16, 7.30-7.31 (m, 2 H, 15-H), 7.33-7.36 (m, 2 H, 19-H), 7.43-7.46 (m, 1 H, 20-H), 7.83-7.84, 7.90-7.92 (m, 2 H, 18-H).  $^{13}\text{C}$ -NMR ( $\text{CDCl}_3$ , 151 MHz):  $\delta$  = 30.17,

30.20 (q, C-11), 34.1, 34.2 (s, C-10), 40.7, 40.8 (q, NMe<sub>2</sub>), 54.1, 54.6 (d, C-5), 58.8, 59.6 (d, C-12), 112.5, 113.1 (d, C-8), 124.4, 125.2 (d, C-3), 126.7, 126.8 (d, C-16), 128.11, 128.25, 128.31, 128.33, 128.34, 128.40, 128.46, 128.99, 129.07, 129.18, (d, C-7, C-14, C-15, C-18, C-19), 131.3, 131.9 (s, C-6), 132.5, 132.6 (d, C-20), 133.4, 134.1 (s, C-4), 134.8, 135.3 (s, C-2), 137.5, 137.8, 138.0, 138.2 (s, C-13, C-17), 148.7, 148.9 (s, C-9), 151.6, 151.8 (s, C-1), 199.1, 200.4 (s, CO). HR-MS (ESI<sup>+</sup>) [M+H]<sup>+</sup>: calcd for [C<sub>37</sub>H<sub>44</sub>NO<sub>2</sub>]<sup>+</sup>: 534.3367, found 534.3347.

Due to *dr* = 1:1, the chemical shifts could not be assigned to the individual isomers.

#### 4.4.2.2. Reaction of the Anion 1-CONEt<sub>2</sub> with the Quinone Methide **3j**

According to GP3, the potassium salt (**1-CONEt<sub>2</sub>**)-K (88.9 mg, 0.345 mmol) and **3j** (106 mg, 0.344 mmol) yielded 2-benzoyl-3-(3,5-di-*tert*-butyl-4-hydroxyphenyl)-*N,N*-diethyl-3-(*p*-tolyl)propanamide **5-CONEt<sub>2</sub>** (165 mg, 0.313 mmol, 91%) as colorless solid.



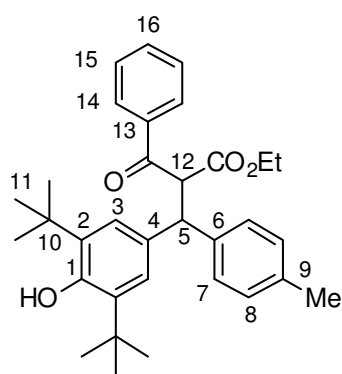
<sup>1</sup>H-NMR (CDCl<sub>3</sub>, 300 MHz):  $\delta$  = 0.72-0.79, 0.84-0.92 (m), 1.00 (t, <sup>3</sup>*J* = 7.1 Hz), 1.25 (s), 1.39 (s), 2.20 (s), 2.28 (s), 3.01-3.46 (m), 3.69 (s), 3.76 (s), 4.85-4.86 (m), 5.02-5.07 (m), 5.14-5.28 (m), 6.79 (d, <sup>3</sup>*J* = 8.7 Hz), 6.81 (d, <sup>3</sup>*J* = 7.8 Hz), 6.82 (d, <sup>3</sup>*J* = 9.0 Hz), 7.07 (d, <sup>3</sup>*J* = 8.1 Hz), 7.11-7.15 (m), 7.28-7.49 (m), 7.80 (d, <sup>3</sup>*J* = 8.4 Hz), 7.93 (d, <sup>3</sup>*J* = 7.2 Hz). <sup>13</sup>C-NMR (CDCl<sub>3</sub>, 75.5 MHz):  $\delta$  = 12.39, 12.43, 13.9, 14.1, 20.9, 21.0, 30.1, 30.3, 40.2, 40.3, 40.61, 40.64, 41.7, 42.0,

50.9, 51.3, 51.6, 52.0, 55.1, 55.2, 59.4, 59.6, 113.73, 113.74, 125.0, 125.1, 125.3, 125.4, 127.8, 127.9, 128.22, 128.23, 128.42, 128.44, 128.96, 129.0, 129.1, 132.3, 132.6, 132.7, 131.7, 131.8, 135.2, 135.3, 135.35, 135.38, 135.4, 135.5, 135.7, 137.5, 137.7, 166.35, 166.38, 195.5, 195.7, 196.4, 196.5. HR-MS (EI): *m/z* calcd for [C<sub>35</sub>H<sub>45</sub>O<sub>3</sub>N]<sup>+</sup> 527.3394 found: 527.3390.

#### 4.4.2.3. Reaction of the Anion 1-CO<sub>2</sub>Et with the Quinone Methide **3j**<sup>[RA]</sup>

According to GP3, the potassium salt (**1-CO<sub>2</sub>Et**)-K (173 mg, 0.751 mmol) and **3j** (154 mg, 0.499 mmol) yielded ethyl 2-benzoyl-3-(3,5-di-*tert*-butyl-4-hydroxyphenyl)-3-(*p*-tolyl)propanoate **5-CO<sub>2</sub>Et** (182 mg, 0.364 mmol, 73%, *dr* ~ 1.3:1) as colorless solid.

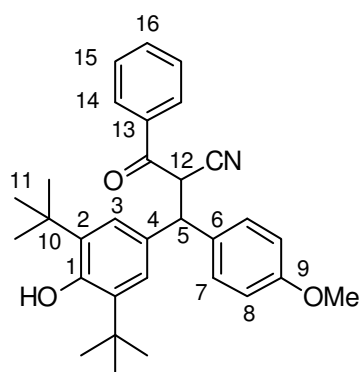




$^1\text{H-NMR}$  ( $\text{CDCl}_3$ , 400 MHz):  $\delta$  = 0.86\*, 1.00 (t, 3 H,  $^3J$  = 7.1 Hz,  $\text{OCH}_2\text{CH}_3$ ), 1.21, 1.41\* (s, 18 H, 11-H), 2.19\*, 2.29 (s, 3 H, Me), 3.80-3.93\*, 3.95-4.00 (m, 2 H,  $\text{OCH}_2\text{CH}_3$ ), 4.86-4.89 (m, 2 H, 5-H, OH major isomer), 4.93\* (d, 1 H,  $^3J$  = 11.8 Hz, 5-H), 5.04\* (s, 1 H, OH), 5.31\*, 5.35\* (d, 1 H,  $^3J$  = 11.8 Hz and 11.9 Hz, 12-H), 6.90\* (s, 2 H, 3-H), 6.96\*, 7.09 (d, 2 H,  $J$  = 7.8 Hz, 8-H), 7.14-7.17\* (m, 4 H, 3-H, 7-H), 7.27 (d, 2 H,  $^3J$  = 8.6 Hz, 7-H, superimposed by  $\text{CDCl}_3$  residual signal), 7.36-7.56 (m, 6 H, 15-H, 16-H, both isomers), 7.84-7.86, 8.00-8.03\* (m, 2 H, 14-H).  $^{13}\text{C-NMR}$  ( $\text{CDCl}_3$ , 101 MHz):  $\delta$  = 13.7\*, 13.8 (q,  $\text{OCH}_2\text{CH}_3$ ), 20.9\*, 21.0 (q, Me), 30.0, 30.3\* (q, C-11), 34.1, 34.3\* (s, C-10), 50.7\*, 51.4 (d, C-5), 59.5, 60.3\* (d, C-12), 61.3\*, 61.4 (t,  $\text{OCH}_2\text{CH}_3$ ), 124.4, 124.8\* (d, C-3), 127.4\*, 127.8 (d, C-7), 128.35, 128.42 (d, C-14, C-15), 128.6\*, 128.7\* (d, C-14, C-15), 129.1, 129.2\* (d, C-8), 131.7, 132.2\* (s, C-4), 133.1, 133.4\* (d, C-16), 135.4, 135.5\* (s, C-2), 135.7\*, 136.0 (s, C-9), 136.7\*, 137.6 (s, C-13), 139.4, 139.5\* (s, C-6), 152.1, 152.4\* (s, C-1), 167.91\*, 167.92 (s, CO of  $\text{CO}_2\text{Et}$ ), 192.9\*, 194.6 (s, CO). HR-MS ( $\text{ESI}^+$ )  $[\text{M}+\text{NH}_4]^+$ : calcd for  $[\text{C}_{33}\text{H}_{44}\text{NO}_4]^+$ : 518.3265, found 518.3249. HR-MS ( $\text{ESI}^-$ )  $[\text{M}-\text{H}]^-$ : calcd for  $[\text{C}_{33}\text{H}_{39}\text{O}_4]^-$ : 499.2854, found 499.2846.

#### 4.4.2.4. Reaction of the Anion 1-CN with the Quinone Methide 3k<sup>[RA]</sup>

According to GP3, the potassium salt (**1-CN**)-K (78.0 mg, 0.426 mmol) and **3k** (138 mg, 0.425 mmol) yielded 2-benzoyl-3-(3,5-di-*tert*-butyl-4-hydroxyphenyl)-3-(4-methoxyphenyl)-propanenitrile **5-CN** (185 mg, 0.394 mmol, 93%, *dr* ~ 1.7:1) as colorless solid.



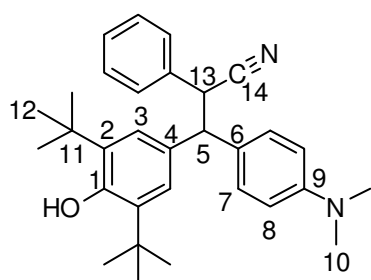
$^1\text{H-NMR}$  ( $\text{CDCl}_3$ , 599 MHz):  $\delta$  = 1.26, 1.40\* (s, 18 H, 11-H), 3.73\*, 3.80 (s, 3H, OMe), 4.69, 4.73\* (d, 1 H,  $^3J$  = 9.8 Hz and 8.9 Hz, 5-H), 4.99\*, 5.06 (d, 1 H,  $^3J$  = 9.8 Hz and 8.9 Hz, 12-H), 5.01, 5.16\* (s, 1 H, OH), 6.77\*, 6.90 (d, 2 H,  $J$  = 8.8 Hz, 8-H), 6.92, 7.07\* (s, 2 H, 3-H), 7.17\*, 7.29 (d, 2 H,  $^3J$  = 8.6 Hz and 8.7 Hz, 7-H), 7.39-7.41, 7.44-7.47\* (m, 2 H, 15-H), 7.54-7.57, 7.58-7.61\* (m, 1 H, 16-H), 7.72-7.73, 7.80-7.82\* (m, 2 H, 14-H).  $^{13}\text{C-NMR}$  ( $\text{CDCl}_3$ , 151 MHz):  $\delta$  = 30.0, 30.2\* (q, C-11), 34.2, 34.4\* (s, C-10), 45.3, 46.2\* (q, C-12), 50.5\*, 51.5 (d, C-5), 55.20\*, 55.23 (q, OMe), 114.1\*, 114.2 (d, C-8), 116.7\*, 116.9 (s, CN), 124.4, 125.1\* (d, C-3), 128.4, 128.6\* (d, C-14), 128.78 (d, C-15), 128.82\*, 128.9\* (2d, C-7, C-15), 129.9 (d, C-7), 129.8\*, 130.0 (s, C-4), 132.0, 132.3\* (s, C-6), 134.0,

134.1\* (d, C-16), 135.1\*, 135.5 (s, C-13), 135.9\*, 136.0 (s, C-2), 152.8, 153.2\* (d, C-1), 158.6\*, 158.9 (s, C-9), 190.7\*, 191.4 (s, CO). HR-MS (ESI<sup>+</sup>) [M+NH<sub>4</sub>]<sup>+</sup>: calcd for [C<sub>31</sub>H<sub>39</sub>N<sub>2</sub>O<sub>3</sub>]<sup>+</sup>: 487.2956, found 487.2938. HR-MS (ESI<sup>-</sup>): calcd for [C<sub>31</sub>H<sub>35</sub>NO<sub>3</sub>]<sup>-</sup>: 469.2622, found 469.2612.

#### 4.4.3. Reaction Products of the Benzyl Anions **2** with the Quinone Methide **3n**

##### 4.4.3.1. Reaction of the Anion **2-CN** with the Quinone Methide **3n**

According to GP3, 2-phenylacetonitrile (48.2 mg, 0.411 mmol), dimsyl potassium (0.457 mmol), and **3n** (115 mg, 0.341 mmol) yielded 3-(3,5-di-tert-butyl-4-hydroxyphenyl)-3-(4-(dimethylamino)phenyl)-2-phenylpropanenitrile **6-CN** (146 mg, 0.321 mmol, 94%, *dr* ~ 1:1.1) as yellow solid.

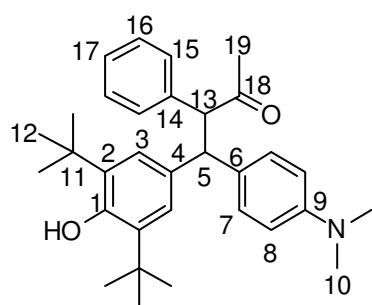


<sup>1</sup>H-NMR (CDCl<sub>3</sub>, 300 MHz):  $\delta$  = 1.34, 1.38\* (s, 18 H, 12-H), 2.92\*, 2.95 (s, 6 H, 10-H), 4.15-4.19 (m, 5-H, both isomers), 4.34, 4.48\* (d, <sup>3</sup>*J* = 9 Hz, <sup>3</sup>*J*\* = 7 Hz, 13-H), 5.04, 5.10\* (s, 1 H, OH), 6.65\*, 6.71 (d, <sup>3</sup>*J* = 9 Hz, 2 H, 8-H), 6.88, 6.95\* (s, 2 H, 3-H), 7.03-7.09 (m, H<sub>arom</sub>), 7.14-7.20 (m, H<sub>arom</sub>), 7.22-7.26 (m, H<sub>arom</sub>). <sup>13</sup>C-NMR (CDCl<sub>3</sub>, 75.5 MHz):  $\delta$  = 30.17, 30.24\* (q, C-12), 34.2, 34.3\* (s, C-11), 40.5 (q, C-10, both isomers), 44.2, 43.9\* (d, C-13), 55.8\*, 56.2 (d, C-5), 112.5\*, 112.6 (d, C-8), 120.4 and 120.6 (s, C-14, both isomers), 124.7, 125.4 (d, C-3), 127.6, 128.3, 128.36, 128.38, 128.4, 128.6, 129.1 (C<sub>arom</sub>), 128.0, 128.8\* (s, C-6), 130.4, 131.4 (s, C-4, both isomers), 135.3\*, 135.5 (s, C-2), 149.4\*, 149.7 (s, C-9), 152.4, 152.8\* (s, C-1). HR-MS (EI) [M-H]<sup>+</sup>: *m/z* calcd for [C<sub>31</sub>H<sub>37</sub>ON<sub>2</sub>]<sup>+</sup>: 453.2911 found: 453.2895.

##### 4.4.3.2. Reaction of the Anion **2-COMe** with the Quinone Methide **3n**

According to GP3, phenylacetone (50.5 mg, 0.376 mmol), KO<sup>*t*</sup>Bu (43.2 mg, 0.385 mmol), and **3n** (112 mg, 0.332 mmol) yielded 4-(3,5-di-tert-butyl-4-hydroxyphenyl)-4-(4-(dimethylamino)phenyl)-3-phenylbutan-2-one **6-COMe** (116 mg, 0.246 mmol, 74%, *dr* ~ 1:1.1) as orange solid.

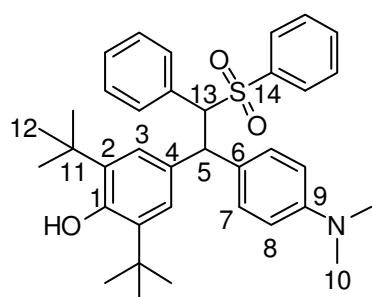
<sup>1</sup>H-NMR (CDCl<sub>3</sub>, 300 MHz):  $\delta$  = 1.16, 1.43\* (s, 18, 12-H), 2.00\*, 2.05 (s, 3 H, 19-H), 2.80\*, 2.91 (s, 6 H, 10-H), 4.46\*, 4.54 (d, <sup>3</sup>*J* = 12 Hz, 1 H, 13-H), 4.58 (bs, 1 H, 5-H both isomers), 4.82, 5.00\* (s, 1 H, OH), 6.48 and 6.93 (d, <sup>3</sup>*J* = 9 Hz, 2 H, 8-H), 6.70-6.73 (m, 4 H, H<sub>arom</sub>),



7.12-7.25 (m, 12 H,  $H_{\text{arom}}$ ), 7.27-7.29 (m, 2 H,  $H_{\text{arom}}$ ).  $^{13}\text{C}$ -NMR ( $\text{CDCl}_3$ , 75.5 MHz):  $\delta$  = 30.2, 30.4\* (q, C-12), 30.5 (q, C-19), 34.1 and 34.3 (s, C-11 both isomers), 40.3\*, 40.7 (q, C-10), 52.85 and 52.91 (d, C-5 both isomers), 64.6, 65.2\* (d, C-13), 112.6 and 113.1 (d, C-8 both isomers), 124.1 and 124.8 (d, C-3 both isomers), 134.9 and 135.6 (s, C-2 both isomers), 126.8, 126.9, 127.0, 128.2, 128.4, 128.71, 128.73, 129, 129.4, 130.0, 134.3, 137.1, 137.3 ( $C_{\text{arom}}$ ), 148.5 and 149.9 (s, C-9 both isomers), 151.5, 152.0\* (s, C-1), 207.8 (s, C-18). HR-MS (EI):  $m/z$  calcd for  $[\text{C}_{32}\text{H}_{41}\text{O}_2\text{N}]^+$ : 471.3132 found: 471.3126.

#### 4.4.3.3. Reaction of the Anion 2-SO<sub>2</sub>Ph with the Quinone Methide 3n

According to GP3, benzyl phenyl sulfone (80.2 mg, 0.345 mmol), KO<sup>t</sup>Bu (39.6 mg, 0.353 mmol), and **3n** (115 mg, 0.341 mmol) yielded 2,6-di-tert-butyl-4-(1-(4-(dimethylamino)phenyl)-2-phenyl-2-(phenylsulfonyl)ethyl)phenol **6-SO<sub>2</sub>Ph** (166 mg, 0.291 mmol, 85%,  $dr \sim 1:1.9$ ) as colorless solid.



$^1\text{H}$ -NMR ( $\text{CDCl}_3$ , 300 MHz):  $\delta$  = 1.26\*, 1.35 (s, 18 H, 12-H), 2.80, 2.90\* (s, 6 H, 10-H), 4.83\*, 4.96 (s, 1 H, OH), 4.97-5.1 (m) and 5.06 (d,  $^3J = 9.3$  Hz, 5-H and 13-H, both isomers), 6.46, 6.58\* (d,  $^3J = 8.7$  Hz, 2 H, 7-H), 6.85\*, 7.05 (s, 2 H, 3-H), 7.03 (d,  $^3J = 8.7$  Hz, 2 H, 8-H, major isomer), 7.15-7.28 (m,  $H_{\text{arom}}$ ), 7.31-7.45 (m,  $H_{\text{arom}}$ ).  $^{13}\text{C}$ -NMR ( $\text{CDCl}_3$ , 75.5 MHz):  $\delta$  = 30.1\*, 30.3 (q, C-12), 34.1\*, 34.2 (s, C-11), 40.4, 40.6\* (q, C-10), 51.0, 51.1\* (d, C-5), 76.2, 76.3\* (d, C-13), 112.2, 122.6\* (d, C-7), 125.0, 125.3\* (d, C-3), 129.3 (d, C-8, major isomer), 126.6, 126.8, 127.7, 127.8, 128.0, 128.10, 128.17, 128.18, 128.20, 128.3, 128.6, 128.7, 130.0, 130.1, 130.8, 131.2, 132.37, 132.42, 133.44, 132.6, 132.8, 133.5 ( $C_{\text{arom}}$ ), 135.0\*, 135.3 (s, C-2), 140.1\*, 140.5 (s, C-14), 148.7, 149.3\* (s, C-9), 151.6\*, 152.3 (s, C-1). HR-MS (EI):  $m/z$  calcd for  $[\text{C}_{36}\text{H}_{43}\text{O}_3\text{NS}]^+$ : 569.2958 found: 569.2948.

### 4.5. Generation and UV-Spectroscopic Characterization of Carbanions 1-X and 2-X

#### 4.5.1. Deprotonation Experiments

The formation of the carbanions **1-Ph** and **2-CN**, **2-COMe** and **2-SO<sub>2</sub>Ph** from their conjugate CH acids were recorded by using diode array UV-Vis spectrometers. The temperature during

all experiments was kept constant by using a circulating bath ( $20.0 \pm 0.02$  °C). Solutions of the CH acids in dry DMSO were added to a solution of KO $t$ Bu (1.05 eq.) or dimsyl potassium (1.05 eq.) in dry DMSO (22–25 mL). After reaching a constant value of the absorbance (within 10 to 90 s) the mixtures were treated subsequently with more base (2–5 equiv. dissolved in DMSO: 0.1–0.3 mL). In all cases a full deprotonation of the CH acid with one equivalent of base was monitored (Figure 13).

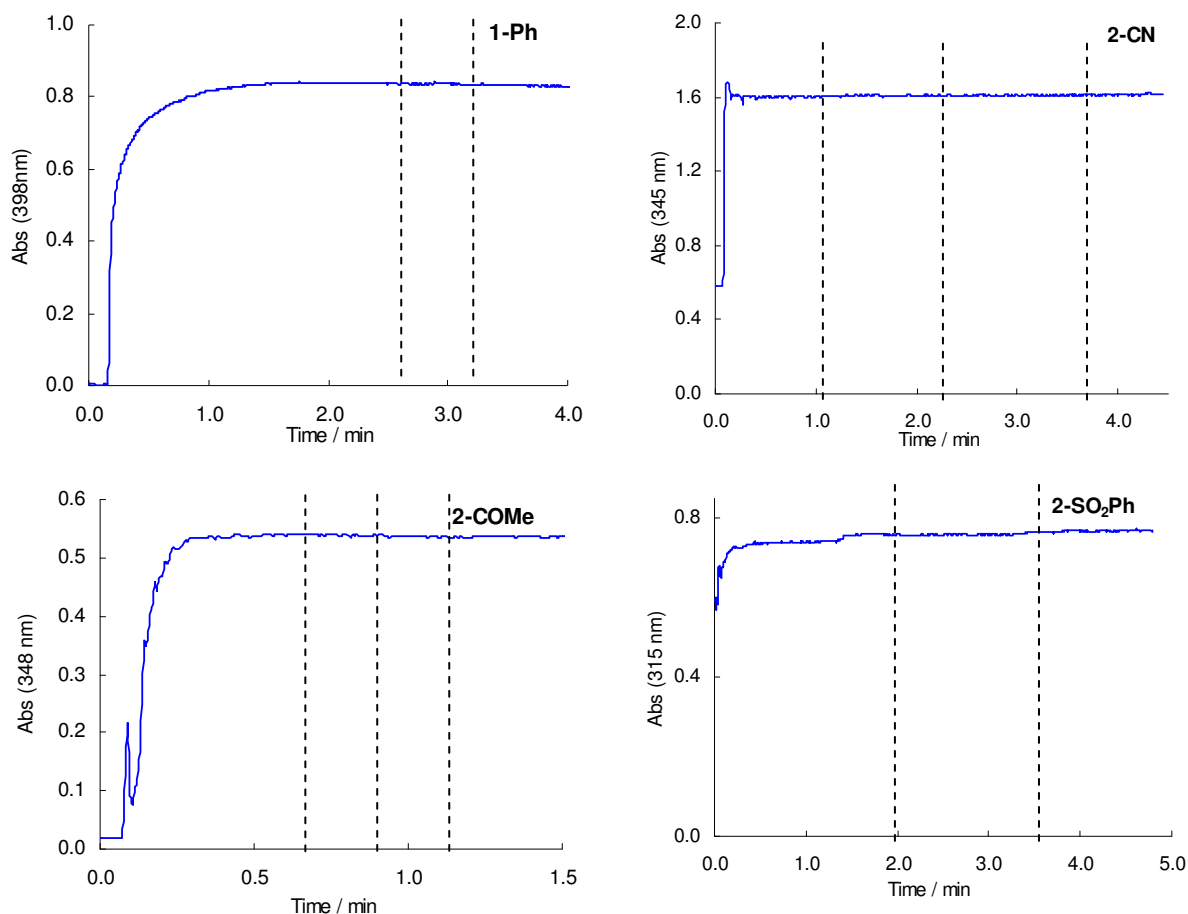


Figure 13: Formation of the anions **1-Ph**, **2-CN**, **2-COMe** and **2-SO<sub>2</sub>Ph** from the corresponding CH acids and KO $t$ Bu (or dimsyl potassium for **2-CN**) in DMSO at 20 °C. Dashed lines mean an additional equivalent of base.

## 4.5.2. UV-Vis Spectra

### 4.5.2.1. UV-Vis Spectra of the Benzoylmethyl Anions 1-X

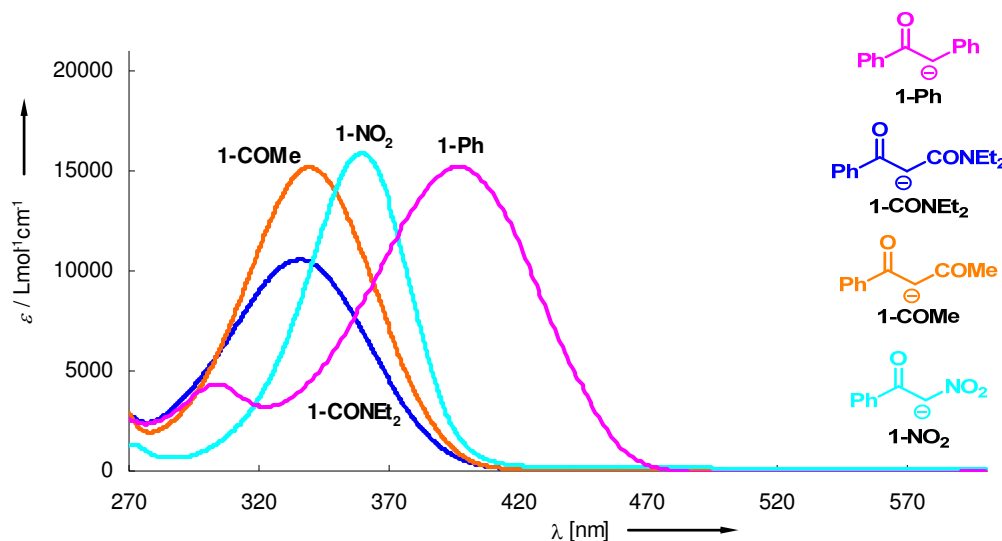


Figure 14: UV-Vis-spectra of the anions **1-Ph**, **1-CONEt<sub>2</sub>**, **1-COMe** and **1-NO<sub>2</sub>** in DMSO (20 °C).

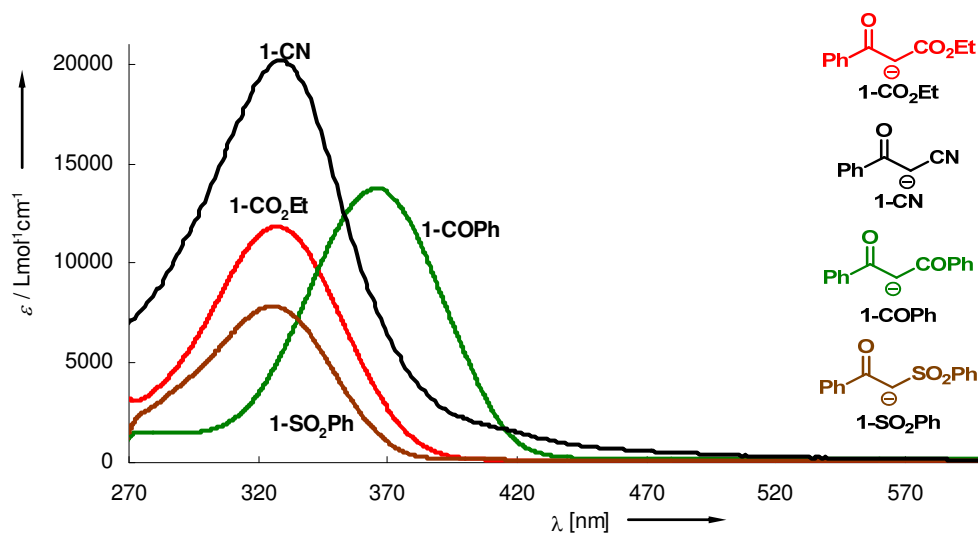
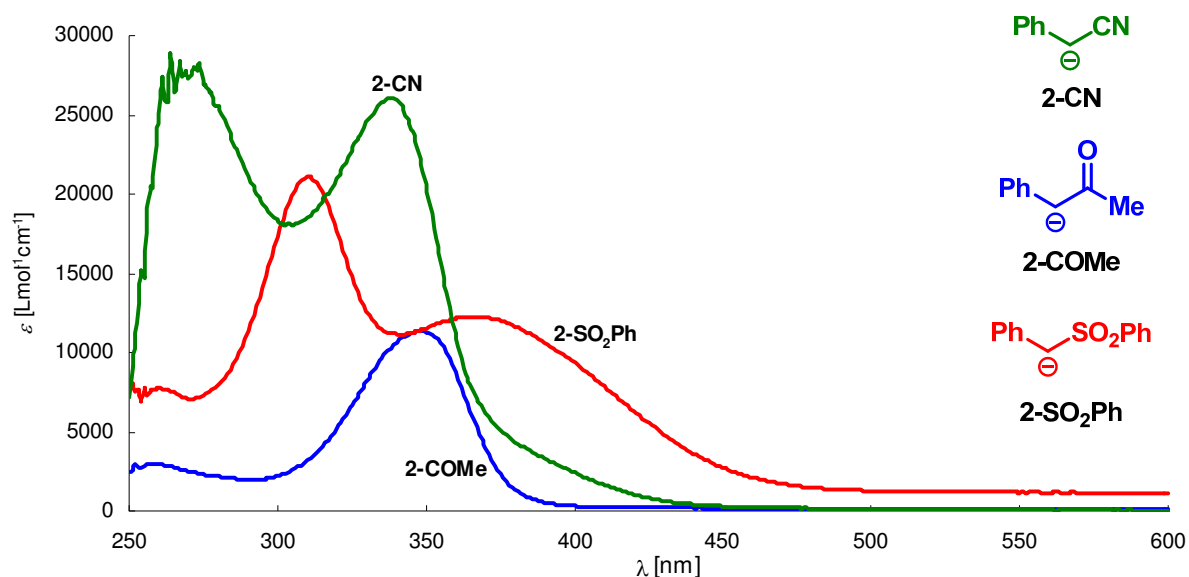


Figure 15: UV-Vis-spectra of the anions **1-CO<sub>2</sub>Et**, **1-CN**, **1-COPh** and **1-SO<sub>2</sub>Ph** in DMSO (20 °C).

## 4.5.2.2. UV-Vis Spectra of the Benzyl Anions 2-X

Figure 16: UV-Vis-spectra of the anions **2** in DMSO (20 °C).

## 4.6. Kinetic Experiments

## 4.6.1. Coordination Experiments with Alkali Metal Salts

Table 7: Pseudo-first-order rate constants for reaction of **1-Ph** (generated from (**1-Ph**)-H by addition of 1.05 equivalents of KOtBu)<sup>[a]</sup> with **3n** at variable concentrations of KBPh<sub>4</sub> (20 °C, stopped-flow, at 486 nm).

[ <b>3n</b> ] / mol L <sup>-1</sup>	[ <b>1-Ph</b> ] / mol L <sup>-1</sup>	[KOtBu] / mol L <sup>-1</sup>	[KBPh <sub>4</sub> ] / mol L <sup>-1</sup>	[K <sup>+</sup> ] <sub>total</sub> / mol L <sup>-1</sup>	<i>k</i> <sub>obs</sub> / s <sup>-1</sup>
	2.12 × 10 <sup>-4</sup>				7.61 × 10 <sup>-1</sup> [a]
1.28 × 10 <sup>-5</sup>	2.12 × 10 <sup>-4</sup>	2.23 × 10 <sup>-4</sup>	1.28 × 10 <sup>-4</sup>	3.51 × 10 <sup>-4</sup>	7.48 × 10 <sup>-1</sup>
1.28 × 10 <sup>-5</sup>	2.12 × 10 <sup>-4</sup>	2.23 × 10 <sup>-4</sup>	2.57 × 10 <sup>-4</sup>	4.80 × 10 <sup>-4</sup>	7.37 × 10 <sup>-1</sup>
1.28 × 10 <sup>-5</sup>	2.12 × 10 <sup>-4</sup>	2.23 × 10 <sup>-4</sup>	5.14 × 10 <sup>-4</sup>	7.36 × 10 <sup>-4</sup>	7.29 × 10 <sup>-1</sup>
1.28 × 10 <sup>-5</sup>	2.12 × 10 <sup>-4</sup>	2.23 × 10 <sup>-4</sup>	1.26 × 10 <sup>-3</sup>	1.48 × 10 <sup>-3</sup>	7.01 × 10 <sup>-1</sup>
1.28 × 10 <sup>-5</sup>	2.12 × 10 <sup>-4</sup>	2.23 × 10 <sup>-4</sup>	2.57 × 10 <sup>-3</sup>	2.79 × 10 <sup>-3</sup>	6.58 × 10 <sup>-1</sup>
1.28 × 10 <sup>-5</sup>	2.12 × 10 <sup>-4</sup>	2.23 × 10 <sup>-4</sup>	5.05 × 10 <sup>-3</sup>	5.27 × 10 <sup>-3</sup>	6.31 × 10 <sup>-1</sup>
1.28 × 10 <sup>-5</sup>	2.12 × 10 <sup>-4</sup>	2.23 × 10 <sup>-4</sup>	7.57 × 10 <sup>-3</sup>	7.79 × 10 <sup>-3</sup>	6.04 × 10 <sup>-1</sup>
1.28 × 10 <sup>-5</sup>	2.12 × 10 <sup>-4</sup>	2.23 × 10 <sup>-4</sup>	1.14 × 10 <sup>-2</sup>	1.16 × 10 <sup>-2</sup>	5.99 × 10 <sup>-1</sup>

[a] Calculated from the second-order rate constants of the free anion (potassium salt in presence of 18-crown-6) given in Table 4.

Table 8: Pseudo-first-order rate constants for reaction of **1-Ph** (generated from (**1-Ph**)-H by addition of 1.05 equivalents of NaOtBu)<sup>[a]</sup> with **3n** at variable concentrations of NaBPh<sub>4</sub> (20 °C, stopped-flow, at 486 nm).

[ <b>3n</b> ] / mol L <sup>-1</sup>	[ <b>1-Ph</b> ] / mol L <sup>-1</sup>	[NaOtBu] / mol L <sup>-1</sup>	[NaBPh <sub>4</sub> ] / mol L <sup>-1</sup>	[Na <sup>+</sup> ] <sub>total</sub> / mol L <sup>-1</sup>	<i>k</i> <sub>obs</sub> / s <sup>-1</sup>
	3.69 × 10 <sup>-4</sup>				1.32 <sup>[a]</sup>
1.59 × 10 <sup>-5</sup>	3.69 × 10 <sup>-4</sup>	3.89 × 10 <sup>-4</sup>	1.80 × 10 <sup>-4</sup>	5.69 × 10 <sup>-4</sup>	0.950
1.59 × 10 <sup>-5</sup>	3.69 × 10 <sup>-4</sup>	3.89 × 10 <sup>-4</sup>	7.20 × 10 <sup>-4</sup>	1.11 × 10 <sup>-3</sup>	0.935
1.59 × 10 <sup>-5</sup>	3.69 × 10 <sup>-4</sup>	3.89 × 10 <sup>-4</sup>	1.32 × 10 <sup>-3</sup>	1.71 × 10 <sup>-3</sup>	0.909
1.59 × 10 <sup>-5</sup>	3.69 × 10 <sup>-4</sup>	3.89 × 10 <sup>-4</sup>	2.70 × 10 <sup>-3</sup>	3.09 × 10 <sup>-3</sup>	0.823
1.59 × 10 <sup>-5</sup>	3.69 × 10 <sup>-4</sup>	3.89 × 10 <sup>-4</sup>	4.41 × 10 <sup>-3</sup>	4.80 × 10 <sup>-3</sup>	0.757
1.59 × 10 <sup>-5</sup>	3.69 × 10 <sup>-4</sup>	3.89 × 10 <sup>-4</sup>	7.35 × 10 <sup>-3</sup>	7.74 × 10 <sup>-3</sup>	0.707
1.59 × 10 <sup>-5</sup>	3.69 × 10 <sup>-4</sup>	3.89 × 10 <sup>-4</sup>	1.18 × 10 <sup>-2</sup>	1.21 × 10 <sup>-2</sup>	0.652
1.59 × 10 <sup>-5</sup>	3.69 × 10 <sup>-4</sup>	3.89 × 10 <sup>-4</sup>	1.78 × 10 <sup>-2</sup>	1.82 × 10 <sup>-2</sup>	0.649

[a] Calculated from the second-order rate constants of the free anion (potassium salt in presence of 18-crown-6) given in Table 4.

Table 9: Pseudo-first-order rate constants for reaction of **1-Ph** (generated from (**1-Ph**)-H by addition of 1.06 equivalents of LiOtBu)<sup>[a]</sup> with **3n** at variable concentrations of LiBF<sub>4</sub> (20 °C, stopped-flow, at 486 nm).

[ <b>3n</b> ] / mol L <sup>-1</sup>	[ <b>1-Ph</b> ] / mol L <sup>-1</sup>	[LiOtBu] / mol L <sup>-1</sup>	[LiBF <sub>4</sub> ] / mol L <sup>-1</sup>	[Li <sup>+</sup> ] <sub>total</sub> / mol L <sup>-1</sup>	<i>k</i> <sub>obs</sub> / s <sup>-1</sup>
	4.39 × 10 <sup>-4</sup>				1.58 <sup>[a]</sup>
3.77 × 10 <sup>-5</sup>	4.39 × 10 <sup>-4</sup>	4.65 × 10 <sup>-4</sup>	0	4.65 × 10 <sup>-4</sup>	1.18
3.77 × 10 <sup>-5</sup>	4.39 × 10 <sup>-4</sup>	4.65 × 10 <sup>-4</sup>	9.03 × 10 <sup>-4</sup>	1.37 × 10 <sup>-3</sup>	1.10
3.77 × 10 <sup>-5</sup>	4.39 × 10 <sup>-4</sup>	4.65 × 10 <sup>-4</sup>	1.81 × 10 <sup>-3</sup>	2.27 × 10 <sup>-3</sup>	0.976
3.77 × 10 <sup>-5</sup>	4.39 × 10 <sup>-4</sup>	4.65 × 10 <sup>-4</sup>	3.61 × 10 <sup>-3</sup>	4.08 × 10 <sup>-3</sup>	0.871
3.77 × 10 <sup>-5</sup>	4.39 × 10 <sup>-4</sup>	4.65 × 10 <sup>-4</sup>	7.23 × 10 <sup>-3</sup>	7.69 × 10 <sup>-3</sup>	0.688
3.77 × 10 <sup>-5</sup>	4.39 × 10 <sup>-4</sup>	4.65 × 10 <sup>-4</sup>	1.08 × 10 <sup>-2</sup>	1.13 × 10 <sup>-2</sup>	0.616
3.77 × 10 <sup>-5</sup>	4.39 × 10 <sup>-4</sup>	4.65 × 10 <sup>-4</sup>	1.69 × 10 <sup>-2</sup>	1.74 × 10 <sup>-2</sup>	0.480
3.77 × 10 <sup>-5</sup>	4.39 × 10 <sup>-4</sup>	4.65 × 10 <sup>-4</sup>	2.62 × 10 <sup>-2</sup>	2.66 × 10 <sup>-2</sup>	0.333
3.77 × 10 <sup>-5</sup>	4.39 × 10 <sup>-4</sup>	4.65 × 10 <sup>-4</sup>	4.25 × 10 <sup>-2</sup>	4.30 × 10 <sup>-2</sup>	0.178
3.77 × 10 <sup>-5</sup>	4.39 × 10 <sup>-4</sup>	4.65 × 10 <sup>-4</sup>	5.88 × 10 <sup>-2</sup>	5.93 × 10 <sup>-2</sup>	0.145

[a] Calculated from the second-order rate constants of the free anion (potassium salt in presence of 18-crown-6) given in Table 4.

Table 10: Pseudo-first-order rate constants for reaction of **1-Ph** (generated from (**1-Ph**)-H by addition of 1.06 equivalents of LiOtBu)<sup>[a]</sup> with **3n** at variable concentrations of LiCl (20 °C, stopped-flow, at 486 nm).

[ <b>3n</b> ] / mol L <sup>-1</sup>	[ <b>1-Ph</b> ] / mol L <sup>-1</sup>	[LiOtBu] / mol L <sup>-1</sup>	[LiCl] / mol L <sup>-1</sup>	[Li <sup>+</sup> ] <sub>total</sub> / mol L <sup>-1</sup>	<i>k</i> <sub>obs</sub> / s <sup>-1</sup>
2.19 × 10 <sup>-5</sup>	9.53 × 10 <sup>-4</sup>				3.42 <sup>[a]</sup>
2.19 × 10 <sup>-5</sup>	9.53 × 10 <sup>-4</sup>	1.01 × 10 <sup>-3</sup>	0	1.01 × 10 <sup>-3</sup>	2.47
2.19 × 10 <sup>-5</sup>	9.53 × 10 <sup>-4</sup>	1.01 × 10 <sup>-3</sup>	5.04 × 10 <sup>-4</sup>	1.51 × 10 <sup>-3</sup>	2.52
2.19 × 10 <sup>-5</sup>	9.53 × 10 <sup>-4</sup>	1.01 × 10 <sup>-3</sup>	1.01 × 10 <sup>-3</sup>	2.01 × 10 <sup>-3</sup>	2.47
2.19 × 10 <sup>-5</sup>	9.53 × 10 <sup>-4</sup>	1.01 × 10 <sup>-3</sup>	2.20 × 10 <sup>-3</sup>	3.21 × 10 <sup>-3</sup>	2.18
2.19 × 10 <sup>-5</sup>	9.53 × 10 <sup>-4</sup>	1.01 × 10 <sup>-3</sup>	5.04 × 10 <sup>-3</sup>	6.05 × 10 <sup>-3</sup>	1.87
2.19 × 10 <sup>-5</sup>	9.53 × 10 <sup>-4</sup>	1.01 × 10 <sup>-3</sup>	1.01 × 10 <sup>-2</sup>	1.11 × 10 <sup>-2</sup>	1.43
2.19 × 10 <sup>-5</sup>	9.53 × 10 <sup>-4</sup>	1.01 × 10 <sup>-3</sup>	2.01 × 10 <sup>-2</sup>	2.12 × 10 <sup>-2</sup>	1.04
2.19 × 10 <sup>-5</sup>	9.53 × 10 <sup>-4</sup>	1.01 × 10 <sup>-3</sup>	3.36 × 10 <sup>-2</sup>	3.46 × 10 <sup>-2</sup>	0.820
2.19 × 10 <sup>-5</sup>	9.53 × 10 <sup>-4</sup>	1.01 × 10 <sup>-3</sup>	5.04 × 10 <sup>-2</sup>	5.14 × 10 <sup>-2</sup>	0.706
2.19 × 10 <sup>-5</sup>	9.53 × 10 <sup>-4</sup>	1.01 × 10 <sup>-3</sup>	7.55 × 10 <sup>-2</sup>	7.65 × 10 <sup>-2</sup>	0.508

[a] Calculated from the second-order rate constants of the free anion (potassium salt in presence of 18-crown-6) given in Table 4.

Table 11: Pseudo-first-order rate constants for reaction of **1-CONEt<sub>2</sub>** with **3g** at variable concentrations of KBPh<sub>4</sub> (20 °C, stopped-flow, at 422 nm).

[ <b>3g</b> ] / mol L <sup>-1</sup>	[ <b>1-CONEt<sub>2</sub></b> ] / mol L <sup>-1</sup>	[KBPh <sub>4</sub> ] / mol L <sup>-1</sup>	[K <sup>+</sup> ] <sub>total</sub> / mol L <sup>-1</sup>	<i>k</i> <sub>obs</sub> / s <sup>-1</sup>
	7.22 × 10 <sup>-4</sup>	0		33.1 <sup>[a]</sup>
1.51 × 10 <sup>-5</sup>	7.22 × 10 <sup>-4</sup>	0	7.22 × 10 <sup>-4</sup>	26.6
1.51 × 10 <sup>-5</sup>	7.22 × 10 <sup>-4</sup>	1.84 × 10 <sup>-4</sup>	9.06 × 10 <sup>-4</sup>	22.3
1.51 × 10 <sup>-5</sup>	7.22 × 10 <sup>-4</sup>	3.68 × 10 <sup>-4</sup>	1.09 × 10 <sup>-3</sup>	19.4
1.51 × 10 <sup>-5</sup>	7.22 × 10 <sup>-4</sup>	7.37 × 10 <sup>-4</sup>	1.46 × 10 <sup>-3</sup>	15.1
1.51 × 10 <sup>-5</sup>	7.22 × 10 <sup>-4</sup>	1.47 × 10 <sup>-3</sup>	2.20 × 10 <sup>-3</sup>	10.6
1.51 × 10 <sup>-5</sup>	7.22 × 10 <sup>-4</sup>	2.46 × 10 <sup>-3</sup>	3.18 × 10 <sup>-3</sup>	7.93
1.51 × 10 <sup>-5</sup>	7.22 × 10 <sup>-4</sup>	3.78 × 10 <sup>-3</sup>	4.50 × 10 <sup>-3</sup>	6.33
1.51 × 10 <sup>-5</sup>	7.22 × 10 <sup>-4</sup>	6.29 × 10 <sup>-3</sup>	7.01 × 10 <sup>-3</sup>	4.86
1.51 × 10 <sup>-5</sup>	7.22 × 10 <sup>-4</sup>	8.81 × 10 <sup>-3</sup>	9.53 × 10 <sup>-3</sup>	3.93
1.51 × 10 <sup>-5</sup>	7.22 × 10 <sup>-4</sup>	1.13 × 10 <sup>-2</sup>	1.20 × 10 <sup>-2</sup>	3.17
1.51 × 10 <sup>-5</sup>	7.22 × 10 <sup>-4</sup>	1.64 × 10 <sup>-2</sup>	1.71 × 10 <sup>-2</sup>	3.07
1.51 × 10 <sup>-5</sup>	7.22 × 10 <sup>-4</sup>	2.13 × 10 <sup>-2</sup>	2.20 × 10 <sup>-2</sup>	3.06

[a] Calculated from the second-order rate constants of the free anion (potassium salt in presence of 18-crown-6) given in Table 4.

Table 12: Pseudo-first-order rate constants for reaction of **1-CO<sub>2</sub>Et** with **3f** at variable concentrations of KBPh<sub>4</sub> (20 °C, stopped-flow, at 630 nm).

[ <b>3f</b> ] / mol L <sup>-1</sup>	[ <b>1-CO<sub>2</sub>Et</b> ] / mol L <sup>-1</sup>	[KBPh <sub>4</sub> ] / mol L <sup>-1</sup>	[K <sup>+</sup> ] <sub>total</sub> / mol L <sup>-1</sup>	<i>k</i> <sub>obs</sub> / s <sup>-1</sup>
	6.58 × 10 <sup>-4</sup>	0		282 <sup>[a]</sup>
1.50 × 10 <sup>-5</sup>	6.58 × 10 <sup>-4</sup>	0	6.58 × 10 <sup>-4</sup>	280
1.50 × 10 <sup>-5</sup>	6.58 × 10 <sup>-4</sup>	2.10 × 10 <sup>-4</sup>	8.68 × 10 <sup>-4</sup>	260
1.50 × 10 <sup>-5</sup>	6.58 × 10 <sup>-4</sup>	4.20 × 10 <sup>-4</sup>	1.08 × 10 <sup>-3</sup>	241
1.50 × 10 <sup>-5</sup>	6.58 × 10 <sup>-4</sup>	9.81 × 10 <sup>-4</sup>	1.64 × 10 <sup>-3</sup>	210
1.50 × 10 <sup>-5</sup>	6.58 × 10 <sup>-4</sup>	1.75 × 10 <sup>-3</sup>	2.41 × 10 <sup>-3</sup>	175
1.50 × 10 <sup>-5</sup>	6.58 × 10 <sup>-4</sup>	2.80 × 10 <sup>-3</sup>	3.46 × 10 <sup>-3</sup>	136
1.50 × 10 <sup>-5</sup>	6.58 × 10 <sup>-4</sup>	4.34 × 10 <sup>-3</sup>	5.00 × 10 <sup>-3</sup>	111
1.50 × 10 <sup>-5</sup>	6.58 × 10 <sup>-4</sup>	7.23 × 10 <sup>-3</sup>	7.89 × 10 <sup>-3</sup>	82.1
1.50 × 10 <sup>-5</sup>	6.58 × 10 <sup>-4</sup>	1.01 × 10 <sup>-2</sup>	1.08 × 10 <sup>-2</sup>	65.2
1.50 × 10 <sup>-5</sup>	6.58 × 10 <sup>-4</sup>	1.30 × 10 <sup>-2</sup>	1.37 × 10 <sup>-2</sup>	55.0
1.50 × 10 <sup>-5</sup>	6.58 × 10 <sup>-4</sup>	1.99 × 10 <sup>-2</sup>	2.08 × 10 <sup>-2</sup>	41.9

[a] Calculated from the second-order rate constants of the free anion (potassium salt in presence of 18-crown-6) given in Table 4.



Table 13: Pseudo-first-order rate constants for reaction of **1-CO<sub>2</sub>Et** with **3f** at variable concentrations of KOTf (20 °C, stopped-flow, at 630 nm).

[ <b>3f</b> ] / mol L <sup>-1</sup>	[ <b>1-CO<sub>2</sub>Et</b> ] / mol L <sup>-1</sup>	[KOTf] / mol L <sup>-1</sup>	[K <sup>+</sup> ] <sub>total</sub> / mol L <sup>-1</sup>	<i>k</i> <sub>obs</sub> / s <sup>-1</sup>
	6.56 × 10 <sup>-4</sup>			281 [a]
1.34 × 10 <sup>-5</sup>	6.56 × 10 <sup>-4</sup>	0	6.56 × 10 <sup>-4</sup>	273
1.34 × 10 <sup>-5</sup>	6.56 × 10 <sup>-4</sup>	2.08 × 10 <sup>-4</sup>	8.63 × 10 <sup>-4</sup>	236
1.34 × 10 <sup>-5</sup>	6.56 × 10 <sup>-4</sup>	4.16 × 10 <sup>-4</sup>	1.07 × 10 <sup>-3</sup>	219
1.34 × 10 <sup>-5</sup>	6.56 × 10 <sup>-4</sup>	1.04 × 10 <sup>-3</sup>	1.69 × 10 <sup>-3</sup>	178
1.34 × 10 <sup>-5</sup>	6.56 × 10 <sup>-4</sup>	2.49 × 10 <sup>-3</sup>	3.15 × 10 <sup>-3</sup>	131
1.34 × 10 <sup>-5</sup>	6.56 × 10 <sup>-4</sup>	3.74 × 10 <sup>-3</sup>	4.40 × 10 <sup>-3</sup>	107
1.34 × 10 <sup>-5</sup>	6.56 × 10 <sup>-4</sup>	5.67 × 10 <sup>-3</sup>	6.32 × 10 <sup>-3</sup>	82.9
1.34 × 10 <sup>-5</sup>	6.56 × 10 <sup>-4</sup>	9.44 × 10 <sup>-3</sup>	1.01 × 10 <sup>-2</sup>	61.0
1.34 × 10 <sup>-5</sup>	6.56 × 10 <sup>-4</sup>	1.32 × 10 <sup>-2</sup>	1.39 × 10 <sup>-2</sup>	50.0
1.34 × 10 <sup>-5</sup>	6.56 × 10 <sup>-4</sup>	1.70 × 10 <sup>-2</sup>	1.77 × 10 <sup>-2</sup>	43.1

[a] Calculated from the second-order rate constants of the free anion (potassium salt in presence of 18-crown-6) given in Table 4.

Table 14: Pseudo-first-order rate constants for reaction of **1-CO<sub>2</sub>Et** (generated from (**1-CO<sub>2</sub>Et**)-H by addition of 1.03 equivalents of NaOtBu)<sup>[a]</sup> with **3f** at variable concentrations of NaBPh<sub>4</sub> (20 °C, stopped-flow, at 630 nm).

[ <b>3f</b> ] / mol L <sup>-1</sup>	[ <b>1-CO<sub>2</sub>Et</b> ] / mol L <sup>-1</sup>	[NaOtBu] / mol L <sup>-1</sup>	[NaBPh <sub>4</sub> ] / mol L <sup>-1</sup>	[Na <sup>+</sup> ] <sub>total</sub> / mol L <sup>-1</sup>	<i>k</i> <sub>obs</sub> / s <sup>-1</sup>
	5.34 × 10 <sup>-4</sup>				229 [a]
1.42 × 10 <sup>-5</sup>	5.34 × 10 <sup>-4</sup>	5.51 × 10 <sup>-4</sup>	1.30 × 10 <sup>-4</sup>	6.81 × 10 <sup>-4</sup>	114
1.42 × 10 <sup>-5</sup>	5.34 × 10 <sup>-4</sup>	5.51 × 10 <sup>-4</sup>	2.59 × 10 <sup>-4</sup>	8.10 × 10 <sup>-4</sup>	95.0
1.42 × 10 <sup>-5</sup>	5.34 × 10 <sup>-4</sup>	5.51 × 10 <sup>-4</sup>	6.49 × 10 <sup>-4</sup>	1.20 × 10 <sup>-3</sup>	64.3
1.42 × 10 <sup>-5</sup>	5.34 × 10 <sup>-4</sup>	5.51 × 10 <sup>-4</sup>	1.30 × 10 <sup>-3</sup>	1.85 × 10 <sup>-3</sup>	41.9
1.42 × 10 <sup>-5</sup>	5.34 × 10 <sup>-4</sup>	5.51 × 10 <sup>-4</sup>	2.59 × 10 <sup>-3</sup>	3.15 × 10 <sup>-3</sup>	26.9
1.42 × 10 <sup>-5</sup>	5.34 × 10 <sup>-4</sup>	5.51 × 10 <sup>-4</sup>	7.17 × 10 <sup>-3</sup>	7.72 × 10 <sup>-3</sup>	23.4
1.42 × 10 <sup>-5</sup>	5.34 × 10 <sup>-4</sup>	5.51 × 10 <sup>-4</sup>	1.43 × 10 <sup>-2</sup>	1.49 × 10 <sup>-2</sup>	15.7
1.42 × 10 <sup>-5</sup>	5.34 × 10 <sup>-4</sup>	5.51 × 10 <sup>-4</sup>	2.15 × 10 <sup>-2</sup>	2.21 × 10 <sup>-2</sup>	11.8
1.42 × 10 <sup>-5</sup>	5.34 × 10 <sup>-4</sup>	5.51 × 10 <sup>-4</sup>	3.23 × 10 <sup>-2</sup>	3.28 × 10 <sup>-2</sup>	11.0

[a] Calculated from the second-order rate constants of the free anion (potassium salt in presence of 18-crown-6) given in Table 4.

Table 15: Pseudo-first-order rate constants for reaction of **1-CO<sub>2</sub>Et** (generated from (**1-CO<sub>2</sub>Et**)-H by addition of 1.04 equivalents of LiOtBu)<sup>[a]</sup> with **3e** at variable concentrations of LiCl (20 °C, stopped-flow, at 635 nm).

[ <b>3e</b> ] / mol L <sup>-1</sup>	[ <b>1-CO<sub>2</sub>Et</b> ] / mol L <sup>-1</sup>	[LiOtBu] / mol L <sup>-1</sup>	[LiCl] / mol L <sup>-1</sup>	[Li <sup>+</sup> ] <sub>total</sub> / mol L <sup>-1</sup>	<i>k</i> <sub>obs</sub> / s <sup>-1</sup>
	6.48 × 10 <sup>-4</sup>				580 [a]
1.28 × 10 <sup>-5</sup>	6.48 × 10 <sup>-4</sup>	6.73 × 10 <sup>-4</sup>	0	6.73 × 10 <sup>-4</sup>	58.1
1.28 × 10 <sup>-5</sup>	6.48 × 10 <sup>-4</sup>	6.73 × 10 <sup>-4</sup>	1.76 × 10 <sup>-4</sup>	8.48 × 10 <sup>-4</sup>	33.5
1.28 × 10 <sup>-5</sup>	6.48 × 10 <sup>-4</sup>	6.73 × 10 <sup>-4</sup>	3.51 × 10 <sup>-4</sup>	1.02 × 10 <sup>-3</sup>	28.7
1.28 × 10 <sup>-5</sup>	6.48 × 10 <sup>-4</sup>	6.73 × 10 <sup>-4</sup>	7.03 × 10 <sup>-4</sup>	1.38 × 10 <sup>-3</sup>	24.7
1.28 × 10 <sup>-5</sup>	6.48 × 10 <sup>-4</sup>	6.73 × 10 <sup>-4</sup>	1.41 × 10 <sup>-3</sup>	2.08 × 10 <sup>-3</sup>	18.0
1.28 × 10 <sup>-5</sup>	6.48 × 10 <sup>-4</sup>	6.73 × 10 <sup>-4</sup>	2.81 × 10 <sup>-3</sup>	3.48 × 10 <sup>-3</sup>	11.7
1.28 × 10 <sup>-5</sup>	6.48 × 10 <sup>-4</sup>	6.73 × 10 <sup>-4</sup>	4.24 × 10 <sup>-3</sup>	4.91 × 10 <sup>-3</sup>	9.56
1.28 × 10 <sup>-5</sup>	6.48 × 10 <sup>-4</sup>	6.73 × 10 <sup>-4</sup>	6.78 × 10 <sup>-3</sup>	7.46 × 10 <sup>-3</sup>	7.04

[a] Calculated from the second-order rate constants of the free anion (potassium salt in presence of 18-crown-6) given in Table 4.

Table 16: Pseudo-first-order rate constants for reaction of **1-CN** with **3f** at variable concentrations of KBPh<sub>4</sub> (20 °C, stopped-flow, at 630 nm).

[ <b>3f</b> ] / mol L <sup>-1</sup>	[ <b>1-CN</b> ] / mol L <sup>-1</sup>	[KBPh <sub>4</sub> ] / mol L <sup>-1</sup>	[K <sup>+</sup> ] <sub>total</sub> / mol L <sup>-1</sup>	<i>k</i> <sub>obs</sub> / s <sup>-1</sup>
	2.71 × 10 <sup>-4</sup>			34.7 <sup>[a]</sup>
1.44 × 10 <sup>-5</sup>	2.71 × 10 <sup>-4</sup>	0	2.71 × 10 <sup>-4</sup>	26.1
1.44 × 10 <sup>-5</sup>	2.71 × 10 <sup>-4</sup>	1.24 × 10 <sup>-4</sup>	3.95 × 10 <sup>-4</sup>	25.1
1.44 × 10 <sup>-5</sup>	2.71 × 10 <sup>-4</sup>	2.49 × 10 <sup>-4</sup>	5.19 × 10 <sup>-4</sup>	24.7
1.44 × 10 <sup>-5</sup>	2.71 × 10 <sup>-4</sup>	4.98 × 10 <sup>-4</sup>	7.68 × 10 <sup>-4</sup>	23.6
1.44 × 10 <sup>-5</sup>	2.71 × 10 <sup>-4</sup>	1.24 × 10 <sup>-3</sup>	1.53 × 10 <sup>-3</sup>	22.3
1.44 × 10 <sup>-5</sup>	2.71 × 10 <sup>-4</sup>	2.49 × 10 <sup>-3</sup>	2.76 × 10 <sup>-3</sup>	20.7
1.44 × 10 <sup>-5</sup>	2.71 × 10 <sup>-4</sup>	4.90 × 10 <sup>-3</sup>	5.17 × 10 <sup>-3</sup>	19.7
1.44 × 10 <sup>-5</sup>	2.71 × 10 <sup>-4</sup>	7.35 × 10 <sup>-3</sup>	7.62 × 10 <sup>-3</sup>	18.2
1.44 × 10 <sup>-5</sup>	2.71 × 10 <sup>-4</sup>	1.10 × 10 <sup>-2</sup>	1.13 × 10 <sup>-2</sup>	17.0

[a] Calculated from the second-order rate constants of the free anion (potassium salt in presence of 18-crown-6) given in Table 4.

Table 17: Pseudo-first-order rate constants for reaction of **1-COMe**<sup>[a]</sup> with **3f** at variable concentrations of KBPh<sub>4</sub> (20 °C, stopped-flow, at 630 nm).

[ <b>3f</b> ] / mol L <sup>-1</sup>	[ <b>1-COMe</b> ] / mol L <sup>-1</sup>	[KBPh <sub>4</sub> ] / mol L <sup>-1</sup>	[K <sup>+</sup> ] <sub>total</sub> / mol L <sup>-1</sup>	<i>k</i> <sub>obs</sub> / s <sup>-1</sup>
	7.88 × 10 <sup>-4</sup>			96.1 <sup>[a]</sup>
1.50 × 10 <sup>-5</sup>	7.88 × 10 <sup>-4</sup>	0	7.88 × 10 <sup>-4</sup>	97.3
1.50 × 10 <sup>-5</sup>	7.88 × 10 <sup>-4</sup>	2.13 × 10 <sup>-4</sup>	1.00 × 10 <sup>-3</sup>	93.3
1.50 × 10 <sup>-5</sup>	7.88 × 10 <sup>-4</sup>	4.26 × 10 <sup>-4</sup>	1.21 × 10 <sup>-3</sup>	92.2
1.50 × 10 <sup>-5</sup>	7.88 × 10 <sup>-4</sup>	9.94 × 10 <sup>-4</sup>	1.78 × 10 <sup>-3</sup>	86.8
1.50 × 10 <sup>-5</sup>	7.88 × 10 <sup>-4</sup>	1.78 × 10 <sup>-3</sup>	2.56 × 10 <sup>-3</sup>	82.1
1.50 × 10 <sup>-5</sup>	7.88 × 10 <sup>-4</sup>	2.84 × 10 <sup>-3</sup>	3.63 × 10 <sup>-3</sup>	77.2
1.50 × 10 <sup>-5</sup>	7.88 × 10 <sup>-4</sup>	4.16 × 10 <sup>-3</sup>	4.95 × 10 <sup>-3</sup>	71.0
1.50 × 10 <sup>-5</sup>	7.88 × 10 <sup>-4</sup>	6.93 × 10 <sup>-3</sup>	7.72 × 10 <sup>-3</sup>	65.0
1.50 × 10 <sup>-5</sup>	7.88 × 10 <sup>-4</sup>	9.70 × 10 <sup>-3</sup>	1.05 × 10 <sup>-2</sup>	59.1
1.50 × 10 <sup>-5</sup>	7.88 × 10 <sup>-4</sup>	1.25 × 10 <sup>-2</sup>	1.33 × 10 <sup>-2</sup>	53.6

[a] Calculated from the second-order rate constants of the free anion (potassium salt in presence of 18-crown-6) given in Table 4.

Table 18: Pseudo-first-order rate constants for reaction of **1-COMe** with **3f** at variable concentrations of KOTf (20 °C, stopped-flow, at 630 nm).

[ <b>3f</b> ] / mol L <sup>-1</sup>	[ <b>1-COMe</b> ] / mol L <sup>-1</sup>	[KOTf] / mol L <sup>-1</sup>	[K <sup>+</sup> ] <sub>total</sub> / mol L <sup>-1</sup>	<i>k</i> <sub>obs</sub> / s <sup>-1</sup>
1.34 × 10 <sup>-5</sup>	6.59 × 10 <sup>-4</sup>			80.3 <sup>[a]</sup>
1.34 × 10 <sup>-5</sup>	6.59 × 10 <sup>-4</sup>	0	6.59 × 10 <sup>-4</sup>	78.5
1.34 × 10 <sup>-5</sup>	6.59 × 10 <sup>-4</sup>	2.20 × 10 <sup>-4</sup>	8.79 × 10 <sup>-4</sup>	79.8
1.34 × 10 <sup>-5</sup>	6.59 × 10 <sup>-4</sup>	4.40 × 10 <sup>-4</sup>	1.10 × 10 <sup>-3</sup>	78.8
1.34 × 10 <sup>-5</sup>	6.59 × 10 <sup>-4</sup>	8.80 × 10 <sup>-4</sup>	1.54 × 10 <sup>-3</sup>	75.6
1.34 × 10 <sup>-5</sup>	6.59 × 10 <sup>-4</sup>	1.83 × 10 <sup>-3</sup>	2.49 × 10 <sup>-3</sup>	71.0
1.34 × 10 <sup>-5</sup>	6.59 × 10 <sup>-4</sup>	2.93 × 10 <sup>-3</sup>	3.59 × 10 <sup>-3</sup>	66.1
1.34 × 10 <sup>-5</sup>	6.59 × 10 <sup>-4</sup>	4.65 × 10 <sup>-3</sup>	5.31 × 10 <sup>-3</sup>	60.4
1.34 × 10 <sup>-5</sup>	6.59 × 10 <sup>-4</sup>	7.75 × 10 <sup>-3</sup>	8.41 × 10 <sup>-3</sup>	53.3
1.34 × 10 <sup>-5</sup>	6.59 × 10 <sup>-4</sup>	1.08 × 10 <sup>-2</sup>	1.15 × 10 <sup>-2</sup>	48.8
1.34 × 10 <sup>-5</sup>	6.59 × 10 <sup>-4</sup>	1.39 × 10 <sup>-2</sup>	1.46 × 10 <sup>-2</sup>	44.1

[a] Calculated from the second-order rate constants of the free anion (potassium salt in presence of 18-crown-6) given in Table 4.

Table 19: Pseudo-first-order rate constants for reaction of **1-COPh** with **3f** at variable concentrations of KBPh<sub>4</sub> (20 °C, stopped-flow, at 630 nm).

[ <b>3f</b> ] / mol L <sup>-1</sup>	[ <b>1-COPh</b> ] / mol L <sup>-1</sup>	[KBPh <sub>4</sub> ] / mol L <sup>-1</sup>	[K <sup>+</sup> ] <sub>total</sub> / mol L <sup>-1</sup>	<i>k</i> <sub>obs</sub> / s <sup>-1</sup>
	5.38 × 10 <sup>-4</sup>			35.0 <sup>[a]</sup>
1.27 × 10 <sup>-5</sup>	5.38 × 10 <sup>-4</sup>	0	5.38 × 10 <sup>-4</sup>	32.5
1.27 × 10 <sup>-5</sup>	5.38 × 10 <sup>-4</sup>	1.23 × 10 <sup>-4</sup>	6.61 × 10 <sup>-4</sup>	30.3
1.27 × 10 <sup>-5</sup>	5.38 × 10 <sup>-4</sup>	3.08 × 10 <sup>-4</sup>	8.46 × 10 <sup>-4</sup>	27.5
1.27 × 10 <sup>-5</sup>	5.38 × 10 <sup>-4</sup>	6.17 × 10 <sup>-4</sup>	1.15 × 10 <sup>-3</sup>	24.6
1.27 × 10 <sup>-5</sup>	5.38 × 10 <sup>-4</sup>	1.23 × 10 <sup>-3</sup>	1.77 × 10 <sup>-3</sup>	20.1
1.27 × 10 <sup>-5</sup>	5.38 × 10 <sup>-4</sup>	2.10 × 10 <sup>-3</sup>	2.64 × 10 <sup>-3</sup>	15.5
1.27 × 10 <sup>-5</sup>	5.38 × 10 <sup>-4</sup>	3.25 × 10 <sup>-3</sup>	3.79 × 10 <sup>-3</sup>	14.1
1.27 × 10 <sup>-5</sup>	5.38 × 10 <sup>-4</sup>	4.55 × 10 <sup>-3</sup>	5.09 × 10 <sup>-3</sup>	13.4
1.27 × 10 <sup>-5</sup>	5.38 × 10 <sup>-4</sup>	5.85 × 10 <sup>-3</sup>	6.39 × 10 <sup>-3</sup>	13.3

[a] Calculated from the second-order rate constants of the free anion (potassium salt in presence of 18-crown-6) given in Table 4.

Table 20: Pseudo-first-order rate constants for reaction of **1-SO<sub>2</sub>Ph** with **3b** at variable concentrations of KBPh<sub>4</sub> (20 °C, stopped-flow, at 620 nm).

[ <b>3b</b> ] / mol L <sup>-1</sup>	[ <b>1-SO<sub>2</sub>Ph</b> ] / mol L <sup>-1</sup>	[KBPh <sub>4</sub> ] / mol L <sup>-1</sup>	[K <sup>+</sup> ] <sub>total</sub> / mol L <sup>-1</sup>	<i>k</i> <sub>obs</sub> / s <sup>-1</sup>
	3.23 × 10 <sup>-4</sup>			73.3 <sup>[a]</sup>
1.10 × 10 <sup>-5</sup>	3.23 × 10 <sup>-4</sup>	0	3.23 × 10 <sup>-4</sup>	75.4
1.10 × 10 <sup>-5</sup>	3.23 × 10 <sup>-4</sup>	1.25 × 10 <sup>-4</sup>	4.48 × 10 <sup>-4</sup>	71.2
1.10 × 10 <sup>-5</sup>	3.23 × 10 <sup>-4</sup>	2.50 × 10 <sup>-4</sup>	5.73 × 10 <sup>-4</sup>	68.1
1.10 × 10 <sup>-5</sup>	3.23 × 10 <sup>-4</sup>	5.00 × 10 <sup>-4</sup>	8.23 × 10 <sup>-4</sup>	63.5
1.10 × 10 <sup>-5</sup>	3.23 × 10 <sup>-4</sup>	1.06 × 10 <sup>-3</sup>	1.39 × 10 <sup>-3</sup>	61.6
1.10 × 10 <sup>-5</sup>	3.23 × 10 <sup>-4</sup>	2.50 × 10 <sup>-3</sup>	2.82 × 10 <sup>-3</sup>	54.7
1.10 × 10 <sup>-5</sup>	3.23 × 10 <sup>-4</sup>	4.25 × 10 <sup>-3</sup>	4.57 × 10 <sup>-3</sup>	49.0
1.10 × 10 <sup>-5</sup>	3.23 × 10 <sup>-4</sup>	6.37 × 10 <sup>-3</sup>	6.70 × 10 <sup>-3</sup>	46.1
1.10 × 10 <sup>-5</sup>	3.23 × 10 <sup>-4</sup>	9.56 × 10 <sup>-3</sup>	9.88 × 10 <sup>-3</sup>	42.5

[a] Calculated from the second-order rate constants of the free anion (potassium salt in presence of 18-crown-6) given in Table 4.

Table 21: Pseudo-first-order rate constants for reaction of **1-NO<sub>2</sub>** with **3d** at variable concentrations of KBPh<sub>4</sub> (20 °C, stopped-flow, at 627 nm).

[ <b>3d</b> ] / mol L <sup>-1</sup>	[ <b>1-NO<sub>2</sub></b> ] / mol L <sup>-1</sup>	[KBPh <sub>4</sub> ] / mol L <sup>-1</sup>	[K <sup>+</sup> ] <sub>total</sub> / mol L <sup>-1</sup>	<i>k</i> <sub>obs</sub> / s <sup>-1</sup>
	3.29 × 10 <sup>-4</sup>			2.01 <sup>[a]</sup>
1.31 × 10 <sup>-5</sup>	3.29 × 10 <sup>-4</sup>	0	3.29 × 10 <sup>-4</sup>	2.05
1.31 × 10 <sup>-5</sup>	3.29 × 10 <sup>-4</sup>	1.27 × 10 <sup>-4</sup>	4.56 × 10 <sup>-4</sup>	2.14
1.31 × 10 <sup>-5</sup>	3.29 × 10 <sup>-4</sup>	2.54 × 10 <sup>-4</sup>	5.83 × 10 <sup>-4</sup>	2.18
1.31 × 10 <sup>-5</sup>	3.29 × 10 <sup>-4</sup>	5.08 × 10 <sup>-4</sup>	8.37 × 10 <sup>-4</sup>	2.07
1.31 × 10 <sup>-5</sup>	3.29 × 10 <sup>-4</sup>	1.24 × 10 <sup>-3</sup>	1.57 × 10 <sup>-3</sup>	1.86
1.31 × 10 <sup>-5</sup>	3.29 × 10 <sup>-4</sup>	2.54 × 10 <sup>-3</sup>	2.87 × 10 <sup>-3</sup>	1.75
1.31 × 10 <sup>-5</sup>	3.29 × 10 <sup>-4</sup>	4.95 × 10 <sup>-3</sup>	5.28 × 10 <sup>-3</sup>	1.37
1.31 × 10 <sup>-5</sup>	3.29 × 10 <sup>-4</sup>	7.42 × 10 <sup>-3</sup>	7.75 × 10 <sup>-3</sup>	1.21
1.31 × 10 <sup>-5</sup>	3.29 × 10 <sup>-4</sup>	1.11 × 10 <sup>-2</sup>	1.15 × 10 <sup>-2</sup>	1.07

[a] Calculated from the second-order rate constants of the free anion (potassium salt in presence of 18-crown-6) given in Table 4.

Table 22: Pseudo-first-order rate constants for reaction of **2-CO<sub>2</sub>Et** (generated from **(2-CO<sub>2</sub>Et)-H** by addition of 1.03 equivalents of KO<sup>t</sup>Bu) with **3n** at variable concentrations of KBPh<sub>4</sub> (20 °C, stopped-flow, at 486 nm).

[ <b>3n</b> ] / mol L <sup>-1</sup>	[ <b>2-CO<sub>2</sub>Et</b> ] / mol L <sup>-1</sup>	[KO <sup>t</sup> Bu] / mol L <sup>-1</sup>	[KBPh <sub>4</sub> ] / mol L <sup>-1</sup>	[K <sup>+</sup> ] <sub>total</sub> / mol L <sup>-1</sup>	<i>k</i> <sub>obs</sub> / s <sup>-1</sup>
	2.45 × 10 <sup>-4</sup>				135 <sup>[a]</sup>
1.59 × 10 <sup>-5</sup>	2.45 × 10 <sup>-4</sup>	3.30 × 10 <sup>-4</sup>	0	3.30 × 10 <sup>-4</sup>	132
1.59 × 10 <sup>-5</sup>	2.45 × 10 <sup>-4</sup>	3.30 × 10 <sup>-4</sup>	1.51 × 10 <sup>-4</sup>	4.81 × 10 <sup>-4</sup>	131
1.59 × 10 <sup>-5</sup>	2.45 × 10 <sup>-4</sup>	3.30 × 10 <sup>-4</sup>	3.03 × 10 <sup>-4</sup>	6.33 × 10 <sup>-4</sup>	129
1.59 × 10 <sup>-5</sup>	2.45 × 10 <sup>-4</sup>	3.30 × 10 <sup>-4</sup>	6.05 × 10 <sup>-4</sup>	9.35 × 10 <sup>-4</sup>	127
1.59 × 10 <sup>-5</sup>	2.45 × 10 <sup>-4</sup>	3.30 × 10 <sup>-4</sup>	1.16 × 10 <sup>-3</sup>	1.49 × 10 <sup>-3</sup>	125
1.59 × 10 <sup>-5</sup>	2.45 × 10 <sup>-4</sup>	3.30 × 10 <sup>-4</sup>	3.03 × 10 <sup>-3</sup>	3.36 × 10 <sup>-3</sup>	120
1.59 × 10 <sup>-5</sup>	2.45 × 10 <sup>-4</sup>	3.30 × 10 <sup>-4</sup>	5.78 × 10 <sup>-3</sup>	6.11 × 10 <sup>-3</sup>	117
1.59 × 10 <sup>-5</sup>	2.45 × 10 <sup>-4</sup>	3.30 × 10 <sup>-4</sup>	8.68 × 10 <sup>-3</sup>	9.01 × 10 <sup>-3</sup>	115
1.59 × 10 <sup>-5</sup>	2.45 × 10 <sup>-4</sup>	3.30 × 10 <sup>-4</sup>	1.30 × 10 <sup>-2</sup>	1.33 × 10 <sup>-2</sup>	111

[a] Calculated from the second-order rate constants of the free anion (potassium salt in presence of 18-crown-6) given in ref.<sup>[2g]</sup>

Table 23: Pseudo-first-order rate constants for reaction of **7a** with **3f** at variable concentrations of KBPh<sub>4</sub> (20 °C, stopped-flow, at 630 nm).

[ <b>3f</b> ] / mol L <sup>-1</sup>	[ <b>7a</b> ] / mol L <sup>-1</sup>	[KBPh <sub>4</sub> ] / mol L <sup>-1</sup>	[K <sup>+</sup> ] <sub>total</sub> / mol L <sup>-1</sup>	<i>k</i> <sub>obs</sub> / s <sup>-1</sup>
	2.72 × 10 <sup>-4</sup>			89.5 <sup>[a]</sup>
1.39 × 10 <sup>-5</sup>	2.72 × 10 <sup>-4</sup>	0	2.72 × 10 <sup>-4</sup>	73.8
1.39 × 10 <sup>-5</sup>	2.72 × 10 <sup>-4</sup>	1.25 × 10 <sup>-4</sup>	3.97 × 10 <sup>-4</sup>	76.8
1.39 × 10 <sup>-5</sup>	2.72 × 10 <sup>-4</sup>	2.50 × 10 <sup>-4</sup>	5.22 × 10 <sup>-4</sup>	71.0
1.39 × 10 <sup>-5</sup>	2.72 × 10 <sup>-4</sup>	5.00 × 10 <sup>-4</sup>	7.73 × 10 <sup>-4</sup>	68.1
1.39 × 10 <sup>-5</sup>	2.72 × 10 <sup>-4</sup>	1.23 × 10 <sup>-3</sup>	1.50 × 10 <sup>-3</sup>	63.1
1.39 × 10 <sup>-5</sup>	2.72 × 10 <sup>-4</sup>	2.50 × 10 <sup>-3</sup>	2.77 × 10 <sup>-3</sup>	58.3
1.39 × 10 <sup>-5</sup>	2.72 × 10 <sup>-4</sup>	4.92 × 10 <sup>-3</sup>	5.20 × 10 <sup>-3</sup>	49.0
1.39 × 10 <sup>-5</sup>	2.72 × 10 <sup>-4</sup>	7.38 × 10 <sup>-3</sup>	7.66 × 10 <sup>-3</sup>	44.0
1.39 × 10 <sup>-5</sup>	2.72 × 10 <sup>-4</sup>	1.11 × 10 <sup>-2</sup>	1.13 × 10 <sup>-2</sup>	39.2
1.39 × 10 <sup>-5</sup>	2.72 × 10 <sup>-4</sup>	1.69 × 10 <sup>-2</sup>	1.71 × 10 <sup>-2</sup>	35.4

[a] Calculated from the second-order rate constants of the free anion (potassium salt in presence of 18-crown-6) given in ref.<sup>[3c]</sup>

Table 24: Pseudo-first-order rate constants for reaction of **7b** with **3f** at variable concentrations of KBPh<sub>4</sub> (20 °C, stopped-flow, at 630 nm).

[ <b>3f</b> ] / mol L <sup>-1</sup>	[ <b>7b</b> ] / mol L <sup>-1</sup>	[KBPh <sub>4</sub> ] / mol L <sup>-1</sup>	[K <sup>+</sup> ] <sub>total</sub> / mol L <sup>-1</sup>	<i>k</i> <sub>obs</sub> / s <sup>-1</sup>
	3.08 × 10 <sup>-4</sup>			18.7 <sup>[a]</sup>
1.37 × 10 <sup>-5</sup>	3.08 × 10 <sup>-4</sup>	0	3.08 × 10 <sup>-4</sup>	18.1
1.37 × 10 <sup>-5</sup>	3.08 × 10 <sup>-4</sup>	1.26 × 10 <sup>-4</sup>	4.34 × 10 <sup>-4</sup>	17.9
1.37 × 10 <sup>-5</sup>	3.08 × 10 <sup>-4</sup>	2.52 × 10 <sup>-4</sup>	5.60 × 10 <sup>-4</sup>	17.7
1.37 × 10 <sup>-5</sup>	3.08 × 10 <sup>-4</sup>	5.05 × 10 <sup>-4</sup>	8.13 × 10 <sup>-4</sup>	17.3
1.37 × 10 <sup>-5</sup>	3.08 × 10 <sup>-4</sup>	1.23 × 10 <sup>-3</sup>	1.54 × 10 <sup>-3</sup>	16.7
1.37 × 10 <sup>-5</sup>	3.08 × 10 <sup>-4</sup>	2.52 × 10 <sup>-3</sup>	2.83 × 10 <sup>-3</sup>	15.5
1.37 × 10 <sup>-5</sup>	3.08 × 10 <sup>-4</sup>	4.93 × 10 <sup>-3</sup>	5.24 × 10 <sup>-3</sup>	14.5
1.37 × 10 <sup>-5</sup>	3.08 × 10 <sup>-4</sup>	7.39 × 10 <sup>-3</sup>	7.70 × 10 <sup>-3</sup>	13.8
1.37 × 10 <sup>-5</sup>	3.08 × 10 <sup>-4</sup>	1.11 × 10 <sup>-2</sup>	1.14 × 10 <sup>-2</sup>	13.6

[a] Calculated from the second-order rate constants of the free anion (potassium salt in presence of 18-crown-6) given in ref.<sup>[3c]</sup>

Table 25: Pseudo-first-order rate constants for reaction of **8-CO<sub>2</sub>Et** with **3h** at variable concentrations of KBPh<sub>4</sub> (20 °C, stopped-flow, at 533 nm).

[ <b>3h</b> ] / mol L <sup>-1</sup>	[ <b>8-CO<sub>2</sub>Et</b> ] / mol L <sup>-1</sup>	[KBPh <sub>4</sub> ] / mol L <sup>-1</sup>	[K <sup>+</sup> ] <sub>total</sub> / mol L <sup>-1</sup>	<i>k</i> <sub>obs</sub> / s <sup>-1</sup>
	2.22 × 10 <sup>-4</sup>			6.57 <sup>[a]</sup>
1.43 × 10 <sup>-5</sup>	2.22 × 10 <sup>-4</sup>	0	2.22 × 10 <sup>-4</sup>	5.79
1.43 × 10 <sup>-5</sup>	2.22 × 10 <sup>-4</sup>	1.24 × 10 <sup>-4</sup>	3.46 × 10 <sup>-4</sup>	5.81
1.43 × 10 <sup>-5</sup>	2.22 × 10 <sup>-4</sup>	2.47 × 10 <sup>-4</sup>	4.69 × 10 <sup>-4</sup>	5.81
1.43 × 10 <sup>-5</sup>	2.22 × 10 <sup>-4</sup>	4.95 × 10 <sup>-4</sup>	7.16 × 10 <sup>-4</sup>	5.58
1.43 × 10 <sup>-5</sup>	2.22 × 10 <sup>-4</sup>	1.24 × 10 <sup>-3</sup>	1.46 × 10 <sup>-3</sup>	4.93
1.43 × 10 <sup>-5</sup>	2.22 × 10 <sup>-4</sup>	2.47 × 10 <sup>-3</sup>	2.69 × 10 <sup>-3</sup>	4.29
1.43 × 10 <sup>-5</sup>	2.22 × 10 <sup>-4</sup>	5.37 × 10 <sup>-3</sup>	5.60 × 10 <sup>-3</sup>	3.41
1.43 × 10 <sup>-5</sup>	2.22 × 10 <sup>-4</sup>	9.40 × 10 <sup>-3</sup>	9.63 × 10 <sup>-3</sup>	2.75
1.43 × 10 <sup>-5</sup>	2.22 × 10 <sup>-4</sup>	1.57 × 10 <sup>-2</sup>	1.59 × 10 <sup>-2</sup>	2.37

[a] Calculated from the second-order rate constants of the free anion (potassium salt in presence of 18-crown-6) given in ref.<sup>[3c]</sup>

Table 26: Pseudo-first-order rate constants for reaction of **8-COMe** with **3h** at variable concentrations of KBPh<sub>4</sub> (20 °C, stopped-flow, at 533 nm).

[ <b>3h</b> ] / mol L <sup>-1</sup>	[ <b>8-COMe</b> ] / mol L <sup>-1</sup>	[KBPh <sub>4</sub> ] / mol L <sup>-1</sup>	[K <sup>+</sup> ] <sub>total</sub> / mol L <sup>-1</sup>	<i>k</i> <sub>obs</sub> / s <sup>-1</sup>
	2.76 × 10 <sup>-4</sup>			1.51 <sup>[a]</sup>
1.32 × 10 <sup>-5</sup>	2.76 × 10 <sup>-4</sup>	0	2.76 × 10 <sup>-4</sup>	1.39
1.32 × 10 <sup>-5</sup>	2.76 × 10 <sup>-4</sup>	1.26 × 10 <sup>-4</sup>	4.01 × 10 <sup>-4</sup>	1.38
1.32 × 10 <sup>-5</sup>	2.76 × 10 <sup>-4</sup>	2.51 × 10 <sup>-4</sup>	5.27 × 10 <sup>-4</sup>	1.35
1.32 × 10 <sup>-5</sup>	2.76 × 10 <sup>-4</sup>	5.02 × 10 <sup>-4</sup>	7.78 × 10 <sup>-4</sup>	1.33
1.32 × 10 <sup>-5</sup>	2.76 × 10 <sup>-4</sup>	1.23 × 10 <sup>-3</sup>	1.51 × 10 <sup>-3</sup>	1.26
1.32 × 10 <sup>-5</sup>	2.76 × 10 <sup>-4</sup>	2.51 × 10 <sup>-3</sup>	2.79 × 10 <sup>-3</sup>	1.16
1.32 × 10 <sup>-5</sup>	2.76 × 10 <sup>-4</sup>	4.93 × 10 <sup>-3</sup>	5.20 × 10 <sup>-3</sup>	1.03
1.32 × 10 <sup>-5</sup>	2.76 × 10 <sup>-4</sup>	5.42 × 10 <sup>-3</sup>	5.69 × 10 <sup>-3</sup>	1.00
1.32 × 10 <sup>-5</sup>	2.76 × 10 <sup>-4</sup>	1.11 × 10 <sup>-2</sup>	1.14 × 10 <sup>-2</sup>	0.770
1.32 × 10 <sup>-5</sup>	2.76 × 10 <sup>-4</sup>	1.71 × 10 <sup>-2</sup>	1.73 × 10 <sup>-2</sup>	0.659

[a] Calculated from the second-order rate constants of the free anion (potassium salt in presence of 18-crown-6) given in ref.<sup>[3c]</sup>

## 4.6.2. Determination of the Nucleophilicity of the Benzoylmethyl Anions 1-X

### 4.6.2.1. Reactions of the Anion of 1,2-Diphenylethanone 1-Ph

Table 27: Kinetics of the reaction of **1-Ph** (generated from (**1-Ph**)-H by addition of 1.05 equivalents of KO<sup>t</sup>Bu) with **3h** (20 °C, stopped-flow, at 533 nm).<sup>[RA]</sup>

[ <b>3h</b> ] / mol L <sup>-1</sup>	[ <b>1-Ph</b> ] / mol L <sup>-1</sup>	[18-Crown-6] / mol L <sup>-1</sup>	[ <b>1-Ph</b> ] / [ <b>3h</b> ]	$k_{\text{obs}}$ / s <sup>-1</sup>
$2.54 \times 10^{-5}$	$2.81 \times 10^{-4}$		11.0	$2.43 \times 10^2$
$2.54 \times 10^{-5}$	$3.51 \times 10^{-4}$	$6.17 \times 10^{-4}$	13.8	$3.25 \times 10^2$
$2.54 \times 10^{-5}$	$4.21 \times 10^{-4}$		16.6	$3.93 \times 10^2$
$2.54 \times 10^{-5}$	$4.91 \times 10^{-4}$	$1.24 \times 10^{-3}$	19.3	$4.70 \times 10^2$
$2.54 \times 10^{-5}$	$5.62 \times 10^{-4}$		22.1	$5.40 \times 10^2$

$$k_2 = 1.05 \times 10^6 \text{ L mol}^{-1} \text{ s}^{-1}$$

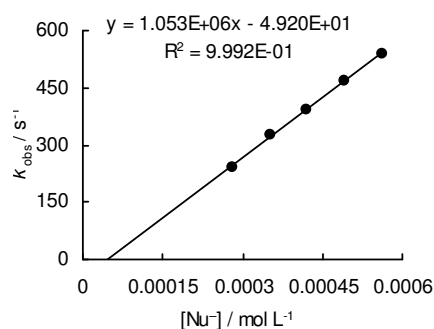


Table 28: Kinetics of the reaction of **1-Ph** (generated from (**1-Ph**)-H by addition of 1.05 equivalents of KO<sup>t</sup>Bu) with **3p** (20 °C, stopped-flow, at 520 nm).<sup>[RA]</sup>

[ <b>3p</b> ] / mol L <sup>-1</sup>	[ <b>1-Ph</b> ] / mol L <sup>-1</sup>	[18-Crown-6] / mol L <sup>-1</sup>	[ <b>1-Ph</b> ] / [ <b>3p</b> ]	$k_{\text{obs}}$ / s <sup>-1</sup>
$2.41 \times 10^{-5}$	$2.92 \times 10^{-4}$	$5.49 \times 10^{-4}$	12.1	21.8
$2.41 \times 10^{-5}$	$3.89 \times 10^{-4}$		16.2	31.3
$2.41 \times 10^{-5}$	$4.87 \times 10^{-4}$	$1.10 \times 10^{-3}$	20.2	40.3
$2.41 \times 10^{-5}$	$5.84 \times 10^{-4}$		24.3	50.2

$$k_2 = 9.68 \times 10^4 \text{ L mol}^{-1} \text{ s}^{-1}$$

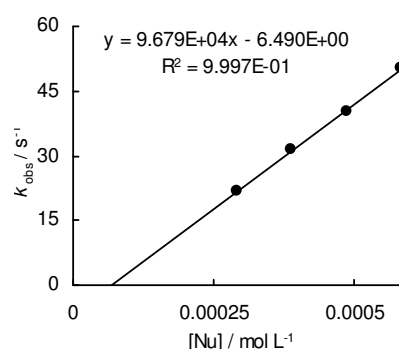


Table 29: Kinetics of the reaction of **1-Ph** (generated from (**1-Ph**)-H by addition of 1.05 equivalents of KO<sup>t</sup>Bu) with **3m** (20 °C, stopped-flow, at 490 nm).

[ <b>3m</b> ] / mol L <sup>-1</sup>	[ <b>1-Ph</b> ] / mol L <sup>-1</sup>	[ <b>1-Ph</b> ] / [ <b>3m</b> ]	$k_{\text{obs}}$ / s <sup>-1</sup>
$1.74 \times 10^{-5}$	$2.12 \times 10^{-4}$	12.2	1.46
$1.74 \times 10^{-5}$	$4.25 \times 10^{-4}$	24.5	3.42
$1.74 \times 10^{-5}$	$6.37 \times 10^{-4}$	36.7	5.69
$1.74 \times 10^{-5}$	$8.50 \times 10^{-4}$	48.9	7.70
$1.74 \times 10^{-5}$	$1.06 \times 10^{-3}$	61.2	9.80

$$k_2 = 9.88 \times 10^3 \text{ L mol}^{-1} \text{ s}^{-1}$$

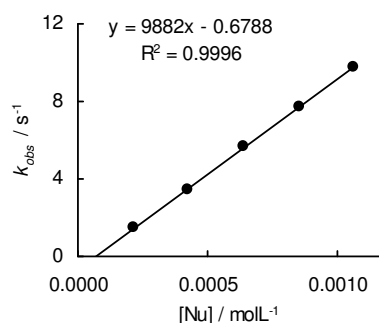
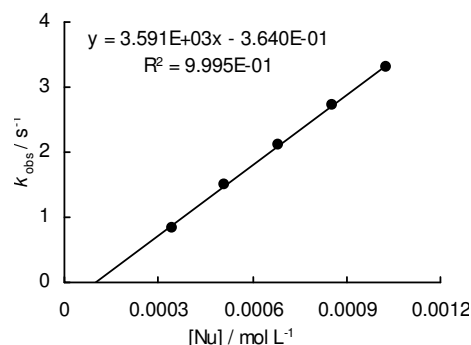


Table 30: Kinetics of the reaction of **1-Ph** (generated from (**1-Ph**)-H by addition of 1.05 equivalents of KO<sup>t</sup>Bu) with **3n** (20 °C, stopped-flow, at 486 nm).<sup>[RA]</sup>

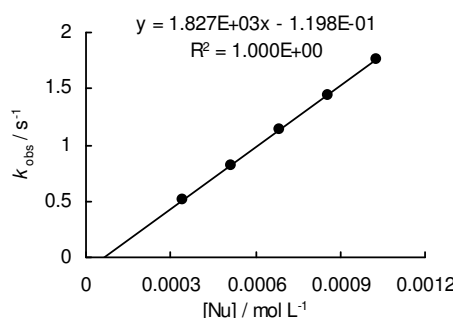
[ <b>3n</b> ] / mol L <sup>-1</sup>	[ <b>1-Ph</b> ] / mol L <sup>-1</sup>	[18-Crown-6] mol L <sup>-1</sup>	[ <b>1-Ph</b> ] /[ <b>3n</b> ]	$k_{\text{obs}}$ / s <sup>-1</sup>
$2.59 \times 10^{-5}$	$3.42 \times 10^{-4}$		13.2	$8.46 \times 10^{-1}$
$2.59 \times 10^{-5}$	$5.14 \times 10^{-4}$	$6.61 \times 10^{-4}$	19.8	1.49
$2.59 \times 10^{-5}$	$6.85 \times 10^{-4}$		26.4	2.11
$2.59 \times 10^{-5}$	$8.56 \times 10^{-4}$	$1.32 \times 10^{-3}$	33.1	2.73
$2.59 \times 10^{-5}$	$1.03 \times 10^{-3}$		39.7	3.30

$$k_2 = 3.59 \times 10^3 \text{ L mol}^{-1} \text{ s}^{-1}$$

Table 31: Kinetics of the reaction of **1-Ph** (generated from (**1-Ph**)-H by addition of 1.05 equivalents of KO<sup>t</sup>Bu) with **3o** (20 °C, stopped-flow, at 521 nm).<sup>[RA]</sup>

[ <b>3o</b> ] / mol L <sup>-1</sup>	[ <b>1-Ph</b> ] / mol L <sup>-1</sup>	[18-Crown-6] mol L <sup>-1</sup>	[ <b>1-Ph</b> ] /[ <b>3o</b> ]	$k_{\text{obs}}$ / s <sup>-1</sup>
$2.59 \times 10^{-5}$	$3.42 \times 10^{-4}$		13.2	$5.05 \times 10^{-1}$
$2.59 \times 10^{-5}$	$5.14 \times 10^{-4}$	$6.61 \times 10^{-4}$	19.8	$8.22 \times 10^{-1}$
$2.59 \times 10^{-5}$	$6.85 \times 10^{-4}$		26.4	1.13
$2.59 \times 10^{-5}$	$8.56 \times 10^{-4}$	$1.32 \times 10^{-3}$	33.1	1.44
$2.59 \times 10^{-5}$	$1.03 \times 10^{-3}$		39.7	1.76

$$k_2 = 1.83 \times 10^3 \text{ L mol}^{-1} \text{ s}^{-1}$$

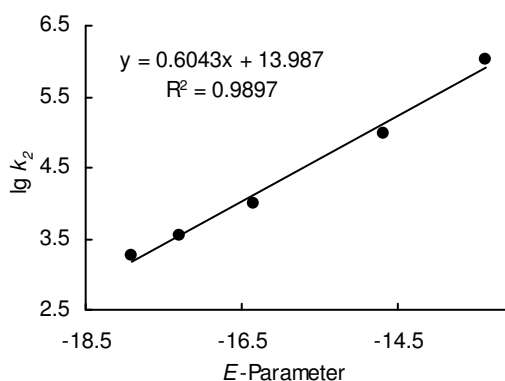


### Determination of Reactivity Parameters $N$ and $s_N$ for the Anion of 1,2-Diphenylethanone (**1-Ph**) in DMSO

Table 32: Rate Constants for the reactions of **1-Ph** with different electrophiles (20 °C).

Electrophile	$E$	$k_2$ / L mol <sup>-1</sup> s <sup>-1</sup>	$\lg k_2$
<b>3h</b>	-13.39	$1.05 \times 10^{6[\text{RA}]}$	6.02
<b>3p</b>	-14.68	$9.68 \times 10^{4[\text{RA}]}$	4.99
<b>3m</b>	-16.36	$9.86 \times 10^3$	3.99
<b>3n</b>	-17.29	$3.59 \times 10^{3[\text{RA}]}$	3.56
<b>3o</b>	-17.90	$1.83 \times 10^{3[\text{RA}]}$	3.26

$$N = 23.15, s_N = 0.60$$

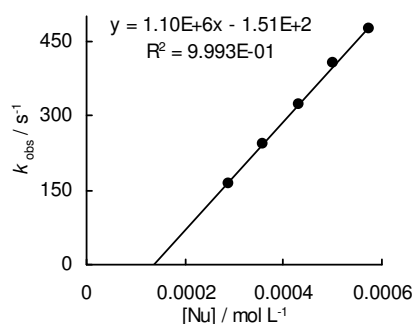


## 4.6.2.2. Reactions of the Sodium Salt of 1,2-Diphenylethanone (1-Ph)-Na

Table 33: Kinetics of the reaction of (1-Ph)-Na (generated from (1-Ph)-H by addition of 1.05 equivalents of NaOtBu) with **3h** (20 °C, stopped-flow, at 533 nm).<sup>[RA]</sup>

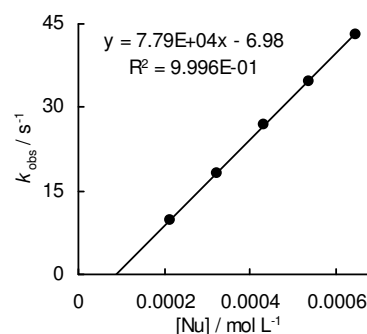
[ <b>3h</b> ] / mol L <sup>-1</sup>	[(1-Ph)-Na] / mol L <sup>-1</sup>	[1-Ph] / [ <b>3h</b> ]	<i>k</i> <sub>obs</sub> / s <sup>-1</sup>
2.38 × 10 <sup>-5</sup>	2.87 × 10 <sup>-4</sup>	12.1	163
2.38 × 10 <sup>-5</sup>	3.59 × 10 <sup>-4</sup>	15.1	242
2.38 × 10 <sup>-5</sup>	4.31 × 10 <sup>-4</sup>	18.1	322
2.38 × 10 <sup>-5</sup>	5.03 × 10 <sup>-4</sup>	21.1	405
2.38 × 10 <sup>-5</sup>	5.75 × 10 <sup>-4</sup>	24.1	475

$$k_2 = 1.10 \times 10^6 \text{ L mol}^{-1} \text{ s}^{-1}$$

Table 34: Kinetics of the reaction of (1-Ph)-Na (generated from (1-Ph)-H by addition of 1.05 equivalents of NaOtBu) with **3p** (20 °C, stopped-flow, at 520 nm).<sup>[RA]</sup>

[ <b>3p</b> ] / mol L <sup>-1</sup>	[(1-Ph)-Na] / mol L <sup>-1</sup>	[1-Ph] / [ <b>3p</b> ]	<i>k</i> <sub>obs</sub> / s <sup>-1</sup>
2.41 × 10 <sup>-5</sup>	2.15 × 10 <sup>-4</sup>	8.94	9.58
2.41 × 10 <sup>-5</sup>	3.23 × 10 <sup>-4</sup>	13.4	18.1
2.41 × 10 <sup>-5</sup>	4.30 × 10 <sup>-4</sup>	17.9	27.0
2.41 × 10 <sup>-5</sup>	5.38 × 10 <sup>-4</sup>	22.3	34.8
2.41 × 10 <sup>-5</sup>	6.45 × 10 <sup>-4</sup>	26.8	43.1

$$k_2 = 7.79 \times 10^4 \text{ L mol}^{-1} \text{ s}^{-1}$$

Table 35: Kinetics of the reaction of (1-Ph)-Na (generated from (1-Ph)-H by addition of 1.06 equivalents of NaOtBu) with **3m** (20 °C, stopped-flow, at 490 nm).<sup>[RA]</sup>

[ <b>3m</b> ] / mol L <sup>-1</sup>	[(1-Ph)-Na] / mol L <sup>-1</sup>	[1-Ph] / [ <b>3m</b> ]	<i>k</i> <sub>obs</sub> / s <sup>-1</sup>
1.45 × 10 <sup>-5</sup>	2.27 × 10 <sup>-4</sup>	15.6	1.16
1.45 × 10 <sup>-5</sup>	4.54 × 10 <sup>-4</sup>	31.2	3.31
1.45 × 10 <sup>-5</sup>	6.80 × 10 <sup>-4</sup>	46.8	5.65
1.45 × 10 <sup>-5</sup>	9.07 × 10 <sup>-4</sup>	62.4	7.69
1.45 × 10 <sup>-5</sup>	1.13 × 10 <sup>-3</sup>	78.1	9.84

$$k_2 = 9.59 \times 10^3 \text{ L mol}^{-1} \text{ s}^{-1}$$

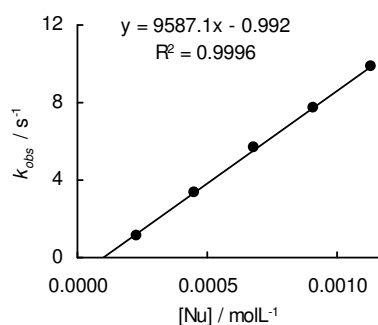
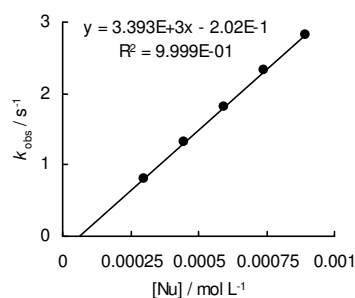




Table 36: Kinetics of the reaction of **(1-Ph)-Na** (generated from **(1-Ph)-H** by addition of 1.05 equivalents of NaOtBu) with **3n** (20 °C, stopped-flow, at 486 nm).<sup>[RA]</sup>

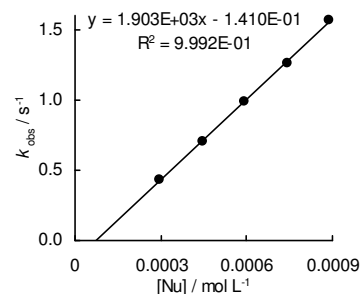
[ <b>3n</b> ] / mol L <sup>-1</sup>	[ <b>(1-Ph)-Na</b> ] / mol L <sup>-1</sup>	[ <b>1-Ph</b> ] /[ <b>3n</b> ]	$k_{\text{obs}}$ / s <sup>-1</sup>
$2.59 \times 10^{-5}$	$2.97 \times 10^{-4}$	11.5	0.800
$2.59 \times 10^{-5}$	$4.46 \times 10^{-4}$	17.2	1.31
$2.59 \times 10^{-5}$	$5.94 \times 10^{-4}$	22.9	1.82
$2.59 \times 10^{-5}$	$7.43 \times 10^{-4}$	28.7	2.33
$2.59 \times 10^{-5}$	$8.91 \times 10^{-4}$	34.4	2.81

$$k_2 = 3.39 \times 10^3 \text{ L mol}^{-1} \text{ s}^{-1}$$

Table 37: Kinetics of the reaction of **(1-Ph)-Na** (generated from **(1-Ph)-H** by addition of 1.05 equivalents of NaOtBu) with **3o** (20 °C, stopped-flow, at 521 nm).<sup>[RA]</sup>

[ <b>3o</b> ] / mol L <sup>-1</sup>	[ <b>(1-Ph)-Na</b> ] / mol L <sup>-1</sup>	[ <b>1-Ph</b> ] /[ <b>3o</b> ]	$k_{\text{obs}}$ / s <sup>-1</sup>
$2.59 \times 10^{-5}$	$2.97 \times 10^{-4}$	11.5	0.436
$2.59 \times 10^{-5}$	$4.46 \times 10^{-4}$	17.2	0.701
$2.59 \times 10^{-5}$	$5.94 \times 10^{-4}$	23.0	0.982
$2.59 \times 10^{-5}$	$7.43 \times 10^{-4}$	28.7	1.26
$2.59 \times 10^{-5}$	$8.91 \times 10^{-4}$	34.4	1.57

$$k_2 = 1.90 \times 10^3 \text{ L mol}^{-1} \text{ s}^{-1}$$



#### 4.6.2.3. Reactions of the Lithium-Salt of 1,2-diphenylethanone (**1-Ph**)-Li

Table 38: Kinetics of the reaction of **(1-Ph)-Li** (generated from **(1-Ph)-H** by addition of 1.05 equivalents of LiOtBu) with **3h** (20 °C, stopped-flow, at 533 nm).<sup>[RA]</sup>

[ <b>3h</b> ] / mol L <sup>-1</sup>	[ <b>(1-Ph)-Li</b> ] / mol L <sup>-1</sup>	[ <b>1-Ph</b> ] /[ <b>3h</b> ]	$k_{\text{obs}}$ / s <sup>-1</sup>
$2.55 \times 10^{-5}$	$2.53 \times 10^{-4}$	9.9	204
$2.55 \times 10^{-5}$	$3.37 \times 10^{-4}$	13.3	285
$2.55 \times 10^{-5}$	$4.22 \times 10^{-4}$	16.6	358
$2.55 \times 10^{-5}$	$5.06 \times 10^{-4}$	19.9	438
$2.55 \times 10^{-5}$	$5.90 \times 10^{-4}$	23.2	512

$$k_2 = 9.12 \times 10^5 \text{ L mol}^{-1} \text{ s}^{-1}$$

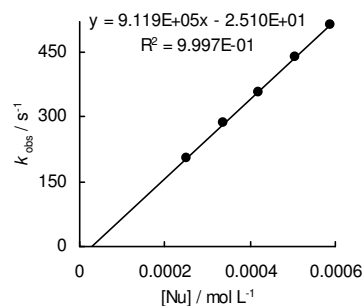
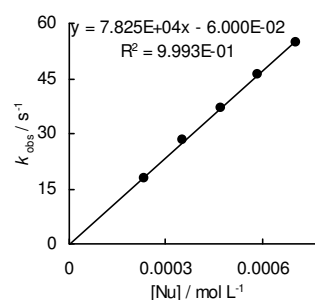


Table 39: Kinetics of the reaction of **(1-Ph)-Li** (generated from **(1-Ph)-H** by addition of 1.05 equivalents of LiOtBu) with **3p** (20 °C, stopped-flow, at 520 nm).<sup>[RA]</sup>

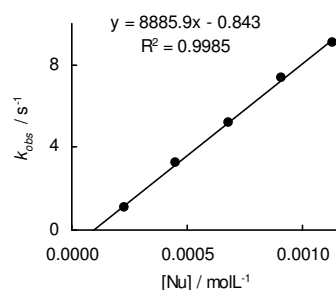
[ <b>3p</b> ] / mol L <sup>-1</sup>	[ <b>(1-Ph)-Li</b> ] / mol L <sup>-1</sup>	[ <b>1-Ph</b> ] /[ <b>3p</b> ]	$k_{\text{obs}}$ / s <sup>-1</sup>
$1.86 \times 10^{-5}$	$2.35 \times 10^{-4}$	12.7	17.9
$1.86 \times 10^{-5}$	$3.53 \times 10^{-4}$	19.0	28.1
$1.86 \times 10^{-5}$	$4.71 \times 10^{-4}$	25.3	36.8
$1.86 \times 10^{-5}$	$5.89 \times 10^{-4}$	31.6	46.2
$1.86 \times 10^{-5}$	$7.06 \times 10^{-4}$	38.0	54.9

$$k_2 = 7.83 \times 10^4 \text{ L mol}^{-1} \text{ s}^{-1}$$

Table 40: Kinetics of the reaction of **(1-Ph)-Li** (generated from **(1-Ph)-H** by addition of 1.04 equivalents of LiOtBu) with **3m** (20 °C, stopped-flow, at 490 nm).

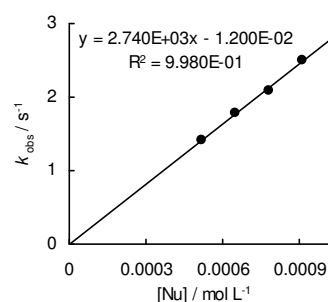
[ <b>3m</b> ] / mol L <sup>-1</sup>	[ <b>(1-Ph)-Li</b> ] / mol L <sup>-1</sup>	[ <b>1-Ph</b> ] /[ <b>3m</b> ]	$k_{\text{obs}}$ / s <sup>-1</sup>
$1.45 \times 10^{-5}$	$2.27 \times 10^{-4}$	15.6	1.08
$1.45 \times 10^{-5}$	$4.54 \times 10^{-4}$	31.2	3.25
$1.45 \times 10^{-5}$	$6.80 \times 10^{-4}$	46.8	5.21
$1.45 \times 10^{-5}$	$9.07 \times 10^{-4}$	62.4	7.38
$1.45 \times 10^{-5}$	$1.13 \times 10^{-3}$	78.1	9.09

$$k_2 = 8.89 \times 10^3 \text{ L mol}^{-1} \text{ s}^{-1}$$

Table 41: Kinetics of the reaction of **(1-Ph)-Li** (generated from **(1-Ph)-H** by addition of 1.05 equivalents of LiOtBu) with **3n** (20 °C, stopped-flow, at 486 nm).<sup>[RA]</sup>

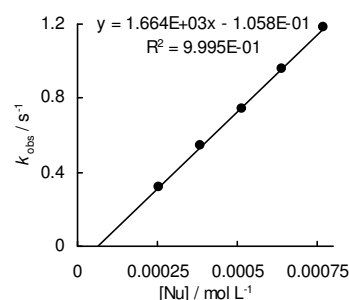
[ <b>3n</b> ] / mol L <sup>-1</sup>	[ <b>(1-Ph)-Li</b> ] / mol L <sup>-1</sup>	[ <b>1-Ph</b> ] /[ <b>3n</b> ]	$k_{\text{obs}}$ / s <sup>-1</sup>
$2.61 \times 10^{-5}$	$5.20 \times 10^{-4}$	19.9	1.42
$2.61 \times 10^{-5}$	$6.50 \times 10^{-4}$	24.9	1.78
$2.61 \times 10^{-5}$	$7.80 \times 10^{-4}$	29.9	2.08
$2.61 \times 10^{-5}$	$9.10 \times 10^{-4}$	34.9	2.50
$2.61 \times 10^{-5}$	$1.04 \times 10^{-3}$	39.9	2.84

$$k_2 = 2.74 \times 10^3 \text{ L mol}^{-1} \text{ s}^{-1}$$

Table 42: Kinetics of the reaction of **(1-Ph)-Li** (generated from **(1-Ph)-H** by addition of 1.05 equivalents of LiOtBu) with **3o** (20 °C, stopped-flow, at 521 nm).<sup>[RA]</sup>

[ <b>3o</b> ] / mol L <sup>-1</sup>	[ <b>(1-Ph)-Li</b> ] / mol L <sup>-1</sup>	[ <b>1-Ph</b> ] /[ <b>3o</b> ]	$k_{\text{obs}}$ / s <sup>-1</sup>
$2.16 \times 10^{-5}$	$2.56 \times 10^{-4}$	11.9	0.320
$2.16 \times 10^{-5}$	$3.84 \times 10^{-4}$	17.8	0.542
$2.16 \times 10^{-5}$	$5.13 \times 10^{-4}$	23.8	0.739
$2.16 \times 10^{-5}$	$6.41 \times 10^{-4}$	29.7	0.954
$2.16 \times 10^{-5}$	$7.69 \times 10^{-4}$	35.7	1.18

$$k_2 = 1.66 \times 10^3 \text{ L mol}^{-1} \text{ s}^{-1}$$

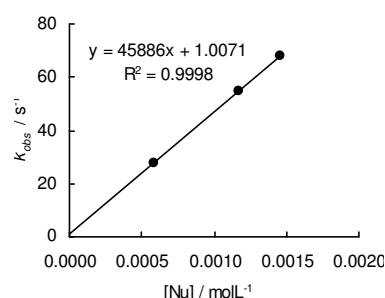


#### 4.6.2.4. Reactions of the Potassium Salt of *N,N*-Diethyl-3-oxo-3-phenylpropanamide (1-CONEt<sub>2</sub>)-K in Presence of 18-Crown-6

Table 43: Kinetics of the reaction of 1-CONEt<sub>2</sub> with 3g (20 °C, stopped-flow, at 422 nm).

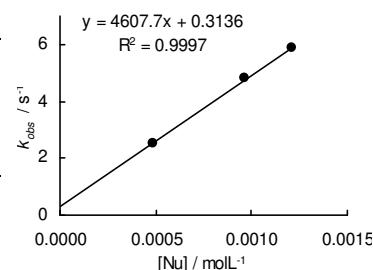
[3g] / mol L <sup>-1</sup>	[1-CONEt <sub>2</sub> ] /mol L <sup>-1</sup>	[18-Crown-6] mol L <sup>-1</sup>	[1-CONEt <sub>2</sub> ] /[3g]	<i>k</i> <sub>obs</sub> / s <sup>-1</sup>
1.38 × 10 <sup>-5</sup>	5.84 × 10 <sup>-4</sup>	6.05 × 10 <sup>-4</sup>	42.3	27.7
1.38 × 10 <sup>-5</sup>	1.17 × 10 <sup>-3</sup>	1.21 × 10 <sup>-3</sup>	84.5	55.0
1.38 × 10 <sup>-5</sup>	1.46 × 10 <sup>-3</sup>	1.54 × 10 <sup>-3</sup>	106	67.8

$$k_2 = 4.59 \times 10^4 \text{ L mol}^{-1} \text{ s}^{-1}$$

Table 44: Kinetics of the reaction of 1-CONEt<sub>2</sub> with 3h (20 °C, stopped-flow, at 533 nm).

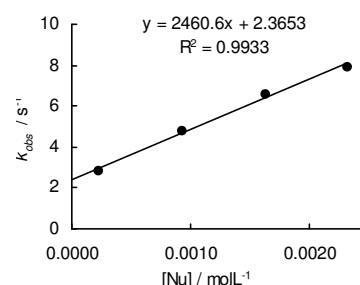
[3h] / mol L <sup>-1</sup>	[1-CONEt <sub>2</sub> ] /mol L <sup>-1</sup>	[18-Crown-6] mol L <sup>-1</sup>	[1-CONEt <sub>2</sub> ] /[3h]	<i>k</i> <sub>obs</sub> / s <sup>-1</sup>
1.57 × 10 <sup>-5</sup>	4.83 × 10 <sup>-4</sup>	5.12 × 10 <sup>-4</sup>	30.8	2.53
1.57 × 10 <sup>-5</sup>	9.67 × 10 <sup>-4</sup>	1.02 × 10 <sup>-3</sup>	61.6	4.80
1.57 × 10 <sup>-5</sup>	1.21 × 10 <sup>-3</sup>	1.30 × 10 <sup>-3</sup>	77.1	5.86

$$k_2 = 4.61 \times 10^3 \text{ L mol}^{-1} \text{ s}^{-1}$$

Table 45: Kinetics of the reaction of 1-CONEt<sub>2</sub> with 3i (20 °C, stopped-flow, at 374 nm).

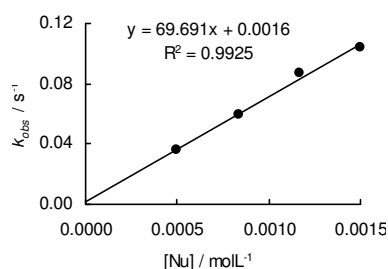
[3i] / mol L <sup>-1</sup>	[1-CONEt <sub>2</sub> ] /mol L <sup>-1</sup>	[18-Crown-6] mol L <sup>-1</sup>	[1-CONEt <sub>2</sub> ] /[3i]	<i>k</i> <sub>obs</sub> / s <sup>-1</sup>
1.81 × 10 <sup>-5</sup>	2.33 × 10 <sup>-4</sup>	2.49 × 10 <sup>-4</sup>	12.8	2.81
1.81 × 10 <sup>-5</sup>	9.31 × 10 <sup>-4</sup>	9.97 × 10 <sup>-4</sup>	51.3	4.74
1.81 × 10 <sup>-5</sup>	1.63 × 10 <sup>-3</sup>	1.75 × 10 <sup>-3</sup>	89.8	6.60
1.81 × 10 <sup>-5</sup>	2.33 × 10 <sup>-3</sup>	2.49 × 10 <sup>-3</sup>	128	7.92

$$k_2 = 2.46 \times 10^3 \text{ L mol}^{-1} \text{ s}^{-1}$$

Table 46: Kinetics of the reaction of 1-CONEt<sub>2</sub> with 3l (20 °C, stopped-flow, at 407 nm).

[3l] / mol L <sup>-1</sup>	[1-CONEt <sub>2</sub> ] /mol L <sup>-1</sup>	[18-Crown-6] mol L <sup>-1</sup>	[1-CONEt <sub>2</sub> ] /[3l]	<i>k</i> <sub>obs</sub> / s <sup>-1</sup>
1.72 × 10 <sup>-5</sup>	5.01 × 10 <sup>-4</sup>	5.36 × 10 <sup>-4</sup>	29.1	3.57 × 10 <sup>-2</sup>
1.72 × 10 <sup>-5</sup>	8.34 × 10 <sup>-4</sup>	8.98 × 10 <sup>-4</sup>	48.5	5.91 × 10 <sup>-2</sup>
1.72 × 10 <sup>-5</sup>	1.17 × 10 <sup>-3</sup>	1.25 × 10 <sup>-3</sup>	68.0	8.68 × 10 <sup>-2</sup>
1.72 × 10 <sup>-5</sup>	1.50 × 10 <sup>-3</sup>	1.62 × 10 <sup>-3</sup>	87.4	1.04 × 10 <sup>-1</sup>

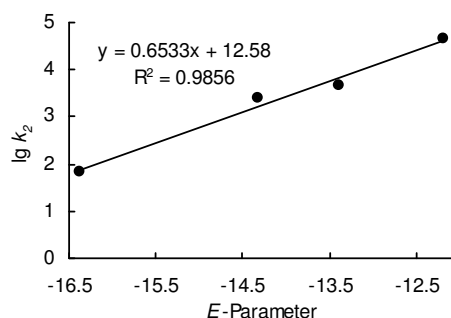
$$k_2 = 6.97 \times 10^1 \text{ L mol}^{-1} \text{ s}^{-1}$$



### Determination of Reactivity Parameters $N$ and $s_N$ for the Anion of $N,N$ -Diethyl-3-oxo-3-phenylpropanamide (**1-CONEt<sub>2</sub>**) in DMSO

Table 47: Rate Constants for the reactions of **1-CONEt<sub>2</sub>** with different electrophiles (20 °C).

Electrophile	$E$	$k_2 / \text{L mol}^{-1} \text{s}^{-1}$	$\lg k_2$
<b>3g</b>	-12.18	$4.59 \times 10^4$	4.66
<b>3h</b>	-13.39	$4.61 \times 10^3$	3.66
<b>3i</b>	-14.36	$2.46 \times 10^3$	3.39
<b>3l</b>	-16.38	$6.97 \times 10^1$	1.84

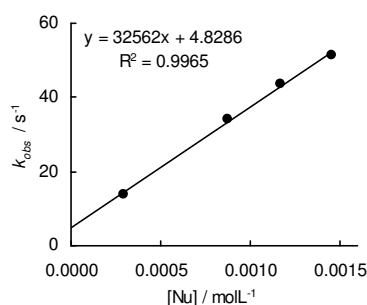


$$N = 19.26, s_N = 0.65$$

### 4.6.2.5. Reactions of the Potassium Salt of $N,N$ -Diethyl-3-oxo-3-phenylpropanamide (**1-CONEt<sub>2</sub>**)-K in Absence of 18-Crown-6

Table 48: Kinetics of the reaction of **1-CONEt<sub>2</sub>** with **3g** (20 °C, stopped-flow, at 422 nm).

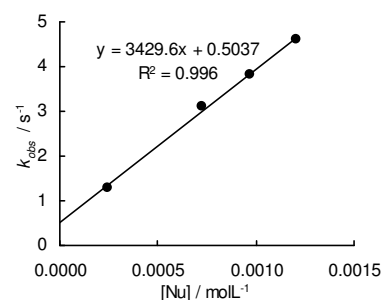
$[\mathbf{3g}] / \text{mol L}^{-1}$	$[\mathbf{1-CONEt_2}] / \text{mol L}^{-1}$	$[\mathbf{1-CONEt_2}]/[\mathbf{3g}]$	$k_{\text{obs}} / \text{s}^{-1}$
$1.38 \times 10^{-5}$	$2.92 \times 10^{-4}$	21.1	13.7
$1.38 \times 10^{-5}$	$8.77 \times 10^{-4}$	63.4	34.3
$1.38 \times 10^{-5}$	$1.17 \times 10^{-3}$	84.5	43.6
$1.38 \times 10^{-5}$	$1.46 \times 10^{-3}$	106	51.4



$$k_2 = 3.26 \times 10^4 \text{ L mol}^{-1} \text{s}^{-1}$$

Table 49: Kinetics of the reaction of **1-CONEt<sub>2</sub>** with **3h** (20 °C, stopped-flow, at 533 nm).

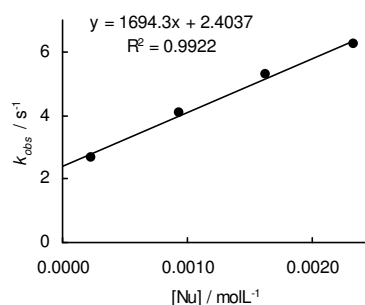
$[\mathbf{3h}] / \text{mol L}^{-1}$	$[\mathbf{1-CONEt_2}] / \text{mol L}^{-1}$	$[\mathbf{1-CONEt_2}]/[\mathbf{3h}]$	$k_{\text{obs}} / \text{s}^{-1}$
$1.57 \times 10^{-5}$	$2.42 \times 10^{-4}$	15.4	1.27
$1.57 \times 10^{-5}$	$7.25 \times 10^{-4}$	46.2	3.12
$1.57 \times 10^{-5}$	$9.67 \times 10^{-4}$	61.6	3.81
$1.57 \times 10^{-5}$	$1.21 \times 10^{-3}$	77.1	4.59



$$k_2 = 3.43 \times 10^3 \text{ L mol}^{-1} \text{s}^{-1}$$

Table 50: Kinetics of the reaction of **1-CONEt<sub>2</sub>** with **3i** (20 °C, stopped-flow, at 374 nm).

$[\mathbf{3i}] / \text{mol L}^{-1}$	$[\mathbf{1-CONEt_2}] / \text{mol L}^{-1}$	$[\mathbf{1-CONEt_2}]/[\mathbf{3i}]$	$k_{\text{obs}} / \text{s}^{-1}$
$1.81 \times 10^{-5}$	$2.33 \times 10^{-4}$	12.8	2.68
$1.81 \times 10^{-5}$	$9.31 \times 10^{-4}$	51.3	4.10
$1.81 \times 10^{-5}$	$1.63 \times 10^{-3}$	89.8	5.28
$1.81 \times 10^{-5}$	$2.33 \times 10^{-3}$	128	6.23

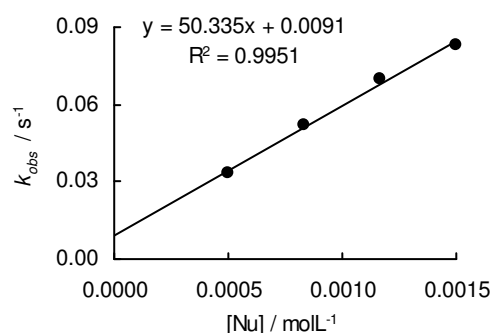


$$k_2 = 1.69 \times 10^3 \text{ L mol}^{-1} \text{s}^{-1}$$

Table 51: Kinetics of the reaction of **1-CONEt<sub>2</sub>** with **3l** (20 °C, stopped-flow, at 374 nm).

[ <b>3l</b> ] / mol L <sup>-1</sup>	[ <b>1-CONEt<sub>2</sub></b> ] / mol L <sup>-1</sup>	[ <b>1-CONEt<sub>2</sub></b> ]/[ <b>3l</b> ]	<i>k</i> <sub>obs</sub> / s <sup>-1</sup>
1.72 × 10 <sup>-5</sup>	5.01 × 10 <sup>-4</sup>	29.1	3.31 × 10 <sup>-2</sup>
1.72 × 10 <sup>-5</sup>	8.34 × 10 <sup>-4</sup>	48.5	5.21 × 10 <sup>-2</sup>
1.72 × 10 <sup>-5</sup>	1.17 × 10 <sup>-3</sup>	68.0	6.95 × 10 <sup>-2</sup>
1.72 × 10 <sup>-5</sup>	1.50 × 10 <sup>-3</sup>	87.4	8.33 × 10 <sup>-2</sup>

$$k_2 = 5.03 \times 10^1 \text{ L mol}^{-1} \text{ s}^{-1}$$

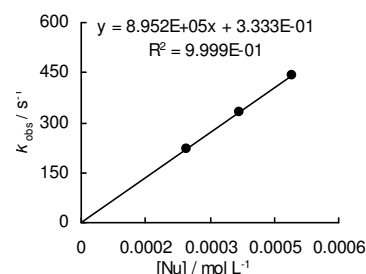


#### 4.6.2.6. Reactions of the Potassium Salt of Ethyl 3-Oxo-3-phenylpropanoate (**1-CO<sub>2</sub>Et**)-K in Presence of 18-Crown-6

Table 52: Kinetics of the reaction of **1-CO<sub>2</sub>Et** with **3e** (20 °C, stopped-flow, at 635 nm).<sup>[RA]</sup>

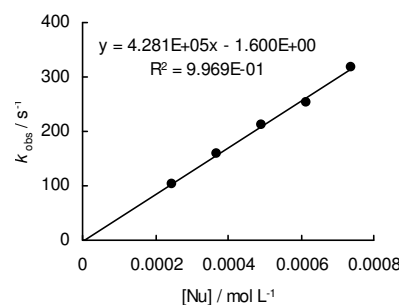
[ <b>3e</b> ] / mol L <sup>-1</sup>	[ <b>1-CO<sub>2</sub>Et</b> ] / mol L <sup>-1</sup>	[18-Crown-6] / mol L <sup>-1</sup>	[ <b>1-CO<sub>2</sub>Et</b> ]/ [ <b>3e</b> ]	<i>k</i> <sub>obs</sub> / s <sup>-1</sup>
1.85 × 10 <sup>-5</sup>	2.46 × 10 <sup>-4</sup>	5.50 × 10 <sup>-4</sup>	13.3	2.21 × 10 <sup>2</sup>
1.85 × 10 <sup>-5</sup>	3.69 × 10 <sup>-4</sup>	7.33 × 10 <sup>-4</sup>	20.0	3.29 × 10 <sup>2</sup>
1.85 × 10 <sup>-5</sup>	4.92 × 10 <sup>-4</sup>	1.28 × 10 <sup>-3</sup>	26.6	4.41 × 10 <sup>2</sup>

$$k_2 = 8.95 \times 10^5 \text{ L mol}^{-1} \text{ s}^{-1}$$

Table 53: Kinetics of the reaction of **1-CO<sub>2</sub>Et** with **3f** (20 °C, stopped-flow, at 630 nm).<sup>[RA]</sup>

[ <b>3f</b> ] / mol L <sup>-1</sup>	[ <b>1-CO<sub>2</sub>Et</b> ] / mol L <sup>-1</sup>	[18-Crown-6] / mol L <sup>-1</sup>	[ <b>1-CO<sub>2</sub>Et</b> ]/ [ <b>3f</b> ]	<i>k</i> <sub>obs</sub> / s <sup>-1</sup>
2.02 × 10 <sup>-5</sup>	2.46 × 10 <sup>-4</sup>	5.50 × 10 <sup>-4</sup>	12.2	1.02 × 10 <sup>2</sup>
2.02 × 10 <sup>-5</sup>	3.69 × 10 <sup>-4</sup>	7.33 × 10 <sup>-4</sup>	18.3	1.58 × 10 <sup>2</sup>
2.02 × 10 <sup>-5</sup>	4.92 × 10 <sup>-4</sup>	1.28 × 10 <sup>-3</sup>	24.4	2.13 × 10 <sup>2</sup>
2.02 × 10 <sup>-5</sup>	6.14 × 10 <sup>-4</sup>	9.17 × 10 <sup>-4</sup>	30.4	2.54 × 10 <sup>2</sup>
2.02 × 10 <sup>-5</sup>	7.37 × 10 <sup>-4</sup>	1.47 × 10 <sup>-4</sup>	36.5	3.17 × 10 <sup>2</sup>

$$k_2 = 4.28 \times 10^5 \text{ L mol}^{-1} \text{ s}^{-1}$$

Table 54: Kinetics of the reaction of **1-CO<sub>2</sub>Et** with **3g** (20 °C, stopped-flow, at 422 nm).<sup>[RA]</sup>

[ <b>3g</b> ] / mol L <sup>-1</sup>	[ <b>1-CO<sub>2</sub>Et</b> ] / mol L <sup>-1</sup>	[18-Crown-6] / mol L <sup>-1</sup>	[ <b>1-CO<sub>2</sub>Et</b> ]/ [ <b>3g</b> ]	<i>k</i> <sub>obs</sub> / s <sup>-1</sup>
2.91 × 10 <sup>-5</sup>	4.16 × 10 <sup>-4</sup>	7.34 × 10 <sup>-4</sup>	14.3	3.36
2.91 × 10 <sup>-5</sup>	6.25 × 10 <sup>-4</sup>	8.26 × 10 <sup>-4</sup>	21.5	5.12
2.91 × 10 <sup>-5</sup>	8.33 × 10 <sup>-4</sup>	1.47 × 10 <sup>-3</sup>	28.6	7.06
2.91 × 10 <sup>-5</sup>	1.04 × 10 <sup>-3</sup>	1.10 × 10 <sup>-3</sup>	35.8	8.69
2.91 × 10 <sup>-5</sup>	1.25 × 10 <sup>-3</sup>	1.84 × 10 <sup>-3</sup>	42.9	10.6

$$k_2 = 8.67 \times 10^3 \text{ L mol}^{-1} \text{ s}^{-1}$$

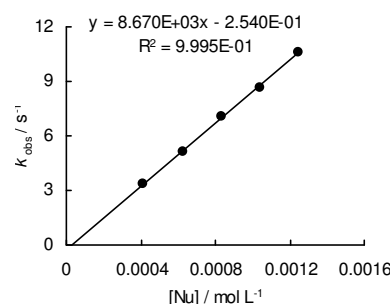
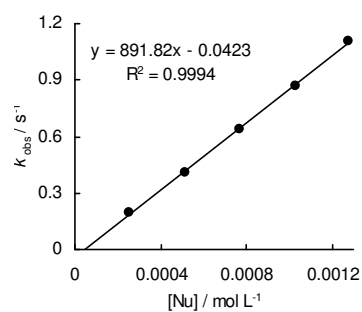


Table 55: Kinetics of the reaction of **1-CO<sub>2</sub>Et** with **3h** (20 °C, stopped-flow, at 533 nm).<sup>[RA]</sup>

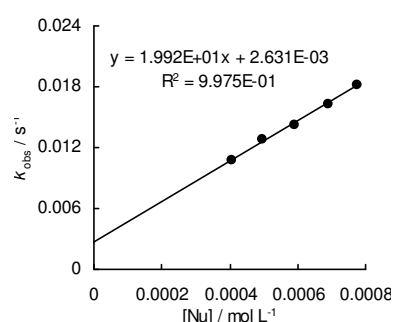
[ <b>3g</b> ] / mol L <sup>-1</sup>	[ <b>1-CO<sub>2</sub>Et</b> ] / mol L <sup>-1</sup>	[18-Crown-6] mol L <sup>-1</sup>	[ <b>1-CO<sub>2</sub>Et</b> ] /[ <b>3g</b> ]	$k_{\text{obs}}$ / s <sup>-1</sup>
$2.55 \times 10^{-5}$	$2.57 \times 10^{-4}$	$7.57 \times 10^{-4}$	10.1	$1.94 \times 10^{-1}$
$2.55 \times 10^{-5}$	$5.13 \times 10^{-4}$	$8.51 \times 10^{-4}$	20.1	$4.11 \times 10^{-1}$
$2.55 \times 10^{-5}$	$7.70 \times 10^{-4}$	$1.51 \times 10^{-3}$	30.2	$6.42 \times 10^{-1}$
$2.55 \times 10^{-5}$	$1.03 \times 10^{-3}$	$1.89 \times 10^{-3}$	40.3	$8.65 \times 10^{-1}$
$2.55 \times 10^{-5}$	$1.28 \times 10^{-3}$	$2.84 \times 10^{-3}$	50.3	1.11

$$k_2 = 8.92 \times 10^2 \text{ L mol}^{-1} \text{ s}^{-1}$$

Table 56: Kinetics of the reaction of **1-CO<sub>2</sub>Et** with **3j** (20 °C, diode array, at 371 nm).<sup>[RA]</sup>

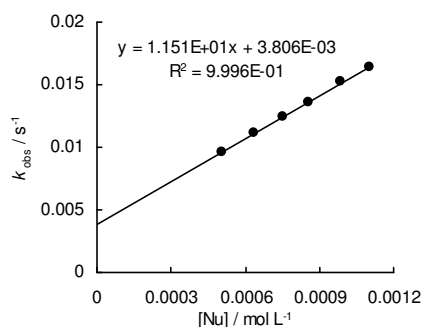
[ <b>3j</b> ] / mol L <sup>-1</sup>	[ <b>1-CO<sub>2</sub>Et</b> ] / mol L <sup>-1</sup>	[18-Crown-6] mol L <sup>-1</sup>	[ <b>1-CO<sub>2</sub>Et</b> ] /[ <b>3j</b> ]	$k_{\text{obs}}$ / s <sup>-1</sup>
$3.69 \times 10^{-5}$	$4.07 \times 10^{-4}$	$5.86 \times 10^{-4}$	11.0	$1.07 \times 10^{-2}$
$3.62 \times 10^{-5}$	$4.99 \times 10^{-4}$	$7.68 \times 10^{-4}$	13.8	$1.27 \times 10^{-2}$
$3.58 \times 10^{-5}$	$5.93 \times 10^{-4}$	$9.51 \times 10^{-4}$	16.6	$1.43 \times 10^{-2}$
$3.58 \times 10^{-5}$	$6.92 \times 10^{-4}$	$1.14 \times 10^{-3}$	19.3	$1.63 \times 10^{-2}$
$3.51 \times 10^{-5}$	$7.76 \times 10^{-4}$	$1.31 \times 10^{-3}$	22.1	$1.82 \times 10^{-2}$

$$k_2 = 1.99 \times 10^1 \text{ L mol}^{-1} \text{ s}^{-1}$$

Table 57: Kinetics of the reaction of **1-CO<sub>2</sub>Et** with **3k** (20 °C, diode array, at 393 nm).<sup>[RA]</sup>

[ <b>3k</b> ] / mol L <sup>-1</sup>	[ <b>1-CO<sub>2</sub>Et</b> ] / mol L <sup>-1</sup>	[18-Crown-6] mol L <sup>-1</sup>	[ <b>1-CO<sub>2</sub>Et</b> ] /[ <b>3k</b> ]	$k_{\text{obs}}$ / s <sup>-1</sup>
$4.30 \times 10^{-5}$	$5.06 \times 10^{-4}$	$5.69 \times 10^{-4}$	11.7	$9.61 \times 10^{-3}$
$4.32 \times 10^{-5}$	$6.34 \times 10^{-4}$	$7.48 \times 10^{-4}$	14.7	$1.11 \times 10^{-2}$
$4.28 \times 10^{-5}$	$7.54 \times 10^{-4}$	$9.26 \times 10^{-4}$	17.6	$1.25 \times 10^{-2}$
$4.15 \times 10^{-5}$	$8.53 \times 10^{-4}$	$1.08 \times 10^{-3}$	20.6	$1.36 \times 10^{-2}$
$4.18 \times 10^{-5}$	$9.83 \times 10^{-4}$	$1.27 \times 10^{-3}$	23.5	$1.52 \times 10^{-2}$
$4.18 \times 10^{-5}$	$1.10 \times 10^{-3}$	$1.45 \times 10^{-3}$	26.4	$1.64 \times 10^{-2}$

$$k_2 = 1.15 \times 10^1 \text{ L mol}^{-1} \text{ s}^{-1}$$

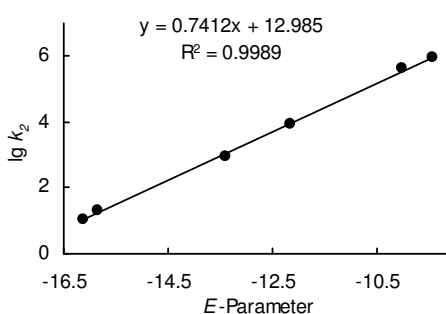


### Determination of Reactivity Parameters $N$ and $s_N$ for the Anion of Ethyl 3-Oxo-3-phenylpropanoate (**1-CO<sub>2</sub>Et**) in DMSO

Table 58: Rate Constants for the reactions of **1-CO<sub>2</sub>Et** with different electrophiles (20 °C).

Electrophile	$E$	$k_2 / \text{L mol}^{-1} \text{ s}^{-1}$	$\lg k_2$
<b>3e</b>	-9.45	$8.95 \times 10^5$ <sup>[RA]</sup>	5.95
<b>3f</b>	-10.04	$4.28 \times 10^5$ <sup>[RA]</sup>	5.63
<b>3g</b>	-12.18	$8.67 \times 10^3$ <sup>[RA]</sup>	3.94
<b>3h</b>	-13.39	$8.92 \times 10^2$ <sup>[RA]</sup>	2.95
<b>3j</b>	-15.83	$1.99 \times 10^1$ <sup>[RA]</sup>	1.30
<b>3k</b>	-16.11	$1.15 \times 10^1$ <sup>[RA]</sup>	1.06

$$N = 17.52, s_N = 0.74$$

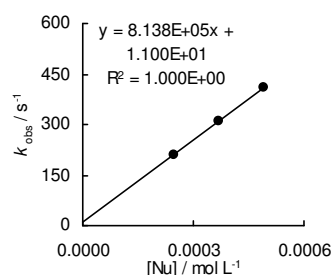


#### 4.6.2.7. Reactions of the Potassium Salt of Ethyl 3-Oxo-3-phenylpropanoate (1-CO<sub>2</sub>Et)-K in Absence of 18-Crown-6

Table 59: Kinetics of the reaction of 1-CO<sub>2</sub>Et with 3e (20 °C, stopped-flow, at 635 nm).<sup>[RA]</sup>

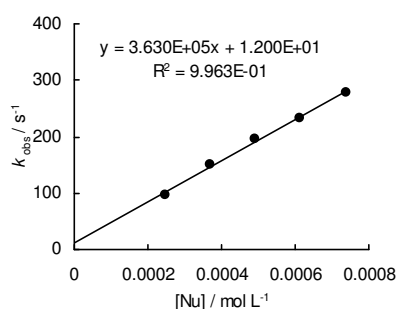
[3e] / mol L <sup>-1</sup>	[1-CO <sub>2</sub> Et] / mol L <sup>-1</sup>	[1-CO <sub>2</sub> Et]/[3e]	<i>k</i> <sub>obs</sub> / s <sup>-1</sup>
1.85 × 10 <sup>-5</sup>	2.46 × 10 <sup>-4</sup>	13.3	2.11 × 10 <sup>2</sup>
1.85 × 10 <sup>-5</sup>	3.69 × 10 <sup>-4</sup>	20.0	3.11 × 10 <sup>2</sup>
1.85 × 10 <sup>-5</sup>	4.92 × 10 <sup>-4</sup>	26.6	4.11 × 10 <sup>2</sup>

$$k_2 = 8.14 \times 10^5 \text{ L mol}^{-1} \text{ s}^{-1}$$

Table 60: Kinetics of the reaction of 1-CO<sub>2</sub>Et with 3f (20 °C, stopped-flow, at 630 nm).<sup>[RA]</sup>

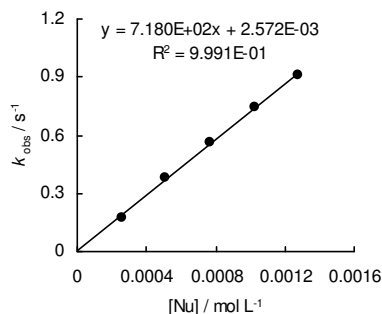
[3f] / mol L <sup>-1</sup>	[1-CO <sub>2</sub> Et] / mol L <sup>-1</sup>	[1-CO <sub>2</sub> Et]/[3f]	<i>k</i> <sub>obs</sub> / s <sup>-1</sup>
2.02 × 10 <sup>-5</sup>	2.46 × 10 <sup>-4</sup>	12.2	9.60 × 10 <sup>1</sup>
2.02 × 10 <sup>-5</sup>	3.69 × 10 <sup>-4</sup>	18.3	1.50 × 10 <sup>2</sup>
2.02 × 10 <sup>-5</sup>	4.92 × 10 <sup>-4</sup>	24.4	1.95 × 10 <sup>2</sup>
2.02 × 10 <sup>-5</sup>	6.14 × 10 <sup>-4</sup>	30.4	2.34 × 10 <sup>2</sup>
2.02 × 10 <sup>-5</sup>	7.37 × 10 <sup>-4</sup>	36.5	2.77 × 10 <sup>2</sup>

$$k_2 = 3.63 \times 10^5 \text{ L mol}^{-1} \text{ s}^{-1}$$

Table 61: Kinetics of the reaction of 1-CO<sub>2</sub>Et with 3g (20 °C, stopped-flow, at 422 nm).<sup>[RA]</sup>

[3g] / mol L <sup>-1</sup>	[1-CO <sub>2</sub> Et] / mol L <sup>-1</sup>	[1-CO <sub>2</sub> Et]/[3g]	<i>k</i> <sub>obs</sub> / s <sup>-1</sup>
2.91 × 10 <sup>-5</sup>	4.16 × 10 <sup>-4</sup>	14.3	3.13
2.91 × 10 <sup>-5</sup>	6.25 × 10 <sup>-4</sup>	21.5	4.69
2.91 × 10 <sup>-5</sup>	8.33 × 10 <sup>-4</sup>	28.6	6.17
2.91 × 10 <sup>-5</sup>	1.04 × 10 <sup>-3</sup>	35.8	7.72
2.91 × 10 <sup>-5</sup>	1.25 × 10 <sup>-3</sup>	42.9	9.08

$$k_2 = 7.18 \times 10^3 \text{ L mol}^{-1} \text{ s}^{-1}$$

Table 62: Kinetics of the reaction of 1-CO<sub>2</sub>Et with 3h (20 °C, stopped-flow, at 533 nm).<sup>[RA]</sup>

[3g] / mol L <sup>-1</sup>	[1-CO <sub>2</sub> Et] / mol L <sup>-1</sup>	[1-CO <sub>2</sub> Et]/[3g]	<i>k</i> <sub>obs</sub> / s <sup>-1</sup>
2.55 × 10 <sup>-5</sup>	2.57 × 10 <sup>-4</sup>	10.1	1.77 × 10 <sup>-1</sup>
2.55 × 10 <sup>-5</sup>	5.13 × 10 <sup>-4</sup>	20.1	3.77 × 10 <sup>-1</sup>
2.55 × 10 <sup>-5</sup>	7.70 × 10 <sup>-4</sup>	30.2	5.65 × 10 <sup>-1</sup>
2.55 × 10 <sup>-5</sup>	1.03 × 10 <sup>-3</sup>	40.3	7.45 × 10 <sup>-1</sup>
2.55 × 10 <sup>-5</sup>	1.28 × 10 <sup>-3</sup>	50.3	9.13 × 10 <sup>-1</sup>

$$k_2 = 7.18 \times 10^2 \text{ L mol}^{-1} \text{ s}^{-1}$$

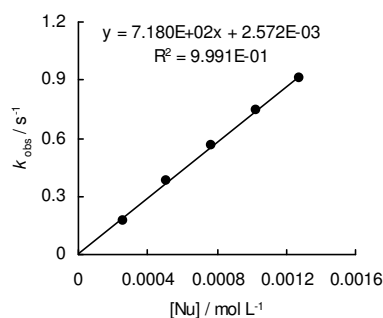
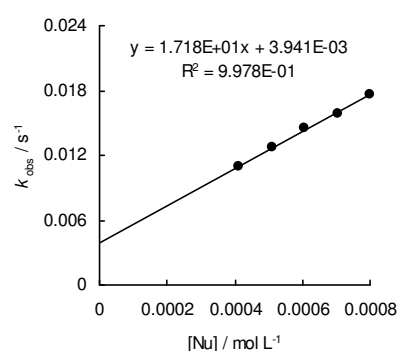


Table 63: Kinetics of the reaction of **1-CO<sub>2</sub>Et** with **3j** (20 °C, diode array, at 371 nm).<sup>[RA]</sup>

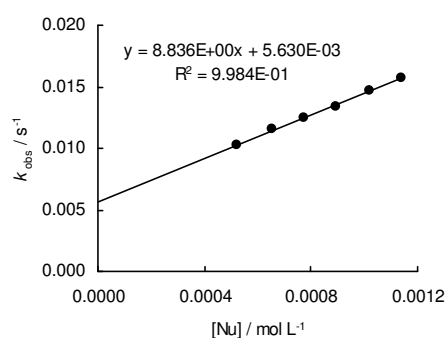
[ <b>3j</b> ] / mol L <sup>-1</sup>	[ <b>1-CO<sub>2</sub>Et</b> ] / mol L <sup>-1</sup>	[ <b>1-CO<sub>2</sub>Et</b> ]/[ <b>3j</b> ]	$k_{\text{obs}}$ / s <sup>-1</sup>
$3.72 \times 10^{-5}$	$4.11 \times 10^{-4}$	11.0	$1.09 \times 10^{-2}$
$3.69 \times 10^{-5}$	$5.09 \times 10^{-4}$	13.8	$1.28 \times 10^{-2}$
$3.67 \times 10^{-5}$	$6.08 \times 10^{-4}$	16.6	$1.45 \times 10^{-2}$
$3.65 \times 10^{-5}$	$7.05 \times 10^{-4}$	19.3	$1.59 \times 10^{-2}$
$3.62 \times 10^{-5}$	$7.99 \times 10^{-4}$	22.1	$1.77 \times 10^{-2}$

$$k_2 = 1.72 \times 10^1 \text{ L mol}^{-1} \text{ s}^{-1}$$

Table 64: Kinetics of the reaction of **1-CO<sub>2</sub>Et** with **3k** (20 °C, diode array, at 393 nm).<sup>[RA]</sup>

[ <b>3k</b> ] / mol L <sup>-1</sup>	[ <b>1-CO<sub>2</sub>Et</b> ] / mol L <sup>-1</sup>	[ <b>1-CO<sub>2</sub>Et</b> ]/[ <b>3k</b> ]	$k_{\text{obs}}$ / s <sup>-1</sup>
$4.46 \times 10^{-5}$	$5.24 \times 10^{-4}$	11.7	$1.02 \times 10^{-2}$
$4.44 \times 10^{-5}$	$6.52 \times 10^{-4}$	14.7	$1.15 \times 10^{-2}$
$4.44 \times 10^{-5}$	$7.75 \times 10^{-4}$	17.6	$1.25 \times 10^{-2}$
$4.34 \times 10^{-5}$	$8.93 \times 10^{-4}$	20.6	$1.34 \times 10^{-2}$
$4.36 \times 10^{-5}$	$1.02 \times 10^{-3}$	23.5	$1.47 \times 10^{-2}$
$4.30 \times 10^{-5}$	$1.14 \times 10^{-3}$	26.4	$1.57 \times 10^{-2}$

$$k_2 = 8.84 \text{ L mol}^{-1} \text{ s}^{-1}$$

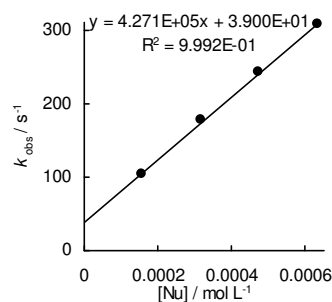


#### 4.6.2.8. Reactions of the Sodium-Salt of Ethyl 3-Oxo-3-phenylpropanoate (**1-CO<sub>2</sub>Et**)-Na

Table 65: Kinetics of the reaction of (**1-CO<sub>2</sub>Et**)-Na with **3e** (20 °C, stopped-flow, at 635 nm).<sup>[RA]</sup>

[ <b>3e</b> ] / mol L <sup>-1</sup>	[( <b>1-CO<sub>2</sub>Et</b> )-Na] / mol L <sup>-1</sup>	[ <b>1-CO<sub>2</sub>Et</b> ]/[ <b>3e</b> ]	$k_{\text{obs}}$ / s <sup>-1</sup>
$1.44 \times 10^{-5}$	$1.58 \times 10^{-4}$	11.0	104
$1.44 \times 10^{-5}$	$3.16 \times 10^{-4}$	21.9	177
$1.44 \times 10^{-5}$	$4.73 \times 10^{-4}$	32.9	242
$1.44 \times 10^{-5}$	$6.31 \times 10^{-4}$	43.8	307

$$k_2 = 4.27 \times 10^5 \text{ L mol}^{-1} \text{ s}^{-1}$$

Table 66: Kinetics of the reaction of (**1-CO<sub>2</sub>Et**)-Na with **3f** (20 °C, stopped-flow, at 630 nm).<sup>[RA]</sup>

[ <b>3f</b> ] / mol L <sup>-1</sup>	[( <b>1-CO<sub>2</sub>Et</b> )-Na] / mol L <sup>-1</sup>	[ <b>1-CO<sub>2</sub>Et</b> ]/[ <b>3f</b> ]	$k_{\text{obs}}$ / s <sup>-1</sup>
$1.30 \times 10^{-5}$	$1.58 \times 10^{-4}$	12.2	46.6
$1.30 \times 10^{-5}$	$3.16 \times 10^{-4}$	24.3	78.8
$1.30 \times 10^{-5}$	$4.73 \times 10^{-4}$	36.5	107
$1.30 \times 10^{-5}$	$6.31 \times 10^{-4}$	48.7	134

$$k_2 = 1.84 \times 10^5 \text{ L mol}^{-1} \text{ s}^{-1}$$

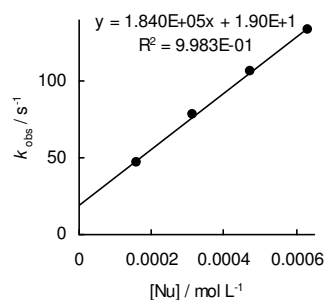
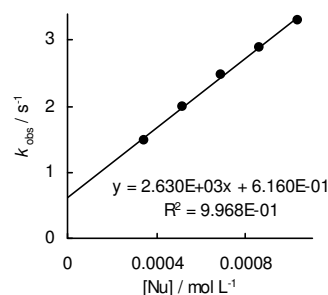




Table 67: Kinetics of the reaction of (1-CO<sub>2</sub>Et)-Na with **3g** (20 °C, stopped-flow, at 422 nm).<sup>[RA]</sup>

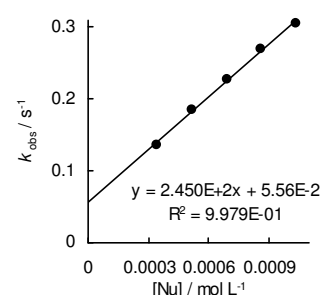
[ <b>3g</b> ] / mol L <sup>-1</sup>	[(1-CO <sub>2</sub> Et)-Na] / mol L <sup>-1</sup>	[1- CO <sub>2</sub> Et] /[ <b>3g</b> ]	$k_{\text{obs}}$ / s <sup>-1</sup>
$2.59 \times 10^{-5}$	$3.45 \times 10^{-4}$	13.3	1.48
$2.59 \times 10^{-5}$	$5.18 \times 10^{-4}$	20.0	2.00
$2.59 \times 10^{-5}$	$6.91 \times 10^{-4}$	26.7	2.48
$2.59 \times 10^{-5}$	$8.63 \times 10^{-4}$	33.3	2.90
$2.59 \times 10^{-5}$	$1.04 \times 10^{-3}$	40.0	3.30

$$k_2 = 2.63 \times 10^3 \text{ L mol}^{-1} \text{ s}^{-1}$$

Table 68: Kinetics of the reaction of (1-CO<sub>2</sub>Et)-Na with **3h** (20 °C, stopped-flow, at 533 nm).<sup>[RA]</sup>

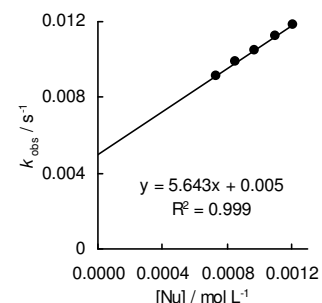
[ <b>3h</b> ] / mol L <sup>-1</sup>	[(1-CO <sub>2</sub> Et)-Na] / mol L <sup>-1</sup>	[1- CO <sub>2</sub> Et] /[ <b>3h</b> ]	$k_{\text{obs}}$ / s <sup>-1</sup>
$2.54 \times 10^{-5}$	$3.45 \times 10^{-4}$	13.6	0.137
$2.54 \times 10^{-5}$	$5.18 \times 10^{-4}$	20.4	0.184
$2.54 \times 10^{-5}$	$6.91 \times 10^{-4}$	27.2	0.228
$2.54 \times 10^{-5}$	$8.63 \times 10^{-4}$	33.9	0.269
$2.54 \times 10^{-5}$	$1.04 \times 10^{-3}$	40.7	0.306

$$k_2 = 2.45 \times 10^2 \text{ L mol}^{-1} \text{ s}^{-1}$$

Table 69: Kinetics of the reaction of (1-CO<sub>2</sub>Et)-Na with **3j** (20 °C, diode array, at 371 nm).<sup>[RA]</sup>

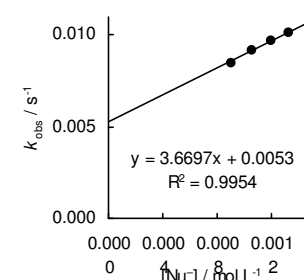
[ <b>3j</b> ] / mol L <sup>-1</sup>	[(1-CO <sub>2</sub> Et)-Na] / mol L <sup>-1</sup>	[1- CO <sub>2</sub> Et] /[ <b>3j</b> ]	$k_{\text{obs}}$ / s <sup>-1</sup>
$3.81 \times 10^{-5}$	$7.35 \times 10^{-4}$	19.3	$9.10 \times 10^{-3}$
$3.81 \times 10^{-5}$	$8.57 \times 10^{-4}$	22.5	$9.87 \times 10^{-3}$
$3.79 \times 10^{-5}$	$9.75 \times 10^{-4}$	25.7	$1.05 \times 10^{-2}$
$3.79 \times 10^{-5}$	$1.10 \times 10^{-3}$	29.0	$1.12 \times 10^{-2}$
$3.77 \times 10^{-5}$	$1.21 \times 10^{-3}$	32.1	$1.18 \times 10^{-2}$

$$k_2 = 5.64 \text{ L mol}^{-1} \text{ s}^{-1}$$

Table 70: Kinetics of the reaction of (1-CO<sub>2</sub>Et)-Na with **3k** (20 °C, diode array, at 393 nm).<sup>[RA]</sup>

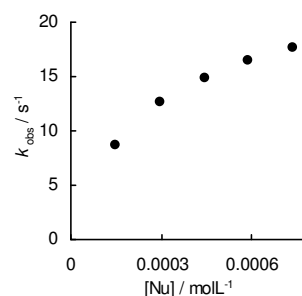
[ <b>3k</b> ] / mol L <sup>-1</sup>	[(1-CO <sub>2</sub> Et)-Na] / mol L <sup>-1</sup>	[1- CO <sub>2</sub> Et] /[ <b>3k</b> ]	$k_{\text{obs}}$ / s <sup>-1</sup>
$4.55 \times 10^{-5}$	$9.00 \times 10^{-4}$	19.8	$8.51 \times 10^{-3}$
$4.57 \times 10^{-5}$	$1.05 \times 10^{-3}$	23.0	$9.20 \times 10^{-3}$
$4.51 \times 10^{-5}$	$1.19 \times 10^{-3}$	26.4	$9.66 \times 10^{-3}$
$4.47 \times 10^{-5}$	$1.33 \times 10^{-3}$	29.8	$1.01 \times 10^{-2}$
$4.48 \times 10^{-5}$	$1.48 \times 10^{-3}$	33.0	$1.07 \times 10^{-2}$

$$k_2 = 3.67 \text{ L mol}^{-1} \text{ s}^{-1}$$



4.6.2.9. Reactions of the Lithium-Salt of Ethyl 3-oxo-3-phenylpropanoate (1-CO<sub>2</sub>Et)-LiTable 71: Kinetics of the reaction of (1-CO<sub>2</sub>Et)-Li with **3f** (20 °C, stopped-flow, at 630 nm).<sup>[RA]</sup>

[ <b>3f</b> ] / mol L <sup>-1</sup>	[(1-CO <sub>2</sub> Et)-Li] / mol L <sup>-1</sup>	[1-CO <sub>2</sub> Et] / [ <b>3f</b> ]	$k_{\text{obs}}$ / s <sup>-1</sup>
$1.35 \times 10^{-5}$	$1.48 \times 10^{-4}$	11.0	8.61
$1.35 \times 10^{-5}$	$2.95 \times 10^{-4}$	21.9	12.6
$1.35 \times 10^{-5}$	$4.43 \times 10^{-4}$	32.9	14.9
$1.35 \times 10^{-5}$	$5.90 \times 10^{-4}$	43.9	16.5
$1.35 \times 10^{-5}$	$7.38 \times 10^{-4}$	54.9	17.7

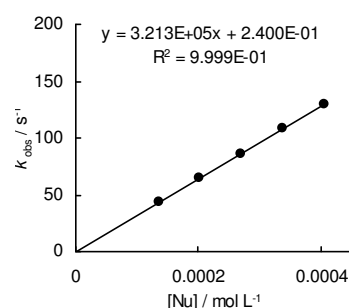


## 4.6.2.10. Reactions of the Anion of 3-Oxo-3-phenylpropanenitrile (1-CN)

Table 72: Kinetics of the reaction of 1-CN with **3e** (20 °C, stopped-flow, at 635 nm).<sup>[RA]</sup>

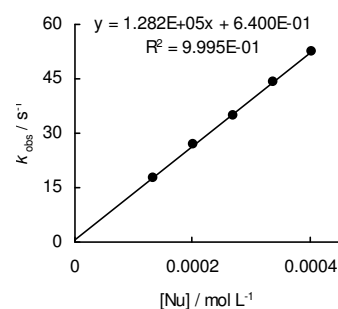
[ <b>3e</b> ] / mol L <sup>-1</sup>	[1-CN] / mol L <sup>-1</sup>	[18-Crown-6] / mol L <sup>-1</sup>	[1-CN] / [ <b>3e</b> ]	$k_{\text{obs}}$ / s <sup>-1</sup>
$1.22 \times 10^{-5}$	$1.35 \times 10^{-4}$		11.1	43.6
$1.22 \times 10^{-5}$	$2.02 \times 10^{-4}$	$5.47 \times 10^{-4}$	16.6	65.3
$1.22 \times 10^{-5}$	$2.70 \times 10^{-4}$		22.2	86.3
$1.22 \times 10^{-5}$	$3.37 \times 10^{-4}$	$9.12 \times 10^{-4}$	27.7	109
$1.22 \times 10^{-5}$	$4.04 \times 10^{-4}$		33.3	130

$$k_2 = 3.21 \times 10^5 \text{ L mol}^{-1} \text{ s}^{-1}$$

Table 73: Kinetics of the reaction of 1-CN with **3f** (20 °C, stopped-flow, at 630 nm).<sup>[RA]</sup>

[ <b>3f</b> ] / mol L <sup>-1</sup>	[1-CN] / mol L <sup>-1</sup>	[18-Crown-6] / mol L <sup>-1</sup>	[1-CN] / [ <b>3f</b> ]	$k_{\text{obs}}$ / s <sup>-1</sup>
$1.71 \times 10^{-5}$	$1.35 \times 10^{-4}$		11.5	17.8
$1.71 \times 10^{-5}$	$2.02 \times 10^{-4}$	$5.47 \times 10^{-4}$	17.3	26.9
$1.71 \times 10^{-5}$	$2.70 \times 10^{-4}$		23.0	34.8
$1.71 \times 10^{-5}$	$3.37 \times 10^{-4}$	$9.12 \times 10^{-4}$	28.8	44.1
$1.71 \times 10^{-5}$	$4.04 \times 10^{-4}$		34.5	52.4

$$k_2 = 1.28 \times 10^5 \text{ L mol}^{-1} \text{ s}^{-1}$$

Table 74: Kinetics of the reaction of 1-CN with **3g** (20 °C, stopped-flow, at 422 nm).<sup>[RA]</sup>

[ <b>3g</b> ] / mol L <sup>-1</sup>	[1-CN] / mol L <sup>-1</sup>	[18-Crown-6] / mol L <sup>-1</sup>	[1-CN] / [ <b>3g</b> ]	$k_{\text{obs}}$ / s <sup>-1</sup>
$2.52 \times 10^{-5}$	$2.73 \times 10^{-4}$		10.8	$4.72 \times 10^{-1}$
$2.52 \times 10^{-5}$	$4.09 \times 10^{-4}$	$9.12 \times 10^{-4}$	16.2	$9.83 \times 10^{-1}$
$2.52 \times 10^{-5}$	$5.46 \times 10^{-4}$		21.6	1.49
$2.52 \times 10^{-5}$	$6.82 \times 10^{-4}$	$1.82 \times 10^{-3}$	27.1	1.99
$2.52 \times 10^{-5}$	$8.19 \times 10^{-4}$		32.5	2.46

$$k_2 = 3.65 \times 10^3 \text{ L mol}^{-1} \text{ s}^{-1}$$

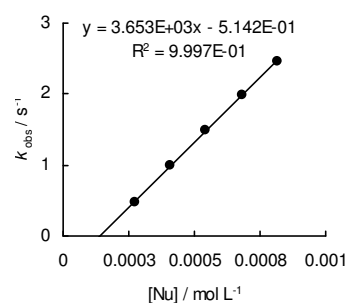
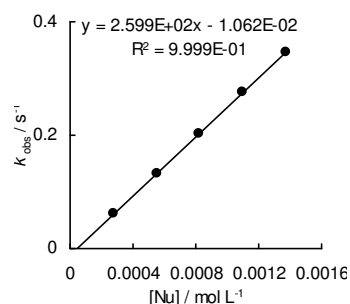


Table 75: Kinetics of the reaction of **1-CN** with **3h** (20 °C, stopped-flow, at 533 nm).<sup>[RA]</sup>

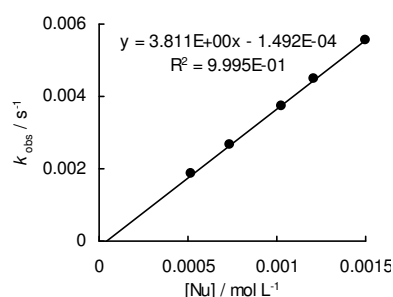
[ <b>3h</b> ] / mol L <sup>-1</sup>	[ <b>1-CN</b> ] / mol L <sup>-1</sup>	[18-Crown-6] / mol L <sup>-1</sup>	[ <b>1-CN</b> ] / [ <b>3h</b> ]	$k_{\text{obs}}$ / s <sup>-1</sup>
$2.55 \times 10^{-5}$	$2.75 \times 10^{-4}$		10.8	$6.21 \times 10^{-2}$
$2.55 \times 10^{-5}$	$5.50 \times 10^{-4}$	$8.99 \times 10^{-4}$	21.6	$1.31 \times 10^{-1}$
$2.55 \times 10^{-5}$	$8.25 \times 10^{-4}$		32.4	$2.03 \times 10^{-1}$
$2.55 \times 10^{-5}$	$1.10 \times 10^{-3}$	$1.80 \times 10^{-3}$	43.2	$2.76 \times 10^{-1}$
$2.55 \times 10^{-5}$	$1.38 \times 10^{-3}$		54.0	$3.47 \times 10^{-1}$

$$k_2 = 2.60 \times 10^2 \text{ L mol}^{-1} \text{ s}^{-1}$$

Table 76: Kinetics of the reaction of **1-CN** with **3j** (20 °C, diode array, at 371 nm).<sup>[RA]</sup>

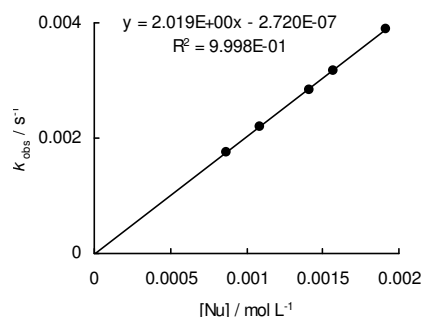
[ <b>3j</b> ] / mol L <sup>-1</sup>	[ <b>1-CN</b> ] / mol L <sup>-1</sup>	[18-Crown-6] / mol L <sup>-1</sup>	[ <b>1-CN</b> ] / [ <b>3j</b> ]	$k_{\text{obs}}$ / s <sup>-1</sup>
$4.34 \times 10^{-5}$	$5.20 \times 10^{-4}$		12.0	$1.86 \times 10^{-3}$
$4.11 \times 10^{-5}$	$7.39 \times 10^{-4}$	$9.99 \times 10^{-4}$	18.0	$2.66 \times 10^{-3}$
$4.29 \times 10^{-5}$	$1.03 \times 10^{-3}$		24.0	$3.72 \times 10^{-3}$
$4.04 \times 10^{-5}$	$1.21 \times 10^{-3}$	$1.64 \times 10^{-3}$	30.0	$4.49 \times 10^{-3}$
$4.16 \times 10^{-5}$	$1.50 \times 10^{-3}$		36.0	$5.57 \times 10^{-3}$

$$k_2 = 3.81 \text{ L mol}^{-1} \text{ s}^{-1}$$

Table 77: Kinetics of the reaction of **1-CN** with **3k** (20 °C, diode array, at 393 nm).<sup>[RA]</sup>

[ <b>3k</b> ] / mol L <sup>-1</sup>	[ <b>1-CN</b> ] / mol L <sup>-1</sup>	[18-Crown-6] / mol L <sup>-1</sup>	[ <b>1-CN</b> ] / [ <b>3k</b> ]	$k_{\text{obs}}$ / s <sup>-1</sup>
$5.22 \times 10^{-5}$	$8.64 \times 10^{-4}$		16.6	$1.76 \times 10^{-3}$
$4.93 \times 10^{-5}$	$1.09 \times 10^{-3}$	$1.67 \times 10^{-3}$	22.1	$2.19 \times 10^{-3}$
$5.10 \times 10^{-5}$	$1.41 \times 10^{-3}$		27.7	$2.84 \times 10^{-3}$
$4.74 \times 10^{-5}$	$1.57 \times 10^{-3}$	$2.40 \times 10^{-3}$	33.1	$3.16 \times 10^{-3}$
$4.98 \times 10^{-5}$	$1.92 \times 10^{-3}$		38.5	$3.89 \times 10^{-3}$

$$k_2 = 2.02 \text{ L mol}^{-1} \text{ s}^{-1}$$

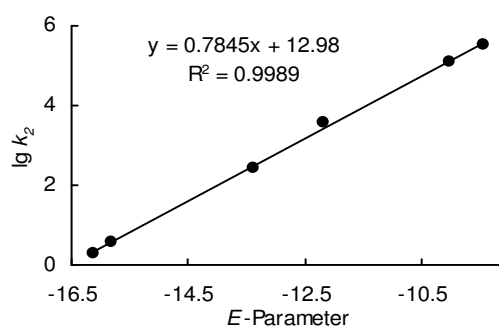


### Determination of Reactivity Parameters $N$ and $s_N$ for the Anion of 3-Oxo-3-phenylpropanitrile (**1-CN**) in DMSO<sup>[RA]</sup>

Table 78: Rate Constants for the reactions of **1-CN** with different electrophiles (20 °C).

Electrophile	$E$	$k_2 / \text{L mol}^{-1} \text{ s}^{-1}$	$\lg k_2$
<b>3e</b>	-9.45	$3.21 \times 10^5$	5.51
<b>3f</b>	-10.04	$1.28 \times 10^5$	5.11
<b>3g</b>	-12.18	$3.65 \times 10^3$	3.56
<b>3h</b>	-13.39	$2.60 \times 10^2$	2.41
<b>3j</b>	-15.83	3.81	0.58
<b>3k</b>	-16.11	2.02	0.30

$$N = 16.55, s_N = 0.78$$

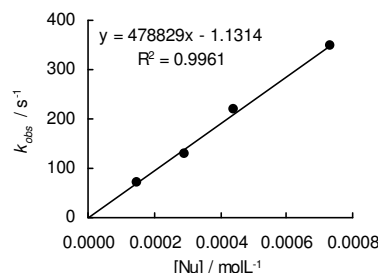


## 4.6.2.11. Reactions of the Anion of 1-Phenylbutane-1,3-dione (1-COMe)

Table 79: Kinetics of the reaction of **1-COMe** with **3e** (20 °C, stopped-flow, at 635 nm).

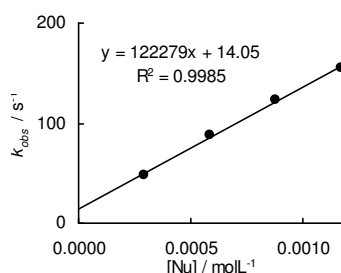
[ <b>3e</b> ] / mol L <sup>-1</sup>	[ <b>1-COMe</b> ] / mol L <sup>-1</sup>	[18-Crown-6] / mol L <sup>-1</sup>	[ <b>1-COMe</b> ] / [ <b>3e</b> ]	$k_{\text{obs}}$ / s <sup>-1</sup>
$1.22 \times 10^{-5}$	$1.47 \times 10^{-4}$		12.1	71.8
$1.22 \times 10^{-5}$	$2.93 \times 10^{-4}$	$3.12 \times 10^{-4}$	24.1	130
$1.22 \times 10^{-5}$	$4.40 \times 10^{-4}$		36.2	218
$1.22 \times 10^{-5}$	$7.33 \times 10^{-4}$		60.3	348

$$k_2 = 4.79 \times 10^5 \text{ L mol}^{-1} \text{ s}^{-1}$$

Table 80: Kinetics of the reaction of **1-COMe** with **3f** (20 °C, stopped-flow, at 630 nm).

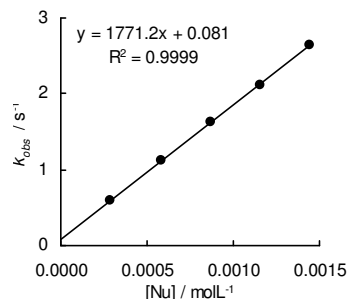
[ <b>3f</b> ] / mol L <sup>-1</sup>	[ <b>1-COMe</b> ] / mol L <sup>-1</sup>	[18-Crown-6] / mol L <sup>-1</sup>	[ <b>1-COMe</b> ] / [ <b>3f</b> ]	$k_{\text{obs}}$ / s <sup>-1</sup>
$1.23 \times 10^{-5}$	$2.93 \times 10^{-4}$		23.8	48.3
$1.23 \times 10^{-5}$	$5.87 \times 10^{-4}$	$6.24 \times 10^{-4}$	47.6	87.5
$1.23 \times 10^{-5}$	$8.80 \times 10^{-4}$		71.4	123
$1.23 \times 10^{-5}$	$1.17 \times 10^{-3}$	$1.25 \times 10^{-3}$	95.2	156

$$k_2 = 1.22 \times 10^5 \text{ L mol}^{-1} \text{ s}^{-1}$$

Table 81: Kinetics of the reaction of **1-COMe** with **3g** (20 °C, stopped-flow, at 422 nm).

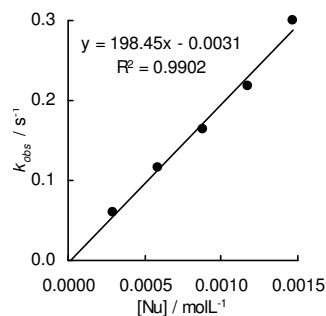
[ <b>3g</b> ] / mol L <sup>-1</sup>	[ <b>1-COMe</b> ] / mol L <sup>-1</sup>	[18-Crown-6] / mol L <sup>-1</sup>	[ <b>1-COMe</b> ] / [ <b>3g</b> ]	$k_{\text{obs}}$ / s <sup>-1</sup>
$1.14 \times 10^{-5}$	$2.90 \times 10^{-4}$		25.5	$5.90 \times 10^{-1}$
$1.14 \times 10^{-5}$	$5.79 \times 10^{-4}$	$6.00 \times 10^{-4}$	51.0	1.11
$1.14 \times 10^{-5}$	$8.69 \times 10^{-4}$		76.5	1.63
$1.14 \times 10^{-5}$	$1.16 \times 10^{-3}$	$1.20 \times 10^{-3}$	102	2.12
$1.14 \times 10^{-5}$	$1.45 \times 10^{-3}$		128	2.65

$$k_2 = 1.77 \times 10^3 \text{ L mol}^{-1} \text{ s}^{-1}$$

Table 82: Kinetics of the reaction of **1-COMe** with **3h** (20 °C, stopped-flow, at 533 nm).

[ <b>3h</b> ] / mol L <sup>-1</sup>	[ <b>1-COMe</b> ] / mol L <sup>-1</sup>	[18-Crown-6] / mol L <sup>-1</sup>	[ <b>1-COMe</b> ] / [ <b>3h</b> ]	$k_{\text{obs}}$ / s <sup>-1</sup>
$1.19 \times 10^{-5}$	$2.93 \times 10^{-4}$		24.6	$5.97 \times 10^{-2}$
$1.19 \times 10^{-5}$	$5.87 \times 10^{-4}$	$6.24 \times 10^{-4}$	49.2	$1.16 \times 10^{-1}$
$1.19 \times 10^{-5}$	$8.80 \times 10^{-4}$		73.8	$1.64 \times 10^{-1}$
$1.19 \times 10^{-5}$	$1.17 \times 10^{-3}$	$1.25 \times 10^{-3}$	98.4	$2.18 \times 10^{-1}$
$1.19 \times 10^{-5}$	$1.47 \times 10^{-3}$		123	$3.00 \times 10^{-1}$

$$k_2 = 1.98 \times 10^2 \text{ L mol}^{-1} \text{ s}^{-1}$$

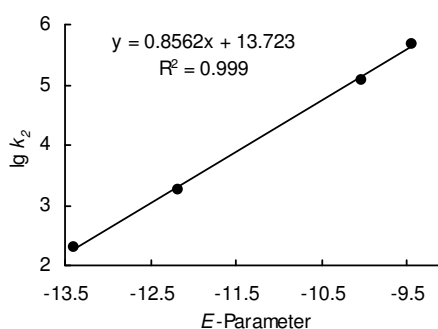


### Determination of Reactivity Parameters $N$ and $s_N$ for the Anion of 1-Phenylbutan-2,3-dione (**1-COMe**) in DMSO

Table 83: Rate Constants for the reactions of **1-COMe** with different electrophiles (20 °C).

Electrophile	$E$	$k_2 / \text{L mol}^{-1} \text{s}^{-1}$	$\lg k_2$
<b>3e</b>	-9.45	$4.79 \times 10^5$	5.68
<b>3f</b>	-10.04	$1.22 \times 10^5$	5.09
<b>3g</b>	-12.18	$1.77 \times 10^3$	3.25
<b>3h</b>	-13.39	$1.98 \times 10^2$	2.30

$$N = 16.03, s_N = 0.86$$

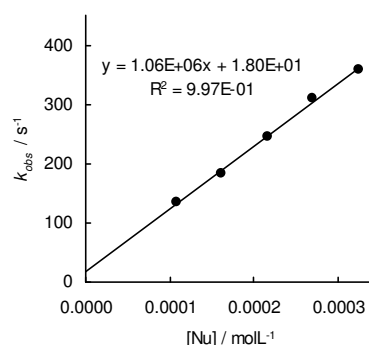


### 4.6.2.12. Reactions of the Anion of Dibenzoylmethane (**1-COPh**)

Table 84: Kinetics of the reaction of **1-COPh** with **3c** (20 °C, stopped-flow, at 618 nm).

$[\mathbf{3c}] / \text{mol L}^{-1}$	$[\mathbf{1-COPh}] / \text{mol L}^{-1}$	$[\mathbf{1-COPh}] / [\mathbf{3c}]$	$k_{\text{obs}} / \text{s}^{-1}$
$1.07 \times 10^{-5}$	$1.08 \times 10^{-4}$	10.1	$1.36 \times 10^2$
$1.07 \times 10^{-5}$	$1.62 \times 10^{-4}$	15.2	$1.84 \times 10^2$
$1.07 \times 10^{-5}$	$2.17 \times 10^{-4}$	20.2	$2.45 \times 10^2$
$1.07 \times 10^{-5}$	$2.71 \times 10^{-4}$	25.3	$3.10 \times 10^2$
$1.07 \times 10^{-5}$	$3.25 \times 10^{-4}$	30.3	$3.59 \times 10^2$

$$k_2 = 1.06 \times 10^6 \text{ L mol}^{-1} \text{s}^{-1}$$

Table 85: Kinetics of the reaction of **1-COPh** with **3d** (20 °C, stopped-flow, at 627 nm).

$[\mathbf{3d}] / \text{mol L}^{-1}$	$[\mathbf{1-COPh}] / \text{mol L}^{-1}$	$[\mathbf{1-COPh}] / [\mathbf{3d}]$	$k_{\text{obs}} / \text{s}^{-1}$
$9.42 \times 10^{-6}$	$1.62 \times 10^{-4}$	17.2	74.0
$9.42 \times 10^{-6}$	$2.17 \times 10^{-4}$	23.0	96.1
$9.42 \times 10^{-6}$	$2.71 \times 10^{-4}$	28.7	122
$9.42 \times 10^{-6}$	$3.25 \times 10^{-4}$	34.5	151

$$k_2 = 4.75 \times 10^5 \text{ L mol}^{-1} \text{s}^{-1}$$

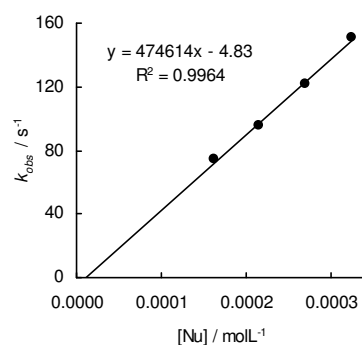
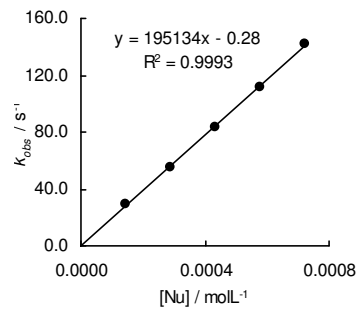


Table 86: Kinetics of the reaction of **1-COPh** with **3e** (20 °C, stopped-flow, at 635 nm).

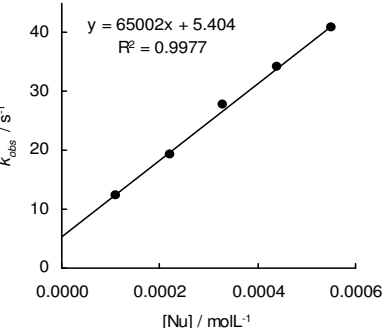
[ <b>3e</b> ] / mol L <sup>-1</sup>	[ <b>1-COPh</b> ] / mol L <sup>-1</sup>	[18-Crown-6] / mol L <sup>-1</sup>	[ <b>1-COPh</b> ] / [ <b>3e</b> ]	$k_{\text{obs}}$ / s <sup>-1</sup>
$1.08 \times 10^{-5}$	$1.45 \times 10^{-4}$		13.4	29.3
$1.08 \times 10^{-5}$	$2.89 \times 10^{-4}$	$3.29 \times 10^{-4}$	26.8	55.1
$1.08 \times 10^{-5}$	$4.30 \times 10^{-4}$		50.2	83.6
$1.08 \times 10^{-5}$	$5.79 \times 10^{-4}$	$6.58 \times 10^{-4}$	53.6	112
$1.08 \times 10^{-5}$	$7.23 \times 10^{-4}$		67.0	142

$k_2 = 1.95 \times 10^5 \text{ L mol}^{-1} \text{ s}^{-1}$


Table 87: Kinetics of the reaction of **1-COPh** with **3f** (20 °C, stopped-flow, at 630 nm).

[ <b>3f</b> ] / mol L <sup>-1</sup>	[ <b>1-COPh</b> ] / mol L <sup>-1</sup>	[18-Crown-6] / mol L <sup>-1</sup>	[ <b>1-COPh</b> ] / [ <b>3f</b> ]	$k_{\text{obs}}$ / s <sup>-1</sup>
$1.06 \times 10^{-5}$	$1.10 \times 10^{-4}$		10.4	12.4
$1.06 \times 10^{-5}$	$2.20 \times 10^{-4}$	$2.88 \times 10^{-4}$	20.8	19.3
$1.06 \times 10^{-5}$	$3.30 \times 10^{-4}$		31.3	27.8
$1.06 \times 10^{-5}$	$4.40 \times 10^{-4}$	$6.73 \times 10^{-4}$	41.7	34.2
$1.06 \times 10^{-5}$	$5.51 \times 10^{-4}$		52.1	40.8

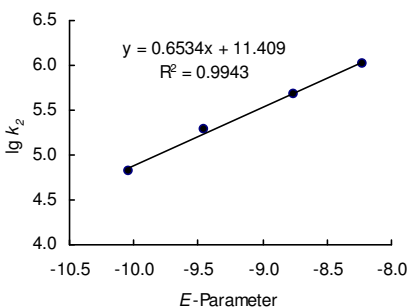
$k_2 = 6.50 \times 10^4 \text{ L mol}^{-1} \text{ s}^{-1}$



### Determination of Reactivity Parameters $N$ and $s_N$ for the Anion of Dibenzoylmethane (**1-COPh**) in DMSO

Table 88: Rate Constants for the reactions of **1-COPh** with different electrophiles (20 °C).

Electrophile	$E$	$k_2 / \text{L mol}^{-1} \text{ s}^{-1}$	$\lg k_2$
<b>3c</b>	-8.22	$1.06 \times 10^6$	6.03
<b>3d</b>	-8.76	$4.75 \times 10^5$	5.68
<b>3e</b>	-9.45	$1.95 \times 10^5$	5.29
<b>3f</b>	-10.04	$6.50 \times 10^4$	4.81



$N = 17.46, s_N = 0.65$

#### 4.6.2.13. Reactions of the Anion of 1-Phenyl-2-(phenylsulfonyl)ethanone (**1-SO<sub>2</sub>Ph**)

Table 89: Kinetics of the reaction of **1-SO<sub>2</sub>Ph** with **3a** (20 °C, stopped-flow, at 613 nm).

[ <b>3a</b> ] / mol L <sup>-1</sup>	[ <b>1-SO<sub>2</sub>Ph</b> ] / mol L <sup>-1</sup>	[ <b>1-SO<sub>2</sub>Ph</b> ] / [ <b>3a</b> ]	$k_{\text{obs}}$ / s <sup>-1</sup>
$1.23 \times 10^{-5}$	$1.27 \times 10^{-4}$	10.3	$7.26 \times 10^1$
$1.23 \times 10^{-5}$	$2.54 \times 10^{-4}$	20.6	$1.36 \times 10^2$
$1.23 \times 10^{-5}$	$3.81 \times 10^{-4}$	30.9	$2.02 \times 10^2$
$1.23 \times 10^{-5}$	$5.08 \times 10^{-4}$	41.1	$2.65 \times 10^2$
$1.23 \times 10^{-5}$	$6.35 \times 10^{-4}$	51.4	$3.31 \times 10^2$

$k_2 = 5.08 \times 10^5 \text{ L mol}^{-1} \text{ s}^{-1}$

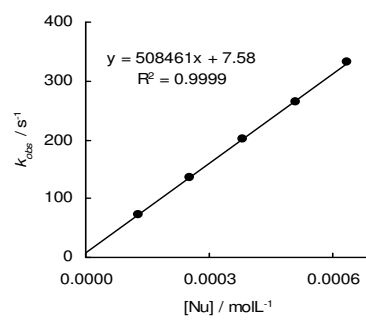
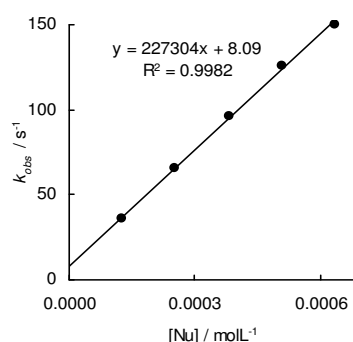


Table 90: Kinetics of the reaction of **1-SO<sub>2</sub>Ph** with **3b** (20 °C, stopped-flow, at 620 nm).

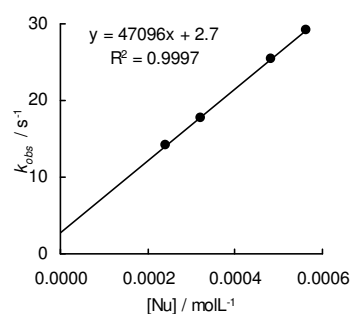
[ <b>3b</b> ] / mol L <sup>-1</sup>	[ <b>1-SO<sub>2</sub>Ph</b> ] / mol L <sup>-1</sup>	[ <b>1-SO<sub>2</sub>Ph</b> ] / [ <b>3b</b> ]	$k_{\text{obs}}$ / s <sup>-1</sup>
$1.18 \times 10^{-5}$	$1.27 \times 10^{-4}$	10.7	$3.57 \times 10^1$
$1.18 \times 10^{-5}$	$2.54 \times 10^{-4}$	21.5	$6.59 \times 10^1$
$1.18 \times 10^{-5}$	$3.81 \times 10^{-4}$	32.2	$9.59 \times 10^1$
$1.18 \times 10^{-5}$	$5.08 \times 10^{-4}$	42.9	$1.26 \times 10^2$
$1.18 \times 10^{-5}$	$6.35 \times 10^{-4}$	53.7	$1.50 \times 10^2$

$$k_2 = 2.27 \times 10^5 \text{ L mol}^{-1} \text{ s}^{-1}$$

Table 91: Kinetics of the reaction of **1-SO<sub>2</sub>Ph** with **3d** (20 °C, stopped-flow, at 627 nm).

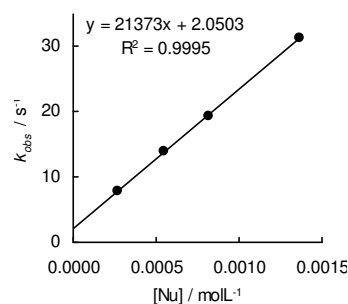
[ <b>3d</b> ] / mol L <sup>-1</sup>	[ <b>1-SO<sub>2</sub>Ph</b> ] / mol L <sup>-1</sup>	[18-Crown-6] / mol L <sup>-1</sup>	[ <b>1-SO<sub>2</sub>Ph</b> ] / [ <b>3d</b> ]	$k_{\text{obs}}$ / s <sup>-1</sup>
$1.19 \times 10^{-5}$	$2.41 \times 10^{-4}$	$2.71 \times 10^{-4}$	20.3	14.1
$1.19 \times 10^{-5}$	$3.21 \times 10^{-4}$		27.1	17.7
$1.19 \times 10^{-5}$	$4.82 \times 10^{-4}$	$5.41 \times 10^{-4}$	40.6	25.5
$1.19 \times 10^{-5}$	$5.62 \times 10^{-4}$		47.4	29.1

$$k_2 = 4.71 \times 10^4 \text{ L mol}^{-1} \text{ s}^{-1}$$

Table 92: Kinetics of the reaction of **1-SO<sub>2</sub>Ph** with **3e** (20 °C, stopped-flow, at 635 nm).

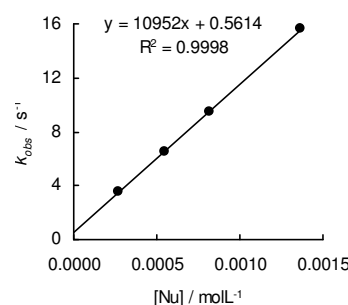
[ <b>3e</b> ] / mol L <sup>-1</sup>	[ <b>1-SO<sub>2</sub>Ph</b> ] / mol L <sup>-1</sup>	[18-Crown-6] / mol L <sup>-1</sup>	[ <b>1-SO<sub>2</sub>Ph</b> ] / [ <b>3e</b> ]	$k_{\text{obs}}$ / s <sup>-1</sup>
$1.13 \times 10^{-5}$	$2.74 \times 10^{-4}$		24.3	7.87
$1.13 \times 10^{-5}$	$5.48 \times 10^{-4}$	$6.32 \times 10^{-4}$	48.7	14.0
$1.13 \times 10^{-5}$	$8.21 \times 10^{-4}$		73.0	19.3
$1.13 \times 10^{-5}$	$1.37 \times 10^{-3}$		122	31.4

$$k_2 = 2.14 \times 10^4 \text{ L mol}^{-1} \text{ s}^{-1}$$

Table 93: Kinetics of the reaction of **1-SO<sub>2</sub>Ph** with **3f** (20 °C, stopped-flow, at 630 nm).<sup>[a]</sup>

[ <b>3f</b> ] / mol L <sup>-1</sup>	[ <b>1-SO<sub>2</sub>Ph</b> ] / mol L <sup>-1</sup>	[18-Crown-6] / mol L <sup>-1</sup>	[ <b>1-SO<sub>2</sub>Ph</b> ] / [ <b>3f</b> ]	$k_{\text{obs}}$ / s <sup>-1</sup>
$9.99 \times 10^{-6}$	$2.74 \times 10^{-4}$		27.4	3.60
$9.99 \times 10^{-6}$	$5.48 \times 10^{-4}$	$6.32 \times 10^{-4}$	54.8	6.57
$9.99 \times 10^{-6}$	$8.21 \times 10^{-4}$		82.2	9.46
$9.99 \times 10^{-6}$	$1.37 \times 10^{-3}$		137	15.6

$$k_2 = 1.10 \times 10^4 \text{ L mol}^{-1} \text{ s}^{-1}$$



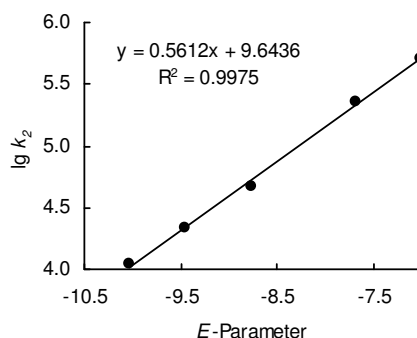
[a] Only the first half-life of the reaction was evaluated.

### Determination of Reactivity Parameters $N$ and $s_N$ for the Anion of 1-Phenyl-2-(phenylsulfonyl)ethanone (**1-SO<sub>2</sub>Ph**) in DMSO

Table 94: Rate Constants for the reactions of **1-SO<sub>2</sub>Ph** with different electrophiles (20 °C).

Electrophile	$E$	$k_2 / \text{L mol}^{-1} \text{s}^{-1}$	$\lg k_2$
<b>3a</b>	-7.02	$5.08 \times 10^5$	5.71
<b>3b</b>	-7.69	$2.27 \times 10^5$	5.36
<b>3d</b>	-8.76	$4.71 \times 10^4$	4.67
<b>3e</b>	-9.45	$2.14 \times 10^4$	4.33
<b>3f</b>	-10.04	$1.10 \times 10^4$	4.08

$$N = 17.18, s_N = 0.56$$

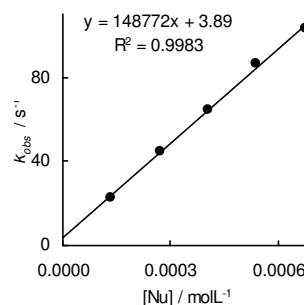


#### 4.6.2.14. Reactions of the Anion of 2-Nitro-1-phenylethanone (**1-NO<sub>2</sub>**)

Table 95: Kinetics of the reaction of **1-NO<sub>2</sub>** with **3a** (20 °C, stopped-flow, at 613 nm).

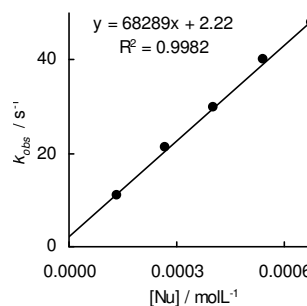
[ <b>3a</b> ] / mol L <sup>-1</sup>	[ <b>1-NO<sub>2</sub></b> ] / mol L <sup>-1</sup>	[18-Crown-6] / mol L <sup>-1</sup>	[ <b>1-NO<sub>2</sub></b> ] / [ <b>3a</b> ]	$k_{\text{obs}} /$ s <sup>-1</sup>
$1.25 \times 10^{-5}$	$1.35 \times 10^{-4}$		10.9	23.1
$1.25 \times 10^{-5}$	$2.71 \times 10^{-4}$	$2.98 \times 10^{-4}$	21.7	44.7
$1.25 \times 10^{-5}$	$4.06 \times 10^{-4}$		32.6	64.4
$1.25 \times 10^{-5}$	$5.41 \times 10^{-4}$	$5.96 \times 10^{-4}$	43.4	86.2
$1.25 \times 10^{-5}$	$6.77 \times 10^{-4}$		54.3	103

$$k_2 = 1.49 \times 10^5 \text{ L mol}^{-1} \text{s}^{-1}$$

Table 96: Kinetics of the reaction of **1-NO<sub>2</sub>** with **3b** (20 °C, stopped-flow, at 620 nm).

[ <b>3b</b> ] / mol L <sup>-1</sup>	[ <b>1-NO<sub>2</sub></b> ] / mol L <sup>-1</sup>	[18-Crown-6] / mol L <sup>-1</sup>	[ <b>1-NO<sub>2</sub></b> ] / [ <b>3b</b> ]	$k_{\text{obs}} /$ s <sup>-1</sup>
$1.12 \times 10^{-5}$	$1.35 \times 10^{-4}$		12.1	11.0
$1.12 \times 10^{-5}$	$2.71 \times 10^{-4}$	$2.98 \times 10^{-4}$	24.1	21.2
$1.12 \times 10^{-5}$	$4.06 \times 10^{-4}$		36.2	29.7
$1.12 \times 10^{-5}$	$5.41 \times 10^{-4}$	$5.96 \times 10^{-4}$	48.2	40.0
$1.12 \times 10^{-5}$	$6.77 \times 10^{-4}$		60.3	47.8

$$k_2 = 6.83 \times 10^4 \text{ L mol}^{-1} \text{s}^{-1}$$

Table 97: Kinetics of the reaction of **1-NO<sub>2</sub>** with **3d** (20 °C, stopped-flow, at 627 nm).

[ <b>3d</b> ] / mol L <sup>-1</sup>	[ <b>1-NO<sub>2</sub></b> ] / mol L <sup>-1</sup>	[18-Crown-6] / mol L <sup>-1</sup>	[ <b>1-NO<sub>2</sub></b> ] / [ <b>3d</b> ]	$k_{\text{obs}} /$ s <sup>-1</sup>
$1.05 \times 10^{-5}$	$2.71 \times 10^{-4}$	$2.98 \times 10^{-4}$	25.7	2.00
$1.05 \times 10^{-5}$	$5.41 \times 10^{-4}$	$5.96 \times 10^{-4}$	51.3	3.83
$1.05 \times 10^{-5}$	$8.12 \times 10^{-4}$		77.0	5.44
$1.05 \times 10^{-5}$	$1.08 \times 10^{-3}$		103	6.96
$1.05 \times 10^{-5}$	$1.35 \times 10^{-3}$		128	8.69

$$k_2 = 6.10 \times 10^3 \text{ L mol}^{-1} \text{s}^{-1}$$

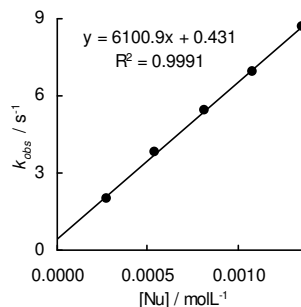
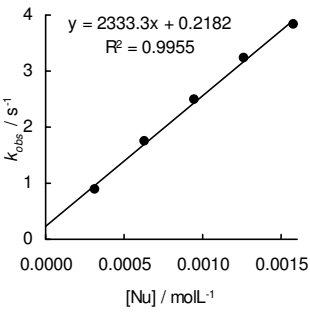




Table 98: Kinetics of the reaction of **1-NO<sub>2</sub>** with **3e** (20 °C, stopped-flow, at 635 nm).

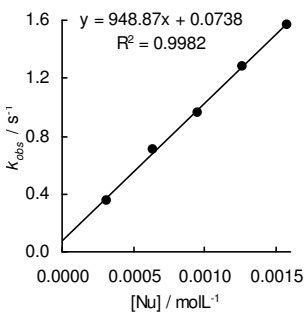
[ <b>3e</b> ] / mol L <sup>-1</sup>	[ <b>1-NO<sub>2</sub></b> ] / mol L <sup>-1</sup>	[18-Crown-6] / mol L <sup>-1</sup>	[ <b>1-NO<sub>2</sub></b> ] / [ <b>3e</b> ]	<i>k</i> <sub>obs</sub> / s <sup>-1</sup>
1.14 × 10 <sup>-5</sup>	3.16 × 10 <sup>-4</sup>		27.8	0.874
1.14 × 10 <sup>-5</sup>	6.33 × 10 <sup>-4</sup>	6.81 × 10 <sup>-4</sup>	55.6	1.75
1.14 × 10 <sup>-5</sup>	9.49 × 10 <sup>-4</sup>		83.3	2.48
1.14 × 10 <sup>-5</sup>	1.27 × 10 <sup>-3</sup>	1.36 × 10 <sup>-3</sup>	111	3.24
1.14 × 10 <sup>-5</sup>	1.58 × 10 <sup>-3</sup>		139	3.81

$k_2 = 2.33 \times 10^3 \text{ L mol}^{-1} \text{ s}^{-1}$


Table 99: Kinetics of the reaction of **1-NO<sub>2</sub>** with **3f** (20 °C, stopped-flow, at 630 nm).

[ <b>3f</b> ] / mol L <sup>-1</sup>	[ <b>1-NO<sub>2</sub></b> ] / mol L <sup>-1</sup>	[18-Crown-6] / mol L <sup>-1</sup>	[ <b>1-NO<sub>2</sub></b> ] / [ <b>3f</b> ]	<i>k</i> <sub>obs</sub> / s <sup>-1</sup>
1.01 × 10 <sup>-5</sup>	3.16 × 10 <sup>-4</sup>		31.4	0.356
1.01 × 10 <sup>-5</sup>	6.33 × 10 <sup>-4</sup>	6.81 × 10 <sup>-4</sup>	62.7	0.706
1.01 × 10 <sup>-5</sup>	9.49 × 10 <sup>-4</sup>		94.1	0.960
1.01 × 10 <sup>-5</sup>	1.27 × 10 <sup>-3</sup>	1.36 × 10 <sup>-3</sup>	125	1.28
1.01 × 10 <sup>-5</sup>	1.58 × 10 <sup>-3</sup>		157	1.57

$k_2 = 9.49 \times 10^2 \text{ L mol}^{-1} \text{ s}^{-1}$

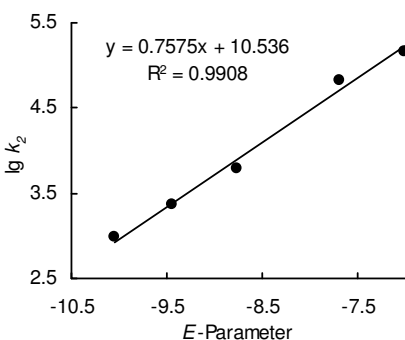


### Determination of Reactivity Parameters *N* and *s<sub>N</sub>* for the Anion of 2-Nitro-1-Phenylethanone (**1-NO<sub>2</sub>**) in DMSO

Table 100: Rate Constants for the reactions of **1-NO<sub>2</sub>** with different electrophiles (20 °C).

Electrophile	<i>E</i>	<i>k</i> <sub>2</sub> / L mol <sup>-1</sup> s <sup>-1</sup>	lg <i>k</i> <sub>2</sub>
<b>3a</b>	-7.02	1.49 × 10 <sup>5</sup>	5.17
<b>3b</b>	-7.69	6.83 × 10 <sup>4</sup>	4.83
<b>3d</b>	-8.76	6.10 × 10 <sup>3</sup>	3.79
<b>3e</b>	-9.45	2.33 × 10 <sup>3</sup>	3.37
<b>3f</b>	-10.04	9.49 × 10 <sup>2</sup>	2.98

$N = 13.91, s_N = 0.76$



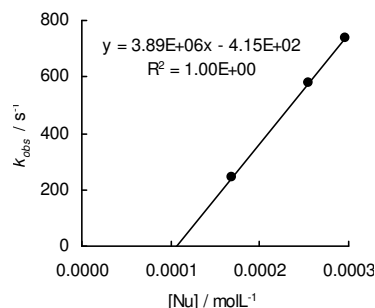
### 4.6.3. Determination of the Nucleophilicity of the Benzyl Anions 2

#### 4.6.3.1. Reactions of the Anion of 2-Phenylacetonitrile (2-CN)

Table 101: Kinetics of the reaction of **2-CN** (generated from (**2-CN**)-H by addition of 1.07 equivalents of dimsyl-K) with **3n** (20 °C, stopped-flow, at 486 nm).<sup>[a]</sup>

[ <b>3n</b> ] / mol L <sup>-1</sup>	[ <b>2-CN</b> ] / mol L <sup>-1</sup>	[18-Crown-6] / mol L <sup>-1</sup>	[ <b>2-CN</b> ] / [ <b>3n</b> ]	$k_{\text{obs}}$ / s <sup>-1</sup>
$1.83 \times 10^{-5}$	$1.70 \times 10^{-4}$		9.3	243
$1.83 \times 10^{-5}$	$2.55 \times 10^{-4}$	$2.76 \times 10^{-4}$	13.9	581
$1.83 \times 10^{-5}$	$2.97 \times 10^{-4}$		16.3	736

$$k_2 = 3.89 \times 10^6 \text{ L mol}^{-1} \text{ s}^{-1}$$

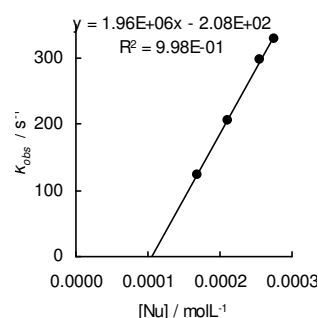


[a] The negative intercept with the abscissa is due to slow/incomplete mixing of the reactants in comparison with the fast reaction.

Table 102: Kinetics of the reaction of **2-CN** (generated from (**2-CN**)-H by addition of 1.07 equivalents of dimsyl-K) with **3o** (20 °C, stopped-flow, at 521 nm).<sup>[a]</sup>

[ <b>3o</b> ] / mol L <sup>-1</sup>	[ <b>2-CN</b> ] / mol L <sup>-1</sup>	[18-Crown-6] / mol L <sup>-1</sup>	[ <b>2-CN</b> ] / [ <b>3o</b> ]	$k_{\text{obs}}$ / s <sup>-1</sup>
$1.82 \times 10^{-5}$	$1.70 \times 10^{-4}$		9.3	124
$1.82 \times 10^{-5}$	$2.12 \times 10^{-4}$	$2.30 \times 10^{-4}$	11.7	206
$1.82 \times 10^{-5}$	$2.55 \times 10^{-4}$		14.0	296
$1.82 \times 10^{-5}$	$2.76 \times 10^{-4}$	$3.04 \times 10^{-4}$	15.2	328

$$k_2 = 1.96 \times 10^6 \text{ L mol}^{-1} \text{ s}^{-1}$$



[a] The negative intercept with the abscissa is due to slow/incomplete mixing of the reactants in comparison with the fast reaction.

#### 4.6.3.2. Reactions of the Anion of Phenylacetone (2-COMe)

Table 103: Kinetics of the reaction of **2-COMe** (generated from (**2-COMe**)-H by addition of 1.05 equivalents of KOtBu) with **3m** (20 °C, stopped-flow, at 490 nm).

[ <b>3m</b> ] / mol L <sup>-1</sup>	[ <b>2-COMe</b> ] / mol L <sup>-1</sup>	[ <b>2-COMe</b> ] / [ <b>3m</b> ]	$k_{\text{obs}}$ / s <sup>-1</sup>
$1.74 \times 10^{-5}$	$2.14 \times 10^{-4}$	12.3	$1.75 \times 10^1$
$1.74 \times 10^{-5}$	$3.21 \times 10^{-4}$	18.5	$3.50 \times 10^1$
$1.74 \times 10^{-5}$	$4.28 \times 10^{-4}$	24.6	$5.04 \times 10^1$
$1.74 \times 10^{-5}$	$6.42 \times 10^{-4}$	36.9	$7.97 \times 10^1$

$$k_2 = 1.44 \times 10^5 \text{ L mol}^{-1} \text{ s}^{-1}$$

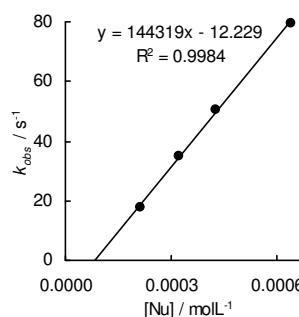
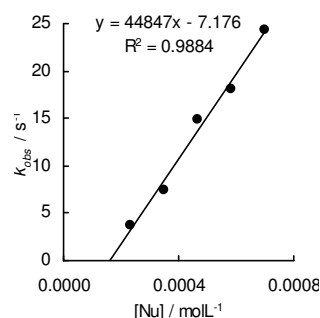


Table 104: Kinetics of the reaction of **2-COMe** (generated from (**2-COMe**)-H by addition of 1.05 equivalents of KO<sup>t</sup>Bu) with **3n** (20 °C, stopped-flow, at 486 nm).

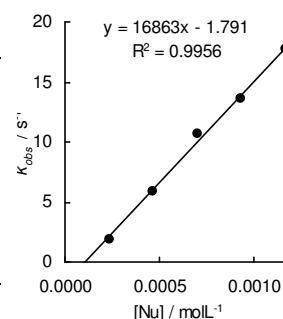
[ <b>3n</b> ] / mol L <sup>-1</sup>	[ <b>2-COMe</b> ] / mol L <sup>-1</sup>	[18-Crown-6] / mol L <sup>-1</sup>	[ <b>2-COMe</b> ] / [ <b>3n</b> ]	$k_{\text{obs}} /$ s <sup>-1</sup>
$1.87 \times 10^{-5}$	$2.33 \times 10^{-4}$		12.4	3.66
$1.87 \times 10^{-5}$	$3.49 \times 10^{-4}$	$3.77 \times 10^{-4}$	18.6	7.44
$1.87 \times 10^{-5}$	$4.65 \times 10^{-4}$		24.8	14.8
$1.87 \times 10^{-5}$	$5.81 \times 10^{-4}$	$6.10 \times 10^{-4}$	31.0	18.1
$1.87 \times 10^{-5}$	$6.98 \times 10^{-4}$		37.3	24.4

$$k_2 = 4.48 \times 10^4 \text{ L mol}^{-1} \text{ s}^{-1}$$

Table 105: Kinetics of the reaction of **2-COMe** (generated from (**2-COMe**)-H by addition of 1.05 equivalents of KO<sup>t</sup>Bu) with **3o** (20 °C, stopped-flow, at 486 nm).

[ <b>3o</b> ] / mol L <sup>-1</sup>	[ <b>2-COMe</b> ] / mol L <sup>-1</sup>	[18-Crown-6] / mol L <sup>-1</sup>	[ <b>2-COMe</b> ] / [ <b>3o</b> ]	$k_{\text{obs}} /$ s <sup>-1</sup>
$1.58 \times 10^{-5}$	$2.33 \times 10^{-4}$		14.7	1.93
$1.58 \times 10^{-5}$	$4.65 \times 10^{-4}$	$5.02 \times 10^{-4}$	29.4	5.93
$1.58 \times 10^{-5}$	$6.98 \times 10^{-4}$		44.1	10.7
$1.58 \times 10^{-5}$	$9.30 \times 10^{-4}$	$1.00 \times 10^{-3}$	58.8	13.6
$1.58 \times 10^{-5}$	$1.16 \times 10^{-3}$		73.5	17.7

$$k_2 = 1.69 \times 10^4 \text{ L mol}^{-1} \text{ s}^{-1}$$

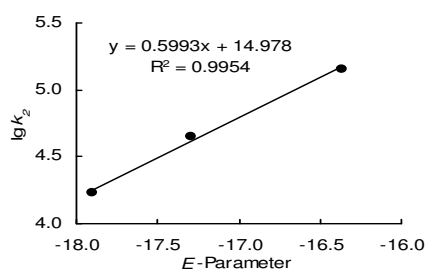


### Determination of Reactivity Parameters $N$ and $s_N$ for the Anion of 2-Phenylacetone (**2-COMe**) in DMSO

Table 106: Rate Constants for the reactions of **2-COMe** with different electrophiles (20 °C).

Electrophile	$E$	$k_2 / \text{L mol}^{-1} \text{ s}^{-1}$	$\lg k_2$
<b>3m</b>	-16.36	$1.44 \times 10^5$	5.16
<b>3n</b>	-17.29	$4.48 \times 10^4$	4.65
<b>3o</b>	-17.90	$1.69 \times 10^4$	4.23

$$N = 24.99, s_N = 0.60$$



### 4.6.3.3. Reactions of the Anion of Benzyl Phenylsulfone (**2-SO<sub>2</sub>Ph**)

Table 107: Kinetics of the reaction of **2-SO<sub>2</sub>Ph** (generated from (**2-SO<sub>2</sub>Ph**)-H by addition of 1.06 equivalents of KO<sup>t</sup>Bu) with **3m** (20 °C, stopped-flow, at 490 nm).

[ <b>3m</b> ] / mol L <sup>-1</sup>	[ <b>2-SO<sub>2</sub>Ph</b> ] / mol L <sup>-1</sup>	[ <b>2-SO<sub>2</sub>Ph</b> ] / [ <b>3m</b> ]	$k_{\text{obs}} /$ s <sup>-1</sup>
$1.78 \times 10^{-5}$	$2.63 \times 10^{-4}$	14.8	$2.77 \times 10^1$
$1.78 \times 10^{-5}$	$3.95 \times 10^{-4}$	22.2	$5.17 \times 10^1$
$1.78 \times 10^{-5}$	$5.27 \times 10^{-4}$	29.7	$8.01 \times 10^1$
$1.78 \times 10^{-5}$	$6.59 \times 10^{-4}$	37.1	$1.04 \times 10^2$

$$k_2 = 1.95 \times 10^5 \text{ L mol}^{-1} \text{ s}^{-1}$$

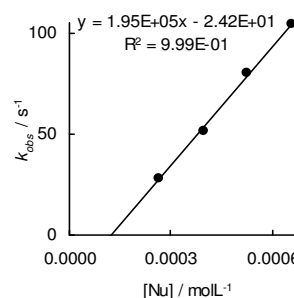


Table 108: Kinetics of the reaction of **2-SO<sub>2</sub>Ph** (generated from (**2-SO<sub>2</sub>Ph**)-H by addition of 1.05 equivalents of KO<sup>t</sup>Bu) with **3n** (20 °C, stopped-flow, at 486 nm).

[ <b>3n</b> ] / mol L <sup>-1</sup>	[ <b>2-SO<sub>2</sub>Ph</b> ] / mol L <sup>-1</sup>	[18-Crown-6] mol L <sup>-1</sup>	[ <b>2-SO<sub>2</sub>Ph</b> ] /[ <b>3n</b> ]	<i>k</i> <sub>obs</sub> / s <sup>-1</sup>
1.58 × 10 <sup>-5</sup>	2.12 × 10 <sup>-4</sup>		13.4	3.62
1.58 × 10 <sup>-5</sup>	4.24 × 10 <sup>-4</sup>	5.23 × 10 <sup>-4</sup>	26.8	17.0
1.58 × 10 <sup>-5</sup>	6.36 × 10 <sup>-4</sup>		40.2	27.5
1.58 × 10 <sup>-5</sup>	8.48 × 10 <sup>-4</sup>	1.05 × 10 <sup>-3</sup>	53.6	41.5
1.58 × 10 <sup>-5</sup>	1.06 × 10 <sup>-3</sup>		67.0	53.3

$k_2 = 5.84 \times 10^4 \text{ L mol}^{-1} \text{ s}^{-1}$

Table 109: Kinetics of the reaction of **2-SO<sub>2</sub>Ph** (generated from (**2-SO<sub>2</sub>Ph**)-H by addition of 1.09 equivalents of KO<sup>t</sup>Bu) with **3o** (20 °C, stopped-flow, at 521 nm).

[ <b>3o</b> ] / mol L <sup>-1</sup>	[ <b>2-SO<sub>2</sub>Ph</b> ] / mol L <sup>-1</sup>	[18-Crown-6] / mol L <sup>-1</sup>	[ <b>2-SO<sub>2</sub>Ph</b> ] /[ <b>3o</b> ]	<i>k</i> <sub>obs</sub> / s <sup>-1</sup>
1.45 × 10 <sup>-5</sup>	2.12 × 10 <sup>-4</sup>		14.6	2.72
1.45 × 10 <sup>-5</sup>	4.24 × 10 <sup>-4</sup>	4.64 × 10 <sup>-4</sup>	29.3	8.74
1.45 × 10 <sup>-5</sup>	6.36 × 10 <sup>-4</sup>		43.9	13.9
1.45 × 10 <sup>-5</sup>	8.48 × 10 <sup>-4</sup>	9.28 × 10 <sup>-4</sup>	58.6	20.4
1.45 × 10 <sup>-5</sup>	1.06 × 10 <sup>-3</sup>		73.2	25.1

$k_2 = 2.66 \times 10^4 \text{ L mol}^{-1} \text{ s}^{-1}$

### Determination of Reactivity Parameters *N* and *s<sub>N</sub>* for the Anion of Benzyl Phenylsulfone (**2-SO<sub>2</sub>Ph**) in DMSO

Table 110: Rate Constants for the reactions of **2-SO<sub>2</sub>Ph** with different electrophiles (20 °C).

Electrophile	<i>E</i>	<i>k</i> <sub>2</sub> / L mol <sup>-1</sup> s <sup>-1</sup>	lg <i>k</i> <sub>2</sub>
<b>3m</b>	-16.36	1.95 × 10 <sup>5</sup>	5.16
<b>3n</b>	-17.29	5.84 × 10 <sup>4</sup>	4.65
<b>3o</b>	-17.90	2.66 × 10 <sup>4</sup>	4.23

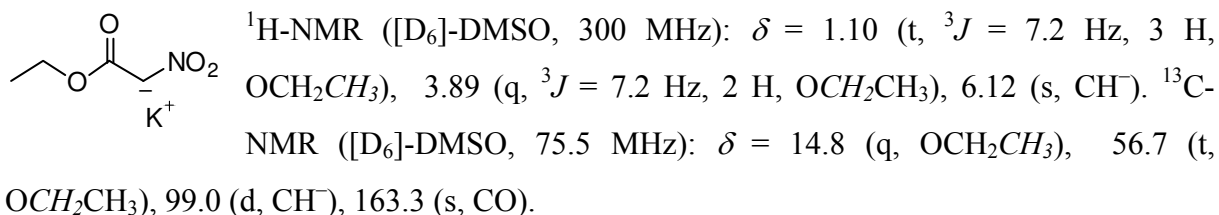
$N = 25.77, s_N = 0.56$

## 5. Appendix

### 5.1. Determination of the Nucleophilic Reactivity of 8-NO<sub>2</sub>

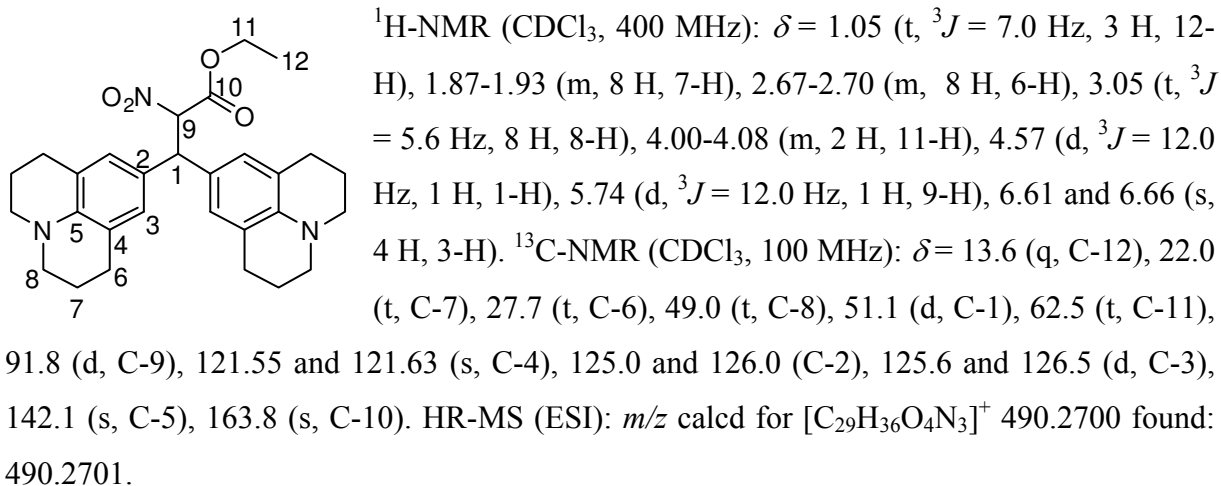
#### 5.1.1. Synthesis of 8-NO<sub>2</sub>

**Potassium 2-ethoxy-1-nitro-2-oxoethan-1-ide (8-NO<sub>2</sub>)-K** was obtained according GP1 from KO<sup>t</sup>Bu (844 mg, 7.88 mmol) and ethyl 2-nitroacetate (**8-H**, 1.08 g, 8.11 mmol) as a colorless solid (948 mg, 5.54 mmol, 70%).



#### 5.1.2. Reaction of 8-NO<sub>2</sub> with 3e-BF<sub>4</sub>

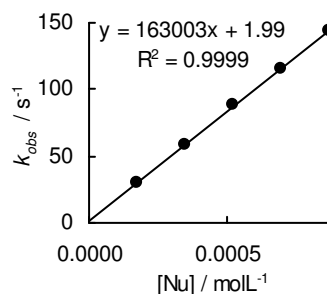
According to GP2, the potassium salt (**8-NO<sub>2</sub>**)-K (43.1 mg, 0.252 mmol) and **3e-BF<sub>4</sub>** (106 mg, 0.299 mmol) yielded ethyl 3,3-bis(1,2,3,5,6,7-hexahydropyrido[3,2,1-ij]quinolin-9-yl)-2-nitropropanoate (96.5 mg, 0.197 mmol, 82%) as yellow solid.



5.1.3. Kinetic Experiments of 8-NO<sub>2</sub> with Benzhdrylium IonsTable 111: Kinetics of the reaction of 8-NO<sub>2</sub> with 3c (20 °C, stopped-flow, at 618 nm).

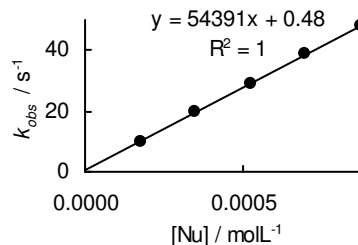
[3c] / mol L <sup>-1</sup>	[8-NO <sub>2</sub> ] / mol L <sup>-1</sup>	[2-NO <sub>2</sub> ] /[3c]	<i>k</i> <sub>obs</sub> / s <sup>-1</sup>
1.66 × 10 <sup>-5</sup>	1.75 × 10 <sup>-4</sup>	10.5	30.2
1.66 × 10 <sup>-5</sup>	3.49 × 10 <sup>-4</sup>	21.1	58.9
1.66 × 10 <sup>-5</sup>	5.24 × 10 <sup>-4</sup>	31.6	87.9
1.66 × 10 <sup>-5</sup>	6.99 × 10 <sup>-4</sup>	42.2	116
1.66 × 10 <sup>-5</sup>	8.73 × 10 <sup>-4</sup>	52.7	114

$$k_2 = 1.63 \times 10^5 \text{ L mol}^{-1} \text{ s}^{-1}$$

Table 112: Kinetics of the reaction of 8-NO<sub>2</sub> with 3d (20 °C, stopped-flow, at 627 nm).

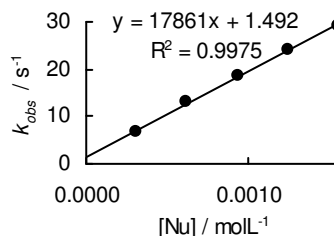
[3d] / mol L <sup>-1</sup>	[8-NO <sub>2</sub> ] / mol L <sup>-1</sup>	[2-NO <sub>2</sub> ] /[3d]	<i>k</i> <sub>obs</sub> / s <sup>-1</sup>
1.43 × 10 <sup>-5</sup>	1.75 × 10 <sup>-4</sup>	12.1	10.0
1.43 × 10 <sup>-5</sup>	3.49 × 10 <sup>-4</sup>	24.5	19.5
1.43 × 10 <sup>-5</sup>	5.24 × 10 <sup>-4</sup>	36.7	28.9
1.43 × 10 <sup>-5</sup>	6.99 × 10 <sup>-4</sup>	48.9	38.5
1.43 × 10 <sup>-5</sup>	8.73 × 10 <sup>-4</sup>	61.2	48.0

$$k_2 = 5.44 \times 10^4 \text{ L mol}^{-1} \text{ s}^{-1}$$

Table 113: Kinetics of the reaction of 8-NO<sub>2</sub> with 3e (20 °C, stopped-flow, at 635 nm).

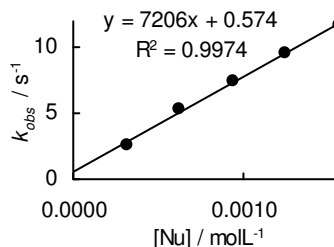
[3e] / mol L <sup>-1</sup>	[8-NO <sub>2</sub> ] / mol L <sup>-1</sup>	[18-Crown-6] / mol L <sup>-1</sup>	[8-NO <sub>2</sub> ] /[3e]	<i>k</i> <sub>obs</sub> / s <sup>-1</sup>
1.19 × 10 <sup>-5</sup>	3.13 × 10 <sup>-4</sup>		26.3	6.59
1.19 × 10 <sup>-5</sup>	6.25 × 10 <sup>-4</sup>	7.08 × 10 <sup>-4</sup>	52.6	12.9
1.19 × 10 <sup>-5</sup>	9.38 × 10 <sup>-4</sup>		78.9	18.8
1.19 × 10 <sup>-5</sup>	1.25 × 10 <sup>-3</sup>	2.12 × 10 <sup>-3</sup>	105	23.9
1.19 × 10 <sup>-5</sup>	1.56 × 10 <sup>-3</sup>		132	29.0

$$k_2 = 1.79 \times 10^4 \text{ L mol}^{-1} \text{ s}^{-1}$$

Table 114: Kinetics of the reaction of 8-NO<sub>2</sub> with 3f (20 °C, stopped-flow, at 630 nm).

[3f] / mol L <sup>-1</sup>	[8-NO <sub>2</sub> ] / mol L <sup>-1</sup>	[18-Crown-6] / mol L <sup>-1</sup>	[8-NO <sub>2</sub> ] /[3f]	<i>k</i> <sub>obs</sub> / s <sup>-1</sup>
1.34 × 10 <sup>-5</sup>	3.13 × 10 <sup>-4</sup>		27.4	2.60
1.34 × 10 <sup>-5</sup>	6.25 × 10 <sup>-4</sup>	7.08 × 10 <sup>-4</sup>	54.9	5.27
1.34 × 10 <sup>-5</sup>	9.38 × 10 <sup>-4</sup>		82.3	7.49
1.34 × 10 <sup>-5</sup>	1.25 × 10 <sup>-3</sup>	2.12 × 10 <sup>-3</sup>	110	9.59
1.34 × 10 <sup>-5</sup>	1.56 × 10 <sup>-3</sup>		137	11.7

$$k_2 = 7.21 \times 10^3 \text{ L mol}^{-1} \text{ s}^{-1}$$

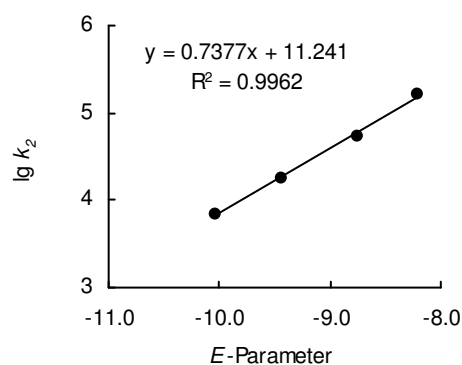


### Determination of Reactivity Parameters $N$ and $s_N$ for the Anion of Benzyl Phenylsulfone ( $\mathbf{8-NO_2}$ ) in DMSO

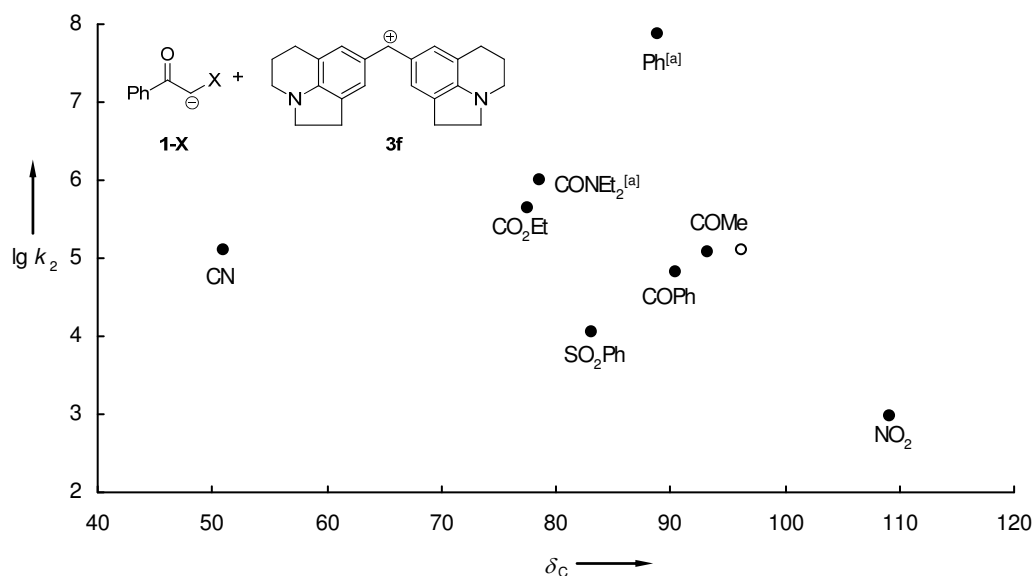
Table 115: Rate Constants for the reactions of  $\mathbf{8-NO_2}$  with different electrophiles (20 °C).

Electrophile	$E$	$k_2 / \text{L mol}^{-1} \text{s}^{-1}$	$\lg k_2$
<b>3c</b>	-8.22	$1.63 \times 10^5$	5.21
<b>3d</b>	-8.76	$5.44 \times 10^4$	4.74
<b>3e</b>	-9.45	$1.79 \times 10^4$	4.25
<b>3f</b>	-10.04	$7.21 \times 10^3$	3.86

$$N = 15.24, s_N = 0.74$$



## 5.2. Correlations

Figure 17: Plot of  $\lg k_2$  of the reactions of the carbanions  $\mathbf{1-X}$  with the benzhydrylium ion  $\mathbf{3f}$  (in DMSO, 20 °C) vs. the  $^{13}\text{C}$  NMR shifts of the their carbanionic center (in  $[\text{D}_6]$  DMSO). [a]  $k_2$  calculated with eq (1).

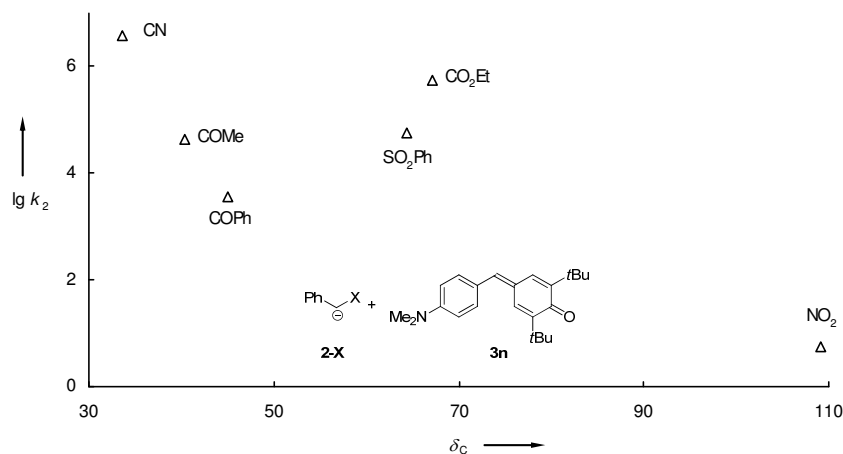


Figure 18: Plot of  $\lg k_2$  of the reactions of the carbanions **2-X** with the quinone methide **3n** (in DMSO, 20 °C) vs. the  $^{13}\text{C}$  NMR shifts of the their carbanionic center (in [D<sub>6</sub>] DMSO).

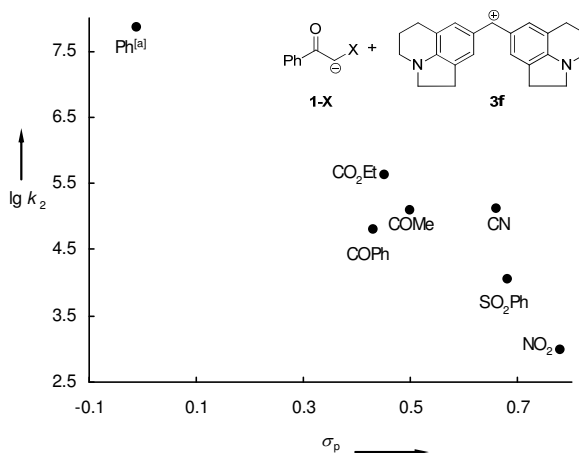


Figure 19: Plot of  $\lg k_2$  of the reactions of the carbanions **1-X** with the benzhydrylium ion **3f** (in DMSO, 20 °C) vs. Hammett's  $\sigma_p$  substituent constants. [a]  $k_2$  calculated with eq (1).

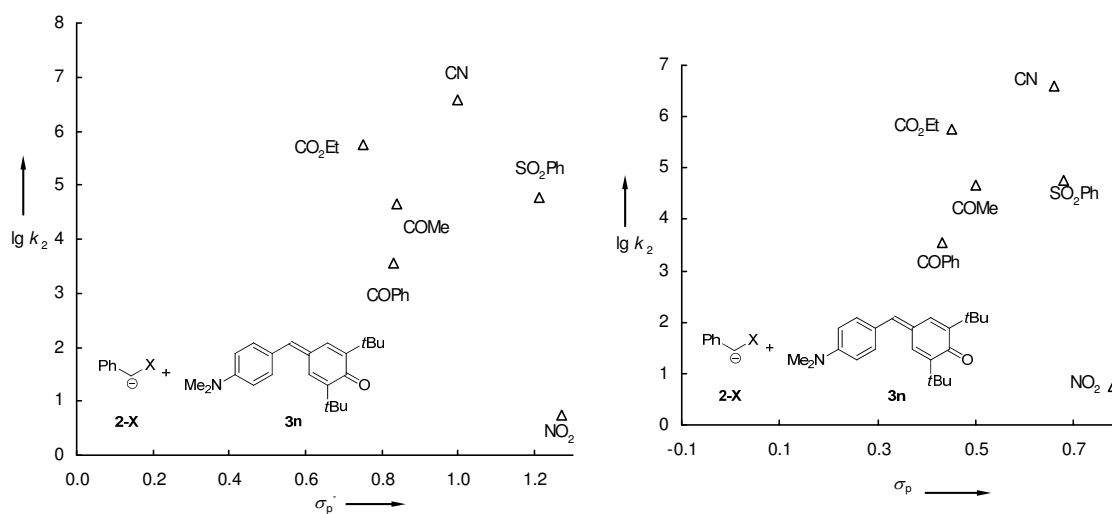


Figure 20: Plot of  $\lg k_2$  of the reactions of the carbanions **2-X** with the electrophile **3n** (in DMSO, 20 °C) vs. Hammett's  $\sigma_p^-$  (left) and  $\sigma_p$  (right) substituent constants.



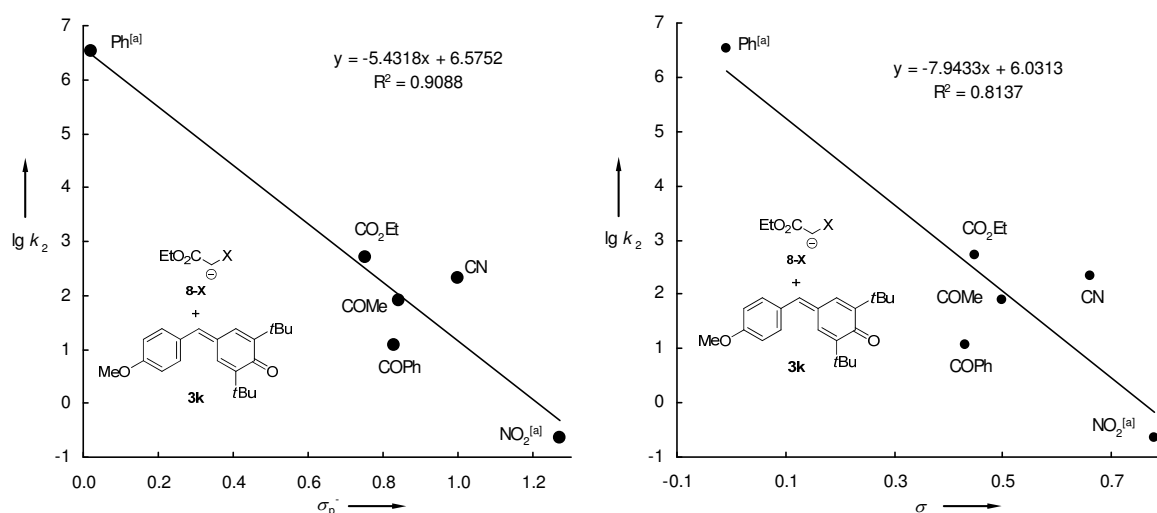


Figure 21: Plot of  $\lg k_2$  of the reactions of the carbanions  $8\text{-X}$  with the electrophile  $3\text{k}$  (in DMSO, 20 °C) vs. Hammett's  $\sigma_p^-$  (left) and  $\sigma$  (right) substituent constants. [a]  $k_2$  calculated with eq (1).

## 6. References

- [1] a) R. B. Bates, C. A. Ogle, *Carbanion Chemistry*, Springer, Berlin, **1983**; b) L. Brandsma, *Preparative Polar Organometallic Chemistry 2*, Springer, Berlin, **1990**, pp. 1-11; c) V. Snieckus, *Advances in Carbanion Chemistry Vol. 1*, JAI Press, Greenwich, CT, **1992**; d) E. Buncl, J. M. Dust, *Carbanion Chemistry*, Oxford, New York, **2003**; e) M. B. Smith, *March's Advanced Organic Chemistry, 7<sup>th</sup> Ed.*, Wiley, Hoboken, **2013**, pp. 221-234.
- [2] Reactivity of Carbanions: a) R. Lucius, H. Mayr, *Angew. Chem.* **2000**, *112*, 2086-2089; *Angew. Chem. Int. Ed.* **2000**, *39*, 1995-1997; b) T. Bug, T. Lemek, H. Mayr, *J. Org. Chem.* **2004**, *69*, 7565-7576; c) T. B. Phan, H. Mayr, *Eur. J. Org. Chem.* **2006**, 2530-2537; d) S. T. A. Berger, A. R. Ofial, H. Mayr, *J. Am. Chem. Soc.* **2007**, *129*, 9753-9761; e) F. Seeliger, H. Mayr, *Org. Biomol. Chem.* **2008**, *6*, 3052-3058; f) O. Kaumanns, R. Appel, T. Lemek, F. Seeliger, H. Mayr, *J. Org. Chem.* **2009**, *74*, 75-81; g) F. Corral-Bautista, H. Mayr, *Eur. J. Org. Chem.* **2013**, 4255-4261.
- [3] Selected publications: a) H. Mayr, M. Patz, *Angew. Chem.* **1994**, *106*, 990-1010; *Angew. Chem. Int. Ed. Engl.* **1994**, *33*, 938-957; b) H. Mayr, T. Bug, M. F. Gotta, N. Hering, B. Irrgang, B. Janker, B. Kempf, R. Loos, A. R. Ofial, G. Remennikov, H. Schimmel, *J. Am. Chem. Soc.* **2001**, *123*, 9500-9512; c) R. Lucius, R. Loos, H. Mayr, *Angew. Chem.* **2002**, *114*, 97-102; *Angew. Chem. Int. Ed.* **2002**, *41*, 91-95; d) H. Mayr, B. Kempf, A. R. Ofial, *Acc. Chem. Res.* **2003**, *36*, 66-77; e) H. Mayr, A. R. Ofial, *Pure Appl. Chem.*

- 2005**, 77, 1807–1821; f) D. Richter, N. Hampel, T. Singer, A. R. Ofial, H. Mayr, *Eur. J. Org. Chem.* **2009**, 3203–3211; g) H. Mayr, A. R. Ofial, *J. Phys. Org. Chem.* **2008**, 21, 584–595; h) H. Mayr, S. Lakhdar, B. Maji, A. R. Ofial, *Beilstein J. Org. Chem.* **2012**, 8, 1458–1478; i) For a comprehensive listing of nucleophilicity parameters  $N$ ,  $s_N$  and electrophilicity parameters  $E$ , see <http://www.cup.uni-muenchen.de/oc/mayr/DBintro.html>.
- [4] S. T. A. Berger, F. H. Seeliger, F. Hofbauer, H. Mayr, *Org. Biomol. Chem.* **2007**, 5, 3020–3026.
- [5] a) W. S. Matthews, J. E. Bares, J. E. Bartmess, F. G. Bordwell, F. J. Cornforth, G. E. Drucker, Z. Margolin, R. J. McCallum, G. J. McCollum, N. R. Vanier, *J. Am. Chem. Soc.* **1975**, 79, 7006–7014; b) F. G. Bordwell, M. Van der Puy, N. R. Vanier, *J. Org. Chem.* **1976**, 41, 1883–1885; c) É. S. Petrov, E. N. Tsvetkov, S. P. Mesyats, A. N. Shatenshtein, M. I. Kabachnik, *Izv. Akad. Nauk SSSR* **1976**, 782–787; d) J. M. Kern, P. Federlin, *Tetrahedron*, **1978**, 66, 661–670; e) F. G. Bordwell, J. E. Bares, J. E. Bartmess, G. J. McCollum, M. Van der Puy, N. R. Vanier, W. S. Matthews, *J. Org. Chem.* **1977**, 42, 321–325; f) W. N. Olmstead, F. G. Bordwell, *J. Org. Chem.* **1980**, 45, 3299–3305; g) F. G. Bordwell, J. A. Harrelson Jr., *Can. J. Chem.* **1990**, 68, 1714–1718.
- [6] M. Raban, E. A. Noe, G. Yamamoto, *J. Am. Chem. Soc.* **1977**, 99, 6527–6531.
- [7] For an overview concerning ion-pairing effects of alkali enolates of  $\beta$ -dicarbonyls: a) H. E. Zaug, A. D. Schaefer, *J. Am. Chem. Soc.* **1965**, 87, 1857–1866; b) M. Raban, D. P. Haritos, *J. Am. Chem. Soc.* **1979**, 101, 5178–5182; c) S. M. Esakov, A. A. Petrov, B. A. Ershov, *J. Org. Chem. USSR (Engl. Trans.)* **1975**, 11, 679–688; d) A. A. Petrov, S. M. Esakov, B. A. Ershov, *J. Org. Chem. USSR (Engl. Trans.)* **1976**, 12, 774–778; e) A. Facchetti, A. Streitwieser, *J. Org. Chem.* **2004**, 69, 8345–8355; f) A. Streitwieser, *J. Mol. Model.* **2006**, 12, 673–680 and references mentioned there.
- [8] For determination of the nucleophilic reactivity of **8**-NO<sub>2</sub> see Appendix of the Supporting Information.
- [6] a) S. Bradamante, G. A. Pagani, *J. Org. Chem.* **1984**, 49, 2863–2870; b) S. Bradamante, G. A. Pagani, *J. Chem. Soc. Perkin Trans. 2* **1986**, 1035–1046; c) E. Barchiesi, S. Bradamante, R. Ferraccioli, G. A. Pagani, *J. Chem. Soc. Perkin Trans. 2* **1990**, 375–383. d) E. Barchiesi, S. Bradamante, R. Ferraccioli, G. A. Pagani, *J. Chem. Soc. Chem. Commun.* **1987**, 1548–1549.

- [10] C. Hansch, A. Leo, D. Hoekman, *Exploring QSAR – Hydrophobic, Electronic, and Steric Constants*, American Chemical Society, Washington, DC, **1995**; and references therein.
- [11] R. Appel, R. Loos, H. Mayr, *J. Am. Chem. Soc.* **2009**, *131*, 704-714.
- [12] H. E. Gottlieb, V. Kotlyar, A. Nudelman, *J. Org. Chem.* **1997**, *62*, 7512-7515.
- [13] R. V. Hoffman, D. J. Huizenga, *J. Org. Chem.* **1991**, *56*, 6435-3439.
- [14] N. Suryakiran, R. Srikanth Reddy, K. Ahalatha, M. Lakshman, Y. Venkateswarlu, *Tetrahedron Lett.* **2006**, *47*, 3853-3856.

## Chapter 4

Quantification of the Nucleophilic Reactivities of Cyclic  $\beta$ -Ketoesters

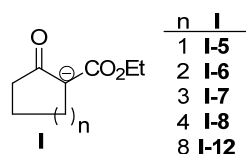
Francisco Corral Bautista and Herbert Mayr

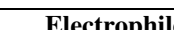
## 1. Introduction

Relationships between ring size and reactivities of cycloalkyl derivatives have attracted the attention of chemists for several decades.<sup>[1-3]</sup> Several investigations dealt with the physical and chemical properties of cyclic  $\beta$ -ketoesters of different ring-size and their anions.<sup>[3]</sup> In extension of our earlier studies on the nucleophilic reactivities of differently substituted carbanions,<sup>[4]</sup> we now report how the nucleophilicities of cyclic  $\beta$ -ketoesters (Scheme 1) depend on ring-size.

For this purpose, we have studied the kinetics of the reactions of the anions of the cyclic  $\beta$ -ketoesters **I** (Scheme 1) with quinone methides **2** (reference electrophiles, Table 1) in DMSO solution and calculated the nucleophilicity parameters of these anions by using the linear free-energy relationship (1).<sup>[5]</sup> In this equation  $E$  is an electrophile-specific parameter,  $N$  and  $s_N$  are nucleophile-specific parameters which are derived from the rates of the reactions of  $\pi$ -,  $n$ -, and  $\sigma$ -nucleophiles with benzydrylium ions and structurally related Michael acceptors (reference electrophiles).<sup>[6]</sup>

$$\lg k_2 (20\text{ }^\circ\text{C}) = s_N (N + E) \quad (1)$$

Scheme 1: Structures of the studied carbanions **I**.Table 1: Quinone methides **2** employed as reference electrophiles in this study.

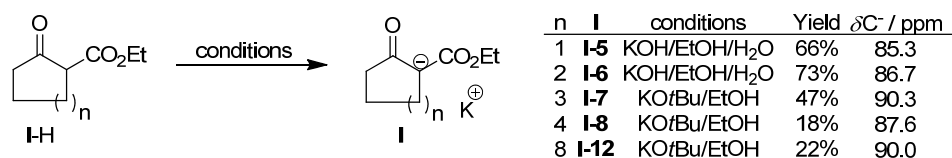
Electrophile			$E^{[a]}$	$\lambda_{\max}$	
	$R^1 = \text{Ph}$	$R^2 = 4\text{-OMe}$	<b>2a</b>	-12.18	422
	$R^1 = \text{Ph}$	$R^2 = 4\text{-NMe}_2$	<b>2b</b>	-13.39	533
	$R^1 = t\text{Bu}$	$R^2 = 4\text{-NO}_2$	<b>2c</b>	-14.36	374
	$R^1 = t\text{Bu}$	$R^2 = 3\text{-F}$	<b>2d</b>	-15.03	354
	$R^1 = t\text{Bu}$	$R^2 = 4\text{-Me}$	<b>2e</b>	-15.83	371
	$R^1 = t\text{Bu}$	$R^2 = 4\text{-OMe}$	<b>2f</b>	-16.11	393

[a]  $E$ -Parameters taken from Ref.<sup>[6b,e]</sup>

## 2. Results and Discussion

### 2.1. Synthesis of the Anions **I**

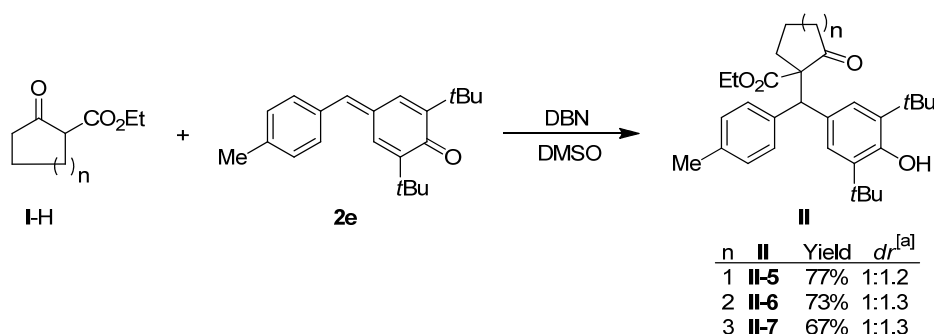
The anions of the 5- and 6-membered rings (**I-5** and **I-6**) were synthesized as described by Mayer and Alder<sup>[7]</sup> by adding the cyclic ketoester to a cold solution (0 °C) of potassium hydroxide in ethanol/water and successive filtration of the precipitated salt (Scheme 2). The anions **I-(7–12)** were synthesized according to a previously described method<sup>[8]</sup> by mixing the corresponding CH acid **I-H** with potassium *tert*-butoxide (KO*t*Bu) in ethanol (Scheme 2). The anions **I-(7–12)** were isolated only in moderate yields because of their solubility in diethyl ether and diethyl ether/pentane mixtures, which were used to purify the precipitated salts.



Scheme 2: Synthesis of the anions **I** and <sup>13</sup>C NMR (in [D<sub>6</sub>]-DMSO) shifts of their anionic center.

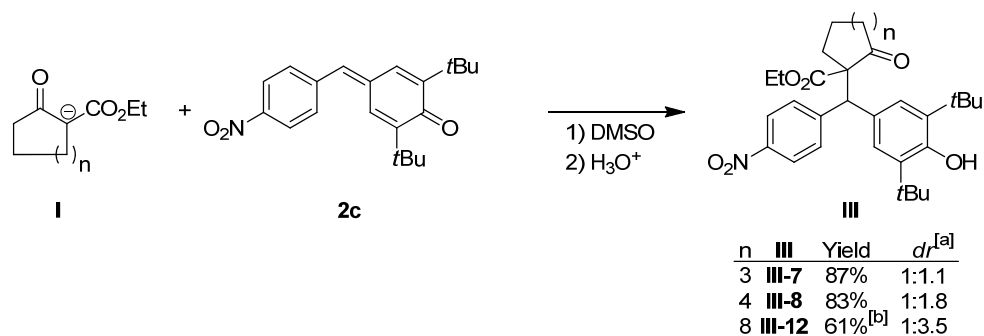
### 2.2. Product Studies

The cyclic ketoesters (**I-(5–7)**)-H were mixed with the quinone methide **2e** and catalytic amounts of 1,5-diazabicyclo[4.3.0]non-5-ene (DBN, 10 mol-%) in DMSO solution. After the reaction solutions turned from yellow to blue (three to six hours), saturated NaCl-solution was added and the products **II** were extracted with diethyl ether and purified by column chromatography (Scheme 3).



Scheme 3: Reactions of the cyclic ketoesters (**I-(5–7)**)-H with the quinone methide **2e**. [a] Derived from <sup>1</sup>H NMR experiments of the crude products.

When the quinone methide **2c** was added to solutions of the potassium salts **I-(7–12)**-K in DMSO, the solutions turned immediately from yellow to blue. After aqueous acidic work up and column-chromatographic purification, the addition products **III** were isolated as shown in Scheme 4.



Scheme 4: Reactions of the anions of the cyclic ketoesters **I-7-12** with the quinone methide **2c**. [a] Derived from  $^1\text{H}$  NMR experiments of the crude products. [b] Only the major isomer was isolated after column chromatographic purification.

### 2.3. Kinetic Investigations

The reactions of the anions **I** with the reference electrophiles **2** were performed in DMSO solution at 20 °C and monitored by UV-Vis spectroscopy at the absorption maxima of the electrophiles. To simplify the evaluation of the kinetic experiments, the carbanions **I** were used in large excess ( $> 10$  equiv.). Thus, their concentrations remained almost constant throughout the reactions, and pseudo-first-order kinetics were obtained in all runs. The first-order rate constants  $k_{\text{obs}}$  were derived by least-squares fitting of the exponential function  $A_t = A_0 \exp(-k_{\text{obs}}t) + C$  to the time-dependent absorbances  $A_t$  of the electrophiles. Second-order rate constants (Tables 2 and 4) were obtained as the slopes of plots of  $k_{\text{obs}}$  versus the nucleophile concentrations (Figure 1).

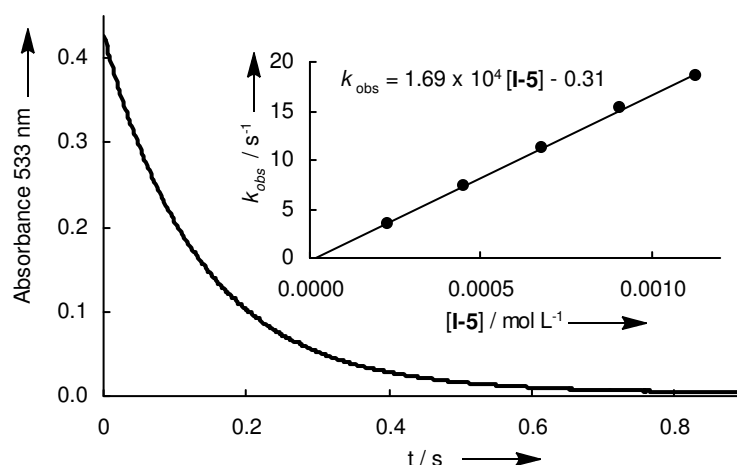


Figure 1: Plot of the absorbance (at 533 nm) vs. time for the reaction of **I-5** ( $4.53 \times 10^{-4}$  mol L $^{-1}$ ) with **2b** ( $1.14 \times 10^{-5}$  mol L $^{-1}$ ) in DMSO at 20 °C in presence of 18-crown-6. Inset: Plot of the first-order rate constants  $k_{\text{obs}}$  vs. the concentration of **I-5**.

As some carbanions derived from  $\beta$ -ketoesters have recently been shown to interact with potassium ions in DMSO solutions even at low concentrations ( $10^{-4}$  mol L $^{-1}$ ),<sup>[8]</sup> kinetic experiments with the potassium salts (**I**-(**5–12**))-K were performed in presence and absence of 18-crown-6 (1.2–2.5 equiv., Table 2).

Table 2: Second-order rate constants of the reactions of **I** with **2** in the presence and absence of 18-crown-6.

Reaction	$k_2 / \text{L mol}^{-1} \text{s}^{-1}$		$k_2(\text{I-K/crown}) / k_2(\text{I-K})$
	I-K/crown	I-K	
<b>I-5 + 2b</b>	$1.69 \times 10^4$	$1.39 \times 10^4$	1.22
<b>I-5 + 2d</b>	$9.34 \times 10^2$	$7.67 \times 10^2$	1.22
<b>I-6 + 2b</b>	$1.33 \times 10^4$	$1.14 \times 10^4$	1.17
<b>I-7 + 2b</b>	$1.09 \times 10^5$	$9.55 \times 10^4$	1.14
<b>I-8 + 2b</b>	$9.38 \times 10^4$	$8.09 \times 10^4$	1.16
<b>I-12 + 2b</b>	$3.09 \times 10^4$	$2.97 \times 10^4$	1.04

The 5- and 6-membered ring compounds (**I-5,6**)-K reacted 1.2 times faster in the presence of crown ether (free anions) than in the absence, as was found for the anion of ethyl benzoylacetate, an acyclic  $\beta$ -ketoester.<sup>[8]</sup> The interactions between the carbanion and the potassium decreases with increasing ring-size (Table 2).

These counter ion effects were studied in more detail by performing kinetic experiments in the presence of variable concentrations of KBPh $_4$ . Plots of the relative reaction rates ( $100 \cdot k_{\text{rel}}$ ) with respect to the rate constant of the free carbanion (potassium salt in presence of 18-crown-6) against the total concentration of potassium ions, show that rate constants of the anion of the 6-membered ring (**I-6**) decreases to around 15% at a potassium-concentration of  $10^{-2}$  mol L $^{-1}$ . The rate constant of the anion of the 12-membered ring (**I-12**), however, remains at around 80% of reactivity with respect to the free carbanion at the same K $^+$ -concentration (Table 3, Figure 2).

As shown in Tables 2 and 3, the anions of the cyclic  $\beta$ -ketoesters **I** interact with their counter ions at the concentration employed for the kinetic measurements ( $10^{-4}$ – $10^{-3}$  mol L $^{-1}$ ). Therefore, 18-crown-6 (1.2–2.5 equiv.) was added to determine the reactivities of the free carbanions towards the reference electrophiles (Table 4).

Table 3:  $k_{\text{obs}}$  values of the reactions of the carbanions **I-6,12** with the quinone methide **2b** with successive addition of  $\text{KBPh}_4$  in DMSO at 20 °C.  $100 \cdot k_{\text{rel}}$  was derived from kinetics of the free carbanions (presence of 18-crown-6).

	$[\text{KBPh}_4] / \text{mol L}^{-1}$	$[\text{K}^+]_{\text{total}} / \text{mol L}^{-1}$	$k_{\text{obs}} / \text{s}^{-1}$	$100 \cdot k_{\text{rel}}$
<chem>CCOC(=O)C1CCCCC1[CH-]</chem> <b>I-6</b> $3.02 \times 10^{-4} \text{ molL}^{-1}$	0		4.06 <sup>[a]</sup>	100
		$3.02 \times 10^{-4}$	2.79	68.7
	$1.28 \times 10^{-4}$	$4.30 \times 10^{-4}$	2.76	68.0
	$2.55 \times 10^{-4}$	$5.57 \times 10^{-4}$	2.59	63.8
	$5.10 \times 10^{-4}$	$8.12 \times 10^{-4}$	2.30	56.7
	$1.23 \times 10^{-3}$	$1.53 \times 10^{-3}$	1.79	44.1
	$2.55 \times 10^{-3}$	$2.85 \times 10^{-3}$	1.23	30.3
	$4.92 \times 10^{-3}$	$5.22 \times 10^{-3}$	0.983	24.2
	$7.37 \times 10^{-3}$	$7.68 \times 10^{-3}$	0.771	19.0
	$1.11 \times 10^{-2}$	$1.14 \times 10^{-2}$	0.591	14.6
<chem>CCOC(=O)C1CCCCC1CCCC1</chem> <b>I-12</b> $2.95 \times 10^{-4} \text{ molL}^{-1}$			9.12 <sup>[a]</sup>	100
		$4.39 \times 10^{-4}$	8.24	90.4
	$1.44 \times 10^{-4}$	$5.83 \times 10^{-4}$	8.06	88.4
	$2.88 \times 10^{-4}$	$8.71 \times 10^{-4}$	7.88	86.4
	$1.45 \times 10^{-3}$	$1.75 \times 10^{-3}$	7.74	84.9
	$2.59 \times 10^{-3}$	$2.89 \times 10^{-3}$	7.63	83.7
	$4.36 \times 10^{-3}$	$4.65 \times 10^{-3}$	7.53	82.6
	$1.02 \times 10^{-2}$	$1.05 \times 10^{-2}$	7.37	80.8
	$1.31 \times 10^{-2}$	$1.34 \times 10^{-2}$	7.32	80.3

[a] Calculated for the free carbanions from the data in Table 4.

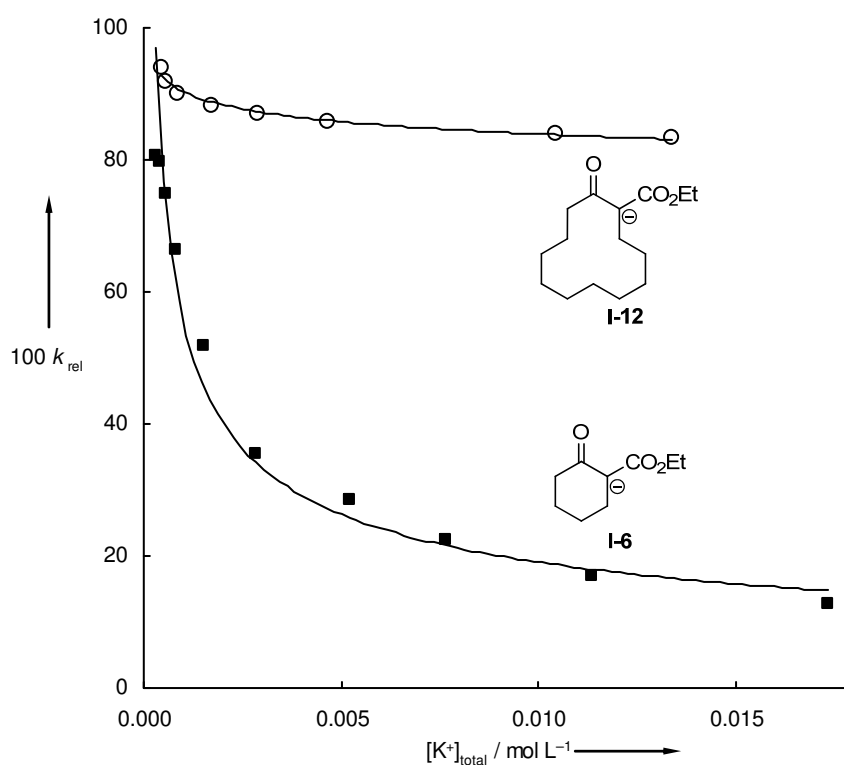
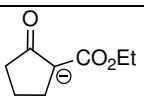
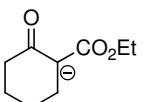
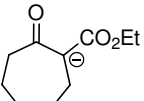
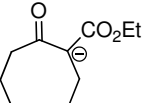
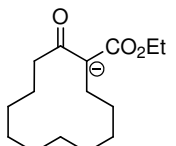


Figure 2: Plot of the relative pseudo-first-order rate constants for the reactions of the carbanions **I-6** and **I-12** with the quinone methide **1b** versus the total concentration of  $\text{K}^+$  in DMSO solution at 20°C.



Table 4: Second-order rate constants  $k_2$  for the reactions of the carbanions **I** with the reference electrophiles **2** in DMSO at 20 °C (in presence of 1.2–2.5 equiv. of 18-crown-6 for the complexation of the  $K^+$  counterion).

Anion	$N$ ( $s_N$ )	Electrophile	$k_2 /$ $L mol^{-1} s^{-1}$
 <b>I-5</b>	18.63 (0.82)	<b>2a</b>	$2.21 \times 10^5$
		<b>2b</b>	$1.69 \times 10^4$
		<b>2c</b>	$3.03 \times 10^3$
		<b>2d</b>	$9.34 \times 10^2$
		<b>2e</b>	$2.06 \times 10^2$
		<b>2f</b>	$1.19 \times 10^2$
 <b>I-6</b>	18.32 (0.84)	<b>2b</b>	$1.33 \times 10^4$
		<b>2c</b>	$2.34 \times 10^3$
		<b>2d</b>	$4.67 \times 10^2$
		<b>2e</b>	$1.24 \times 10^2$
		<b>2f</b>	$7.47 \times 10^1$ [a]
 <b>I-7</b>	19.53 (0.83)	<b>2b</b>	$1.09 \times 10^5$
		<b>2c</b>	$2.46 \times 10^4$
		<b>2d</b>	$5.11 \times 10^3$
		<b>2e</b>	$1.10 \times 10^3$
		<b>2f</b>	$6.89 \times 10^2$
 <b>I-8</b>	20.02 (0.76)	<b>2b</b>	$9.38 \times 10^4$
		<b>2c</b>	$3.12 \times 10^4$
		<b>2d</b>	$6.75 \times 10^3$
		<b>2e</b>	$1.37 \times 10^3$
 <b>I-12</b>	20.60 (0.63)	<b>2b</b>	$3.09 \times 10^4$
		<b>2c</b>	$9.39 \times 10^3$
		<b>2d</b>	$2.95 \times 10^3$
		<b>2e</b>	$1.01 \times 10^3$
		<b>2f</b>	$6.24 \times 10^2$ [a]

[a] Rate constants were acquired by addition of variable concentrations (3–5 equiv.) of CH acid.

## 2.4. Correlation Analysis

Plots of  $\lg k_2$  for the reactions of the carbanions **I** with the reference electrophiles **2** against the electrophilicity parameters  $E$  were linear, as shown in Figure 3, indicating that equation (1) is applicable to these reactions. From the slopes of these correlations, the nucleophile-specific parameters  $s_N$  were derived, and the negative intercepts on the abscissa ( $\lg k_2 = 0$ ) correspond to the nucleophilicity parameters  $N$  (Table 4).

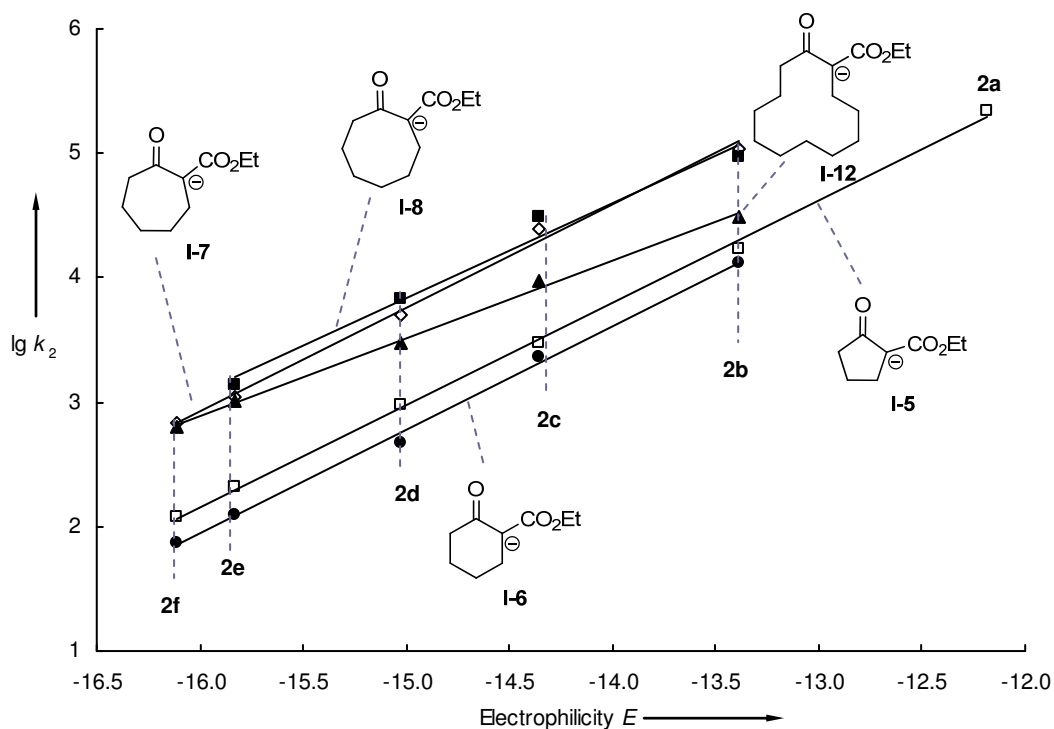


Figure 3: Correlation of the second-order rate constants  $\lg k_2$  for the reactions of the nucleophiles **I** with the electrophiles **2** in DMSO with their electrophilicity parameters  $E$ .

## 2.5. Structure-Reactivity Relationships

The  $s_N$ -parameters of the 5-, 6- and 7-membered rings **I-5–7** are almost identical (0.82, 0.83, 0.84) which is illustrated by the parallel lines in Figure 3, i.e. the relative reaction rates are independent of the nature of the electrophile. When the ring-size increases further, the sensitivity parameter ( $s_N$ ) decreases to 0.76 for **I-8** and 0.63 for **I-12**.

The different  $s_N$  parameters are also responsible for the reactivity order. If one just looks at the nucleophilicity parameters  $N$  one would see that the reactivity increases with the ring size (Table 4). However when the reaction rates towards a certain electrophile are compared, as done in Figure 4 for the quinone methides **2b,c,e** one can see that this trend is not valid.

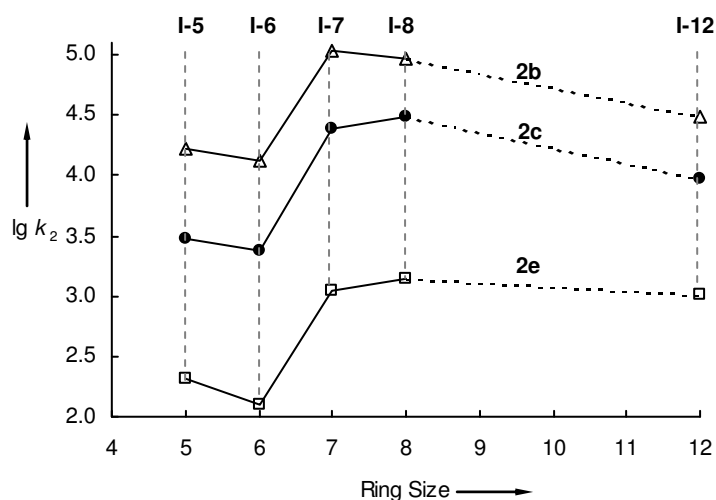


Figure 4: Plot of the rate constants  $\lg k_2$  of the reaction of the nucleophiles **I** with the electrophiles **2b,c,e** against the ring size.

Plots of the reported rate constants for the oxygen attack (black triangles) and the carbon attack (white squares) of the reactions of **I-5,6,8** with isopropyl iodine in DMSO against the rate constant for the reactions of **I-5,6,8** with the quinone methide **2c** is shown in Figure 5.<sup>[3d]</sup> From these correlations, one can see that the rate constants of the carbon-attack in the alkylation reactions increase with the rate constants for the reactions with the quinone methide **2c**. However, the rate constant for the oxygen attack do not show a trend when they are correlated with the rate constants towards the quinone methide **2c**.

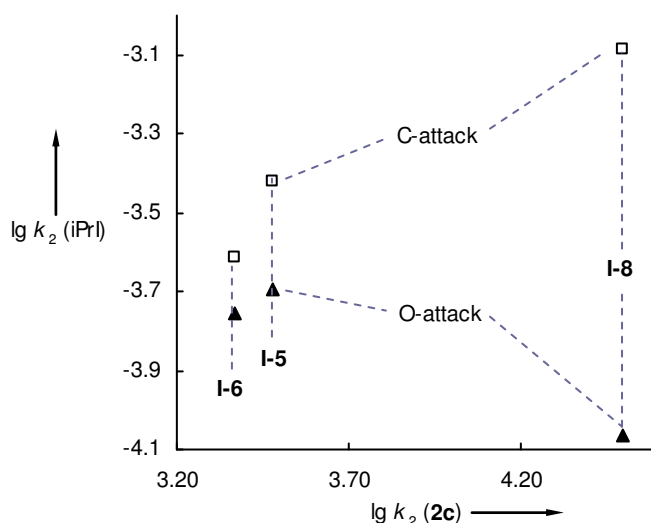


Figure 5: Plot of the rate constants  $\lg k_2$  of the reactions of **I** with isopropyl iodide in DMSO vs. the rate constants of the reactions with the quinone methide **2c** in DMSO. Black triangles: oxygen attack; white squares: carbon attack.<sup>[3d]</sup>

The carbanions **I-5–12** react with methyl iodide in methanol yielding exclusively the carbon-alkylated products.<sup>[3c]</sup> When the rate constants of the methylations in methanol are correlated with the rate constants of the reactions of **I-5–12** with the quinone methide **2c**, a plot of low quality is obtained (Figure 7, Appendix). The ordering of the reactivities of the carbanions **I-5** to **I-12** from this work, do not correlate either with other reactivities of cycloalkyl-derivatives, e.g. hydrolysis of lactones (Figure 8, Appendix),<sup>[9]</sup> hydroboration of cycloalkenes (Figure 9, Appendix),<sup>[2a]</sup> or solvolysis of cycloalkyl chlorides (Figure 10, Appendix)<sup>[1a]</sup> and tosylates (Figure 11, Appendix)<sup>[1d]</sup>. It might be expected that no correlations are obtained in Figures 8–11 since in some cases the cycloalkyl-derivatives are acting as electrophiles, however, as no trends are found, one can see that the ordering of the reactivities caused by the ring size of the cycloalkyl-derivative, is different for each system and reaction.

### 3. Conclusion

The rate constants for the reactions of the anions of the cyclic  $\beta$ -ketoesters **I-5–12** with quinone methides in DMSO follow the linear free-energy relationship [Equation (1)], allowing us to include these compounds in our comprehensive nucleophilicity scale.<sup>[6f]</sup> Their nucleophilic reactivities cover a range of about 1.5 orders of magnitude and are comparable to ethyl acetylacrylate (Figure 6). We found that the reactivity of these cyclic carbanions does not correlate with their ring size, however, we found that the counter ion effect depends on the ring size.

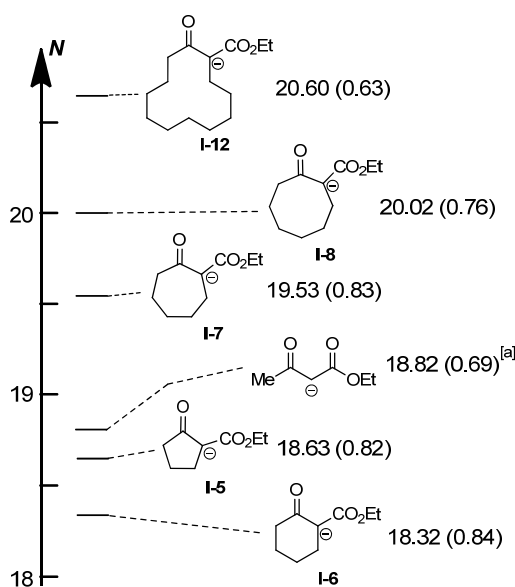


Figure 6: Nucleophilic reactivities,  $N$  ( $s_N$ ), of the cyclic  $\beta$ -ketoesters **I** in comparison to an acyclic  $\beta$ -ketoester. [a]  $N$  and  $s_N$  parameters from Ref.<sup>[5b]</sup>

Additionally, the rate constants obtained in this work were correlated with the rate constants of different reactions of other cyclic reagents in dependency of their ring size concluding that each reaction is affected differently by the ring size.

## 4. Experimental Section

### 4.1. General

#### Materials

Commercially available DMSO ( $\text{H}_2\text{O}$  content < 50 ppm) was used without further purification. The reference electrophiles used in this work were synthesized according to literature procedures.<sup>[6b,e]</sup> The cyclic ketoesters (**I-5**)-H and (**I-6**)-H were purchased from Merck-Suchard, (**I-8**)-H was purchased from Sigma-Aldrich. (**I-7**)-H and (**I-12**)-H were synthesized as described below.

#### NMR spectroscopy

In the  $^1\text{H}$  and  $^{13}\text{C}$  NMR spectra chemical shifts are given in ppm and refer to tetramethylsilane ( $\delta_{\text{H}} = 0.00$ ,  $\delta_{\text{C}} = 0.0$ ),  $[\text{D}_6]\text{-DMSO}$  ( $\delta_{\text{H}} = 2.50$ ,  $\delta_{\text{C}} = 39.5$ ) or to  $\text{CDCl}_3$  ( $\delta_{\text{H}} = 7.26$ ,  $\delta_{\text{C}} = 77.0$ ),<sup>[10]</sup> as internal standards. The coupling constants are given in Hz. For reasons of simplicity, the  $^1\text{H}$ -NMR signals of AA'BB'-spin systems of *p*-disubstituted aromatic rings are treated as doublets. Signal assignments are based on additional COSY, gHSQC, and gHMBC experiments. Chemical shifts marked with (\*) refer to the minor isomer when the product was obtained as a mixture of two diastereomers.

#### Kinetics

As the reactions of colored quinone methides **2** with colorless nucleophiles **I** yield colorless products (or products with a different absorption range than the reactants), the reactions could be followed by UV-Vis spectroscopy. As all reactions were fast ( $\tau_{1/2} < 10$  s), the kinetics were monitored using stopped-flow techniques. The temperature of all solutions was kept constant at  $20.0 \pm 0.1$  °C by using a circulating bath thermostat. In all runs the concentration of the nucleophile was at least 10 times higher than the concentration of the electrophile, resulting in pseudo-first-order kinetics with an exponential decay of the concentration of the minor compound. First-order rate constants  $k_{\text{obs}}$  were obtained by least-squares fitting of the

exponential function  $A_t = A_0 \exp(-k_{\text{obs}}t) + C$  to the time-depending absorbances. The second-order rate constants  $k_2$  were obtained from the slopes of the linear plots of  $k_{\text{obs}}$  against the nucleophile concentrations.

## 4.2. Synthesis of the Cyclic Ketoesters (I-H) and their Anions (I-K)

### 4.2.1. Synthesis of the Cyclic Ketoesters (I-H)

#### 4.2.1.1. Ethyl 2-Oxocycloheptanecarboxylate ((I-7)-H)

A mixture of sodium hydride (1.23 g, 51.2 mmol) and diethyl carbonate (4.3 mL, 35.3 mmol) in 40 mL of toluene were heated up to 100 °C. A solution of cycloheptanone (2.0 mL, 17.0 mmol) in 20 mL of toluene was added drop wise to the hot suspension during 2 h. The reaction mixture was stirred at 100 °C for further 45 min. After cool down, aqueous HCl (2 mol L<sup>-1</sup>, 40 mL) was added and the mixture was extracted with ethyl acetate (2 x 40 mL). The combined organic layers were washed with brine and dried over sodium sulfate before the solvent was removed. After column chromatography (silica/pentane/ethyl acetate), ethyl 2-oxocycloheptanecarboxylate ((I-7)-H, 2.75 g, 14.9 mmol, 88%) was yielded as a colorless liquid.

<sup>1</sup>H NMR-Signals as in Literature.<sup>[11]</sup>

#### 4.2.1.2. Ethyl 2-Oxocyclododecanecarboxylate ((I-12)-H)

A mixture of sodium hydride (4.66 g, 194 mmol) and diethyl carbonate (12.0 mL, 99.9 mmol) in 45 mL of toluene were heated up to 110 °C. A solution of cyclododecanone (11.9 g, 65.3 mmol) in 25 mL of toluene was added drop wise to the hot suspension during 1.5 h. The reaction mixture was stirred at 110 °C for further 3 h. After cool down, aqueous HCl (2 mol L<sup>-1</sup>, 60 mL) was added and the mixture was extracted with diethyl ether (3 x 30 mL). The combined organic layers were washed with brine and dried over sodium sulfate before the solvent was removed. After distillation ( $4 \times 10^{-3}$  mbar, 108-110 °C) ethyl 2-oxocyclododecanecarboxylate ((I-12)-H, 12.8 g, 50.3 mmol, 77%) was yielded as a colorless liquid.

<sup>1</sup>H NMR-Signals as in Literature.<sup>[12]</sup>

### 4.2.2. Synthesis of the Anions (I-K)

#### 4.2.2.1. Potassium 1-(Ethoxycarbonyl)-2-oxocyclopentan-1-ide ((I-5)-K)<sup>[7]</sup>

Following the procedure of Mayer and Alder:<sup>[7]</sup> potassium hydroxide (5.60 g, 99.8 mmol) were dissolved in 25 mL of ethanol and 1.5 mL water. Ethyl 2-oxocyclopentanecarboxylate ((I-5)-H, 15.6 g, 99.9 mmol) was added drop wise at 0 °C. 15 mL of diethyl ether were added to the formed precipitate before filtration. The obtained solid was recrystallized from ethanol yielding potassium 1-(ethoxycarbonyl)-2-oxocyclopentan-1-ide ((I-5)-K, 12.7 g, 65.4 mmol, 66%) as a light yellow solid.

<sup>1</sup>H-NMR ([D<sub>6</sub>]-DMSO, 400 MHz)  $\delta$  = 1.08 (t, <sup>3</sup>*J* = 7.0 Hz, 3 H, OCH<sub>2</sub>CH<sub>3</sub>), 1.50-1.58 (m, 2 H, CH<sub>2</sub>), 1.84-1.88 (m, 2 H, CH<sub>2</sub>), 2.36-2.39 (m, 2 H, CH<sub>2</sub>), 3.84 (q, <sup>3</sup>*J* = 7.0 Hz, 2 H, OCH<sub>2</sub>CH<sub>3</sub>). <sup>13</sup>C-NMR ([D<sub>6</sub>]-DMSO, 101 MHz)  $\delta$  = 15.4 (q, OCH<sub>2</sub>CH<sub>3</sub>), 20.0 (t, CH<sub>2</sub>), 29.2 (t, CH<sub>2</sub>), 40.0 (t, CH<sub>2</sub>), 55.5 (t, OCH<sub>2</sub>CH<sub>3</sub>), 85.3 (s, C<sup>-</sup>), 165.8 (s, COOEt), 190.0 (CO).

#### 4.2.2.2. Potassium 1-(Ethoxycarbonyl)-2-oxocyclohexan-1-ide ((I-6)-K)

Following the procedure of Mayer and Alder:<sup>[7]</sup> potassium hydroxide (1.96 g, 34.9 mmol) were dissolved in 25 mL of ethanol and 1.5 mL water. Ethyl 2-oxocyclohexanecarboxylate ((I-6)-H, 15.6 g, 99.9 mmol) was added drop wise at 0 °C. 15 mL of diethyl ether were added to the formed precipitate before filtration. The obtained solid was recrystallized from ethanol yielding potassium 1-(ethoxycarbonyl)-(2-oxocyclohexyl)methanide ((I-6)-K, 5.32 g, 25.6 mmol, 73%) as a light yellow solid.

<sup>1</sup>H-NMR ([D<sub>6</sub>]-DMSO, 400 MHz)  $\delta$  = 1.08 (t, <sup>3</sup>*J* = 6.8 Hz, 3 H, OCH<sub>2</sub>CH<sub>3</sub>), 1.45-1.50 (m, 4 H, CH<sub>2</sub>CH<sub>2</sub>), 1.85 (b, 2 H, CH<sub>2</sub>), 2.23 (b, 2 H, CH<sub>2</sub>), 3.83 (q, <sup>3</sup>*J* = 6.8 Hz, 2 H, OCH<sub>2</sub>CH<sub>3</sub>). <sup>13</sup>C-NMR ([D<sub>6</sub>]-DMSO, 101 MHz)  $\delta$  = 15.3 (q, OCH<sub>2</sub>CH<sub>3</sub>), 24.1 (t, CH<sub>2</sub>), 24.7 (t, CH<sub>2</sub>), 26.2 (t, CH<sub>2</sub>), 38.3 (t, CH<sub>2</sub>), 55.5 (t, OCH<sub>2</sub>CH<sub>3</sub>), 86.7 (s, C<sup>-</sup>), 167.5 (s, COOEt), 182.8 (CO).

#### 4.2.2.3. Potassium 1-(Ethoxycarbonyl)-2-oxocycloheptan-1-ide ((I-7)-K)

Potassium *tert*-butoxide (226 mg, 2.01 mmol) was dissolved in ethanol (5 mL) and ethyl 2-oxocycloheptanecarboxylate ((I-7)-H, 379 mg, 2.06 mmol) was added dropwise. After 10 min. the solvent was removed under reduced pressure and the residue was washed several times with dry pentane/ diethyl ether yielding potassium 1-(ethoxycarbonyl)-2-oxocycloheptan-1-ide ((I-7)-K, 212 mg, 0.954 mmol, 47%) as a colorless solid.

$^1\text{H-NMR}$  ( $[\text{D}_6]$ -DMSO, 400 MHz)  $\delta$  = 1.08 (t,  $^3J$  = 7.0 Hz, 3 H,  $\text{OCH}_2\text{CH}_3$ ), 1.34-1.40 (m, 2 H,  $\text{CH}_2$ ), 1.43-1.48 (m, 2 H,  $\text{CH}_2$ ), 1.54-1.60 (m, 2 H,  $\text{CH}_2$ ), 2.15-2.17 (m, 2 H,  $\text{CH}_2$ ), 2.35-2.38 (m, 2 H,  $\text{CH}_2$ ), 3.81 (q,  $^3J$  = 7.0 Hz, 2 H,  $\text{OCH}_2\text{CH}_3$ ).  $^{13}\text{C-NMR}$  ( $[\text{D}_6]$ -DMSO, 101 MHz)  $\delta$  = 15.4 (q,  $\text{OCH}_2\text{CH}_3$ ), 25.2 (t,  $\text{CH}_2$ ), 27.1 (t,  $\text{CH}_2$ ), 31.0 (t,  $\text{CH}_2$ ), 32.1 (t,  $\text{CH}_2$ ), 44.5 (t,  $\text{CH}_2$ ), 55.5 (t,  $\text{OCH}_2\text{CH}_3$ ), 90.3 (s,  $\text{C}^-$ ), 167.0 (s,  $\text{COOEt}$ ), 190.6 (CO).

#### 4.2.2.4. Potassium 1-(Ethoxycarbonyl)-2-oxocyclooctan-1-ide ((**I-8**)-K)

Potassium *tert*-butoxide (905 mg, 8.07 mmol) was dissolved in ethanol (5 mL) and ethyl 2-oxocyclooctanecarboxylate ((**I-8**)-H, 1.62 g, 8.26 mmol) was added dropwise. After 10 min. the solvent was removed under reduced pressure and the residue was washed several times with dry pentane/diethyl ether yielding potassium 1-(ethoxycarbonyl)-2-oxocyclooctan-1-ide ((**I-8**)-K, 340 mg, 1.44 mmol, 18%) as a colorless solid.

$^1\text{H-NMR}$  ( $[\text{D}_6]$ -DMSO, 400 MHz)  $\delta$  = 1.07 (t,  $^3J$  = 7.0 Hz, 3 H,  $\text{OCH}_2\text{CH}_3$ ), 1.33-1.46 (m, 6 H,  $\text{CH}_2$ ), 1.48-1.57 (m, 2 H,  $\text{CH}_2$ ), 2.13-2.20 (m, 2 H,  $\text{CH}_2$ ), 2.31-2.50 (m, 2 H,  $\text{CH}_2$ ), 3.82 (q,  $^3J$  = 7.2 Hz, 2 H,  $\text{OCH}_2\text{CH}_3$ ).  $^{13}\text{C-NMR}$  ( $[\text{D}_6]$ -DMSO, 101 MHz)  $\delta$  = 15.3 (q,  $\text{OCH}_2\text{CH}_3$ ), 25.9 (t,  $\text{CH}_2$ ), 26.6 (t,  $\text{CH}_2$ ), 27.0 (t,  $\text{CH}_2$ ), 28.9 (t,  $\text{CH}_2$ ), 31.5 (t,  $\text{CH}_2$ ), 40.3 (t,  $\text{CH}_2$ ), 55.3 (t,  $\text{OCH}_2\text{CH}_3$ ), 87.6 (s,  $\text{C}^-$ ), 167.2 (s,  $\text{COOEt}$ ), 187.8 (CO).

#### 4.2.2.5. Potassium 1-(Ethoxycarbonyl)-2-oxocyclododecan-1-ide ((**I-12**)-K)

Potassium *tert*-butoxide (384 mg, 3.42 mmol) was dissolved in ethanol (5 mL) and ethyl 2-oxocyclododecanecarboxylate ((**I-12**)-H, 876 mg, 3.44 mmol) was added dropwise. After 10 min. the solvent was removed under reduced pressure and the residue was washed several times with dry pentane/diethyl ether yielding potassium 1-(ethoxycarbonyl)-2-oxocyclododecan-1-ide ((**I-12**)-K, 221 mg, 0.756 mmol, 22%) as a colorless solid.

$^1\text{H-NMR}$  ( $[\text{D}_6]$ -DMSO, 400 MHz)  $\delta$  = 1.06 (t,  $^3J$  = 7.2 Hz, 3 H,  $\text{OCH}_2\text{CH}_3$ ), 1.10-1.44 (m,  $\text{CH}_2$ ), 1.49-1.59 (m,  $\text{CH}_2$ ), 1.85-1.91 (m,  $\text{CH}_2$ ), 2.51-2.56 (m,  $\text{CH}_2$ ), 3.65-3.78 (m,  $\text{CH}_2$ ), 3.82-3.90 (m,  $\text{CH}_2$ ).  $^{13}\text{C-NMR}$  ( $[\text{D}_6]$ -DMSO, 101 MHz)  $\delta$  = 15.5 (q,  $\text{OCH}_2\text{CH}_3$ ), 23.2, 24.1, 24.56, 24.61, 25.2, 25.4, 25.7, 26.0, 26.4 (all t,  $\text{CH}_2$ ), 39.5 (t,  $\text{CH}_2$ , superimposed with solvent), 55.1 (t,  $\text{OCH}_2\text{CH}_3$ ), 90.0 (s,  $\text{C}^-$ ), 169.5 (s,  $\text{COOEt}$ ), 190.0 (CO).



### 4.3. Reaction Products

#### 4.3.1. Reactions of Cyclic Ketoesters (I) with Quinone Methides (2)

##### General Procedure 1 (GP1):

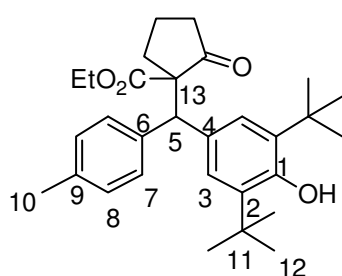
The cyclic ketoester (**I-H**, 50-100 mg, 0.32-0.35 mmol) and the quinone methide (**2e**, 95-110 mg, 0.31-0.32 mmol) were dissolved in 10-15 mL of dry DMSO and 2-3 drops of 1,5-Diazabicyclo(4.3.0)non-5-ene (DBN) were added. After 3 to 5 hours, 20 mL of brine were added and the mixture was extracted with diethyl ether (3 x 20 mL). The combined organic layers were washed with brine and dried over sodium sulfate. After removing the solvent by distillation, the crude products were purified by column chromatography (silica/pentane/dichloromethane).

##### General Procedure 2 (GP2):

The potassium salt of the cyclic ketoester (**I-K**, ~100 mg, 0.30-0.35 mmol) was dissolved in 5-10 mL of dry DMSO and a solution of the quinone methide **2c** (~100 mg, 0.29-0.31 mmol in 5 mL DMSO) was added. When the solution turned dark blue, 30 mL of aqueous acetic acid (0.5%) was added and the mixture was extracted with diethyl ether (3 x 15 mL). The combined organic layers were washed with brine and dried over sodium sulfate before the solvent was removed under reduced pressure. The crude products were purified by column chromatography (silica/pentane/dichloromethane).

##### 4.3.1.1. Reaction of (I-5)-H with the Quinonemethide 2e

According to GP1, ethyl 2-oxocyclopentanecarboxylate ((**I-5**)-H, 54.1 mg, 0.346 mmol), and **2e** (95.4 mg, 0.309 mmol) yielded ethyl 1-((3,5-di-tert-butyl-4-hydroxyphenyl)(p-tolyl)methyl)-2-oxocyclopentanecarboxylate **II-5** (110 mg, 0.237 mmol, 77%, *dr* ~ 1:1.2) as yellow oil.

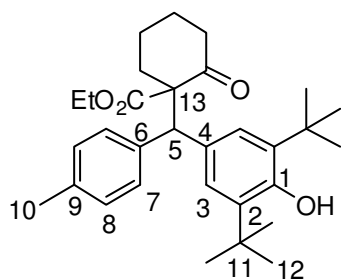


$^1\text{H-NMR}$  ( $\text{CDCl}_3$ , 300 MHz)  $\delta$  = 0.74, 0.84\* (t,  $^3J$  = 7.2 Hz, 3 H,  $\text{OCH}_2\text{CH}_3$ ), 1.34\*, 1.40 (s, 18 H, 12-H), 1.49-1.89 (m,  $\text{CH}_2$ ), 2.11-2.25 (m,  $\text{CH}_2$ ), 2.27, 2.28\* (s, 3 H, 10-H), 2.94-3.05 (m,  $\text{CH}_2$ ), 3.72-4.05 (m,  $\text{OCH}_2\text{CH}_3$ ), 5.04, 5.06\* (s, 1 H, OH), 5.10 (bs, 1 H, 5-H), 6.96-7.00 (m,  $\text{H}_{\text{arom}}$ ), 7.04-7.06 (m,  $\text{H}_{\text{arom}}$ ), 7.16 (d,  $^3J$  = 8.1 Hz, 2 H,  $\text{H}_{\text{arom}}$ ).  $^{13}\text{C-NMR}$  ( $\text{CDCl}_3$ , 75.5 MHz)  $\delta$  =

13.4, 13.5\* (q,  $\text{OCH}_2\text{CH}_3$ ), 19.5\*, 19.8 (t,  $\text{CH}_2$ ), 20.93, 20.96\* (q, C-10), 29.38, 29.43\* (t,  $\text{CH}_2$ ), 30.29\*, 30.32 (q, C-12), 34.3 (t,  $\text{CH}_2$ ), 38.65, 38.73\* (s, C-11), 54.85, 54.94\* (d, C-5), 61.4, 61.5\* (t,  $\text{OCH}_2\text{CH}_3$ ), 66.5\*, 67.0 (s, C-13), 125.6, 126.5\* (d, C-3), 128.8, 128.9, 129.8 (d, C-7, C-8, both isomers), 131.6, 131.9\* (s, C-4), 135.3+, 135.4 (s, C-2), 135.6\*, 136.0 (s, C-9), 137.9, 138.0\* (s, C-6), 152.2, 152.3\* (s, C-1), 168.4, 169.0\* (s,  $\text{COOEt}$ ), 214.4\*, 214.4 (s, CO). HR-MS (EI):  $m/z$  calcd for  $[\text{C}_{30}\text{H}_{40}\text{O}_4]^+$ : 464.2921 found: 464.2912.

#### 4.3.1.2. Reaction of (I-6)-H with the Quinonemethide 2e

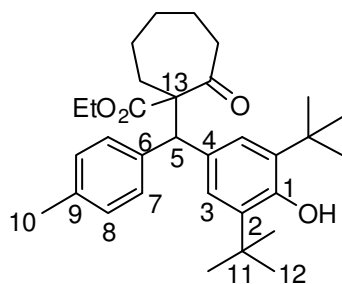
According to GP1, ethyl 2-oxocyclohexanecarboxylate ((I-6)-H, 55.0 mg, 0.323 mmol), and **2e** (98.9 mg, 0.321 mmol) yielded ethyl 1-((3,5-di-tert-butyl-4-hydroxyphenyl)(p-tolyl)methyl)-2-oxocyclohexanecarboxylate **II-6** (113 mg, 0.236 mmol, 73%,  $dr \sim 1:1.4$ ) as yellow oil.



$^1\text{H-NMR}$  ( $\text{CDCl}_3$ , 300 MHz)  $\delta$  = 0.82, 0.91\* (t,  $^3J$  = 7.2 Hz, 3 H,  $\text{OCH}_2\text{CH}_3$ ), 1.25-1.35 (m,  $\text{CH}_2$ ), 1.390\*, 1.393 (s, 18 H, 12-H), 1.43-1.60 (m,  $\text{CH}_2$ ), 1.69-1.96 (m,  $\text{CH}_2$ ), 2.26\*, 2.27 (s, 3 H, 10-H), 2.34-2.45 (m,  $\text{CH}_2$ ), 2.57-2.67 (m,  $\text{CH}_2$ ), 3.67-3.93 (m,  $\text{OCH}_2\text{CH}_3$ ), 4.84\*, 5.06 (s, 1 H, 5-H), 5.006, 5.014\* (s, 1 H, OH), 7.01-7.05 (m, 2 H, 8-H), 7.20, 7.22\* (s, 2 H, 3-H), 7.29-7.32 (m, 2 H, 7-H).  $^{13}\text{C-NMR}$  ( $\text{CDCl}_3$ , 75.5 MHz)  $\delta$  = 13.45, 13.54\* (q,  $\text{OCH}_2\text{CH}_3$ ), 20.9 (q, C-10), 22.9, 26.7, 34.5, 35.6, 41.9, 42.0 (t,  $\text{CH}_2$ ), 30.41\*, 30.35 (q, C-12), 34.3, 34.4\* (s, C-11), 52.9, 54.3\* (d, C-5), 61.0, 61.1 (t,  $\text{OCH}_2\text{CH}_3$ ), 66.36\*, 66.42 (s, C-13), 126.8, 127.3\* (d, C-3), 128.45\*, 128.54 (d, C-8), 130.2\*, 130.5 (d, C-7), 131.1\*, 131.4 (s, C-4), 134.8\*, 134.9 (s, C-2), 135.6, 135.8\* (s, C-9), 138.2, 138.4\* (s, C-6), 152.1\*, 152.2 (s, C-1), 170.5, 171.0\* (s,  $\text{COOEt}$ ), 206.4, 206.6\* (s, CO). HR-MS (ESI):  $m/z$  calcd for  $\text{C}_{31}\text{H}_{42}\text{O}_4\text{Na}$ : 501.2981 found: 501.2974.

#### 4.3.1.3. Reaction of (I-7)-H with the Quinonemethide 2e

According to GP1, ethyl 2-oxocycloheptanecarboxylate ((I-7)-H, 62.0 mg, 0.337 mmol), and **2e** (105 mg, 0.341 mmol) yielded ethyl 1-((3,5-di-tert-butyl-4-hydroxyphenyl)(p-tolyl)methyl)-2-oxocycloheptanecarboxylate **II-7** (113 mg, 0.229 mmol, 67%,  $dr \sim 1:1$ ) as yellow oil.

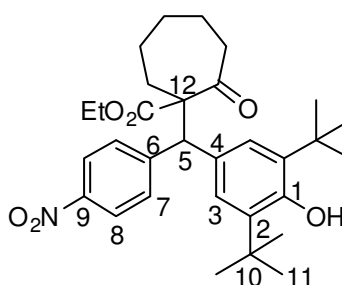


$^1\text{H-NMR}$  ( $\text{CDCl}_3$ , 400 MHz)  $\delta$  = 0.54-0.68 (m,  $\text{CH}_2$ ), 0.77, 0.87 (t,  $^3J$  = 7.2 Hz, 3 H,  $\text{OCH}_2\text{CH}_3$ ), 1.38, 1.39 (s, 18 H, 12-H), 1.40-1.46 (m,  $\text{CH}_2$ ), 1.58-1.48 (m,  $\text{CH}_2$ ), 2.26, 2.27 (s, 3 H, 10-H), 2.30-2.50 (m,  $\text{CH}_2$ ), 3.76-3.89 (m, 2 H,  $\text{OCH}_2\text{CH}_3$ ), 4.97, 5.02 (s, 1 H, OH), 5.01, 5.03 (s, 1 H, 5-H), 7.03, (d,  $^3J$  = 7.6 Hz, 2 H, 8-H, both isomers), 7.12, 7.24 (s, 2 H, 3-H), 7.26, 7.33 (d,  $^3J$  = 8.0 Hz, 2 H, 7-H).  $^{13}\text{C-NMR}$  ( $\text{CDCl}_3$ , 101 MHz)  $\delta$  = 13.4, 13.5 (q,  $\text{OCH}_2\text{CH}_3$ ), 20.9, 21.0 (q, C-10), 24.9 (b,  $\text{CH}_2$ ), 26.1, 26.2, 26.3, 26.5, 31.5, 31.7, 42.1, 42.3 (t,  $\text{CH}_2$ ), 30.3, 30.4 (q, C-12), 34.31, 34.35 (s, C-11), 53.6, 54.4 (d, C-5), 61.0, 61.1 (t,  $\text{OCH}_2\text{CH}_3$ ), 68.3, 68.4 (s, C-13), 126.3, 126.9 (d, C-3), 128.61, 128.63 (d, C-8), 129.2, 130.2 (d, C-7), 131.1, 132.0 (s, C-4), 135.0, 135.1 (s, C-2), 135.66, 135.68 (s, C-9), 138.2, 138.6 (s, C-6), 152.1, 152.2 (s, C-1), 171.7 (s, COOEt), 207.9, 208.2 (s, CO). HR-MS (EI):  $m/z$  calcd for  $[\text{C}_{32}\text{H}_{45}\text{O}_6\text{N}]^+$ : 493.3312 found: 493.3318.

Due to  $dr \sim 1:1$ , the NMR-signals could not be assigned to the isomers.

#### 4.3.1.4. Reaction of the Potassium Salt (I-7)-K with the Quinonemethide 2c

According to GP2, potassium 1-(ethoxycarbonyl)-2-oxocycloheptan-1-ide ((I-7)-K, 78.0 mg, 0.351 mmol), and **2c** (104 mg, 0.306 mmol) yielded ethyl 1-((3,5-di-tert-butyl-4-hydroxyphenyl)(4-nitrophenyl)methyl)-2-oxocycloheptanecarboxylate **III-7** (139 mg, 0.265 mmol, 87%,  $dr \sim 1:1.2$ ) as yellow oil.

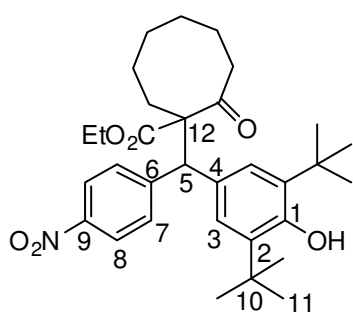


$^1\text{H-NMR}$  ( $\text{CDCl}_3$ , 300 MHz)  $\delta$  = 0.40-0.63 (m,  $\text{CH}_2$ ), 0.77\*, 0.88 (t,  $^3J$  = 7.2 Hz, 3 H,  $\text{OCH}_2\text{CH}_3$ ), 1.38\*, 1.40 (s, 18 H, 11-H), 1.42-1.47 (m,  $\text{CH}_2$ ), 1.63-1.75 (m,  $\text{CH}_2$ ), 2.17-2.54 (m,  $\text{CH}_2$ ), 3.78-3.96 (m,  $\text{OCH}_2\text{CH}_3$ ), 5.126 (s, OH), 5.16, 5.133 (s, 1 H, 5-H, both isomers), 7.07, 7.15\* (s, 2 H, 3-H), 7.56\* (d,  $^3J$  = 9.0 Hz, 2 H, 7\*-H), 7.67 (d,  $^3J$  = 8.7 Hz, 2 H, 7-H), 8.08 (d,  $^3J$  = 8.7 Hz, 2 H, 8-H), 8.10\* (d,  $^3J$  = 9.0 Hz, 2 H, 8\*-H).  $^{13}\text{C-NMR}$  ( $\text{CDCl}_3$ , 75.5 MHz)  $\delta$  = 13.4, 13.5\* (q,  $\text{OCH}_2\text{CH}_3$ ), 24.8, 24.9, 26.1, 26.3, 29.7, 30.0, 31.76, 31.83, 41.9, 42.2 (t,  $\text{CH}_2$ ), 30.26, 30.31\* (q, C-11), 34.37, 34.38 (s, C-10, both isomers), 53.9\*, 54.1 (d, C-5), 61.45, 61.47 (t,  $\text{OCH}_2\text{CH}_3$ , both isomers), 67.90, 67.94 (s, C-12, both isomers), 123.0, 123.1\* (d, C-8), 126.2, 127.0\* (s, C-3), 129.2, 130.1 (s, C-4, both isomers), 130.4\*, 131.2 (d, C-7), 146.2, 146.3 (s, C-9, both isomers), 149.6, 150.1 (s, C-6, both isomers), 152.7, 152.8 (s, C-1, both

isomers), 171.3, 171.4 (s, COOEt, both isomers), 207.3, 207.7 (s, CO, both isomers). HR-MS (EI):  $m/z$  calcd for  $[C_{32}H_{41}O_6N]^+$ : 523.2928 found: 523.2916.

#### 4.3.1.5. Reaction of the Potassium Salt (I-8)-K with the Quinonemethide 2c

According to GP2, potassium 1-(ethoxycarbonyl)-2-oxocyclooctan-1-ide ((I-8)-K, 82.5 mg, 0.349 mmol), and **2c** (103 mg, 0.303 mmol) yielded ethyl 1-((3,5-di-tert-butyl-4-hydroxyphenyl)(4-nitrophenyl)methyl)-2-oxocyclooctanecarboxylate **III-8** (135 mg, 0.251 mmol, 83%,  $dr \sim 1:1.7$ ) as yellow oil.

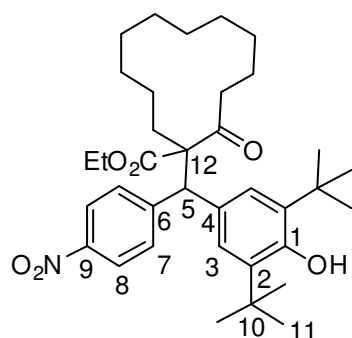


$^1\text{H-NMR}$  ( $\text{CDCl}_3$ , 600 MHz)  $\delta$  = 0.79\*, 0.93 (t,  $^3J$  = 7.2 Hz, 3 H,  $\text{OCH}_2\text{CH}_3$ ), 0.84-0.89 (m,  $\text{CH}_2$ ), 1.11-1.19 (m,  $\text{CH}_2$ ), 1.23-1.35 (m,  $\text{CH}_2$ ), 1.37\*, 1.41 (s, 18 H, 11-H), 1.45-1.58 (m,  $\text{CH}_2$ ), 1.62-1.68 (m,  $\text{CH}_2$ ), 1.77-1.83 (m,  $\text{CH}_2$ ), 2.12-2.18 (m,  $\text{CH}_2$ ), 2.27-2.32 (m,  $\text{CH}_2$ ), 2.44-2.61 (m,  $\text{CH}_2$ ), 3.65\*-3.61\*, 3.76-3.82, 3.89\*-3.94\*, 4.00-4.06 (m,  $\text{OCH}_2\text{CH}_3$ ), 4.94 (s, 1 H, 5-H), 5.08\* (1 H, OH), 5.13 (s, 5\*-H and OH major isomer), 7.19\*, 7.24 (s, 2 H, 3-H), 7.63, 7.82\* (d,  $^3J$  = 8.4 Hz, 2 H, 7-H), 8.05, 8.15\* (d,  $^3J$  = 9.0 Hz, 2 H, 8-H).  $^{13}\text{C-NMR}$  ( $\text{CDCl}_3$ , 151 MHz)  $\delta$  = 13.3\*, 13.5 (q,  $\text{OCH}_2\text{CH}_3$ ), 22.85, 22.90, 24.5, 24.7, 25.7, 26.3, 27.4, 28.0, 30.8, 32.5, 40.3, 40.6 (t,  $\text{CH}_2$ ), 30.2\*, 30.3 (q, C-11), 34.37\*, 34.43 (s, C-10), 52.2\*, 53.6 (d, C-5), 61.1\*, 61.2 (t,  $\text{OCH}_2\text{CH}_3$ ), 66.8\*, 67.0 (s, C-12), 122.8, 123.3\* (d, C-8), 126.6, 126.7\* (d, C-3), 129.9, 130.1\* (s, C-4), 130.8, 131.2\* (d, C-7), 135.2\*, 135.7 (s, C-2), 146.0, 146.4\* (s, C-9), 149.7\*, 150.5 (s, C-6), 152.4\*, 152.8 (s, C-1), 171.8 (bs, COOEt, both isomers), 210.4\*, 211.3 (s, CO). HR-MS (EI):  $m/z$  calcd for  $[C_{32}H_{43}O_6N]^+$ : 537.3085 found: 537.3077.

#### 4.3.1.6. Reaction of the Potassium Salt (I-12)-K with the Quinonemethide 2c

According to GP2, potassium 1-(ethoxycarbonyl)-2-oxocyclododecan-1-ide ((I-12)-K, 103 mg, 0.352 mmol), and **2c** (97.0 mg, 0.286 mmol) yielded ethyl 1-((3,5-di-tert-butyl-4-hydroxyphenyl)(4-nitrophenyl)methyl)-2-oxocyclododecanecarboxylate **III-12** (104 mg, 0.175 mmol, 61%) as yellow oil.

$^1\text{H-NMR}$  ( $\text{CDCl}_3$ , 300 MHz)  $\delta$  = 1.00 (t,  $^3J$  = 7.1 Hz, 3 H,  $\text{OCH}_2\text{CH}_3$ ), 1.06-1.37 (m, 15 H,  $\text{CH}_2$ ), 1.41 (s, 18 H, 11-H), 1.93-2.02 (m, 2 H,  $\text{CH}_2$ ), 2.05-2.15 (m, 1 H,  $\text{CH}_2$ ), 2.26-2.37 (m, 1 H,  $\text{CH}_2$ ), 2.67-2.80 (m, 1 H,  $\text{CH}_2$ ), 3.87-4.13 (m,  $\text{OCH}_2\text{CH}_3$ ), 5.00 (s, 1 H, 5-H), 5.14 (s, 1 H, OH), 7.10 (s, 2 H, 3-H), 7.54 (s,  $^3J$  = 8.7 Hz, 2 H, 7-H), 8.03 (s,  $^3J$  = 9.0 Hz, 2 H, 8-H).  $^{13}\text{C-}$



NMR ( $\text{CDCl}_3$ , 75.5 MHz)  $\delta$  = 13.5 (q,  $\text{OCH}_2\text{CH}_3$ ), 18.9, 21.8, 22.0, 22.2, 22.7, 23.4, 26.5, 26.8, 31.6, 35.5 (t,  $\text{CH}_2$ ), 30.3 (q, C-11), 34.3 (s, C-10), 51.3 (d, C-5), 61.3 (t,  $\text{OCH}_2\text{CH}_3$ ), 68.3 (s, C-12), 122.5 (d, C-8), 126.3 (d, C-3), 129.5 (s, C-4), 131.2 (s, C-7), 135.8 (s, C-2), 145.8 (s, C-9), 150.7 (s, C-6), 152.7 (s, C-1), 172.4 (s,  $\text{COOEt}$ ), 205.9 (s, CO). HR-MS (EI):  $m/z$  calcd for  $[\text{C}_{36}\text{H}_{51}\text{NO}_6]^+$ : 593.3711 found: 593.3697.

## 4.4. Kinetic Experiments

### 4.4.1. Determination of the Nucleophilicity of Cyclic $\beta$ -Ketoester Anions I-K

#### 4.4.1.1. Reactions of Potassium 1-(Ethoxycarbonyl)-2-oxocyclopentan-1-ide ((I-5)-K)

Table 5: Kinetics of the reaction of (I-5)-K with **2a** (20 °C, stopped-flow, at 422 nm).

[ <b>2a</b> ] / mol L <sup>-1</sup>	[I-5] / mol L <sup>-1</sup>	[18-crown-6] / mol L <sup>-1</sup>	[I-5] / [ <b>2a</b> ]	$k_{\text{obs}}$ / s <sup>-1</sup>
$9.22 \times 10^{-6}$	$9.78 \times 10^{-5}$	$1.22 \times 10^{-4}$	10.6	8.81
$9.22 \times 10^{-6}$	$1.22 \times 10^{-5}$	$1.83 \times 10^{-4}$	13.3	14.2
$9.22 \times 10^{-6}$	$1.47 \times 10^{-4}$	$1.83 \times 10^{-4}$	15.9	19.6
$9.22 \times 10^{-6}$	$1.96 \times 10^{-4}$	$2.44 \times 10^{-4}$	21.2	30.4

$$k_2 = 2.21 \times 10^5 \text{ L mol}^{-1} \text{ s}^{-1}$$

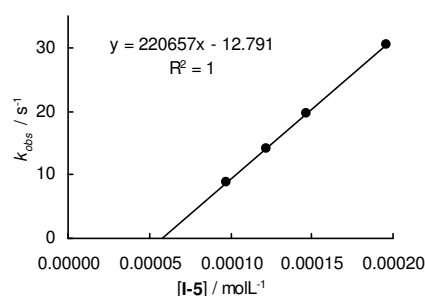


Table 6: Kinetics of the reaction of (I-5)-K with **2b** (20 °C, stopped-flow, at 533 nm).

[ <b>2b</b> ] / mol L <sup>-1</sup>	[I-5] / mol L <sup>-1</sup>	[18-crown-6] / mol L <sup>-1</sup>	[I-5] / [ <b>2b</b> ]	$k_{\text{obs}}$ / s <sup>-1</sup>
$1.14 \times 10^{-5}$	$2.27 \times 10^{-4}$	$3.57 \times 10^{-4}$	19.8	3.42
$1.14 \times 10^{-5}$	$4.53 \times 10^{-4}$	$9.51 \times 10^{-4}$	39.6	7.36
$1.14 \times 10^{-5}$	$6.80 \times 10^{-4}$	$9.51 \times 10^{-4}$	59.4	11.2
$1.14 \times 10^{-5}$	$9.06 \times 10^{-4}$	$2.38 \times 10^{-3}$	79.2	15.3
$1.14 \times 10^{-5}$	$1.13 \times 10^{-3}$	$1.66 \times 10^{-3}$	99.0	18.6

$$k_2 = 1.69 \times 10^4 \text{ L mol}^{-1} \text{ s}^{-1}$$

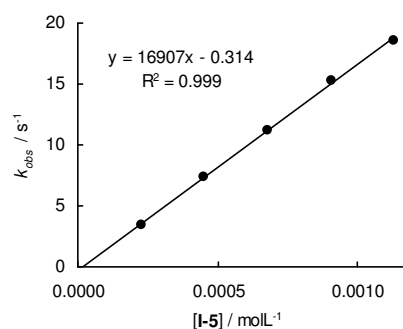
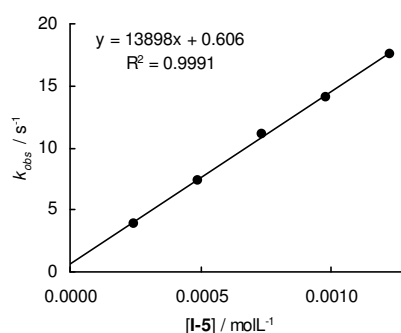


Table 7: Kinetics of the reaction of (**I-5**)-K with **2b** (20 °C, stopped-flow, at 533 nm).

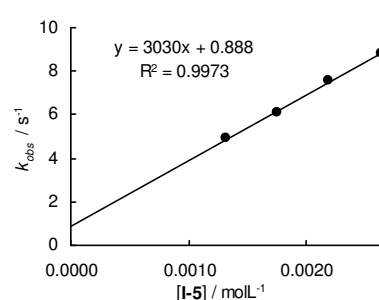
[ <b>2b</b> ] / mol L <sup>-1</sup>	[ <b>I-5</b> ] / mol L <sup>-1</sup>	[ <b>I-5</b> ] / [ <b>2b</b> ]	$k_{\text{obs}}$ / s <sup>-1</sup>
$1.21 \times 10^{-5}$	$2.45 \times 10^{-4}$	20.3	3.92
$1.21 \times 10^{-5}$	$4.90 \times 10^{-4}$	40.6	7.40
$1.21 \times 10^{-5}$	$7.35 \times 10^{-4}$	60.9	11.1
$1.21 \times 10^{-5}$	$9.80 \times 10^{-4}$	81.2	14.1
$1.21 \times 10^{-5}$	$1.23 \times 10^{-3}$	101	17.6

$$k_2 = 1.39 \times 10^4 \text{ L mol}^{-1} \text{ s}^{-1}$$

Table 8: Kinetics of the reaction of (**I-5**)-K with **2c** (20 °C, stopped-flow, at 374 nm).

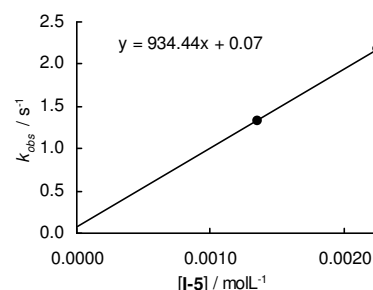
[ <b>2c</b> ] / mol L <sup>-1</sup>	[ <b>I-5</b> ] / mol L <sup>-1</sup>	[18-crown-6] / mol L <sup>-1</sup>	[ <b>I-5</b> ] / [ <b>2c</b> ]	$k_{\text{obs}}$ / s <sup>-1</sup>
$9.90 \times 10^{-6}$	$1.31 \times 10^{-3}$	$1.73 \times 10^{-3}$	136	4.91
$9.90 \times 10^{-6}$	$1.75 \times 10^{-3}$	$1.97 \times 10^{-3}$	177	6.08
$9.90 \times 10^{-6}$	$2.19 \times 10^{-3}$	$2.71 \times 10^{-3}$	221	7.61
$9.90 \times 10^{-6}$	$2.63 \times 10^{-3}$	$2.96 \times 10^{-3}$	265	8.82

$$k_2 = 3.03 \times 10^3 \text{ L mol}^{-1} \text{ s}^{-1}$$

Table 9: Kinetics of the reaction of (**I-5**)-K with **2d** (20 °C, stopped-flow, at 354 nm).

[ <b>2d</b> ] / mol L <sup>-1</sup>	[ <b>I-5</b> ] / mol L <sup>-1</sup>	[18-crown-6] / mol L <sup>-1</sup>	[ <b>I-5</b> ] / [ <b>2d</b> ]	$k_{\text{obs}}$ / s <sup>-1</sup>
$1.33 \times 10^{-5}$	$1.35 \times 10^{-3}$	$1.43 \times 10^{-3}$	101	1.33
$1.33 \times 10^{-5}$	$2.25 \times 10^{-3}$	$2.37 \times 10^{-3}$	169	2.17

$$k_2 = 9.34 \times 10^2 \text{ L mol}^{-1} \text{ s}^{-1}$$

Table 10: Kinetics of the reaction of (**I-5**)-K with **2d** (20 °C, stopped-flow, at 354 nm).

[ <b>2d</b> ] / mol L <sup>-1</sup>	[ <b>I-5</b> ] / mol L <sup>-1</sup>	[ <b>I-5</b> ] / [ <b>2d</b> ]	$k_{\text{obs}}$ / s <sup>-1</sup>
$1.33 \times 10^{-5}$	$8.99 \times 10^{-4}$	67.5	0.681
$1.33 \times 10^{-5}$	$1.80 \times 10^{-3}$	135	1.38
$1.33 \times 10^{-5}$	$2.70 \times 10^{-3}$	203	2.06

$$k_2 = 7.67 \times 10^2 \text{ L mol}^{-1} \text{ s}^{-1}$$

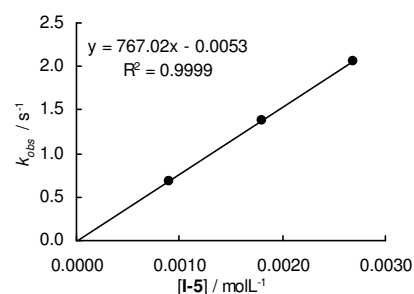
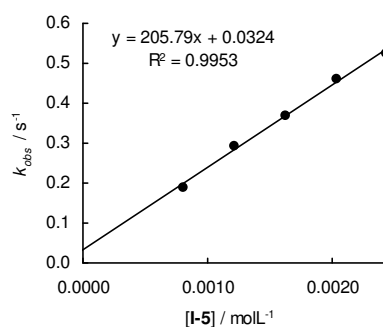


Table 11: Kinetics of the reaction of (**I-5**)-K with **2e** (20 °C, stopped-flow, at 371 nm).

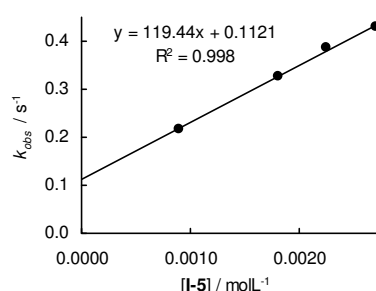
[ <b>2e</b> ] / mol L <sup>-1</sup>	[ <b>I-5</b> ] / mol L <sup>-1</sup>	[18-crown-6] / mol L <sup>-1</sup>	[ <b>I-5</b> ] /[ <b>2e</b> ]	$k_{\text{obs}}$ / s <sup>-1</sup>
$1.66 \times 10^{-5}$	$8.13 \times 10^{-4}$	$9.28 \times 10^{-4}$	49.0	$1.90 \times 10^{-1}$
$1.66 \times 10^{-5}$	$1.22 \times 10^{-3}$	$1.74 \times 10^{-3}$	73.5	$2.92 \times 10^{-1}$
$1.66 \times 10^{-5}$	$1.63 \times 10^{-3}$	$1.86 \times 10^{-3}$	98.0	$3.70 \times 10^{-1}$
$1.66 \times 10^{-5}$	$2.03 \times 10^{-3}$	$2.90 \times 10^{-3}$	123	$4.59 \times 10^{-1}$
$1.66 \times 10^{-5}$	$2.44 \times 10^{-3}$	$2.78 \times 10^{-3}$	147	$5.25 \times 10^{-1}$

$$k_2 = 2.06 \times 10^2 \text{ L mol}^{-1} \text{ s}^{-1}$$

Table 12: Kinetics of the reaction of (**I-5**)-K with **2f** (20 °C, stopped-flow, at 393 nm).

[ <b>2f</b> ] / mol L <sup>-1</sup>	[ <b>I-5</b> ] / mol L <sup>-1</sup>	[18-crown-6] / mol L <sup>-1</sup>	[ <b>I-5</b> ] /[ <b>2f</b> ]	$k_{\text{obs}}$ / s <sup>-1</sup>
$1.31 \times 10^{-5}$	$8.99 \times 10^{-4}$	$9.43 \times 10^{-4}$	68.5	$2.18 \times 10^{-1}$
$1.31 \times 10^{-5}$	$1.80 \times 10^{-3}$	$2.00 \times 10^{-3}$	137	$3.27 \times 10^{-1}$
$1.31 \times 10^{-5}$	$2.25 \times 10^{-3}$	$2.95 \times 10^{-3}$	171	$3.86 \times 10^{-1}$
$1.31 \times 10^{-5}$	$2.70 \times 10^{-3}$	$3.06 \times 10^{-3}$	205	$4.30 \times 10^{-1}$

$$k_2 = 1.19 \times 10^2 \text{ L mol}^{-1} \text{ s}^{-1}$$

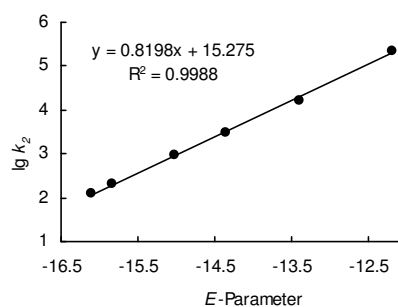


### Determination of Reactivity Parameters $N$ and $s_N$ for Potassium 1-(Ethoxycarbonyl)-2-oxocyclopentan-1-ide ((**I-5**)-K) in DMSO

Table 13: Rate constants for the reactions of (**I-5**)-K with different electrophiles (20 °C, in presence of 18-crown-6).

Electrophile	$E$	$k_2$ / L mol <sup>-1</sup> s <sup>-1</sup>	$\log k_2$
<b>2a</b>	-12.18	$2.21 \times 10^5$	5.34
<b>2b</b>	-13.39	$1.69 \times 10^4$	4.23
<b>2c</b>	-14.36	$3.03 \times 10^3$	3.48
<b>2d</b>	-15.03	$9.34 \times 10^2$	2.97
<b>2e</b>	-15.83	$2.06 \times 10^2$	2.31
<b>2f</b>	-16.11	$1.19 \times 10^2$	2.08

$$N = 18.63, s_N = 0.82$$

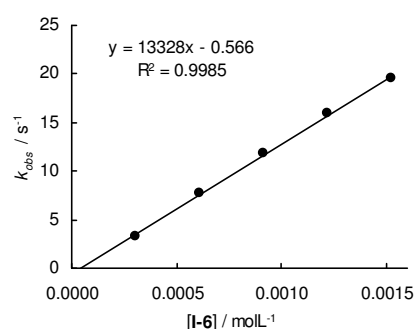


## 4.4.1.2. Reactions of Potassium 1-(Ethoxycarbonyl)-2-oxocyclohexan-1-ide ((I-6)-K)

Table 14: Kinetics of the reaction of (I-6)-K with **2b** (20 °C, stopped-flow, at 533 nm).

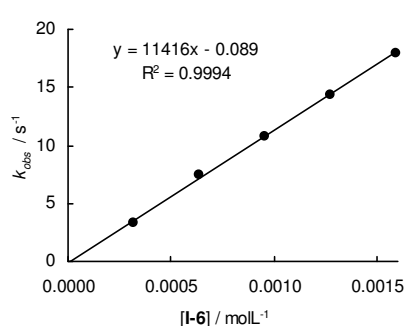
[ <b>2b</b> ] / mol L <sup>-1</sup>	[ <b>I-6</b> ] / mol L <sup>-1</sup>	[18-crown-6] / mol L <sup>-1</sup>	[ <b>I-6</b> ] /[ <b>2b</b> ]	$k_{\text{obs}}$ / s <sup>-1</sup>
$1.14 \times 10^{-5}$	$3.05 \times 10^{-4}$	$4.76 \times 10^{-4}$	26.7	3.23
$1.14 \times 10^{-5}$	$6.10 \times 10^{-4}$	$1.90 \times 10^{-3}$	53.3	7.76
$1.14 \times 10^{-5}$	$9.16 \times 10^{-4}$	$1.43 \times 10^{-3}$	80.0	11.8
$1.14 \times 10^{-5}$	$1.22 \times 10^{-3}$	$4.76 \times 10^{-3}$	107	15.9
$1.14 \times 10^{-5}$	$1.53 \times 10^{-3}$	$2.38 \times 10^{-3}$	133	19.5

$$k_2 = 1.33 \times 10^4 \text{ L mol}^{-1} \text{ s}^{-1}$$

Table 15: Kinetics of the reaction of (I-6)-K with **2b** (20 °C, stopped-flow, at 533 nm).

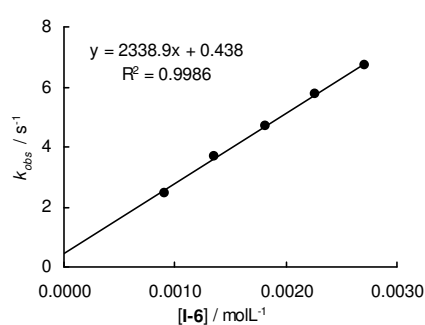
[ <b>2b</b> ] / mol L <sup>-1</sup>	[ <b>I-6</b> ] / mol L <sup>-1</sup>	[ <b>I-6</b> ] /[ <b>2b</b> ]	$k_{\text{obs}}$ / s <sup>-1</sup>
$1.21 \times 10^{-5}$	$3.18 \times 10^{-4}$	26.3	3.37
$1.21 \times 10^{-5}$	$6.35 \times 10^{-4}$	52.6	7.39
$1.21 \times 10^{-5}$	$9.53 \times 10^{-4}$	78.9	10.8
$1.21 \times 10^{-5}$	$1.27 \times 10^{-3}$	105	14.4
$1.21 \times 10^{-5}$	$1.59 \times 10^{-3}$	132	18.0

$$k_2 = 1.14 \times 10^4 \text{ L mol}^{-1} \text{ s}^{-1}$$

Table 16: Kinetics of the reaction of (I-6)-K with **2c** (20 °C, stopped-flow, at 374 nm).

[ <b>2c</b> ] / mol L <sup>-1</sup>	[ <b>I-6</b> ] / mol L <sup>-1</sup>	[18-crown-6] / mol L <sup>-1</sup>	[ <b>I-6</b> ] /[ <b>2c</b> ]	$k_{\text{obs}}$ / s <sup>-1</sup>
$1.52 \times 10^{-5}$	$9.06 \times 10^{-4}$	$1.08 \times 10^{-3}$	59.5	2.48
$1.52 \times 10^{-5}$	$1.36 \times 10^{-3}$	$2.03 \times 10^{-3}$	89.2	3.69
$1.52 \times 10^{-5}$	$1.81 \times 10^{-3}$	$2.16 \times 10^{-3}$	119	4.70
$1.52 \times 10^{-5}$	$2.26 \times 10^{-3}$	$3.25 \times 10^{-3}$	149	5.76
$1.52 \times 10^{-5}$	$2.72 \times 10^{-3}$	$3.25 \times 10^{-3}$	178	6.74

$$k_2 = 2.34 \times 10^3 \text{ L mol}^{-1} \text{ s}^{-1}$$

Table 17: Kinetics of the reaction of (I-6)-K with **2d** (20 °C, stopped-flow, at 354 nm).

[ <b>2d</b> ] / mol L <sup>-1</sup>	[ <b>I-6</b> ] / mol L <sup>-1</sup>	[18-crown-6] / mol L <sup>-1</sup>	[ <b>I-6</b> ]/[ <b>2d</b> ]	$k_{\text{obs}}$ / s <sup>-1</sup>
$1.86 \times 10^{-5}$	$1.01 \times 10^{-3}$	$1.06 \times 10^{-3}$	54.4	$5.59 \times 10^{-1}$
$1.86 \times 10^{-5}$	$1.51 \times 10^{-3}$	$1.98 \times 10^{-3}$	81.6	$8.24 \times 10^{-1}$
$1.86 \times 10^{-5}$	$2.02 \times 10^{-3}$	$2.11 \times 10^{-3}$	109	1.07
$1.86 \times 10^{-5}$	$2.52 \times 10^{-3}$	$3.17 \times 10^{-3}$	136	1.28
$1.86 \times 10^{-5}$	$3.03 \times 10^{-3}$	$3.17 \times 10^{-3}$	163	1.51

$$k_2 = 4.67 \times 10^2 \text{ L mol}^{-1} \text{ s}^{-1}$$

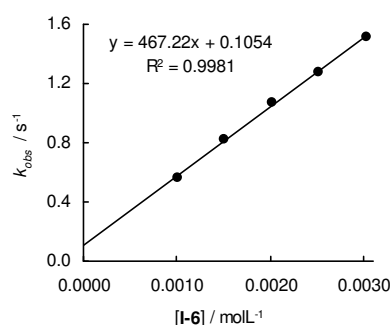
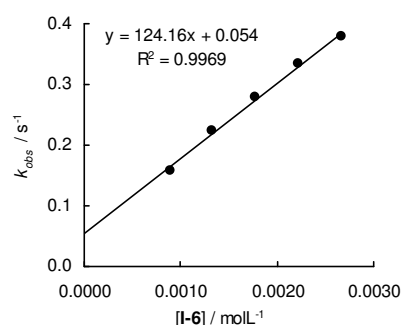




Table 18: Kinetics of the reaction of (**I-6**)-K with **2e** (20 °C, stopped-flow, at 371 nm).

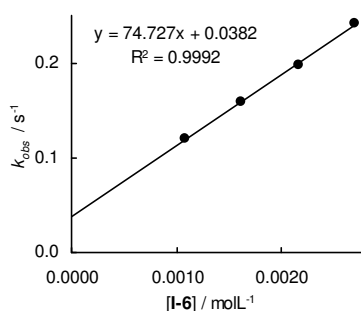
[ <b>2e</b> ] / mol L <sup>-1</sup>	[ <b>I-6</b> ] / mol L <sup>-1</sup>	[18-crown-6] / mol L <sup>-1</sup>	[ <b>I-6</b> ] / [ <b>2e</b> ]	$k_{\text{obs}}$ / s <sup>-1</sup>
$1.76 \times 10^{-5}$	$8.89 \times 10^{-4}$	$1.09 \times 10^{-3}$	50.4	$1.59 \times 10^{-1}$
$1.76 \times 10^{-5}$	$1.33 \times 10^{-3}$	$1.63 \times 10^{-3}$	75.6	$2.23 \times 10^{-1}$
$1.76 \times 10^{-5}$	$1.78 \times 10^{-3}$	$2.18 \times 10^{-3}$	101	$2.79 \times 10^{-1}$
$1.76 \times 10^{-5}$	$2.22 \times 10^{-3}$	$2.72 \times 10^{-3}$	126	$3.33 \times 10^{-1}$
$1.76 \times 10^{-5}$	$2.67 \times 10^{-3}$	$3.27 \times 10^{-3}$	151	$3.80 \times 10^{-1}$

$$k_2 = 1.24 \times 10^2 \text{ L mol}^{-1} \text{ s}^{-1}$$

Table 19: Kinetics of the reaction of (**I-6**)-K with **2f** (20 °C, stopped-flow, at 393 nm, with addition of CH acid).

[ <b>2f</b> ] / mol L <sup>-1</sup>	[ <b>I-6</b> ] / mol L <sup>-1</sup>	[ <b>(I-6)</b> -H] / mol L <sup>-1</sup>	[ <b>(I-6)</b> -H] / [ <b>I-6</b> ]	[18-crown-6] / mol L <sup>-1</sup>	[ <b>I-6</b> ]/[ <b>2f</b> ]	$k_{\text{obs}}$ / s <sup>-1</sup>
$1.72 \times 10^{-5}$	$1.08 \times 10^{-3}$	$4.50 \times 10^{-3}$	4.17	$1.64 \times 10^{-3}$	62.7	$1.20 \times 10^{-1}$
$1.72 \times 10^{-5}$	$1.62 \times 10^{-3}$	$5.40 \times 10^{-3}$	3.34	$1.85 \times 10^{-3}$	94.1	$1.58 \times 10^{-1}$
$1.72 \times 10^{-5}$	$2.16 \times 10^{-3}$	$9.89 \times 10^{-3}$	4.59	$3.29 \times 10^{-3}$	125	$1.98 \times 10^{-1}$
$1.72 \times 10^{-5}$	$2.70 \times 10^{-3}$	$8.99 \times 10^{-3}$	3.34	$3.08 \times 10^{-3}$	157	$2.41 \times 10^{-1}$

$$k_2 = 7.47 \times 10^1 \text{ L mol}^{-1} \text{ s}^{-1}$$

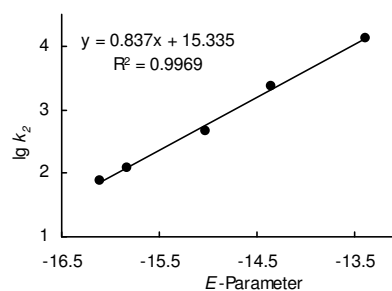


### Determination of Reactivity Parameters $N$ and $s_N$ for Potassium 1-(Ethoxycarbonyl)-2-oxocyclohexan-1-ide ((**I-6**)-K) in DMSO

Table 20: Rate constants for the reactions of (**I-6**)-K with different electrophiles (20 °C, in presence of 18-crown-6).

Electrophile	$E$	$k_2$ / L mol <sup>-1</sup> s <sup>-1</sup>	$\log k_2$
<b>2b</b>	-13.39	$1.33 \times 10^4$	4.12
<b>2c</b>	-14.36	$2.34 \times 10^3$	3.37
<b>2d</b>	-15.03	$4.67 \times 10^2$	2.67
<b>2e</b>	-15.83	$1.24 \times 10^2$	2.09
<b>2f</b>	-16.11	$7.47 \times 10^1$	1.87

$$N = 18.32, s_N = 0.84$$

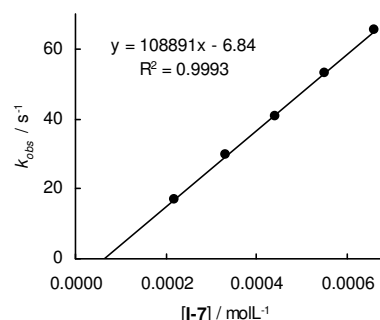


## 4.4.1.3. Reactions of Potassium 1-(Ethoxycarbonyl)-2-oxocycloheptan-1-ide ((I-7)-K)

Table 21: Kinetics of the reaction of (I-7)-K with **2b** (20 °C, stopped-flow, at 533 nm).

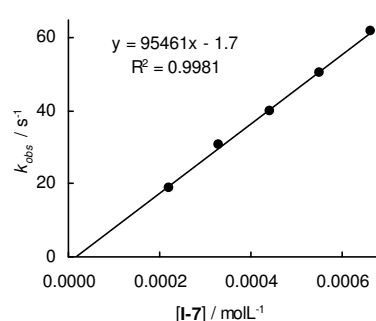
[ <b>2b</b> ] / mol L <sup>-1</sup>	[ <b>I-7</b> ] / mol L <sup>-1</sup>	[18-crown-6] / mol L <sup>-1</sup>	[ <b>I-7</b> ] /[ <b>2b</b> ]	$k_{\text{obs}}$ / s <sup>-1</sup>
$1.27 \times 10^{-5}$	$2.20 \times 10^{-4}$	$2.82 \times 10^{-4}$	17.3	16.9
$1.27 \times 10^{-5}$	$3.31 \times 10^{-4}$	$7.05 \times 10^{-4}$	26.0	29.9
$1.27 \times 10^{-5}$	$4.41 \times 10^{-4}$	$5.64 \times 10^{-4}$	34.7	40.5
$1.27 \times 10^{-5}$	$5.51 \times 10^{-4}$	$1.41 \times 10^{-3}$	43.3	53.3
$1.27 \times 10^{-5}$	$6.61 \times 10^{-4}$	$8.46 \times 10^{-4}$	52.0	65.2

$$k_2 = 1.09 \times 10^5 \text{ L mol}^{-1} \text{ s}^{-1}$$

Table 22: Kinetics of the reaction of (I-7)-K with **2b** (20 °C, stopped-flow, at 533 nm).

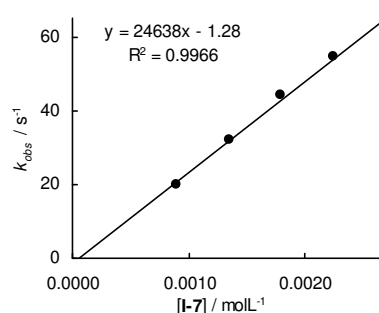
[ <b>2b</b> ] / mol L <sup>-1</sup>	[ <b>I-7</b> ] / mol L <sup>-1</sup>	[ <b>I-7</b> ] /[ <b>2c</b> ]	$k_{\text{obs}}$ / s <sup>-1</sup>
$1.27 \times 10^{-5}$	$2.20 \times 10^{-4}$	17.3	19.0
$1.27 \times 10^{-5}$	$3.31 \times 10^{-4}$	26.0	30.9
$1.27 \times 10^{-5}$	$4.41 \times 10^{-4}$	34.7	39.8
$1.27 \times 10^{-5}$	$5.51 \times 10^{-4}$	43.3	50.3
$1.27 \times 10^{-5}$	$6.61 \times 10^{-4}$	52.0	61.9

$$k_2 = 9.55 \times 10^4 \text{ L mol}^{-1} \text{ s}^{-1}$$

Table 23: Kinetics of the reaction of (I-7)-K with **2c** (20 °C, stopped-flow, at 374 nm).

[ <b>2c</b> ] / mol L <sup>-1</sup>	[ <b>I-7</b> ] / mol L <sup>-1</sup>	[18-crown-6] / mol L <sup>-1</sup>	[ <b>I-7</b> ] /[ <b>2c</b> ]	$k_{\text{obs}}$ / s <sup>-1</sup>
$1.73 \times 10^{-5}$	$8.98 \times 10^{-4}$	$9.53 \times 10^{-4}$	51.8	20.0
$1.73 \times 10^{-5}$	$1.35 \times 10^{-3}$	$1.43 \times 10^{-3}$	77.7	31.9
$1.73 \times 10^{-5}$	$1.80 \times 10^{-3}$	$1.91 \times 10^{-3}$	104	44.4
$1.73 \times 10^{-5}$	$2.24 \times 10^{-3}$	$2.38 \times 10^{-3}$	130	54.5
$1.73 \times 10^{-5}$	$2.69 \times 10^{-3}$	$2.86 \times 10^{-3}$	156	64.0

$$k_2 = 2.46 \times 10^4 \text{ L mol}^{-1} \text{ s}^{-1}$$

Table 24: Kinetics of the reaction of (I-7)-K with **2d** (20 °C, stopped-flow, at 354 nm).

[ <b>2d</b> ] / mol L <sup>-1</sup>	[ <b>I-7</b> ] / mol L <sup>-1</sup>	[18-crown-6] / mol L <sup>-1</sup>	[ <b>I-7</b> ] /[ <b>2d</b> ]	$k_{\text{obs}}$ / s <sup>-1</sup>
$2.15 \times 10^{-5}$	$1.05 \times 10^{-3}$	$1.17 \times 10^{-3}$	49.0	6.51
$2.15 \times 10^{-5}$	$1.58 \times 10^{-3}$	$2.04 \times 10^{-3}$	73.5	9.22
$2.15 \times 10^{-5}$	$2.10 \times 10^{-3}$	$2.33 \times 10^{-3}$	98.0	11.8
$2.15 \times 10^{-5}$	$2.63 \times 10^{-3}$	$3.21 \times 10^{-3}$	123	14.6

$$k_2 = 5.11 \times 10^3 \text{ L mol}^{-1} \text{ s}^{-1}$$

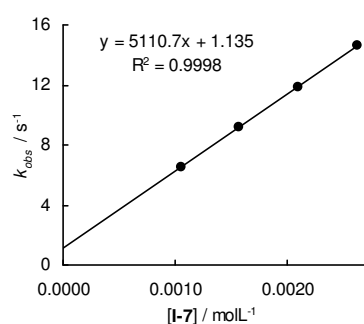
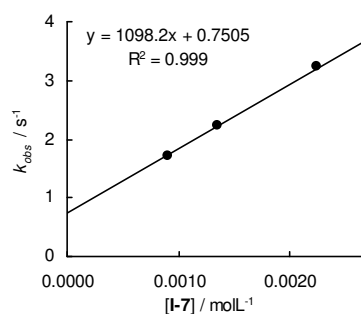


Table 25: Kinetics of the reaction of (I-7)-K with **2e** (20 °C, stopped-flow, at 371 nm).

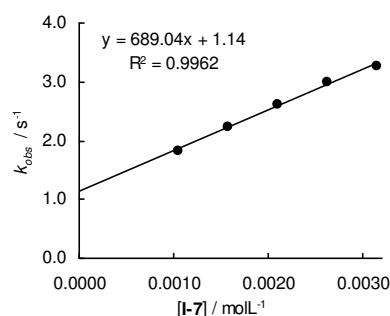
[ <b>2e</b> ] / mol L <sup>-1</sup>	[I-7] / mol L <sup>-1</sup>	[18-crown-6] / mol L <sup>-1</sup>	[I-7] / [ <b>2e</b> ]	$k_{\text{obs}}$ / s <sup>-1</sup>
$1.72 \times 10^{-5}$	$8.98 \times 10^{-4}$	$9.53 \times 10^{-4}$	52.3	1.72
$1.72 \times 10^{-5}$	$1.35 \times 10^{-3}$	$1.43 \times 10^{-3}$	78.4	2.24
$1.72 \times 10^{-5}$	$2.24 \times 10^{-3}$	$2.38 \times 10^{-3}$	131	3.25
$1.72 \times 10^{-5}$	$2.69 \times 10^{-3}$	$2.86 \times 10^{-3}$	157	3.68

$$k_2 = 1.10 \times 10^3 \text{ L mol}^{-1} \text{ s}^{-1}$$

Table 26: Kinetics of the reaction of (I-7)-K with **2f** (20 °C, stopped-flow, at 393 nm).

[ <b>2f</b> ] / mol L <sup>-1</sup>	[I-7] / mol L <sup>-1</sup>	[18-crown-6] / mol L <sup>-1</sup>	[I-7] / [ <b>2f</b> ]	$k_{\text{obs}}$ / s <sup>-1</sup>
$1.43 \times 10^{-5}$	$1.05 \times 10^{-3}$	$1.17 \times 10^{-3}$	73.5	1.83
$1.43 \times 10^{-5}$	$1.58 \times 10^{-3}$	$2.04 \times 10^{-3}$	110	2.24
$1.43 \times 10^{-5}$	$2.10 \times 10^{-3}$	$2.33 \times 10^{-3}$	147	2.62
$1.43 \times 10^{-5}$	$2.63 \times 10^{-3}$	$3.21 \times 10^{-3}$	184	2.98
$1.43 \times 10^{-5}$	$3.15 \times 10^{-3}$	$3.50 \times 10^{-3}$	220	3.27

$$k_2 = 6.89 \times 10^2 \text{ L mol}^{-1} \text{ s}^{-1}$$

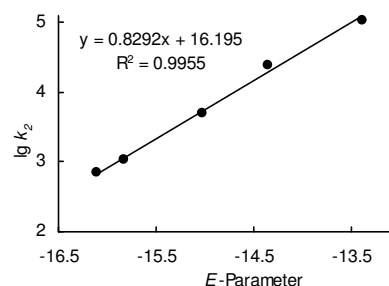


### Determination of Reactivity Parameters $N$ and $s_N$ for Potassium 1-(Ethoxycarbonyl)-2-oxocycloheptan-1-ide ((I-7)-K) in DMSO

Table 27: Rate constants for the reactions of (I-7)-K with different electrophiles (20 °C, in presence of 18-crown-6).

Electrophile	$E$	$k_2$ / L mol <sup>-1</sup> s <sup>-1</sup>	$\log k_2$
<b>2b</b>	-13.39	$1.09 \times 10^5$	5.04
<b>2c</b>	-14.36	$2.46 \times 10^4$	4.39
<b>2d</b>	-15.03	$5.11 \times 10^3$	3.71
<b>2e</b>	-15.83	$1.10 \times 10^3$	3.04
<b>2f</b>	-16.11	$6.89 \times 10^2$	2.84

$$N = 19.53, s_N = 0.83$$

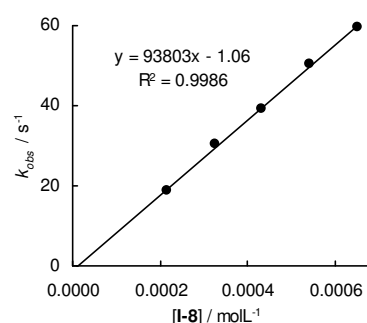


## 4.4.1.4. Reactions of Potassium 1-(Ethoxycarbonyl)-2-oxocyclooctan-1-ide ((I-8)-K)

Table 28: Kinetics of the reaction of (I-8)-K with **2b** (20 °C, stopped-flow, at 533 nm).

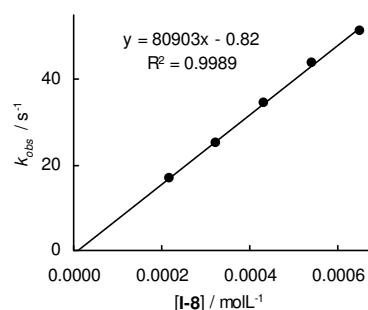
[ <b>2b</b> ] / mol L <sup>-1</sup>	[ <b>I-8</b> ] / mol L <sup>-1</sup>	[18-crown-6] / mol L <sup>-1</sup>	[ <b>I-8</b> ] / [ <b>2d</b> ]	$k_{\text{obs}}$ / s <sup>-1</sup>
$1.27 \times 10^{-5}$	$2.17 \times 10^{-4}$	$2.82 \times 10^{-4}$	17.1	18.7
$1.27 \times 10^{-5}$	$3.26 \times 10^{-4}$	$7.05 \times 10^{-4}$	25.6	30.3
$1.27 \times 10^{-5}$	$4.34 \times 10^{-4}$	$5.64 \times 10^{-4}$	34.1	39.4
$1.27 \times 10^{-5}$	$5.43 \times 10^{-4}$	$1.13 \times 10^{-3}$	42.7	50.3
$1.27 \times 10^{-5}$	$6.51 \times 10^{-4}$	$8.46 \times 10^{-4}$	51.2	59.6

$$k_2 = 9.38 \times 10^4 \text{ L mol}^{-1} \text{ s}^{-1}$$

Table 29: Kinetics of the reaction of (I-8)-K with **2b** (20 °C, stopped-flow, at 533 nm).

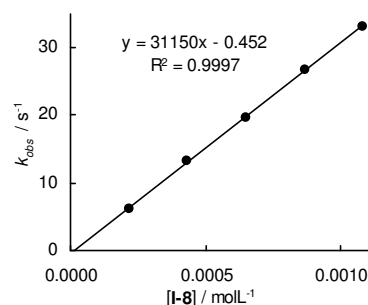
[ <b>2b</b> ] / mol L <sup>-1</sup>	[ <b>I-8</b> ] / mol L <sup>-1</sup>	[ <b>I-8</b> ] / [ <b>2d</b> ]	$k_{\text{obs}}$ / s <sup>-1</sup>
$1.27 \times 10^{-5}$	$2.17 \times 10^{-4}$	17.1	16.8
$1.27 \times 10^{-5}$	$3.26 \times 10^{-4}$	25.6	25.2
$1.27 \times 10^{-5}$	$4.34 \times 10^{-4}$	34.1	34.3
$1.27 \times 10^{-5}$	$5.43 \times 10^{-4}$	42.7	43.8
$1.27 \times 10^{-5}$	$6.51 \times 10^{-4}$	51.2	51.4

$$k_2 = 8.09 \times 10^4 \text{ L mol}^{-1} \text{ s}^{-1}$$

Table 30: Kinetics of the reaction of (I-8)-K with **2c** (20 °C, stopped-flow, at 374 nm).

[ <b>2c</b> ] / mol L <sup>-1</sup>	[ <b>I-8</b> ] / mol L <sup>-1</sup>	[18-crown-6] / mol L <sup>-1</sup>	[ <b>I-8</b> ] / [ <b>2c</b> ]	$k_{\text{obs}}$ / s <sup>-1</sup>
$1.41 \times 10^{-5}$	$2.17 \times 10^{-4}$	$2.58 \times 10^{-4}$	15.3	6.16
$1.41 \times 10^{-5}$	$4.33 \times 10^{-4}$	$6.45 \times 10^{-4}$	30.6	13.3
$1.41 \times 10^{-5}$	$6.50 \times 10^{-4}$	$7.74 \times 10^{-4}$	46.0	19.6
$1.41 \times 10^{-5}$	$8.67 \times 10^{-4}$	$1.29 \times 10^{-3}$	61.3	26.7
$1.41 \times 10^{-5}$	$1.08 \times 10^{-3}$	$1.29 \times 10^{-3}$	76.6	33.2

$$k_2 = 3.12 \times 10^4 \text{ L mol}^{-1} \text{ s}^{-1}$$

Table 31: Kinetics of the reaction of (I-8)-K with **2d** (20 °C, stopped-flow, at 354 nm).

[ <b>2d</b> ] / mol L <sup>-1</sup>	[ <b>I-8</b> ] / mol L <sup>-1</sup>	[18-crown-6] / mol L <sup>-1</sup>	[ <b>I-8</b> ] / [ <b>2d</b> ]	$k_{\text{obs}}$ / s <sup>-1</sup>
$1.47 \times 10^{-5}$	$2.17 \times 10^{-4}$	$2.58 \times 10^{-4}$	14.7	2.17
$1.47 \times 10^{-5}$	$4.33 \times 10^{-4}$	$6.45 \times 10^{-4}$	29.4	3.79
$1.47 \times 10^{-5}$	$6.50 \times 10^{-4}$	$7.74 \times 10^{-4}$	44.1	5.22
$1.47 \times 10^{-5}$	$8.67 \times 10^{-4}$	$1.29 \times 10^{-3}$	58.9	6.66
$1.47 \times 10^{-5}$	$1.08 \times 10^{-3}$	$1.29 \times 10^{-3}$	73.6	8.05

$$k_2 = 6.75 \times 10^3 \text{ L mol}^{-1} \text{ s}^{-1}$$

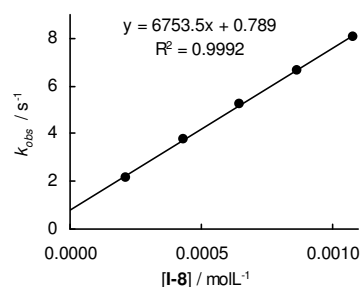
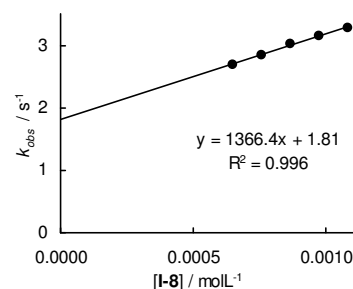


Table 32: Kinetics of the reaction of (I-8)-K with **2e** (20 °C, stopped-flow, at 371 nm).

[ <b>2e</b> ] / mol L <sup>-1</sup>	[ <b>I-8</b> ] / mol L <sup>-1</sup>	[18-crown-6] / mol L <sup>-1</sup>	[ <b>I-8</b> ] / [ <b>2e</b> ]	$k_{\text{obs}}$ / s <sup>-1</sup>
$1.38 \times 10^{-5}$	$6.50 \times 10^{-4}$	$7.74 \times 10^{-4}$	47.1	2.69
$1.38 \times 10^{-5}$	$7.58 \times 10^{-4}$	$1.16 \times 10^{-3}$	54.9	2.84
$1.38 \times 10^{-5}$	$8.67 \times 10^{-4}$	$1.03 \times 10^{-3}$	62.7	3.02
$1.38 \times 10^{-5}$	$9.75 \times 10^{-4}$	$1.42 \times 10^{-3}$	70.6	3.14
$1.38 \times 10^{-5}$	$1.08 \times 10^{-3}$	$1.29 \times 10^{-3}$	78.4	3.28

$$k_2 = 1.37 \times 10^3 \text{ L mol}^{-1} \text{ s}^{-1}$$

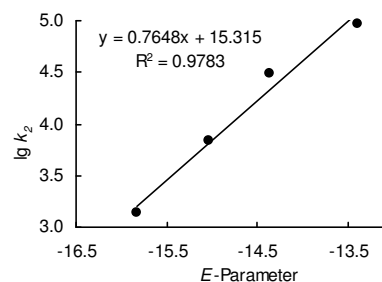


### Determination of Reactivity Parameters $N$ and $s_N$ for Potassium 1-(Ethoxycarbonyl)-2-oxocyclooctan-1-ide ((I-8)-K) in DMSO

Table 33: Rate constants for the reactions of (I-8)-K with different electrophiles (20 °C, in presence of 18-crown-6).

Electrophile	$E$	$k_2$ / L mol <sup>-1</sup> s <sup>-1</sup>	$\log k_2$
<b>2b</b>	-13.39	$9.38 \times 10^4$	4.97
<b>2c</b>	-14.36	$3.12 \times 10^4$	4.49
<b>2d</b>	-15.03	$6.75 \times 10^3$	3.83
<b>2e</b>	-15.83	$1.37 \times 10^3$	3.14

$$N = 20.02, s_N = 0.76$$



#### 4.4.1.5. Reactions of Potassium 1-(Ethoxycarbonyl)-2-oxododecan-1-ide ((I-12)-K)

Table 34: Kinetics of the reaction of (I-12)-K with **2b** (20 °C, stopped-flow, at 533 nm).

[ <b>2b</b> ] / mol L <sup>-1</sup>	[ <b>I-12</b> ] / mol L <sup>-1</sup>	[18-crown-6] / mol L <sup>-1</sup>	[ <b>I-12</b> ] / [ <b>2d</b> ]	$k_{\text{obs}}$ / s <sup>-1</sup>
$1.27 \times 10^{-5}$	$2.11 \times 10^{-4}$	$3.07 \times 10^{-4}$	16.6	5.05
$1.27 \times 10^{-5}$	$4.22 \times 10^{-4}$	$7.68 \times 10^{-4}$	33.2	11.5
$1.27 \times 10^{-5}$	$6.33 \times 10^{-4}$	$9.22 \times 10^{-4}$	49.8	17.7
$1.27 \times 10^{-5}$	$8.44 \times 10^{-4}$	$1.84 \times 10^{-3}$	66.4	24.7
$1.27 \times 10^{-5}$	$1.06 \times 10^{-3}$	$1.54 \times 10^{-3}$	83.0	31.0

$$k_2 = 3.09 \times 10^4 \text{ L mol}^{-1} \text{ s}^{-1}$$

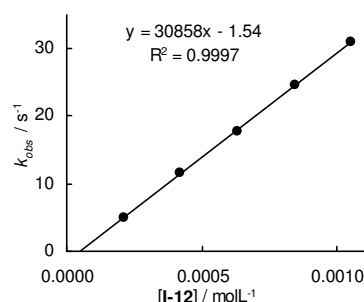
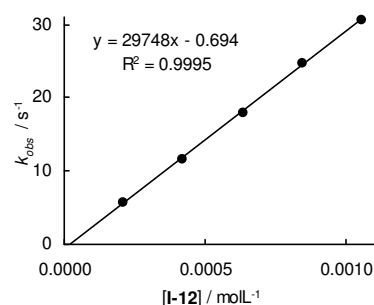


Table 35: Kinetics of the reaction of (I-12)-K with **2b** (20 °C, stopped-flow, at 533 nm).

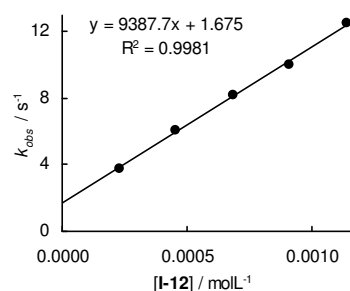
[ <b>2b</b> ] / mol L <sup>-1</sup>	[I-12] / mol L <sup>-1</sup>	[I-12] / [ <b>2d</b> ]	$k_{\text{obs}}$ / s <sup>-1</sup>
$1.27 \times 10^{-5}$	$2.11 \times 10^{-4}$	16.6	5.77
$1.27 \times 10^{-5}$	$4.22 \times 10^{-4}$	33.2	11.6
$1.27 \times 10^{-5}$	$6.33 \times 10^{-4}$	49.8	18.0
$1.27 \times 10^{-5}$	$8.44 \times 10^{-4}$	66.4	24.7
$1.27 \times 10^{-5}$	$1.06 \times 10^{-3}$	83.0	30.6

$$k_2 = 2.97 \times 10^4 \text{ L mol}^{-1} \text{ s}^{-1}$$

Table 36: Kinetics of the reaction of (I-12)-K with **2c** (20 °C, stopped-flow, at 374 nm).

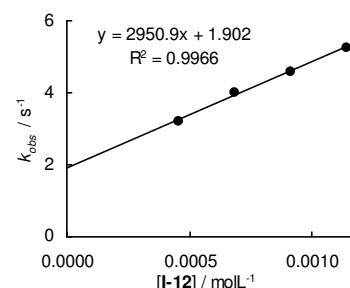
[ <b>2c</b> ] / mol L <sup>-1</sup>	[I-12] / mol L <sup>-1</sup>	[18-crown-6] / mol L <sup>-1</sup>	[I-12] / [ <b>2c</b> ]	$k_{\text{obs}}$ / s <sup>-1</sup>
$1.52 \times 10^{-5}$	$2.28 \times 10^{-4}$	$2.52 \times 10^{-4}$	15.0	3.77
$1.52 \times 10^{-5}$	$4.56 \times 10^{-4}$	$8.40 \times 10^{-4}$	30.0	6.05
$1.52 \times 10^{-5}$	$6.84 \times 10^{-4}$	$7.56 \times 10^{-4}$	45.0	8.17
$1.52 \times 10^{-5}$	$9.12 \times 10^{-4}$	$1.68 \times 10^{-3}$	60.0	10.0
$1.52 \times 10^{-5}$	$1.14 \times 10^{-3}$	$1.26 \times 10^{-3}$	75.0	12.5

$$k_2 = 9.39 \times 10^3 \text{ L mol}^{-1} \text{ s}^{-1}$$

Table 37: Kinetics of the reaction of (I-12)-K with **2d** (20 °C, stopped-flow, at 354 nm).

[ <b>2d</b> ] / mol L <sup>-1</sup>	[I-12] / mol L <sup>-1</sup>	[18-crown-6] / mol L <sup>-1</sup>	[I-12] / [ <b>2d</b> ]	$k_{\text{obs}}$ / s <sup>-1</sup>
$1.46 \times 10^{-5}$	$4.56 \times 10^{-4}$	$8.40 \times 10^{-4}$	31.3	3.20
$1.46 \times 10^{-5}$	$6.84 \times 10^{-4}$	$1.01 \times 10^{-3}$	47.0	3.99
$1.46 \times 10^{-5}$	$9.12 \times 10^{-4}$	$1.68 \times 10^{-3}$	62.6	4.60
$1.46 \times 10^{-5}$	$1.14 \times 10^{-3}$	$1.68 \times 10^{-3}$	78.3	5.24

$$k_2 = 2.95 \times 10^3 \text{ L mol}^{-1} \text{ s}^{-1}$$

Table 38: Kinetics of the reaction of (I-12)-K with **2e** (20 °C, stopped-flow, at 371 nm).

[ <b>2d</b> ] / mol L <sup>-1</sup>	[I-12] / mol L <sup>-1</sup>	[18-crown-6] / mol L <sup>-1</sup>	[I-12] / [ <b>2d</b> ]	$k_{\text{obs}}$ / s <sup>-1</sup>
$1.39 \times 10^{-5}$	$1.52 \times 10^{-3}$	$1.66 \times 10^{-3}$	109	6.03
$1.39 \times 10^{-5}$	$2.27 \times 10^{-3}$	$3.56 \times 10^{-3}$	163	6.76
$1.39 \times 10^{-5}$	$3.03 \times 10^{-3}$	$3.33 \times 10^{-3}$	217	7.41
$1.39 \times 10^{-5}$	$3.79 \times 10^{-3}$	$7.13 \times 10^{-3}$	272	8.36

$$k_2 = 1.01 \times 10^3 \text{ L mol}^{-1} \text{ s}^{-1}$$

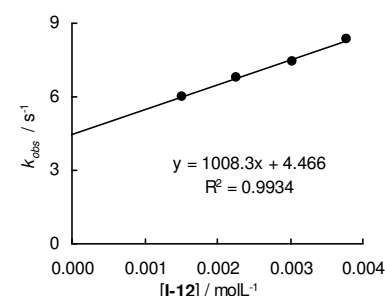
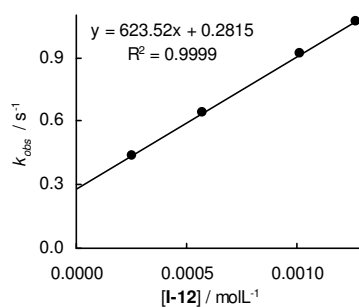


Table 39: Kinetics of the reaction of (**I-12**)-K with **2f** (20 °C, stopped-flow, at 393 nm, with addition of CH acid).

[ <b>2f</b> ] / mol L <sup>-1</sup>	[ <b>I-12</b> ] / mol L <sup>-1</sup>	[( <b>I-12</b> )-H] / mol L <sup>-1</sup>	[( <b>I-12</b> )-H] / [ <b>I-12</b> ]	[18-crown-6] / mol L <sup>-1</sup>	[ <b>I-12</b> ] / [ <b>2f</b> ]	$k_{\text{obs}}$ / s <sup>-1</sup>
$1.72 \times 10^{-5}$	$2.54 \times 10^{-4}$	$9.84 \times 10^{-4}$	3.88	$3.14 \times 10^{-4}$	14.8	$4.38 \times 10^{-1}$
$1.72 \times 10^{-5}$	$5.71 \times 10^{-4}$	$2.46 \times 10^{-3}$	4.31	$8.37 \times 10^{-4}$	33.2	$6.39 \times 10^{-1}$
$1.72 \times 10^{-5}$	$1.01 \times 10^{-3}$	$4.92 \times 10^{-3}$	4.85	$1.67 \times 10^{-3}$	59.0	$9.17 \times 10^{-1}$
$1.72 \times 10^{-5}$	$1.27 \times 10^{-3}$	$4.92 \times 10^{-3}$	3.88	$1.57 \times 10^{-3}$	73.8	1.07

$$k_2 = 6.24 \times 10^2 \text{ L mol}^{-1} \text{ s}^{-1}$$

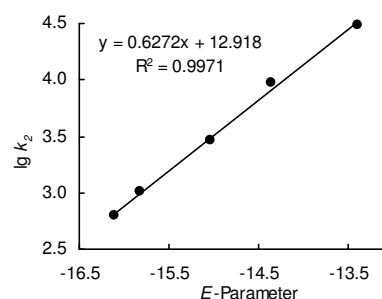


### Determination of Reactivity Parameters $N$ and $s_N$ for Potassium 1-(Ethoxycarbonyl)-2-oxocyclododecan-1-ide ((**I-12**)-K) in DMSO

Table 40: Rate constants for the reactions of (**I-12**)-K with different electrophiles (20 °C, in presence of 18-crown-6).

Electrophile	$E$	$k_2$ / L mol <sup>-1</sup> s <sup>-1</sup>	$\log k_2$
<b>2b</b>	-13.39	$3.09 \times 10^4$	4.49
<b>2c</b>	-14.36	$9.39 \times 10^3$	3.97
<b>2d</b>	-15.03	$2.95 \times 10^3$	3.47
<b>2e</b>	-15.83	$1.01 \times 10^3$	3.00
<b>2f</b>	-16.11	$6.24 \times 10^{-1}$	2.79

$$N = 20.60, s_N = 0.63$$



4.4.4.2. Coordination Experiments with KBPh<sub>4</sub>Table 41: Pseudo-first-order rate constants for reaction of (**I-6**)-K<sup>[a]</sup> with **2b** with variable concentrations of KBPh<sub>4</sub> (20 °C, stopped-flow, at 533 nm).

[ <b>2b</b> ] / mol L <sup>-1</sup>	[ <b>I-6</b> ] / mol L <sup>-1</sup>	[KBPh <sub>4</sub> ] / mol L <sup>-1</sup>	[K <sup>+</sup> ] <sub>total</sub> / mol L <sup>-1</sup>	<i>k</i> <sub>obs</sub> / s <sup>-1</sup>
	3.02 × 10 <sup>-4</sup>			4.02 <sup>[a]</sup>
1.46 × 10 <sup>-5</sup>	3.02 × 10 <sup>-4</sup>	0	3.02 × 10 <sup>-4</sup>	2.79
1.46 × 10 <sup>-5</sup>	3.02 × 10 <sup>-4</sup>	1.28 × 10 <sup>-4</sup>	4.30 × 10 <sup>-4</sup>	2.76
1.46 × 10 <sup>-5</sup>	3.02 × 10 <sup>-4</sup>	2.55 × 10 <sup>-4</sup>	5.57 × 10 <sup>-4</sup>	2.59
1.46 × 10 <sup>-5</sup>	3.02 × 10 <sup>-4</sup>	5.10 × 10 <sup>-4</sup>	8.12 × 10 <sup>-4</sup>	2.30
1.46 × 10 <sup>-5</sup>	3.02 × 10 <sup>-4</sup>	1.23 × 10 <sup>-3</sup>	1.53 × 10 <sup>-3</sup>	1.79
1.46 × 10 <sup>-5</sup>	3.02 × 10 <sup>-4</sup>	2.55 × 10 <sup>-3</sup>	2.85 × 10 <sup>-3</sup>	1.23
1.46 × 10 <sup>-5</sup>	3.02 × 10 <sup>-4</sup>	4.92 × 10 <sup>-3</sup>	5.22 × 10 <sup>-3</sup>	9.83 × 10 <sup>-1</sup>
1.46 × 10 <sup>-5</sup>	3.02 × 10 <sup>-4</sup>	7.37 × 10 <sup>-3</sup>	7.68 × 10 <sup>-3</sup>	7.71 × 10 <sup>-1</sup>
1.46 × 10 <sup>-5</sup>	3.02 × 10 <sup>-4</sup>	1.11 × 10 <sup>-2</sup>	1.14 × 10 <sup>-2</sup>	5.91 × 10 <sup>-1</sup>
1.46 × 10 <sup>-5</sup>	3.02 × 10 <sup>-4</sup>	1.70 × 10 <sup>-2</sup>	1.73 × 10 <sup>-2</sup>	4.41 × 10 <sup>-1</sup>

[a] Calculated from the second-order rate constant of the free anion (potassium salt in presence of 18-crown-6) given in Table 4.

Table 42: Pseudo-first-order rate constants for reaction of (**I-12**)-K<sup>[a]</sup> with **2b** with variable concentrations of KBPh<sub>4</sub> (20 °C, stopped-flow, at 533 nm).

[ <b>2b</b> ] / mol L <sup>-1</sup>	[ <b>I-12</b> ] / mol L <sup>-1</sup>	[KBPh <sub>4</sub> ] / mol L <sup>-1</sup>	[K <sup>+</sup> ] <sub>total</sub> / mol L <sup>-1</sup>	<i>k</i> <sub>obs</sub> / s <sup>-1</sup>
	2.95 × 10 <sup>-4</sup>			9.12 <sup>[a]</sup>
1.30 × 10 <sup>-5</sup>	2.95 × 10 <sup>-4</sup>	1.44 × 10 <sup>-4</sup>	4.39 × 10 <sup>-4</sup>	8.24
1.30 × 10 <sup>-5</sup>	2.95 × 10 <sup>-4</sup>	2.88 × 10 <sup>-4</sup>	5.83 × 10 <sup>-4</sup>	8.06
1.30 × 10 <sup>-5</sup>	2.95 × 10 <sup>-4</sup>	5.76 × 10 <sup>-4</sup>	8.71 × 10 <sup>-4</sup>	7.88
1.30 × 10 <sup>-5</sup>	2.95 × 10 <sup>-4</sup>	1.45 × 10 <sup>-3</sup>	1.75 × 10 <sup>-3</sup>	7.74
1.30 × 10 <sup>-5</sup>	2.95 × 10 <sup>-4</sup>	2.59 × 10 <sup>-3</sup>	2.89 × 10 <sup>-3</sup>	7.63
1.30 × 10 <sup>-5</sup>	2.95 × 10 <sup>-4</sup>	4.36 × 10 <sup>-3</sup>	4.65 × 10 <sup>-3</sup>	7.53
1.30 × 10 <sup>-5</sup>	2.95 × 10 <sup>-4</sup>	1.02 × 10 <sup>-2</sup>	1.05 × 10 <sup>-2</sup>	7.37
1.30 × 10 <sup>-5</sup>	2.95 × 10 <sup>-4</sup>	1.31 × 10 <sup>-2</sup>	1.34 × 10 <sup>-2</sup>	7.32

[a] Calculated from the second-order rate constant of the free anion (potassium salt in presence of 18-crown-6) given in Table 4.



## 5. Appendix

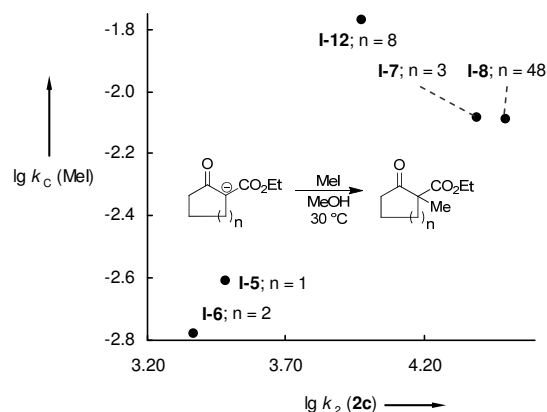


Figure 6: Reaction rate of the methylation of **I-5–12** in methanol (30 °C) vs. the reaction rates of **I-5–12** with the quinone methide **2c** in DMSO (20 °C).<sup>[3c]</sup>

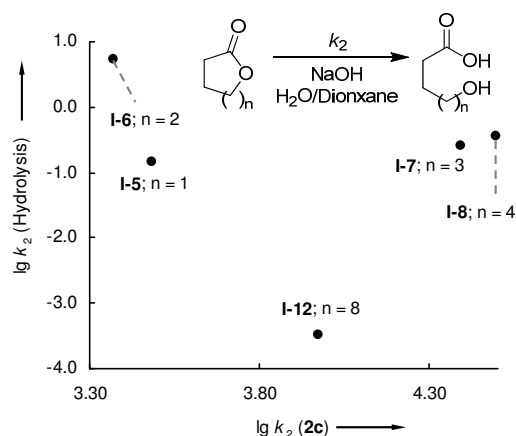


Figure 7: Reaction rate of the solvolysis of lactones vs. the reaction rates of the cyclic  $\beta$ -ketoester anions **I** with the quinone methide **2c**.<sup>[9]</sup>

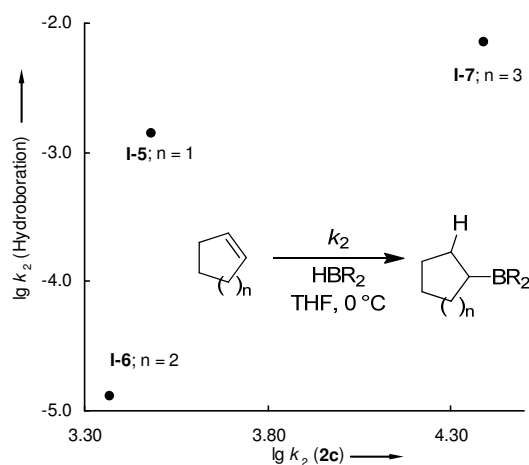


Figure 8: Reaction rate of the hydroboration of cycloalkenes vs. the reaction rates of the cyclic  $\beta$ -ketoester anions **I** with the quinone methide **2c**.<sup>[2a]</sup>  $\text{HBR}_2$  = Disiamylborane.

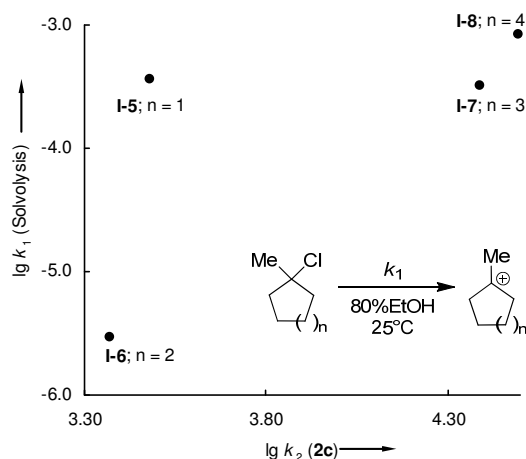


Figure 9: Reaction rate of the solvolysis of 1-chloro-1-methylcycloalkanes vs. the reaction rates of the cyclic  $\beta$ -ketoester anions **I** with the quinone methide **2c**.<sup>[1a]</sup>

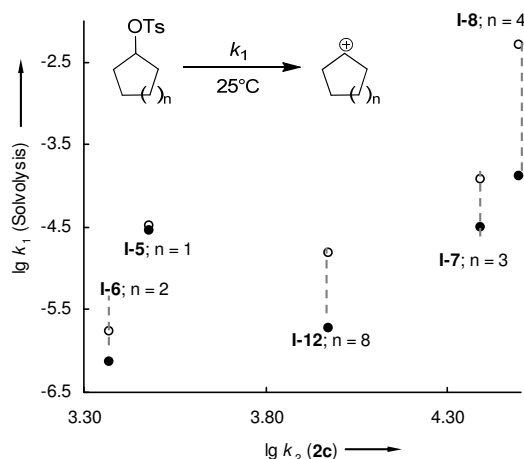


Figure 10: Reaction rate of the solvolysis of cycloalkyl tosylates vs. the reaction rates of the cyclic  $\beta$ -ketoester anions **I** with the quinone methide **2c**.<sup>[1d]</sup> Filled circles: solvolysis in EtOH/H<sub>2</sub>O. Empty circles: solvolysis in TFE.

## 6. References

- [1] Examples of solvolysis reactions: a) H. C. Brown, M. Borkowski, *J. Am. Chem. Soc.* **1952**, *74*, 1894-1902; b) R. C. Hahn, T. F. Corbin, H. Shechter, *J. Am. Chem. Soc.* **1968**, *90*, 3404-3415; c) A. P. Krapcho, R. G. Johanson, *J. Org. Chem.* **1971**, *36*, 146-157; d) H.-J. Schneider, G. Schmidt, F. Thomas, *J. Am. Chem. Soc.* **1983**, *105*, 3556-3563.
- [2] Examples for electrophilic additions: a) H. C. Brown, A. W. Moerikofer, *J. Am. Chem. Soc.* **1961**, *83*, 3417-3422; b) M. Roth, H. Mayr, *J. Org. Chem.* **1994**, *59*, 169-172.
- [3] Properties of cyclic  $\beta$ -ketoesters: a) S. J. Rhoads, R. D. Reynolds, R. Raulins, *J. Am. Chem. Soc.* **1952**, *74*, 2889-2892; b) S. J. Rhoads, J. C. Gilbert, A. W. Decora, T. R. Garland, *Tetrahedron*, **1963**, *19*, 1625-1644; c) S. J. Rhoads, A. W. Decora,

- Tetrahedron*, **1963**, 19, 1654-1659; d) S. J. Rhoads, R. W. Hasbrouck, *Tetrahedron*, **1966**, 22, 3557-3570; e) A. Chatterjee, D. Banerjee, S. Banerjee, *Tetrahedron Lett.* **1965**, 43, 3851-3860.
- [4] Reactivity of Carbanions: a) R. Loos, S. Kobayashi, H. Mayr, *J. Am. Chem. Soc.* **2003**, 125, 14126-14132; b) T. Bug, T. Lemek, H. Mayr, *J. Org. Chem.* **2004**, 69, 7565-7576; c) T. B. Phan, H. Mayr, *Eur. J. Org. Chem.* **2006**, 2530-2537; d) S. T. A. Berger, A. R. Ofial, H. Mayr, *J. Am. Chem. Soc.* **2007**, 129, 9753-9761; e) F. Seeliger, H. Mayr, *Org. Biomol. Chem.* **2008**, 6, 3052-3058; f) O. Kaumanns, R. Appel, T. Lemek, F. Seeliger, H. Mayr, *J. Org. Chem.* **2009**, 74, 75-81; g) F. Corral-Bautista, H. Mayr, *Eur. J. Org. Chem.* **2013**, 4255-4261.
- [5] H. Mayr, M. Patz, *Angew. Chem.* **1994**, 106, 990-1010; *Angew. Chem. Int. Ed. Engl.* **1994**, 33, 938-957.
- [6] Selected Publications: a) H. Mayr, T. Bug, M. F. Gotta, N. Hering, B. Irrgang, B. Janker, B. Kempf, R. Loos, A. R. Ofial, G. Remennikov, H. Schimmel, *J. Am. Chem. Soc.* **2001**, 123, 9500-9512; b) R. Lucius, R. Loos, H. Mayr, *Angew. Chem.* **2002**, 114, 97-102; *Angew. Chem. Int. Ed.* **2002**, 41, 91-95; c) H. Mayr, B. Kempf, A. R. Ofial, *Acc. Chem. Res.* **2003**, 36, 66-77; d) H. Mayr, A. R. Ofial, *Pure Appl. Chem.* **2005**, 77, 1807-1821; e) D. Richter, N. Hampel, T. Singer, A. R. Ofial, H. Mayr, *Eur. J. Org. Chem.* **2009**, 3203-3211; f) For a comprehensive listing of nucleophilicity parameters  $N$ ,  $s_N$  and electrophilicity parameters  $E$ , see <http://www.cup.uni-muenchen.de/oc/mayr/DBintro.html>.
- [7] R. Mayer, E. Alder, *Chem. Ber.* **1955**, 88, 1866-1868.
- [8] Compare the results described in Chapter 3 of this thesis.
- [9] R. Huisgen, H. Ott, *Tetrahedron* **1959**, 6, 253-267.
- [10] H. E. Gottlieb, V. Kotlyar, A. Nudelman, *J. Org. Chem.* **1997**, 62, 7512-7515.
- [11] B. Darses, I. N. Michaelides, F. Sladojevich, J. W. Ward, P. R. Rzepa, D. J. Dixon, *Org. Lett.* **2012**, 14, 1684-1687.
- [12] J. Marshall, V. H. Audia, *J. Org. Chem.* **1987**, 52, 1106-1113.

## Chapter 5

# From Carbanions to Organometallic Compounds: Quantification of Metal-Ion-Effects on Nucleophilic Reactivities

*Francisco Corral Bautista, Roland Appel, Lydia Klier, Paul Knochel and Herbert Mayr*

### 1. Introduction

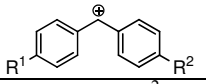
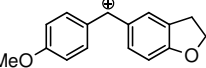
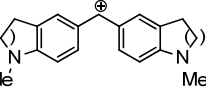
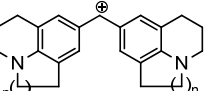
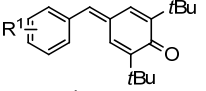
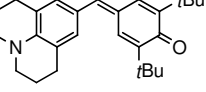
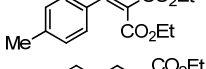
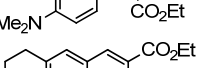
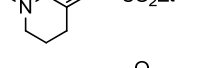
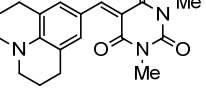
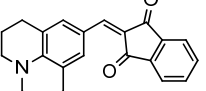
Organometallic compounds belong to the most important reagents in organic synthesis, which allow chemo- and stereoselective transformations.<sup>[1]</sup> Depending on the nature of the metal, the carbon-metal bond is more or less covalent and influences drastically various properties, such as reactivity, selectivity, and tolerance towards functional groups.<sup>[1a,2]</sup> Organolithium compounds, for example, are easily accessible and highly reactive towards a wide range of functional groups,<sup>[3]</sup> whereas organo-zinc or organo-tin compounds are much less reactive, but show higher selectivity and tolerance towards functional groups.<sup>[2c,4]</sup> Though these huge differences in reactivity are well-known to any organic chemist, a quantitative comparison between the reactivities of free carbanions and different organometallics has to our knowledge so far not been described.

The linear-free energy relationship (1),<sup>[5]</sup> where  $E$  is an electrophile-specific parameter, and  $N$  and  $s_N$  are nucleophile-specific parameters, which are derived from the rates of the reactions of  $\pi$ -,  $n$ -, and  $\sigma$ -nucleophiles with benzhydrylium ions **1**, quinone methides **2**, and structurally related Michael acceptors **3–5** (reference electrophiles, Table 1),<sup>[6]</sup> has previously been used to characterize the nucleophilic reactivities of a variety of organo-silicon<sup>[6a,6c,7]</sup> and organo-tin<sup>[6a,6c]</sup> compounds, as well as of carbanions.<sup>[8]</sup>

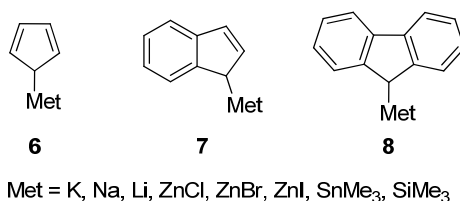
$$\lg k_2(20\text{ }^\circ\text{C}) = s_N(N + E) \quad (1)$$

In this study, we report about the kinetics of a series of organometallic derivatives (Li, Na, K, Zn, Sn, Si) of cyclopentadiene, indene and fluorene (Scheme 1) towards reference electrophiles (Table 1) of widely differing reactivity. In this way it will become possible to quantify the influence of increasing covalent character of the carbon-metal bond on its nucleophilic reactivity.

Table 1: Reference electrophiles applied in this study.

		$E^{[a]}$	$\lambda / \text{nm}$
<b>1a</b>	$R^1 = \text{Me}$ $R^2 = \text{Me}$	3.63	
<b>1b</b>	$R^1 = \text{OPh}$ $R^2 = \text{Me}$	2.16	475
<b>1c</b>	$R^1 = \text{OMe}$ $R^2 = \text{Me}$	1.48	488
<b>1d</b>	$R^1 = \text{OMe}$ $R^2 = \text{OPh}$	0.61	517
<b>1e</b>	$R^1 = \text{OMe}$ $R^2 = \text{OMe}$	0.00	513
<b>1f</b>		-0.81	520
<b>1g</b>	$R^1 = R^2 = \text{N(Ph)(CH}_2\text{CF}_3\text{)}$	-3.14	601
<b>1h</b>	$R^1 = R^2 = \text{N(Me)(CH}_2\text{CF}_3\text{)}$	-3.85	593
<b>1j</b>	$R^1 = R^2 = \text{N(Ph)}_2$	-4.72	672
<b>1k</b>	$R^1 = R^2 = N\text{-morpholino}$	-5.53	620
<b>1l</b>	$R^1 = R^2 = \text{N(Me)(Ph)}$	-5.89	622
<b>1m</b>	$R^1 = R^2 = \text{N(Me)}_2$	-7.02	613
<b>1n</b>	$R^1 = R^2 = N\text{-pyrrolidino}$	-7.69	620
			
<b>1o</b>	$n = 2$	-8.22	618
<b>1p</b>	$n = 1$	-8.76	627
			
<b>1q</b>	$n = 2$	-9.45	635
<b>1r</b>	$n = 1$	-10.04	630
			
<b>2a</b>	$R^1 = 3\text{-F}$	-15.03	354
<b>2b</b>	$R^1 = 4\text{-Me}$	-15.83	371
<b>2c</b>	$R^1 = 4\text{-OMe}$	-16.11	393
<b>2d</b>	$R^1 = 4\text{-N(Me)}_2$	-17.29	486
<b>2e</b>		-17.90	521
<b>3a</b>		-21.11	
<b>3b</b>		-23.10	400
<b>3c</b>		-23.80	407
<b>4</b>		-13.84	520
<b>5</b>		-14.68	520

[a] From ref. [6a-c,e,9]

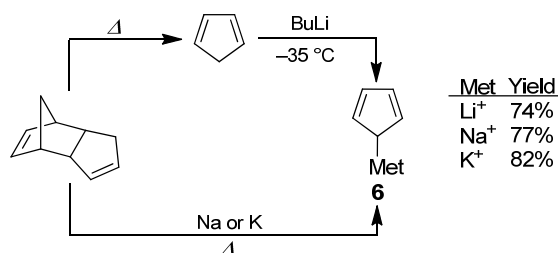


Scheme 1: Nucleophiles studied in this work.

## 2. Results and Discussion

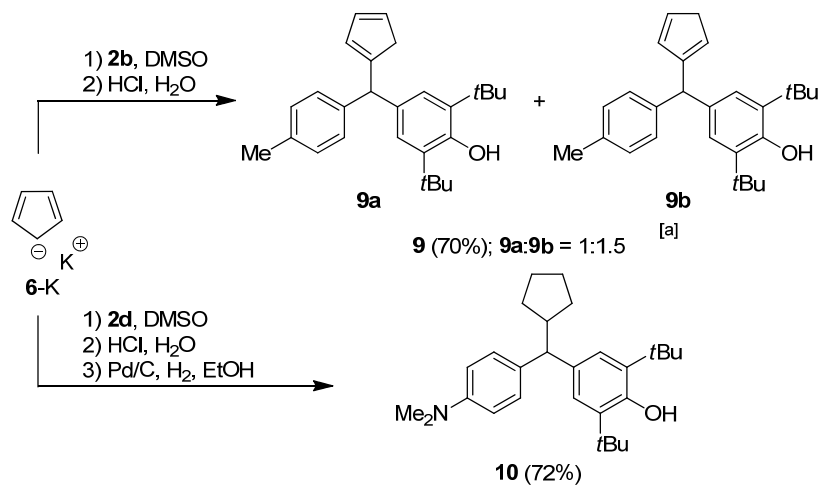
### 2.1. Alkali Metals

All investigations of the alkali derivatives of the nucleophiles **6–8** were performed in DMSO solution. The alkali salts of **6** were synthesized by deprotonation of freshly distilled cyclopentadiene with butyl lithium at  $-35\text{ }^{\circ}\text{C}$  or by direct heating of sodium or potassium in dicyclopentadiene and washing the precipitated alkali salts with dry pentane (Scheme 2).<sup>[10]</sup> As the alkali salts of **7** and **8** are highly reactive and have a low stability, they were not isolated in substance, but generated in solution by treating the corresponding hydrocarbons with  $\sim 1.05$  equivalents of alkali *tert*-butoxide (KO*t*Bu, NaO*t*Bu, LiO*t*Bu).

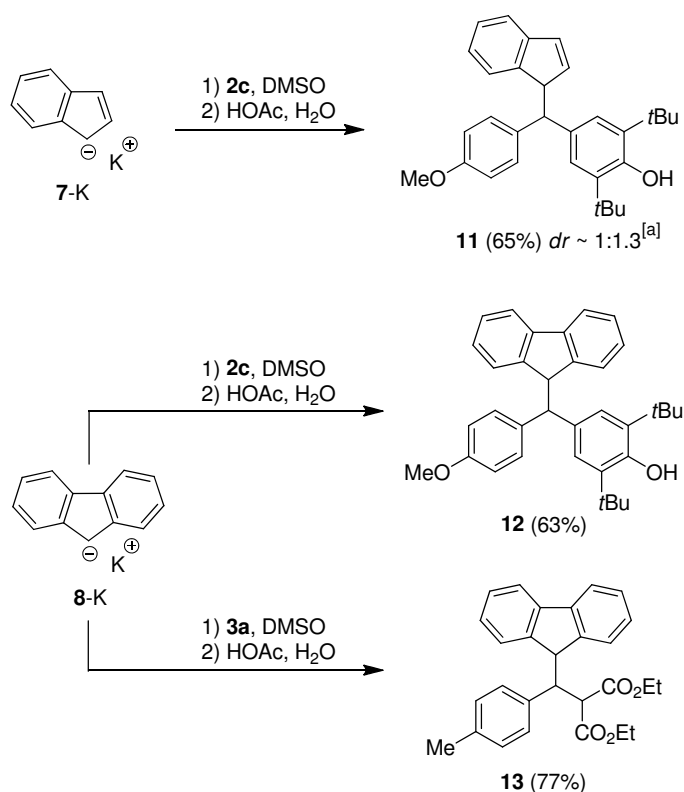
Scheme 2: Synthesis of the alkali derivatives of **6**.

To elucidate the course of the reactions, which have been studied kinetically, representative product analyses for the reactions of the potassium salts (**6–8**)-K with quinone methides (**2**) and diethyl benzylidenemalonates (**3**) were performed. For that purpose, potassium cyclopentadienide (**6**-K) was combined with a solution of the quinone methide **2b** in DMSO; after aqueous acidic work up, 70% of the addition products **9a** and **9b** were isolated as a mixture of two regioisomers. The initially formed cyclopentadiene derivative with the substituent at the  $\text{sp}^3$ -carbon of the cyclopentadiene ring was not detected but underwent rapid 1,5-sigmatropic hydrogen shifts to give **9a** and **9b**. In order to facilitate the product analysis, the addition product from **6**-K and **2d** was hydrogenated to yield 72% of **10** (Scheme 3). The alkali salts **7**-K and **8**-K were generated by adding KO*t*Bu to the corresponding CH acids in DMSO and a solution of the quinone methide **2c** or the diethyl benzylidene malonate **3a** was

added subsequently. After aqueous acidic work up, the products **11**, **12** and **13** were obtained (Scheme 4).



Scheme 3: Reaction of **6-K** with the quinone methides **2b** and **2d** in DMSO at ambient temperature. [a] Determined by <sup>1</sup>H NMR-spectroscopy after purification by chromatography.



Scheme 4: Reaction of **7-K** and **8-K** with the reference electrophiles **2c** and **3a** in DMSO at ambient temperature. [a] Determined by <sup>1</sup>H NMR-spectroscopy after purification by chromatography.

The kinetic studies of the reactions of the alkali derivatives **6–8** with the reference electrophiles **2–5** were performed in DMSO solution at 20 °C and monitored by UV-Vis spectroscopy at or close to the absorption maxima of the electrophiles. To simplify the

evaluation of the kinetic experiments, the nucleophiles were used in large excess ( $> 10$  equiv.). Thus, the concentrations of the nucleophiles remained almost constant throughout the reactions, and pseudo-first-order kinetics were observed in all runs. The first-order rate constants  $k_{\text{obs}}$  were obtained by least-squares fitting of the exponential function  $A_t = A_0 \exp(-k_{\text{obs}}t) + C$  to the time-dependent absorbances  $A_t$  of the electrophile.

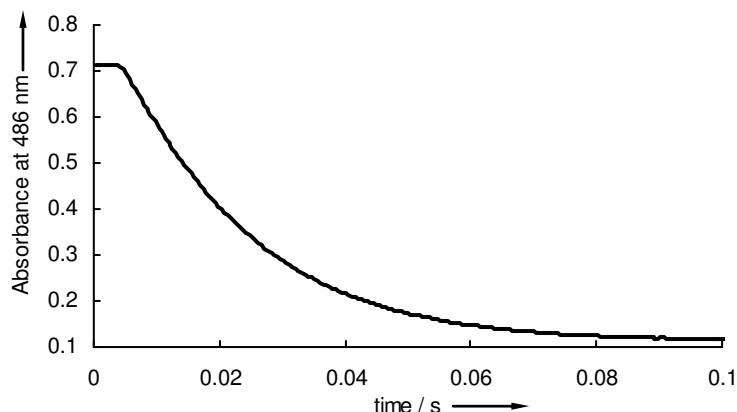


Figure 1: Plot of the absorbance (at 486 nm) vs. time for the reaction of **7-K** ( $9.78 \times 10^{-4}$  mol L $^{-1}$ ) with **2d** ( $2.03 \times 10^{-5}$  mol L $^{-1}$ ) in DMSO at 20 °C.

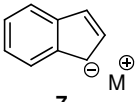
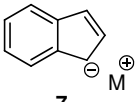
To investigate the influence of cation concentrations on the rates of the reactions, the pseudo-first-order rate constants for the reactions of **7-Li** with the quinone methide **2d** were determined while the Li $^{+}$ -concentration in solution was subsequently increased by addition of LiCl or LiBF $_4$  (Table 2, Figure 2). The  $k_{\text{obs}}$  values are also given as relative rate constants ( $k_{\text{rel}} = 1$ ) with respect to the rate constant of the free carbanion, which corresponds to the reactivity of **7-K** in the presence of 18-crown-6.

Figure 2 illustrates that in a  $10^{-3}$  mol L $^{-1}$  solution indenyl lithium (**7-Li**), obtained by treatment of **7-H** with LiOtBu, shows around 60% of the reactivity of the free carbanion. Addition of LiBF $_4$  causes a moderate increase of reactivity from 65 to 69 % at  $[\text{Li}^{+}] \approx 6 \times 10^{-3}$  mol L $^{-1}$ ; further addition of LiBF $_4$  reduces the first-order rate constant to 62% of the reactivity of the free carbanion, which remains almost constant at LiBF $_4$  concentrations between  $2 \times 10^{-2}$  and  $5 \times 10^{-2}$  mol L $^{-1}$ . The addition of LiCl to **7-Li** ( $10^{-3}$  mol L $^{-1}$ ) causes a decrease of reactivity to 30% of the reactivity of the free carbanion at  $[\text{Li}^{+}] \approx 2 \times 10^{-3}$  mol L $^{-1}$ ; at higher concentrations of LiCl, the reactivity increases again, and at  $[\text{Li}^{+}]$  between  $5 \times 10^{-2}$  and  $7 \times 10^{-2}$  mol L $^{-1}$ , the rate constants in both series approach each other at around 50–60% of the reactivity of the free carbanion. This behavior indicates the formation of different aggregates at different concentrations, which have not been investigated in detail. As the first-order rate constants  $k_{\text{obs}}$  of the reactions of **7-Li** with quinone methides correlate linearly with



[7-Li] at concentrations  $\leq 3 \times 10^{-3} \text{ mol L}^{-1}$ , as shown in the left part of Figure 3, one can assume that indenyl lithium (7-Li) does not form aggregates in this concentration range when the stoichiometric ratio carbanion/lithium is one.

Table 2:  $k_{\text{obs}}$  values for the reactions of 7-Li with the quinone methide **2d** with variable concentrations of LiCl or LiBF<sub>4</sub> in DMSO at 20 °C.  $k_{\text{rel}} = 1$  was derived from kinetics of 7-K in presence of 18-crown-6.

	M	Additive	[Li <sup>+</sup> ] <sub>total</sub> / mol L <sup>-1</sup>	$k_{\text{obs}} / \text{s}^{-1}$	100· $k_{\text{rel}}$
 <b>7</b> $9.52 \times 10^{-4} \text{ mol L}^{-1}$	K	18-crown-6	0	44.6 <sup>[a]</sup>	100
	Li	none	$1.00 \times 10^{-3}$ [b]	25.8	58
	Li	LiCl	$1.62 \times 10^{-3}$	14.0	31
	Li	LiCl	$1.99 \times 10^{-3}$	17.6	39
	Li	LiCl	$3.17 \times 10^{-3}$	19.4	43
	Li	LiCl	$5.97 \times 10^{-3}$	20.7	46
	Li	LiCl	$1.09 \times 10^{-2}$	23.3	52
	Li	LiCl	$2.00 \times 10^{-2}$	23.4	52
	Li	LiCl	$3.28 \times 10^{-2}$	23.3	52
	Li	LiCl	$6.92 \times 10^{-2}$	26.0	58
 <b>7</b> $9.42 \times 10^{-4} \text{ mol L}^{-1}$	K	18-crown-6	0	44.2 <sup>[a]</sup>	100
	Li	none	$9.89 \times 10^{-4}$ [b]	28.6	65
	Li	LiBF <sub>4</sub>	$1.53 \times 10^{-3}$	29.0	66
	Li	LiBF <sub>4</sub>	$2.08 \times 10^{-3}$	30.0	68
	Li	LiBF <sub>4</sub>	$3.60 \times 10^{-3}$	30.6	69
	Li	LiBF <sub>4</sub>	$6.43 \times 10^{-3}$	30.3	69
	Li	LiBF <sub>4</sub>	$1.12 \times 10^{-2}$	27.6	62
	Li	LiBF <sub>4</sub>	$2.14 \times 10^{-2}$	27.3	62
	Li	LiBF <sub>4</sub>	$3.51 \times 10^{-2}$	26.9	61
	Li	LiBF <sub>4</sub>	$5.55 \times 10^{-2}$	27.6	62

[a] Calculated from the second-order rate constant of the free carbanions (potassium salts + 18-crown-6) in Table 3. [b] Corresponds to the concentration of LiOtBu which was used for the deprotonation of 7-H.

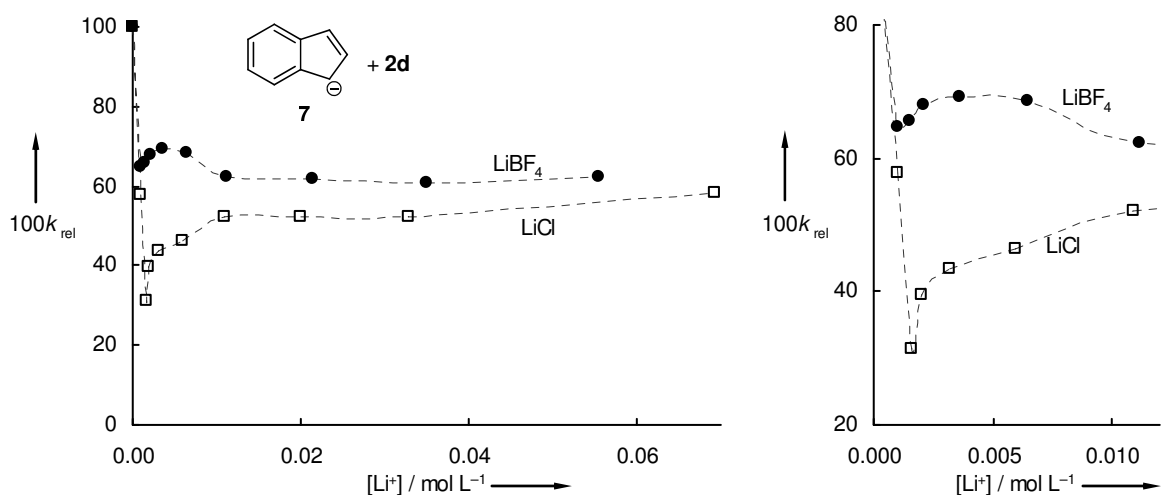
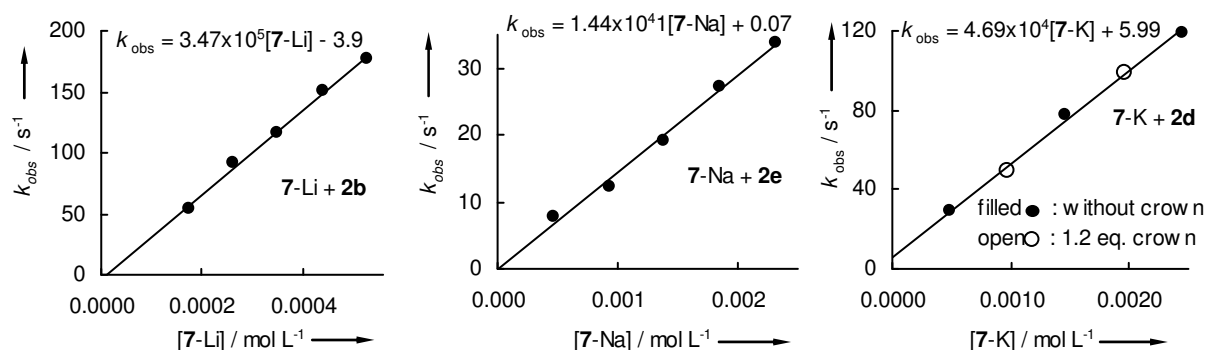

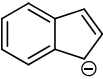
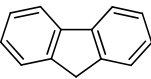


Figure 2: Left: Plot of the relative first-order rate constants ( $100k_{\text{rel}}$ ) of 7-Li ( $10^{-3} \text{ mol L}^{-1}$ ) versus the total concentration of lithium in the solution (DMSO, 20 °C). Right: Amplification of the diluted region (dashed square).

Figure 3: Plots of the first-order rate constants  $k_{\text{obs}}$  vs. the concentration of 7-Met.

Linear correlations of  $k_{\text{obs}}$  with the concentrations of the organoalkali compounds are obtained for all alkali derivatives of cyclopentadiene, indene and fluorene, as shown for representative examples in Figure 3 and for all studied systems in the Experimental Section. As the  $k_{\text{obs}}$  values for the reactions of 6-K, 7-K and 8-K with reference electrophiles, which are measured in the presence and in the absence of 18-crown-6, are on the same  $k_{\text{obs}}$  versus carbanion-concentration plots (compare right part of Figure 3 and Experimental Section), we conclude that the kinetics of the reactions of these potassium salts reflect the reactivities of the free carbanions.

Table 3: Second-order rate constants  $k_2$  of the reaction of the alkali metal derivatives 6–8 with reference electrophiles in DMSO at 20 °C.

Nucleophile	Electrophile	Li <sup>+</sup> $k_2 / \text{L mol}^{-1} \text{s}^{-1}$	Na <sup>+</sup> $k_2 / \text{L mol}^{-1} \text{s}^{-1}$	K <sup>+</sup> [a] $k_2 / \text{L mol}^{-1} \text{s}^{-1}$
 <b>6</b>	<b>4</b>	$4.86 \times 10^5$	$4.74 \times 10^5$	$5.07 \times 10^5$
	<b>5</b>	$1.64 \times 10^5$	$1.60 \times 10^5$	$1.69 \times 10^5$
	<b>2b</b>	$1.28 \times 10^4$	$1.32 \times 10^4$	$1.21 \times 10^4$
	<b>2c</b>	$6.23 \times 10^3$	$6.85 \times 10^3$	$6.39 \times 10^3$
	<b>2d</b>	$6.49 \times 10^2$	$6.52 \times 10^2$	$6.74 \times 10^2$
	<i>N</i> ( <i>s<sub>N</sub></i> )	20.59 (0.86)	20.64 (0.85)	20.58 (0.86)
 <b>7</b>	<b>2a</b>	$1.41 \times 10^6$	$1.90 \times 10^6$	$2.16 \times 10^6$
	<b>2b</b>	$3.47 \times 10^5$	$3.36 \times 10^5$	$5.70 \times 10^5$
	<b>2c</b>	$1.77 \times 10^5$	$2.37 \times 10^5$	$2.82 \times 10^5$
	<b>2d</b>	$2.85 \times 10^4$	$3.35 \times 10^4$	$4.69 \times 10^4$
	<b>2e</b>	$1.14 \times 10^4$	$1.44 \times 10^4$	$2.04 \times 10^4$
	<i>N</i> ( <i>s<sub>N</sub></i> )	23.44 (0.73)	23.54 (0.73)	23.93 (0.71)
 <b>8</b>	<b>2d</b>	$4.03 \times 10^5$	$7.00 \times 10^5$	$7.86 \times 10^5$
	<b>2e</b>	$2.67 \times 10^5$	$2.02 \times 10^5$	$5.83 \times 10^5$
	<b>3b</b>	$4.90 \times 10^1$	$7.44 \times 10^1$	$8.89 \times 10^1$
	<b>3c</b>	$4.11 \times 10^1$	$4.63 \times 10^1$	$7.34 \times 10^1$
	<i>N</i> ( <i>s<sub>N</sub></i> )	26.00 (0.65)	26.18 (0.65)	26.35 (0.66)

[a] Rate constants, *N* and *s<sub>N</sub>* parameters correspond to the free anions.

Table 3 shows that the alkali counter ions influence the reactivities of the carbanions in different ways. While the second-order rate constants ( $k_2$ ) for 6-Na and 6-Li are almost

identical to those the free anion **6-K**, the rate constants for **7-Na** are about 0.7–0.8 times and those for **7-Li** about 0.6 times of the rate constants of **7-K**. In the fluorenyl-series **8**, the sodium salt **8-Na** reacts about 0.6–0.8 and the lithium-salt **8-Li** around 0.5 times as fast as the free anion (**8-K**). The increase of the counter ion effect from the cyclopentadienyl- (**6**) to the indenyl- (**7**) and the fluorenyl-derived alkali salts (**8**) can be explained by increasing concentration of the negative charge on the nucleophilic center along this series.

Plots of  $\lg k_2$  for the reactions of the alkali derivatives **6–8** with the reference electrophiles against their electrophilicity parameters  $E$  are linear, as shown for the potassium-derivatives (**6–8**)-K in Figure 4. As depicted in the Experimental Section, all reactions of this type followed analogous linear correlations, indicating that equation (1) is applicable. From the slopes of these correlations, the nucleophile-specific parameters  $s_N$  were derived, and the negative intercepts on the abscissa ( $\lg k_2 = 0$ ) correspond to the nucleophilicity parameters  $N$  (Table 3).

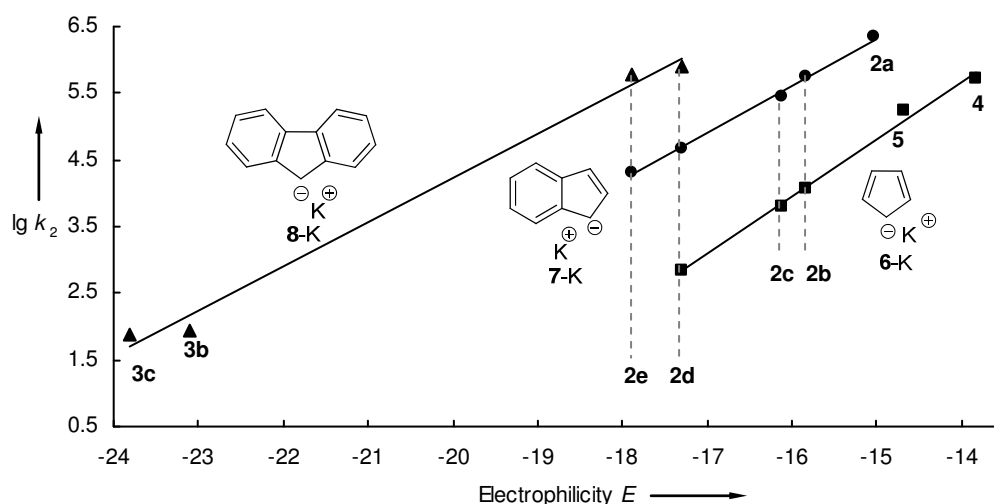
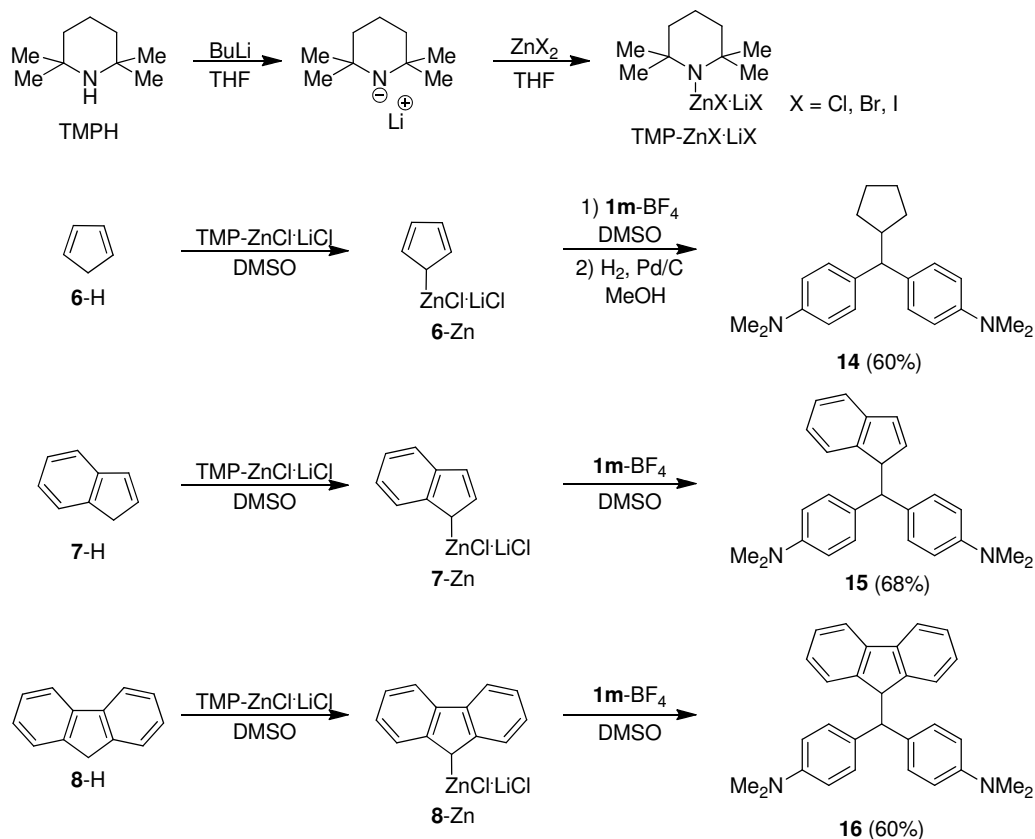


Figure 4: Correlation of the  $\lg k_2$  values for the reactions of the potassium salts (**6–8**)-K with reference electrophiles vs. their electrophilicity parameters  $E$ .

## 2.2. Organozinc Compounds

As described in detail in the Appendix, attempts to study the kinetics of LiX-free solutions of (**6–8**)-ZnX ( $X = \text{Cl}, \text{Br}$ ) failed. For that reason, also the product studies were performed with (**6–8**)-ZnCl·LiCl. Treatment of solutions of the CH acids (**6–8**)-H in DMSO with a solution of TMP·ZnCl·LiCl (~1.1 equiv.) and subsequent combination with the benzhydrylium tetrafluoroborate **1m**-BF<sub>4</sub> gave the crude products **15** and **16** after aqueous work-up, which were recrystallized from dichloromethane/ethanol (Scheme 5). As the combination of **6**-Zn with **1m**-BF<sub>4</sub> led to a mixture of two isomers (compare reaction of the potassium salt **6-K**

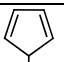
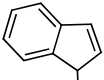
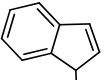
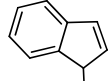
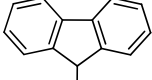
with quinone methides, Scheme 3), the addition product was hydrogenated to give **14** in 60% yield (Scheme 5).



Scheme 5: Reactions of the organozinc-compounds (**6–8**)-ZnCl with the benzhydrylium tetrafluoroborate **1m**-BF<sub>4</sub> in DMSO at ambient temperature.

For the kinetic studies, the organozinc compounds were not isolated in substance, but generated by treating the CH acids with 1.05–1.10 equiv. of TMP-ZnX·LiX (X = Cl, Br, I) in DMSO prior to the kinetic measurements. The generation of the zinc species can be followed by UV-Vis-spectroscopy as the absorptions of (**6–8**)-ZnCl differ from those of their hydrocarbon precursors. As the absorbances of (**6–8**)-ZnCl generated from (**6–8**)-H and 1.05–1.10 equiv. of TMP-ZnCl·LiCl remain constant when additional 2–4 equiv. of TMP-base were added, one can conclude that 1.05–1.10 equiv. of TMP-base are sufficient for the complete deprotonation of the CH acids (plots depicted in the Experimental Section). The kinetic studies were performed as described above for the alkali salts, using pseudo-first-order conditions with an excess of the organozinc compounds and monitoring the UV-Vis absorbances of the electrophiles. The second-order rate constants were derived from linear plots of the pseudo-first-order rate constants versus the nucleophile concentrations (Table 4).

Table 4: Second-order rate constants  $k_2$  for the reactions of the zinc derivatives (6–8)-ZnX with reference electrophiles in DMSO at 20 °C.

Nucleophile	$N$ ( $s_N$ )	Electrophile	$k_2 /$ $\text{L mol}^{-1} \text{s}^{-1}$
 6-ZnCl	16.46 (0.48)	<b>1m</b>	$2.89 \times 10^4$
		<b>1n</b>	$1.50 \times 10^4$
		<b>1p</b>	$5.26 \times 10^3$
		<b>1q</b>	$1.92 \times 10^3$
 7-ZnCl	18.09 (0.46)	<b>1m</b>	$1.38 \times 10^5$
		<b>1n</b>	$6.85 \times 10^4$
		<b>1p</b>	$1.90 \times 10^4$
		<b>1q</b>	$1.08 \times 10^4$
		<b>1r</b>	$5.46 \times 10^3$
 7-ZnBr	15.52 (0.51)	<b>1m</b>	$2.03 \times 10^4$
		<b>1n</b>	$1.19 \times 10^4$
		<b>1o</b>	$5.24 \times 10^3$
		<b>1p</b>	$2.75 \times 10^3$
 7-ZnI	14.36 (0.49)	<b>1m</b>	$3.69 \times 10^3$
		<b>1n</b>	$2.39 \times 10^3$
		<b>1o</b>	$1.20 \times 10^3$
		<b>1p</b>	$5.12 \times 10^2$
 8-ZnCl	14.05 (0.66)	<b>1m</b>	$3.38 \times 10^4$
		<b>1n</b>	$1.78 \times 10^4$
		<b>1p</b>	$3.26 \times 10^3$
		<b>1q</b>	$9.00 \times 10^2$

To exclude that reactions of the chloride anions with the benzhydrylium ions affect the kinetic measurements, the benzhydrylium salt **1n**-BF<sub>4</sub> ( $1.3\text{--}1.4 \times 10^{-5} \text{ mol L}^{-1}$ ) was combined with excess LiCl ( $3.8 \times 10^{-3} \text{ mol L}^{-1}$ ) or Bu<sub>4</sub>NCl ( $2.1 \times 10^{-3} \text{ mol L}^{-1}$ ) in DMSO while the absorbance of the electrophile was followed. The absorbance of the benzhydrylium ion decreased to 40–50% within 30 min, probably because of a slow reaction of **1n**-BF<sub>4</sub> with DMSO. As the reactions of **1n**-BF<sub>4</sub> with the organozinc reagents (6–8)-ZnX proceed within less than 1–5 s under the conditions of the kinetic experiments, one can exclude that parallel reactions of **1n** with either DMSO or Cl<sup>−</sup> affect the rate constants listed in Table 4.

As secondary amines such as piperidine ( $N = 17.19$ ) and morpholine ( $N = 16.96$ ) have similar nucleophilicity parameters as the zinc-nucleophiles,<sup>[11]</sup> we have also examined whether tetramethylpiperidine (TMPH) which is formed during deprotonation of the hydrocarbons affects the kinetic experiments. Therefore the benzhydrylium salt **1n**-BF<sub>4</sub> ( $1.43 \times 10^{-5} \text{ mol L}^{-1}$ ) was combined with TMPH ( $0.9\text{--}3.8 \times 10^{-3} \text{ mol L}^{-1}$ ) in DMSO and the kinetics of the reactions were followed by monitoring the absorbance of **1n** by UV-Vis spectroscopy. Since only slow decreases, which remain in a plateau at around 60–70% of the initial absorbance of

the benzhydrylium ion are observable, a quantitative reaction of TMPH and **1n** could be excluded. Though the reason of the decrease of the absorbance is not clear yet, the consumption of the electrophile in this reaction is that small and slow compared to the reactions in Table 4, that a participation of TMPH in the kinetic experiments of Table 4 can be excluded. In order to examine whether TMPH interacts with the organozinc compounds, kinetic experiments were performed in which the TMPH-concentration was varied while keeping the concentration of the electrophile (**1n**) and the nucleophile (**7-Zn**) constant. As shown in Figure 5, the influence of TMPH on the reaction rates is marginal; in view of the fact that the TMPH concentrations in these control experiments were 10–100 times higher than in the experiments described in Table 4, one can conclude that the presence of TMPH in our kinetic experiments can be neglected.

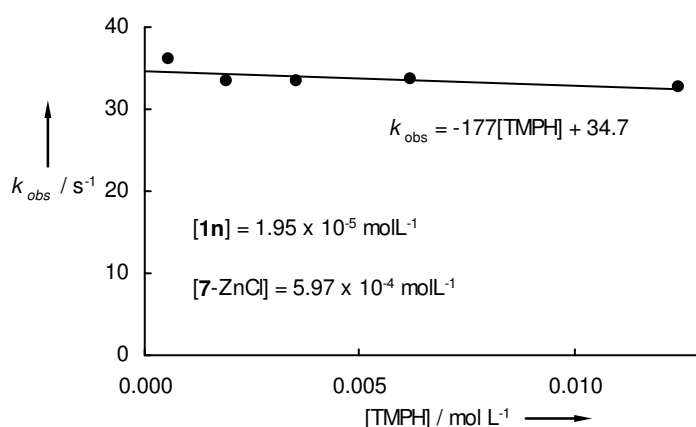


Figure 5:  $k_{obs}$  values for the reaction of **7-ZnCl** with **1n** in DMSO in the presence of variable concentrations of TMPH.

The nucleophilicity parameters  $N$  and  $s_N$  were derived from linear plots of  $\lg k_2$  versus the  $E$ -parameters of the corresponding electrophiles as shown for **7-Zn** and **8-Zn** in Figure 6. Analogous correlations for the other systems listed in Table 4 are shown in the Experimental Section (Tables 66, 72, 82, 87).

The nucleophilic reactivities of the organozinc reagents (**6–8**)-ZnX in Table 4 show that the indenyl derivative **7-ZnCl** is about one order of magnitude more reactive than the cyclopentadienyl **6-ZnCl** and the fluorenyl analogue **8-ZnCl**. Because of the significantly different values of the sensitivity  $s_N$ , the relative reactivities will change when looking at reactions with weaker or stronger electrophiles. Table 4 also shows the influence of the halide on the reactivity of the different zinc-derivatives. Thus **7-ZnCl** is 6 to 7 times more reactive than **7-ZnBr** and 20–40 times more reactive than **7-ZnI**. The different  $s_N$  parameters again indicate that these reactivity ratios depend on the electrophile.

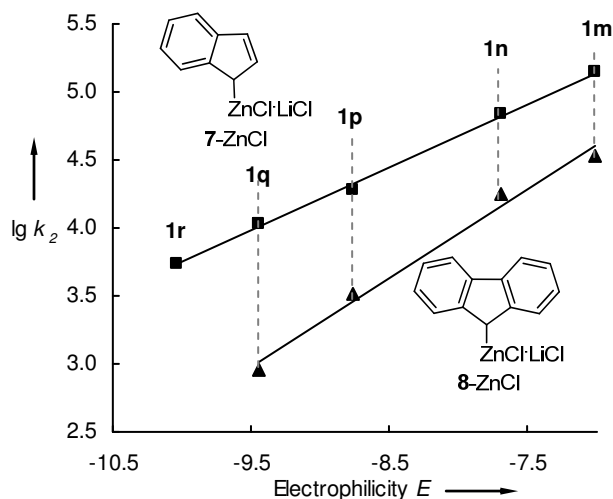
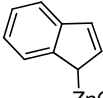
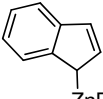
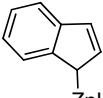
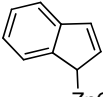
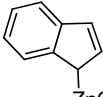
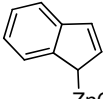


Figure 6: Correlation of  $\lg k_2$  for the reactions of **7-Zn** and **8-Zn** with reference electrophiles vs. their electrophilicity parameters  $E$ .

As lithium or magnesium salts are known to improve the yields of palladium- and nickel-catalyzed cross-couplings of organozinc reagents, and generally enhance the reactivity of organometallic reagents,<sup>[12]</sup> we also studied the influence of different additives (LiCl, LiBr, Bu<sub>4</sub>NCl, MgCl<sub>2</sub>) on the reactivity of the zinc-nucleophiles **7-ZnX**·LiX (X = Cl, Br, I). For that purpose, rate constants for the reactions of the nucleophiles **7-ZnX** with the benzhydrylium ion **1n** were determined at variable concentrations of additives while the concentration of the organozinc compound and of the electrophile remained constant (Table 5).

Table 5 shows that all additives increase the reactivities of the investigated organozinc reagents, however to different extent. While 7 equiv. of LiCl increase the reactivity of **7-ZnCl** by a factor of 4 (entries 7 versus 1), the reactivity of **7-ZnBr** is increased by a factor of 16 by 7 equiv. of LiCl (entries 14 versus 9) and the reactivity of **7-ZnI**·LiI increases even 82 times when 8 equiv. of LiCl are added (entries 24 versus 17). As **7-ZnI** is approximately 30 times less reactive than **7-ZnCl**, the larger effect of LiCl additives on the reactivity of **7-ZnI** can be explained by halide exchange.

Table 5:  $k_{\text{obs}}$  values and  $k_{\text{rel}}$  for the reactions of **7**-ZnCl·LiCl, **7**-ZnBr·LiBr and **7**-ZnI·LiI with the benzhydrylium ion **1n** with successive addition of additives in DMSO at 20 °C.

	Entry	Additive	[Additive]/mol L <sup>-1</sup>	$k_{\text{obs}}/\text{s}^{-1}$	$k_{\text{rel}}$
 <b>7</b> -ZnCl $c = 8.63 \times 10^{-4} \text{ mol L}^{-1}$	1	none	0	62.9	1
	2	LiCl	$1.66 \times 10^{-4}$	72.1	1.15
	3	LiCl	$3.32 \times 10^{-4}$	79.3	1.26
	4	LiCl	$6.64 \times 10^{-4}$	87.2	1.39
	5	LiCl	$1.66 \times 10^{-3}$	117	1.86
	6	LiCl	$3.32 \times 10^{-3}$	156	2.48
	7	LiCl	$6.64 \times 10^{-3}$	243	3.86
	8	LiCl	$1.66 \times 10^{-2}$	415	6.60
 <b>7</b> -ZnBr $c = 4.73 \times 10^{-4} \text{ mol L}^{-1}$	9	none	0	5.53	1
	10	LiCl	$1.66 \times 10^{-4}$	6.62	1.20
	11	LiCl	$3.32 \times 10^{-4}$	8.73	1.58
	12	LiCl	$6.64 \times 10^{-4}$	14.3	2.59
	13	LiCl	$1.66 \times 10^{-3}$	35.4	6.40
	14	LiCl	$3.32 \times 10^{-3}$	87.1	15.8
	15	LiCl	$4.98 \times 10^{-3}$	135	24.4
	16	LiCl	$6.64 \times 10^{-3}$	196	35.4
 <b>7</b> -ZnI $c = 8.33 \times 10^{-4} \text{ mol L}^{-1}$	17	none	0	2.13	1
	18	LiCl	$3.32 \times 10^{-4}$	2.38	1.12
	19	LiCl	$6.64 \times 10^{-4}$	3.14	1.47
	20	LiCl	$1.66 \times 10^{-3}$	16.5	7.75
	21	LiCl	$2.49 \times 10^{-3}$	50.5	23.7
	22	LiCl	$3.32 \times 10^{-3}$	78.1	36.6
	23	LiCl	$4.98 \times 10^{-3}$	110	51.6
	24	LiCl	$6.64 \times 10^{-3}$	176	82.6
 <b>7</b> -ZnCl $c = 4.52 \times 10^{-4} \text{ mol L}^{-1}$	25	none	0	30.8	1
	26	LiBr	$1.77 \times 10^{-4}$	29.3	0.95
	27	LiBr	$3.55 \times 10^{-4}$	28.4	0.92
	28	LiBr	$7.09 \times 10^{-4}$	30.7	1.00
	29	LiBr	$1.77 \times 10^{-3}$	36.4	1.18
	30	LiBr	$4.26 \times 10^{-3}$	54.8	1.78
	31	LiBr	$8.87 \times 10^{-3}$	71.8	2.33
	32	LiBr	$1.77 \times 10^{-2}$	82.3	2.67
 <b>7</b> -ZnCl $c = 3.89 \times 10^{-4} \text{ mol L}^{-1}$	33	none	0	26.5	1
	34	Bu <sub>4</sub> NCl	$1.80 \times 10^{-4}$	31.3	1.18
	35	Bu <sub>4</sub> NCl	$3.60 \times 10^{-4}$	35.3	1.33
	36	Bu <sub>4</sub> NCl	$7.20 \times 10^{-4}$	42.8	1.62
	37	Bu <sub>4</sub> NCl	$1.26 \times 10^{-3}$	51.4	1.94
	38	Bu <sub>4</sub> NCl	$2.16 \times 10^{-3}$	58.9	2.22
	39	Bu <sub>4</sub> NCl	$4.32 \times 10^{-3}$	77.9	2.94
	40	Bu <sub>4</sub> NCl	$9.00 \times 10^{-3}$	94.8	3.58
 <b>7</b> -ZnCl $c = 3.53 \times 10^{-4} \text{ mol L}^{-1}$	41	Bu <sub>4</sub> NCl	$1.44 \times 10^{-2}$	115	4.34
	42	none	0	23.8	1
	43	MgCl <sub>2</sub>	$2.00 \times 10^{-4}$	34.1	1.43
	44	MgCl <sub>2</sub>	$3.99 \times 10^{-4}$	43.7	1.84
	45	MgCl <sub>2</sub>	$7.98 \times 10^{-4}$	60.0	2.52
	46	MgCl <sub>2</sub>	$1.40 \times 10^{-3}$	78.8	3.31
	47	MgCl <sub>2</sub>	$2.39 \times 10^{-3}$	90.6	3.81
	48	MgCl <sub>2</sub>	$4.79 \times 10^{-3}$	100	4.20
	49	MgCl <sub>2</sub>	$9.98 \times 10^{-3}$	104	4.37
	50	MgCl <sub>2</sub>	$1.60 \times 10^{-2}$	114	4.79

According to the literature, alkylzinc halides form ate-complexes of the type  $[\text{RZnX}_2]^-$  when lithium-salts are added.<sup>[12c,13]</sup> Fleckenstein and Koszinowski reported that BuZnI does not



undergo significant ionic disproportionation with formation of zincates in pure THF, but zincates  $[\text{RZnX}_2]^-$  are observed when LiCl is added and their concentration increase with the concentration of the added LiCl. Furthermore, the ESI mass spectrometry experiments of Fleckenstein and Koszinowski show for the system  $\text{BuZnI}/(\text{LiCl})_2$  signals of the zincates  $\text{BuZnI}_2^- : \text{BuZnICl}^- : \text{BuZnCl}_2^-$  with a intensity ratio of 50 : 5 : 1, indicating that at low excess of  $\text{Cl}^-$  over  $\text{I}^-$ , iodide rich complexes still predominate.<sup>[13]</sup> In line with this observation, comparison of entries 20 and 5 (Table 5) show that the  $7\text{-ZnCl}\cdot(\text{LiCl})_3$  system is approximately 7 times more reactive than the  $7\text{-ZnI}\cdot(\text{LiI})(\text{LiCl})_2$  system. However, further addition of LiCl results in an approximation of the reactivities of both systems (Figure 7).

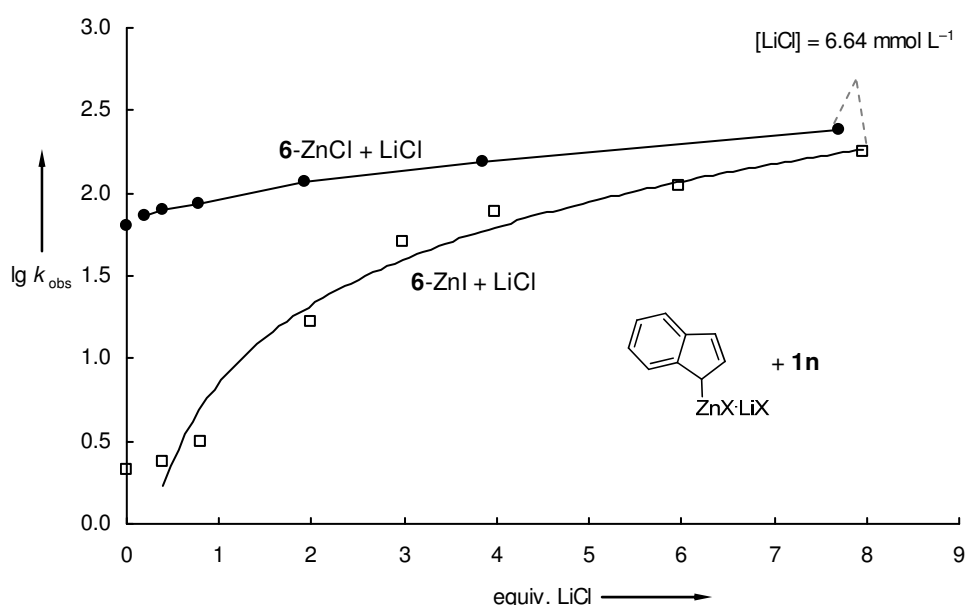


Figure 7: Plots of  $\lg k_{\text{obs}}$  of the reactions of different zinc-derivatives of **7** with the electrophile **1n** versus the concentration of added lithium chloride (DMSO, 20 °C).

Figure 8 shows how the reactivity of  $7\text{-ZnCl}$  is affected by addition of LiCl, LiBr,  $\text{Bu}_4\text{NCl}$  or  $\text{MgCl}_2$ . One can see, that 20 equiv. of LiBr accelerate by a factor of 2, the same amount of  $\text{Bu}_4\text{NCl}$  by a factor of 3,  $\text{MgCl}_2$  by factor of 4 and LiCl by factor of 7. The relative accelerations by these additives vary when other concentrations are considered, and it is most remarkable that  $\text{MgCl}_2$  is the best activator when less than 5 equiv. are employed. Small quantities of LiBr even reduce the reactivity due to the replacement of the chlorozincate  $[7\text{-ZnCl}_2]^-$  by the less reactive complexes  $[7\text{-ZnClBr}]^-$  or  $[7\text{-ZnBr}_2]^-$ .

In summary, the present experiments show that additives enhance the nucleophilic reactivity of organozinc reagents. However, the magnitude of the acceleration of the reaction rates was different depending on the organozinc reagent and on the nature of the additive.

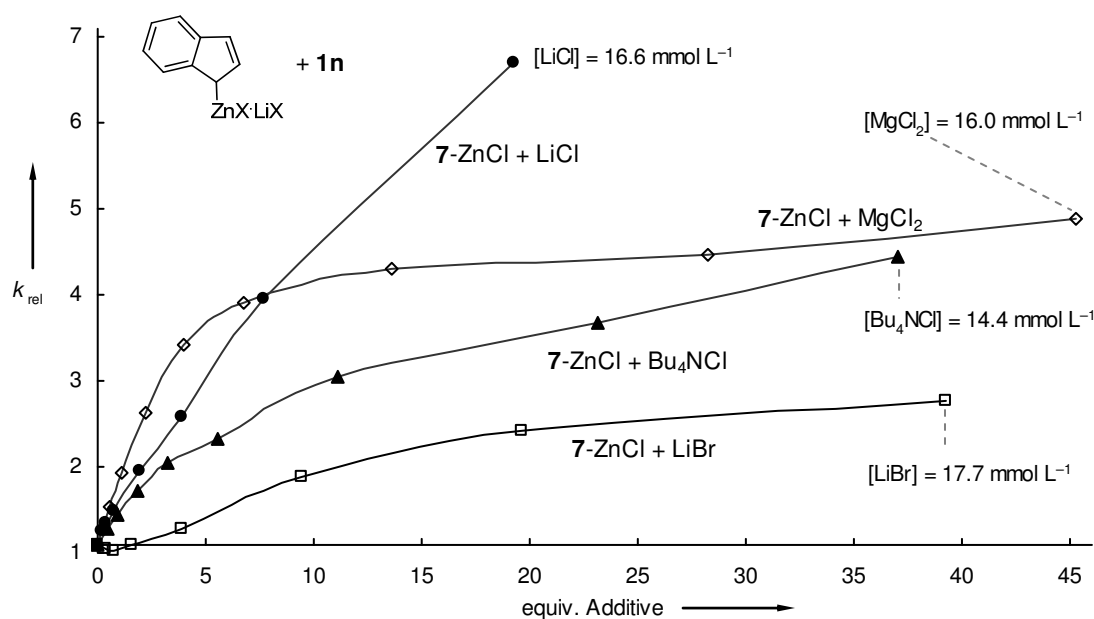
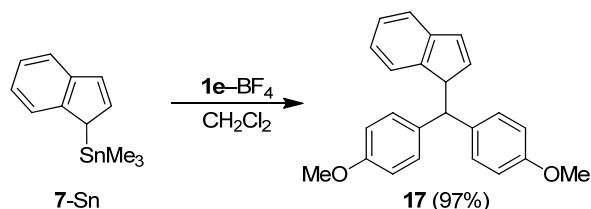


Figure 8: Plots of  $k_{rel}$  of the reactions of 7-Zn with the electrophile **1n** versus the concentration of different additives (DMSO, 20 °C).

### 2.3. Organotin and Organosilicon Compounds

(1*H*-Inden-1-yl)trimethylstannane (**7-Sn**) was synthesized in analogy to the reported procedure for the corresponding tributylstannyl compound<sup>[14]</sup> by deprotonation of indene with butyl lithium and subsequent addition of trimethyltin chloride. After distillation, **7-Sn** was isolated in 52% yield. (1*H*-Inden-1-yl)trimethylsilane (**7-Si**) was synthesized analogously by adding trimethylsilyl chloride to a solution of lithium indenide (**7-Li**) in THF. The crude product was distilled to yield 79% of **7-Si**.<sup>[15]</sup>

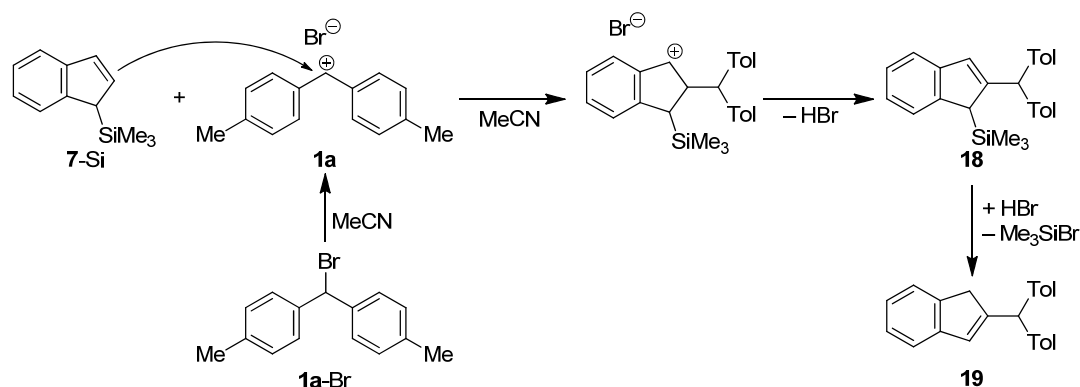
Combination of indenyl-tin (**7-Sn**) with **1e**-BF<sub>4</sub> in dichloromethane at ambient temperature yielded 97% of **17** after filtration over Al<sub>2</sub>O<sub>3</sub> and chromatographic purification (Scheme 6).



Scheme 6: Reaction of **7-Sn** with the benzhydrylium salt **1e**-BF<sub>4</sub> in dichloromethane at ambient temperature.

As the reaction of **7-Si** with the pregenerated benzhydrylium salts used for the kinetic investigations (see below) led to complex product mixtures, **7-Si** was combined with the covalent benzhydryl bromide **1a**-Br in acetonitrile. GC/MS monitoring of the reaction

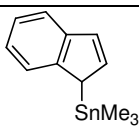
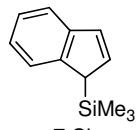
progress showed that the formation of product **18** was completed after 4 to 6 hours. The hydrodesilylation which leads to product **19** is much slower. Though traces of **19** were already observed after two hours, the subsequent transformation of **18** into **19** was not even complete after 5 days. Pure **18** was obtained in 46% yield, when  $\text{NaHCO}_3$  was added to the reaction mixture after 4 hours, before the solvent was evaporated and the residue was purified by column chromatography. Stirring the mixture of **7-Si** and **1a-Br** in acetonitrile for 5 days, evaporation of the solvent, and column chromatography (silica/pentane/ $\text{CH}_2\text{Cl}_2$ ) of the residue yielded 49% of **19**.



Scheme 7: Reaction of **7-Si** with the benzhydrylium bromide **1a-Br** in acetonitrile at ambient temperature.

The kinetic studies of the reactions of **7-Sn** and **7-Si** with the benzhydrylium ions **1** were performed in dichloromethane at 20 °C applying the same method as described above (UV-Vis-techniques and pseudo-first-order conditions) to give the second order rate constants listed in Table 6. The nucleophilicity parameters  $N$  and  $s_N$  were derived in the usual way from linear plots of  $\lg k_2$  versus the  $E$ -parameters of the corresponding electrophiles. The high quality of these correlations is demonstrated in section 2.4.

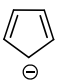
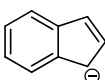
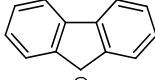
Table 6: Second-order rate constants  $k_2$  of the reaction of **7-Sn** and **7-Si** with reference electrophiles in  $\text{CH}_2\text{Cl}_2$  at 20 °C.

Nucleophile	$N$ ( $s_N$ )	Electro- phile	$k_2 /$ $\text{L mol}^{-1} \text{s}^{-1}$
 <b>7-Sn</b>	6.68 (0.81)	<b>1g</b>	$7.36 \times 10^2$
		<b>1h</b>	$1.92 \times 10^2$
		<b>1j</b>	$3.74 \times 10^1$
		<b>1k</b>	7.70
		<b>1l</b>	4.79
 <b>7-Si</b>	-0.10 (1.05)	<b>1b</b>	$1.15 \times 10^2$
		<b>1c</b>	$3.77 \times 10^1$
		<b>1d</b>	3.38
		<b>1e</b>	$7.69 \times 10^{-1}$
		<b>1f</b>	$1.04 \times 10^{-1}$

## 2.4. Structure-Reactivity Relationships and Correlation Analysis

Table 7 summarizes that benzo-annulation of the cyclopentadienyl anion increases the nucleophilic reactivity of the carbanions. While the mono-benzoannulated system **7** is two orders of magnitude more reactive than the cyclopentadienyl anion **6**, the bis-benzoannulated fluorenyl anion **8** is even three orders of magnitude more reactive than **6**. Bordwell reported an analogous increase of Brønsted basicity in the series **6**  $\rightarrow$  **7**  $\rightarrow$  **8** (Table 7) and explained this trend by decreasing aromaticity along this series.<sup>[16]</sup> This interpretation was supported by Schleyer's NICS parameters<sup>[17]</sup> for the five-membered rings (Table 7),<sup>[18]</sup> which also indicate that benzoannulation of the cyclopentadienyl anion **6** is associated with a decrease of aromaticity. The Brønsted plot in Figure 10 with a slope of  $\alpha = 0.63$  shows that roughly  $\frac{2}{3}$  of the increase of basicity in the series **6**  $\rightarrow$  **7**  $\rightarrow$  **8** is reflected by the nucleophilic reactivities of these carbanions toward the quinone methide **2d**, which serves as a reference electrophile.

Table 7: Nucleophilic reactivities, Brønsted basicities, and NICS values of the Carbanions **6–8**.

			
	<b>6</b>	<b>7</b>	<b>8</b>
$\lg k_2$ vs. <b>2d</b>	2.83	4.67	5.90
$\text{p}K_{\text{a}}$ (DMSO) <sup>[19]</sup>	18.0	20.1	22.6
NICS <sup>[18]</sup>	-21.5	-19.9	-16.3

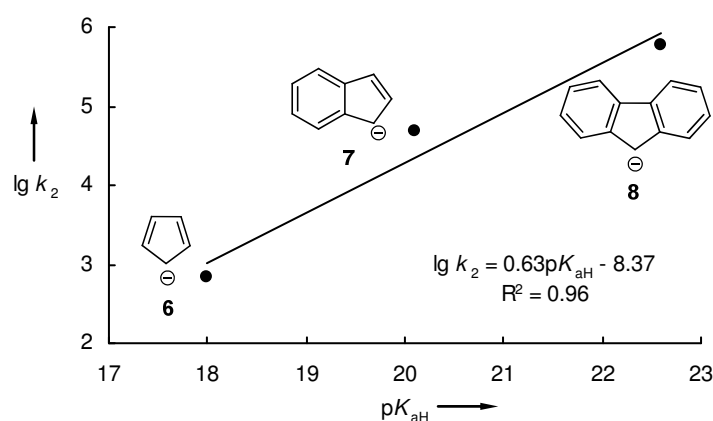


Figure 10:  $\lg k_2$  for the reaction of the potassium derivatives (free carbanions) of **6–8** with the quinone methide **2d** in DMSO at 20 °C versus the  $\text{p}K_{\text{aH}}$  values (in DMSO) of the conjugated acids.<sup>[19]</sup>

As illustrated in Figure 11, a different reactivity order is found for the organozinc compounds (**6–8**)-ZnCl. Using **1p** as the reference electrophile, the second-order rate constants listed in Table 4 yield the relative reactivities **6**-ZnCl : **7**-ZnCl : **8**-ZnCl = 1.0 : 3.6 : 0.62. Though this ratio changes when the reference electrophile is varied, in all investigated reactions the

indenyl compound **7**-ZnCl is 3–5 times more reactive than the cyclopentadienyl derivative **6**-ZnCl, while the fluorenyl compound **8**-ZnCl has a similar, even slightly lower reactivity than the corresponding cyclopentadienyl derivative **6**-ZnCl. While the reactivity increase from **6**-ZnCl to **7**-ZnCl (though attenuated compared to the free carbanions **6** and **7**), which can again be explained by the higher localization of the negative charge in the indenyl compound **7**-ZnCl, the lower reactivity of **8**-ZnCl compared with **7**-ZnCl can be assigned to the more covalent character of the C–Zn bonds. As shown in Scheme 8, both cyclopentadienyl- (**6**-ZnCl) and indenyl zinc chloride (**7**-ZnCl) can react via a  $S_E2'$  mechanism, where breaking of the C–Zn bond can be delayed with respect to the formation of the new C–C bond. In case the fluorenyl compound, the electrophile has to attack at the Zn-substituted carbon center which is obviously somewhat slower despite the higher charge density at this position.

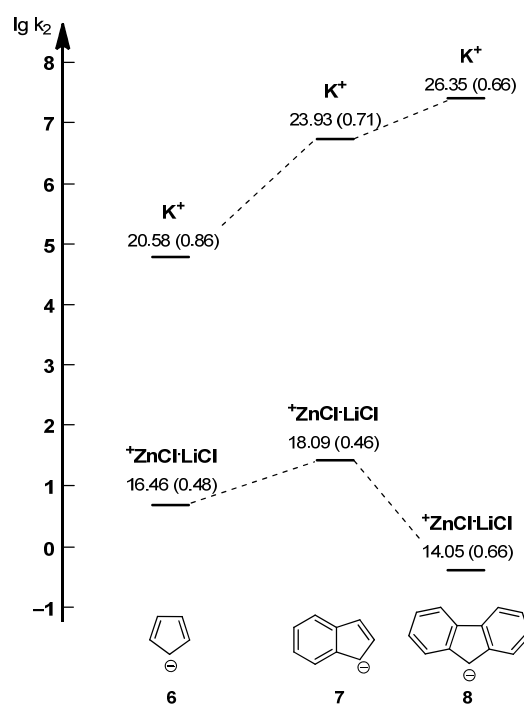
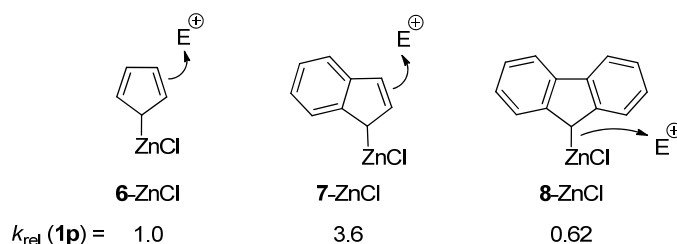


Figure 11: Second-order rate constants for the reactions of the carbanions **6–8** and the organozinc compounds (**6–8**)-ZnCl with the quinone methide **2a** ( $E = -15.03$ ) calculated by eq. (1) using the  $N(s_N)$  parameters in Tables 3 and 4.



Scheme 8:  $S_E2'$  and  $S_E2$ -reactions of organozinc chlorides with electrophiles.

Since cyclopentadienylsilyl and -stannyl compounds exist as mixtures of constitutional isomers,<sup>[20]</sup> as described for compounds **9a** and **9b** in Scheme 4, and fluorenyl-stannyl and -silyl compounds only react with highly reactive carbocations ( $E > 2$ ), giving complicated product mixtures (subsequent Friedel-Crafts reactions), only the indenylstannyl **7-Sn** and -silyl compounds **7-Si** were investigated for the comparison of the reactivities of carbanions with those of the corresponding organotin and silicon compounds.

We thus use the indenyl compounds **7-Met** as model system for quantify the influence of metal-coordination on the reactivities of C-nucleophiles. Figure 12 illustrates that an unambiguous graduation of relative reactivities is impossible. Because of the huge differences in reactivity, one cannot find a single electrophile which allows one to compare all compounds. While strong electrophiles will undergo diffusion-controlled reactions with the highly reactive nucleophiles (e.g. the organoalkali compounds) and thus will not differentiate their nucleophilic reactivities, weaker electrophiles will not react at all with the weaker nucleophiles e.g. the tin- and silicon derivatives.

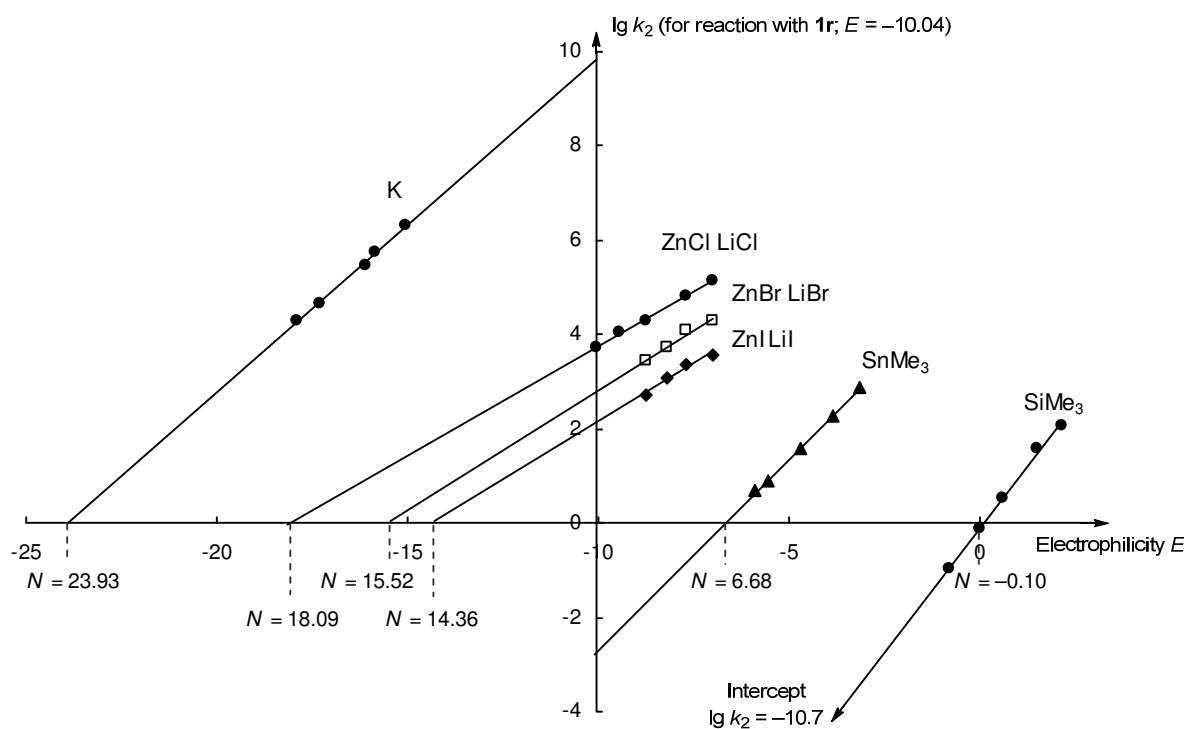


Figure 12: Plot of  $\lg k_2$  for the reactions of **7-Met** with reference electrophiles versus their electrophilicity parameters  $E$ . Intercepts with the abscissa correspond to the negative  $N$  values of **7-Met**. The vertical line at  $E = -10.04$  gives  $\lg k_2$  for the reaction of the corresponding **7-Met** with **1r**.

If we select an electrophile of intermediate reactivity (**1r**,  $E = -10.04$ ) as reference, for example, and extrapolate the correlation lines to the intersection with the vertical line at  $E = -10.04$ , one can see that the relative reactivities toward this electrophile extend over more

than 20 orders of magnitude. It should be noted, however, that the largest rate constant of this comparison ( $\lg k_2 = 9.8$ ) as well as the smallest rate constant ( $\lg k_2 = -10.6$ ) are hypothetical, because they are either beyond the diffusion limit or too small to be observable.

In order to base nucleophilic reactivities on rate constants, which can actually be measured, we have been using eq. (1), which defines nucleophilicity as the negative intercepts on the abscissa of  $\lg k_2$  versus  $E$  plots, as shown in Figures 4, 6, and 12. With  $-0.1 < N < 24$  for **7-K** to **7-Si** a similar reactivity range is indicated as by considering the relative reactivities toward **1r**. As indenylsilane **7-Si** reacts with electrophiles at C-2, we have to conclude that the attack at the carbanionoid position C-3 is even slower indicating that coordination with a  $\text{SiMe}_3$  group reduces the nucleophilic reactivity of the indenyl anion even more than indicated by the correlations in Figure 12.

### 3. Conclusion

The rate constants for the reactions of different organometallic derivatives of cyclopentadiene (**6**), indene (**7**) and fluorene (**8**) with benzhydrylium ions, quinone methides and structurally related Michael acceptors were determined. As the potassium derivatives (**6–8**)-K behaved as free carbanions in DMSO solution, the nucleophilic reactivities of the cyclopentadienyl, indenyl, and fluorenyl anion could be compared directly showing an increase of reactivity from **6**  $\rightarrow$  **7**  $\rightarrow$  **8** due to benzoannulation. The counter ion effects in the sodium and lithium derivatives of **6–8** also increased from the cyclopentadienyl- to the indenyl- and the fluorenyl compounds as a result of the stronger concentration of charge at the nucleophilic centers in the 5-membered rings. The zinc derivatives (**6–8**)-ZnCl show a more moderate nucleophilic reactivity and a different ordering of reactivity; being here the indenyl derivative the most reactive and fluorenyl-zinc the least reactive reagent in this series, which is explained by a change from the  $\text{S}_{\text{E}}2'$  mechanism for **6**-ZnCl and **7**-ZnCl to the  $\text{S}_{\text{E}}2$  mechanism for **8**-ZnCl. Furthermore, kinetic experiments of **7**-ZnX (X = Cl, Br, I) in presence of different additives showed that LiCl, LiBr,  $\text{MgCl}_2$ , and  $\text{Bu}_4\text{NCl}$  enhance, though with different magnitudes, the reactivity of organozinc reagents.

Figure 13 illustrates the common rule that the reactivities of main group organometallic reagents generally increase with increasing difference of electronegativity.<sup>[1a,2]</sup> One can see, however, that there is no linear relationship and that in this series of compounds, differences in electronegativities have only a large effect on nucleophilic reactivities for the less

electronegative metals and not for the highly electropositive metals which give rise to ionic compounds.

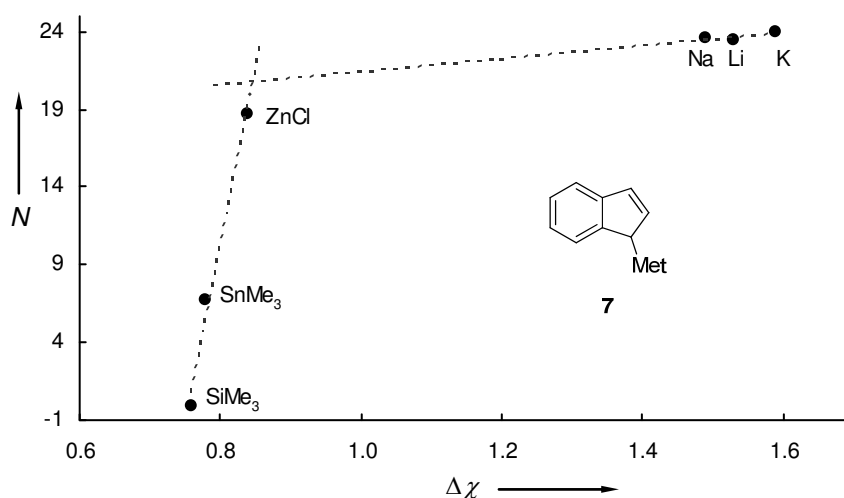


Figure 13: Nucleophilic reactivities of different organometallic derivatives of indene (**7-Met**) vs. the electronegativity-difference between carbon and metal ( $\Delta\chi$ ).<sup>[21]</sup>

## 4. Experimental Section

This chapter contains contributions from different authors. Experiments which were not performed by the author of this thesis are marked as follows: contributions from Roland Appel<sup>[RA]</sup> and contributions from Lydia Klier<sup>[LK]</sup>.

### 4.1. General

#### Materials

Commercially available DMSO (H<sub>2</sub>O content < 50 ppm) was used without further purification. Dichloromethane was successively treated with concentrated sulfuric acid, water, 10% NaHCO<sub>3</sub> solution, and water. After drying with CaCl<sub>2</sub>, it was freshly distilled over CaH<sub>2</sub> under exclusion of moisture (N<sub>2</sub> atmosphere). THF and Et<sub>2</sub>O were freshly distilled from sodium/benzophenone previous to use. The reference electrophiles used in this work were synthesized according to literature procedures.<sup>[6a-c,e,9]</sup>

#### NMR spectroscopy

In the <sup>1</sup>H and <sup>13</sup>C NMR spectra chemical shifts are given in ppm and refer to tetramethylsilane ( $\delta_{\text{H}} = 0.00$ ,  $\delta_{\text{C}} = 0.0$ ), [D<sub>6</sub>]-DMSO ( $\delta_{\text{H}} = 2.50$ ,  $\delta_{\text{C}} = 39.5$ ) or to CDCl<sub>3</sub> ( $\delta_{\text{H}} = 7.26$ ,  $\delta_{\text{C}} = 77.0$ ).<sup>[22]</sup>



as internal standards. The coupling constants are given in Hz. For reasons of simplicity, the  $^1\text{H}$ -NMR signals of AA'BB'-spin systems of *p*-disubstituted aromatic rings are treated as doublets. Signal assignments are based on additional COSY, gHSQC, and gHMBC experiments. Chemical shifts marked with (\*) refer to the minor isomer when the product was obtained as a mixture of two diastereomers.

### Kinetics

As the reactions of colored electrophiles **1–5** with colorless nucleophiles **6–8** yield colorless products (or products with a different absorption range than the reactants), the reactions could be followed by UV-Vis spectroscopy. Slow reactions ( $\tau_{1/2} > 10$  s) were determined by using conventional UV-Vis-spectrophotometers. Stopped-flow techniques were used for the investigation of rapid reactions ( $\tau_{1/2} < 10$  s). The temperature of all solutions was kept constant at  $20.0 \pm 0.1$  °C during all kinetic studies by using a circulating bath thermostat. In all runs the concentration of the nucleophile was at least 10 times higher than the concentration of the electrophile, resulting in pseudo-first-order kinetics with an exponential decay of the concentration of the minor compound. First-order rate constants  $k_{\text{obs}}$  were obtained by least-squares fitting of the exponential function  $A_t = A_0 \exp(-k_{\text{obs}}t) + C$  to the time-depending absorbances. The second-order rate constants  $k_2$  were obtained from the slopes of the linear plots of  $k_{\text{obs}}$  against the nucleophile concentrations.

## **4.2. Synthesis of the Nucleophiles**

### **4.2.1. Synthesis of the Cyclopentadienides **6****

#### **4.2.1.1. Lithium Cyclopentadienide (**6-Li**)<sup>[RA]</sup>**

According to den Besten *et al.*<sup>[10a]</sup>, **6-Li** was obtained from cyclopentadiene (1.61 g, 24.4 mmol) and butyl lithium (25.0 mmol) as a colorless solid (1.30 g, 18.0 mmol, 74%).

#### **4.2.1.2. Sodium Cyclopentadienide (**6-Na**)<sup>[RA]</sup>**

According to Panda *et al.*<sup>[10b]</sup>, **6-Na** was obtained from dicyclopentadiene (40 mL) and sodium (1.32 g, 57.0 mmol) as a colorless solid (3.87 g, 43.9 mmol, 77%).

#### 4.2.1.3. Potassium Cyclopentadienide (6-K)<sup>[RA]</sup>

According to Panda *et al.*<sup>[10b]</sup>, **6-K** was obtained from dicyclopentadiene (40 mL) and potassium (2.20 g, 56.3 mmol) as a colorless solid (4.83 g, 46.4 mmol, 82%).

### 4.2.2. Synthesis of the Indenes **7**

#### 4.2.2.1. (1*H*-Inden-1-yl)trimethylstannane (**7-Sn**)

Indene (4.0 mL, 34.1 mmol) was dissolved in 40 mL dry THF and cooled to  $-10\text{ }^{\circ}\text{C}$  where butyl lithium (30.0 mmol,  $2.5\text{ mol L}^{-1}$  solution in hexane) was added drop wise. After 5 min, chloro-trimethyl-stannane (6.0 mL, 30.1 mmol) was added. The mixture was stirred at ambient temperature for 18 h before the solvent was removed at reduced pressure. Pentane (30 mL) was added to the residue and the solution was separated from the precipitate by a syringe. After distillation ( $7 \times 10^{-3}$  mbar,  $55\text{ }^{\circ}\text{C}$ ), (1*H*-inden-1-yl)trimethylstannane (**7-Sn**, 4.36 g, 15.6 mmol, 52%) was obtained as light yellow liquid.

$^1\text{H-NMR}$  ( $\text{CDCl}_3$ , 300 MHz)  $\delta$  = 0.02 (s, 9 H,  $\text{Sn}(\text{CH}_3)_3$ ), 4.10 (bs, 1 H), 6.76 (t,  $^3J = 3.5\text{ Hz}$ , 1 H), 6.90 (bs, 1 H), 7.16-7.24 (m, 2 H), 7.50 (broad, 2 H).  $^{13}\text{C-NMR}$  ( $\text{CDCl}_3$ , 75.5 MHz)  $\delta$  =  $-9.5$  ( $\text{Sn}(\text{CH}_3)_3$ ), 121.1, 123.1 (broad) 123.4 (broad), 124.5, 135.0.

#### 4.2.2.2. (1*H*-Inden-1-yl)trimethylsilane (**7-Si**)

Indene (12.0 mL, 102 mmol) was dissolved in 40 mL dry THF and cooled to  $-10\text{ }^{\circ}\text{C}$  where butyl lithium (113 mmol,  $1.3\text{ mol L}^{-1}$  solution in hexane) was added drop wise. After 5 min, chloro-trimethyl-silane (17.0 mL, 134 mmol) was added. The mixture was stirred at ambient temperature for 16 h before the solvent was removed at reduced pressure. Pentane (30 mL) was added to the residue and the precipitated salts were filtrated. After distillation ( $4 \times 10^{-3}$  mbar,  $42\text{ }^{\circ}\text{C}$ ), (1*H*-inden-1-yl)trimethylsilane (**7-Si**, 14.7 g, 78.0 mmol, 76%) was obtained as light yellow liquid.

$^1\text{H NMR}$ -Signals as in Literature.<sup>[15]</sup>

### 4.2.3. Synthesis of the TMP-ZnX Bases<sup>[23]</sup>

#### 4.2.3.1. TMP-ZnCl·LiCl<sup>[LK]</sup>

TMP-ZnCl·LiCl was synthesized as described before.<sup>[23]</sup>

**4.2.3.2. TMP-ZnBr·LiBr<sup>[LK]</sup>**

According to ref.<sup>[23]</sup>, TMP-ZnBr·LiBr was synthesized from 2,2,6,6-tetramethylpiperidine (10.2 mL, 8.54 g, 60 mmol), *n*-butyl lithium (60 mmol) and zinc bromide (13.5 g, 60 mmol, dissolved in THF).

**4.2.3.3. TMP-ZnI·LiI<sup>[LK]</sup>**

According to ref.<sup>[23]</sup>, TMP-ZnI·LiI was synthesized from 2,2,6,6-tetramethylpiperidine (10.2 mL, 8.54 g, 60 mmol), *n*-butyl lithium (60 mmol) and zinc iodide\* (19.2 g, 60 mmol, dissolved in THF).

\*Zinc iodide was previously synthesized by a slowly addition of equimolar amounts of iodine (solution in THF) to a suspension of zinc in THF at  $-60\text{ }^{\circ}\text{C}$ .

**4.3. Product Studies****4.3.1. Alkali Metals****4.3.1.1. Reaction of Potassium Cyclopentadienide (6-K) with the Quinone Methide 2d<sup>[RA]</sup>**

Potassium cyclopentadienide (**6-K**, 31.3 mg, 0.300 mmol) was dissolved in 5 mL of dry DMSO and a solution of **2d** (100 mg, 0.324 mmol) in 5 mL DMSO was added. 50 mL of aqueous HCl ( $c = 1\text{ mol L}^{-1}$ ) was added after 5 min and the resulting mixture was extracted with dichloromethane (2 x 30 mL). The combined organic layers were washed with water and brine and dried over sodium sulfate before the solvent was removed by distillation. Purification by column chromatography (silica/ethyl acetate/pentane) yielded 2,6-di-*tert*-butyl-4-(cyclopenta-1,3-dien-1-yl(*p*-tolyl)methyl)phenol (**9a**) and 2,6-di-*tert*-butyl-4-(cyclopenta-1,4-dien-1-yl(*p*-tolyl)methyl)phenol (**9b**) as a pale yellow oil (80 mg, 0.21 mmol, 70 %, **9a** : **9b** ~ 1.5 : 1).

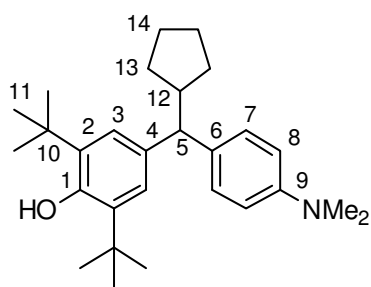
<sup>1</sup>H-NMR (CDCl<sub>3</sub>, 300 MHz):  $\delta = 1.40$  (s,  $2 \times 18\text{ H}$ , *t*Bu<sup>\*</sup>, *t*Bu<sup>#</sup>), 2.33 (s,  $2 \times 3\text{ H}$ , Me<sup>\*</sup>, Me<sup>#</sup>), 2.91-2.93<sup>#</sup> (m, 2 H, CH<sub>2</sub>), 3.00-3.02<sup>\*</sup> (m, 2 H, CH<sub>2</sub>), 5.02-5.05 (m, 4 H, CH<sup>\*</sup>, CH<sup>#</sup>, OH<sup>\*</sup>, OH<sup>#</sup>), 5.82-5.84<sup>\*</sup> (m, 1 H, CH<sub>olefin</sub><sup>\*</sup>), 5.99-6.00<sup>#</sup> (m, 1 H, CH<sub>olefin</sub><sup>#</sup>), 6.30-6.32<sup>#</sup> (m, 1 H, CH<sub>olefin</sub><sup>#</sup>), 6.38-6.43 (m, 3 H,  $2 \times$  CH<sub>olefin</sub><sup>\*</sup>, CH<sub>olefin</sub><sup>#</sup>), 6.98 (d, 4 H,  $J = 4.3\text{ Hz}$ , CH<sub>aryl</sub><sup>\*</sup>, CH<sub>aryl</sub><sup>#</sup>), 7.06-7.12 (m, 8 H, CH<sub>aryl</sub><sup>\*</sup>, CH<sub>aryl</sub><sup>#</sup>). <sup>13</sup>C-NMR (CDCl<sub>3</sub>, 75.5 MHz):  $\delta = 21.02^{\#}$  (q, Me), 21.04<sup>\*</sup> (q, Me), 30.3 (q, *t*Bu, signals of the two isomers superimposed), 34.31<sup>#</sup> (s, *t*Bu), 34.32<sup>\*</sup> (s, *t*Bu), 41.0<sup>\*</sup> (t, CH<sub>2</sub>), 43.2<sup>#</sup> (t, CH<sub>2</sub>), 51.9<sup>\*</sup> (d, CH), 52.9<sup>#</sup> (d, CH), 125.3<sup>#</sup> (d, CH<sub>aryl</sub>), 125.5<sup>\*</sup> (d, CH<sub>aryl</sub>),

128.57 (d), 128.60 (d), 128.7 (d), 128.80 (d), 128.82 (d), 129.6 (d), 131.6<sup>#</sup> (d, CH<sub>olefin</sub>), 132.0<sup>#</sup> (d, CH<sub>olefin</sub>), 133.3<sup>\*</sup> (d, CH<sub>olefin</sub>), 133.8<sup>\*</sup> (s), 134.5<sup>#</sup> (s), 134.9<sup>\*</sup> (d, CH<sub>olefin</sub>), 135.3 (s, two signals superimposed), 135.32 (s), 135.34 (s), 141.1<sup>\*</sup> (s), 141.8<sup>#</sup> (s), 150.0<sup>\*</sup> (s), 151.97<sup>#</sup> (s), 151.98<sup>\*</sup> (s), 152.64<sup>#</sup> (s). MS (EI):  $m/e$  (%) = 375 (31), 374 (100) [M]<sup>+</sup>, 360 (12), 359 (38), 318 (11), 317 (38), 310 (16), 309 (57), 269 (29), 261 (15), 219 (52), 169 (14), 154 (11), 57 (35). HR-MS (EI) [M]<sup>+</sup>: calcd for [C<sub>27</sub>H<sub>34</sub>O]<sup>+</sup>: 374.2605, found 374.2604.

\* can be assigned to **9a**; # can be assigned to **9b**

#### 4.3.1.2. Reaction of Potassium Cyclopentadienide (6-K) with the Quinone Methide **2g**<sup>[RA]</sup>

Potassium cyclopentadienide (**6-K**, 50.0 mg, 0.480 mmol) was dissolved in 10 mL of dry DMSO. Subsequently, a solution of the quinone methide **2g** (160 mg, 0.474 mmol) in 3 mL of CH<sub>2</sub>Cl<sub>2</sub> was added and the resulting reaction mixture was stirred for 2 min. The reaction was quenched by the addition of diluted aqueous HCl and extracted with CH<sub>2</sub>Cl<sub>2</sub> (2 x 10 mL). The combined organic layers were washed with water and brine, dried over Na<sub>2</sub>SO<sub>4</sub> and evaporated under reduced pressure. The remaining residue was dissolved in 15 mL of EtOH and Pd/C(10 %)-catalyst (10 mg) was added. After vigorous stirring for 15 h under H<sub>2</sub>, the reaction mixture was filtrated over celite and evaporated under reduced pressure. Purification by column chromatography (*n*-pentane/EtOAc), yielded 2,6-di-*tert*-butyl-4-(cyclopentyl(4-(dimethylamino)phenyl)methyl)phenol (**10**, 140 mg, 0.343 mmol, 72%) as yellow solid.



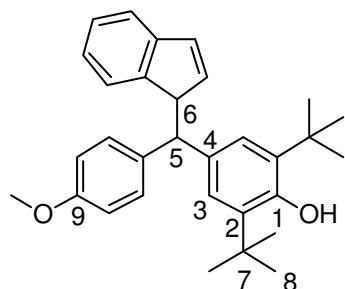
R<sub>f</sub> (*n*-pentane/EtOAc 10:1, *v/v*): 0.69. M.p.: 143-146 °C. <sup>1</sup>H-NMR (CDCl<sub>3</sub>, 599 MHz):  $\delta$  = 1.10-1.14 (m, 2 H, 13-H), 1.40 (s, 18 H, 11-H), 1.49-1.53 (m, 2 H, 14-H), 1.58-1.63 (m, 4 H, 13-H, 14-H), 2.54-2.61 (m, 1 H, 12-H), 2.88 (s, 6 H, NMe<sub>2</sub>), 3.35 (d, 1 H,  $J$  = 11.1 Hz, 5-H), 4.91 (s, 1 H, OH), 6.66 (d, 2 H,  $J$  = 8.7 Hz, 8-H), 7.04 (s, 2 H, 3-H), 7.15 (d, 2 H,  $J$  = 8.7 Hz, 7-

H). <sup>13</sup>C-NMR (CDCl<sub>3</sub>, 151 MHz):  $\delta$  = 25.42 (t, C-14), 25.45 (t, C-14), 30.4 (q, C-11), 32.3 (t, C-13), 32.4 (t, C-13), 34.3 (s, C-10), 40.8 (q, NMe<sub>2</sub>), 45.3 (d, C-12), 57.6 (d, C-5), 112.8 (d, C-8), 124.2 (d, C-3), 128.4 (d, C-7), 135.1 (2s, C-2, C-6), 136.7 (s, C-4), 148.7 (s, C-9), 151.5 (s, C-1). MS (EI):  $m/e$  (%) = 407 (5) [M]<sup>+</sup>, 339 (22), 338 (100). HR-MS (EI) [M]<sup>+</sup>: calc. for [C<sub>28</sub>H<sub>41</sub>NO]<sup>+</sup>: 407.3182, found: 407.3190.

#### 4.3.1.3. Reaction of Potassium Indenide (7-K) with the Quinone Methide 2e

Potassium *tert*-butoxyde (42.6 mg, 0.38 mmol) was dissolved in 5 mL dry DMSO and indene (0.1 mL, 0.85 mmol) was added. Subsequently, a solution of **2e** (110 mg, 0.339 mmol) in 5 mL DMSO was added. 50 mL of aqueous acetic acid (0.5%) was added after 10 min and the resulting mixture was extracted with ethyl acetate (2 x 30 mL). The combined organic layers were washed with brine and dried over sodium sulfate before the solvent was removed by distillation. Purification by column chromatography (silica/ethyl acetate:hexane = 1:4) yielded 2,6-di-*tert*-butyl-4-((2,3-dihydro-1H-inden-1-yl)(4-methoxyphenyl)methyl)phenol (**11**, 97.7 mg, 0.222 mmol, 65%, *dr* ~ 1:1.4) as pale yellow solid.

<sup>1</sup>H-NMR (CDCl<sub>3</sub>, 400 MHz):  $\delta$  = 1.39, 1.40\* (s, 18 H, 8-H), 3.65-3.71 (m, 1 H, 5-H, both isomers), 3.77\*, 3.81 (s, 1 H, OMe), 4.19-4.25 (m, 1 H, 6-H, both isomers), 5.02, 5.10\* (s, 1

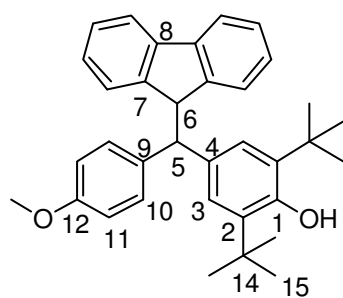


H, OH), 6.30 (td, <sup>3</sup>*J* = 5.6 Hz, <sup>4</sup>*J* = 1.6 Hz, 2 H), 6.35 (d, <sup>3</sup>*J* = 7.6 Hz, 1 H), 6.48 (d, <sup>3</sup>*J* = 7.6 Hz, 1 H), 6.74 (d, <sup>3</sup>*J* = 5.6 Hz, 2 H), 6.83\*, 6.83 (d, <sup>3</sup>*J* = 8.8, 2 H, H<sub>anisyl</sub>), 6.90-6.94 (m, 2 H), 7.07, 7.10\* (s, 2 H, 3-H), 7.18 (t, <sup>3</sup>*J* = 7.4 Hz, 2 H), 7.24-7.30 (m, 6 H).

<sup>13</sup>C-NMR (CDCl<sub>3</sub>, 101 MHz):  $\delta$  = 30.33, 30.35\* (q, C-8), 34.3, 34.4\* (s, C-7), 53.0, 53.1 (d, C-5), 55.18, 55.5 (d, C-6), 55.21, 55.3\* (q, OMe), 113.68, 113.74\* (d, C<sub>anisyl</sub>), 124.1, 124.9\* (d, C-3), 120.87 (2 C), 124.1, 124.2, 124.3, 124.9, 126.5, 128.7, 129.3, 130.8, 131.0, 134.5, 134.9, 135.4, 135.6, 136.9, 137.0, 139.1, 139.4, 144.68, 144.70, 146.2, 146.4, 152.0, 152.3\* (s, C-1), 157.9\*, 158.1 (s, C-9). HR-MS (EI) [*M*]: calc. for [C<sub>31</sub>H<sub>36</sub>O<sub>2</sub>]<sup>+</sup>: 440.2710, found: 440.2705.

#### 4.3.1.2. Reaction of Potassium fluorenone (8-K) with the Quinone Methide 2e

Potassium *tert*-butoxyde (69.6 mg, 0.62 mmol) was dissolved in 5 mL dry DMSO and fluorenone (143 mg, 0.862 mmol) was added. Subsequently, a solution of **2e** (91.8 mg, 0.283 mmol) in 5 mL DMSO was added. 50 mL of aqueous acetic acid (0.5%) was added after 10 min and the resulting mixture was extracted with ethyl acetate (2 x 30 mL). The combined organic layers were washed with brine and dried over sodium sulfate before the solvent was removed by distillation. Purification by column chromatography (silica/ethyl acetate:hexane = 1:9) yielded 4-((9H-fluoren-9-yl)(4-methoxyphenyl)methyl)-2,6-di-*tert*-butylphenol (**12**, 87.8 mg, 0.179 mmol, 63%) as yellow oil.

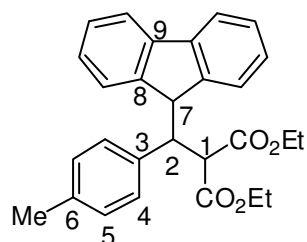


$^1\text{H-NMR}$  ( $\text{CDCl}_3$ , 300 MHz):  $\delta$  = 1.30 (s, 18 H, 15-H), 3.79, (s, 3 H, OMe), 4.17 (d,  $^3J$  = 8.1 Hz, 1 H, 5-H), 4.70 (d,  $^3J$  = 8.1 Hz, 1 H, 6-H), 5.00 (s, 1 H, OH), 6.53 (d,  $^3J$  = 7.8 Hz, 1 H), 6.77 (s, 2 H, 3-H), 6.79 (d,  $^3J$  = 7.8 Hz, 1 H), 6.84 (s, 2 H, 11-H), 6.96-7.07 (m, 2 H), 7.21-7.29 (m, 4 H), 7.63 (d,  $^3J$  = 7.5 Hz, 2 H).  $^{13}\text{C-NMR}$  ( $\text{CDCl}_3$ , 75.5 MHz):  $\delta$  = 30.3 (q, C-15), 34.3 (s, C-14),

52.6 (d, C-6), 54.5 (d, C-5), 55.2 (q, OMe), 113.6 (d, C-11), 119.3, 125.5, 125.7, 126.0, 126.1, 126.2, 126.84, 126.87, 129.8 (d,  $\text{C}_{\text{arom}}$ ), 132.9, 135.7 (s, C-4 and C-9), 141.2, 141.4 (s, C-8), 145.7, 146.2 (s, C-7), 152.1 (s, C-1), 158.0 (s, C-12).

#### 4.3.1.3. Reaction of Potassium fluorenone (8-K) with the Diethyl Benzylidenemalonate 3a

Potassium *tert*-butoxyde (87.5 mg, 0.780 mmol) was dissolved in 5 mL of dry DMSO and fluorene (145 mg, 0.872 mmol) was added. Subsequently, a solution of **3a** (130 mg, 0.496 mmol) in 5 mL DMSO was added. 50 mL of aqueous acetic acid (0.5%) was added after 5 min and the resulting mixture was extracted with ethyl acetate (2 x 30 mL). The combined organic layers were washed with brine (2 x 20 mL) and dried over sodium sulfate before the solvent was removed by distillation. Purification by column chromatography (silica/ethyl acetate:hexane = 1:9) yielded diethyl 2-((9*H*-fluorene-9-yl)(*p*-tolyl)methyl)malonate (**13**, 163 mg, 0.380 mmol, 77%) as colorless solid.



Melting Point: 94.2-95.1 °C.  $^1\text{H-NMR}$  ( $\text{CDCl}_3$ , 300 MHz):  $\delta$  = 0.90 (t,  $^3J$  = 7.1 Hz, 3 H,  $\text{OCH}_2\text{CH}_3$ ), 1.36 (t,  $^3J$  = 7.2 Hz, 3 H,  $\text{OCH}_2\text{CH}_3$ ), 2.01 (s, 3 H, Me), 3.85-3.93 (m, 2 H,  $\text{OCH}_2\text{CH}_3$ ), 4.25-4.37 (m, 4 H,  $\text{OCH}_2\text{CH}_3$ , 2-H, 7-H), 4.44 (d,  $^3J$  = 12.0 Hz, 1 H, 1-H), 6.41 (d,  $^3J$  = 8.1 Hz, 2 H, 4-H), 6.56 (d,  $^3J$  = 8.1 Hz, 2 H, 5-H),

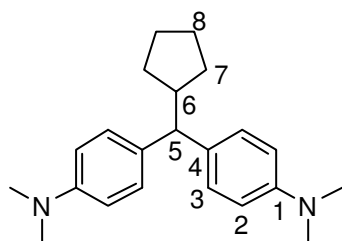
7.17-7.29 (m, 2 H), 7.32-7.35 (m, 2 H), 7.43 (d,  $^3J$  = 7.2 Hz, 1 H), 7.52-7.55 (m, 1 H), 7.65 (d,  $^3J$  = 7.5 Hz, 1 H), 7.81-7.84 (m, 1 H).  $^{13}\text{C-NMR}$  ( $\text{CDCl}_3$ , 75.5 MHz):  $\delta$  = 13.7, 14.2 (q,  $\text{OCH}_2\text{CH}_3$ ), 20.8 (q, Me), 48.7 (d, C-2), 49.8 (d, C-7), 56.3 (d, C-1), 61.3, 61.9 (t,  $\text{OCH}_2\text{CH}_3$ ), 119.5, 120.0, 124.8, 125.8, 126.5, 126.7, 127.0, 127.4 (d,  $\text{C}_{\text{fluorenyl}}$ ), 127.6 (d, C-5), 128.5 (d, C-4), 132.9 (s, C-3), 135.9 (s, C-6), 141.0, 142.3 (s, C-9), 143.7, 145.2 (s, C-8), 167.6, 168.6 (s,  $\text{CO}_2\text{Et}$ ). HR-MS (EI) [ $\text{M}^+$ ]: calc. for  $[\text{C}_{28}\text{H}_{28}\text{O}_4]^+$ : 428.1982, found: 428.1974.

### 4.3.2. Zink Derivatives

General Procedure 2 (GP2): The reactions were performed under argon-atmosphere. The CH acid is dissolved in 5 mL dry DMSO and 1.5-1.1 equiv. of TMP-ZnCl·LiCl (solution in THF ~ 1.3 mol L<sup>-1</sup>) is added and stirred for 5 min at room temperature. In a separated flask, a solution of the benzhydrylium tetrafluoroborate **1m**-BF<sub>4</sub> in 10 mL DMSO is prepared. The solution of the Zn-derivatives (**6**–**8**)-ZnCl is added dropwise (with a syringe) to the cation solution until the blue solution turned yellow. After 5 min at room temperature, 15 mL of aqueous K<sub>2</sub>CO<sub>3</sub> (~1%) is added and the mixture is extracted with ethyl acetate (3 x 15 mL). The combined organic layers were washed with brine and dried over sodium sulfate and the solvent was removed by distillation. The crude products were recrystallized from dichloromethane/pentane.

#### 4.3.2.1. Reaction of **6**-ZnCl with the Benzhydrylium Tetrafluoroborate **1m**-BF<sub>4</sub>

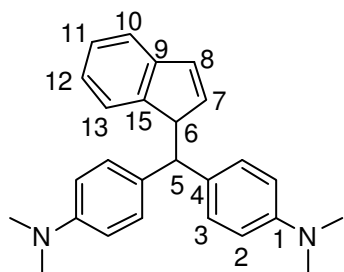
Cyclopentadiene (100 µg, 1.21 mmol), TMP-ZnCl·LiCl (1.29 mmol) and **1m**-BF<sub>4</sub> (150 mg, 0.441 mmol) were mixed according to GP2. The obtained crude product (yellow oil) was dissolved in 10 mL of ethanol where Pd/C-catalyst (10 mg) was added. Under an atmosphere of hydrogen, the mixture was stirred at ambient temperature. The reaction process was controlled by GC-MS. After 16 h, another portion of catalyst (10 mg) was added and the reaction was stirred for further 22 h. After filtration over celite, the solvent was removed and the crude residue was purified by column chromatography on silica (pentane:ethyl acetate = 2:1) yielding 4,4'-(cyclopentylmethylene)bis(*N,N*-dimethylaniline) (**14**, 85.1, 264 mmol, 60%) as an oil.



<sup>1</sup>H-NMR (CDCl<sub>3</sub>, 300 MHz):  $\delta$  = 1.10-1.20 and 1.47-1.69 (m, 4 H, 7-H and 8-H), 2.86 (s, 12 H, NMe<sub>2</sub>), 2.54-2.64 (m, 1 H, 6-H), 3.39 (d, <sup>3</sup>*J* = 11.4 Hz, 1 H, 5-H), 6.66 (d, <sup>3</sup>*J* = 8.7 Hz, 2 H, 2-H), 7.13 (d, <sup>3</sup>*J* = 8.7 Hz, 2 H, 3-H). <sup>13</sup>C-NMR (CDCl<sub>3</sub>, 75.5 MHz):  $\delta$  = 24.4 (d, C-8), 31.3 (d, C-7), 39.9 (q, NMe<sub>2</sub>), 43.8 (d, C-6), 55.6 (d, C-5), 112.0 (d, C-2), 127.4 (d, C-3), 134.1 (s, C-4), 147.6 (s, C-1). HR-MS (EI) [M]: calc. for [C<sub>22</sub>H<sub>30</sub>N<sub>2</sub>]<sup>+</sup>: 322.2404, found: 322.2395.

**4.3.2.2. Reaction of 7-ZnCl with the Benzhydrylium Tetrafluoroborate 1m-BF<sub>4</sub>**

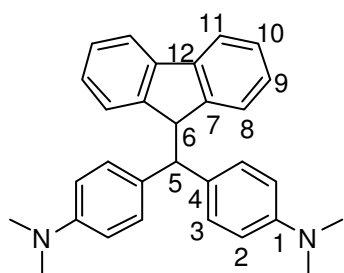
Indene (0.35 mL, 2.99 mmol), TMP-ZnCl·LiCl (3.13 mmol) and **1m**-BF<sub>4</sub> (100 mg, 0.294 mmol), yielded according to GP2 4,4'-((1*H*-inden-1-yl)methylene)bis(*N,N*-dimethylaniline) (**15**, 74.0 mg, 0.201 mmol, 68%) as colorless solid.



M.p.: 172.8-173.4 °C. <sup>1</sup>H-NMR (CDCl<sub>3</sub>, 300 MHz):  $\delta$  = 2.80, 2.84 (s, 12 H, NMe<sub>2</sub>), 3.53 (d, <sup>3</sup>*J* = 10.5 Hz, 1 H, 5-H), 4.19 (d, <sup>3</sup>*J* = 10.5 Hz, 1 H, 6-H), 6.27 (dd, <sup>3</sup>*J* = 5.4 Hz, <sup>4</sup>*J* = 1.8 Hz, 1 H, 7-H), 6.51 (d, <sup>3</sup>*J* = 7.6 Hz, 1 H, 8-H), 6.75-6.67 (m, 5 H, 2-H and 12-H), 6.84 (t, <sup>3</sup>*J* = 7.5 Hz, 1 H, 11-H), 7.07-7.16 (m, 5 H, 3-H and 13-H), 7.21 (d, <sup>3</sup>*J* = 7.4 Hz, 1 H, 10-H). <sup>13</sup>C-NMR (CDCl<sub>3</sub>, 75.5 MHz):  $\delta$  = 39.8 (q, NMe<sub>2</sub>), 51.3 (d, C-5), 54.0 (d, C-6), 111.9 (d, C-2), 119.8 (d, C-10), 123.2 (d, C-11), 123.5 (d, C-8), 125.4 (d, C-13), 127.8 (d, C-3), 129.7 (d, C-12), 132.1 and 132.6 (s, C-4), 138.6 (d, C-7), 143.7 (s, C-15), 145.6 (s, C-9), 147.9 and 148.2 (s, C-1). HR-MS (EI) [*M*]: calc. for [C<sub>26</sub>H<sub>28</sub>N<sub>2</sub>]<sup>+</sup>: 368.2247, found: 368.2241.

**4.3.2.3. Reaction of 8-ZnCl with the Benzhydrylium Tetrafluoroborate 1m-BF<sub>4</sub>**

Fluorene (444 mg, 2.67 mmol), TMP-ZnCl·LiCl (2.72 mmol) and **1m**-BF<sub>4</sub> (111 mg, 0.326 mmol), yielded according to GP2 4,4'-((9*H*-fluoren-9-yl)methylene)bis(*N,N*-dimethylaniline) (**16**, 82.3 mg, 0.197 mmol, 60%) as colorless solid.



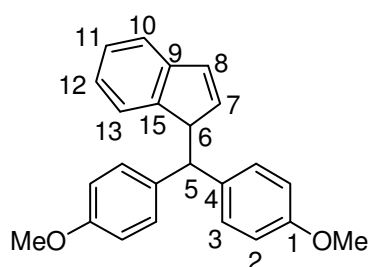
Decomposition at 237 °C. <sup>1</sup>H-NMR (CDCl<sub>3</sub>, 400 MHz):  $\delta$  = 2.89 (s, 12 H, NMe<sub>2</sub>), 3.97 (d, <sup>3</sup>*J* = 9.3 Hz, 1 H, 5-H), 4.73 (d, <sup>3</sup>*J* = 9.3 Hz, 1 H, 6-H), 6.64 (d, <sup>3</sup>*J* = 6.8 Hz, 2 H, 2-H), 6.88 (d, <sup>3</sup>*J* = 7.6 Hz, 2 H, 8-H), 7.00 and 7.26 (each: t, <sup>3</sup>*J* = 7.6 Hz, 2 H, 9-H and 10-H), 7.12 (d, <sup>3</sup>*J* = 6.8 Hz, 2 H, 3-H), 7.68 (d, <sup>3</sup>*J* = 7.5 Hz, 2 H, 11-H). <sup>13</sup>C-NMR (CDCl<sub>3</sub>, 101 MHz):  $\delta$  = 40.8 (q, NMe<sub>2</sub>), 52.1 (d, C-6), 53.8 (d, C-5), 112. (d, C-2), 119.3 (d, C-11), 126.0 (d, C-8), 126.2 and 126.8 (d, C-9 and C-10), 129.4 (d, C-3), 132.4 (s, C-4), 141.2 (s, C-12), 146.2 (s, C-7), 149.2 (s, C-1). HR-MS (EI) [*M*]<sup>2+</sup>: calc. for [C<sub>30</sub>H<sub>28</sub>N<sub>2</sub>]<sup>2+</sup>: 416.2252, found: 416.2240.



### 4.3.3. Tin Derivative

#### 4.3.3.1. Reaction of 7-Sn with the Benzhydrylium Tetrafluoroborate 1m-BF<sub>4</sub>

Bis(4-methoxyphenyl)methanol (**1e**-OH, 125 mg, 0.512 mmol) was dissolved in 10 mL of dry diethyl ether and cooled to  $-60\text{ }^{\circ}\text{C}$  where HBF<sub>4</sub> (0.5 mL, v/v = 50% in Et<sub>2</sub>O), was added drop wise. After 5 min, the solvent was removed by filtration (under Ar-atmosphere), and the red precipitate (**1e**-BF<sub>4</sub>) was washed three times with dry Et<sub>2</sub>O and dried in vacuum (at  $-60\text{ }^{\circ}\text{C}$ ). **1e**-BF<sub>4</sub> was dissolved in 10 mL of dry dichloromethane and a solution of 7-Sn (220 mg, 0.789 mmol) in 3 mL of CH<sub>2</sub>Cl<sub>2</sub> was added and the mixture was allowed to warm up to room temperature where it was filtered over Al<sub>2</sub>O<sub>3</sub> (with CH<sub>2</sub>Cl<sub>2</sub> as eluent). After evaporate of the solvent, the crude product was purified by column chromatography on silica (pentane:ethyl acetate = 9:1) yielding 1-(bis(4-methoxyphenyl)methyl)-1*H*-indene (**17**, 171 mg, 499 μmol, 97%) as colorless solid.

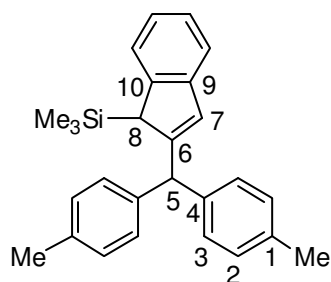


M.p.:  $175.2\text{--}176.2\text{ }^{\circ}\text{C}$ . <sup>1</sup>H-NMR (CDCl<sub>3</sub>, 300 MHz):  $\delta$  = 3.70 (d, <sup>3</sup>*J* = 10.5 Hz, 1 H, 5-H), 3.75, 3.80 (s, 6 H, OMe), 4.26 (d, <sup>3</sup>*J* = 10.5 Hz, 1 H, 6-H), 6.30 (dd, <sup>3</sup>*J* = 5.6 Hz, <sup>4</sup>*J* = 1.8 Hz, 1 H, 7-H), 6.75 (d, <sup>3</sup>*J* = 7.5 Hz, 1 H, 8-H), 6.54 (d, <sup>3</sup>*J* = 7.8 Hz, 1 H, H<sub>arom</sub>), 6.78–6.89 (m, 4 H, 2-H), 6.93 (t, <sup>3</sup>*J* = 7.5 Hz, 1 H, H<sub>arom</sub>), 7.16–7.31 (m, 6 H, 3-H and H<sub>arom</sub>). <sup>13</sup>C-NMR (CDCl<sub>3</sub>, 75.5 MHz):  $\delta$  = 54.4 (d, C-5), 54.7 (d, C-6), 55.19 and 55.24 (q, OMe), 113.8, 113.9 (d, C-2), 121.0, 124.31, 124.34, 126.6 (d, C<sub>arom</sub>), 128.6, 129.2 (d, C-3), 131.2 (d, C-8), 136.5, 138.8 (s, C-4), 138.9 (d, C-7), 144.5 (s, C-9), 146.2 (s, C-15), 158.0, 158.2 (s, C-1). HR-MS (EI) [*M*]: calc. for [C<sub>24</sub>H<sub>22</sub>O<sub>2</sub>]<sup>+</sup>: 342.1614, found: 342.1614.

### 4.3.4. Silicon Derivative

#### 4.3.4.1. Reaction of 7-Si with the Benzhydryl bromide 1a-Br

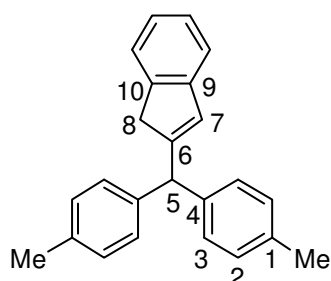
Under nitrogen atmosphere, bis(4-methylphenyl)-bromomethane (**1a**-Br, 108 mg, 0.392 mmol) were dissolved in 8 mL of dry acetonitrile and a solution of 7-Si (83.1 mg, 0.441 mmol) in 4 mL acetonitrile was added. The reaction mixture was stirred at ambient temperature for 4 h, controlling the reaction progress by GC/MS, before NaHCO<sub>3</sub> (solid, ~50 mg) was added and the solvent was removed under reduced pressure. Column chromatography on silica with pentane/dichloromethane as eluent yielded (2-(di-*p*-tolylmethyl)-1*H*-inden-1-yl)trimethylsilane (**18**, 69.5 mg, 0.182 mmol, 46%) as colorless oil.



$^1\text{H-NMR}$  ( $\text{CDCl}_3$ , 300 MHz):  $\delta$  = 0.08 (s, 9 H,  $\text{SiMe}_3$ ), 2.35 (s, 3 H, Me), 2.38 (s, 3 H, Me), 3.51 (s, 1 H, 8-H), 5.29 (s, 1 H, 5-H), 6.23 (s, 1 H, 7-H), 7.03-7.24 (m, 10 H,  $\text{H}_{\text{arom}}$ ), 7.29-7.37 (m, 2 H,  $\text{H}_{\text{arom}}$ ).  $^{13}\text{C-NMR}$  ( $\text{CDCl}_3$ , 75.5 MHz):  $\delta$  = -1.7 (q,  $\text{SiMe}_3$ ), 21.20, 21.21 (q, Me), 47.5 (d, C-8), 52.8 (d, C-5), 120.6, 122.9, 123.2, 124.9 (d,  $\text{CH}_{\text{indene}}$ ), 128.2 (d, C-7), 128.9, 129.1, 129.2, 129.3 (d, C-2 and C-3), 135.9, 136.1 (s, C-1), 140.3, 140.8 (s, C-4), 144.0, 145.8 (s, C-9 and C-10), 155.3 (s, C-6). HR-MS (EI): calc. for  $[\text{C}_{27}\text{H}_{30}\text{Si}]^+$ : 382.2111, found: 382.2120.

#### 4.3.4.2. Reaction of 7-Si with the Benzhydryl bromide 1a-Br with Hydrodesililation

Under nitrogen atmosphere, bis(4-methylphenyl)-bromomethane (**1a-Br**, 130 mg, 0.472 mmol) were dissolved in 8 mL of dry acetonitrile and a solution of **7-Si** (106 mg, 0.563 mmol) in 4 mL acetonitrile was added. The reaction mixture was stirred at ambient temperature for 120 h controlling the reaction progress by GC/MS, before the solvent was removed under reduced pressure. Column chromatography on silica with pentane/dichloromethane as eluent yielded 2-(di-*p*-tolylmethyl)-1*H*-indene (**19**, 71.0 mg, 0.229 mmol, 49%) as colorless oil.



$^1\text{H-NMR}$  ( $\text{CDCl}_3$ , 300 MHz):  $\delta$  = 2.32 (s, 6 H, Me), 3.34 (s, 2 H, 8-H), 5.15 (s, 1 H, 5-H), 6.31 (s, 1 H, 7-H), 7.02-7.14 (m, 9 H,  $\text{H}_{\text{arom}}$ ), 7.17-7.23 (m, 1 H,  $\text{H}_{\text{arom}}$ ), 7.31 (d,  $^3J$  = 7.2 Hz, 1 H,  $\text{H}_{\text{arom}}$ ).  $^{13}\text{C-NMR}$  ( $\text{CDCl}_3$ , 75.5 MHz):  $\delta$  = 21.0 (q, Me), 41.0 (t, C-8), 53.0 (d, C-5), 120.5, 123.5, 124.1, 126.3 (d,  $\text{C}_{\text{arom}}$ ), 128.8, 129.1 (d, C-2 and C-3), 129.8 (d, C-7), 135.9 (s, C-1), 140.3 (s, C-4), 143.5, 144.9 (s, C-7 and C-8), 152.7 (s, C-6). HR-MS (EI)  $[M]$ : calc. for  $[\text{C}_{24}\text{H}_{22}]^+$ : 310.1722, found: 310.1724.

## 4.4. Kinetic Experiments

### 4.4.1. Kinetic Experiments on the Alkali Metal Derivatives of 6–8

#### 4.4.1.1. Kinetic Experiments at Variable Concentrations of Li<sup>+</sup>

Table 8: Pseudo-first-order rate constants for reactions of 7-Li (generated from 7-H by addition of 1.05 equivalents of LiOtBu) with **2d** at variable concentrations of LiCl (20 °C, stopped-flow, at 486 nm).

[ <b>2d</b> ] / mol L <sup>-1</sup>	[7-H] / mol L <sup>-1</sup>	[LiOtBu] / mol L <sup>-1</sup>	[LiCl] / mol L <sup>-1</sup>	[Li <sup>+</sup> ] <sub>total</sub> / mol L <sup>-1</sup>	<i>k</i> <sub>obs</sub> / s <sup>-1</sup>
	9.52 × 10 <sup>-4</sup>				36.6 <sup>[a]</sup>
2.42 × 10 <sup>-5</sup>	9.52 × 10 <sup>-4</sup>	1.00 × 10 <sup>-3</sup>	0	1.00 × 10 <sup>-3</sup>	25.8
2.42 × 10 <sup>-5</sup>	9.52 × 10 <sup>-4</sup>	1.00 × 10 <sup>-3</sup>	6.20 × 10 <sup>-4</sup>	1.62 × 10 <sup>-3</sup>	14.0
2.42 × 10 <sup>-5</sup>	9.52 × 10 <sup>-4</sup>	1.00 × 10 <sup>-3</sup>	9.93 × 10 <sup>-4</sup>	1.99 × 10 <sup>-3</sup>	17.6
2.42 × 10 <sup>-5</sup>	9.52 × 10 <sup>-4</sup>	1.00 × 10 <sup>-3</sup>	2.17 × 10 <sup>-3</sup>	3.17 × 10 <sup>-3</sup>	19.4
2.42 × 10 <sup>-5</sup>	9.52 × 10 <sup>-4</sup>	1.00 × 10 <sup>-3</sup>	4.96 × 10 <sup>-3</sup>	5.97 × 10 <sup>-3</sup>	20.7
2.42 × 10 <sup>-5</sup>	9.52 × 10 <sup>-4</sup>	1.00 × 10 <sup>-3</sup>	9.93 × 10 <sup>-3</sup>	1.09 × 10 <sup>-2</sup>	23.3
2.42 × 10 <sup>-5</sup>	9.52 × 10 <sup>-4</sup>	1.00 × 10 <sup>-3</sup>	1.90 × 10 <sup>-2</sup>	2.00 × 10 <sup>-2</sup>	23.4
2.42 × 10 <sup>-5</sup>	9.52 × 10 <sup>-4</sup>	1.00 × 10 <sup>-3</sup>	3.18 × 10 <sup>-2</sup>	3.28 × 10 <sup>-2</sup>	23.3
2.42 × 10 <sup>-5</sup>	9.52 × 10 <sup>-4</sup>	1.00 × 10 <sup>-3</sup>	6.82 × 10 <sup>-2</sup>	6.92 × 10 <sup>-2</sup>	26.0

[a] Calculated from the second-order rate constants of the free anion (potassium salt in presence of 18-crown-6) given in Table 3.

Table 9: Pseudo-first-order rate constants for reactions of 7-Li (generated from 7-H by addition of 1.05 equivalents of LiOtBu) with **2d** at variable concentrations of LiBF<sub>4</sub> (20 °C, stopped-flow, at 486 nm).

[ <b>2d</b> ] / mol L <sup>-1</sup>	[7-H] / mol L <sup>-1</sup>	[LiOtBu] / mol L <sup>-1</sup>	[LiBF <sub>4</sub> ] / mol L <sup>-1</sup>	[Li <sup>+</sup> ] <sub>total</sub> / mol L <sup>-1</sup>	<i>k</i> <sub>obs</sub> / s <sup>-1</sup>
	9.42 × 10 <sup>-4</sup>				50.2 <sup>[a]</sup>
2.57 × 10 <sup>-5</sup>	9.42 × 10 <sup>-4</sup>	9.89 × 10 <sup>-4</sup>	0	9.89 × 10 <sup>-4</sup>	28.6
2.57 × 10 <sup>-5</sup>	9.42 × 10 <sup>-4</sup>	9.89 × 10 <sup>-4</sup>	5.44 × 10 <sup>-4</sup>	1.53 × 10 <sup>-3</sup>	29.0
2.57 × 10 <sup>-5</sup>	9.42 × 10 <sup>-4</sup>	9.89 × 10 <sup>-4</sup>	1.09 × 10 <sup>-3</sup>	2.08 × 10 <sup>-3</sup>	30.0
2.57 × 10 <sup>-5</sup>	9.42 × 10 <sup>-4</sup>	9.89 × 10 <sup>-4</sup>	2.61 × 10 <sup>-3</sup>	3.60 × 10 <sup>-3</sup>	30.6
2.57 × 10 <sup>-5</sup>	9.42 × 10 <sup>-4</sup>	9.89 × 10 <sup>-4</sup>	5.44 × 10 <sup>-3</sup>	6.43 × 10 <sup>-3</sup>	30.3
2.57 × 10 <sup>-5</sup>	9.42 × 10 <sup>-4</sup>	9.89 × 10 <sup>-4</sup>	1.02 × 10 <sup>-2</sup>	1.12 × 10 <sup>-2</sup>	27.6
2.57 × 10 <sup>-5</sup>	9.42 × 10 <sup>-4</sup>	9.89 × 10 <sup>-4</sup>	2.05 × 10 <sup>-2</sup>	2.14 × 10 <sup>-2</sup>	27.3
2.57 × 10 <sup>-5</sup>	9.42 × 10 <sup>-4</sup>	9.89 × 10 <sup>-4</sup>	3.41 × 10 <sup>-2</sup>	3.51 × 10 <sup>-2</sup>	26.9
2.57 × 10 <sup>-5</sup>	9.42 × 10 <sup>-4</sup>	9.89 × 10 <sup>-4</sup>	5.45 × 10 <sup>-3</sup>	5.55 × 10 <sup>-2</sup>	27.6

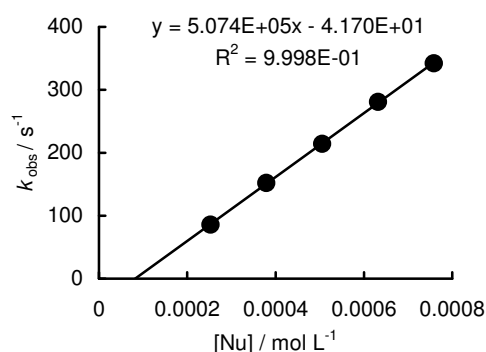
[a] Calculated from the second-order rate constants of the free anion (potassium salt in presence of 18-crown-6) given in Table 3.

## 4.4.1.2. Reactions of Potassium Cyclopentadienide (6-K)

Table 10: Kinetics of the reaction of **6-K** with **4** (20 °C, stopped-flow, at 520 nm).<sup>[RA]</sup>

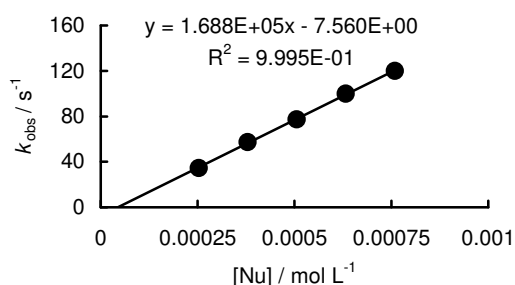
[ <b>4</b> ] / mol L <sup>-1</sup>	[ <b>6-K</b> ] / mol L <sup>-1</sup>	[18-crown-6] / mol L <sup>-1</sup>	$k_{\text{obs}}$ / s <sup>-1</sup>
$2.45 \times 10^{-5}$	$2.53 \times 10^{-4}$		$8.58 \times 10^1$
$2.45 \times 10^{-5}$	$3.79 \times 10^{-4}$	$1.70 \times 10^{-3}$	$1.52 \times 10^2$
$2.45 \times 10^{-5}$	$5.06 \times 10^{-4}$		$2.14 \times 10^2$
$2.45 \times 10^{-5}$	$6.32 \times 10^{-4}$	$1.70 \times 10^{-3}$	$2.81 \times 10^2$
$2.45 \times 10^{-5}$	$7.59 \times 10^{-4}$		$3.42 \times 10^2$

$$k_2 = 5.07 \times 10^5 \text{ L mol}^{-1} \text{ s}^{-1}$$

Table 11: Kinetics of the reaction of **6-K** with **5** (20 °C, stopped-flow, at 520 nm).<sup>[RA]</sup>

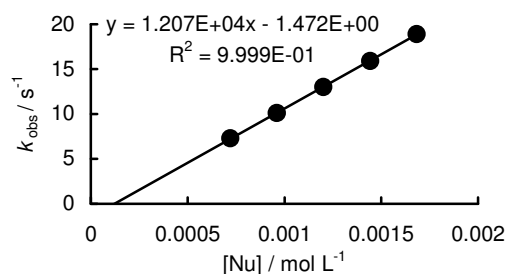
[ <b>5</b> ] / mol L <sup>-1</sup>	[ <b>6-K</b> ] / mol L <sup>-1</sup>	[18-crown-6] / mol L <sup>-1</sup>	$k_{\text{obs}}$ / s <sup>-1</sup>
$2.37 \times 10^{-5}$	$2.53 \times 10^{-4}$		$3.45 \times 10^1$
$2.37 \times 10^{-5}$	$3.79 \times 10^{-4}$	$8.48 \times 10^{-4}$	$5.74 \times 10^1$
$2.37 \times 10^{-5}$	$5.06 \times 10^{-4}$		$7.73 \times 10^1$
$2.37 \times 10^{-5}$	$6.32 \times 10^{-4}$	$1.70 \times 10^{-3}$	$9.98 \times 10^1$
$2.37 \times 10^{-5}$	$7.59 \times 10^{-4}$		$1.20 \times 10^2$

$$k_2 = 1.69 \times 10^5 \text{ L mol}^{-1} \text{ s}^{-1}$$

Table 12: Kinetics of the reaction of **6-K** with **2b** (20 °C, stopped-flow, at 371 nm).<sup>[RA]</sup>

[ <b>2d</b> ] / mol L <sup>-1</sup>	[ <b>6-K</b> ] / mol L <sup>-1</sup>	[18-crown-6] / mol L <sup>-1</sup>	$k_{\text{obs}}$ / s <sup>-1</sup>
$2.50 \times 10^{-5}$	$7.21 \times 10^{-4}$		7.29
$2.50 \times 10^{-5}$	$9.62 \times 10^{-4}$	$8.53 \times 10^{-4}$	$1.01 \times 10^1$
$2.50 \times 10^{-5}$	$1.20 \times 10^{-3}$		$1.30 \times 10^1$
$2.50 \times 10^{-5}$	$1.44 \times 10^{-3}$	$1.71 \times 10^{-3}$	$1.59 \times 10^1$
$2.50 \times 10^{-5}$	$1.68 \times 10^{-4}$		$1.89 \times 10^2$

$$k_2 = 1.21 \times 10^4 \text{ L mol}^{-1} \text{ s}^{-1}$$

Table 13: Kinetics of the reaction of **6-K** with **2c** (20 °C, stopped-flow, at 393 nm).<sup>[RA]</sup>

[ <b>2c</b> ] / mol L <sup>-1</sup>	[ <b>6-K</b> ] / mol L <sup>-1</sup>	[18-crown-6] / mol L <sup>-1</sup>	$k_{\text{obs}}$ / s <sup>-1</sup>
$2.54 \times 10^{-5}$	$6.91 \times 10^{-4}$		3.68
$2.54 \times 10^{-5}$	$9.21 \times 10^{-4}$	$9.35 \times 10^{-4}$	5.15
$2.54 \times 10^{-5}$	$1.15 \times 10^{-3}$		6.64
$2.54 \times 10^{-5}$	$1.38 \times 10^{-3}$	$1.87 \times 10^{-3}$	8.16
$2.54 \times 10^{-5}$	$1.61 \times 10^{-4}$		9.53

$$k_2 = 6.39 \times 10^4 \text{ L mol}^{-1} \text{ s}^{-1}$$

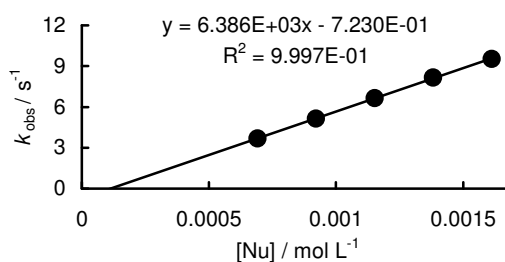
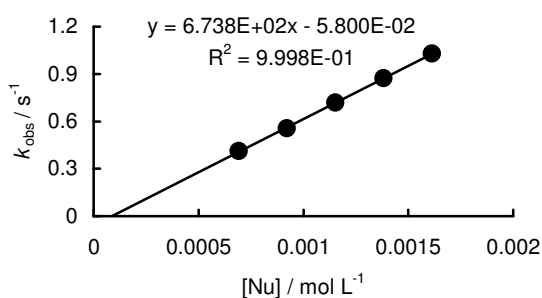


Table 14: Kinetics of the reaction of **6-K** with **2d** (20 °C, stopped-flow, at 486 nm).<sup>[RA]</sup>

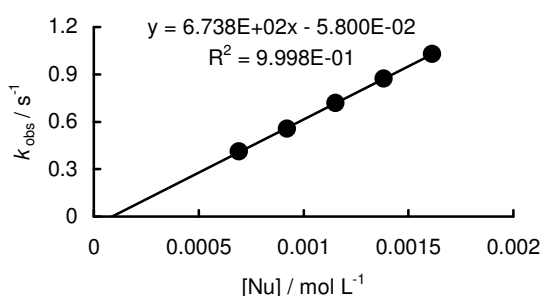
[ <b>2d</b> ] / mol L <sup>-1</sup>	[ <b>6-K</b> ] / mol L <sup>-1</sup>	[18-crown-6] / mol L <sup>-1</sup>	$k_{\text{obs}}$ / s <sup>-1</sup>
$2.58 \times 10^{-5}$	$6.91 \times 10^{-4}$		$4.12 \times 10^{-1}$
$2.58 \times 10^{-5}$	$9.21 \times 10^{-4}$	$9.35 \times 10^{-4}$	$5.57 \times 10^{-1}$
$2.58 \times 10^{-5}$	$1.15 \times 10^{-3}$		$7.18 \times 10^{-1}$
$2.58 \times 10^{-5}$	$1.38 \times 10^{-3}$	$1.87 \times 10^{-3}$	$8.73 \times 10^{-1}$
$2.58 \times 10^{-5}$	$1.61 \times 10^{-4}$		1.03

$$k_2 = 6.74 \times 10^4 \text{ L mol}^{-1} \text{ s}^{-1}$$

Table 15: Kinetics of the reaction of **6-K** with **2e** (20 °C, stopped-flow, at 521 nm).<sup>[RA]</sup>

[ <b>2e</b> ] / mol L <sup>-1</sup>	[ <b>6-K</b> ] / mol L <sup>-1</sup>	[18-crown-6] / mol L <sup>-1</sup>	$k_{\text{obs}}$ / s <sup>-1</sup>
$2.58 \times 10^{-5}$	$6.91 \times 10^{-4}$		$4.12 \times 10^{-1}$
$2.58 \times 10^{-5}$	$9.21 \times 10^{-4}$	$9.35 \times 10^{-4}$	$5.57 \times 10^{-1}$
$2.58 \times 10^{-5}$	$1.15 \times 10^{-3}$		$7.18 \times 10^{-1}$
$2.58 \times 10^{-5}$	$1.38 \times 10^{-3}$	$1.87 \times 10^{-3}$	$8.73 \times 10^{-1}$
$2.58 \times 10^{-5}$	$1.61 \times 10^{-4}$		1.03

$$k_2 = 6.74 \times 10^4 \text{ L mol}^{-1} \text{ s}^{-1}$$

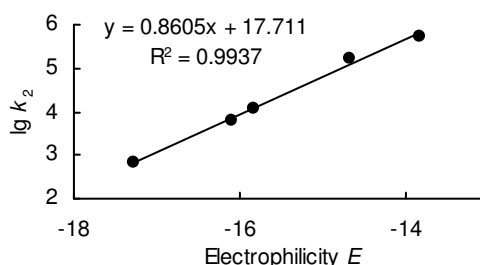


### Determination of Reactivity Parameters $N$ and $s_N$ for Potassium Cyclopentadienide (**6-K**) in DMSO

Table 16: Rate Constants for the reactions of **6-K** with different electrophiles.<sup>[RA]</sup>

Electrophile	$E$	$k_2 / \text{L mol}^{-1} \text{ s}^{-1}$	$\lg k_2$
<b>4</b>	-13.84	$5.07 \times 10^5$	5.71
<b>5</b>	-14.68	$1.69 \times 10^5$	5.23
<b>2b</b>	-15.83	$1.21 \times 10^4$	4.08
<b>2c</b>	-16.11	$6.39 \times 10^3$	3.81
<b>2d</b>	-17.29	$6.74 \times 10^2$	2.83

$$N = 20.58, s_N = 0.86$$



#### 4.4.1.3. Reactions of Sodium Cyclopentadienide (**6-Na**)

Table 17: Kinetics of the reaction of **6-Na** with **4** (20 °C, stopped-flow, at 520 nm).<sup>[RA]</sup>

[ <b>4</b> ] / mol L <sup>-1</sup>	[ <b>6-Na</b> ] / mol L <sup>-1</sup>	$k_{\text{obs}}$ / s <sup>-1</sup>
$2.53 \times 10^{-5}$	$2.95 \times 10^{-4}$	$1.31 \times 10^2$
$2.53 \times 10^{-5}$	$4.43 \times 10^{-4}$	$2.00 \times 10^2$
$2.53 \times 10^{-5}$	$5.90 \times 10^{-4}$	$2.69 \times 10^2$
$2.53 \times 10^{-5}$	$7.38 \times 10^{-4}$	$3.41 \times 10^2$
$2.53 \times 10^{-5}$	$8.86 \times 10^{-4}$	$4.10 \times 10^2$

$$k_2 = 4.74 \times 10^5 \text{ L mol}^{-1} \text{ s}^{-1}$$

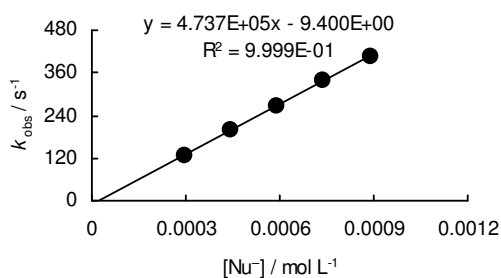
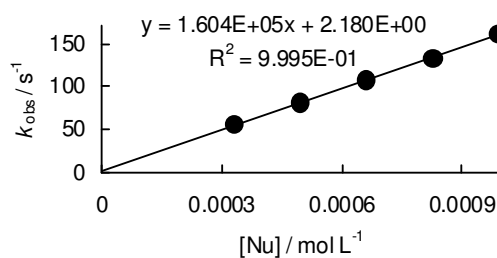


Table 18: Kinetics of the reaction of **6**-Na with **5** (20 °C, stopped-flow, at 520 nm).<sup>[RA]</sup>

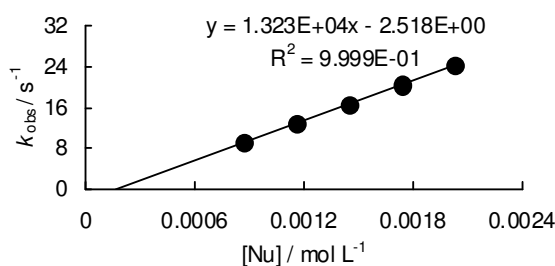
[ <b>5</b> ] / mol L <sup>-1</sup>	[ <b>6</b> -Na] / mol L <sup>-1</sup>	$k_{\text{obs}}$ / s <sup>-1</sup>
$2.56 \times 10^{-5}$	$3.30 \times 10^{-4}$	$5.56 \times 10^1$
$2.56 \times 10^{-5}$	$4.95 \times 10^{-4}$	$8.13 \times 10^1$
$2.56 \times 10^{-5}$	$6.60 \times 10^{-4}$	$1.08 \times 10^2$
$2.56 \times 10^{-5}$	$8.24 \times 10^{-4}$	$1.33 \times 10^2$
$2.56 \times 10^{-5}$	$9.89 \times 10^{-4}$	$1.62 \times 10^2$

$$k_2 = 1.60 \times 10^5 \text{ L mol}^{-1} \text{ s}^{-1}$$

Table 19: Kinetics of the reaction of **6**-Na with **2b** (20 °C, stopped-flow, at 371 nm).<sup>[RA]</sup>

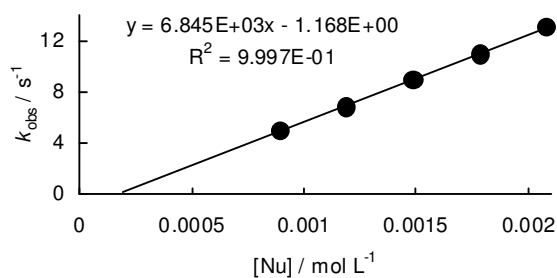
[ <b>2b</b> ] / mol L <sup>-1</sup>	[ <b>6</b> -Na] / mol L <sup>-1</sup>	$k_{\text{obs}}$ / s <sup>-1</sup>
$2.50 \times 10^{-5}$	$8.70 \times 10^{-4}$	9.06
$2.50 \times 10^{-5}$	$1.16 \times 10^{-3}$	12.8
$2.50 \times 10^{-5}$	$1.45 \times 10^{-3}$	16.6
$2.50 \times 10^{-5}$	$1.74 \times 10^{-3}$	2.05
$2.50 \times 10^{-5}$	$2.03 \times 10^{-3}$	24.4

$$k_2 = 1.32 \times 10^4 \text{ L mol}^{-1} \text{ s}^{-1}$$

Table 20: Kinetics of the reaction of **6**-Na with **2c** (20 °C, stopped-flow, at 393 nm).<sup>[RA]</sup>

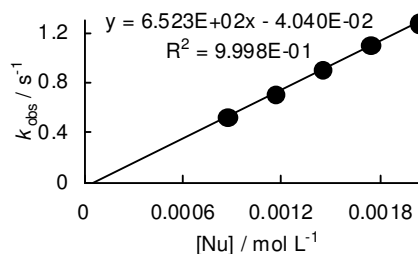
[ <b>2c</b> ] / mol L <sup>-1</sup>	[ <b>6</b> -Na] / mol L <sup>-1</sup>	$k_{\text{obs}}$ / s <sup>-1</sup>
$2.50 \times 10^{-5}$	$8.91 \times 10^{-4}$	4.99
$2.50 \times 10^{-5}$	$1.19 \times 10^{-3}$	6.90
$2.50 \times 10^{-5}$	$1.48 \times 10^{-3}$	8.97
$2.50 \times 10^{-5}$	$1.78 \times 10^{-3}$	11.0
$2.50 \times 10^{-5}$	$2.08 \times 10^{-3}$	13.1

$$k_2 = 6.85 \times 10^3 \text{ L mol}^{-1} \text{ s}^{-1}$$

Table 21: Kinetics of the reaction of **6**-Na with **2d** (20 °C, stopped-flow, at 486 nm).<sup>[RA]</sup>

[ <b>2d</b> ] / mol L <sup>-1</sup>	[ <b>6</b> -Na] / mol L <sup>-1</sup>	$k_{\text{obs}}$ / s <sup>-1</sup>
$2.58 \times 10^{-5}$	$8.70 \times 10^{-4}$	$5.28 \times 10^{-1}$
$2.58 \times 10^{-5}$	$1.16 \times 10^{-3}$	$7.12 \times 10^{-1}$
$2.58 \times 10^{-5}$	$1.45 \times 10^{-3}$	$9.08 \times 10^{-1}$
$2.58 \times 10^{-5}$	$1.74 \times 10^{-3}$	1.10
$2.58 \times 10^{-5}$	$2.03 \times 10^{-3}$	1.28

$$k_2 = 6.52 \times 10^2 \text{ L mol}^{-1} \text{ s}^{-1}$$

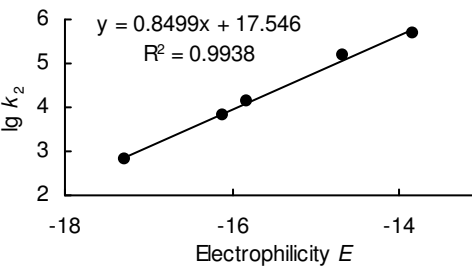


### Determination of Reactivity Parameters $N$ and $s_N$ for Sodium Cyclopentadienide (**6-Na**) in DMSO

Table 22: Rate Constants for the reactions of **6-Na** with different electrophiles.<sup>[RA]</sup>

Electrophile	$E$	$k_2 / \text{L mol}^{-1} \text{s}^{-1}$	$\lg k_2$
<b>4</b>	-13.84	$4.74 \times 10^5$	5.68
<b>5</b>	-14.68	$1.60 \times 10^5$	5.20
<b>2b</b>	-15.83	$1.32 \times 10^4$	4.12
<b>2c</b>	-16.11	$6.85 \times 10^3$	3.84
<b>2d</b>	-17.29	$6.52 \times 10^2$	2.81

$N = 20.64, s_N = 0.85$

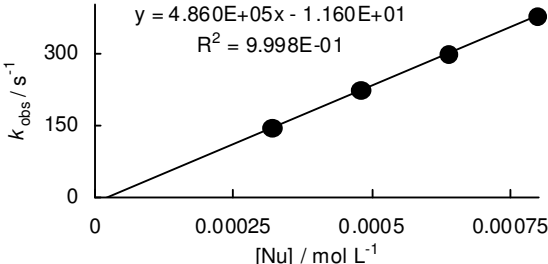


#### 4.4.1.4. Reactions of Lithium Cyclopentadienide (**6-Li**)

Table 23: Kinetics of the reaction of **6-Li** with **4** (20 °C, stopped-flow, at 520 nm).<sup>[RA]</sup>

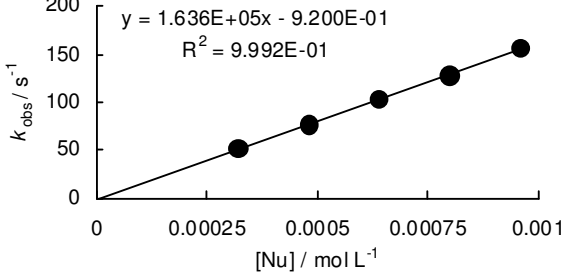
$[\mathbf{4}] / \text{mol L}^{-1}$	$[\mathbf{6-Li}] / \text{mol L}^{-1}$	$k_{\text{obs}} / \text{s}^{-1}$
$2.51 \times 10^{-5}$	$3.19 \times 10^{-4}$	$1.43 \times 10^2$
$2.51 \times 10^{-5}$	$4.79 \times 10^{-4}$	$2.23 \times 10^2$
$2.51 \times 10^{-5}$	$6.39 \times 10^{-4}$	$2.97 \times 10^2$
$2.51 \times 10^{-5}$	$7.98 \times 10^{-4}$	$3.77 \times 10^2$

$k_2 = 4.86 \times 10^5 \text{ L mol}^{-1} \text{s}^{-1}$


Table 24: Kinetics of the reaction of **6-Li** with **5** (20 °C, stopped-flow, at 520 nm).<sup>[RA]</sup>

$[\mathbf{5}] / \text{mol L}^{-1}$	$[\mathbf{6-Li}] / \text{mol L}^{-1}$	$k_{\text{obs}} / \text{s}^{-1}$
$2.56 \times 10^{-5}$	$3.19 \times 10^{-4}$	$5.20 \times 10^1$
$2.56 \times 10^{-5}$	$4.79 \times 10^{-4}$	$7.68 \times 10^1$
$2.56 \times 10^{-5}$	$6.39 \times 10^{-4}$	$1.04 \times 10^2$
$2.56 \times 10^{-5}$	$7.98 \times 10^{-4}$	$1.28 \times 10^2$
$2.56 \times 10^{-5}$	$9.58 \times 10^{-4}$	$1.58 \times 10^2$

$k_2 = 1.64 \times 10^5 \text{ L mol}^{-1} \text{s}^{-1}$


Table 25: Kinetics of the reaction of **6-Li** with **2b** (20 °C, stopped-flow, at 371 nm).<sup>[RA]</sup>

$[\mathbf{2b}] / \text{mol L}^{-1}$	$[\mathbf{6-Li}] / \text{mol L}^{-1}$	$k_{\text{obs}} / \text{s}^{-1}$
$2.49 \times 10^{-5}$	$9.87 \times 10^{-4}$	$1.06 \times 10^1$
$2.49 \times 10^{-5}$	$1.32 \times 10^{-3}$	$1.45 \times 10^1$
$2.49 \times 10^{-5}$	$1.65 \times 10^{-3}$	$1.86 \times 10^1$
$2.49 \times 10^{-5}$	$1.97 \times 10^{-3}$	$2.29 \times 10^1$
$2.49 \times 10^{-5}$	$2.30 \times 10^{-3}$	$2.74 \times 10^1$

$k_2 = 1.28 \times 10^4 \text{ L mol}^{-1} \text{s}^{-1}$

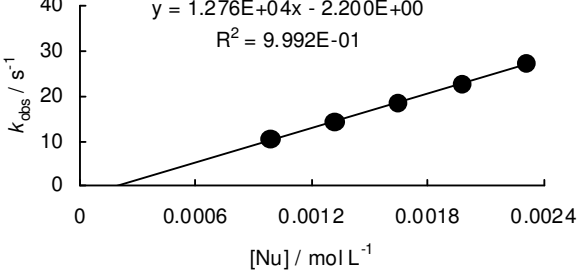
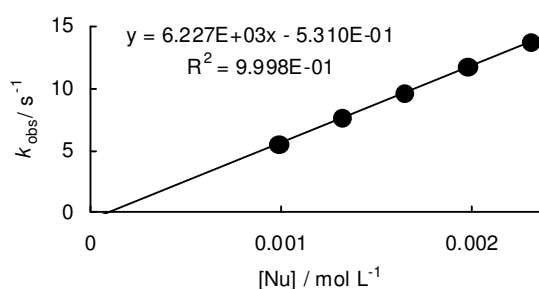


Table 26: Kinetics of the reaction of **6**-Li with **2c** (20 °C, stopped-flow, at 393 nm).<sup>[RA]</sup>

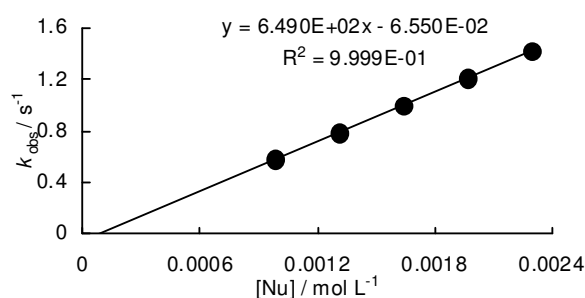
[ <b>2c</b> ] / mol L <sup>-1</sup>	[ <b>6</b> -Li] / mol L <sup>-1</sup>	$k_{\text{obs}}$ / s <sup>-1</sup>
$2.55 \times 10^{-5}$	$9.87 \times 10^{-4}$	5.60
$2.55 \times 10^{-5}$	$1.32 \times 10^{-3}$	7.71
$2.55 \times 10^{-5}$	$1.65 \times 10^{-3}$	9.66
$2.55 \times 10^{-5}$	$1.97 \times 10^{-3}$	11.8
$2.55 \times 10^{-5}$	$2.30 \times 10^{-3}$	13.8

$$k_2 = 6.23 \times 10^4 \text{ L mol}^{-1} \text{ s}^{-1}$$

Table 27: Kinetics of the reaction of **6**-Li with **2d** (20 °C, stopped-flow, at 486 nm).<sup>[RA]</sup>

[ <b>2d</b> ] / mol L <sup>-1</sup>	[ <b>6</b> -Li] / mol L <sup>-1</sup>	$k_{\text{obs}}$ / s <sup>-1</sup>
$2.58 \times 10^{-5}$	$9.85 \times 10^{-4}$	$5.78 \times 10^{-1}$
$2.58 \times 10^{-5}$	$1.31 \times 10^{-3}$	$7.83 \times 10^{-1}$
$2.58 \times 10^{-5}$	$1.64 \times 10^{-3}$	$9.99 \times 10^{-1}$
$2.58 \times 10^{-5}$	$1.97 \times 10^{-3}$	1.21
$2.58 \times 10^{-5}$	$2.30 \times 10^{-3}$	1.43

$$k_2 = 6.49 \times 10^2 \text{ L mol}^{-1} \text{ s}^{-1}$$

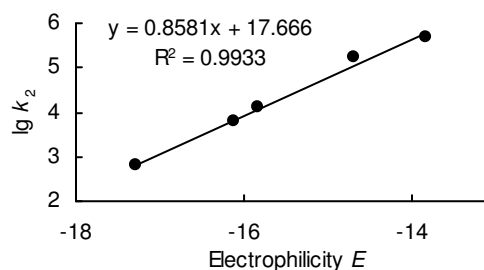


### Determination of Reactivity Parameters $N$ and $s_N$ for Lithium Cyclopentadienide (**6**-Li) in DMSO

Table 28: Rate Constants for the reactions of **6**-Li with different electrophiles.<sup>[RA]</sup>

Electrophile	$E$	$k_2$ / L mol <sup>-1</sup> s <sup>-1</sup>	$\lg k_2$
<b>4</b>	-13.84	$4.86 \times 10^5$	5.69
<b>5</b>	-14.68	$1.64 \times 10^5$	5.21
<b>2b</b>	-15.83	$1.28 \times 10^4$	4.11
<b>2c</b>	-16.11	$6.23 \times 10^3$	3.79
<b>2d</b>	-17.29	$6.49 \times 10^2$	2.81

$$N = 20.59, s_N = 0.86$$



#### 4.4.1.5. Reactions of Potassium Indenide (**7**-K)

Table 29: Kinetics of the reaction of **7**-K (generated from **7**-H by addition of 1.05 equiv. KO<sup>t</sup>Bu) with **2a** (20 °C, stopped-flow, at 354 nm).

[ <b>2a</b> ] / mol L <sup>-1</sup>	[ <b>7</b> -K] / mol L <sup>-1</sup>	[ <b>7</b> -K]/[ <b>2c</b> ]	$k_{\text{obs}}$ / s <sup>-1</sup>
$9.41 \times 10^{-6}$	$5.83 \times 10^{-5}$	6.20	68.3
$9.41 \times 10^{-6}$	$7.00 \times 10^{-5}$	7.44	83.9
$9.41 \times 10^{-6}$	$8.17 \times 10^{-5}$	8.68	113
$9.41 \times 10^{-6}$	$9.33 \times 10^{-5}$	9.92	140
$9.41 \times 10^{-6}$	$1.28 \times 10^{-4}$	13.64	216

$$k_2 = 2.16 \times 10^6 \text{ L mol}^{-1} \text{ s}^{-1}$$

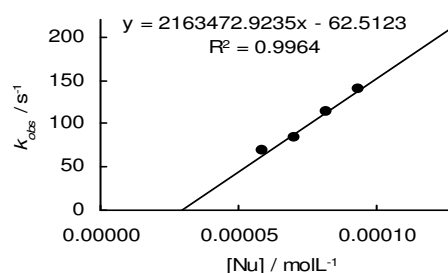
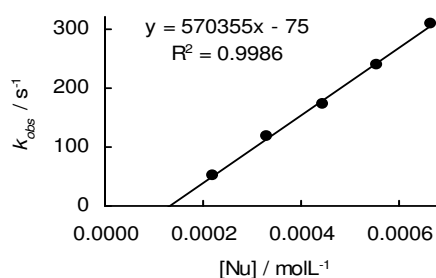




Table 30: Kinetics of the reaction of **7-K** (generated from **7-H** by addition of 1.05 equiv. KO<sup>t</sup>Bu) with **2b** (20 °C, stopped-flow, at 371 nm).

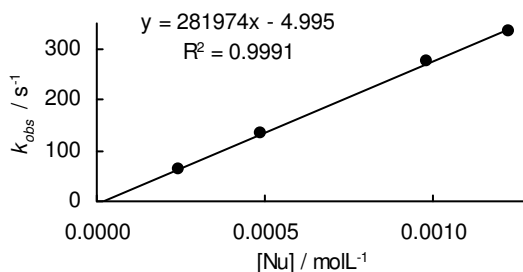
[ <b>2b</b> ] / mol L <sup>-1</sup>	[ <b>7-K</b> ] / mol L <sup>-1</sup>	[ <b>7-K</b> ]/[ <b>2d</b> ]	$k_{\text{obs}} /$ s <sup>-1</sup>
$2.27 \times 10^{-5}$	$2.22 \times 10^{-4}$	9.79	51.8
$2.27 \times 10^{-5}$	$3.33 \times 10^{-4}$	14.7	119
$2.27 \times 10^{-5}$	$4.44 \times 10^{-4}$	19.6	173
$2.27 \times 10^{-5}$	$5.55 \times 10^{-4}$	24.5	240
$2.27 \times 10^{-5}$	$6.66 \times 10^{-4}$	29.4	308

$$k_2 = 5.70 \times 10^5 \text{ L mol}^{-1} \text{ s}^{-1}$$

Table 31: Kinetics of the reaction of **7-K** (generated from **7-H** by addition of 1.05 equiv. KO<sup>t</sup>Bu) with **2c** (20 °C, stopped-flow, at 393 nm).

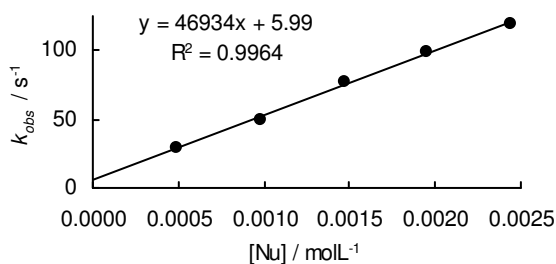
[ <b>2c</b> ] / mol L <sup>-1</sup>	[ <b>7-K</b> ] / mol L <sup>-1</sup>	[18-crown-6] / mol L <sup>-1</sup>	$k_{\text{obs}} /$ s <sup>-1</sup>
$2.11 \times 10^{-5}$	$2.44 \times 10^{-4}$		63.3
$2.11 \times 10^{-5}$	$4.89 \times 10^{-4}$	$5.77 \times 10^{-4}$	132
$2.11 \times 10^{-5}$	$9.78 \times 10^{-4}$	$1.15 \times 10^{-3}$	276
$2.11 \times 10^{-5}$	$1.22 \times 10^{-3}$		336

$$k_2 = 2.82 \times 10^5 \text{ L mol}^{-1} \text{ s}^{-1}$$

Table 32: Kinetics of the reaction of **7-K** (generated from **7-H** by addition of 1.05 equiv. KO<sup>t</sup>Bu) with **2d** (20 °C, stopped-flow, at 486 nm).

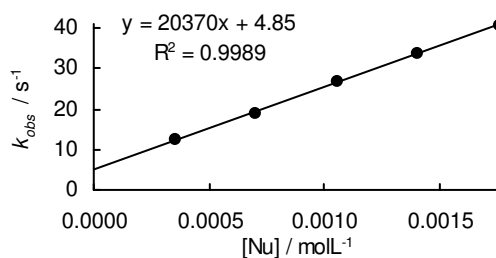
[ <b>2d</b> ] / mol L <sup>-1</sup>	[ <b>7-K</b> ] / mol L <sup>-1</sup>	[18-crown-6] / mol L <sup>-1</sup>	$k_{\text{obs}} /$ s <sup>-1</sup>
$2.03 \times 10^{-5}$	$4.89 \times 10^{-4}$		29.2
$2.03 \times 10^{-5}$	$9.78 \times 10^{-4}$	$1.09 \times 10^{-3}$	49.3
$2.03 \times 10^{-5}$	$1.47 \times 10^{-3}$		77.5
$2.03 \times 10^{-5}$	$1.96 \times 10^{-3}$	$2.19 \times 10^{-3}$	99.2
$2.03 \times 10^{-5}$	$2.44 \times 10^{-3}$		119

$$k_2 = 4.69 \times 10^4 \text{ L mol}^{-1} \text{ s}^{-1}$$

Table 33: Kinetics of the reaction of **7-K** (generated from **7-H** by addition of 1.06 equiv. KO<sup>t</sup>Bu) with **2e** (20 °C, stopped-flow, at 521 nm).

[ <b>2e</b> ] / mol L <sup>-1</sup>	[ <b>7-K</b> ] / mol L <sup>-1</sup>	[18-crown-6] / mol L <sup>-1</sup>	$k_{\text{obs}} /$ s <sup>-1</sup>
$1.87 \times 10^{-5}$	$3.53 \times 10^{-4}$		12.2
$1.87 \times 10^{-5}$	$7.06 \times 10^{-4}$	$7.87 \times 10^{-4}$	18.7
$1.87 \times 10^{-5}$	$1.06 \times 10^{-3}$		26.9
$1.87 \times 10^{-5}$	$1.41 \times 10^{-3}$	$1.57 \times 10^{-3}$	33.6
$1.87 \times 10^{-5}$	$1.76 \times 10^{-3}$		40.7

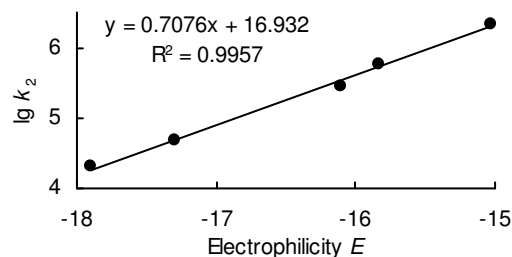
$$k_2 = 2.04 \times 10^4 \text{ L mol}^{-1} \text{ s}^{-1}$$



Determination of Reactivity Parameters  $N$  and  $s_N$  for Potassium Indenide (**7-K**) in DMSOTable 34: Rate Constants for the reactions of **7-K** with different electrophiles.

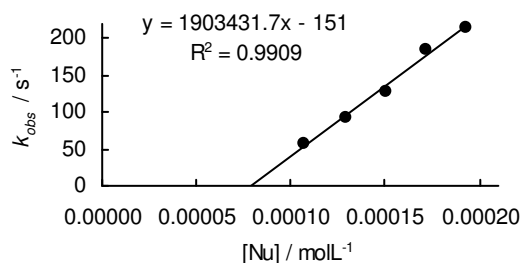
Electrophile	$E$	$k_2 / \text{L mol}^{-1} \text{s}^{-1}$	$\lg k_2$
<b>2a</b>	-15.03	$2.16 \times 10^6$	6.33
<b>2b</b>	-15.83	$5.70 \times 10^5$	5.76
<b>2c</b>	-16.11	$2.82 \times 10^5$	5.45
<b>2d</b>	-17.29	$4.69 \times 10^4$	4.67
<b>2e</b>	-17.90	$2.04 \times 10^4$	4.31

$$N = 23.93, s_N = 0.71$$

**4.4.1.6. Reactions of Sodium Indenide (**7-Na**)**Table 35: Kinetics of the reaction of **7-Na** (generated from **7-H** by addition of 1.07 equiv. NaOtBu) with **2a** (20 °C, stopped-flow, at 354 nm).

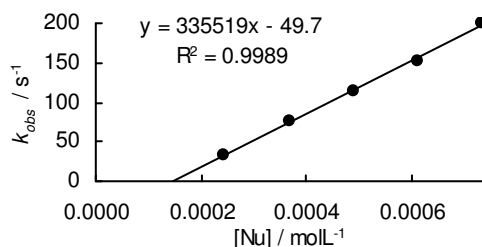
$[\mathbf{2a}] / \text{mol L}^{-1}$	$[\mathbf{7-Na}] / \text{mol L}^{-1}$	$[\mathbf{7-Na}]/[\mathbf{2a}]$	$k_{\text{obs}} / \text{s}^{-1}$
$9.41 \times 10^{-6}$	$1.07 \times 10^{-4}$	11.4	56.5
$9.41 \times 10^{-6}$	$1.29 \times 10^{-4}$	13.7	91.3
$9.41 \times 10^{-6}$	$1.50 \times 10^{-4}$	16.0	128
$9.41 \times 10^{-6}$	$1.72 \times 10^{-4}$	18.3	185
$9.41 \times 10^{-6}$	$1.93 \times 10^{-4}$	20.5	214

$$k_2 = 1.90 \times 10^6 \text{ L mol}^{-1} \text{s}^{-1}$$

Table 36: Kinetics of the reaction of **7-Na** (generated from **7-H** by addition of 1.05 equiv. NaOtBu) with **2b** (20 °C, stopped-flow, at 371 nm).

$[\mathbf{2b}] / \text{mol L}^{-1}$	$[\mathbf{7-Na}] / \text{mol L}^{-1}$	$[\mathbf{7-Na}]/[\mathbf{2b}]$	$k_{\text{obs}} / \text{s}^{-1}$
$2.45 \times 10^{-5}$	$2.45 \times 10^{-4}$	10.0	31.7
$2.45 \times 10^{-5}$	$3.68 \times 10^{-4}$	15.0	76.0
$2.45 \times 10^{-5}$	$4.91 \times 10^{-4}$	20.0	115
$2.45 \times 10^{-5}$	$6.13 \times 10^{-4}$	25.0	153
$2.45 \times 10^{-5}$	$7.36 \times 10^{-4}$	30.0	199

$$k_2 = 3.36 \times 10^5 \text{ L mol}^{-1} \text{s}^{-1}$$

Table 37: Kinetics of the reaction of **7-Na** (generated from **7-H** by addition of 1.06 equiv. NaOtBu) with **2c** (20 °C, stopped-flow, at 371 nm).

$[\mathbf{2c}] / \text{mol L}^{-1}$	$[\mathbf{7-Na}] / \text{mol L}^{-1}$	$[\mathbf{7-Na}]/[\mathbf{2c}]$	$k_{\text{obs}} / \text{s}^{-1}$
$2.45 \times 10^{-5}$	$2.31 \times 10^{-4}$	10.1	52.0
$2.45 \times 10^{-5}$	$4.61 \times 10^{-4}$	20.1	113
$2.45 \times 10^{-5}$	$7.50 \times 10^{-4}$	32.7	182
$2.45 \times 10^{-5}$	$9.23 \times 10^{-4}$	40.3	221
$2.45 \times 10^{-5}$	$1.15 \times 10^{-3}$	50.3	271

$$k_2 = 2.37 \times 10^5 \text{ L mol}^{-1} \text{s}^{-1}$$

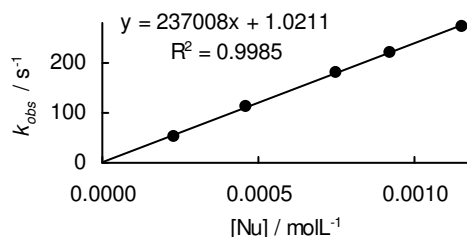
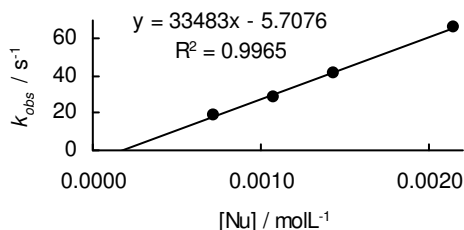


Table 38: Kinetics of the reaction of **7**-Na (generated from **7**-H by addition of 1.04 equiv. NaOtBu) with **2d** (20 °C, stopped-flow, at 393 nm).

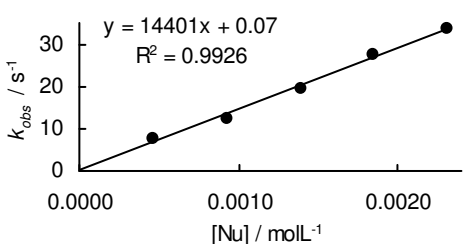
[ <b>2d</b> ] / mol L <sup>-1</sup>	[ <b>7</b> -Na] / mol L <sup>-1</sup>	[ <b>7</b> -Na]/[ <b>2d</b> ]	$k_{\text{obs}} /$ s <sup>-1</sup>
$2.96 \times 10^{-5}$	$7.15 \times 10^{-4}$	24.1	19.5
$2.96 \times 10^{-5}$	$1.07 \times 10^{-3}$	36.2	28.6
$2.96 \times 10^{-5}$	$1.43 \times 10^{-3}$	48.2	42.1
$2.96 \times 10^{-5}$	$2.14 \times 10^{-3}$	72.3	66.5

$$k_2 = 3.35 \times 10^4 \text{ L mol}^{-1} \text{ s}^{-1}$$

Table 39: Kinetics of the reaction of **7**-Na (generated from **7**-H by addition of 1.06 equiv. NaOtBu) with **2d** (20 °C, stopped-flow, at 521 nm).

[ <b>2e</b> ] / mol L <sup>-1</sup>	[ <b>7</b> -Na] / mol L <sup>-1</sup>	[ <b>7</b> -Na]/[ <b>2e</b> ]	$k_{\text{obs}} /$ s <sup>-1</sup>
$1.83 \times 10^{-5}$	$4.63 \times 10^{-4}$	25.3	7.80
$1.83 \times 10^{-5}$	$9.26 \times 10^{-4}$	50.5	12.4
$1.83 \times 10^{-5}$	$1.39 \times 10^{-3}$	75.8	19.2
$1.83 \times 10^{-5}$	$1.85 \times 10^{-3}$	101	27.3
$1.83 \times 10^{-5}$	$2.32 \times 10^{-3}$	126	33.7

$$k_2 = 1.44 \times 10^4 \text{ L mol}^{-1} \text{ s}^{-1}$$

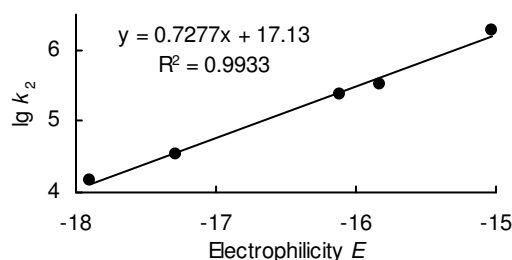


#### Determination of Reactivity Parameters $N$ and $s_N$ for Sodium Indenide (**7**-Na) in DMSO

Table 40: Rate Constants for the reactions of **7**-Na with different electrophiles.

Electrophile	$E$	$k_2 / \text{L mol}^{-1} \text{ s}^{-1}$	$\lg k_2$
<b>2a</b>	-15.03	$1.90 \times 10^6$	6.28
<b>2b</b>	-15.83	$3.36 \times 10^5$	5.53
<b>2c</b>	-16.11	$2.37 \times 10^5$	5.37
<b>2d</b>	-17.29	$3.35 \times 10^4$	5.43
<b>2e</b>	-17.90	$1.44 \times 10^4$	4.16

$$N = 23.54, s_N = 0.73$$



#### 4.4.1.7. Reactions of Lithium Indenide (**7**-Li)

Table 41: Kinetics of the reaction of **7**-Li (generated from **7**-H by addition of 1.06 equiv. LiOtBu) with **2a** (20 °C, stopped-flow, at 354 nm).

[ <b>2a</b> ] / mol L <sup>-1</sup>	[ <b>7</b> -Li] / mol L <sup>-1</sup>	[ <b>7</b> -Li]/[ <b>2a</b> ]	$k_{\text{obs}} /$ s <sup>-1</sup>
$9.41 \times 10^{-6}$	$8.32 \times 10^{-5}$	8.84	33.6
$9.41 \times 10^{-6}$	$9.01 \times 10^{-5}$	9.57	41.3
$9.41 \times 10^{-6}$	$1.04 \times 10^{-4}$	11.0	62.0
$9.41 \times 10^{-6}$	$1.11 \times 10^{-4}$	11.8	72.0

$$k_2 = 1.41 \times 10^6 \text{ L mol}^{-1} \text{ s}^{-1}$$

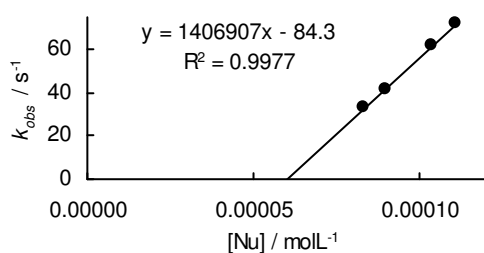
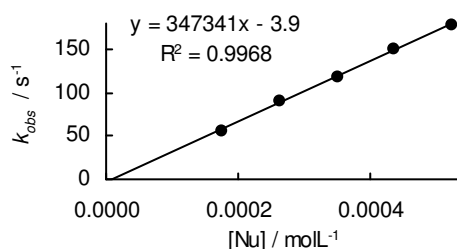


Table 42: Kinetics of the reaction of **7**-Li (generated from **7**-H by addition of 1.05 equiv. LiOtBu) with **2b** (20 °C, stopped-flow, at 371 nm).

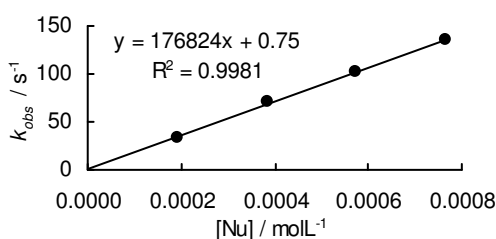
[ <b>2b</b> ] / mol L <sup>-1</sup>	[ <b>7</b> -Li] / mol L <sup>-1</sup>	[ <b>7</b> -Li]/[ <b>2b</b> ]	$k_{\text{obs}} /$ s <sup>-1</sup>
$1.88 \times 10^{-5}$	$1.76 \times 10^{-4}$	9.34	54.5
$1.88 \times 10^{-5}$	$2.63 \times 10^{-4}$	14.0	91.0
$1.88 \times 10^{-5}$	$3.51 \times 10^{-4}$	18.7	117
$1.88 \times 10^{-5}$	$4.39 \times 10^{-4}$	23.4	151
$1.88 \times 10^{-5}$	$5.27 \times 10^{-4}$	28.0	177

$$k_2 = 3.47 \times 10^5 \text{ L mol}^{-1} \text{ s}^{-1}$$

Table 43: Kinetics of the reaction of **7**-Li (generated from **7**-H by addition of 1.08 equiv. LiOtBu) with **2c** (20 °C, stopped-flow, at 393 nm).

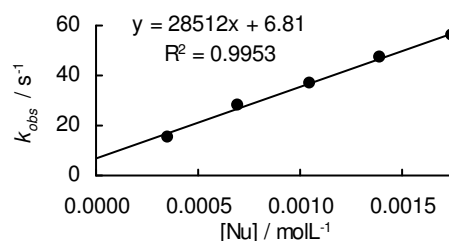
[ <b>2c</b> ] / mol L <sup>-1</sup>	[ <b>7</b> -Li] / mol L <sup>-1</sup>	[ <b>7</b> -Li]/[ <b>2c</b> ]	$k_{\text{obs}} /$ s <sup>-1</sup>
$1.90 \times 10^{-5}$	$1.92 \times 10^{-4}$	10.1	32.8
$1.90 \times 10^{-5}$	$3.83 \times 10^{-4}$	20.2	70.9
$1.90 \times 10^{-5}$	$5.75 \times 10^{-4}$	30.3	103
$1.90 \times 10^{-5}$	$7.66 \times 10^{-4}$	40.4	135

$$k_2 = 1.77 \times 10^4 \text{ L mol}^{-1} \text{ s}^{-1}$$

Table 44: Kinetics of the reaction of **7**-Li (generated from **7**-H by addition of 1.13 equiv. LiOtBu) with **2d** (20 °C, stopped-flow, at 486 nm).

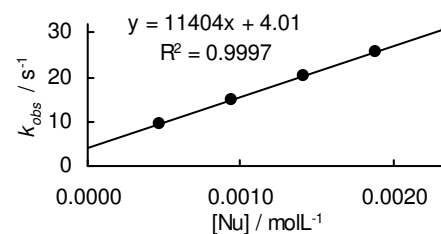
[ <b>2d</b> ] / mol L <sup>-1</sup>	[ <b>7</b> -Li] / mol L <sup>-1</sup>	[ <b>7</b> -Li]/[ <b>2d</b> ]	$k_{\text{obs}} /$ s <sup>-1</sup>
$1.78 \times 10^{-5}$	$3.50 \times 10^{-4}$	19.7	15.5
$1.78 \times 10^{-5}$	$7.01 \times 10^{-4}$	39.4	28.2
$1.78 \times 10^{-5}$	$1.05 \times 10^{-3}$	59.1	37.0
$1.78 \times 10^{-5}$	$1.40 \times 10^{-3}$	78.8	47.3
$1.78 \times 10^{-5}$	$1.75 \times 10^{-3}$	98.5	55.9

$$k_2 = 2.85 \times 10^4 \text{ L mol}^{-1} \text{ s}^{-1}$$

Table 45: Kinetics of the reaction of **7**-Li (generated from **7**-H by addition of 1.05 equiv. LiOtBu) with **2e** (20 °C, stopped-flow, at 521 nm).

[ <b>2e</b> ] / mol L <sup>-1</sup>	[ <b>7</b> -Li] / mol L <sup>-1</sup>	[ <b>7</b> -Li]/[ <b>2e</b> ]	$k_{\text{obs}} /$ s <sup>-1</sup>
$1.69 \times 10^{-5}$	$4.72 \times 10^{-4}$	27.9	9.25
$1.69 \times 10^{-5}$	$9.44 \times 10^{-4}$	55.9	14.8
$1.69 \times 10^{-5}$	$1.42 \times 10^{-3}$	83.8	20.4
$1.69 \times 10^{-5}$	$1.89 \times 10^{-3}$	112	25.5
$1.69 \times 10^{-5}$	$2.36 \times 10^{-3}$	140	30.8

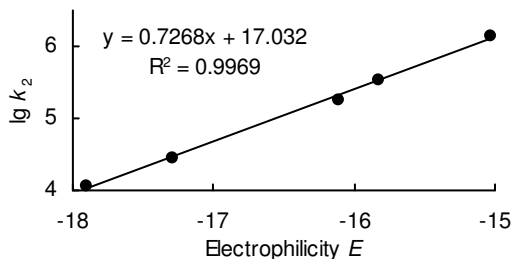
$$k_2 = 1.14 \times 10^4 \text{ L mol}^{-1} \text{ s}^{-1}$$



Determination of Reactivity Parameters  $N$  and  $s_N$  for Lithium Indenide (**7**-Li) in DMSOTable 46: Rate Constants for the reactions of **7**-Li with different electrophiles.

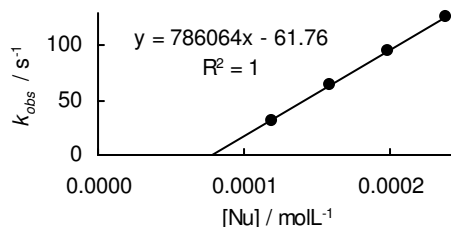
Electrophile	$E$	$k_2 / \text{L mol}^{-1} \text{s}^{-1}$	$\lg k_2$
<b>2a</b>	-15.03	$1.41 \times 10^6$	6.15
<b>2b</b>	-15.83	$3.47 \times 10^5$	5.54
<b>2c</b>	-16.11	$1.77 \times 10^5$	5.25
<b>2d</b>	-17.29	$2.85 \times 10^4$	4.45
<b>2e</b>	-17.90	$1.14 \times 10^4$	4.06

$N = 23.44, s_N = 0.73$

**4.4.1.8. Reactions of Potassium Fluorenone (8-K)**Table 47: Kinetics of the reaction of **8**-K (generated from **8**-H by addition of 1.05 equiv. KO $t$ Bu) with **2d** (20 °C, stopped-flow, at 486 nm).

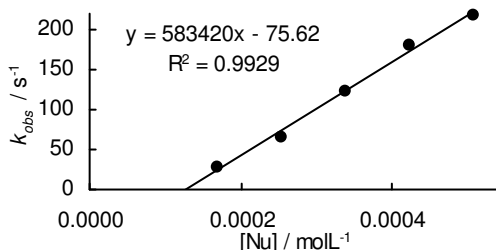
$[\mathbf{2d}] / \text{mol L}^{-1}$	$[\mathbf{8-K}] / \text{mol L}^{-1}$	$[\mathbf{8-K}]/[\mathbf{2d}]$	$k_{\text{obs}} / \text{s}^{-1}$
$8.06 \times 10^{-6}$	$1.20 \times 10^{-4}$	9.34	54.5
$8.06 \times 10^{-6}$	$1.59 \times 10^{-4}$	14.0	91.0
$8.06 \times 10^{-6}$	$1.99 \times 10^{-4}$	18.7	117
$8.06 \times 10^{-6}$	$2.39 \times 10^{-4}$	23.4	151

$k_2 = 7.86 \times 10^5 \text{ L mol}^{-1} \text{s}^{-1}$

Table 48: Kinetics of the reaction of **8**-K (generated from **8**-H by addition of 1.05 equiv. KO $t$ Bu) with **2e** (20 °C, stopped-flow, at 521 nm).

$[\mathbf{2e}] / \text{mol L}^{-1}$	$[\mathbf{8-K}] / \text{mol L}^{-1}$	$[\mathbf{18-crown-6}] / \text{mol L}^{-1}$	$k_{\text{obs}} / \text{s}^{-1}$
$1.45 \times 10^{-5}$	$1.70 \times 10^{-4}$		27.4
$1.45 \times 10^{-5}$	$2.54 \times 10^{-4}$	$2.83 \times 10^{-4}$	64.3
$1.45 \times 10^{-5}$	$3.39 \times 10^{-4}$		123
$1.45 \times 10^{-5}$	$4.24 \times 10^{-4}$	$4.71 \times 10^{-4}$	180
$1.45 \times 10^{-5}$	$5.09 \times 10^{-4}$		217

$k_2 = 5.83 \times 10^5 \text{ L mol}^{-1} \text{s}^{-1}$

Table 49: Kinetics of the reaction of **8**-K (generated from **8**-H by addition of 1.05 equiv. KO $t$ Bu) with **3b** (20 °C, stopped-flow, at 400 nm).

$[\mathbf{3b}] / \text{mol L}^{-1}$	$[\mathbf{8-K}] / \text{mol L}^{-1}$	$[\mathbf{8-K}]/[\mathbf{3b}]$	$k_{\text{obs}} / \text{s}^{-1}$
$2.18 \times 10^{-5}$	$7.25 \times 10^{-4}$	34.8	$4.85 \times 10^{-2}$
$2.18 \times 10^{-5}$	$1.45 \times 10^{-3}$	69.6	$1.22 \times 10^{-1}$
$2.18 \times 10^{-5}$	$2.90 \times 10^{-3}$	139	$2.57 \times 10^{-1}$
$2.18 \times 10^{-5}$	$3.62 \times 10^{-3}$	174	$3.03 \times 10^{-1}$

$k_2 = 8.89 \times 10^1 \text{ L mol}^{-1} \text{s}^{-1}$

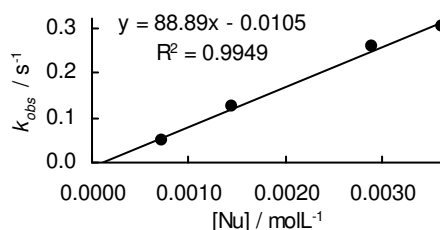
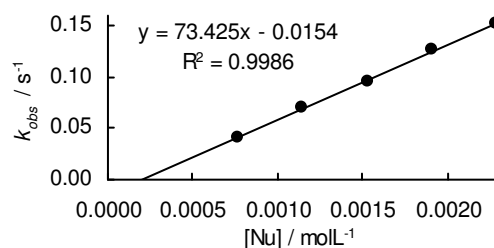


Table 50: Kinetics of the reaction of **8-K** (generated from **8-H** by addition of 1.05 equiv. KOtBu) with **3c** (20 °C, stopped-flow, at 407 nm).

[ <b>3c</b> ] / mol L <sup>-1</sup>	[ <b>8-K</b> ] / mol L <sup>-1</sup>	[18-crown-6] / mol L <sup>-1</sup>	$k_{\text{obs}}$ / s <sup>-1</sup>
$1.60 \times 10^{-5}$	$7.64 \times 10^{-4}$		$4.03 \times 10^{-2}$
$1.60 \times 10^{-5}$	$1.15 \times 10^{-3}$	$1.30 \times 10^{-3}$	$6.99 \times 10^{-2}$
$1.60 \times 10^{-5}$	$1.53 \times 10^{-3}$		$9.48 \times 10^{-2}$
$1.60 \times 10^{-5}$	$1.91 \times 10^{-3}$	$2.13 \times 10^{-3}$	$1.27 \times 10^{-1}$
$1.60 \times 10^{-5}$	$2.29 \times 10^{-3}$		$1.52 \times 10^{-1}$

$$k_2 = 7.34 \times 10^1 \text{ L mol}^{-1} \text{ s}^{-1}$$

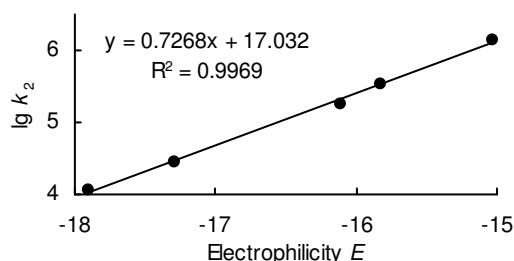


### Determination of Reactivity Parameters $N$ and $s_N$ for Potassium Fluorene (**8-K**) in DMSO

Table 51: Rate Constants for the reactions of **8-K** with different electrophiles.

Electrophile	$E$	$k_2 / \text{L mol}^{-1} \text{ s}^{-1}$	$\lg k_2$
<b>2d</b>	-17.29	$7.86 \times 10^5$	5.90
<b>2e</b>	-17.90	$5.83 \times 10^5$	5.77
<b>3b</b>	-23.10	$8.89 \times 10^1$	1.95
<b>3c</b>	-23.80	$7.37 \times 10^1$	1.87

$$N = 26.35, s_N = 0.66$$

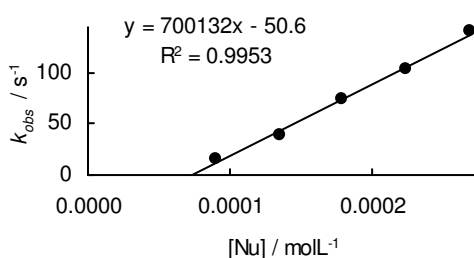


#### 4.4.1.9. Reactions of Sodium Fluorene (**8-Na**)

Table 52: Kinetics of the reaction of **8-Na** (generated from **8-H** by addition of 1.05 equiv. NaOtBu) with **2d** (20 °C, stopped-flow, at 486 nm).

[ <b>2d</b> ] / mol L <sup>-1</sup>	[ <b>8-Na</b> ] / mol L <sup>-1</sup>	[ <b>8-Na</b> ]/[ <b>2d</b> ]	$k_{\text{obs}}$ / s <sup>-1</sup>
$8.09 \times 10^{-6}$	$8.96 \times 10^{-5}$	11.7	16.1
$8.09 \times 10^{-6}$	$1.34 \times 10^{-4}$	17.6	40.0
$8.09 \times 10^{-6}$	$1.79 \times 10^{-4}$	23.4	73.5
$8.09 \times 10^{-6}$	$2.24 \times 10^{-4}$	29.3	104
$8.09 \times 10^{-6}$	$2.69 \times 10^{-4}$	35.1	141

$$k_2 = 7.00 \times 10^5 \text{ L mol}^{-1} \text{ s}^{-1}$$

Table 53: Kinetics of the reaction of **8-Na** (generated from **8-H** by addition of 1.05 equiv. NaOtBu) with **2e** (20 °C, stopped-flow, at 521 nm).

[ <b>2e</b> ] / mol L <sup>-1</sup>	[ <b>8-Na</b> ] / mol L <sup>-1</sup>	[ <b>8-Na</b> ]/[ <b>2e</b> ]	$k_{\text{obs}}$ / s <sup>-1</sup>
$1.69 \times 10^{-5}$	$1.74 \times 10^{-4}$	10.8	29.9
$1.69 \times 10^{-5}$	$3.48 \times 10^{-4}$	21.7	70.4
$1.69 \times 10^{-5}$	$5.22 \times 10^{-4}$	32.5	106
$1.69 \times 10^{-5}$	$6.95 \times 10^{-4}$	43.4	139
$1.69 \times 10^{-5}$	$8.69 \times 10^{-4}$	54.2	171

$$k_2 = 2.02 \times 10^5 \text{ L mol}^{-1} \text{ s}^{-1}$$

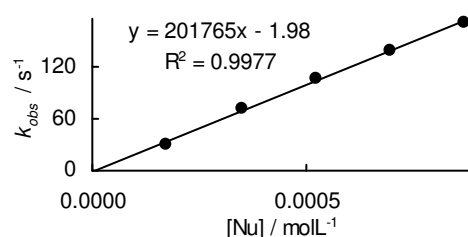
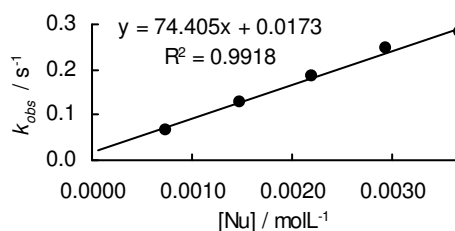


Table 54: Kinetics of the reaction of **8**-Na (generated from **8**-H by addition of 1.06 equiv. NaOtBu) with **3b** (20 °C, stopped-flow, at 400 nm).

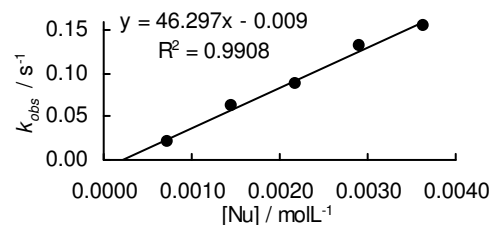
[ <b>3b</b> ] / mol L <sup>-1</sup>	[ <b>8</b> -Na] / mol L <sup>-1</sup>	[ <b>8</b> -Na]/[ <b>3b</b> ]	$k_{\text{obs}}$ / s <sup>-1</sup>
$2.18 \times 10^{-5}$	$7.35 \times 10^{-4}$	35.6	$6.60 \times 10^{-2}$
$2.18 \times 10^{-5}$	$1.47 \times 10^{-4}$	71.1	0.129
$2.18 \times 10^{-5}$	$2.21 \times 10^{-3}$	107	0.185
$2.18 \times 10^{-5}$	$2.94 \times 10^{-3}$	142	0.246
$2.18 \times 10^{-5}$	$3.68 \times 10^{-3}$	178	0.281

$$k_2 = 7.44 \times 10^1 \text{ L mol}^{-1} \text{ s}^{-1}$$

Table 55: Kinetics of the reaction of **8**-Na (generated from **8**-H by addition of 1.04 equiv. NaOtBu) with **3c** (20 °C, stopped-flow, at 407 nm).

[ <b>3c</b> ] / mol L <sup>-1</sup>	[ <b>8</b> -Na] / mol L <sup>-1</sup>	[ <b>8</b> -Na]/[ <b>3c</b> ]	$k_{\text{obs}}$ / s <sup>-1</sup>
$1.61 \times 10^{-5}$	$7.29 \times 10^{-4}$	46.9	$2.17 \times 10^{-2}$
$1.61 \times 10^{-5}$	$1.46 \times 10^{-3}$	93.9	$6.23 \times 10^{-2}$
$1.61 \times 10^{-5}$	$2.19 \times 10^{-3}$	141	$8.90 \times 10^{-2}$
$1.61 \times 10^{-5}$	$2.91 \times 10^{-3}$	188	$1.33 \times 10^{-1}$
$1.61 \times 10^{-5}$	$3.64 \times 10^{-3}$	235	$1.55 \times 10^{-1}$

$$k_2 = 4.63 \times 10^1 \text{ L mol}^{-1} \text{ s}^{-1}$$

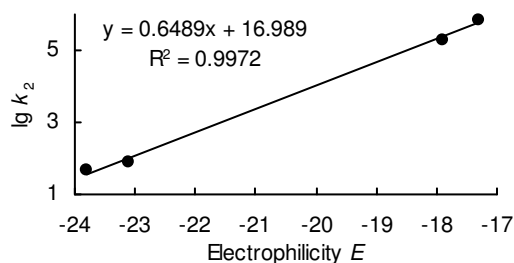


### Determination of Reactivity Parameters $N$ and $s_N$ for Sodium Fluorenyl (8-Na) in DMSO

Table 56: Rate Constants for the reactions of **8**-Na with different electrophiles.

Electrophile	$E$	$k_2$ / L mol <sup>-1</sup> s <sup>-1</sup>	$\lg k_2$
<b>2d</b>	-17.29	$7.00 \times 10^5$	5.85
<b>2e</b>	-17.90	$2.02 \times 10^5$	5.31
<b>3b</b>	-23.10	$7.44 \times 10^1$	1.87
<b>3c</b>	-23.80	$4.63 \times 10^1$	1.67

$$N = 26.18, s_N = 0.65$$



#### 4.4.1.10. Reactions of Lithium Fluorenyl (8-Li)

Table 57: Kinetics of the reaction of **8**-Li (generated from **8**-H by addition of 1.02 equiv. LiOtBu) with **2d** (20 °C, stopped-flow, at 486 nm).

[ <b>2d</b> ] / mol L <sup>-1</sup>	[ <b>8</b> -Li] / mol L <sup>-1</sup>	[ <b>8</b> -Li]/[ <b>2d</b> ]	$k_{\text{obs}}$ / s <sup>-1</sup>
$8.30 \times 10^{-6}$	$1.37 \times 10^{-4}$	16.8	28.0
$8.30 \times 10^{-6}$	$1.83 \times 10^{-4}$	22.4	46.9
$8.30 \times 10^{-6}$	$2.29 \times 10^{-4}$	28.0	69.4
$8.30 \times 10^{-6}$	$2.74 \times 10^{-4}$	33.7	82.0

$$k_2 = 4.03 \times 10^5 \text{ L mol}^{-1} \text{ s}^{-1}$$

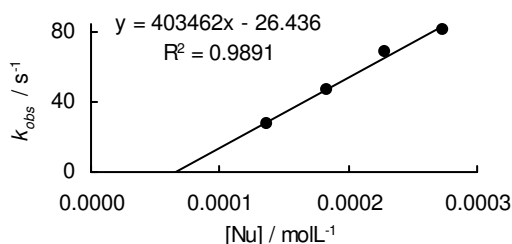
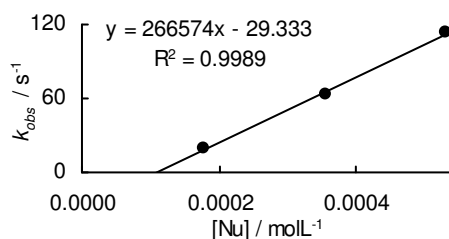


Table 58: Kinetics of the reaction of **8**-Li (generated from **8**-H by addition of 1.05 equiv. LiOtBu) with **2e** (20 °C, stopped-flow, at 521 nm).

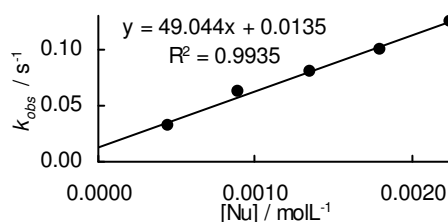
[ <b>2e</b> ] / mol L <sup>-1</sup>	[ <b>8</b> -Li] / mol L <sup>-1</sup>	[ <b>8</b> -Li]/[ <b>2e</b> ]	$k_{\text{obs}}$ / s <sup>-1</sup>
$1.45 \times 10^{-5}$	$1.77 \times 10^{-4}$	12.9	18.7
$1.45 \times 10^{-5}$	$3.54 \times 10^{-4}$	25.7	63.2
$1.45 \times 10^{-5}$	$5.31 \times 10^{-4}$	38.6	113

$$k_2 = 2.67 \times 10^5 \text{ L mol}^{-1} \text{ s}^{-1}$$

Table 59: Kinetics of the reaction of **8**-Li (generated from **8**-H by addition of 1.06 equiv. LiOtBu) with **3b** (20 °C, stopped-flow, at 400 nm).

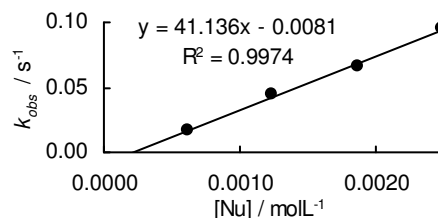
[ <b>3b</b> ] / mol L <sup>-1</sup>	[ <b>8</b> -Li] / mol L <sup>-1</sup>	[ <b>8</b> -Li]/[ <b>3b</b> ]	$k_{\text{obs}}$ / s <sup>-1</sup>
$1.51 \times 10^{-5}$	$4.50 \times 10^{-4}$	31.6	$3.26 \times 10^{-2}$
$1.51 \times 10^{-5}$	$9.00 \times 10^{-4}$	63.2	$6.21 \times 10^{-2}$
$1.51 \times 10^{-5}$	$1.35 \times 10^{-3}$	94.8	$7.97 \times 10^{-2}$
$1.51 \times 10^{-5}$	$1.80 \times 10^{-3}$	126	$1.00 \times 10^{-1}$
$1.51 \times 10^{-5}$	$2.25 \times 10^{-3}$	158	$1.24 \times 10^{-1}$

$$k_2 = 4.90 \times 10^1 \text{ L mol}^{-1} \text{ s}^{-1}$$

Table 60: Kinetics of the reaction of **8**-Li (generated from **8**-H by addition of 1.05 equiv. LiOtBu) with **3c** (20 °C, stopped-flow, at 407 nm).

[ <b>3c</b> ] / mol L <sup>-1</sup>	[ <b>8</b> -Li] / mol L <sup>-1</sup>	[ <b>8</b> -Li]/[ <b>3c</b> ]	$k_{\text{obs}}$ / s <sup>-1</sup>
$1.61 \times 10^{-5}$	$6.21 \times 10^{-4}$	40.5	$1.70 \times 10^{-2}$
$1.61 \times 10^{-5}$	$1.24 \times 10^{-3}$	81.0	$4.47 \times 10^{-2}$
$1.61 \times 10^{-5}$	$1.86 \times 10^{-3}$	122	$6.64 \times 10^{-2}$
$1.61 \times 10^{-5}$	$2.48 \times 10^{-3}$	162	$9.49 \times 10^{-2}$

$$k_2 = 4.11 \times 10^1 \text{ L mol}^{-1} \text{ s}^{-1}$$

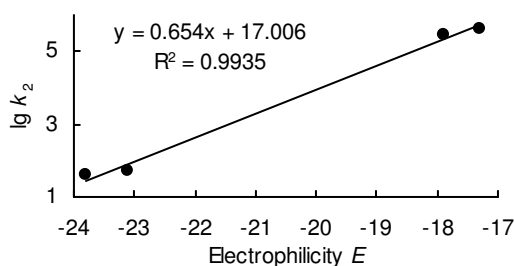


### Determination of Reactivity Parameters $N$ and $s_N$ for Lithium Fluorenyl (8-Li) in DMSO

Table 61: Rate Constants for the reactions of **8**-Li with different electrophiles.

Electrophile	$E$	$k_2$ / L mol <sup>-1</sup> s <sup>-1</sup>	$\lg k_2$
<b>2d</b>	-17.29	$4.03 \times 10^5$	5.61
<b>2e</b>	-17.90	$2.67 \times 10^5$	5.43
<b>3b</b>	-23.10	$4.90 \times 10^1$	1.69
<b>3c</b>	-23.80	$4.11 \times 10^1$	1.61

$$N = 26.00, s_N = 0.65$$





## 4.4.2. Kinetic Experiments of the Zinc Derivatives of 6–8

### 4.4.2.1. Deprotonation Experiments

The formation of the organozinc compounds (6–8)-ZnCl from their conjugate CH acids (6–8)-H, were recorded by using diode array UV-Vis spectrometers. The temperature during all experiments was kept constant by using a circulating bath ( $20.0 \pm 0.02$  °C). Solutions of the CH acids (6–8)-H in dry DMSO were added to a solution of TMP-ZnCl·LiCl (1.06–1.08 eq.) in dry DMSO respectively. After the equilibration of the absorption (4 to 7 min) the mixtures were treated subsequently with various equivalents of TMP-ZnCl·LiCl (dissolved in DMSO). In all cases a full deprotonation of the CH acid with one equivalent of base was monitored (Figure 14).

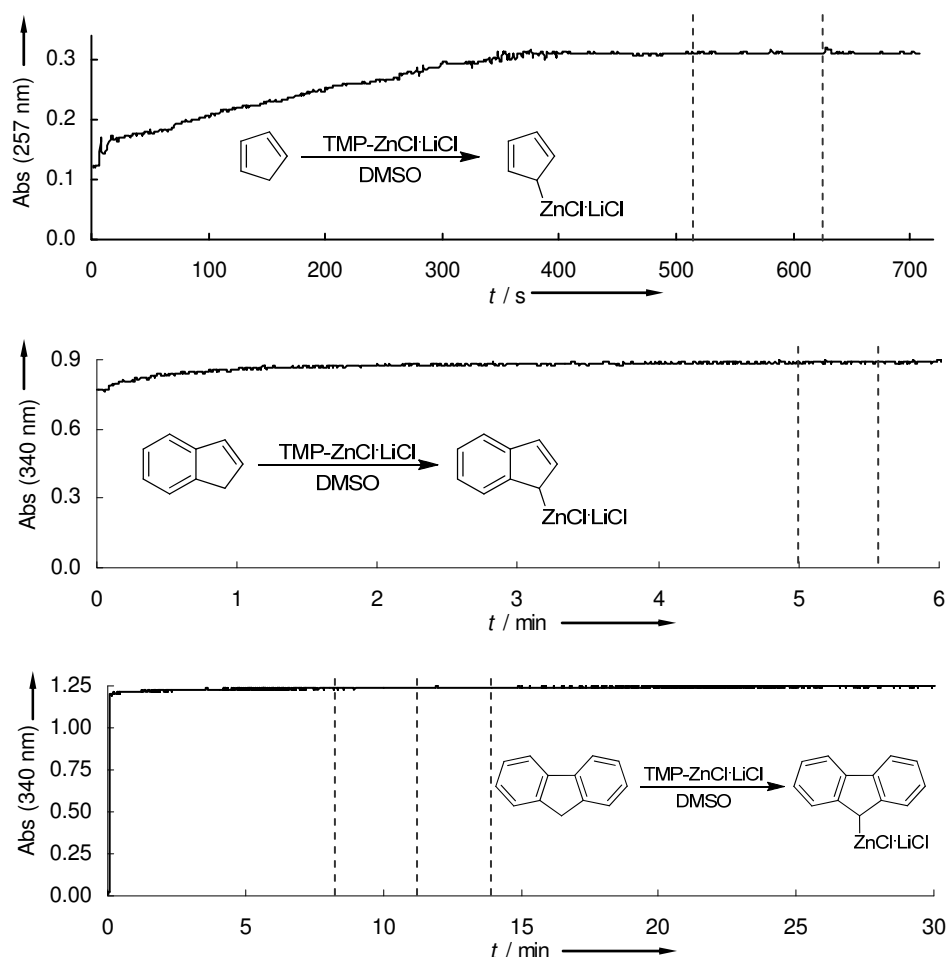
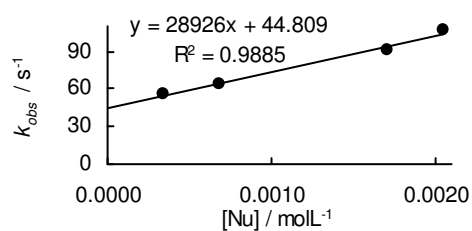


Figure 14: Formation of the organozinc compounds (6–8)-ZnCl from the corresponding CH acid by addition of TMP-ZnCl·LiCl in DMSO at 20 °C. Dashed lines mean an addition equiv. of TMP-ZnCl·LiCl.

4.4.2.2. Reactions of **6**-ZnClTable 62: Kinetics of the reaction of **6**-ZnCl (generated from **6**-H by addition of 1.09 equiv. TMP-ZnCl·LiCl) with **1m** (20 °C, stopped-flow, at 613 nm).

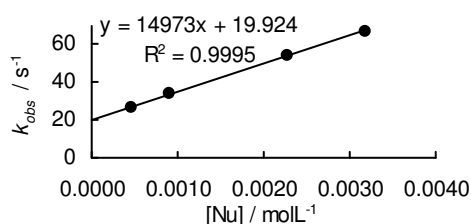
[ <b>1m</b> ] / mol L <sup>-1</sup>	[ <b>6</b> -ZnCl] / mol L <sup>-1</sup>	[ <b>6</b> -ZnCl]/[ <b>1m</b> ]	$k_{\text{obs}} /$ s <sup>-1</sup>
$2.28 \times 10^{-5}$	$3.43 \times 10^{-4}$	15.0	55.5
$2.28 \times 10^{-5}$	$6.85 \times 10^{-4}$	30.1	64.5
$2.28 \times 10^{-5}$	$1.71 \times 10^{-3}$	75.2	91.0
$2.28 \times 10^{-5}$	$2.06 \times 10^{-3}$	90.2	107

$$k_2 = 2.89 \times 10^4 \text{ L mol}^{-1} \text{ s}^{-1}$$

Table 63: Kinetics of the reaction of **6**-ZnCl (generated from **6**-H by addition of 1.05 equiv. TMP-ZnCl·LiCl) with **1n** (20 °C, stopped-flow, at 620 nm).

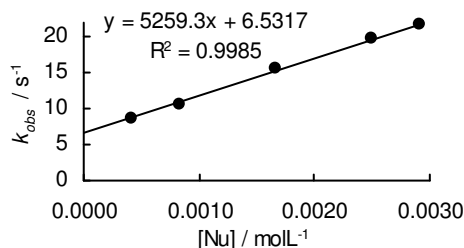
[ <b>1n</b> ] / mol L <sup>-1</sup>	[ <b>6</b> -ZnCl] / mol L <sup>-1</sup>	[ <b>6</b> -ZnCl]/[ <b>1n</b> ]	$k_{\text{obs}} /$ s <sup>-1</sup>
$1.87 \times 10^{-5}$	$4.54 \times 10^{-4}$	24.2	26.4
$1.87 \times 10^{-5}$	$9.08 \times 10^{-4}$	48.4	33.7
$1.87 \times 10^{-5}$	$2.27 \times 10^{-3}$	121	54.4
$1.87 \times 10^{-5}$	$3.18 \times 10^{-3}$	170	67.1

$$k_2 = 1.50 \times 10^4 \text{ L mol}^{-1} \text{ s}^{-1}$$

Table 64: Kinetics of the reaction of **6**-ZnCl (generated from **6**-H by addition of 1.06 equiv. TMP-ZnCl·LiCl) with **1p** (20 °C, stopped-flow, at 627 nm).

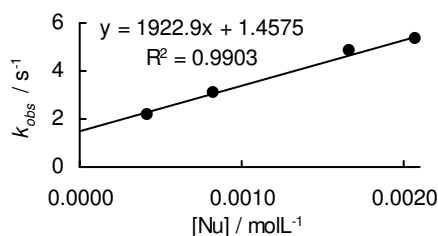
[ <b>1p</b> ] / mol L <sup>-1</sup>	[ <b>6</b> -ZnCl] / mol L <sup>-1</sup>	[ <b>6</b> -ZnCl]/[ <b>1p</b> ]	$k_{\text{obs}} /$ s <sup>-1</sup>
$2.22 \times 10^{-5}$	$4.16 \times 10^{-4}$	18.7	8.77
$2.22 \times 10^{-5}$	$8.32 \times 10^{-4}$	37.4	10.7
$2.22 \times 10^{-5}$	$1.66 \times 10^{-3}$	74.8	15.6
$2.22 \times 10^{-5}$	$2.50 \times 10^{-3}$	112	19.7
$2.22 \times 10^{-5}$	$2.91 \times 10^{-3}$	131	21.7

$$k_2 = 5.26 \times 10^3 \text{ L mol}^{-1} \text{ s}^{-1}$$

Table 65: Kinetics of the reaction of **6**-ZnCl (generated from **6**-H by addition of 1.06 equiv. TMP-ZnCl·LiCl) with **1q** (20 °C, stopped-flow, at 635 nm).

[ <b>1q</b> ] / mol L <sup>-1</sup>	[ <b>6</b> -ZnCl] / mol L <sup>-1</sup>	[ <b>6</b> -ZnCl]/[ <b>1q</b> ]	$k_{\text{obs}} /$ s <sup>-1</sup>
$1.69 \times 10^{-5}$	$4.16 \times 10^{-4}$	24.6	2.18
$1.69 \times 10^{-5}$	$8.32 \times 10^{-4}$	49.3	3.10
$1.69 \times 10^{-5}$	$1.66 \times 10^{-3}$	98.6	4.84
$1.69 \times 10^{-5}$	$2.08 \times 10^{-3}$	123	5.31

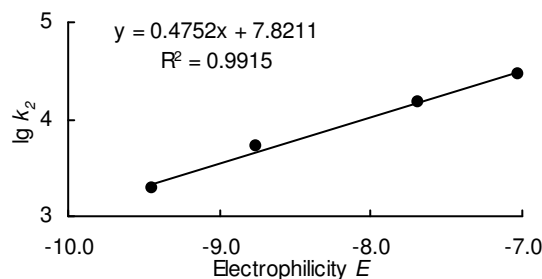
$$k_2 = 1.92 \times 10^3 \text{ L mol}^{-1} \text{ s}^{-1}$$



Determination of Reactivity Parameters  $N$  and  $s_N$  for **6**-Zn in DMSOTable 66: Rate Constants for the reactions of **6**-ZnCl with different electrophiles.

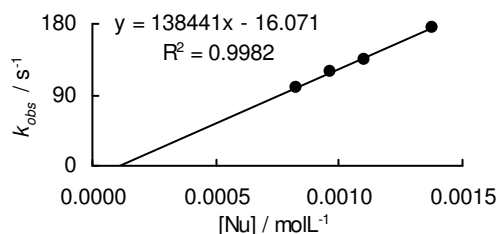
Electrophile	$E$	$k_2 / \text{L mol}^{-1} \text{s}^{-1}$	$\lg k_2$
<b>1m</b>	-7.02	$2.89 \times 10^4$	4.46
<b>1n</b>	-7.69	$1.50 \times 10^4$	4.18
<b>1p</b>	-8.76	$5.26 \times 10^3$	3.72
<b>1q</b>	-9.45	$1.92 \times 10^3$	3.28

$$N = 16.46, s_N = 0.48$$

**4.4.2.3. Reactions of **7**-ZnCl**Table 67: Kinetics of the reaction of **7**-ZnCl (generated from **7**-H by addition of 1.08 equiv. TMP-ZnCl·LiCl) with **1m** (20 °C, stopped-flow, at 613 nm).

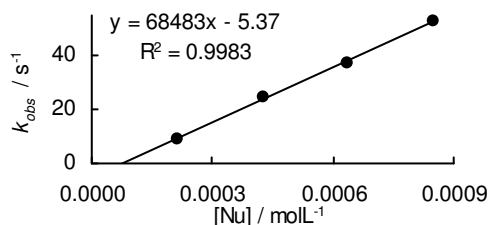
$[\mathbf{1m}] / \text{mol L}^{-1}$	$[\mathbf{7-ZnCl}] / \text{mol L}^{-1}$	$[\mathbf{7-ZnCl}]/[\mathbf{1m}]$	$k_{\text{obs}} / \text{s}^{-1}$
$2.20 \times 10^{-5}$	$8.29 \times 10^{-4}$	37.6	98.8
$2.20 \times 10^{-5}$	$9.67 \times 10^{-4}$	43.9	119
$2.20 \times 10^{-5}$	$1.11 \times 10^{-3}$	50.1	135
$2.20 \times 10^{-5}$	$1.38 \times 10^{-3}$	62.7	176

$$k_2 = 1.38 \times 10^5 \text{ L mol}^{-1} \text{s}^{-1}$$

Table 68: Kinetics of the reaction of **7**-ZnCl (generated from **7**-H by addition of 1.09 equiv. TMP-ZnCl·LiCl) with **1n** (20 °C, stopped-flow, at 620 nm).

$[\mathbf{1n}] / \text{mol L}^{-1}$	$[\mathbf{7-ZnCl}] / \text{mol L}^{-1}$	$[\mathbf{7-ZnCl}]/[\mathbf{1n}]$	$k_{\text{obs}} / \text{s}^{-1}$
$2.04 \times 10^{-5}$	$2.13 \times 10^{-4}$	10.4	8.82
$2.04 \times 10^{-5}$	$4.25 \times 10^{-4}$	20.9	24.7
$2.04 \times 10^{-5}$	$6.38 \times 10^{-4}$	31.3	37.5
$2.04 \times 10^{-5}$	$8.51 \times 10^{-4}$	41.7	53.1

$$k_2 = 6.85 \times 10^4 \text{ L mol}^{-1} \text{s}^{-1}$$

Table 69: Kinetics of the reaction of **7**-ZnCl (generated from **7**-H by addition of 1.05 equiv. TMP-ZnCl·LiCl) with **1p** (20 °C, stopped-flow, at 627 nm).

$[\mathbf{1p}] / \text{mol L}^{-1}$	$[\mathbf{7-ZnCl}] / \text{mol L}^{-1}$	$[\mathbf{7-ZnCl}]/[\mathbf{1p}]$	$k_{\text{obs}} / \text{s}^{-1}$
$1.65 \times 10^{-5}$	$2.20 \times 10^{-4}$	13.3	2.70
$1.65 \times 10^{-5}$	$4.39 \times 10^{-4}$	26.6	6.24
$1.65 \times 10^{-5}$	$6.59 \times 10^{-4}$	40.0	11.3
$1.65 \times 10^{-5}$	$8.78 \times 10^{-4}$	53.3	15.1
$1.65 \times 10^{-5}$	$1.10 \times 10^{-3}$	66.6	19.1

$$k_2 = 1.90 \times 10^4 \text{ L mol}^{-1} \text{s}^{-1}$$

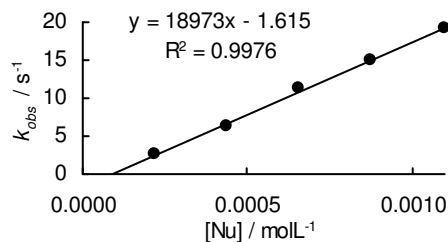
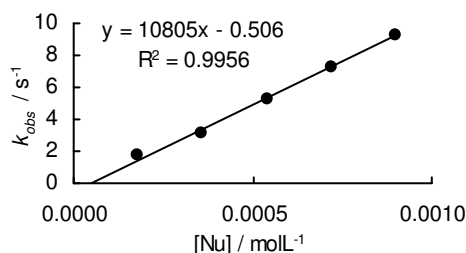


Table 70: Kinetics of the reaction of **7**-ZnCl (generated from **7**-H by addition of 1.06 equiv. TMP-ZnCl·LiCl) with **1q** (20 °C, stopped-flow, at 635 nm).

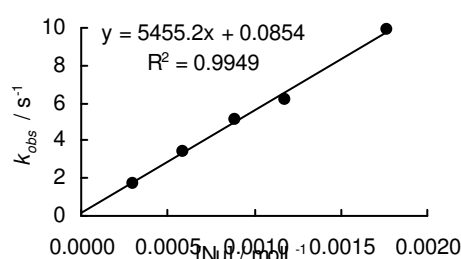
[ <b>1q</b> ] / mol L <sup>-1</sup>	[ <b>7</b> -ZnCl] / mol L <sup>-1</sup>	[ <b>7</b> -ZnCl]/[ <b>1q</b> ]	$k_{\text{obs}}$ / s <sup>-1</sup>
$1.55 \times 10^{-5}$	$1.80 \times 10^{-4}$	11.6	1.69
$1.55 \times 10^{-5}$	$3.60 \times 10^{-4}$	23.2	3.08
$1.55 \times 10^{-5}$	$5.40 \times 10^{-4}$	34.9	5.26
$1.55 \times 10^{-5}$	$7.20 \times 10^{-4}$	46.5	7.30
$1.55 \times 10^{-5}$	$9.00 \times 10^{-4}$	58.1	9.30

$$k_2 = 1.08 \times 10^4 \text{ L mol}^{-1} \text{ s}^{-1}$$

Table 71: Kinetics of the reaction of **7**-ZnCl (generated from **7**-H by addition of 1.06 equiv. TMP-ZnCl·LiCl) with **1r** (20 °C, stopped-flow, at 630 nm).

[ <b>1r</b> ] / mol L <sup>-1</sup>	[ <b>7</b> -ZnCl] / mol L <sup>-1</sup>	[ <b>7</b> -ZnCl]/[ <b>1r</b> ]	$k_{\text{obs}}$ / s <sup>-1</sup>
$1.72 \times 10^{-5}$	$2.95 \times 10^{-4}$	17.1	1.65
$1.72 \times 10^{-5}$	$5.91 \times 10^{-4}$	34.3	3.42
$1.72 \times 10^{-5}$	$8.86 \times 10^{-4}$	51.4	5.09
$1.72 \times 10^{-5}$	$1.18 \times 10^{-3}$	68.5	6.16
$1.72 \times 10^{-5}$	$1.77 \times 10^{-3}$	103	9.88

$$k_2 = 5.46 \times 10^4 \text{ L mol}^{-1} \text{ s}^{-1}$$

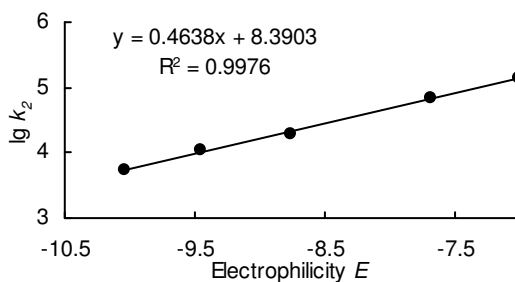


### Determination of Reactivity Parameters $N$ and $s_N$ for **7**-ZnCl in DMSO

Table 72: Rate Constants for the reactions of **7**-ZnCl with different electrophiles.

Electrophile	$E$	$k_2$ / L mol <sup>-1</sup> s <sup>-1</sup>	$\lg k_2$
<b>1m</b>	-7.02	$1.38 \times 10^5$	5.14
<b>1n</b>	-7.69	$6.85 \times 10^4$	4.84
<b>1p</b>	-8.76	$1.90 \times 10^4$	4.28
<b>1q</b>	-9.45	$1.08 \times 10^4$	4.03
<b>1r</b>	-10.04	$5.46 \times 10^3$	3.74

$$N = 18.09, s_N = 0.46$$



#### 4.4.2.4. Reactions of **7**-ZnBr

Table 73: Kinetics of the reaction of **7**-ZnBr (generated from **7**-H by addition of 1.06 equiv. TMP-ZnBr·LiBr) with **1m** (20 °C, stopped-flow, at 613 nm).

[ <b>1m</b> ] / mol L <sup>-1</sup>	[ <b>7</b> -ZnBr] / mol L <sup>-1</sup>	[ <b>7</b> -ZnBr]/[ <b>1m</b> ]	$k_{\text{obs}}$ / s <sup>-1</sup>
$1.65 \times 10^{-5}$	$5.54 \times 10^{-4}$	33.5	11.0
$1.65 \times 10^{-5}$	$8.32 \times 10^{-4}$	50.3	17.2
$1.65 \times 10^{-5}$	$1.11 \times 10^{-3}$	67.1	23.3
$1.65 \times 10^{-5}$	$1.39 \times 10^{-3}$	83.8	27.8
$1.65 \times 10^{-5}$	$1.66 \times 10^{-3}$	101	33.8

$$k_2 = 2.03 \times 10^4 \text{ L mol}^{-1} \text{ s}^{-1}$$

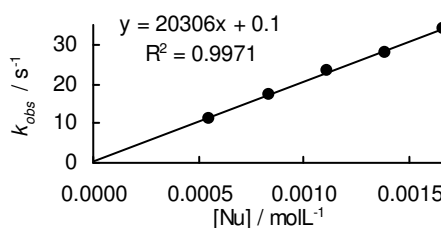
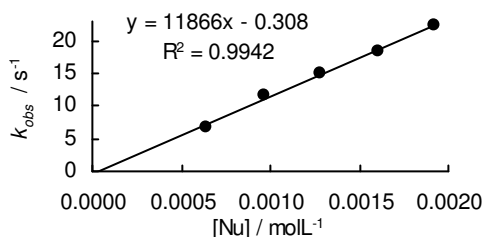


Table 74: Kinetics of the reaction of **7**-ZnBr (generated from **7**-H by addition of 1.06 equiv. TMP-ZnBr·LiBr) with **1n** (20 °C, stopped-flow, at 620 nm).

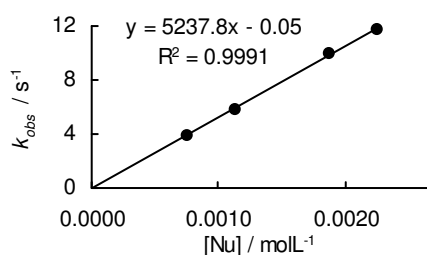
[ <b>1n</b> ] / mol L <sup>-1</sup>	[ <b>7</b> -ZnBr] / mol L <sup>-1</sup>	[ <b>7</b> -ZnBr]/[ <b>1n</b> ]	$k_{\text{obs}}$ / s <sup>-1</sup>
$1.82 \times 10^{-5}$	$6.40 \times 10^{-4}$	35.3	6.80
$1.82 \times 10^{-5}$	$9.61 \times 10^{-4}$	52.9	11.7
$1.82 \times 10^{-5}$	$1.28 \times 10^{-3}$	70.5	15.2
$1.82 \times 10^{-5}$	$1.60 \times 10^{-3}$	88.2	18.3
$1.82 \times 10^{-5}$	$1.92 \times 10^{-3}$	106	22.5

$$k_2 = 1.19 \times 10^4 \text{ L mol}^{-1} \text{ s}^{-1}$$

Table 75: Kinetics of the reaction of **7**-ZnBr (generated from **7**-H by addition of 1.05 equiv. TMP-ZnBr·LiBr) with **1o** (20 °C, stopped-flow, at 618 nm).

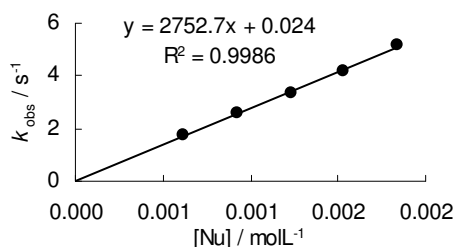
[ <b>1o</b> ] / mol L <sup>-1</sup>	[ <b>7</b> -ZnBr] / mol L <sup>-1</sup>	[ <b>7</b> -ZnBr]/[ <b>1o</b> ]	$k_{\text{obs}}$ / s <sup>-1</sup>
$1.68 \times 10^{-5}$	$7.54 \times 10^{-4}$	44.8	3.92
$1.68 \times 10^{-5}$	$1.13 \times 10^{-3}$	67.2	5.80
$1.68 \times 10^{-5}$	$1.89 \times 10^{-3}$	112	9.97
$1.68 \times 10^{-5}$	$2.26 \times 10^{-3}$	135	11.7

$$k_2 = 5.24 \times 10^3 \text{ L mol}^{-1} \text{ s}^{-1}$$

Table 76: Kinetics of the reaction of **7**-ZnBr (generated from **7**-H by addition of 1.05 equiv. TMP-ZnBr·LiBr) with **1p** (20 °C, stopped-flow, at 627 nm).

[ <b>1p</b> ] / mol L <sup>-1</sup>	[ <b>7</b> -ZnBr] / mol L <sup>-1</sup>	[ <b>7</b> -ZnBr]/[ <b>1p</b> ]	$k_{\text{obs}}$ / s <sup>-1</sup>
$1.78 \times 10^{-5}$	$6.15 \times 10^{-4}$	34.4	1.76
$1.78 \times 10^{-5}$	$9.22 \times 10^{-4}$	51.7	2.55
$1.78 \times 10^{-5}$	$1.23 \times 10^{-3}$	68.9	3.36
$1.78 \times 10^{-5}$	$1.54 \times 10^{-3}$	86.1	4.21
$1.78 \times 10^{-5}$	$1.84 \times 10^{-3}$	103	5.16

$$k_2 = 2.75 \times 10^3 \text{ L mol}^{-1} \text{ s}^{-1}$$

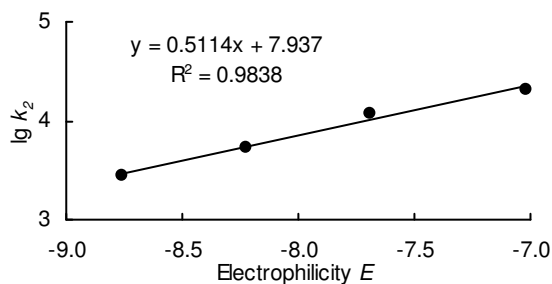


### Determination of Reactivity Parameters $N$ and $s_N$ for **7**-ZnBr in DMSO

Table 77: Rate Constants for the reactions of **7**-ZnBr with different electrophiles.

Electrophile	$E$	$k_2$ / L mol <sup>-1</sup> s <sup>-1</sup>	$\lg k_2$
<b>1m</b>	-7.02	$2.03 \times 10^4$	4.31
<b>1n</b>	-7.69	$1.19 \times 10^4$	4.08
<b>1o</b>	-8.22	$5.24 \times 10^3$	3.72
<b>1p</b>	-8.76	$2.75 \times 10^3$	3.44

$$N = 15.52, s_N = 0.51$$

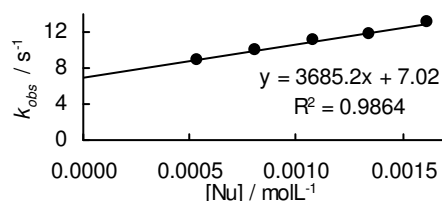


## 4.4.2.5. Reactions of 7-ZnI

Table 78: Kinetics of the reaction of 7-ZnI (generated from 7-H by addition of 1.07 equiv. TMP-ZnI·LiI) with **1m** (20 °C, stopped-flow, at 613 nm).

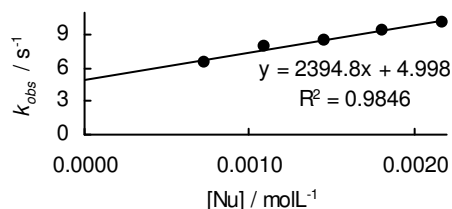
[ <b>1m</b> ] / mol L <sup>-1</sup>	[7-ZnI] / mol L <sup>-1</sup>	[7-ZnI]/[ <b>1m</b> ]	<i>k</i> <sub>obs</sub> / s <sup>-1</sup>
1.83 × 10 <sup>-5</sup>	5.39 × 10 <sup>-4</sup>	29.4	9.00
1.83 × 10 <sup>-5</sup>	8.08 × 10 <sup>-4</sup>	44.2	9.97
1.83 × 10 <sup>-5</sup>	1.08 × 10 <sup>-3</sup>	58.9	11.2
1.83 × 10 <sup>-5</sup>	1.35 × 10 <sup>-3</sup>	73.6	11.7
1.83 × 10 <sup>-5</sup>	1.62 × 10 <sup>-3</sup>	88.3	13.1

$$k_2 = 3.69 \times 10^3 \text{ L mol}^{-1} \text{ s}^{-1}$$

Table 79: Kinetics of the reaction of 7-ZnI (generated from 7-H by addition of 1.06 equiv. TMP-ZnI·LiI) with **1n** (20 °C, stopped-flow, at 620 nm).

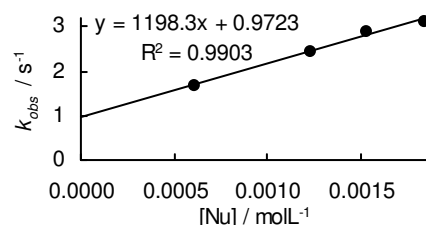
[ <b>1n</b> ] / mol L <sup>-1</sup>	[7-ZnI] / mol L <sup>-1</sup>	[7-ZnI]/[ <b>1n</b> ]	<i>k</i> <sub>obs</sub> / s <sup>-1</sup>
1.72 × 10 <sup>-5</sup>	7.27 × 10 <sup>-4</sup>	42.2	6.54
1.72 × 10 <sup>-5</sup>	1.09 × 10 <sup>-3</sup>	63.3	7.85
1.72 × 10 <sup>-5</sup>	1.45 × 10 <sup>-3</sup>	84.4	8.47
1.72 × 10 <sup>-5</sup>	1.82 × 10 <sup>-3</sup>	106	9.43
1.72 × 10 <sup>-5</sup>	2.18 × 10 <sup>-3</sup>	127	10.1

$$k_2 = 2.39 \times 10^3 \text{ L mol}^{-1} \text{ s}^{-1}$$

Table 80: Kinetics of the reaction of 7-ZnI (generated from 7-H by addition of 1.06 equiv. TMP-ZnI·LiI) with **1o** (20 °C, stopped-flow, at 618 nm).

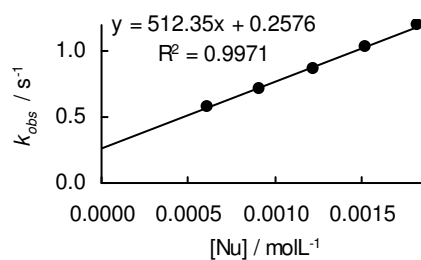
[ <b>1o</b> ] / mol L <sup>-1</sup>	[7-ZnI] / mol L <sup>-1</sup>	[7-ZnI]/[ <b>1o</b> ]	<i>k</i> <sub>obs</sub> / s <sup>-1</sup>
1.82 × 10 <sup>-5</sup>	6.15 × 10 <sup>-4</sup>	33.8	1.69
1.82 × 10 <sup>-5</sup>	1.23 × 10 <sup>-3</sup>	67.7	2.44
1.82 × 10 <sup>-5</sup>	1.54 × 10 <sup>-3</sup>	84.6	2.90
1.82 × 10 <sup>-5</sup>	1.84 × 10 <sup>-3</sup>	102	3.12

$$k_2 = 1.20 \times 10^3 \text{ L mol}^{-1} \text{ s}^{-1}$$

Table 81: Kinetics of the reaction of 7-ZnI (generated from 7-H by addition of 1.07 equiv. TMP-ZnI·LiI) with **1p** (20 °C, stopped-flow, at 627 nm).

[ <b>1p</b> ] / mol L <sup>-1</sup>	[7-ZnI] / mol L <sup>-1</sup>	[7-ZnI]/[ <b>1p</b> ]	<i>k</i> <sub>obs</sub> / s <sup>-1</sup>
1.65 × 10 <sup>-5</sup>	6.08 × 10 <sup>-4</sup>	36.9	0.584
1.65 × 10 <sup>-5</sup>	9.12 × 10 <sup>-4</sup>	55.3	0.715
1.65 × 10 <sup>-5</sup>	1.22 × 10 <sup>-3</sup>	73.8	0.863
1.65 × 10 <sup>-5</sup>	1.52 × 10 <sup>-3</sup>	92.2	1.04
1.65 × 10 <sup>-5</sup>	1.82 × 10 <sup>-3</sup>	111	1.20

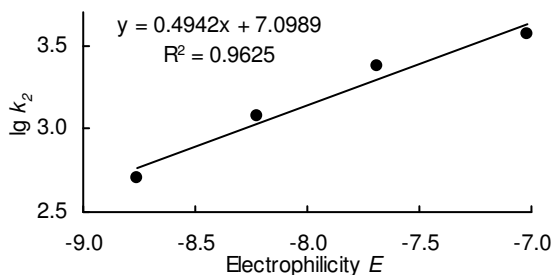
$$k_2 = 5.12 \times 10^2 \text{ L mol}^{-1} \text{ s}^{-1}$$



Determination of Reactivity Parameters  $N$  and  $s_N$  for **7**-ZnI in DMSOTable 82: Rate Constants for the reactions of **7**-ZnI with different electrophiles.

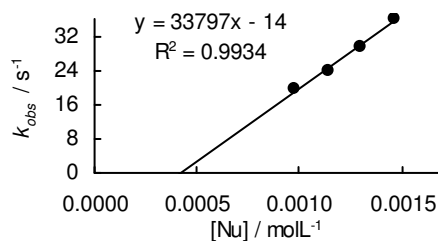
Electrophile	$E$	$k_2 / \text{L mol}^{-1} \text{s}^{-1}$	$\lg k_2$
<b>1m</b>	-7.02	$3.69 \times 10^3$	3.57
<b>1n</b>	-7.69	$2.39 \times 10^3$	3.38
<b>1o</b>	-8.22	$1.20 \times 10^3$	3.08
<b>1p</b>	-8.76	$5.12 \times 10^2$	2.71

$$N = 14.36, s_N = 0.49$$

**4.4.2.6. Reactions of **8**-ZnCl**Table 83: Kinetics of the reaction of **8**-ZnCl (generated from **8**-H by addition of 1.04 equiv. TMP-ZnCl·LiCl) with **1m** (20 °C, stopped-flow, at 613 nm).

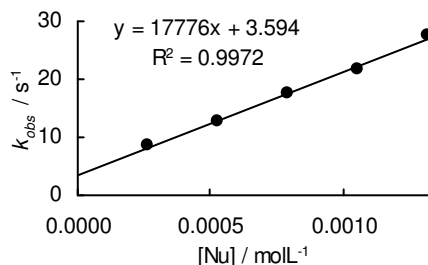
$[\mathbf{1m}] / \text{mol L}^{-1}$	$[\mathbf{8-ZnCl}] / \text{mol L}^{-1}$	$[\mathbf{8-ZnCl}]/[\mathbf{1m}]$	$k_{\text{obs}} / \text{s}^{-1}$
$2.20 \times 10^{-5}$	$9.76 \times 10^{-4}$	44.3	19.5
$2.20 \times 10^{-5}$	$1.14 \times 10^{-3}$	51.7	24.0
$2.20 \times 10^{-5}$	$1.30 \times 10^{-3}$	59.0	29.5
$2.20 \times 10^{-5}$	$1.46 \times 10^{-3}$	66.4	36.0

$$k_2 = 3.38 \times 10^4 \text{ L mol}^{-1} \text{s}^{-1}$$

Table 84: Kinetics of the reaction of **8**-ZnCl (generated from **8**-H by addition of 1.08 equiv. TMP-ZnCl·LiCl) with **1n** (20 °C, stopped-flow, at 620 nm).

$[\mathbf{1n}] / \text{mol L}^{-1}$	$[\mathbf{8-ZnCl}] / \text{mol L}^{-1}$	$[\mathbf{8-ZnCl}]/[\mathbf{1n}]$	$k_{\text{obs}} / \text{s}^{-1}$
$2.64 \times 10^{-5}$	$2.64 \times 10^{-4}$	12.9	8.53
$2.64 \times 10^{-5}$	$5.27 \times 10^{-4}$	25.9	12.9
$2.64 \times 10^{-5}$	$7.91 \times 10^{-4}$	38.8	17.5
$2.64 \times 10^{-5}$	$1.05 \times 10^{-3}$	51.7	21.8
$2.64 \times 10^{-5}$	$1.32 \times 10^{-3}$	64.6	27.5

$$k_2 = 1.78 \times 10^4 \text{ L mol}^{-1} \text{s}^{-1}$$

Table 85: Kinetics of the reaction of **8**-ZnCl (generated from **8**-H by addition of 1.07 equiv. TMP-ZnCl·LiCl) with **1p** (20 °C, stopped-flow, at 627 nm).

$[\mathbf{1p}] / \text{mol L}^{-1}$	$[\mathbf{8-ZnCl}] / \text{mol L}^{-1}$	$[\mathbf{8-ZnCl}]/[\mathbf{1p}]$	$k_{\text{obs}} / \text{s}^{-1}$
$2.65 \times 10^{-5}$	$2.53 \times 10^{-4}$	15.4	4.31
$2.65 \times 10^{-5}$	$5.07 \times 10^{-4}$	30.7	5.10
$2.65 \times 10^{-5}$	$1.01 \times 10^{-3}$	61.5	6.74
$2.65 \times 10^{-5}$	$1.27 \times 10^{-3}$	76.9	7.62

$$k_2 = 3.26 \times 10^3 \text{ L mol}^{-1} \text{s}^{-1}$$

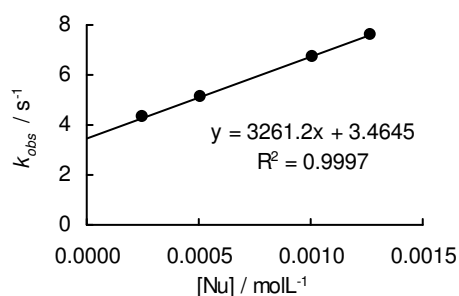
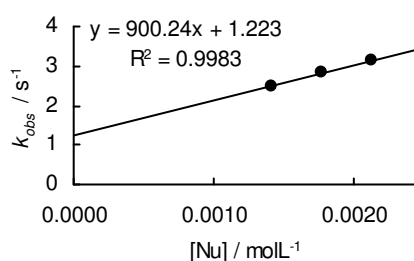


Table 86: Kinetics of the reaction of **8**-ZnCl (generated from **8**-H by addition of 1.07 equiv. TMP-ZnCl·LiCl) with **1q** (20 °C, stopped-flow, at 627 nm).

[ <b>1q</b> ] / mol L <sup>-1</sup>	[ <b>8</b> -ZnCl] / mol L <sup>-1</sup>	[ <b>8</b> -ZnCl]/[ <b>1q</b> ]	$k_{\text{obs}}$ / s <sup>-1</sup>
$1.96 \times 10^{-5}$	$1.06 \times 10^{-3}$	54.3	2.44
$1.96 \times 10^{-5}$	$1.42 \times 10^{-3}$	72.4	2.49
$1.96 \times 10^{-5}$	$1.77 \times 10^{-3}$	90.5	2.84
$1.96 \times 10^{-5}$	$2.13 \times 10^{-3}$	109	3.12

$$k_2 = 9.00 \times 10^2 \text{ L mol}^{-1} \text{ s}^{-1}$$

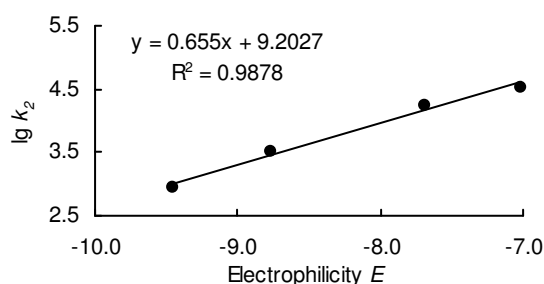


### Determination of Reactivity Parameters $N$ and $s_N$ for **8**-ZnCl in DMSO

Table 87: Rate Constants for the reactions of **8**-ZnCl with different electrophiles.

Electrophile	$E$	$k_2$ / L mol <sup>-1</sup> s <sup>-1</sup>	lg $k_2$
<b>1m</b>	-7.02	$3.38 \times 10^4$	4.53
<b>1n</b>	-7.69	$1.78 \times 10^4$	4.25
<b>1p</b>	-8.76	$3.26 \times 10^3$	3.51
<b>1q</b>	-9.45	$9.00 \times 10^2$	2.95

$$N = 14.05, s_N = 0.66$$



### 4.4.2.7. Control Experiments

#### Reaction of **1n** with LiCl and Bu<sub>4</sub>NCl

Table 88: Reactions of **1n** with LiCl and Bu<sub>4</sub>NCl in DMSO (20 °C, diode array, at 620 nm).

[ <b>1n</b> ] / mol L <sup>-1</sup>	Salt	[Salt] / mol L <sup>-1</sup>	$k_{\text{obs}}$ / s <sup>-1</sup>
$1.44 \times 10^{-5}$	LiCl	$1.91 \times 10^{-3}$	-
$1.41 \times 10^{-5}$	LiCl	$3.75 \times 10^{-3}$	-
$1.35 \times 10^{-5}$	Bu <sub>4</sub> NCl	$1.53 \times 10^{-3}$	-
$1.3 \times 10^{-5}$	Bu <sub>4</sub> NCl	$2.06 \times 10^{-3}$	-

#### Reaction of **1n** with TMPH

Table 89: Reactions of TMPH with **1n** in DMSO (20 °C, stopped-flow, at 620 nm).

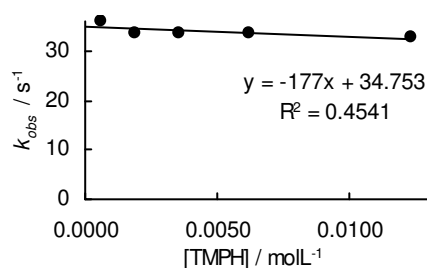
[ <b>1n</b> ] / mol L <sup>-1</sup>	[TMPH] / mol L <sup>-1</sup>	[TMPH]/[ <b>1n</b> ]	$k_{\text{obs}}$ / s <sup>-1</sup>
$1.43 \times 10^{-5}$	$1.31 \times 10^{-3}$	92.0	-
$1.43 \times 10^{-5}$	$1.69 \times 10^{-3}$	118	-
$1.43 \times 10^{-5}$	$2.81 \times 10^{-3}$	197	-
$1.43 \times 10^{-5}$	$3.75 \times 10^{-3}$	263	-



Reaction of **7**-ZnCl with **1n** presence of variable concentrations of TMPHTable 90: Kinetics of the reaction of **7**-ZnCl (generated from **7**-H by addition of 1.08 equiv. TMP-ZnCl·LiCl) with **1n** (20 °C, stopped-flow, at 620 nm).

[ <b>1n</b> ] / mol L <sup>-1</sup>	[ <b>7</b> -ZnCl] / mol L <sup>-1</sup>	[TMPH] / mol L <sup>-1</sup>	[TMPH] <sub>total</sub> / mol L <sup>-1</sup>	<i>k</i> <sub>obs</sub> / s <sup>-1</sup>
1.95 × 10 <sup>-5</sup>	5.79 × 10 <sup>-4</sup>	0	5.79 × 10 <sup>-4</sup>	36.0
1.95 × 10 <sup>-5</sup>	5.79 × 10 <sup>-4</sup>	1.31 × 10 <sup>-3</sup>	1.89 × 10 <sup>-3</sup>	33.4
1.95 × 10 <sup>-5</sup>	5.79 × 10 <sup>-4</sup>	5.63 × 10 <sup>-3</sup>	6.21 × 10 <sup>-3</sup>	33.7
1.95 × 10 <sup>-5</sup>	5.79 × 10 <sup>-4</sup>	2.96 × 10 <sup>-3</sup>	3.54 × 10 <sup>-3</sup>	33.5
1.95 × 10 <sup>-5</sup>	5.79 × 10 <sup>-4</sup>	1.19 × 10 <sup>-3</sup>	1.24 × 10 <sup>-3</sup>	32.8

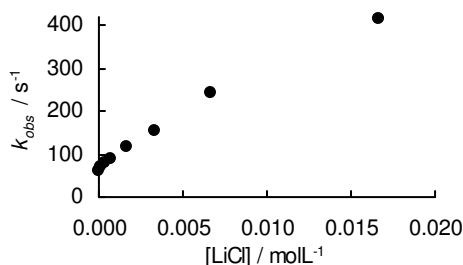
$$k_2 = 1.78 \times 10^4 \text{ L mol}^{-1} \text{ s}^{-1}$$



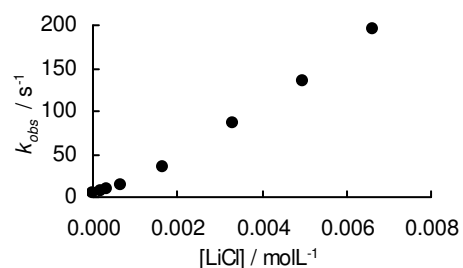
## 4.4.2.8. Experiments with Additives

Table 91: Kinetics of the reaction of **7**-ZnCl (generated from **7**-H by addition of 1.04 equiv. TMP-ZnCl·LiCl) with **1n** in presence of variable concentrations of LiCl (20 °C, stopped-flow, at 620 nm).

[ <b>1n</b> ] / mol L <sup>-1</sup>	[ <b>7</b> -ZnCl] / mol L <sup>-1</sup>	[LiCl] / mol L <sup>-1</sup>	<i>k</i> <sub>obs</sub> / s <sup>-1</sup>
2.04 × 10 <sup>-5</sup>	8.63 × 10 <sup>-4</sup>	0	62.9
2.04 × 10 <sup>-5</sup>	8.63 × 10 <sup>-4</sup>	1.66 × 10 <sup>-4</sup>	72.1
2.04 × 10 <sup>-5</sup>	8.63 × 10 <sup>-4</sup>	3.32 × 10 <sup>-4</sup>	79.3
2.04 × 10 <sup>-5</sup>	8.63 × 10 <sup>-4</sup>	6.64 × 10 <sup>-4</sup>	87.2
2.04 × 10 <sup>-5</sup>	8.63 × 10 <sup>-4</sup>	1.66 × 10 <sup>-3</sup>	117
2.04 × 10 <sup>-5</sup>	8.63 × 10 <sup>-4</sup>	3.32 × 10 <sup>-3</sup>	156
2.04 × 10 <sup>-5</sup>	8.63 × 10 <sup>-4</sup>	6.64 × 10 <sup>-3</sup>	243
2.04 × 10 <sup>-5</sup>	8.63 × 10 <sup>-4</sup>	1.66 × 10 <sup>-2</sup>	415

Table 92: Kinetics of the reaction of **7**-ZnBr (generated from **7**-H by addition of 1.06 equiv. TMP-ZnBr·LiBr) with **1n** in presence of variable concentrations of LiCl (20 °C, stopped-flow, at 620 nm).

[ <b>1n</b> ] / mol L <sup>-1</sup>	[ <b>7</b> -ZnBr] / mol L <sup>-1</sup>	[LiCl] / mol L <sup>-1</sup>	<i>k</i> <sub>obs</sub> / s <sup>-1</sup>
2.04 × 10 <sup>-5</sup>	4.73 × 10 <sup>-4</sup>	0	5.53
2.04 × 10 <sup>-5</sup>	4.73 × 10 <sup>-4</sup>	1.66 × 10 <sup>-4</sup>	6.62
2.04 × 10 <sup>-5</sup>	4.73 × 10 <sup>-4</sup>	3.32 × 10 <sup>-4</sup>	8.73
2.04 × 10 <sup>-5</sup>	4.73 × 10 <sup>-4</sup>	6.64 × 10 <sup>-4</sup>	14.3
2.04 × 10 <sup>-5</sup>	4.73 × 10 <sup>-4</sup>	1.66 × 10 <sup>-3</sup>	35.4
2.04 × 10 <sup>-5</sup>	4.73 × 10 <sup>-4</sup>	3.32 × 10 <sup>-3</sup>	87.1
2.04 × 10 <sup>-5</sup>	4.73 × 10 <sup>-4</sup>	4.98 × 10 <sup>-3</sup>	135
2.04 × 10 <sup>-5</sup>	4.73 × 10 <sup>-4</sup>	6.64 × 10 <sup>-3</sup>	196

Table 93: Kinetics of the reaction of **7**-ZnI (generated from **7**-H by addition of 1.09 equiv. TMP-ZnI·LiI) with **1n** in presence of variable concentrations of LiCl (20 °C, stopped-flow, at 620 nm).

[ <b>1n</b> ] / mol L <sup>-1</sup>	[ <b>7</b> -ZnI] / mol L <sup>-1</sup>	[LiCl] / mol L <sup>-1</sup>	<i>k</i> <sub>obs</sub> / s <sup>-1</sup>
2.04 × 10 <sup>-5</sup>	8.33 × 10 <sup>-4</sup>	0	2.13
2.04 × 10 <sup>-5</sup>	8.33 × 10 <sup>-4</sup>	3.32 × 10 <sup>-4</sup>	2.38
2.04 × 10 <sup>-5</sup>	8.33 × 10 <sup>-4</sup>	6.64 × 10 <sup>-4</sup>	3.14
2.04 × 10 <sup>-5</sup>	8.33 × 10 <sup>-4</sup>	1.66 × 10 <sup>-3</sup>	16.5
2.04 × 10 <sup>-5</sup>	8.33 × 10 <sup>-4</sup>	2.49 × 10 <sup>-3</sup>	50.5
2.04 × 10 <sup>-5</sup>	8.33 × 10 <sup>-4</sup>	3.32 × 10 <sup>-3</sup>	78.1
2.04 × 10 <sup>-5</sup>	8.33 × 10 <sup>-4</sup>	4.98 × 10 <sup>-3</sup>	110
2.04 × 10 <sup>-5</sup>	8.33 × 10 <sup>-4</sup>	6.64 × 10 <sup>-3</sup>	176

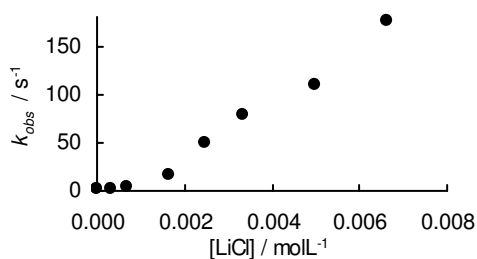
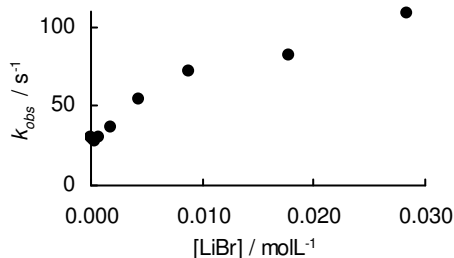
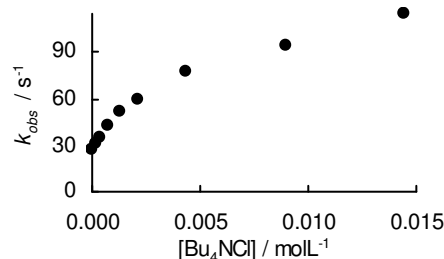


Table 94: Kinetics of the reaction of **7**-ZnCl (generated from **7**-H by addition of 1.07 equiv. TMP-ZnCl·LiCl) with **1n** in presence of variable concentrations of LiBr (20 °C, stopped-flow, at 620 nm).

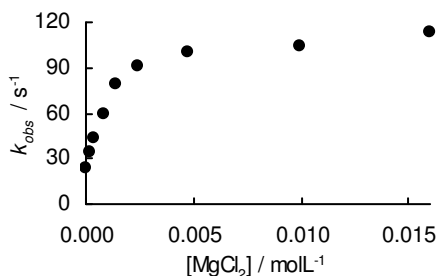
[ <b>1n</b> ] / mol L <sup>-1</sup>	[ <b>7</b> -ZnCl] / mol L <sup>-1</sup>	[LiBr] / mol L <sup>-1</sup>	<i>k</i> <sub>obs</sub> / s <sup>-1</sup>
2.04 × 10 <sup>-5</sup>	4.52 × 10 <sup>-4</sup>	0	30.8
2.04 × 10 <sup>-5</sup>	4.52 × 10 <sup>-4</sup>	1.77 × 10 <sup>-4</sup>	29.3
2.04 × 10 <sup>-5</sup>	4.52 × 10 <sup>-4</sup>	3.55 × 10 <sup>-4</sup>	28.4
2.04 × 10 <sup>-5</sup>	4.52 × 10 <sup>-4</sup>	7.09 × 10 <sup>-4</sup>	30.7
2.04 × 10 <sup>-5</sup>	4.52 × 10 <sup>-4</sup>	1.77 × 10 <sup>-3</sup>	36.4
2.04 × 10 <sup>-5</sup>	4.52 × 10 <sup>-4</sup>	4.26 × 10 <sup>-3</sup>	54.8
2.04 × 10 <sup>-5</sup>	4.52 × 10 <sup>-4</sup>	8.87 × 10 <sup>-3</sup>	71.8
2.04 × 10 <sup>-5</sup>	4.52 × 10 <sup>-4</sup>	1.77 × 10 <sup>-2</sup>	82.3

Table 95: Kinetics of the reaction of **7**-ZnCl (generated from **7**-H by addition of 1.03 equiv. TMP-ZnCl·LiCl) with **1n** in presence of variable concentrations of Bu<sub>4</sub>NCl (20 °C, stopped-flow, at 620 nm).

[ <b>1n</b> ] / mol L <sup>-1</sup>	[ <b>7</b> -ZnCl] / mol L <sup>-1</sup>	[Bu <sub>4</sub> NCl] / mol L <sup>-1</sup>	<i>k</i> <sub>obs</sub> / s <sup>-1</sup>
2.36 × 10 <sup>-5</sup>	3.89 × 10 <sup>-4</sup>	0	26.5
2.36 × 10 <sup>-5</sup>	3.89 × 10 <sup>-4</sup>	1.80 × 10 <sup>-4</sup>	31.3
2.36 × 10 <sup>-5</sup>	3.89 × 10 <sup>-4</sup>	3.60 × 10 <sup>-4</sup>	35.3
2.36 × 10 <sup>-5</sup>	3.89 × 10 <sup>-4</sup>	7.20 × 10 <sup>-4</sup>	42.8
2.36 × 10 <sup>-5</sup>	3.89 × 10 <sup>-4</sup>	1.26 × 10 <sup>-3</sup>	51.4
2.36 × 10 <sup>-5</sup>	3.89 × 10 <sup>-4</sup>	2.16 × 10 <sup>-3</sup>	58.9
2.36 × 10 <sup>-5</sup>	3.89 × 10 <sup>-4</sup>	4.32 × 10 <sup>-3</sup>	77.9
2.36 × 10 <sup>-5</sup>	3.89 × 10 <sup>-4</sup>	9.00 × 10 <sup>-3</sup>	94.8
2.36 × 10 <sup>-5</sup>	3.89 × 10 <sup>-4</sup>	1.44 × 10 <sup>-2</sup>	115

Table 96: Kinetics of the reaction of **7**-ZnCl (generated from **7**-H by addition of 1.09 equiv. TMP-ZnCl·LiCl) with **1n** in presence of variable concentrations of MgCl<sub>2</sub> (20 °C, stopped-flow, at 620 nm).

[ <b>1n</b> ] / mol L <sup>-1</sup>	[ <b>7</b> -ZnCl] / mol L <sup>-1</sup>	[MgCl <sub>2</sub> ] / mol L <sup>-1</sup>	<i>k</i> <sub>obs</sub> / s <sup>-1</sup>
2.83 × 10 <sup>-5</sup>	3.53 × 10 <sup>-4</sup>	0	23.8
2.83 × 10 <sup>-5</sup>	3.53 × 10 <sup>-4</sup>	2.00 × 10 <sup>-4</sup>	34.1
2.83 × 10 <sup>-5</sup>	3.53 × 10 <sup>-4</sup>	3.99 × 10 <sup>-4</sup>	43.7
2.83 × 10 <sup>-5</sup>	3.53 × 10 <sup>-4</sup>	7.98 × 10 <sup>-4</sup>	60.0
2.83 × 10 <sup>-5</sup>	3.53 × 10 <sup>-4</sup>	1.40 × 10 <sup>-3</sup>	78.8
2.83 × 10 <sup>-5</sup>	3.53 × 10 <sup>-4</sup>	2.39 × 10 <sup>-3</sup>	90.6
2.83 × 10 <sup>-5</sup>	3.53 × 10 <sup>-4</sup>	4.79 × 10 <sup>-3</sup>	100
2.83 × 10 <sup>-5</sup>	3.53 × 10 <sup>-4</sup>	9.98 × 10 <sup>-3</sup>	104
2.83 × 10 <sup>-5</sup>	3.53 × 10 <sup>-4</sup>	1.60 × 10 <sup>-2</sup>	114



#### 4.4.3. Kinetic Experiments of the Tin and Silicon Derivatives of **7**

##### 4.4.3.1. Reactions of **7**-Sn

Table 97: Kinetics of the reaction of **7**-Sn with **1g** in CH<sub>2</sub>Cl<sub>2</sub> (20 °C, stopped-flow, at 601 nm).

[ <b>1g</b> ] / mol L <sup>-1</sup>	[ <b>7</b> -Sn] / mol L <sup>-1</sup>	[ <b>7</b> -Sn]/[ <b>1g</b> ]	<i>k</i> <sub>obs</sub> / s <sup>-1</sup>
1.09 × 10 <sup>-5</sup>	1.05 × 10 <sup>-3</sup>	96.1	0.894
1.09 × 10 <sup>-5</sup>	1.47 × 10 <sup>-3</sup>	135	1.22
1.09 × 10 <sup>-5</sup>	2.31 × 10 <sup>-3</sup>	211	1.84
1.09 × 10 <sup>-5</sup>	2.73 × 10 <sup>-3</sup>	250	2.13

$$k_2 = 7.36 \times 10^2 \text{ L mol}^{-1} \text{ s}^{-1}$$

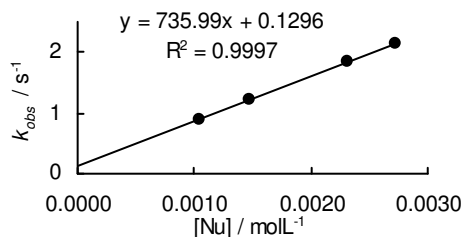
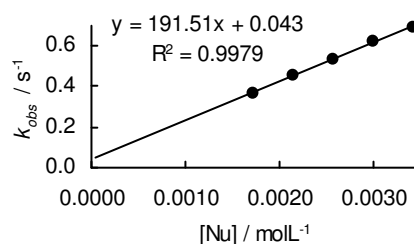


Table 98: Kinetics of the reaction of **7-Sn** with **1h** in CH<sub>2</sub>Cl<sub>2</sub> (20 °C, stopped-flow, at 593 nm).

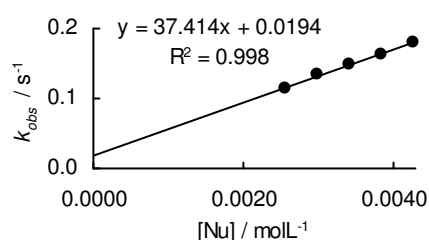
[ <b>1h</b> ] / mol L <sup>-1</sup>	[ <b>7-Sn</b> ] / mol L <sup>-1</sup>	[ <b>7-Sn</b> ]/[ <b>1h</b> ]	$k_{\text{obs}} /$ s <sup>-1</sup>
$1.01 \times 10^{-5}$	$1.71 \times 10^{-3}$	170	0.369
$1.01 \times 10^{-5}$	$2.14 \times 10^{-3}$	212	0.453
$1.01 \times 10^{-5}$	$2.57 \times 10^{-3}$	255	0.532
$1.01 \times 10^{-5}$	$2.99 \times 10^{-3}$	297	0.626
$1.01 \times 10^{-5}$	$3.42 \times 10^{-3}$	339	0.692

$$k_2 = 1.92 \times 10^2 \text{ L mol}^{-1} \text{ s}^{-1}$$

Table 99: Kinetics of the reaction of **7-Sn** with **1j** in CH<sub>2</sub>Cl<sub>2</sub> (20 °C, stopped-flow, at 672 nm).

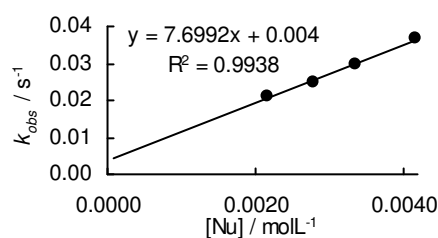
[ <b>1j</b> ] / mol L <sup>-1</sup>	[ <b>7-Sn</b> ] / mol L <sup>-1</sup>	[ <b>7-Sn</b> ]/[ <b>1j</b> ]	$k_{\text{obs}} /$ s <sup>-1</sup>
$8.97 \times 10^{-6}$	$2.57 \times 10^{-3}$	286	0.114
$8.97 \times 10^{-6}$	$2.99 \times 10^{-3}$	334	0.133
$8.97 \times 10^{-6}$	$3.42 \times 10^{-3}$	381	0.148
$8.97 \times 10^{-6}$	$3.85 \times 10^{-3}$	429	0.163
$8.97 \times 10^{-6}$	$4.28 \times 10^{-3}$	477	0.179

$$k_2 = 3.74 \times 10^1 \text{ L mol}^{-1} \text{ s}^{-1}$$

Table 100: Kinetics of the reaction of **7-Sn** with **1k** in CH<sub>2</sub>Cl<sub>2</sub> (20 °C, diode array, at 620 nm).

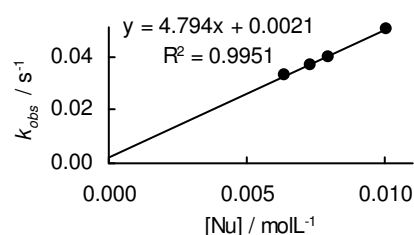
[ <b>1k</b> ] / mol L <sup>-1</sup>	[ <b>7-Sn</b> ] / mol L <sup>-1</sup>	[ <b>7-Sn</b> ]/[ <b>1k</b> ]	$k_{\text{obs}} /$ s <sup>-1</sup>
$1.11 \times 10^{-5}$	$2.16 \times 10^{-3}$	194	$2.12 \times 10^{-2}$
$1.08 \times 10^{-5}$	$2.79 \times 10^{-3}$	259	$2.50 \times 10^{-2}$
$1.04 \times 10^{-5}$	$3.36 \times 10^{-3}$	324	$2.96 \times 10^{-2}$
$1.07 \times 10^{-5}$	$4.17 \times 10^{-3}$	388	$3.65 \times 10^{-2}$

$$k_2 = 7.70 \text{ L mol}^{-1} \text{ s}^{-1}$$

Table 101: Kinetics of the reaction of **7-Sn** with **1l** in CH<sub>2</sub>Cl<sub>2</sub> (20 °C, diode array, at 622 nm).

[ <b>1l</b> ] / mol L <sup>-1</sup>	[ <b>7-Sn</b> ] / mol L <sup>-1</sup>	[ <b>7-Sn</b> ]/[ <b>1l</b> ]	$k_{\text{obs}} /$ s <sup>-1</sup>
$1.07 \times 10^{-5}$	$6.40 \times 10^{-3}$	599	$3.33 \times 10^{-2}$
$1.07 \times 10^{-5}$	$7.33 \times 10^{-3}$	685	$3.69 \times 10^{-2}$
$1.06 \times 10^{-5}$	$7.93 \times 10^{-3}$	748	$3.95 \times 10^{-2}$
$1.07 \times 10^{-5}$	$1.00 \times 10^{-2}$	942	$5.05 \times 10^{-2}$

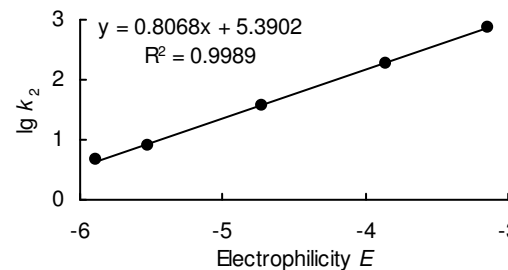
$$k_2 = 4.79 \text{ L mol}^{-1} \text{ s}^{-1}$$



Determination of Reactivity Parameters  $N$  and  $s_N$  for **7-Sn** in  $\text{CH}_2\text{Cl}_2$ Table 102: Rate Constants for the reactions of **7-Sn** with different electrophiles.

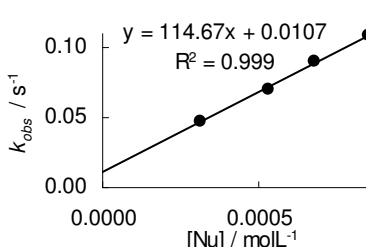
Electrophile	$E$	$k_2 / \text{L mol}^{-1} \text{s}^{-1}$	$\lg k_2$
<b>1g</b>	-3.14	736	2.87
<b>1h</b>	-3.85	192	2.28
<b>1j</b>	-4.72	37.4	1.57
<b>1k</b>	-5.53	7.70	0.89
<b>1l</b>	-5.89	4.79	0.68

$N = 6.68, s_N = 0.81$


**4.4.3.2. Reactions of 7-Si**Table 103: Kinetics of the reaction of **7-Si** with **1b** in  $\text{CH}_2\text{Cl}_2$  (20 °C, diode array, at 475 nm).

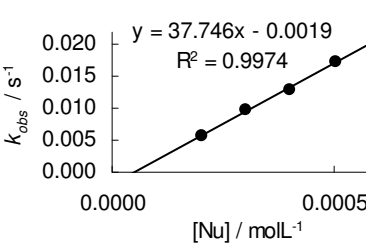
$[\mathbf{1b}] / \text{mol L}^{-1}$	$[\mathbf{7-Si}] / \text{mol L}^{-1}$	$[\mathbf{7-Si}]/[\mathbf{1b}]$	$k_{\text{obs}} / \text{s}^{-1}$
$2.44 \times 10^{-5}$	$3.16 \times 10^{-4}$	13.0	$4.73 \times 10^{-2}$
$2.74 \times 10^{-5}$	$5.32 \times 10^{-4}$	19.4	$7.05 \times 10^{-2}$
$2.62 \times 10^{-5}$	$6.79 \times 10^{-4}$	25.9	$8.93 \times 10^{-2}$
$2.62 \times 10^{-5}$	$8.49 \times 10^{-4}$	32.4	$1.08 \times 10^{-1}$

$k_2 = 115 \text{ L mol}^{-1} \text{s}^{-1}$


Table 104: Kinetics of the reaction of **7-Si** with **1c** in  $\text{CH}_2\text{Cl}_2$  (20 °C, diode array, at 488 nm).

$[\mathbf{1c}] / \text{mol L}^{-1}$	$[\mathbf{7-Si}] / \text{mol L}^{-1}$	$[\mathbf{7-Si}]/[\mathbf{1c}]$	$k_{\text{obs}} / \text{s}^{-1}$
$1.90 \times 10^{-5}$	$2.01 \times 10^{-4}$	10.6	$5.81 \times 10^{-3}$
$1.91 \times 10^{-5}$	$3.02 \times 10^{-4}$	15.9	$9.80 \times 10^{-3}$
$1.90 \times 10^{-5}$	$4.02 \times 10^{-4}$	21.1	$1.28 \times 10^{-2}$
$1.91 \times 10^{-5}$	$5.04 \times 10^{-4}$	26.4	$1.72 \times 10^{-2}$
$1.90 \times 10^{-5}$	$6.03 \times 10^{-4}$	31.7	$2.11 \times 10^{-2}$

$k_2 = 37.7 \text{ L mol}^{-1} \text{s}^{-1}$


Table 105: Kinetics of the reaction of **7-Si** with **1d** in  $\text{CH}_2\text{Cl}_2$  (20 °C, diode array, at 517 nm).

$[\mathbf{1d}] / \text{mol L}^{-1}$	$[\mathbf{7-Si}] / \text{mol L}^{-1}$	$[\mathbf{7-Si}]/[\mathbf{1d}]$	$k_{\text{obs}} / \text{s}^{-1}$
$1.56 \times 10^{-5}$	$3.76 \times 10^{-4}$	24.1	$1.69 \times 10^{-3}$
$1.56 \times 10^{-5}$	$7.53 \times 10^{-4}$	48.2	$2.90 \times 10^{-3}$
$1.56 \times 10^{-5}$	$1.13 \times 10^{-3}$	72.3	$4.08 \times 10^{-3}$
$1.56 \times 10^{-5}$	$1.51 \times 10^{-3}$	96.4	$5.47 \times 10^{-3}$
$1.56 \times 10^{-5}$	$1.88 \times 10^{-3}$	121	$6.77 \times 10^{-3}$

$k_2 = 3.38 \text{ L mol}^{-1} \text{s}^{-1}$

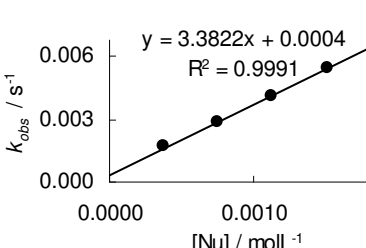
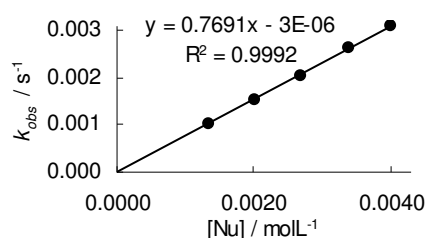


Table 106: Kinetics of the reaction of **7-Si** with **1e** in CH<sub>2</sub>Cl<sub>2</sub> (20 °C, diode array, at 513 nm).

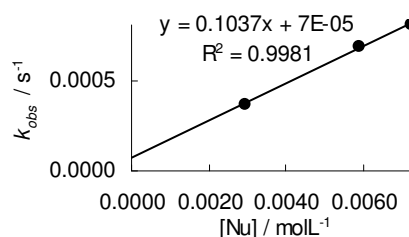
[ <b>1e</b> ] / mol L <sup>-1</sup>	[ <b>7-Si</b> ] / mol L <sup>-1</sup>	[ <b>7-Si</b> ]/[ <b>1e</b> ]	<i>k</i> <sub>obs</sub> / s <sup>-1</sup>
2.02 × 10 <sup>-5</sup>	1.33 × 10 <sup>-3</sup>	66.0	1.04 × 10 <sup>-3</sup>
2.04 × 10 <sup>-5</sup>	2.02 × 10 <sup>-3</sup>	98.9	1.53 × 10 <sup>-3</sup>
2.03 × 10 <sup>-5</sup>	2.68 × 10 <sup>-3</sup>	132	2.04 × 10 <sup>-3</sup>
2.05 × 10 <sup>-5</sup>	3.38 × 10 <sup>-3</sup>	165	2.63 × 10 <sup>-3</sup>
2.03 × 10 <sup>-5</sup>	4.02 × 10 <sup>-3</sup>	198	3.08 × 10 <sup>-3</sup>

$$k_2 = 7.69 \times 10^{-1} \text{ L mol}^{-1} \text{ s}^{-1}$$

Table 107: Kinetics of the reaction of **7-Si** with **1f** in CH<sub>2</sub>Cl<sub>2</sub> (20 °C, diode array, at 520 nm).

[ <b>1f</b> ] / mol L <sup>-1</sup>	[ <b>7-Si</b> ] / mol L <sup>-1</sup>	[ <b>7-Si</b> ]/[ <b>1f</b> ]	<i>k</i> <sub>obs</sub> / s <sup>-1</sup>
2.47 × 10 <sup>-5</sup>	2.93 × 10 <sup>-3</sup>	118.4	3.74 × 10 <sup>-4</sup>
2.48 × 10 <sup>-5</sup>	5.88 × 10 <sup>-3</sup>	236.8	6.95 × 10 <sup>-4</sup>
2.45 × 10 <sup>-5</sup>	7.25 × 10 <sup>-3</sup>	296.0	8.18 × 10 <sup>-4</sup>

$$k_2 = 1.04 \times 10^{-1} \text{ L mol}^{-1} \text{ s}^{-1}$$

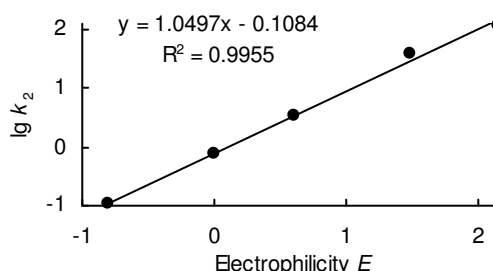


### Determination of Reactivity Parameters *N* and *s<sub>N</sub>* for **7-Si** in CH<sub>2</sub>Cl<sub>2</sub>

Table 108: Rate Constants for the reactions of **7-Sn** with different electrophiles.

Electrophile	<i>E</i>	<i>k</i> <sub>2</sub> / L mol <sup>-1</sup> s <sup>-1</sup>	lg <i>k</i> <sub>2</sub>
<b>1b</b>	2.16	115	2.06
<b>1c</b>	1.48	37.7	1.58
<b>1d</b>	0.61	3.38	0.53
<b>1e</b>	0.00	7.69 × 10 <sup>-1</sup>	-0.11
<b>1f</b>	-0.81	1.04 × 10 <sup>-1</sup>	-0.98

$$N = -0.10, s_N = 1.05$$



## 5. Appendix

### 5.1. LiCl-free Organozinc Compounds

1) Transmetallation: As ZnCl<sub>2</sub> forms complexes with DMSO, the direct transmetallation by treatment of **7-K** with ZnCl<sub>2</sub> (**7-K** → **7-ZnCl**) in DMSO solution was not successful. The transmetallation (**7-K** → **7-ZnCl**) could be performed in THF or in Et<sub>2</sub>O. When the generated organozinc reagent was diluted with DMSO, and combined with benzhydrylium tetrafluoroborates, the decays of the absorbances of the benzhydrylium ions were not mono-exponential.

2) Isolation of the Organozinc Reagent: **7-K** was generated by addition of KO<sup>*t*</sup>Bu to a solution of **7-H** in THF. Subsequent addition of ZnCl<sub>2</sub> (solution in Et<sub>2</sub>O) formed **7-ZnCl**. The

precipitated KCl was filtered off, and the solution was evaporated to yield **7**-ZnCl as a yellow solid. Analysis by NMR spectroscopy showed that **7**-ZnCl was not pure (probably as THF/Et<sub>2</sub>O-complex). Pure **7**-ZnCl also was not obtained when the synthesis was performed in THF or in Et<sub>2</sub>O.

3) Zinc Insertion: **7**-Br was added to a suspension of Zn in dry DMSO and heated for 5 min to 120 °C. After sedimentation over night, the clear solution was separated, and the concentration of **7**-ZnBr was determined by titration with iodine. When the kinetic experiments with these solutions were performed under pseudo-first order conditions (large excesses of **7**-ZnBr), the decays of the absorbance of the electrophiles were not mono-exponential. However, the experiments were not reproducible, and  $k_{\text{obs}}$  derived from the initial rates (usually one half-life could be evaluated as a mono-exponential decay), did not correlate with the concentrations of the organozinc reagent.

## 6. References

- [1] a) N. Negishi, *Organometallics in Organic Synthesis*, VCH, Weinheim, **1996**; b) I. Omae, *Applications of Organometallic Compounds*, Wiley, Chichester, **1998**; c) P. Knochel, *Handbook of Functionalized Organometallics*, Wiley-VCH, Weinheim **2005**.
- [2] a) E. G. Rochow, D. T. Hurd, R. N. Lewis, *The Chemistry of Organometallic Compounds*, Wiley, New York, **1957**; b) P. Powell, *Principles of Organometallic Chemistry*, Chapman and Hall, London, **1988**; c) B. Haag, M. Mosrin, H. Ila, V. Malakhov, P. Knochel, *Angew. Chem.* **2011**, *123*, 9968-9999; *Angew. Chem. Int. Ed.* **2011**, *50*, 9794-9824.
- [3] G. Wu, M. Huang, *Chem. Rev.* **2006**, *106*, 2596-2616.
- [4] a) A. Boudier, L. O. Bromm, M. Lotz and P. Knochel, *Angew. Chem.* **2000**, *112*, 4584-4606; *Angew. Chem. Intl. Ed.* **2000**, *39*, 4414-4435; b) I. Coldham, *J. Chem. Soc., Perkin Trans. 1* **1998**, 1343-1364; c) T. Klatt, J. T. Markiewicz, C. Sämman, P. Knochel, *J. Org. Chem.* **2014**, *79*, 4253-4269.
- [5] H. Mayr, M. Patz, *Angew. Chem.* **1994**, *106*, 990-1010; *Angew. Chem. Int. Ed. Engl.* **1994**, *33*, 938-957.
- [6] Selected Publications: a) H. Mayr, T. Bug, M. F. Gotta, N. Hering, B. Irrgang, B. Janker, B. Kempf, R. Loos, A. R. Ofial, G. Remennikov, H. Schimmel, *J. Am. Chem. Soc.* **2001**, *123*, 9500-9512; b) R. Lucius, R. Loos, H. Mayr, *Angew. Chem.* **2002**, *114*,

- 97–102; *Angew. Chem. Int. Ed.* **2002**, *41*, 91–95; c) H. Mayr, B. Kempf, A. R. Ofial, *Acc. Chem. Res.* **2003**, *36*, 66–77; d) H. Mayr, A. R. Ofial, *Pure Appl. Chem.* **2005**, *77*, 1807–1821; e) D. Richter, N. Hampel, T. Singer, A. R. Ofial, H. Mayr, *Eur. J. Org. Chem.* **2009**, 3203–3211; f) H. Mayr, S. Lakhdar, B. Maji, A. R. Ofial, *Beilstein, J. Org. Chem.* **2012**, *8*, 1458–1478; f) For a comprehensive listing of nucleophilicity parameters  $N$ ,  $s_N$  and electrophilicity parameters  $E$ , see <http://www.cup.uni-muenchen.de/oc/mayr/DBintro.html>.
- [7] Reactivity of Organo-Silicon: a) G. Haben, H. Mayr, *J. Am. Chem. Soc.* **1991**, *113*, 4954–4961; b) H. Laub, H. Yamamoto, H. Mayr, *Org. Lett.* **2010**, *12*, 5206–5209; c) H. Laub, H. Mayr, *Chem. Eur. J.* **2014**, *20*, 1103–1110.
- [8] Reactivity of Carbanions: a) R. Loos, S. Kobayashi, H. Mayr, *J. Am. Chem. Soc.* **2003**, *125*, 14126–14132; b) T. Bug, T. Lemek, H. Mayr, *J. Org. Chem.* **2004**, *69*, 7565–7576; c) T. B. Phan, H. Mayr, *Eur. J. Org. Chem.* **2006**, 2530–2537; d) S. T. A. Berger, A. R. Ofial, H. Mayr, *J. Am. Chem. Soc.* **2007**, *129*, 9753–9761; e) F. Seeliger, H. Mayr, *Org. Biomol. Chem.* **2008**, *6*, 3052–3058; f) O. Kaumanns, R. Appel, T. Lemek, F. Seeliger, H. Mayr, *J. Org. Chem.* **2009**, *74*, 75–81; g) F. Corral-Bautista, H. Mayr, *Eur. J. Org. Chem.* **2013**, 4255–4261.
- [9] a) F. Seeliger, S. T. A. Berger, G. Y. Remenikov, K. Polborn, H. Mayr, *J. Org. Chem.* **2007**, *72*, 9170–9180; b) O. Kaumanns, R. Lucius, H. Mayr, *Chem. Eur. J.* **2008**, *14*, 9675–9682.
- [10] Synthesis of **6**-Li: R. den Besten, S. Harder, L. Brandsma, *J. Organometal. Chem.* **1990**, *385*, 153–159. Synthesis of **6**-Na and **6**-K: T. K. Panda, M. T. Gamer, P. W. Roesky, *Organometallics* **2003**, *22*, 877–878.
- [11] S. Minegishi, H. Mayr, *J. Am. Chem. Soc.* **2003**, *125*, 286–295.
- [12] a) L. Jin, C. Liu, J. Jiu, F. Hu, Y. Lan, A. S. Batsanov, J. A. K. Howard, T. B. Marder, A. Lei, *J. Am. Chem. Soc.* **2009**, *131*, 16656–16657; b) G. T. Achonduh, N. Hadei, C. Valente, S. Avola, C. J. O'Brien, M. G. Organ, *Chem. Comm.* **2010**, *46*, 4109–4111; c) H. N. Hunter, N. Hadei, V. Blagojevic, P. Patschinski, G. T. Achonduh, S. Avola, D. K. Bohme, M. G. Organ, *Chem. Eur. J.* **2011**, *17*, 7845–7851; d) D. R. Armstrong, W. Clegg, P. Garcia-Alvarez, A. R. Kennedy, M. D. McCall, L. Russo, E. Hevia, *Chem. Eur. J.* **2011**, *17*, 8333–8341.
- [13] J. E. Fleckenstein, K. Koszinowski, *Organometallics* **2011**, *30*, 5018–5026.

- [14] W. A. Herrmann, F. E. Kühn, C. C. Romão, *J. Organometal. Chem.* **1995**, 489, C56-C59.
- [15] J. A. Murphy, C. W. Patterson, *J. Chem. Soc. Perkin Trans. I* **1993**, 405-410.
- [16] F. G. Bordwell, G. E. Drucker, H. E. Fried, *J. Org. Chem.* **1981**, 46, 632-635.
- [17] P. v. R. Schleyer, C. Maeker, A. Dramsfeld, H. Jiao, N. J. R. van Eikema Hommes, *J. Am. Chem. Soc.* **1996**, 118, 6317-6318.
- [18] S. Patchkovskii, W. Thiel, *J. Mol. Model.* **2000**, 6, 67-75.
- [19] a) F. G. Bordwell, G. E. Drucker, *J. Org. Chem.* **1980**, 45, 3325-3328; b) W. S. Matthews, J. E. Bares, J. E. Bartmes, F. G. Bordwell, F. J. Cornforth, G. E. Drucker, Z. Margolin, R. J. McCallum, G. J. McCollum, N. R. Vanier, *J. Am. Chem. Soc.* **1975**, 97, 7006-7014.
- [20] a) C. S. Kraihanzel, M. L. Losee, *J. Am. Chem. Soc.* **1968**, 90, 4701-4705; b) A. J. Ashe, III, *J. Am. Chem. Soc.* **1970**, 92, 1233-1235; c) A. Davison, P. E. Rakita, *Inorg. Chem.* **1970**, 9, 289-294; d) K. W. Egger, T. L. James, *J. Organometal. Chem.* **1971**, 26, 335-343; e) N. M. Segeyev, G. I. Avramenko, A. V. Kisin, V. A. Korenevsky, Y. A. Ustinyuk, *J. Organometal. Chem.* **1971**, 32, 55-77; f) D. Nori-Sharg, F. Roohi, F. Deyhimi, R. Naeem-Abyaneh, *THEOCHEM* **2006**, 763, 21-28.
- [21] A. L. Allred, E. G. Rochow, *J. Inorg. Nucl. Chem.* **1958**, 5, 264-268.
- [22] H. E. Gottlieb, V. Kotlyar, A. Nudelman, *J. Org. Chem.* **1997**, 62, 7512-7515.
- [23] M. Mosrin, P. Knochel, *Org. Lett.* **2009**, 11, 1837-1840.



## Chapter 6

# Ambident Reactivity of Enolates in Polar Aprotic Solvents

*Francisco Corral Bautista and Herbert Mayr*

### 1. Introduction

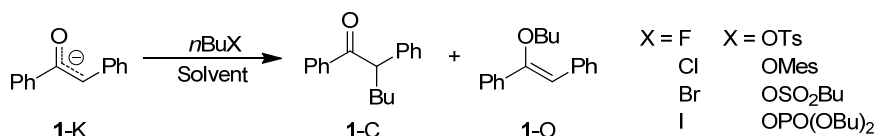
Enolate ions are probably the most used ambident nucleophiles in organic synthesis as they react with a large variety of electrophiles allowing numerous transformations, which lead to a wide range of products.<sup>[1]</sup> However, controlling their regioselectivity has been a dilemma for chemist during decades. Pearson's principle of hard and soft acids and bases (HSAB) was a first attempt to describe the regioselectivity of ambident reactivity.<sup>[2]</sup> Thereby, electrophiles with a high polarized bond between the carbon and leaving-group were terminated as "hard electrophiles", and should yield enol ethers as main product when they are combined with enolate ions. Accordingly showed Zimmerman that enolate ions are protonated at the "hard" oxygen in a fast, reversible step, whereas the thermodynamically more stable ketone is formed by a slow reaction.<sup>[3]</sup> However, the combination of enolate ions with carbocations, which are "hard" electrophiles as well, yield exclusively the carbon-alkylated products.<sup>[4]</sup> Furthermore, Buncel *et al.* reported on the attack of the "hard" oxygen of the acetophenone derived enolate at one of the "soft" carbon-atoms of trinitrobenzene.<sup>[5]</sup>

Gompper concluded that changes in selectivity (O- versus C-attack) are a result of the change in polarity in the transition from one system to another (solvent, counter ion, electrophile, etc.) rejecting the assumption that the ratio of the O/C-alkylation increases with the reactivity of the alkylating agent as the oxygen alkylation increased in the row BuI → BuBr → BuCl → BuF while the reactivity of the electrophiles decrease in the same row.<sup>[6]</sup>

As to our knowledge, until nowadays no concept or theory is able to describe the regioselectivity of enolate ions, we study herein systematically the ambident reactivity of enolate ions.

Therefore, the influence of different parameters on the alkylation of the anion of deoxybenzoin (**1**) is studied systematically (Scheme 1). For this purpose, alkylation reactions of the potassium salt of deoxybenzoin (**1-K**) with different butyl derivates were performed under constant conditions by successive change of one parameter (electrophile, solvent, temperature, counter ion, etc). The results are compared with those reported in the literature.

Furthermore, kinetic experiments will show if there is a relationship between reactivity and the regioselectivity.



Scheme 1: Butylation of the anion of deoxybenzoin (**1-K**).

## 2. Results and Discussion

### 2.1. General

**Alkylation Reactions:** The alkylation reactions were performed under argon-atmosphere. Potassium *tert*-butoxide (KO*t*Bu, 33–35 mg, 0.29–0.31 mmol) was dissolved in 8.0 mL of solvent and deoxybenzoin (**1-H**, 54–57 mg, 0.28–0.29 mmol) was added to the KO*t*Bu solution before the electrophile (~0.32 mmol) was added. The reaction mixtures were stirred until **1-K** was consumed which was indicated by decoloration of the intense yellow color of the carbanion (from 10 min for BuI in DMSO to 3 days for BuCl in THF). After an aqueous work up, the crude reactions products were analyzed by  $^1\text{H}$  NMR in  $\text{CDCl}_3$ . The given O/C ratios were obtained as the average of two experiments.. In general, the conversions of all reactions were above 70%.

**Analytical Method:** To determine the ratio between the carbon-alkylated (C-alkylated, **1-C**) and oxygen-alkylated (O-alkylated, **1-O**) product,  $^1\text{H}$  NMR spectroscopy was used. Thereby, the integrals of the signals at 4.54 ppm (triplet, **1-C**) and 6.06 ppm (singlet, **1-O**)<sup>[7]</sup> were compared. To verify the accurateness of this method, well defined amounts of **1-C** and **1-O** were mixed in  $\text{CDCl}_3$  and the obtained ratios of the  $^1\text{H}$  NMR experiments were plotted against the calculated ratio in the respective sample (Figure 1).

As shown in Figure 1, the analysis by NMR furnishes accurate results even when the ratio of the products is small or large.

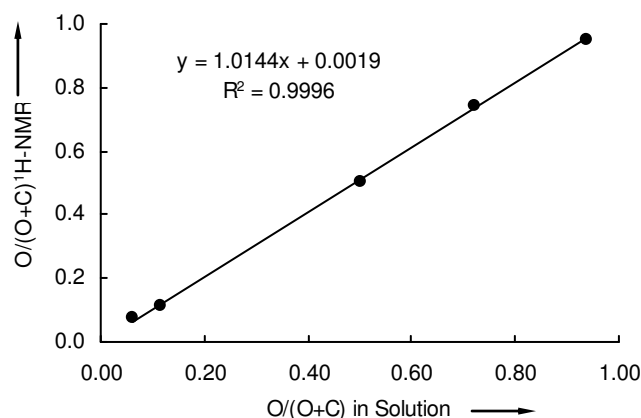


Figure 1: Ratio of **1**-O derived by <sup>1</sup>H NMR experiments versus ratio of **1**-O present in the respective NMR-tube (CDCl<sub>3</sub>, 200 MHz).

## 2.2. Experiments Varying the Concentration

First, the influence of the concentration of the electrophile on the regioselectivity was studied. Therefore, experiments with different amounts/excesses of electrophile were performed in DMSO (Table 1).

Table 1: O/C-Ratio for alkylation reactions of **1**-K with BuI, BuCl and BuOTs in DMSO at different concentrations of the electrophile ([**1**-K] ~ 34-35 mmol L<sup>-1</sup>).

[BuI] / mmol L <sup>-1</sup>	[BuI] / [ <b>1</b> -K]	O/C	[BuCl] / mmol L <sup>-1</sup>	[BuCl] / [ <b>1</b> -K]	O/C	[BuOTs] / mmol L <sup>-1</sup>	[BuOTs] / [ <b>1</b> -K]	O/C
44	1.3	5:95	48	1.4	19:81	40	1.2	62:38
220	7	4:96	250	7	22:78	245	7	63:37
550	15	4:96	590	17	24:76	614	18	59:41
1100	30	5:95	1190	35	24:76			

When the electrophile concentration was varied between 40 and 1200 mmol L<sup>-1</sup>, i.e. from 1.2 to 35 equiv. of electrophile with respect to **1**-K, the O/C-ratio remained almost constant. Thus, the electrophile concentration has no influence on the product ratio.

In the next experiment-series, the overall concentration is varied. Therefore, the amount of solvent (DMSO) is varied for the alkylation reactions of **1**-K with butyl iodide and butyl tosylate (Table 2, Figure 2).

Table 2: O/C Ratio of the alkylation reactions of **1-K** with BuI and BuOTs in DMSO at different concentrations ( $[\text{BuI}] / [\text{1-K}] = 1.2\text{--}1.3$ ;  $[\text{BuOTs}] / [\text{1-K}] = 1.1\text{--}1.2$ ).

BuI		BuOTs	
$[\text{1-K}] / \text{mmol L}^{-1}$	O/C <sup>[a]</sup>	$[\text{1-K}] / \text{mmol L}^{-1}$	O/C <sup>[a]</sup>
2.62	2:98	2.63	51:49
2.74	3:97	2.70	50:50
6.82	3:97	6.65	50:50
6.96	4:96	7.08	54:46
16.1	4:96	1.71	53:47
16.5	4:96	16.2	55:45
34.5	5:95	3.74	61:39
34.8	5:95	35.5	62:38

[a] O/C Ratios are given for a single experiment.

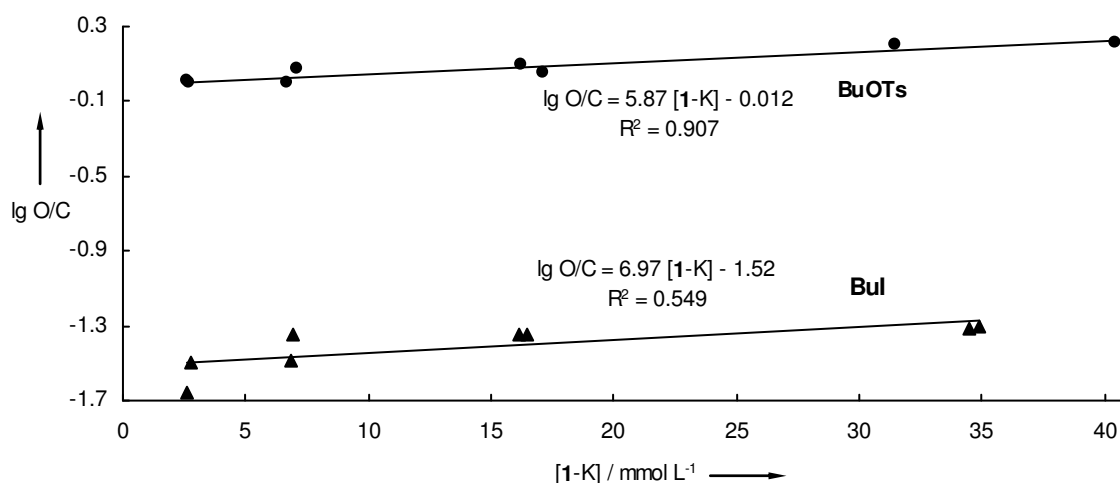
Figure 2: lg O/C of the alkylation reactions of **1-K** with BuI (triangles) and BuOTs (circles) in DMSO at different concentrations versus the concentration of **1-K**.

Table 2 and Figure 2 show that the O/C ratio for the alkylation reactions of **1-K** with BuI and BuOTs in DMSO increases with the concentration. These results are in contrast to Le Noble's conclusion: "*the freer the anion, the larger the O/C ratio*",<sup>[8]</sup> if we assume that the carbanions are better solvated, and the ion-pairs better separated at higher dilution. However, as Table 3 shows, examples in which the oxygen alkylation increases as well as examples in which the carbon alkylation increases with the concentration are reported in the literature.<sup>[9]</sup>

Table 3: O/C Ratio of the methylation reactions of the anions of propiophenone and phenylacetone in HMPT at different concentrations.<sup>[9]</sup>

<i>c</i> (Enolate)				
	+ MeI in HMPT	+ (MeO) <sub>2</sub> SO <sub>2</sub> in HMPT	+ (MeO) <sub>3</sub> PO in HMPT	+ (MeO) <sub>2</sub> SO <sub>2</sub> in HMPT
	O/C	O/C	O/C	O/C
0.1 mol L <sup>-1</sup>	5:95	90:10	50:50	
0.2 mol L <sup>-1</sup>	6:94	87:13		69:31
0.5 mol L <sup>-1</sup>	7:97	86:14	44:56	50:50
1.0 mol L <sup>-1</sup>	9:91	83:17	41:59	50:50

Though the effects of the concentration on the regioselectivity of the alkylation of enolate ions are small, the results found in this work and those reported in the literature are contradictory and no general rule is observed.

### 2.3. Experiments Varying the Solvent and the Electrophile

Reactions of **1-K** with different butylation agents (BuI, BuBr, BuCl, BuF, BuOTs, BuOMes, (BuO)<sub>2</sub>SO<sub>2</sub> and (BuO)<sub>3</sub>PO), were performed in different solvents (DMSO, DMF, acetone, THF and Et<sub>2</sub>O). The resulting O/C ratios are summarized in Table 4.

Table 4: O/C Ratios for alkylation reactions of **1-K** with different butylation agents in different solvents ([**1-K**]  $\approx$  0.28–0.29 mmol L<sup>-1</sup>, [BuX]  $\approx$  0.32 mmol L<sup>-1</sup>).

	DMSO	DMF	Acetone	THF	Et <sub>2</sub> O
BuI	5:95	4:96	5:95	4:96	
BuBr	15:85	12:88	15:85	17:83	— <sup>[a]</sup>
BuCl	19:81	28:72	31:69	20:80	— <sup>[a]</sup>
BuF	— <sup>[b]</sup>	— <sup>[b]</sup>		— <sup>[b]</sup>	
BuOTs	62:38	65:35	60:40	39:61	— <sup>[a]</sup>
BuOMes	69:31	70:30	65:35	30:70	
(BuO) <sub>2</sub> SO <sub>2</sub>	66:34	69:31	64:36	29:71	14:86 <sup>[c]</sup>
(BuO) <sub>3</sub> PO	— <sup>[d]</sup>	— <sup>[d]</sup>			

[a] No product formation was observed. Heterogeneous mixture. [b] No product formation was observed after two weeks. [c] Reaction in heterogenic media. [d] No product formation was observed with [(BuO)<sub>3</sub>PO]  $\approx$  0.3–0.7 mmol L<sup>-1</sup>.

In general, the reactions in DMSO and DMF showed conversions above 70%. The reactions in THF and acetone showed lower conversions for the reactions with BuCl (54% in THF and 35% in acetone, compare Experimental Section). The reactions of **1-K** with BuF did not show any product formation independent of the solvent. For these reactions, no product formation was observed by GC/MS analysis even after two weeks. The reactions with tributyl phosphate did not show any product formation as well, even when an excess of electrophile was applied (1.2–2.5 equiv.). The reactions performed in Et<sub>2</sub>O were only successful for (BuO)<sub>2</sub>SO<sub>2</sub>. In general, **1-K** forms in diethyl ether a heterogenic system and obviously, only dibutyl sulfate is electrophilic enough to undergo a reaction with the poorly soluble salt under these conditions.

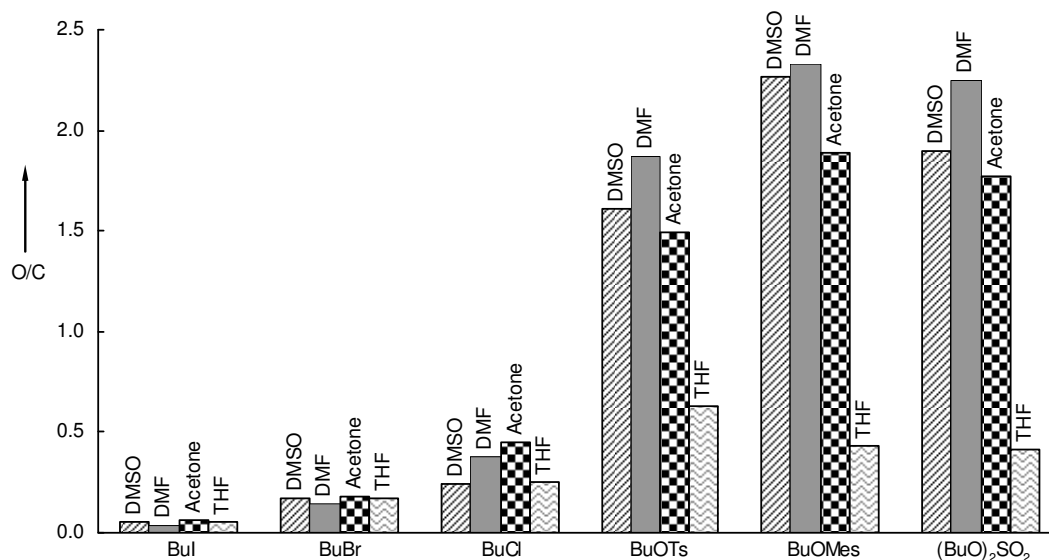


Figure 3: O/C Ratios for butylation reactions of **1-K** in different solvents.

Figure 3 visualizes how the product ratios of the alkylation reactions of **1-K** are affected by different electrophiles and different solvents. Though the main product of the alkylation reactions with butyl halides is the carbon-alkylated **1-C**, the amount of oxygen alkylated product **1-O** increases from BuI to BuBr to BuCl. If the butyl-group of the electrophile is bounded to an oxygen, as it is in butyl tosylate, -mesylate and -sulfate, the major product is the oxygen-alkylated one. Exceptions are the reactions in THF, where carbon-attack was predominant for all reagents. Furthermore, while alkylations with butyl iodide and butyl bromide yielded similar product ratios in the different solvents, differences between the solvents are more noticeable for the alkylations of **1-K** with butyl chloride, where higher O/C ratios are obtained. The different solvents showed the biggest effect in the alkylation reactions of **1-K** with BuOTs, BuOMes and (BuO)<sub>2</sub>SO<sub>2</sub>.

From plots of the O/C ratios of the alkylation reactions of **1-K** with different alkylation agents with the solvent polarity parameters  $E_T^N$ ,<sup>[10]</sup> as done for three examples in Figure 4, one can see that the solvent polarity has no direct influence on the carbon- or oxygen-attack. While the amount of oxygen-alkylated product decreases with increasing solvent polarity for the reactions of **1-K** with BuBr, the O/C ratio for the reactions of **1-K** with BuCl increases with the polarity from acetone to THF, but decreases again when the solvent polarity increases further (from THF to DMF to DMSO). A similar behavior is found for the reactions of **1-K** with (BuO)<sub>2</sub>SO<sub>2</sub>: a strong increase of the O/C ratio from diethyl ether to DMF followed by a decrease from DMF to DMSO. An analogous plot as in Figure 4 was reported by Gompper

and Wagner for the alkylation of the sodium salt of propiophenone, but here, a linear relation between  $\lg O/C$  and solvent polarity was found.<sup>[6]</sup>

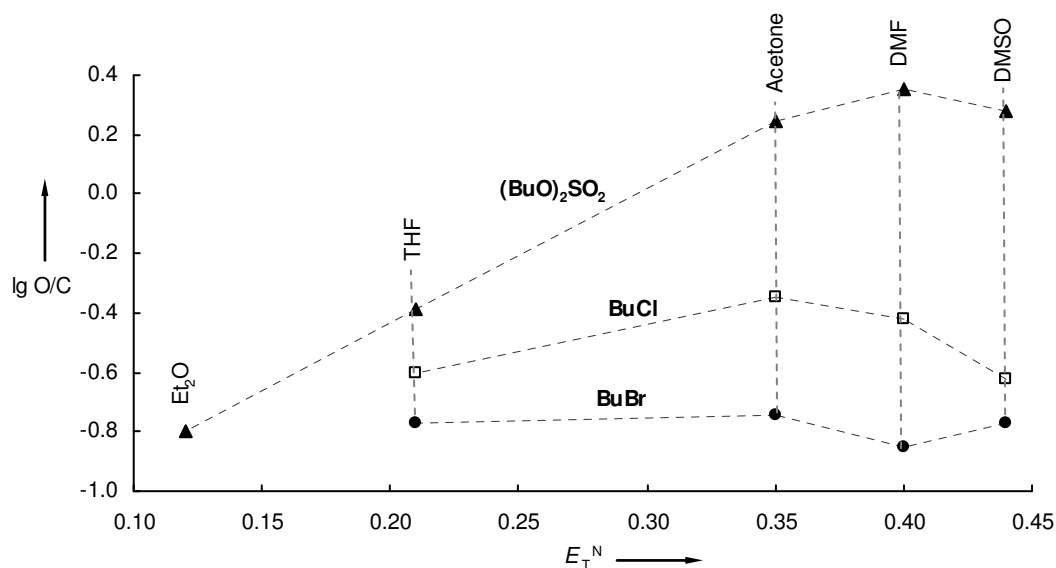


Figure 4: O/C Ratios for butylation reactions of **1-K** with BuBr, BuCl and  $(BuO)_2SO_2$  in different solvents versus the solvent polarity parameter  $E_T^N$  of the solvent.<sup>[10]</sup>

When product ratios are correlated with the acceptor number ( $AN$ , Figure 5) or the relative permittivity (dielectric constant  $\epsilon_r$ , Figure 6), plots with analogous shapes as in Figure 4 are obtained, indicating that an increase of solvent polarity does not generally lead to an increase in oxygen alkylation.

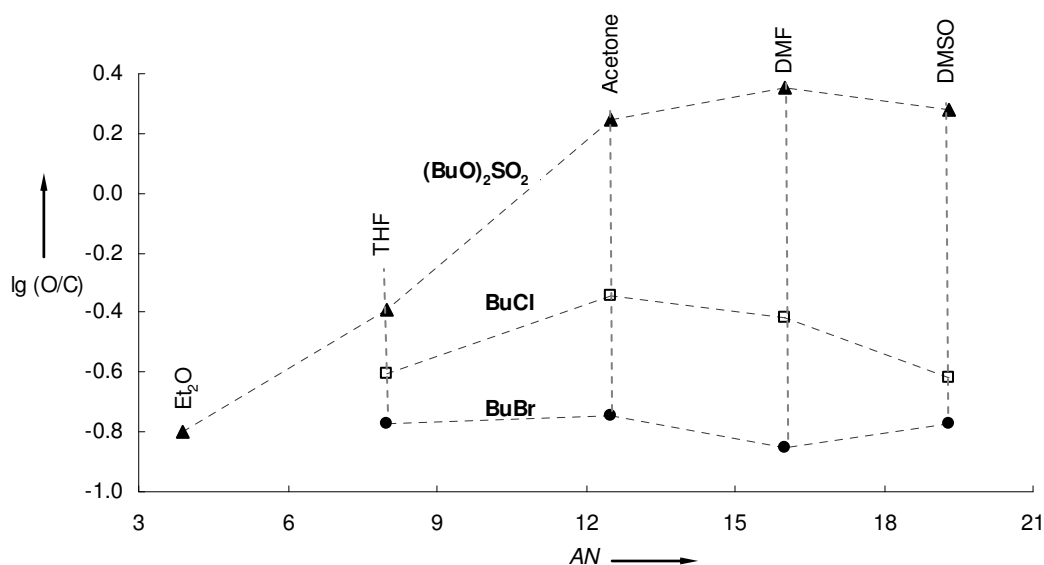


Figure 5: O/C Ratios for butylation reactions of **1-K** with BuBr, BuCl and  $(BuO)_2SO_2$  in different solvents versus the Acceptor Number  $AN$  (polarity parameter) of the solvent.<sup>[10]</sup>

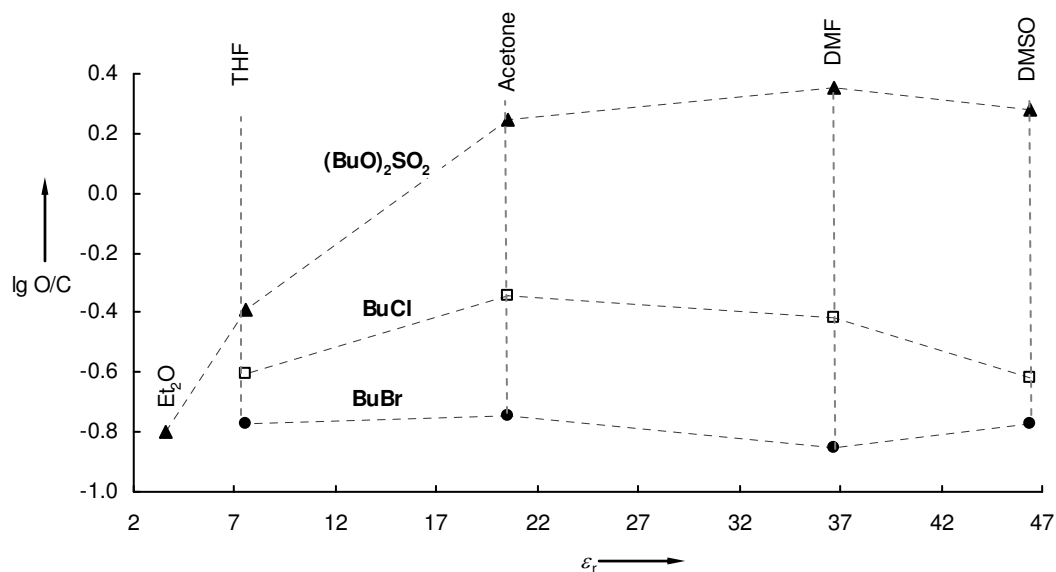


Figure 6: O/C Ratios for butylation reactions of **1-K** with BuBr, BuCl and  $(BuO)_2SO_2$  in different solvents versus the relative permittivity (dielectric constant)  $\epsilon_r$  of the solvent.<sup>[10]</sup>

Various publications reported an increase of oxygen alkylation with increasing solvent polarity, which is explained by a better solvation of the carbanion and the counter ion.<sup>[8,11]</sup> Furthermore is reported, that small amounts of water in the solvent, which affects the solvation properties of the solvent, have an influence on the regioselectivity of the alkylation of sodium naphthalen-2-olate with benzyl bromide in THF.<sup>[12]</sup> Another factor which has to be considered is whether the reaction takes place in a heterogeneous or homogeneous medium. Kornblum and Lurie studied this based on the alkylation of sodium phenolate and potassium *tert*-octyl-phenolate, concluding that a homogenous reaction mixture yields exclusively oxygen alkylation,<sup>[13]</sup> whereas a heterogeneous reaction lead to mixtures of oxygen- and carbon-alkylated products.<sup>[14]</sup> Moreover, the regioselectivity of the alkylations of enolate ions which are performed in heterogeneous media, can be influenced by phase-transfer catalysts<sup>[7]</sup> or by additives as quaternary ammonium salts.<sup>[15]</sup> Therefore, the influence of the heterogeneity on the reaction has to be considered, when product ratio for the alkylation of **1-K** with  $(BuO)_2SO_2$  in diethyl ether is compared with those obtained in the more polar solvents.

## 2.4. Variation of the Counter Ion

As shown in previous works, the counter ion can have a strong influence on the reactivity of carbanions.<sup>[4b]</sup> Therefore, alkylation reactions with different alkali salts of deoxybenzoin (**1-M**, M = Li, Na, K), as well as alkylations adding dicyclohexano-18-crown-6 to **1-K**



([crown] / [**1-K**]  $\approx$  1.2–1.5), were performed in DMSO and in THF (Table 5, Figure 7). The different alkali derivatives were generated by mixing deoxybenzoin (**1-H**) with a solution of the corresponding alkali *tert*-butoxide (LiOtBu, NaOtBu, KOtBu) in DMSO or THF.

Table 5: O/C Ratios for the alkylation of **1-M**, (M = Li, Na, K, K/crown) with BuI, BuCl and BuOTs in DMSO and THF.

	<b>M<sup>+</sup></b>	<b>O/C</b>	<b>BuI</b>	<b>O/C</b>	<b>BuCl</b>	<b>O/C</b>	<b>BuOTs</b>
			<b>conversion<sup>[a]</sup></b>		<b>conversion<sup>[a]</sup></b>		<b>conversion<sup>[a]</sup></b>
DMSO	Li <sup>+</sup>	4:96	97%	24:76	96%	60:40	88%
	Na <sup>+</sup>	4:96	98%	24:76	98%	60:40	95%
	K <sup>+</sup>	5:95	88%	19:81	83%	62:38	80%
	K <sup>+</sup> /crown	4:96	> 60% <sup>[b]</sup>	23:77	> 60% <sup>[b]</sup>	60:40	>50% <sup>[b]</sup>
THF	Li <sup>+</sup>	0:100 <sup>[c]</sup>	70%	— <sup>[d]</sup>	0%	— <sup>[d]</sup>	0%
	Na <sup>+</sup>	0:100 <sup>[c]</sup>	82%	— <sup>[d]</sup>	0%	0:100 <sup>[c]</sup>	19%
	K <sup>+</sup>	4:96	87%	20:80	54%	39:61	35%
	K <sup>+</sup> /crown	7:93	100%	40:60	33%	77:23	> 50% <sup>[b]</sup>

[a] Average of two runs (for each run see Experimental Section). [b] Exact conversion could no be derived from <sup>1</sup>H NMR experiments as signals are superimposed. [c] Only carbon-alkylation was observed. [d] No reaction was observed.

As shown in Table 5, not only the O/C ratios are affected by changing the counter ion of the nucleophile, but also the conversions of the reactions are influenced. Whereas all reactions in DMSO show almost quantitative conversions, in THF, **1-Li** only reacted with BuI and **1-Na** only showed a good conversion with BuI, but only 19% with BuOTs and no reaction with BuCl. The potassium derivative showed moderate conversions, whereas the free carbanion (K/crown) reacts with BuI quantitatively and with BuCl and BuOTs with moderate yields.

As visualized by Figure 7, the counter ion effect is in THF more pronounced than in DMSO. Previous studies showed that the potassium salt of deoxybenzoin (**1-K**) behaves as the free carbanion in DMSO solution at [**1-K**]  $\approx$  0.1–1 mmol L<sup>-1</sup>, and that increasing the potassium concentration over 10 mmol L<sup>-1</sup>, only had moderate effects on the reactivity of **1-K**.<sup>[4b]</sup> Accordingly, Table 5 shows that the O/C ratios of the reactions of **1-M** in DMSO are poorly affected by the counter ion M = K<sup>+</sup>/crown, K<sup>+</sup>, Na<sup>+</sup>, Li<sup>+</sup>. When the reactions are performed in THF, the effects are stronger, for example, the reactions of BuI with the lithium and sodium derivatives of **1** only lead to carbon-alkylation. The strongest counter-ion effect, however, is obtained when crown ether is added to the potassium salt **1-K** in THF. Thus, addition of 18-crown-6 increases the O/C ratio for the reactions by a factor of two.

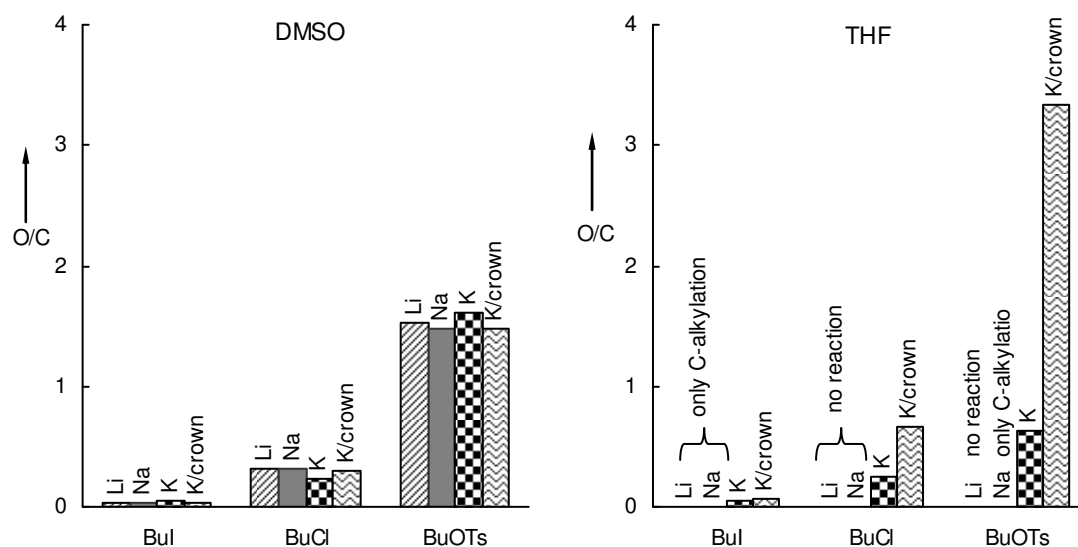


Figure 7: O/C Ratios for the alkylation reactions of **1**-M (M = Li, Na, K, K/crown) with BuI, BuCl and BuOTs in DMSO (left) and THF (right).

The results in this work are in accord to the observations of Arnett and de Palma, who report that the lithium salts of dibenzoylmethane and dipivaloylmethane do not react with methylfluorosulfonate in propylene carbonate, whereas the sodium, potassium and cesium derivatives of the diketones yield the oxygen alkylated products almost quantitatively.<sup>[16]</sup> Brieger and Pelletier reported for the reactions of ethyl acetoacetate with butyl chloride in DMF under addition of different alkali carbonates, that the O/C ratio of the products increase from lithium to sodium or potassium (Table 6).<sup>[11b]</sup> A further example describes the ambident reactivity of ethyl acetoacetate anions towards allyl chloride in HMPT (Table 6).<sup>[8]</sup> The counter ion effect in this example is not that pronounced as HMPT has good solvating properties and can separate the ion pairs. However, a slight increase of the O/C ratio from lithium over sodium to potassium is observable. Though the product ratio is moderately affected by the counter ion, the decrease of the reaction time from the lithium derivative to the sodium salt by a factor of 42 is remarkable.

Table 6: O/C Ratios for the alkylations of alkali salts of ethyl acetoacetate under different conditions in dependence of the counter ion.

M <sup>+</sup>	Ethyl acetoacetate and butyl chloride in DMF (130 °C) <sup>[a]</sup>	Ethyl acetoacetate and allyl chloride in HMPT (95 °C) <sup>[b]</sup>	
	O/C	O/C	Reaction time
Li <sup>+</sup>	19:81	12:88	210 min
Na <sup>+</sup>	61:39	17:87	5 min
K <sup>+</sup>	53:57	17:87	3 min
K <sup>+</sup> /tetraglyme		17:87	3 min
Bu <sub>4</sub> N <sup>+</sup>		16:84	3 min

[a] From ref.<sup>[11b]</sup> [b] From ref.<sup>[8]</sup>

Sarthou, Bram and Guibe, moreover, reported the effects of alkali salt additives on the product ratio of the alkylation of the lithium and sodium salts of ethyl acetoacetate with ethyl bromide and ethyl tosylate in DMF at 25 °C. As expected, the oxygen-alkylation decreased with the concentration of the added  $\text{LiClO}_4$  or  $\text{NaClO}_4$ .<sup>[17]</sup>

The counter ion has not only an influence on the product ratio, but also on the reaction rate. Smaller cations are stronger coordinated by enolate ions,<sup>[18]</sup> and therefore the oxygen alkylation increases in the row  $\text{Li}^+ > \text{Na}^+ > \text{K}^+$ . However, solvents coordinate the metal cations as well and therefore the role of the solvent can not be neglected. Thus, highly polar solvents, such as DMSO and HMPT, decrease the counter ion effect compared to, for example, THF.

## 2.5. Experiments Varying the Temperature

To study the influence of the temperature on the product ratio of the alkylation of **1-K**, reactions were performed in DMSO and in THF at different temperatures (Table 7). To exclude a temperature induced isomerisation of the reaction products, **1-C** and **1-O** were heated to 80–100 °C in  $[\text{D}_6]$ -DMSO during 5–7 hours.  $^1\text{H}$  NMR experiments showed that both, **1-C** and **1-O** are stable compounds and that no isomerisation takes place.

Table 7: O/C Ratios for the alkylation of **1-K** with different butyl derivatives in DMSO and THF at different temperatures.

	DMSO					THF	
	20 °C	40 °C	60 °C	80 °C	100 °C	20 °C	50 °C
BuI	5:95	6:94	10:90	11:89	14:86	4:96	5:95
BuBr	15:85			22:78		17:83	18:82
BuCl	19:81	30:70	34:66	35:65	43:57		
BuOTs	63:57	62:58	59:41	53:47	48:52	39:61	28:72
BuOMes	69:31			64:36			
$(\text{BuO})_2\text{SO}_2$	66:34			57:43		29:71	26:74

Table 7 shows that the oxygen attack is favored by increasing the temperature for the alkylations with butyl halides, whereas the O/C ratio for the alkylations with butyl- tosylate, mesylate and sulfate decrease by increasing the temperature.

Eyring-type plots of the O/C ratios versus temperature for the reactions of **1-K** with BuI, BuCl and BuOTs in DMSO, from which the activation parameters and the isoselective temperature ( $\mathcal{G}_{\text{iso}}$ ;  $\text{O/C} = 1$ ) were calculated, are shown in Figure 8. As the experiments were performed below the isoselective temperature, the O/C ratios approach 1 [ $\ln(\text{O/C}) = 0$ ] by increasing the temperature independent from the electrophile.

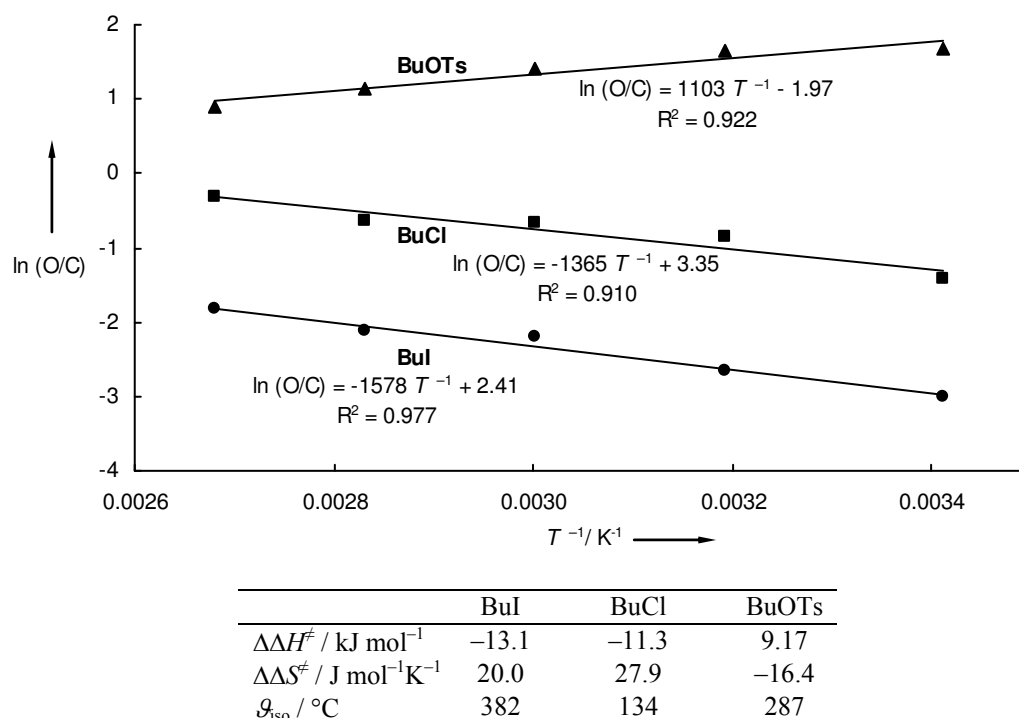


Figure 8: Plots of the O/C ratios for the alkylation reactions of **1-K** with BuI, BuCl and BuOTs in DMSO at different temperatures versus  $T^{-1}$  and calculated activation parameter for the respective reactions.

The Eyring-type plots for the alkylation of the potassium salt of ethyl acetoacetate with butyl chloride in DMSO and *N*-methyl pyrrolidone which are shown in Figure 9, show in contrast a positive slope for the reaction in *N*-methyl pyrrolidone, and no linear relationship for the reaction in DMSO.<sup>[11b]</sup> One possible reason could be, that the experiments shown in Figure 9 cross the isoselective temperature.

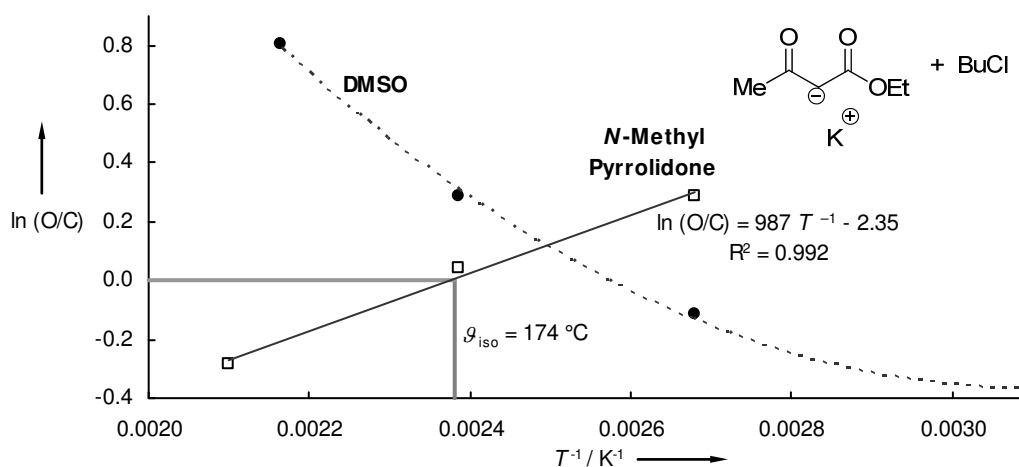
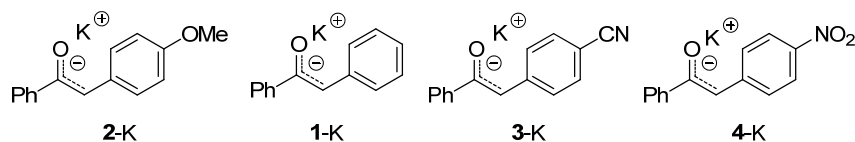


Figure 9: Plots of the O/C ratios for the alkylation reactions of the potassium salt of ethyl acetoacetate with BuCl in DMSO and *N*-methyl pyrrolidone at different temperatures versus  $T^{-1}$ .<sup>[11b]</sup>

## 2.6. Variation of the Substituent on Deoxybenzoin Anions

Introducing electron withdrawing or electron donating groups in *para*-position of the benzylic moiety of deoxybenzoin (**1**) changes the electronic structure without affecting the steric situation at the carbanionic center (Scheme 2).



Scheme 2: Substituted deoxybenzoin anions (**1–4**)-K.

The alkylation experiments of the potassium salts of the substituted deoxybenzoins (**1–4**)-K in DMSO were performed in analogy to the above mentioned experiments ( $[(\mathbf{1-4})\text{-K}] \approx 0.28 - 0.30 \text{ mmol L}^{-1}$ ;  $[\text{BuX}] \approx 0.32 - 0.35 \text{ mmol L}^{-1}$ ; Table 8, Figure 10).

Table 8: O/C Ratios for the alkylation of different substituted deoxybenzoin anions (**1–4**)-K with BuI and BuOTs in DMSO.

	$\sigma_p^{-[\text{a}]}$	BuI	BuOTs
<b>2-K</b> (R = OMe)	-0.27	6:94	67:33
<b>1-K</b> (R = H)	0	5:95	62:38
<b>3-K</b> (R = CN)	0.56	4:96	51:39
<b>4-K</b> (R = NO <sub>2</sub> )	0.78	3:97	59:41

[a] From ref.<sup>[19]</sup>

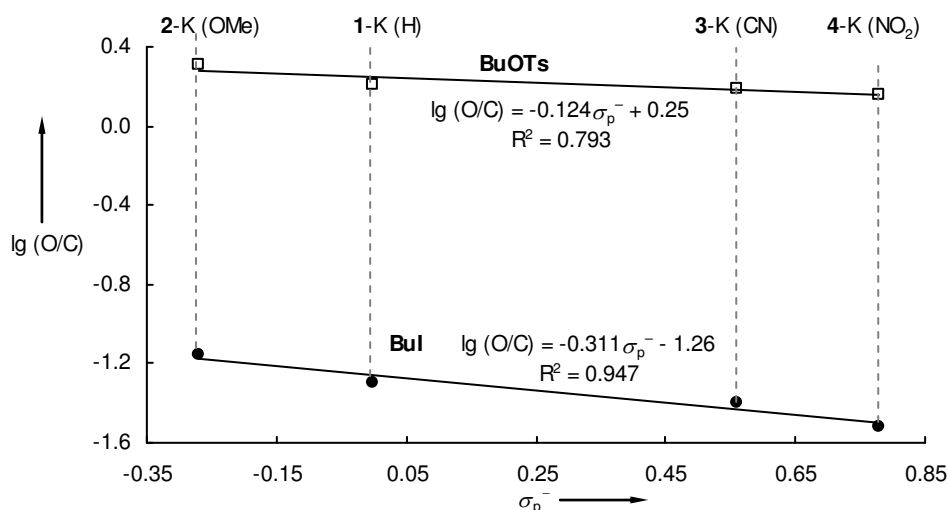


Figure 10: O/C Ratios for the alkylation reactions of substituted deoxybenzoins (**1–4**)-K with BuI and BuOTs in DMSO versus Hammett's substituent parameters  $\sigma_p^-$ .

As shown in Table 8, the O/C ratios decrease when electron withdrawing groups are introduced. Thus, a decrease in electron density at the carbanionic center results in an increase of carbon-alkylation. Figure 10 shows a correlation of the O/C ratios of these reactions with Hammett's substituent parameters  $\sigma_p^-$ <sup>[19]</sup> which visualizes these effects.

In contrast to the results of this work, plots of the same type for the methylation reactions of the sodium salts of substituted aryl acetones in HMPT or THF do not show any correlation (Figure 11).<sup>[9,20]</sup> Though the shapes of both plots look similar, a relationship between the regioselectivity of the reactions and the electronic structure of the nucleophiles could not be derived.

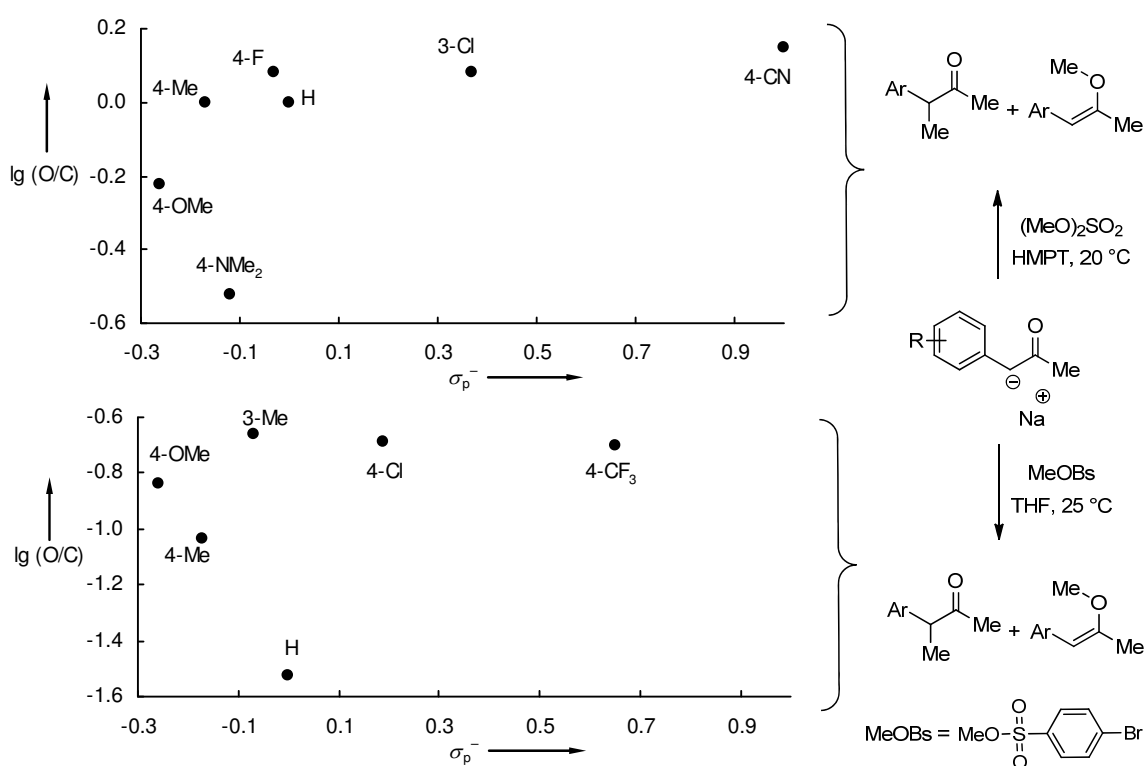


Figure 11: O/C Ratios for the alkylation reactions of the sodium salts of substituted aryl acetones with dimethyl sulfate in HMPT (top) and MeOBs in THF (bottom) versus Hammett's substituent parameters  $\sigma_p^-$ .<sup>[9,20]</sup>

A further example for the influence of substituents on the regioselectivity is shown for the alkylation of the sodium salt of propiophenone with dimethyl sulfate in Figure 12.<sup>[9]</sup> As the carbanionic center of propiophenone anion is not in direct conjugation with the substituents, the product ratio ( $\lg(O/C)$ ) is correlated with  $\sigma$  instead of  $\sigma_p^-$ . But even, when the data of Gompper *et al.* is correlated with  $\sigma_p^-$ , it is obvious that the slope of this plot is positive and of a higher magnitude than that obtained from the data of this work. A Hammett-type plot with a

positive slope is obtained as well for the reaction of the potassium salts of substituted acetophenones with 2,6-difluorobenzonitrile in DMSO at 25 °C (correlation shown in the Appendix).<sup>[21]</sup>

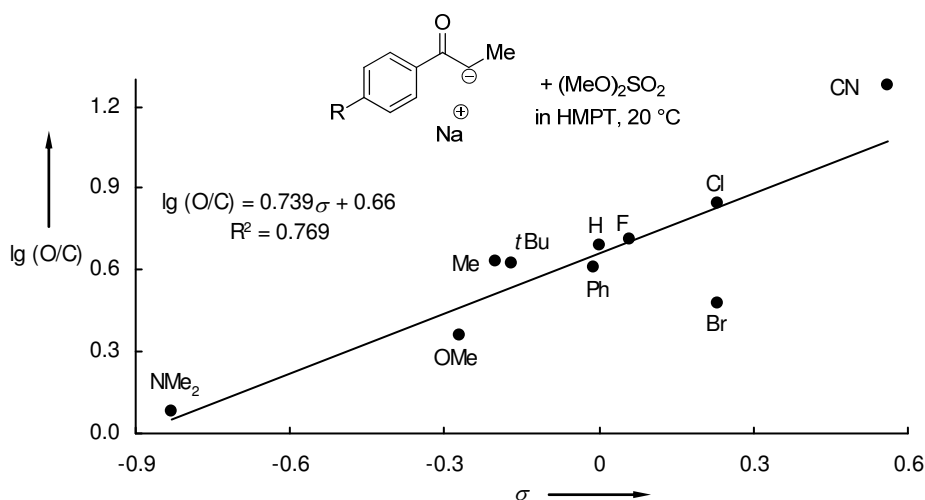


Figure 12: O/C Ratios for the alkylation reactions of substituted propiophenones with dimethyl sulfate in HMPT versus Hammett's substituent parameters  $\sigma$ .<sup>[9]</sup>

The allopolarization principle says that the change in regioselectivity is induced by a change of the polarity of the ambident system due to modifications in the substitution pattern.<sup>[6,23]</sup> However, the presented examples show some discrepancies. While the “polarity of the ambident system” (by introduction of substituents in the aromatic moiety) should change in the same way in all examples, the response of the regioselectivity is quite different.

## 2.7. Kinetic Studies

The relation between regioselectivity and reactivity is studied in this section. First, the nucleophilicity of the anion of deoxybenzoin in different solvents is compared with the product ratios obtained in the first part of this work. Secondly, the nucleophilicities (in DMSO solution) of the substituted deoxybenzoins (**2–4**) are determined and in the third part, kinetic studies of the alkylation reactions are described.

### 2.7.1. Alkylation and Nucleophilicity

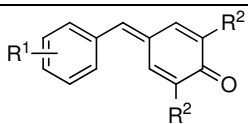
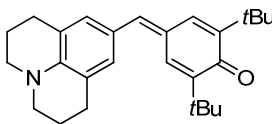
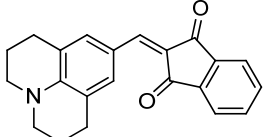
Based on the reactions of  $\pi$ -,  $n$ -, and  $\sigma$ -nucleophiles with benzhydrylium ions and structurally related Michael acceptors (reference electrophiles), the linear free-energy relationship (1),<sup>[23]</sup> is a useful tool for the quantification of the nucleophilic and electrophilic reactivity.<sup>[4,24]</sup> In

this equation,  $E$  is an electrophile-specific parameter, and  $N$  and  $s_N$  are nucleophile-specific parameters.

$$\lg k_2(20\text{ }^\circ\text{C}) = s_N(N + E) \quad (1)$$

Applying (1), the nucleophilic reactivity of **1-K** in DMSO was characterized.<sup>[4b]</sup> To examine how the nucleophilic reactivity of the enolate **1-K** changes in different solvents, the rate constants of the reactions of **1-K** with Michael acceptors **5** (reference electrophiles, Table 9) were determined in order to calculate the nucleophilicity parameters  $N$  and  $s_N$  in different solvents.

Table 9: Michael acceptors used as reference electrophiles.

	<b>5</b>	<b>R<sup>1</sup></b>	<b>R<sup>2</sup></b>	<b>E<sup>[a]</sup></b>	<b><math>\lambda_{\max}^{[b]}</math></b>
	<b>5a</b>	4-OMe	Ph	-12.18	422
	<b>5b</b>	4-NMe <sub>2</sub>	Ph	-13.39	533
	<b>5c</b>	4-NO <sub>2</sub>	<i>t</i> Bu	-14.36	374
	<b>5d</b>	3-F	<i>t</i> Bu	-15.03	354
	<b>5e</b>	4-Me	<i>t</i> Bu	-15.83	371
	<b>5f</b>	4-OMe	<i>t</i> Bu	-16.11	393
	<b>5g</b>	4-NMe <sub>2</sub>	Me	-16.36	490
	<b>5h</b>	4-NMe <sub>2</sub>	<i>t</i> Bu	-17.29	486
	<b>5i</b>			-17.90	521
	<b>5j</b>			-14.68	[c]
[a] From ref. <sup>[4a,24d,25]</sup> [b] In nm in DMSO. [c] Not used in this study. See Table 10.					

The reactions of **1-K** with the reference electrophiles **5** were performed in DMF, acetone and THF solution at 20 °C and monitored by UV-Vis spectroscopy at or close to the absorption maxima of the electrophiles. To simplify the evaluation of the kinetic experiments, the carbanion was used in large excess (> 10 equiv.). Thus, the concentrations of the nucleophile remained almost constant throughout the reactions, and pseudo-first-order kinetics were obtained in all runs. The first-order rate constants  $k_{\text{obs}}$  were derived by least-squares fitting of the exponential function  $A_t = A_0 \exp(-k_{\text{obs}}t) + C$  to the time-dependent absorbances  $A_t$  of the electrophiles. Second-order rate constants (Table 10) were obtained as the slopes of plots of  $k_{\text{obs}}$  versus the nucleophile concentrations (Figure 13).

As acetone is not stable towards strong bases for a long time, the KO*t*Bu stock solution which was used for the deprotonation of the ketone **1-H** was prepared in DMSO and both solutions



were combined just before the measurements. Generally, the kinetic experiments were finished in less than 5 min after the deprotonation. The concentration of the KO $t$ Bu solution was chosen in that way, that the amount of DMSO was less than 3%.

As the anion of deoxybenzoin can interact with potassium in the different solvents, 18-crown-6 was added to complex the cation. The ratio [crown ether]/[**1-K**]  $\approx$  1.2 – 2.5 was varied for the determination of the different first-order rate constants. As the obtained first-order rate constants correlate linearly with the concentration of the nucleophile, it can be assumed that the obtained second-order rate constants correspond to those of the free anion in the respective solvent. Furthermore, for some examples, rate constants in absence of 18-crown-6 were determined (Table 10).

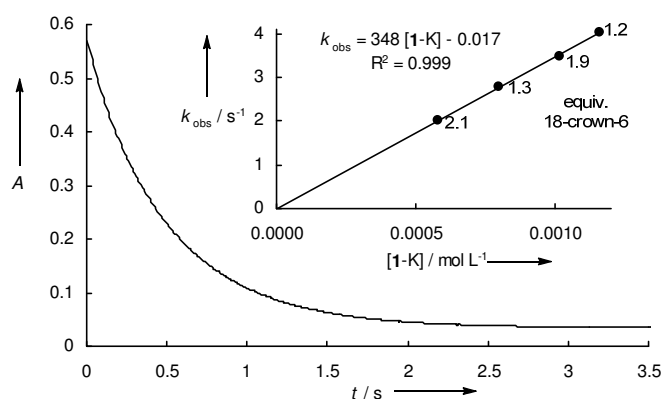


Figure 13: Plot of the absorbance  $A$  (486 nm) versus time for the reaction of **1-K** ( $5.80 \times 10^{-4} \text{ mol L}^{-1}$ ) and **5h** ( $1.33 \times 10^{-5} \text{ mol L}^{-1}$ ) in acetone at 20 °C. Inset: Plot of  $k_{\text{obs}}$  versus  $[1-K]$ .

Table 10 shows that the counter-ion effect is negligible in DMF. Here, first-order rate constants  $k_{\text{obs}}$  which were obtained in presence and in absence of 18-crown-6 correlate linearly with the concentration of the nucleophile. The reactions in acetone and in THF, however, show remarkable differences between the second-order rate constants which were obtained in presence or in absence of crown ether.

Correlations of  $\lg k_2$  for the reactions of **1** with quinone methides **5** (in the respective solvent) versus the electrophilicity parameters of the electrophiles were linear (Figure 14). From these plots, the nucleophilicity parameter  $N$  could be derived from the negative intercept with the abscissa and the sensitivity parameters  $s_N$  correspond to the slopes of the correlations. As the rate constants which were obtained in presence of 18-crown-6 were correlated with the electrophilicity of the quinone methides, the nucleophilicity parameters of the free carbanion **1** were obtained (Figure 14, Table 10).

Table 10: Second-order rate constants for the reactions of **1-K** with quinone methides **5**,  $N$  and  $s_N$  parameters of the free carbanion of deoxybenzoin **1** (potassium salts/18-crown-6) in different solvents at 20 °C.

Solvent	$N^{[a]}$ $s_N^{[a]}$	Electrophile	$k_2 / \text{Lmol}^{-1}\text{s}^{-1}$
DMSO	23.14 <sup>[b]</sup> 0.60 <sup>[b]</sup>	<b>5b</b>	$1.05 \times 10^6$ <sup>[b]</sup>
		<b>5j</b>	$9.79 \times 10^4$ <sup>[b]</sup>
		<b>5g</b>	$9.86 \times 10^3$ <sup>[b]</sup>
		<b>5h</b>	$3.59 \times 10^3$ <sup>[b]</sup>
		<b>5i</b>	$1.83 \times 10^3$ <sup>[b]</sup>
DMF	26.69 0.39	<b>5g</b>	$9.84 \times 10^3$
		<b>5g</b>	$9.88 \times 10^3$ <sup>[c]</sup>
		<b>5h</b>	$4.04 \times 10^3$ <sup>[d]</sup>
		<b>5i</b>	$2.53 \times 10^3$ <sup>[d]</sup>
Acetone	24.39 0.50	<b>5g</b>	$1.02 \times 10^4$
		<b>5h</b>	$3.48 \times 10^3$
		<b>5h</b>	$1.26 \times 10^3$ <sup>[c]</sup>
		<b>5i</b>	$1.74 \times 10^3$
		<b>5i</b>	$4.86 \times 10^2$ <sup>[c]</sup>
THF	21.93 0.60	<b>5g</b>	$2.11 \times 10^3$
		<b>5g</b>	$5.52 \times 10^2$ <sup>[c]</sup>
		<b>5h</b>	$6.36 \times 10^2$
		<b>5i</b>	$2.50 \times 10^2$
		<b>5i</b>	$8.93$ <sup>[c]</sup>

[a] Of the free carbanions. [b] From ref.<sup>[4b]</sup> [c] In absence of 18-crown-6. Not used for the calculation of  $N$  and  $s_N$ . [d] Calculated from first-order rate constants in presence and in absence of 18-crown-6.

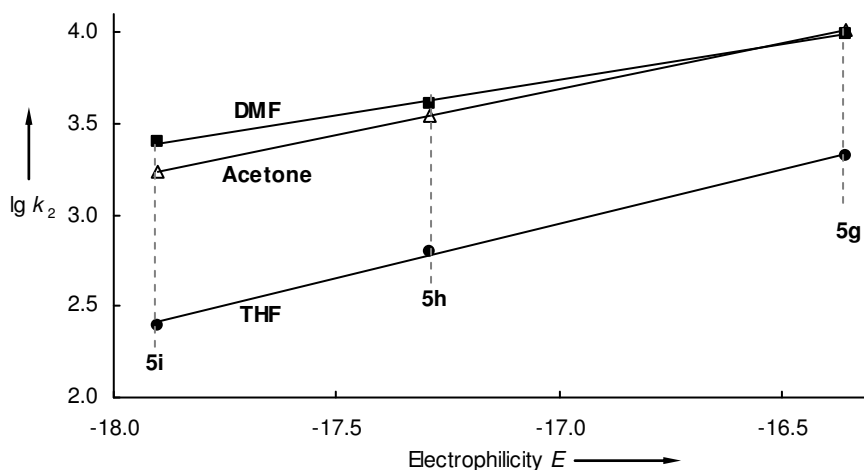


Figure 14: Plot of  $\lg k_2$  of the reactions of **1** with quinone methides **5** in different solvents at 20 °C versus the electrophilicity  $E$  of the quinone methides.

When the second-order rate constants for the reactions of the free anion of deoxybenzoin **1** with quinone methides **5g–i** are correlated with the solvent polarity parameters  $E_T^N$ ,  $AN$  or  $\epsilon_r$  (Figure 15), plots with a similar shape as those in Figures 4–6, where the O/C ratios of the alkylation reactions of **1-K** were correlated with the solvent polarity, are obtained. In general,

the reactivity increases with the polarity from THF to acetone, followed by a slight increase to DMF and DMSO. In case of the most reactive quinone methide **5g**, the rate constants increased from THF to acetone, but remained constant in DMF and DMSO. It can be concluded, that from a certain solvent polarity (here acetone), the reactivity of the free carbanion is only slightly affected by further increase of the solvent polarity.

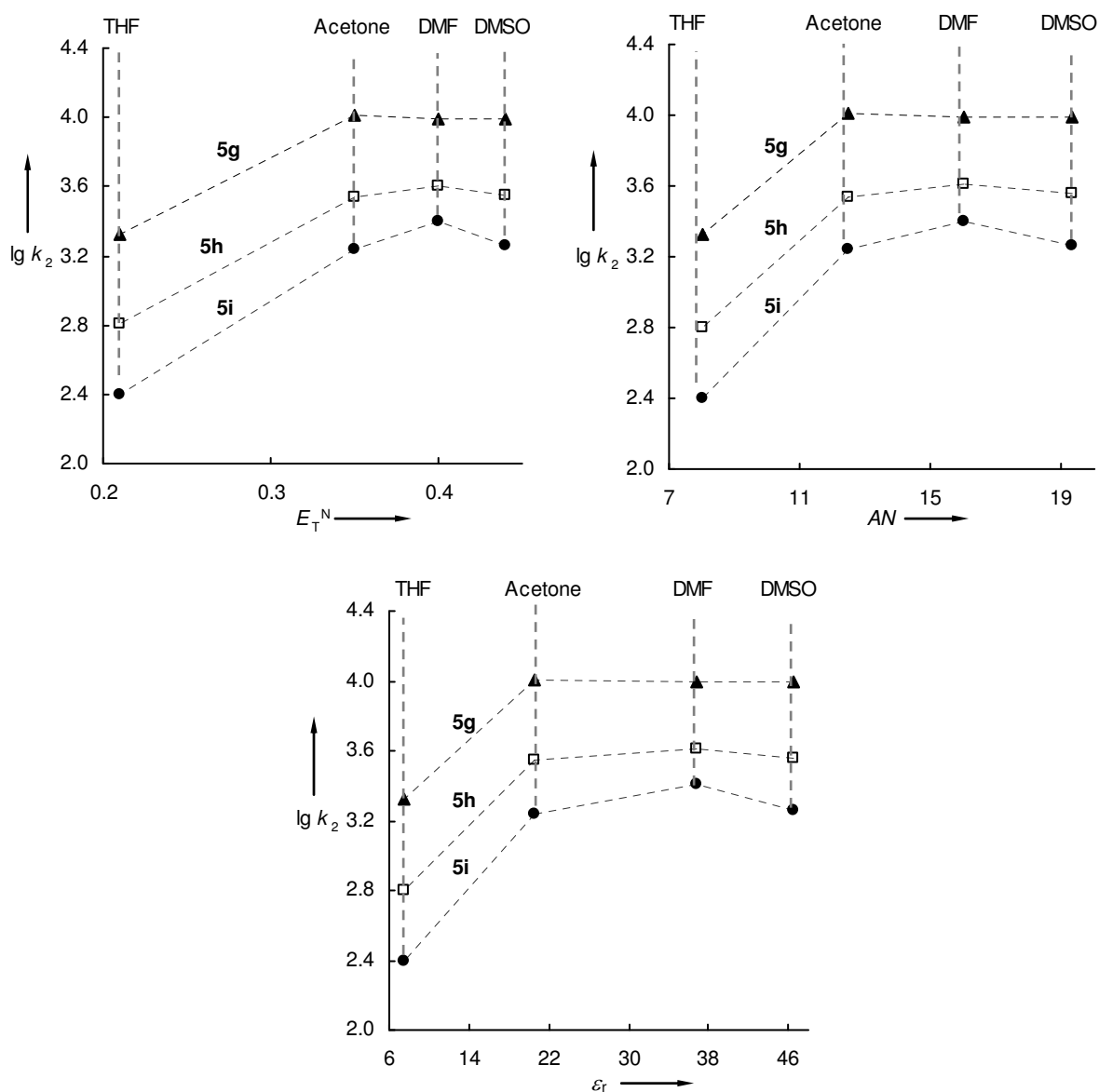


Figure 15:  $\lg k_2$  of the reactions of **1** with quinone methides **5** in different solvents at 20 °C versus the solvent polarity parameters  $E_T^N$  (top, left),  $AN$  (top, right) and  $\epsilon_r$  (bottom, center).<sup>[10]</sup>

When the product ratios (O/C) of the alkylation reactions of **1-K** in different solvents (Table 4) are compared with the nucleophilic reactivities of **1** in the respective solvent, one has to consider that the rate constants in Table 10, and therefore the nucleophilicities, correspond to

the carbon attack of the carbanion at the reference electrophile as shown by product studies.<sup>[4b]</sup> Therefore, a plots of poor quality are obtained when the product ratios of the reactions of **1-K** with BuI, BuCl and BuOTs are correlated with the rate constants of the reaction of the free carbanion **1** with the reference electrophile **5i** (Figure 16 left). As **1-K** showed counter-ion effects in the alkylation experiments (compare section 2.4) and in the kinetic experiments (Table 10), the O/C ratios, which were obtained for the potassium salts, are also plotted against rate constants of the potassium salt **1-K** with **5i** (Figure 16 right).

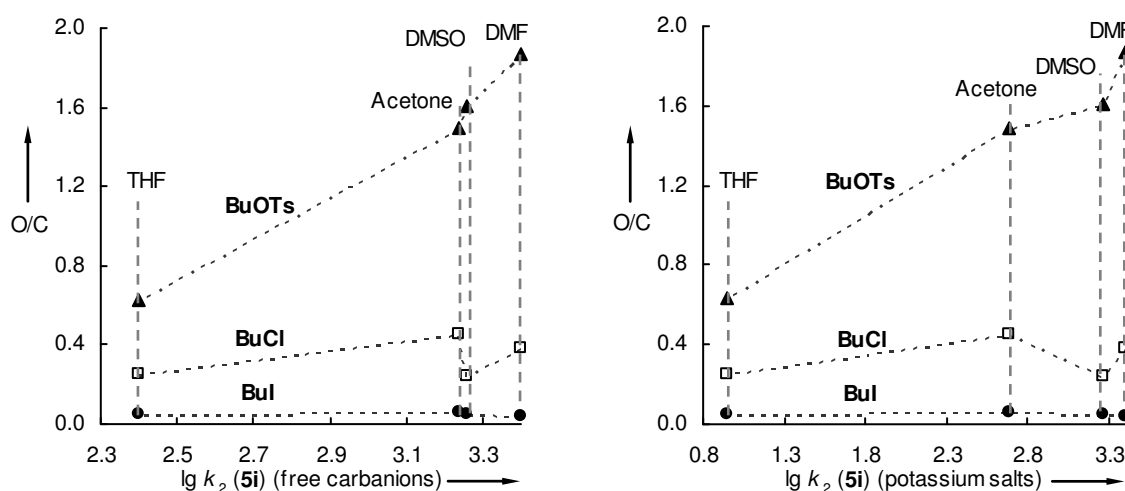


Figure 16: Correlation of the O/C ratio of the alkylation reactions of **1-K** with BuI, BuCl and BuOTs in different solvents with  $\lg k_2$  for the reaction of free carbanion **1** with **5i** (left) and of the potassium salt **1-K** with **5i** (right) in different solvents.

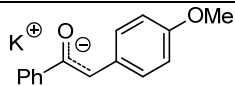
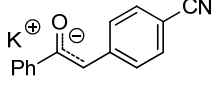
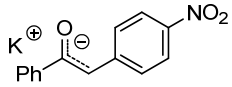
The plots in Figure 16 do not show a trend between the regioselectivity and the reactivity. However, the product ratios were correlated with the rate constants for the reactions of **1** and **1-K** with a reference electrophile (**5i**), and therefore, one has to consider, as the sensitivity parameters  $s_N$  differ in the studied solvents, that plotting the O/C ratios versus a different reference reaction, correlations with different shapes might be obtained. Nevertheless, comparing both plots in Figure 16, one can see that the counter ion effect is not negligible.

In section 2.6 it has been shown, that the product ratios of the alkylation reactions of the anions of the substituted deoxybenzoins **1–4** correlate well with Hammett's substituent parameters.

For this purpose, the second-order rate constants for the reactions of the anions of the substituted deoxybenzoins **2–4** with reference electrophiles **5** in DMSO solution were determined applying the same method as described above (UV-Vis-techniques and pseudo-first-order conditions, Table 11). As the carbanions are intensely colored (UV-Vis-spectra of

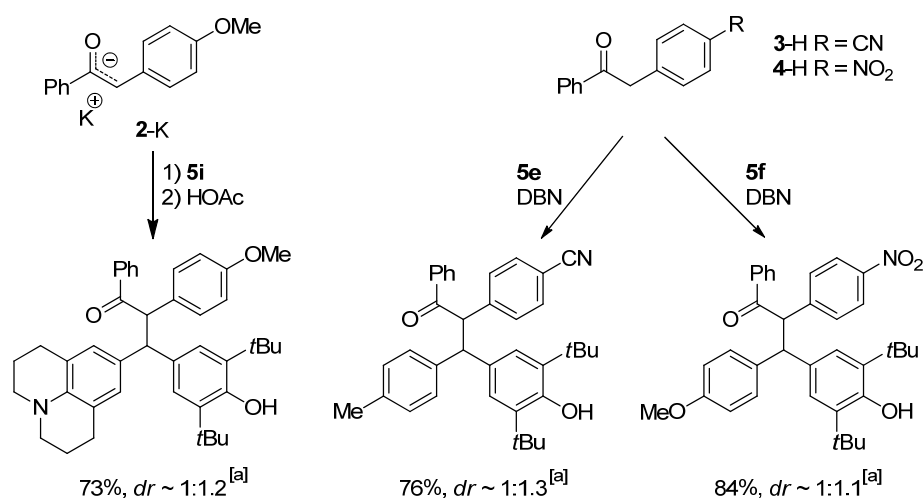
(1–4)-K are shown in the Appendix), the absorbance of the electrophile which was monitored during the kinetic experiment was not the absorbance maximum in all runs. The wavelengths which were used for the evaluation of the experiments are also listed in Table 11.

Table 11: Second-order rate constants for the reactions of the potassium salts of *p*-substituted deoxybenzoins with the reference electrophiles **5** in DMSO at 20 °C and the resulting *N* and *s<sub>N</sub>* parameters.  $\lambda$  corresponds to the wavelength which was monitored during the kinetic experiment.

Nucleophile	$N$ $s_N$	Electrophile	$k_2 / \text{Lmol}^{-1}\text{s}^{-1}$	$\lambda / \text{nm}$
 <b>2-K</b>	27.46 0.41	<b>5g</b>	$3.62 \times 10^4$	500
		<b>5h</b>	$1.45 \times 10^4$	500
		<b>5i</b>	$8.50 \times 10^3$	521
 <b>3-K</b>	20.20 0.70	<b>5b</b>	$5.01 \times 10^4$	533
		<b>5c</b>	$1.38 \times 10^4$	360
		<b>5d</b>	$3.93 \times 10^3$	354
		<b>5e</b>	$1.04 \times 10^3$	354
 <b>4-K</b>	19.14 0.64	<b>5a</b>	$3.07 \times 10^4$	422
		<b>5c</b>	$1.19 \times 10^3$	374
		<b>5d</b>	$3.47 \times 10^2$	374
		<b>5f</b>	$1.02 \times 10^2$	405

As the  $k_{\text{obs}}$  values for the reactions of (2–4)-K with reference electrophiles which are measured in the presence and in the absence of 18-crown-6 are on the same  $k_{\text{obs}}$  versus carbanion-concentration plots (compare Experimental Section), we conclude that the kinetics of these potassium salts reflect the reactivities of the free carbanions. The nucleophilicity *N* and the sensitivity *s<sub>N</sub>* in Table 11 were obtained from plots of  $\lg k_2$  with the electrophilicity *E* of the corresponding quinone methide as explained above (the respective correlations are shown in the Experimental Section).

Representative product studies, which were performed by mixing a DMSO solutions of the potassium salt **2-K** with a DMSO solution of quinone methide **5i** or by combining (3,4)-H with **5e** or **5f** in DMSO in presence of catalytic amounts of 1,5-Diazabicyclo (4.3.0)non-5-ene (DBN) and subsequent aqueous acidic work up, showed that the rate constants in Table 11 correspond to carbon attack, and consequently the nucleophile-specific parameters *N* and *s<sub>N</sub>* refer to the carbon centers of **2–4** (Scheme 3).



Scheme 3: Reactions of the carbanions **2–4** with quinone methides **5** in DMSO. [a] Derived from  $^1\text{H}$  NMR experiments after purification by column chromatography. DBN = 1,5-Diazabicyclo (4.3.0)non-5-ene.

The plots in Figure 17, where the O/C ratios of the alkylation of the carbanions (**1–4**)-K with BuI and BuOTs in DMSO were correlated with the nucleophilic reactivities of the carbanions, show that the amount of oxygen-alkylation increases with the reactivity of the carbanion, which is in accord to the correlations in Figure 10 (section 2.6).

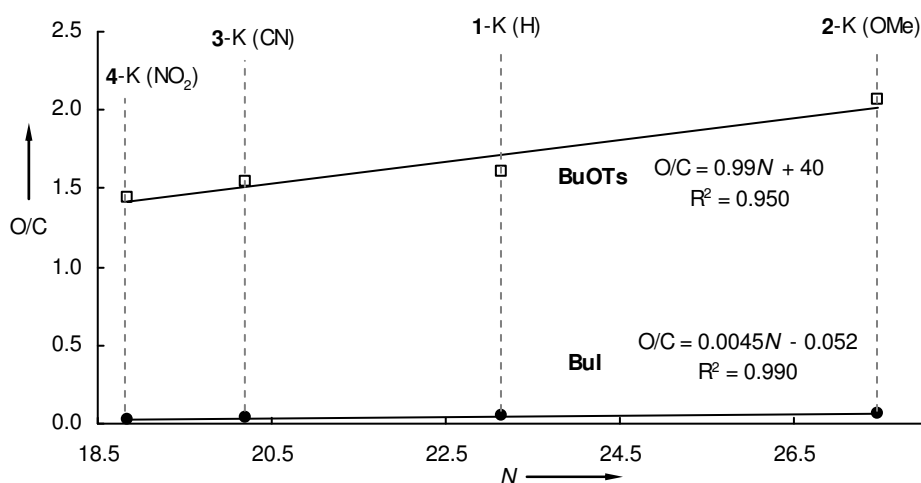


Figure 17: Correlation of the O/C ratio of the alkylation reactions of (**1–4**)-K with BuI and BuOTs in DMSO with the nucleophilic reactivities of the carbanions.

### 2.7.2. Kinetic Studies of the Alkylation Reactions

The reaction rates of the alkylation reactions of **1-K** with butyl iodide were determined in different solvents at 20 °C. As carbanion **1-K** is colored, the reactions were followed using UV-Vis-techniques following the consumption of **1-K** during the reaction. Applying pseudo-

first-order conditions (excess of BuI), the second rate constants were derived from linear plots of the pseudo-first-order reaction rates and the electrophile concentrations (Table 12). As BuI can react with DMSO,<sup>[26]</sup> the stock solution of the electrophile was prepared in THF. The concentrations were selected in that way, that the THF concentration in the reaction-solution was less than 4%. For the reactions in DMF, acetone and THF, pseudo-first-order rate constants were only obtained when at least one equivalent, with respect to potassium, of 18-crown-6 was present. Additionally, varying the concentration of crown ether showed that the amount of 18-crown-6 has no effect on the kinetics, at least when more than one equiv. is present. As the kinetics of the potassium salt of deoxybenzoin in DMSO correspond to the free anion, and the kinetic experiments in the other solvents were performed in presence of crown ether, the rate constants in Table 12 correspond to those of the free carbanion.

Table 12: Rate constants for the reactions of **1-K** with BuI in different solvents at 20 °C.

	DMSO	DMF	Acetone	THF
$k_2 / \text{Lmol}^{-1}\text{s}^{-1}$	11.5	11.4 <sup>[a]</sup>	5.92 <sup>[a]</sup>	0.477 <sup>[a]</sup>
[a] In presence of 18-crown-6 (1.2–1.6 equiv.).				

The second-order rate constants of the reactions of **1-K** with BuI in THF, acetone and DMF correlated linearly with the solvent polarity parameter  $E_T^N$  (Figure 18). Although the  $E_T^N$  value of DMSO is higher than that of DMF, the same rate constant was obtained for the reaction of **1-K** with butyl iodide in both solvents.

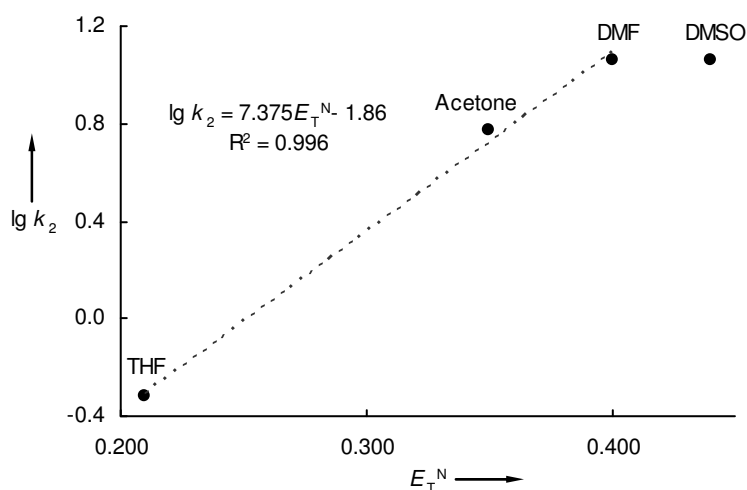


Figure 18: Correlation of  $\lg k_2$  for the alkylation of **1-K** with BuI in different solvents with the solvent polarity parameter  $E_T^N$ .<sup>[10]</sup>

Figure 19 shows analogous plots of the rate constants of the reactions of **1-K** with BuI in different solvents with the acceptor number ( $AN$ ) and the relative permittivity ( $\epsilon_r$ ). In both cases, the plots show a flattening towards increasing solvent polarity, as was found when the

rate constants of the reaction of **1-K** with quinone methides were correlated with the solvent polarity (compare Figure 15).

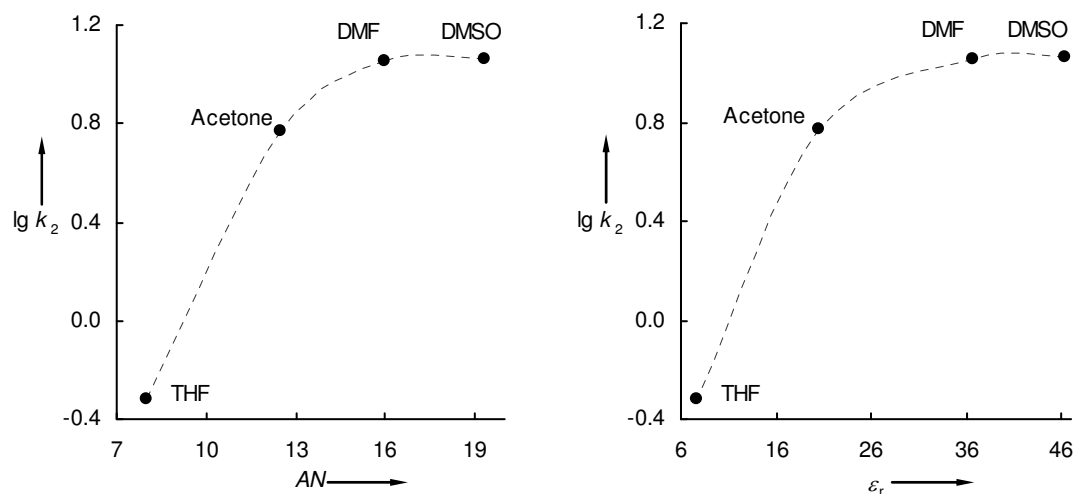


Figure 19: Correlation of  $\lg k_2$  for the alkylation of **1-K** with BuI in different solvents with the acceptor number (AN, left) and the relative permittivity ( $\epsilon_r$ , right).<sup>[10]</sup>

Plotting the rate constants for the reaction of **1-K** with BuI versus the O/C ratios obtained for these reactions (Figure 20), the counter ion effect has to be considered. As shown in section 2.4, the O/C ratio is more or less not influenced by the counter ion when the reactions are performed in DMSO. As shown in Table 10, the kinetics experiments of **1-K** in DMF are also not affected by the addition of crown ether. Therefore, the rate constants of these reactions (free carbanions) can be correlated with the obtained O/C ratios from Table 4. However, the reactions in THF showed strong counter ion effects in the alkylation reactions as well as in the kinetic studies. Therefore shows Figure 20 the product ratio for the alkylation of **1-K** with BuI in the presence of 18-crown-6 (from Table 5). As the kinetic studies in acetone showed a counter ion effect as well, one has to consider that the data point of the O/C ratio (the alkylation was carried out in absence of crown ether) should be shifted to the right as indicated by the dashed arrow in Figure 20, implying that the oxygen-alkylation increases when the counter-ion is complexed as it has been found for the reactions in THF.



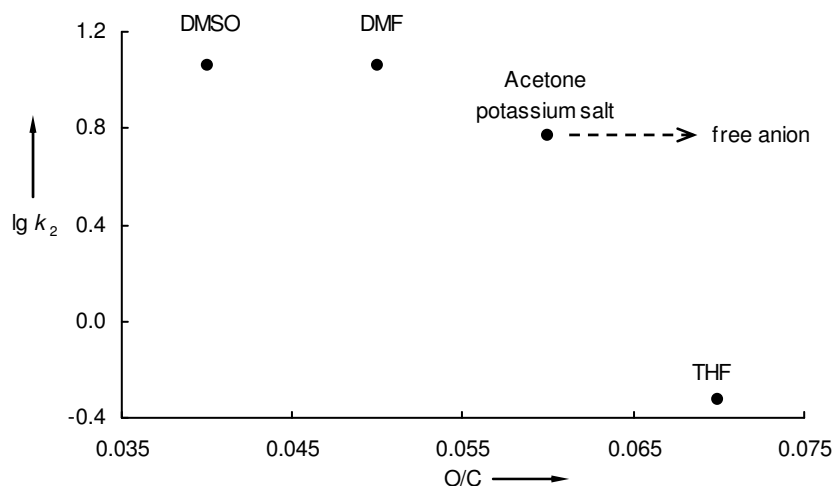


Figure 20: Correlation of  $\lg k_2$  for the alkylation of **1-K** with BuI in different solvents with the O/C ratio of the alkylation reactions.

As the rate constants of the alkylations of **1-K** with BuI in different solvents can not be compared so easily due to the counter ion effect, rate constants of the reactions of **1-K** with different butylation agents were determined in THF solution at 20 °C (Table 13). The kinetic experiments were performed as described before, applying pseudo-first-order conditions (excess of the electrophile) and monitoring the reaction progress by UV-Vis-spectroscopy. All kinetic experiments were performed in presence of 18-crown-6 (1.2–2.5 equiv.). As plots of the first-order rate constants, which were obtained with different amounts of 18-crown-6 (at least 1.2 equiv.), with the electrophile concentrations were linear, the second-order rate constants ( $k_2$ ) which were derived from the slope of these correlations, correspond to the alkylation of the free carbanion.

Table 13: Rate constants for the reactions of **1-K** with BuX in THF at 20 °C.

Electrophile	$k_2 / \text{Lmol}^{-1}\text{s}^{-1}$	O/C <sup>[a]</sup>
BuI	$4.77 \times 10^{-1}$	4:96
BuBr	$2.68 \times 10^{-1}$	17:83
BuCl	$3.72 \times 10^{-2}$	20:80
BuOTs	$2.11 \times 10^3$	39:61
BuOMes	$2.30 \times 10^{-1}$	30:70
(BuO) <sub>2</sub> SO <sub>2</sub>	— <sup>[b]</sup>	29:71

[a] From Table 4. [b] Rate constant too high for the determination by stopped-flow-techniques.

Table 13 shows that the rate constants of the reactions of **1-K** with butyl halides decrease from BuI over BuBr to BuCl and that butyl mesylate and butyl bromide react with a similar rate constant with the anion of deoxybenzoin. Noticeable is the rate constant of BuOTs with **1-K**, which is 4 orders of magnitude higher than the remaining. The rate constant for the

reaction of **1-K** with  $(\text{BuO})_2\text{SO}_2$  could not be determined as the reaction is too fast for the applied technique (stopped-flow). From the applied concentrations ( $[\mathbf{1-K}] = 5.5 \times 10^{-5} - 1.1 \times 10^{-4} \text{ mol L}^{-1}$ ;  $[(\text{BuO})_2\text{SO}_2] = 10^{-4} - 10^{-3} \text{ mol L}^{-1}$ ) and the time limit of the used device ( $\sim 50 \text{ ms}$ ) the magnitude of the rate constant can be estimated. The rate constant should be at least  $10^5 \text{ L mol}^{-1} \text{ s}^{-1}$ .

As the rate constants for the reactions of **1-K** with the butylation agents in THF were obtained in the presence of 18-crown-6, they could only be correlated with the product ratios of the reaction which were performed in presence of crown ether as well. However, Figure 21 does not show any trend between reactivity and the regioselectivity.

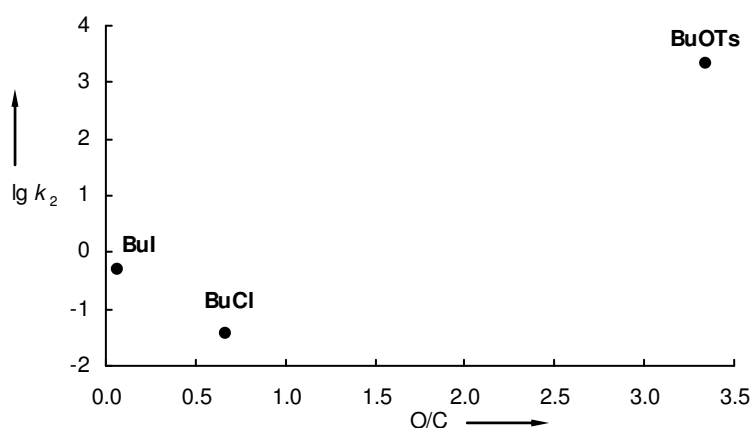


Figure 21: Correlation of  $\lg k_2$  for the alkylation of **1-K** with different butyl derivatives in THF at  $20^\circ \text{C}$  with the O/C ratio of these alkylation reactions. Synthetic and the kinetic studies were performed in presence of 18-crown-6.

A similar study is shown in Figure 22, where the rate constants for the alkylation reactions of the sodium salt of ethyl  $\alpha$ -ethyl acetoacetate with different ethylation agents in DMF are correlated with the product ratios.<sup>[27]</sup> In contrast to the results in this work, the rate constant of the reaction with ethyl tosylate is two orders of magnitude lower than those of the ethyl halides (EtI and EtBr).

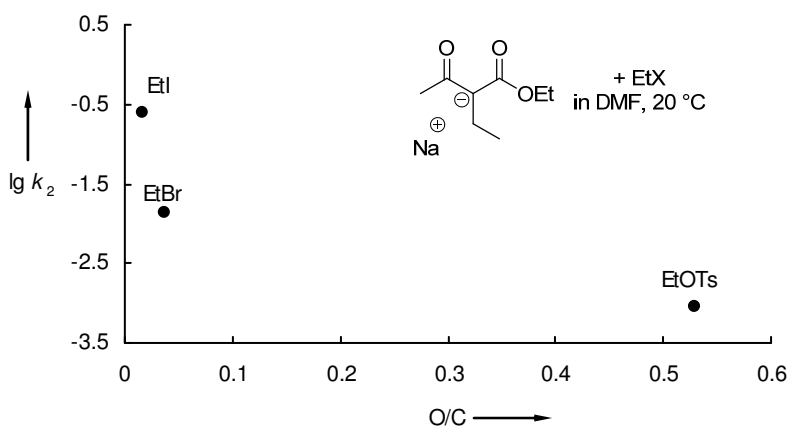


Figure 22: Correlation of  $\lg k_2$  for the alkylation of the sodium salt of ethyl  $\alpha$ -ethyl acetoacetate with different ethyl derivatives in DMF at 20 °C with the O/C ratio of these alkylation reactions.<sup>[27]</sup>

### 3. Conclusion

The regioselectivity of the alkylation of enolate ions has been studied based on reactions of the anion of deoxybenzoin (**1**) with different butyl derivatives in dependency of the concentration, the leaving group, the solvent, the counter ion, the temperature and substituents on the aromatic moiety. Kinetic experiments of these alkylation reactions were performed. Furthermore, the obtained data was compared to analogous experiments reported in the literature.

In this work was found that the oxygen alkylation of **1-K** is favored when the concentration is increased, which is in contrast to Le Noble's results. However, Gompper *et al.* reported examples in which the oxygen alkylation was favored by increasing concentration as well as examples in which the carbon alkylation was favored by increasing the concentration. When the influences of the solvent and the leaving-group were studied, general relationships were found; the O/C ratio increases with the solvent polarity as well as with a better leaving-group. However, no direct correlation was found between the product ratio and the solvent polarity. Furthermore has to be considered, that only polar aprotic solvents were used in this study and with one exception, all reactions were in homogeneous media. These two factors, heterogeneity/homogeneity and protic/aprotic solvents influence the regioselectivity of the alkylation of enolate ions as well.

Experiments which studied the counter ion effect on the alkylation of enolate ions showed that solvent separated carbanions yield more oxygen alkylation than ion pairs. In general, the O/C ratio increases from lithium enolates over sodium enolates and potassium enolates to the

free enolates. Nevertheless, the role of the solvent can not be neglected. While the counter ion effects of **1** in DMSO are marginal, considerable effects were observed in THF.

It was found that the regioselectivity of the alkylations decreases by increasing the temperature. As the isoselective temperature is above the studied temperature-interval, the yields of oxygen alkylation increased for the alkylations with butyl halides and decreased for the reactions with butyl tosylate, mesylate and sulfate while the temperature was increased.

The study of the influence of substituents in the aromatic moiety of the anion of deoxybenzoin showed that electron withdrawing groups decrease the O/C ratio independent of the electrophile used for the alkylation. However, reported examples with contrary results were shown, as well as reported studies in which the substituents have no clear influence on the regioselectivity of the alkylation of enolates were discussed.

With kinetic experiments of the reactions of the anion of deoxybenzoin (**1**) with reference electrophiles, the nucleophilicity parameters of **1** in DMF, acetone and THF were determined. In this context, not insignificant counter ion effects in acetone and THF were found. The obtained rate constants did not correlate with the solvent polarity parameters as well as the product ratios (O/C) of the alkylation experiments with the nucleophilic reactivities in the different solvents. The kinetic studies of the reactions of the alkylation of **1** with BuI in different solvents showed that the rate constants increase with the solvent polarity, however, not linearly. The rate constants for the alkylations of **1** with the different butylation agents in THF showed no correlation with the O/C ratios.

In this study, it has been shown that the successive study of the different parameters which influence the regioselectivity of the alkylation of enolate ions is partly conflicting. For example, factors like the solvent polarity and the counter ion effects can not be treated separately, or the fact that highly reactive alkylating agents can react with the solvent (e.g. dimethyl sulfate and DMSO) forming a reactive intermediate which alkylates the enolate as well, can not be neglected. Furthermore, for each study presented in this work, literature examples with contrary results were discussed. This concludes that no general rules can predict how the regioselectivity of the alkylation of enolate ions can be influenced and each system has to be studied independently.

## 4. Experimental Section

### 4.1. General

#### Materials

Commercially available DMSO (H<sub>2</sub>O content < 50 ppm), DMF (H<sub>2</sub>O content < 50 ppm), Acetone (H<sub>2</sub>O content < 50 ppm), was used without further purification. THF was distilled from sodium/benzophenone and stored over molecular sieve. Deoxybenzoin (**1-H**) was purchased from Sigma-Aldrich (Germany). *p*-Substituted deoxybenzoins (**2–4**)-H were synthesized following literature procedures. The reference electrophiles used in this work were synthesized according to literature procedures.<sup>[4a,24d,25]</sup>

#### NMR spectroscopy

In the <sup>1</sup>H and <sup>13</sup>C NMR spectra chemical shifts are given in ppm and refer to tetramethylsilane ( $\delta_{\text{H}} = 0.00$ ,  $\delta_{\text{C}} = 0.0$ ), [D<sub>6</sub>]-DMSO ( $\delta_{\text{H}} = 2.50$ ,  $\delta_{\text{C}} = 39.5$ ) or to CDCl<sub>3</sub> ( $\delta_{\text{H}} = 7.26$ ,  $\delta_{\text{C}} = 77.0$ ),<sup>[28]</sup> as internal standards. The coupling constants are given in Hz. For reasons of simplicity, the <sup>1</sup>H NMR signals of AA'BB'-spin systems of *p*-disubstituted aromatic rings are treated as doublets. Signal assignments are based on additional COSY, gHSQC, and gHMBC experiments.

#### Alkylation Reactions

All the reactions were carried out under inert atmosphere (argon or dried nitrogen) at ambient temperature. For the temperature depending experiments, the reactions were carried out in thermostats.

#### Kinetics

As the reactions of colored quinone methides **5** with the carbanions (**1–4**)-K or of the anion of deoxybenzoin (**1-K**) with butyl derivatives yield colorless products (or products with a different absorption range than the reactants), the reactions could be followed by UV-Vis spectroscopy. The kinetics of fast reactions ( $\tau_{1/2} < 10$  s) were monitored using stopped-flow techniques, slow reactions ( $\tau_{1/2} > 10$  s) were monitored by using conventional UV-Vis-techniques (diode array). The temperature of all solutions was kept constant at  $20.0 \pm 0.1$  °C by using a circulating bath thermostat. In all runs the concentration of the nucleophile was at least 10

times higher than the concentration of the electrophile, resulting in pseudo-first-order kinetics with an exponential decay of the concentration of the minor compound. First-order rate constants  $k_{\text{obs}}$  were obtained by least-squares fitting of the exponential function  $A_t = A_0 \exp(-k_{\text{obs}}t) + C$  to the time-dependent absorbances. The second-order rate constants  $k_2$  were obtained from the slopes of the linear plots of  $k_{\text{obs}}$  against the nucleophile concentrations.

## 4.2. Synthesis of the Substituted Deoxybenzoins and their Alkylated Derivates

### 4.2.1. Synthesis of the Substituted Deoxybenzoins 2–4

#### 4.2.1.1. 2-(4-Methoxyphenyl)-1-phenylethanone 2-H<sup>[29]</sup>

$\text{AlCl}_3$  (4.5 g, 33.7 mmol) was suspended in 20 mL benzene and cooled to 0 °C. A solution of 2-(4-methoxyphenyl)acetyl chloride (2.0 mL, 13.1 mmol) in 5 mL benzene were added slowly at 0 °C during 1 h. The reaction mixture was stirred at 0 °C for further 4 h and at ambient temperature over night. The mixture was poured on ice and conc. HCl and  $\text{CH}_2\text{Cl}_2$  were added until a solution was obtained. The organic layer was separated and the aqueous layer was extracted twice with  $\text{CH}_2\text{Cl}_2$ . The combined organic layers were washed with HCl ( $c = 2 \text{ mol L}^{-1}$ ), water and NaOH ( $c = 2 \text{ mol L}^{-1}$ ), dried over sodium sulfate and the solvent was removed by evaporation. After recrystallization from ethanol/ $\text{CH}_2\text{Cl}_2$  2-(4-methoxyphenyl)-1-phenylethanone (2-H, 2.56 g, 86%) was obtained as a light yellow solid.

#### 4.2.1.2. 4-(2-Oxo-2-phenylethyl)benzonitrile 3-H<sup>[30]</sup>

((Benzoyloxy)(phenyl)methyl)triphenylphosphonium chloride: Benzaldehyde (5.0 mL, 49.5 mmol), benzoylchloride (5.7 mL, 49.5 mmol) and triphenylphosphine (13.0 g, 49.5 mmol) were heated at 120 °C for 2 h. After cooling, the crude product was stirred in 60 mL of a pentane : diethylether = 1 : 1 mixture for 1 h and filtrated (20.1 g, 39.5 mmol, 80%).

4-(4-Oxo-2,4-diphenylbut-1-en-1-yl)benzonitrile: ((Benzoyloxy)(phenyl)methyl)triphenylphosphonium chloride (4.7 g, 9.23 mmol) was suspended in 50 mL THF. Butyl lithium (10.3 mmol) was added slowly at –60 °C and the mixture was stirred for 20 min. 4-Formylbenzonitrile (1.40 g, 10.7 mmol, dissolved in 10 mL of THF) was added at –60 °C. After 15 min. the reaction mixture was allowed to warm up to ambient temperature, then, HCl was added and the mixture was extracted with diethylether (3 x 30 mL). The combined organic layers were washed with aqueous HCl ( $0.2 \text{ mol L}^{-1}$ ), water and sodium bicarbonate solution

and dried over sodium sulfate. After removing the solvent, the crude product was recrystallized from ethanol/pentane (4.23 g, 13.0 mmol, 55%).

4-(2-Oxo-2-phenylethyl)benzonitrile: 4-(4-Oxo-2,4-diphenylbut-1-en-1-yl)benzonitrile (740 mg, 2.27 mmol) were dissolved in 30 mL of methanolic potassium hydroxid (5%) while heating slightly. After 15 min, the solution was poured to 100 mL of water. 4-(2-Oxo-2-phenylethyl)benzonitrile (**3-H**) crystallized as colorless solid within 10 min (395 mg, 1.79 mmol, 79%).

The analytical data of the tree steps was according to literature.<sup>[30]</sup>

#### 4.2.1.3. 2-(4-Nitrophenyl)-1-phenylethanone **4-H**

Thionylchloride (3.0 mL, 41.3 mmol) were added slowly to a solution of 2-(4-nitrophenyl)acetic acid (5.00 g, 27.6 mmol) in 10 mL of dry THF. The reaction mixture was heated to 50 °C for 40 min and after cooling, the solvent and the excess of thionylchloride were removed by evaporation. The residue was dissolved in 50 mL benzene and AlCl<sub>3</sub> (4.50 g, 33.7 mmol) was added in small portions at 0 °C during 2 h. Then, the mixture was refluxed for 50 min. After cooling, the mixture was poured on ice and conc. HCl and CH<sub>2</sub>Cl<sub>2</sub> were added until a solution was obtained. The organic layer was separated and the aqueous layer was extracted twice with CH<sub>2</sub>Cl<sub>2</sub>. The combined organic layers were washed with HCl (c = 2 mol L<sup>-1</sup>), water and NaOH (c = 2 mol L<sup>-1</sup>), dried over sodium sulfate and the solvent was removed by evaporation. After recrystallization from ethanol/CH<sub>2</sub>Cl<sub>2</sub> 2-(4-nitrophenyl)-1-phenylethanone (**4-H**, 4.87 g, 73%) was obtained as a light yellow solid.

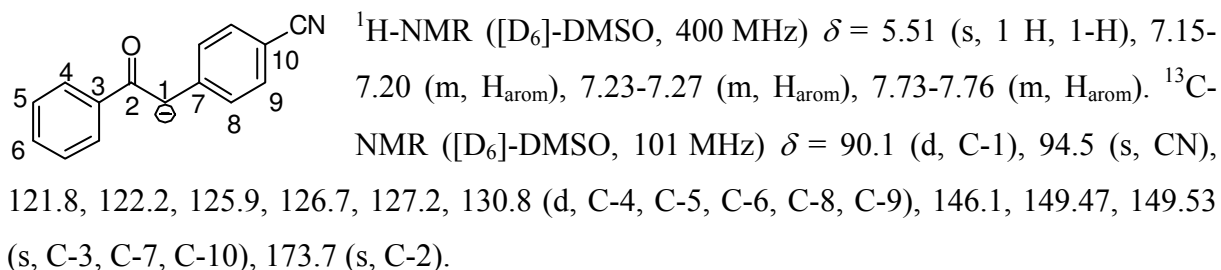
<sup>1</sup>H NMR is according to literature.<sup>[31]</sup>

#### 4.2.2. Synthesis of the Carbanions (**3,4**)-K

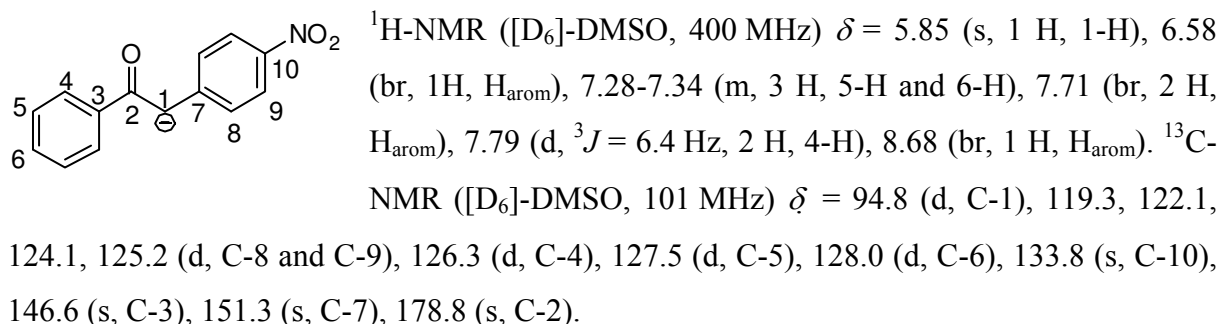
General Procedure 1 (GP1): Potassium *tert*-butoxide was dissolved in absolute ethanol and the corresponding amount of substituted deoxybenzoin (**3,4**)-H was added. After 10 min. of stirring at ambient temperature, the solvent was removed under reduced atmosphere. The resulting solid was washed several times (3 to 4) with dry diethyl ether.

**4.2.2.1. Potassium 1-(4-cyanophenyl)-2-oxo-2-phenylethan-1-ide (3-K)**

According to GP1, 4-(2-Oxo-2-phenylethyl)benzonitrile (**3-H**, 350 mg, 1.58 mmol) and KO<sup>t</sup>Bu (177 mg, 1.58 mmol) yielded potassium 1-(4-cyanophenyl)-2-oxo-2-phenylethan-1-ide (**3-K**, 320 mg, 1.23 mmol, 78%) as yellow solid.

**4.2.2.2. Potassium 1-(4-nitrophenyl)-2-oxo-2-phenylethan-1-ide (4-K)**

According to GP1, 2-(4-nitrophenyl)-1-phenylethanone (**4-H**, 1.31 g, 5.43 mmol) and KO<sup>t</sup>Bu (600 mg, 5.35 mmol) yielded potassium 1-(4-nitrophenyl)-2-oxo-2-phenylethan-1-ide (**4-K**, 1.35 g, 4.83 mmol, 90%) as violet-black solid.

**4.2.3. Synthesis of the Alkylated Derivatives****4.2.3.1. Synthesis of 1,2-diphenylhexan-1-one (1-C)<sup>[7]</sup>**

Potassium *tert*-butoxide (1.01 g, 9.00 mmol) was suspended in 50 mL of dry diethylether and deoxybenzoin (**1-H**, 1.68 g, 8.56 mmol) was added at 0 °C. After 5 min of stirring at 0 °C, butyl iodide (1.00 mL, 1.62 g, 8.80 mmol) was added. After three hours, 50 mL of water were added, the organic layer was separated and the aqueous layer was extracted with diethyl ether (2 x 30 mL). The combined organic phase was washed with brine, dried over sodium sulfate and the solvent was removed under reduced pressure. The light yellow solid (yield ~ 90%) was recrystallized four times from ethanol to obtained the pure carbon alkylated product 1,2-diphenylhexan-1-one (**1-C**, 835 mg, 3.31 mmol, 39%).



The NMR Data is according to literature.<sup>[7]</sup>

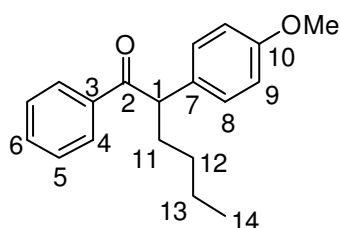
#### 4.2.3.2. Synthesis of (Z)-(1-butoxyethene-1,2-diyl)dibenzene (1-O)<sup>[7]</sup>

Deoxybenzoin (**1-H**, 1.00g, 5.10 mmol), *n*-butyl tosylate (1.17 g, 5.12 mmol), and 18-crown-6 (822 mg, 2.24 mmol) were added to a mixture of potassium hydroxide (6.60 g, 118 mmol) and 8.00 mL of water and 20 mL of toluene. After 20 hours, 40 mL of water were added and the mixture was extracted with diethyl ether (2 x 40 mL). The combined organic layers were washed with brine and dried over sodium sulfate before the solvent was removed by distillation. The crude product was purified by chromatography (silica gel/CH<sub>2</sub>Cl<sub>2</sub> : pentane = 1.5 : 2) yielding (Z)-(1-butoxyethene-1,2-diyl)dibenzene (**1-O**, 915 mg, 3.63 mmol, 71%) as an light yellow oil.

The NMR Data is according to literature.<sup>[7]</sup>

#### 4.2.3.3. Synthesis of 2-(4-methoxyphenyl)-1-phenylhexan-1-one (2-C)

2-(4-Methoxyphenyl)-1-phenylethanone (**2-H**, 139 mg, 0.614 mmol), KO<sup>t</sup>Bu (77.2 mg, 0.688 mmol) and butyl iodide (810 mg, 4.40 mmol) were mixed with 20 mL of diethyl ether and stirred for 4 days. After adding 25 mL of brine, the organic layer was separated. The aqueous layer was extracted with diethyl ether (2 x 15 mL), the combined organic layers were dried over sodium sulfate and the solvent was evaporated. After purification by column chromatography (silica/dichloromethane/pentane) 2-(4-methoxyphenyl)-1-phenylhexan-1-one (**2-C**, 87.9 mg, 0.311 mmol, 51%) was obtained as a yellow oil.

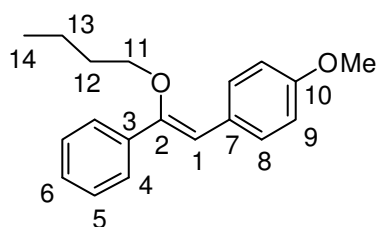


<sup>1</sup>H-NMR (CDCl<sub>3</sub>, 300 MHz)  $\delta$  = 0.86 (t, <sup>3</sup>J = 7.1 Hz, 3 H, 14-H), 1.14-1.40 (m, 4 H, 12-H, 13-H), 1.71-1.86 (m, 1 H, 11-H), 2.08-2.20 (m, 1 H, 11-H), 3.74 (s, 3 H, OMe), 4.48 (t, <sup>3</sup>J = 7.4 Hz, 1 H, 1-H), 6.82 (d, <sup>3</sup>J = 8.7 Hz, 2 H, 9-H), 7.21 (d, <sup>3</sup>J = 8.7 Hz, 2 H, 8-H), 7.35-7.47 (m, 3 H, 5-H, 6-H), 7.93-7.97 (m, 2 H, 4-H). <sup>13</sup>C-

NMR (CDCl<sub>3</sub>, 75.5 MHz)  $\delta$  = 14.0 (q, C-14), 22.7 (t, C-13), 29.9 (t, C-12), 33.8 (t, C-11), 52.7 (d, C-1), 55.2 (q, OMe), 114.3 (d, C-9), 128.5 (d, C-5), 128.6 (d, C-4), 129.2 (d, C-8), 131.8 (s, C-7), 132.7 (d, C-6), 137.1 (s, C-3), 158.5 (s, C-10), 200.4 (s, C-2). HR-MS (EI): *m/z* calcd for [C<sub>19</sub>H<sub>22</sub>O<sub>2</sub>]<sup>+</sup>: 282.1614, found 282.1620.

**4.2.3.4. Synthesis of (Z)-1-(2-butoxy-2-phenylvinyl)-4-methoxybenzene (2-O)**

Potassium *tert*-butoxide (87.7 mg, 0.782 mmol) and dicyclohexano-18-crown-6 (328 mg, 0.874 mmol) were dissolved in 10 mL THF and 2-(4-methoxyphenyl)-1-phenylethanone (**2-H**, 173 mg, 0.765 mmol) and butyl tosylate (202 mg, 0.885 mmol) were added. The mixture was stirred at room temperature for 5 days before 15 mL of aqueous acid (HCl, 2 mol L<sup>-1</sup>) were added and extracted with diethyl ether (3 x 10 mL). The combined organic layers were washed with brine, dried over sodium sulfate and the solvent was removed by distillation. The crude product was purified by column chromatography on silica with pentane/dichloromethane as eluent yielding (Z)-1-(2-butoxy-2-phenylvinyl)-4-methoxybenzene (**2-O**, 51.9 mg, 0.184 mmol, 24%) as a yellow oil.



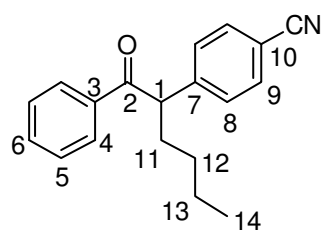
<sup>1</sup>H-NMR (CDCl<sub>3</sub>, 300 MHz)  $\delta$  = 0.93 (t, <sup>3</sup>J = 7.4 Hz, 3 H, 14-H), 1.39-1.52 (m, 2 H, 13-H), 1.69-1.79 (m, 2 H, 12-H), 3.73 (t, <sup>3</sup>J = 6.8 Hz, 2 H, 11-H), 3.82 (s, 3 H, OMe), 6.05 (s, 1 H, 1-H), 6.89 (d, <sup>3</sup>J = 9.0 Hz, 2 H, 9-H), 7.29-7.40 (m, 3 H, 5-H and 6-H), 7.52-7.56 (m, 2 H, 4-H), 7.69 (d, <sup>3</sup>J = 8.7 Hz, 2 H, 8-H).

<sup>13</sup>C-NMR (CDCl<sub>3</sub>, 75.5 MHz)  $\delta$  = 13.9 (q, C-14), 19.3 (t, C-13), 32.2 (t, C-12), 55.2 (q, OMe), 69.9 (t, C-11), 112.7 (d, C-1), 113.7 (d, C-9), 126.3 (d, C-4), 127.9 (s, C-7), 128.4 (s, C-5), 128.9 (s, C-6), 129.8 (d, C-8), 137.2 (s, C-3), 153.7 (s, C-2), 158.1 (s, C-10). HR-MS (EI): *m/z* calcd for [C<sub>19</sub>H<sub>22</sub>O<sub>2</sub>]<sup>+</sup>: 282.1614, found 282.1608.

**4.2.3.5. Synthesis of 4-(1-oxo-1-phenylhexan-2-yl)benzonitrile (3-C)**

Potassium 1-(4-cyanophenyl)-2-oxo-2-phenylethan-1-ide (**3-K**, 157 mg, 0.605 mmol) and butyl iodide (810 mg, 4.40 mmol) were dissolved in a mixture of 20 mL DMSO and 20 mL dry diethyl ether and stirred at ambient temperature for 4 days. Then, 40 mL of brine were added and extracted with diethyl ether (3 x 20 mL). The combined organic layers were washed with brine and dried over sodium sulfate. After removing the solvent by distillation, the crude product was purified by column chromatography on silica with pentane/dichloromethane as eluent. 4-(1-oxo-1-phenylhexan-2-yl)benzonitrile (**3-C**, 98.2 mg, 0.354 mmol, 59%) was obtained as a yellow oil.

<sup>1</sup>H-NMR (CDCl<sub>3</sub>, 300 MHz)  $\delta$  = 0.86 (t, <sup>3</sup>J = 7.1 Hz, 3 H, 14-H), 1.15-1.51 (m, 4 H, 12-H and 13-H), 1.72-1.98 (m, 1 H, 11-H), 2.14-2.26 (m, 1 H, 11-H), 4.63 (t, <sup>3</sup>J = 7.2 Hz, 1 H, 1-H), 7.40-7.46 (m, 3 H, H<sub>arom</sub>), 7.50-7.54 (m, 2 H, H<sub>arom</sub>), 7.58 (d, <sup>3</sup>J = 8.1 Hz, 2 H, H<sub>arom</sub>), 7.94 (d,

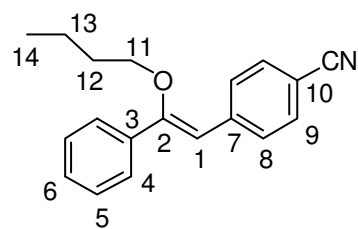


$^3J = 7.2$  Hz, 2 H, 4-H).  $^{13}\text{C-NMR}$  ( $\text{CDCl}_3$ , 75.5 MHz)  $\delta = 13.9$  (q, C-14), 22.6 (t, C-13), 29.8 (t, C-12), 33.8 (t, C-11), 53.4 (d, C-1), 111.0 (s, CN), 118.7 (s, C-10), 128.5, 128.7, 129.1, 132.6 (d, C-4, C-5, C-8, C-9), 133.3 (d, C-6), 136.5, 145.2 (s, C-3, C-7), 199.1 (s, C-2). HR-MS (EI):  $m/z$  calcd for  $[\text{C}_{19}\text{H}_{19}\text{NO}]^+$ : 277.1461, found

277.1474.

#### 4.2.3.6. Synthesis of (Z)-4-(2-Butoxy-2-phenylvinyl)benzonitrile (3-O)

Potassium *tert*-butoxide (65.3 mg, 0.582 mmol) and dicyclohexano-18-crown-6 (233 mg, 0.621 mmol) were dissolved in 10 mL THF and 4-(2-Oxo-2-phenylethyl)benzonitrile (**3-H**, 128 mg, 0.579 mmol) and butyl tosylate (146 mg, 0.639 mmol) were added. The mixture was stirred at room temperature for 14 days before 15 mL of aqueous acid ( $\text{HCl}$ , 2 mol  $\text{L}^{-1}$ ) were added and extracted with diethyl ether (3 x 10 mL). The combined organic layers were washed with brine, dried over sodium sulfate and the solvent was removed by distillation. The crude product was purified by column chromatography on silica with pentane/dichloromethane as eluent yielding (Z)-4-(2-butoxy-2-phenylvinyl)benzonitrile (**3-O**, 63.2 mg, 0.228 mmol, 39%) as a yellow oil.



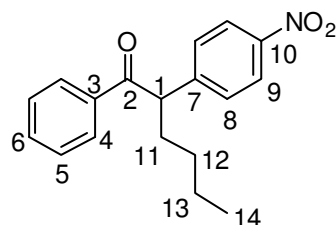
$^1\text{H-NMR}$  ( $\text{CDCl}_3$ , 300 MHz)  $\delta = 0.92$  (t,  $^3J = 7.4$  Hz, 3 H, 14-H), 1.36-1.48 (m, 2 H, 13-H), 1.66-1.76 (m, 2 H, 12-H), 3.78 (t,  $^3J = 6.8$  Hz, 2 H, 11-H), 5.94 (s, 1 H, 1-H), 7.37-3.44 (m, 3 H, 5-H, 6-H), 7.49-7.57 (m, 2 H, 4-H), 7.59 (d,  $^3J = 8.4$  Hz, 2 H, 9-H), 7.80 (d,  $^3J = 8.4$  Hz, 2 H, 8-H).  $^{13}\text{C-NMR}$  ( $\text{CDCl}_3$ ,

75.5 MHz)  $\delta = 13.8$  (q, C-14), 19.2 (t, C-13), 32.1 (t, C-12), 70.6 (t, C-11), 109.0 (s, C-10), 111.0 (d, C-1), 119.4 (s, CN), 127.1 (d, C-4), 128.6 (d, C-5), 128.7 (d, C-8), 129.0 (d, C-6), 132.0 (d, C-9), 136.1 (s, C-3), 141.0 (s, C-7), 159.0 (s, C-2). HR-MS (EI):  $m/z$  calcd for  $[\text{C}_{18}\text{H}_{19}\text{NO}]^+$ : 277.1459, found 277.1462.

#### 4.2.3.7. Synthesis of 2-(4-nitrophenyl)-1-phenylhexan-1-one (4-C)

Potassium 1-(4-nitrophenyl)-2-oxo-2-phenylethan-1-ide (**4-K**, 162 mg, 0.580 mmol) and butyl iodide (810 mg, 4.40 mmol) were dissolved in a mixture of 20 mL DMSO and 20 mL of dry diethyl ether and stirred at ambient temperature for 4 days. Then, 40 mL of brine were added and extracted with diethyl ether (3 x 20 mL). The combined organic layers were washed with

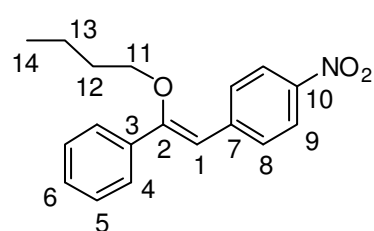
brine and dried over sodium sulfate. After removing the solvent by distillation, the crude product was purified by column chromatography on silica with pentane/dichloromethane as eluent. 2-(4-Nitrophenyl)-1-phenylhexan-1-one (**4-C**, 134 mg, 0.451 mmol, 78%) was obtained as yellow oil.



$^1\text{H-NMR}$  ( $\text{CDCl}_3$ , 400 MHz)  $\delta$  = 0.87 (t,  $^3J$  = 7.2 Hz, 3 H, 14-H), 1.16-1.40 (m, 4 H, 12-H and 13-H), 1.81-1.90 (m, 1 H, 11-H), 2.18-2.27 (m, 1 H, 11-H), 4.69 (t,  $^3J$  = 7.4 Hz, 1 H, 1-H), 7.41-7.46 (m, 2 H, 8-H), 7.49-7.56 (m, 3 H, 5-H and 6-H), 7.93-7.96 (m, 2 H, 4-H), 8.14-8.18 (m, 2 H, 9-H).  $^{13}\text{C-NMR}$  ( $\text{CDCl}_3$ , 101 MHz)  $\delta$  = 13.9 (q, C-14), 22.6 (t, C-13), 29.8 (t, C-12), 33.9 (t, C-11), 53.2 (d, C-1), 124.0 (d, C-9), 128.5 and 129.5 (d, C-4 and C-5), 128.8 (d, C-8), 133.4 (d, C-6), 136.5 (s, C-10), 147.0, 147.2 (s, C-3 and C-7), 199.0 (s, C-2). HR-MS (EI):  $m/z$  calcd for  $[\text{C}_{18}\text{H}_{19}\text{NO}_3]$ : 297.1365, found 297.1365.

#### 4.2.3.8. Synthesis of 1-(2-butoxy-2-phenylvinyl)-4-nitrobenzene (**4-O**)

Potassium 1-(4-nitrophenyl)-2-oxo-2-phenylethan-1-ide (**4-K**, 135 mg, 0.483 mmol) and butyl tosylate (168 mg, 0.736 mmol) were dissolved in 10 mL of DMSO. After 4 days of stirring, the mixture turned to a clear red solution where 20 mL of aqueous acetic acid (0.5%) were added. After extraction with diethyl ether (3 x 10 mL), the combined organic layers were washed with brine and dried over sodium sulfate. After removing the solvent, the crude product was purified by column chromatography on silica with pentane/dichloromethane as eluent yielding 1-(2-butoxy-2-phenylvinyl)-4-nitrobenzene (**4-O**, 21.0 mg, 0.0706 mmol, 15%) as yellow oil.



$^1\text{H-NMR}$  ( $\text{CDCl}_3$ , 300 MHz)  $\delta$  = 0.93, 0.99\* (t,  $^3J$  = 7.4 Hz, 3 H, 14-H), 1.37-1.347, 1.48\*-1.56\* (m, 2 H, 13-H), 1.68-1.76, 1.76\*-1.85\* (m 2 H, 12-H), 3.81 (t,  $^3J$  = 6.6 Hz, 2 H, 11-H), 3.99\* (t,  $^3J$  = 6.3 Hz, 2 H, 11\*-H), 5.82\*, 5.99 (s, 1 H, 1-H), 7.01\*, 7.86 (d,  $^3J$  = 9.0 Hz, 2 H, 8-H), 7.31-7.36, 7.39-7.46, 7.51-7.55 (m, 4-H, 5-H, 6-H, both isomers), 7.93\*, 8.18 (d,  $^3J$  = 9.0 Hz, 2 H, 9-H).  $^{13}\text{C-NMR}$  ( $\text{CDCl}_3$ , 75.5 MHz)  $\delta$  = 13.8 (q, C-14), 19.2, 19.4\* (t, C-13), 32.1 (t, C-12), 68.4\*, 70.7 (t, C-11), 100.6\*, 110.6 (d, C-1), 123.4\*, 123.7 (d, C-9), 127.2, 128.3, 128.6, 128.7, 128.8, 129.2, 129.3, 129.4, 129.5 (C-4, C-5, C-6, C-7, C-8, both isomers), 135.5\*, 136.0 (s, C-3), 143.2,

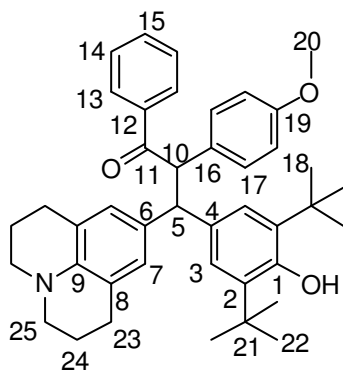
145.4\* (s, C-10), 159.7, 160.5\* (s, C-2). HR-MS (EI):  $m/z$  calcd for  $[C_{18}H_{19}NO_3]$ : 297.1365, found 297.1366.

#### 4.2.4. Reactions of the Substituted Deoxybenzoins (2–4)-K with Quinone Methides in DMSO

**General Procedure 2 (PG2):** The substituted deoxybenzoin (**3–4**) and the quinone methide **5** were dissolved in 10 mL dry DMSO. 1,5-Diazabicyclo(4.3.0)non-5-ene (5 drops) was added and the mixture was stirred at ambient temperature for 24 h. After the addition of 30 mL of brine, the mixture was extracted with dichloromethane (3 x 15 mL). The combined organic layers were washed with brine, dried over sodium sulfate and the solvent was removed by distillation. The obtained crude products were purified by means of column chromatography (silica/pentane/dichloromethane).

##### 4.2.4.1. Reaction of 2-K with 5i

KOtBu (40.2 mg, 0.358 mmol) was dissolved in 10 mL dry DMSO and 2-(4-methoxyphenyl)-1-phenylethanone (**2-H**, 77.1 mg, 0.341 mmol) was added before a solution of **5i** (131 mg, 0.336 mmol) in 5 mL DMSO was added. Aqueous acetic acid (0.5%, 40 mL) was added after 40 min and the mixture was extracted with ethyl acetate (2 x 30 mL). The combined organic layers were washed with brine, dried over sodium sulfate and the solvent was removed by distillation. Column chromatography (Silica/ethyl acetate/pentane) yielded 3-(3,5-di-tert-butyl-4-hydroxyphenyl)-3-(1,2,3,5,6,7-hexahydropyrido[3,2,1-ij]quinolin-9-yl)-2-(4-methoxyphenyl)-1-phenylpropan-1-one (151 mg, 0.245 mmol, 73%,  $dr \sim 1:1.2$ ) as orange oil.



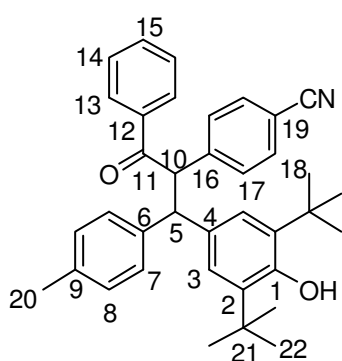
$^1\text{H-NMR}$  ( $\text{CDCl}_3$ , 300 MHz):  $\delta$  = 1.18 (s, 18 H, 22-H), 1.73-1.89 (m, 2 H, 24-H), 2.41-2.59 (m, 2 H, 23-H), 2.92 (t,  $^3J$  = 5.6 Hz, 2 H, 25-H), 3.64 (s, 3 H, 20-H), 4.45 (d,  $^3J$  = 11.7 Hz, 1 H, 5-H), 4.77 (s, 1 H, OH), 5.23 (d,  $^3J$  = 11.7 Hz, 1 H, 10-H), 6.35 (s, 2 H, 7-H), 6.60-6.66 (m, 3 H,  $\text{H}_{\text{arom}}$ ), 6.94 (s, 2 H, 3-H), 7.14-7.17 (m, 2 H,  $\text{H}_{\text{arom}}$ ), 7.24-7.27 (m, 2 H,  $\text{H}_{\text{arom}}$ ), 7.69-7.73 (m, 2 H,  $\text{H}_{\text{arom}}$ ).

$^{13}\text{C-NMR}$  ( $\text{CDCl}_3$ , 75.5 MHz):  $\delta$  = 21.2 (t, C-24), 26.5 (t, C-23), 29.2 (q, C-22), 33.2 (s, c-21), 49.0 (t, C-25), 53.7 (d, C-5), 54.1 (q, C-20), 56.9 (d, C-10), 120.1 (s, C-8), 123.5 (d, C-3), 125.9 (s, C-7), 133.3 (s, C-2), 139.9 (s, C-9), 150.7 (s, C-1), 157.3 (s, C-19), 199.9 (s, C-11), 112.7, 127.0, 127.2, 129.2, 131.3 (d,

$C_{\text{arom}}$ ), 129.1, 129.4, 134.1, 137.4 (s,  $C_{\text{arom}}$ ). HR-MS (EI):  $m/z$  calcd for  $[C_{42}H_{49}NO_3]^{++}$ : 615.3707, found 615.3644.

#### 4.2.4.2. Reaction of 3-K with 5e

According to GP2, 4-(2-Oxo-2-phenylethyl)benzonitrile (**3-H**, 125 mg, 0.566 mmol) and **5e** (127 mg, 0.412 mmol) yielded 4-(1-(3,5-di-tert-butyl-4-hydroxyphenyl)-3-oxo-3-phenyl-1-(p-tolyl)propan-2-yl)benzonitrile (166 mg, 0.313 mmol, 76%,  $dr \sim 1:1.3$ ) as yellow oil.

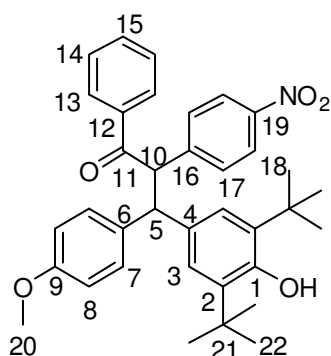


$^1\text{H-NMR}$  ( $\text{CDCl}_3$ , 300 MHz):  $\delta$  = 1.24, 1.26\* (s, 18 H, 22-H), 2.19, 2.22\* (s, 3 H, 20-H), 4.74\* (d,  $^3J = 11.5$  Hz, 1 H, 5\*-H), 4.78 (d,  $^3J = 11.7$  Hz, 1 H, 5-H), 4.92, 4.93\* (s, 1 H, OH), 5.35\* (d,  $^3J = 11.5$  Hz, 1 H, 10\*-H), 5.50 (d,  $^3J = 11.7$  Hz, 1 H, 10-H), 6.66\*, 7.00 (s, 2 H, 3-H), 6.91-6.92 (m,  $H_{\text{arom}}$ ), 7.19-7.24 (m,  $H_{\text{arom}}$ ), 7.33-7.41 (m,  $H_{\text{arom}}$ ), 7.45-7.51 (m,  $H_{\text{arom}}$ ), 7.79-7.81 (m,  $H_{\text{arom}}$ ), 7.85-7.87 (m,  $H_{\text{arom}}$ ).  $^{13}\text{C-NMR}$  ( $\text{CDCl}_3$ , 75.5 MHz):  $\delta$  = 20.9 (q, C-20), 30.06, 30.14\* (q, C-22), 34.08\*, 34.13 (s, C-21), 54.8\*, 55.2 (d, C-5), 58.3, 59.2\* (d, C-10), 110.6, 110.7 (s, CN, both isomers), 124.2, 125.0\* (d, C-3), 135.4, 135.57 (s, C-9, both isomers), 135.66, 135.74 (s, C-2, both isomers), 151.95, 152.11 (s, both isomers), 127.4, 128.0, 128.1, 128.3, 128.5, 128.6, 128.9, 129.2, 129.7, 129.8, 131.9, 132.1, 133.1, 133.2, 132.7, 136.9, 137.5, 139.0, 139.6, 143.6, 143.2 ( $C_{\text{arom}}$ ), 198.0, 199.2 (C-11, both isomers). HR-MS (EI):  $m/z$  calcd for  $[C_{37}H_{39}NO_2]^{++}$ : 529.2975, found 529.2974.

#### 4.2.4.3. Reaction of 4-K with 5f

According to GP2, 2-(4-nitrophenyl)-1-phenylethanone (**4-H**, 91.5 mg, 0.379 mmol) and **5f** (121 mg, 0.373 mmol) yielded 3-(3,5-di-tert-butyl-4-hydroxyphenyl)-3-(4-methoxyphenyl)-2-(4-nitrophenyl)-1-phenylpropan-1-one (177 mg, 0.313 mmol, 84%,  $dr \sim 1:1.1$ ) as yellow oil.

$^1\text{H-NMR}$  ( $\text{CDCl}_3$ , 300 MHz):  $\delta$  = 1.26 (s, 18 H, 22-H, both isomers), 3.68, 3.72\* (s, 3 H, 20-H), 4.80\* (d,  $^3J = 11.4$  Hz, 1 H, 5\*-H), 4.83 (d,  $^3J = 11.7$  Hz, 1 H, 5-H), 4.96 (s, 1 H, OH, both isomers), 5.41\* (d,  $^3J = 11.4$  Hz, 1 H, 10\*-H), 5.56 (d,  $^3J = 11.7$  Hz, 1 H, 10-H), 6.68\*, 7.01 (s, 2 H, 3-H), 7.25-7.32 (m,  $H_{\text{arom}}$ ), 7.36-7.41 (m,  $H_{\text{arom}}$ ), 7.48-7.52 (m,  $H_{\text{arom}}$ ), 7.81-7.90 (m,  $H_{\text{arom}}$ ), 7.98-8.04 (m,  $H_{\text{arom}}$ ).  $^{13}\text{C-NMR}$  ( $\text{CDCl}_3$ , 75.5



MHz):  $\delta$  = 30.2, 30.3\* (q, C-22), 34.2\*, 34.3 (s, C-21), 55.16, 55.23\* (q, C-20), 54.6\*, 55.6 (d, C-5), 58.4, 59.2\* (d, C-10), 124.4, 125.1\* (d, C-3), 113.8, 114.0, 123.5, 123.7, 128.2, 128.5, 128.68, 128.74, 128.8, 129.3, 129.9, 130.0, 132.2, 132.8, (d, C<sub>arom</sub>, both isomers), 135.6\*, 135.8 (s, C-2), 133.3, 133.4, 134.4, 137.0, 137.6, 146.9, 147.0, 145.5, 145.8 (s, C<sub>arom</sub>, both isomers), 152.2\*, 152.3 (s, C-1), 158.0, 158.1 (s, C-9), 198.2\*, 199.2 (s, C-11). HR-MS (EI):  $m/z$  calcd for [C<sub>36</sub>H<sub>39</sub>NO<sub>5</sub>]<sup>+</sup>: 565.2823, found 565.2823.

#### 4.2.5. Verification of the Accurateness of Determining the Ratios by NMR

Solutions of the C-alkylated **1-C** and the O-alkylated **1-O** in CDCl<sub>3</sub> were combined in different ratios in different NMR tubes as shown in Table 14.

Table 14: Real ratios and analyzed ratios (by <sup>1</sup>H NMR) in NMR tubes.

Entry	in NMR Tube			NMR Exp.
	1-C / mg	1-O / mg	1-O / (1-C + 1-O)	1-O / (1-C + 1-O)
1	2.00	30.3	93.8	94.3
2	9.09	23.2	71.9	74.1
3	16.0	16.2	50.2	50.3
4	23.0	3.03	11.6	11.3
5	30.0	2.02	6.30	7.40

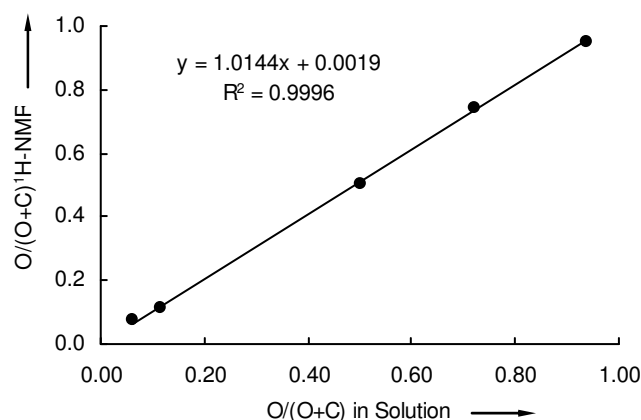


Figure 23: Analyzed ratios (by <sup>1</sup>H NMR) versus real ratios and in NMR tubes.

#### 4.3. Alkylation Reactions of Deoxybenzoin

General Procedure: KO<sup>t</sup>Bu (31-35 mg, ~1.05 equiv.) were dissolved in 8.0 mL of dry solvent. Two min after adding deoxybenzoin (**1-H**, 50-60 mg, 1 equiv.), the electrophile was added and the reaction mixture was stirred at ambient temperature. After decoloration of the solution (color of **1-K**), 15 mL brine were added and the reaction mixture was extracted with diethyl ether (2 x 15 mL). The combined organic layers were dried over sodium sulfate and the

solvent was removed by evaporation at reduced pressure. The O/C-ratio was calculated by integration of the signals of the C-alkylated product (**1-C**, t, 4.54 ppm) and the O-alkylated product (**1-O**, s, 6.06 ppm) of the  $^1\text{H}$  NMR spectra of the samples. Each reaction was performed twice and averaged (see Tables).

### 4.3.1. Alkylation Reactions of Deoxybenzoin Varying Concentrations

#### 4.3.1.1. Varying the Concentration of the Reaction

General Procedure: All the reactions were performed in DMSO as described above using the solvent amounts as shown in Table 15.

Table 15: Reactions of the potassium salt of deoxybenzoin (**1-K**) with BuI and BuOTs in DMSO at different concentrations.

Entry	Deoxybenzoin		KOtBu		Electrophile		Volumen	Conversion %	$c / \text{molL}^{-1}$	O : C	
	mg	mmol	mg	mmol		mmol	DMSO / mL				
1	54.7	0.279	32.8	0.292	<i>n</i> BuI	0.352	8.0	84	$3.48 \times 10^{-2}$	5	95
2	54.1	0.276	32.5	0.290	<i>n</i> BuI	0.352	8.0	90	$3.45 \times 10^{-2}$	5	95
3	51.8	0.264	31.2	0.278	<i>n</i> BuI	0.352	16.0	95	$1.65 \times 10^{-2}$	4	96
4	50.5	0.257	30.5	0.272	<i>n</i> BuI	0.352	16.0	100	$1.61 \times 10^{-2}$	4	96
5	54.6	0.278	32.7	0.291	<i>n</i> BuI	0.352	40.0	94	$6.96 \times 10^{-3}$	4	96
6	53.5	0.273	32.2	0.287	<i>n</i> BuI	0.352	40.0	84	$6.82 \times 10^{-3}$	3	97
7	53.7	0.274	32.5	0.290	<i>n</i> BuI	0.352	100.0	83	$2.74 \times 10^{-3}$	3	97
8	51.5	0.262	31.0	0.276	<i>n</i> BuI	0.352	100.0	91	$2.62 \times 10^{-3}$	2	98
9	55.8	0.284	32.5	0.290	<i>n</i> BuOTs	0.319	8.0	80	$3.55 \times 10^{-2}$	61	39
10	58.7	0.299	35.2	0.314	<i>n</i> BuOTs	0.319	8.0	79	$3.74 \times 10^{-2}$	62	38
11	50.8	0.259	30.7	0.274	<i>n</i> BuOTs	0.319	16.0	79	$1.62 \times 10^{-2}$	55	45
12	53.8	0.274	32.3	0.288	<i>n</i> BuOTs	0.319	16.0	78	$1.71 \times 10^{-2}$	53	47
13	55.6	0.283	33.5	0.299	<i>n</i> BuOTs	0.319	40.0	82	$7.08 \times 10^{-3}$	54	46
14	52.2	0.266	31.5	0.281	<i>n</i> BuOTs	0.319	40.0	71 <sup>[a]</sup>	$6.65 \times 10^{-3}$	50	50
15	53.0	0.270	31.9	0.284	<i>n</i> BuOTs	0.319	100.0	87	$2.70 \times 10^{-3}$	50	50
16	51.6	0.263	31.1	0.277	<i>n</i> BuOTs	0.319	100.0	>65 <sup>[a]</sup>	$2.63 \times 10^{-3}$	51	49

[a] Signals of deoxybenzoin and BuOTs are superimposed.

#### 4.3.1.2. Varying the Excess of the Electrophile

General Procedure: All the reactions were performed as described above using 8.0 mL of solvent and adding the amount of electrophile as described in Table 16.



Table 16: Reactions of the potassium salt of deoxybenzoin (**1-K**) with BuI, BuCl and BuOTs in DMSO varying the concentrations of the electrophile.

Entry	Deoxybenzoin		KOtBu		Electrophile		Solvent	Conversion %	O : C			
	mg	mmol	mg	mmol		mmol			O : C	Average		
1a	54.7	0.279	32.8	0.292	<i>n</i> BuI	0.352	DMSO	84	4.8	95.2	5	95
1b	54.1	0.276	32.5	0.290	<i>n</i> BuI	0.352	DMSO	90	4.7	95.3		
2a	47.6	0.243	31.2	0.278	<i>n</i> BuI	1.76	DMSO	90	4.4	95.6	4	96
2b	51.7	0.263	30.8	0.275	<i>n</i> BuI	1.76	DMSO	70	4.2	95.8		
3a	57.2	0.291	34.3	0.306	<i>n</i> BuI	4.40	DMSO	74	4.7	95.3	4	96
3b	56.7	0.289	33.9	0.302	<i>n</i> BuI	4.40	DMSO	77	3.4	96.6		
4a	52.8	0.269	31.7	0.283	<i>n</i> BuI	8.80	DMSO	75	4.2	95.8	5	95
4b	57.5	0.293	34.2	0.305	<i>n</i> BuI	8.80	DMSO	77	6.1	93.9		
5a	61.2	0.312	36.2	0.323	<i>n</i> BuCl	0.380	DMSO	55	18.0	82.0	19	81
5b	56.3	0.287	33.4	0.298	<i>n</i> BuCl	0.380	DMSO	61	20.9	79.1		
6a	54.7	0.279	32.6	0.291	<i>n</i> BuCl	2.00	DMSO	100	22.2	77.8	22	78
6b	51.8	0.264	31.4	0.280	<i>n</i> BuCl	2.00	DMSO	100	21.6	78.4		
7a	51.3	0.261	30.9	0.275	<i>n</i> BuCl	4.75	DMSO	83	23.5	76.5	24	76
7b	54.4	0.277	32.7	0.291	<i>n</i> BuCl	4.75	DMSO	89	24.2	75.8		
8a	52.0	0.265	30.9	0.275	<i>n</i> BuCl	9.51	DMSO	86	24.5	75.5	24	76
8b	50.8	0.259	30.6	0.273	<i>n</i> BuCl	9.51	DMSO	80	22.6	77.4		
9a	55.8	0.284	32.5	0.290	<i>n</i> BuOTs	0.319	DMSO	80	61.3	38.7	62	38
9b	58.7	0.299	35.2	0.314	<i>n</i> BuOTs	0.319	DMSO	79	62.1	37.9		
10a	56.1	0.286	33.6	0.299	<i>n</i> BuOTs	1.96	DMSO	75	63.3	36.7	63	37
10b	52.3	0.267	31.3	0.279	<i>n</i> BuOTs	1.96	DMSO	[a]	62.9	37.1		
11a	54.3	0.277	32.3	0.288	<i>n</i> BuOTs	4.91	DMSO	81	58.8	41.2	59	41
11b	52.8	0.269	31.8	0.283	<i>n</i> BuOTs	4.91	DMSO	[a]	[a]			

[a] Signals of the products are superimposed with the signals of the electrophile.

### 4.3.2. Reactions Varying the Solvent and the Electrophile

#### 4.3.2.1. Reactions in DMSO

Table 17: Reactions of the potassium salt of deoxybenzoin (**1-K**) with different electrophiles in DMSO.

Entry	Deoxybenzoin		KOtBu		Electrophile	mmol	Conversion %	O : C			
	mg	mmol	mg	mmol				O : C	Average		
1a	58.1	0.296	34.3	0.306	<i>n</i> BuI	0.352	84	4.8	95.2	5	95
1b	55.3	0.282	32.3	0.288	<i>n</i> BuI	0.352	90	4.7	95.3		
2a	57.6	0.294	33.5	0.299	<i>n</i> BuBr	0.371	86	14.5	85.5	15	85
2b	53.6	0.273	31.2	0.278	<i>n</i> BuBr	0.371	81	15.1	84.9		
3a	61.2	0.312	36.2	0.323	<i>n</i> BuCl	0.380	55	18.0	82.0	19	81
3b	56.3	0.287	33.4	0.298	<i>n</i> BuCl	0.380	61	20.9	79.1		
4a	55.8	0.284	32.5	0.290	<i>n</i> BuOTs	0.319	80	61.3	38.7	62	38
4b	58.7	0.299	35.2	0.314	<i>n</i> BuOTs	0.319	79	62.1	37.9		
5a	53.3	0.272	31.6	0.282	<i>n</i> BuOMes	0.328	[a]	69.4	30.6	69	31
5b	55.8	0.284	32.9	0.293	<i>n</i> BuOMes	0.328	[a]	69.4	30.6		
6a	60.7	0.309	35.4	0.316	( <i>n</i> BuO) <sub>2</sub> SO <sub>2</sub>	0.328	[a]	65.4	34.6	66	34
6b	55.8	0.284	32.4	0.289	( <i>n</i> BuO) <sub>2</sub> SO <sub>2</sub>	0.328	[a]	65.8	34.2		

[a] Signals of deoxybenzoin and the electrophile are superimposed.

## 4.3.2.2. Reactions in DMF

Table 18: Reactions of the potassium salt of deoxybenzoin (**1-K**) with different electrophiles in DMF.

Entry	Deoxybenzoin		KOtBu		Electrophile	Conversion %	O : C				
	mg	mmol	mg	mmol	mmol		O : C	Average			
1a	54.0	0.275	32.5	0.290	<i>n</i> BuI	0.352	81	4.0	96.0	4	96
1b	51.5	0.262	30.9	0.275	<i>n</i> BuI	0.352	85	4.5	95.5		
2a	52.2	0.266	31.6	0.282	<i>n</i> BuBr	0.371	78	11.9	88.1	12	88
2b	50.9	0.259	30.7	0.274	<i>n</i> BuBr	0.371	83	12.6	87.4		
3a	51.4	0.262	30.9	0.275	<i>n</i> BuCl	0.380	81	27.9	72.1	28	72
3b	52.5	0.268	31.5	0.281	<i>n</i> BuCl	0.380	60	27.3	72.7		
4a	56.0	0.285	33.6	0.299	<i>n</i> BuOTs	0.319	76	64.9	35.1	65	35
4b	51.5	0.262	31.1	0.277	<i>n</i> BuOTs	0.319	89	65.4	34.6		
5a	50.9	0.259	31.1	0.277	<i>n</i> BuOMes	0.328	[a]	69.9	30.1	70	30
5b	54.3	0.277	33.0	0.294	<i>n</i> BuOMes	0.328	[a]	69.9	30.1		
6a	55.2	0.281	33.2	0.296	( <i>n</i> BuO) <sub>2</sub> SO <sub>2</sub>	0.328	[a]	69.0	31.0	69	31
6b	54.3	0.277	32.5	0.290	( <i>n</i> BuO) <sub>2</sub> SO <sub>2</sub>	0.328	[a]	69.4	30.6		

[a] Signals of deoxybenzoin and the electrophile are superimposed.

## 4.3.2.3. Reactions in Acetone

Table 19: Reactions of the potassium salt of deoxybenzoin (**1-K**) with different electrophiles in acetone.

Entry	Deoxybenzoin		KOtBu		Electrophile	Conversion %	O : C				
	mg	mmol	mg	mmol	mmol		O : C	Average			
1a	54.7	0.279	33.2	0.296	<i>n</i> BuI	0.352	77	5.3	94.7	5	95
1b	56.8	0.289	34.2	0.305	<i>n</i> BuI	0.352	93	5.3	94.7		
2a	57.0	0.290	34.0	0.303	<i>n</i> BuBr	0.371	100	15.6	84.4	15	85
2b	56.5	0.288	34.1	0.304	<i>n</i> BuBr	0.371	87	15.0	85.0		
3a	57.3	0.292	34.1	0.304	<i>n</i> BuCl	0.380	35	31.6	68.4	31	69
3b	56.8	0.289	33.8	0.301	<i>n</i> BuCl	0.380	33	30.8	69.2		
4a	56.7	0.289	34.0	0.303	<i>n</i> BuOTs	0.319	93	59.9	40.1	60	40
4b	56.3	0.287	34.0	0.303	<i>n</i> BuOTs	0.319	94	59.9	40.1		
5a	56.1	0.286	33.9	0.302	<i>n</i> BuOMes	0.328	[a]	65.4	34.6	65	35
5b	56.9	0.290	34.1	0.304	<i>n</i> BuOMes	0.328	[a]	65.4	34.6		
6a	56.6	0.288	33.4	0.298	( <i>n</i> BuO) <sub>2</sub> SO <sub>2</sub>	0.328	[a]	64.1	35.9	64	36
6b	56.6	0.288	33.4	0.298	( <i>n</i> BuO) <sub>2</sub> SO <sub>2</sub>	0.328	[a]	63.7	36.3		

[a] Signals of deoxybenzoin and the electrophile are superimposed.

## 4.3.2.4. Reactions in THF

Table 20: Reactions of the potassium salt of deoxybenzoin (**1-K**) with different electrophiles in THF.

Entry	Deoxybenzoin		KOtBu		Electrophile	Conversion %	O : C				
	mg	mmol	mg	mmol			mmol	O : C	Average		
1a	48.5	0.247	29.2	0.260	<i>n</i> BuI	0.352	78	4.8	95.2	4	96
1b	54.6	0.278	32.8	0.292	<i>n</i> BuI	0.352	95	4.1	95.9		
2a	51.0	0.260	30.6	0.273	<i>n</i> BuBr	0.371	49	13.6	86.4	14	86
2b	52.3	0.267	31.7	0.283	<i>n</i> BuBr	0.371	91	15.2	84.8		
3a	52.0	0.265	31.2	0.278	<i>n</i> BuCl	0.380	55	21.8	78.2	20	80
3b	52.6	0.268	31.6	0.282	<i>n</i> BuCl	0.380	53	18.2	81.8		
4a	51.7	0.263	31.0	0.276	<i>n</i> BuOTs	0.319	35	38.8	61.2	39	61
4b	50.6	0.258	30.3	0.270	<i>n</i> BuOTs	0.319	27	38.5	61.5		
5a	50.6	0.258	30.3	0.270	<i>n</i> BuOMes	0.328	79 <sup>[a]</sup>	29.9	70.1	30	70
5b	56.6	0.288	34.2	0.305	<i>n</i> BuOMes	0.328	85 <sup>[a]</sup>	30.3	69.7		
6a	50.6	0.258	30.4	0.271	( <i>n</i> BuO) <sub>2</sub> SO <sub>2</sub>	0.328	[a]	28.2	71.8	29	71
6b	51.3	0.261	30.9	0.275	( <i>n</i> BuO) <sub>2</sub> SO <sub>2</sub>	0.328	[a]	30.2	69.8		

[a] Signals of deoxybenzoin and the electrophile are superimposed.

### 4.3.3. Reactions Varying the Counter Ion

General Procedure: All the reactions were performed as described above using different alkali metal butoxides (NaOtBu, LiOtBu) for the generation of the anion of deoxybenzoin.

#### 4.3.3.1. Reactions in DMSO

Table 21: Reactions of different alkali salt of deoxybenzoin with different electrophiles in DMSO.

Entry	Deoxybenzoin		MOtBu			Electrophile		Conversion %	O : C			
	mg	mmol	M <sup>+</sup>	mg	mmol	mmol	O : C		Average			
1a	45.2	0.230	Na	23.6	0.246	<i>n</i> BuI	0.352	100	4.6	95.4	4	96
1b	44.6	0.227	Na	23.1	0.240	<i>n</i> BuI	0.352	96	4.0	96.0		
2a	57.0	0.290	Na	29.4	0.306	<i>n</i> BuCl	0.380	100	25.1	74.9	24	76
2b	52.8	0.269	Na	26.8	0.279	<i>n</i> BuCl	0.380	95	23.9	76.1		
3a	59.2	0.302	Na	30.5	0.317	<i>n</i> BuOTs	0.319	93	60.6	39.4	60	40
3b	54.9	0.280	Na	28.3	0.294	<i>n</i> BuOTs	0.319	97	58.5	41.5		
4a	51.7	0.263	Li	22.2	0.277	<i>n</i> BuI	0.352	96	3.8	96.2	4	96
4b	52.3	0.267	Li	22.5	0.281	<i>n</i> BuI	0.352	97	4.1	95.9		
5a	51.0	0.260	Li	22.1	0.276	<i>n</i> BuCl	0.380	98	23.2	76.8	24	76
5b	51.5	0.262	Li	22.2	0.277	<i>n</i> BuCl	0.380	92	24.8	75.2		
6a	51.8	0.264	Li	22.4	0.280	<i>n</i> BuOTs	0.319	85	60.2	39.8	60	40
6b	52.4	0.267	Li	22.5	0.281	<i>n</i> BuOTs	0.319	91	60.6	39.4		
7a	55.8	0.284	K/Crown	33.5	0.299	<i>n</i> BuI	0.352	>60 <sup>[a]</sup>	4.1	95.9	4	96
7b	55.5	0.283	K/Crown	33.4	0.298	<i>n</i> BuI	0.352	>60 <sup>[a]</sup>	4.0	96.0		
8a	56.6	0.288	K/Crown	34.2	0.305	<i>n</i> BuCl	0.380	>50 <sup>[a]</sup>	22.8	77.2	23	77
8b	55.8	0.284	K/Crown	33.5	0.299	<i>n</i> BuCl	0.380	>50 <sup>[a]</sup>	23.8	76.2		
9a	56.4	0.287	K/Crown	33.7	0.300	<i>n</i> BuOTs	0.319	>50 <sup>[a]</sup>	59.5	40.5	60	40
9b	55.6	0.283	K/Crown	33.4	0.298	<i>n</i> BuOTs	0.319	>50 <sup>[a]</sup>	59.9	40.1		

[a] Signals of deoxybenzoin and crown ether are superimposed.

#### 4.3.3.2. Reactions in THF

Table 22: Reactions of different alkali salt of deoxybenzoin with different electrophiles in THF.

Entry	Deoxybenzoin		MO/ <i>t</i> Bu			Electrophile		Conversion	O : C			
	mg	mmol	M <sup>+</sup>	mg	mmol	mmol	mmol	%	O : C		Average	
1a	56.4	0.287	Na	28.8	0.300	<i>n</i> BuI	0.352	78	0	100	only carbon	
1b	56.5	0.288	Na	28.4	0.296	<i>n</i> BuI	0.352	88	0	100		
2a	55.5	0.283	Na	28.7	0.299	<i>n</i> BuCl	0.380	0			no reaction	
2b	55.9	0.285	Na	29.0	0.302	<i>n</i> BuCl	0.380	0				
3a	51.3	0.261	Na	26.4	0.275	<i>n</i> BuOTs	0.319	17	0	100	only carbon	
3b	51.1	0.260	Na	26.4	0.275	<i>n</i> BuOTs	0.319	20	0	100		
4a	52.4	0.267	Li	22.4	0.280	<i>n</i> BuI	0.352	58	0.2	99.8	0	100
4b	52.3	0.267	Li	22.4	0.280	<i>n</i> BuI	0.352	73	0.3	99.7		
5a	56.4	0.287	Li	24.5	0.306	<i>n</i> BuCl	0.380	0			no reaction	
5b	55.8	0.284	Li	24.3	0.304	<i>n</i> BuCl	0.380	0				
6a	55.8	0.284	Li	24.6	0.307	<i>n</i> BuOTs	0.319	0			no reaction	
6b	56.1	0.286	Li	24.7	0.309	<i>n</i> BuOTs	0.319	0				
7a	56.2	0.286	K/Crown	34.3	0.306	<i>n</i> BuI	0.352	100	6.8	93.2	7	93
7b	56.4	0.287	K/Crown	34.5	0.307	<i>n</i> BuI	0.352	100	6.3	93.7		
8a	56.1	0.286	K/Crown	33.9	0.302	<i>n</i> BuCl	0.380	34	40.5	59.5	40	60
8b	56.3	0.287	K/Crown	34.1	0.304	<i>n</i> BuCl	0.380	32	39.7	60.3		
9a	56.7	0.289	K/Crown	34.8	0.310	<i>n</i> BuOTs	0.319	>50 <sup>[a]</sup>	76.3	23.7	77	23
9b	56.2	0.286	K/Crown	34.5	0.307	<i>n</i> BuOTs	0.319	>50 <sup>[a]</sup>	77.5	22.5		

[a] Signals of deoxybenzoin and crown ether are superimposed.

### 4.3.4. Reactions Varying the Temperature

**General Procedure:** The anion solutions were prepared from deoxybenzoin and KO<sup>t</sup>Bu in 8.0 mL of solvent as previously described. Before the electrophile was added, the solutions were cooled or heated in a thermostat and the temperature of the solution was controlled with a digital thermometer. When the solutions reached, and kept the correspondent temperature for 10 min. the electrophile was added. After decoloration of the solution (consumption of **1-K**), the reactions were stopped adding water at the reaction-temperature. After cool down to ambient temperature, the reaction mixtures were treated as described above.

#### 4.3.4.1. Reactions in DMSO

Table 23: Reactions of the potassium salt of deoxybenzoin (**1-K**) with different electrophiles in DMSO at different temperatures.

Entry	Deoxybenzoin		KO <sup>t</sup> Bu		Electrophile	<i>g</i> / °C	Conversion %	O : C				
	mg	mmol	mg	mmol	mmol			O : C	Average			
1a	54.7	0.279	32.8	0.292	<i>n</i> BuI	0.352	20	84	4.8	95.2	5	95
1b	54.1	0.276	32.5	0.290	<i>n</i> BuI	0.352	20	90	4.7	95.3		
2a	55.8	0.284	33.1	0.295	<i>n</i> BuI	0.352	40	81	6.1	93.9	6	94
2b	55.0	0.280	32.8	0.292	<i>n</i> BuI	0.352	40	100	6.9	93.1		
3a	51.6	0.263	31.0	0.276	<i>n</i> BuI	0.352	60	100	9.1	90.9	10	90
3b	51.4	0.262	30.6	0.273	<i>n</i> BuI	0.352	60	100	11.3	88.7		
4a	53.1	0.271	31.8	0.283	<i>n</i> BuI	0.352	80	100	10.3	89.7	11	89
4b	53.7	0.274	32.3	0.288	<i>n</i> BuI	0.352	80	100	10.7	89.3		
5a	53.9	0.275	32.1	0.286	<i>n</i> BuI	0.352	100	100	13.7	86.3	14	86
5b	51.4	0.262	30.5	0.272	<i>n</i> BuI	0.352	100	100	14.0	86.0		
6a	53.2	0.271	31.5	0.281	<i>n</i> BuCl	0.380	20	55	18.0	82.0	19	81
6b	56.0	0.285	33.6	0.299	<i>n</i> BuCl	0.380	20	61	20.9	79.1		
7a	58.4	0.298	35.3	0.315	<i>n</i> BuCl	0.380	40	56	30.0	70.0	30	70
7b	58.2	0.297	34.7	0.309	<i>n</i> BuCl	0.380	40	59	29.7	70.3		
8a	56.3	0.287	33.4	0.298	<i>n</i> BuCl	0.380	60	71	33.6	66.4	34	66
8b	56.5	0.288	33.5	0.299	<i>n</i> BuCl	0.380	60	78	33.7	66.3		
9a	53.7	0.274	32.0	0.285	<i>n</i> BuCl	0.380	80	34	34.0	66.0	35	65
9b	54.4	0.277	32.5	0.290	<i>n</i> BuCl	0.380	80	49	35.5	64.5		
10a	53.7	0.274	32.1	0.286	<i>n</i> BuCl	0.380	100	26	42.7	57.3	43	57
10b	54.4	0.277	32.6	0.291	<i>n</i> BuCl	0.380	100	23	42.6	57.4		
11a	57.2	0.291	34.4	0.307	<i>n</i> BuOTs	0.319	20	78	62.5	37.5	63	37
11b	56.7	0.289	34.2	0.305	<i>n</i> BuOTs	0.319	20	82	62.9	37.1		
12a	56.4	0.287	33.9	0.302	<i>n</i> BuOTs	0.319	40	>60 <sup>[a]</sup>	62.1	37.9	62	38
12b	55.6	0.283	33.4	0.298	<i>n</i> BuOTs	0.319	40	>60 <sup>[a]</sup>	62.5	37.5		
13a	53.1	0.271	31.8	0.283	<i>n</i> BuOTs	0.319	60	78	59.5	40.5	59	41
13b	53.7	0.274	32.3	0.288	<i>n</i> BuOTs	0.319	60	84	57.8	42.2		
14a	56.5	0.288	34.1	0.304	<i>n</i> BuOTs	0.319	80	82	53.8	46.2	53	47
14b	55.9	0.285	33.7	0.300	<i>n</i> BuOTs	0.319	80	78	52.6	47.4		
15a	57.0	0.290	34.8	0.310	<i>n</i> BuOTs	0.319	100	[a]	47.8	52.2	48	52
15b	56.7	0.289	34.5	0.307	<i>n</i> BuOTs	0.319	100	[a]	47.2	52.8		
16a	57.0	0.290	34.3	0.306	<i>n</i> BuBr	0.371	80	78	21.7	78.3	22	78
16b	56.6	0.288	34.0	0.303	<i>n</i> BuBr	0.371	80	86	22.7	77.3		
17a	56.2	0.286	34.0	0.303	<i>n</i> BuOMes	0.328	80	100	64.9	35.1	64	36
17b	56.0	0.285	33.9	0.302	<i>n</i> BuOMes	0.328	80	100	63.3	36.7		
18a	56.0	0.285	34.0	0.303	( <i>n</i> BuO) <sub>2</sub> SO <sub>2</sub>	0.328	80	100	57.5	42.5	57	43
18b	55.6	0.283	33.8	0.301	( <i>n</i> BuO) <sub>2</sub> SO <sub>2</sub>	0.328	80	100	57.1	42.9		

[a] Signals of deoxybenzoin and the electrophile are superimposed.

## 4.3.4.1. Reactions in THF

Table 24: Reactions of the potassium salt of deoxybenzoin (**1-K**) with different electrophiles in THF at different temperatures.

Entry	Deoxybenzoin		KOtBu		Electrophile	$\theta / ^\circ\text{C}$	Conversion %	O : C		
	mg	mmol	mg	mmol	mmol			O : C	Average	
1a	55.6	0.283	33.3	0.297	<i>n</i> BuI	0.352	50	82	4.9	95.1
1b	56.2	0.286	33.6	0.299	<i>n</i> BuI	0.352	50	87	5.1	94.9
2a	56.2	0.286	33.9	0.302	<i>n</i> BuBr	0.371	50	74	18.1	81.9
2b	55.7	0.284	33.4	0.298	<i>n</i> BuBr	0.371	50	76	18.5	81.5
3a	55.3	0.282	33.2	0.296	<i>n</i> BuOTs	0.319	50	65	28.0	72.0
3b	55.5	0.283	33.3	0.297	<i>n</i> BuOTs	0.319	50	67	27.6	72.4
4a	55.6	0.283	33.3	0.297	( <i>n</i> BuO) <sub>2</sub> SO <sub>2</sub>	0.328	50	[a]	26.0	74.0
4b	56.6	0.288	33.9	0.302	( <i>n</i> BuO) <sub>2</sub> SO <sub>2</sub>	0.328	50	[a]	25.5	74.5

[a] Signals of deoxybenzoin and the electrophile are superimposed.

4.3.5. Reactions of *p*-Substituted Deoxybenzoines

The reactions were performed in DMSO as described above using *p*-OMe, *p*-CN and *p*-NO<sub>2</sub> substituted deoxybenzoines as nucleophiles and *n*BuI and *n*BuOTs as electrophiles. The O/C-ratio was calculated from the integrals in <sup>1</sup>H NMR-experiments. *p*-OMe: 4.48 ppm (**2-C**), 6.05 ppm (**2-O**); *p*-CN: 4.63 ppm (**3-C**), 5.94 ppm (**3-O**); *p*-NO<sub>2</sub>: 4.69 ppm (**4-C**), 5.82, 5.99 ppm (**4-O**, two isomers). Each reaction was performed twice and averaged (Table 12).

Table 25: Reactions of the potassium salt of *p*-substituted deoxybenzoines (**2–4-K**) with different electrophiles in DMSO.

Entry	Deoxybenzoin R	Deoxybenzoin		KOtBu		Electrophile	Conversion %	O : C		
		mg	mmol	mg	mmol	mmol		O : C	Average	
1a	NO <sub>2</sub>	80.2	0.287	[a]		<i>n</i> BuI	0.352	100	2.7	97.3
1b	NO <sub>2</sub>	79.3	0.284	[a]		<i>n</i> BuI	0.352	100	2.5	97.5
2a	NO <sub>2</sub>	80.2	0.287	[a]		<i>n</i> BuOTs	0.319	55	60.6	39.4
2b	NO <sub>2</sub>	80.1	0.287	[a]		<i>n</i> BuOTs	0.319	57	57.1	42.9
3a	CN	74.0	0.285	[a]		<i>n</i> BuI	0.352	100	3.1	96.9
3b	CN	73.7	0.284	[a]		<i>n</i> BuI	0.352	100	4.1	95.9
4a	CN	74.3	0.286	[a]		<i>n</i> BuOTs	0.319	> 90 <sup>[b]</sup>	60.6	39.4
4b	CN	73.7	0.284	[a]		<i>n</i> BuOTs	0.319	> 90 <sup>[b]</sup>	60.6	39.4
5a	OMe	65.4	0.289	34.2	0.305	<i>n</i> BuI	0.352	92	6.5	93.5
5b	OMe	65.0	0.287	34.0	0.303	<i>n</i> BuI	0.352	85	6.3	93.7
6a	OMe	65.3	0.289	34.1	0.304	<i>n</i> BuOTs	0.319	> 90 <sup>[b]</sup>	67.6	32.4
6b	OMe	66.0	0.292	34.4	0.307	<i>n</i> BuOTs	0.319	> 90 <sup>[b]</sup>	67.1	32.9

[a] Potassium salt of the substituted deoxybenzoin was used. [b] Signals of deoxybenzoin and *n*BuOTs are superimposed.

## 4.4. Kinetic Experiments

### 4.4.1. Reactions of the Potassium Salt of Deoxybenzoin (1-K) in Different Solvents

#### 4.4.1.1. Reactions of 1-K in DMF

Table 26: Kinetics of the reaction of **1-K** (generated from **1-H** by addition of 1.05 equiv. KO $t$ Bu) with **5g** in presence of 18-crown-6 (20 °C, stopped-flow, at 490 nm).

[ <b>5g</b> ] / mol L <sup>-1</sup>	[ <b>1-K</b> ] / mol L <sup>-1</sup>	[18-crown-6] / mol L <sup>-1</sup>	[ <b>1-K</b> ] / [ <b>5g</b> ]	$k_{\text{obs}}$ / s <sup>-1</sup>
$1.42 \times 10^{-5}$	$4.60 \times 10^{-4}$	$5.48 \times 10^{-4}$	32.3	2.06
$1.42 \times 10^{-5}$	$6.89 \times 10^{-4}$	$8.22 \times 10^{-4}$	48.5	3.88
$1.42 \times 10^{-5}$	$9.19 \times 10^{-4}$	$1.10 \times 10^{-3}$	64.7	6.85
$1.42 \times 10^{-5}$	$1.15 \times 10^{-3}$	$1.37 \times 10^{-3}$	80.9	8.61

$$k_2 = 9.84 \times 10^3 \text{ L mol}^{-1} \text{ s}^{-1}$$

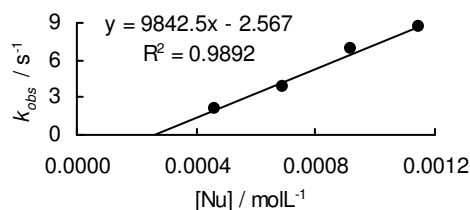


Table 27: Kinetics of the reaction of **1-K** (generated from **1-H** by addition of 1.05 equiv. KO $t$ Bu) with **5g** in absence of 18-crown-6 (20 °C, stopped-flow, at 490 nm).

[ <b>5g</b> ] / mol L <sup>-1</sup>	[ <b>1-K</b> ] / mol L <sup>-1</sup>	[ <b>1-K</b> ] / [ <b>5g</b> ]	$k_{\text{obs}}$ / s <sup>-1</sup>
$1.42 \times 10^{-5}$	$4.60 \times 10^{-4}$	32.3	1.99
$1.42 \times 10^{-5}$	$6.89 \times 10^{-4}$	48.5	3.65
$1.42 \times 10^{-5}$	$9.19 \times 10^{-4}$	64.7	6.40
$1.42 \times 10^{-5}$	$1.15 \times 10^{-3}$	80.9	8.64

$$k_2 = 9.88 \times 10^3 \text{ L mol}^{-1} \text{ s}^{-1} \text{ [a]}$$

[a] Not used for the calculation of  $N$  and  $s_N$ .

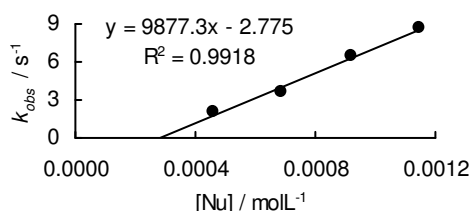


Table 28: Kinetics of the reaction of **1-K** (generated from **1-H** by addition of 1.05 equiv. KO $t$ Bu) with **5h** (20 °C, stopped-flow, at 486 nm).

[ <b>5h</b> ] / mol L <sup>-1</sup>	[ <b>1-K</b> ] / mol L <sup>-1</sup>	[18-crown-6] / mol L <sup>-1</sup>	[ <b>1-K</b> ] / [ <b>5h</b> ]	$k_{\text{obs}}$ / s <sup>-1</sup>
$1.30 \times 10^{-5}$	$7.29 \times 10^{-4}$	$8.64 \times 10^{-4}$	55.9	1.76
$1.30 \times 10^{-5}$	$9.72 \times 10^{-4}$	$1.03 \times 10^{-3}$	74.6	2.94
$1.30 \times 10^{-5}$	$1.23 \times 10^{-3}$		93.2	3.70
$1.30 \times 10^{-5}$	$1.46 \times 10^{-3}$	$1.73 \times 10^{-3}$	112	5.08
$1.30 \times 10^{-5}$	$1.70 \times 10^{-3}$		131	5.60

$$k_2 = 4.04 \times 10^3 \text{ L mol}^{-1} \text{ s}^{-1}$$

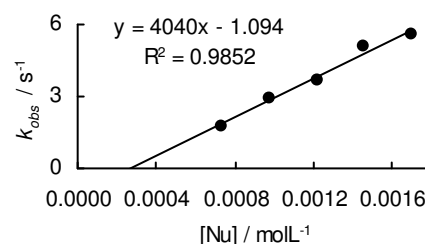
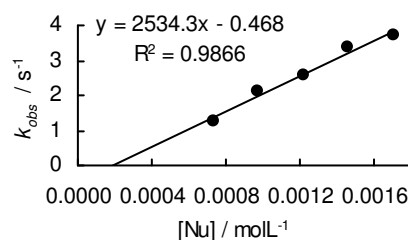


Table 29: Kinetics of the reaction of **1-K** (generated from **1-H** by addition of 1.05 equiv. KO $t$ Bu) with **5i** (20 °C, stopped-flow, at 521 nm).

[ <b>5i</b> ] / mol L <sup>-1</sup>	[ <b>1-K</b> ] / mol L <sup>-1</sup>	[18-crown-6] / mol L <sup>-1</sup>	[ <b>1-K</b> ] / [ <b>5i</b> ]	$k_{\text{obs}}$ / s <sup>-1</sup>
$1.21 \times 10^{-5}$	$7.29 \times 10^{-4}$		60.1	1.28
$1.21 \times 10^{-5}$	$9.72 \times 10^{-4}$	$1.15 \times 10^{-3}$	80.1	2.10
$1.21 \times 10^{-5}$	$1.22 \times 10^{-3}$		100	2.59
$1.21 \times 10^{-5}$	$1.46 \times 10^{-3}$	$1.73 \times 10^{-3}$	120	3.36
$1.21 \times 10^{-5}$	$1.70 \times 10^{-3}$		140	3.73

$$k_2 = 2.53 \times 10^3 \text{ L mol}^{-1} \text{ s}^{-1}$$

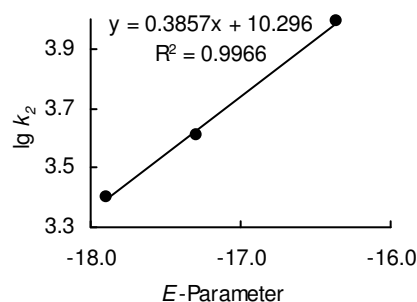


### Determination of Reactivity Parameters $N$ and $s_N$ of Potassium 2-Oxo-1,2-diphenylethan-1-ide (**1-K**) in DMF

Table 30: Rate Constants for the reactions of **1-K** with different electrophiles (20 °C, in presence of 18-crown-6).

Electrophile	$E$	$k_2 / \text{L mol}^{-1} \text{s}^{-1}$	$\log k_2$
<b>5g</b>	-16.36	$9.84 \times 10^3$	3.99
<b>5h</b>	-17.29	$4.04 \times 10^3$	3.61
<b>5i</b>	-17.90	$2.53 \times 10^3$	3.40

$$N = 26.69, s_N = 0.39$$

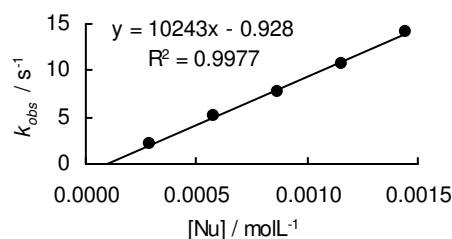


#### 4.4.1.2. Reactions of **1-K** in Acetone

Table 31: Kinetics of the reaction of **1-K** (generated from **1-H** by addition of 1.05 equiv. KOtBu) with **5g** (20 °C, stopped-flow, at 490 nm).

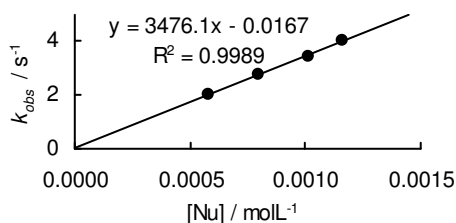
[ <b>5g</b> ] / $\text{mol L}^{-1}$	[ <b>1-K</b> ] / $\text{mol L}^{-1}$	[18-crown-6] / $\text{mol L}^{-1}$	[ <b>1-K</b> ] / [ <b>5g</b> ]	$k_{\text{obs}} / \text{s}^{-1}$
$1.52 \times 10^{-5}$	$2.90 \times 10^{-4}$	$3.49 \times 10^{-3}$	19.1	2.17
$1.52 \times 10^{-5}$	$5.80 \times 10^{-4}$	$6.97 \times 10^{-4}$	38.3	5.06
$1.52 \times 10^{-5}$	$8.70 \times 10^{-4}$	$1.05 \times 10^{-2}$	57.4	7.78
$1.52 \times 10^{-5}$	$1.16 \times 10^{-3}$	$1.39 \times 10^{-3}$	76.5	10.7
$1.52 \times 10^{-5}$	$1.45 \times 10^{-3}$	$1.74 \times 10^{-3}$	95.6	14.2

$$k_2 = 1.02 \times 10^4 \text{ L mol}^{-1} \text{s}^{-1}$$

Table 32: Kinetics of the reaction of **1-K** (generated from **1-H** by addition of 1.05 equiv. KOtBu) with **5h** (20 °C, stopped-flow, at 486 nm).

[ <b>5h</b> ] / $\text{mol L}^{-1}$	[ <b>1-K</b> ] / $\text{mol L}^{-1}$	[18-crown-6] / $\text{mol L}^{-1}$	[ <b>1-K</b> ] / [ <b>5h</b> ]	$k_{\text{obs}} / \text{s}^{-1}$
$1.33 \times 10^{-5}$	$5.80 \times 10^{-4}$	$1.23 \times 10^{-3}$	43.7	2.00
$1.33 \times 10^{-5}$	$7.94 \times 10^{-4}$	$1.05 \times 10^{-4}$	60.1	2.77
$1.33 \times 10^{-5}$	$1.01 \times 10^{-3}$	$1.90 \times 10^{-2}$	76.5	3.47
$1.33 \times 10^{-5}$	$1.16 \times 10^{-3}$	$1.39 \times 10^{-3}$	87.4	4.04

$$k_2 = 3.48 \times 10^3 \text{ L mol}^{-1} \text{s}^{-1}$$

Table 33: Kinetics of the reaction of **1-K** (generated from **1-H** by addition of 1.05 equiv. KOtBu) with **5h** (20 °C, stopped-flow, at 486 nm).

[ <b>5h</b> ] / $\text{mol L}^{-1}$	[ <b>1-K</b> ] / $\text{mol L}^{-1}$	[18-crown-6] / $\text{mol L}^{-1}$	[ <b>1-K</b> ] / [ <b>5h</b> ]	$k_{\text{obs}} / \text{s}^{-1}$
$1.33 \times 10^{-5}$	$2.90 \times 10^{-4}$	0	21.8	0.417
$1.33 \times 10^{-5}$	$8.70 \times 10^{-4}$	0	65.5	1.45
$1.33 \times 10^{-5}$	$1.45 \times 10^{-3}$	0	109	1.88

$$k_2 = 1.26 \times 10^3 \text{ L mol}^{-1} \text{s}^{-1}$$

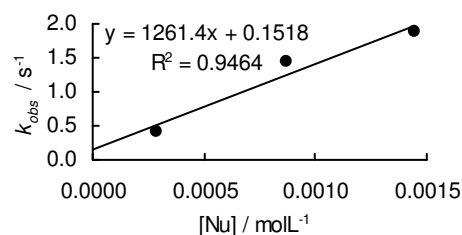
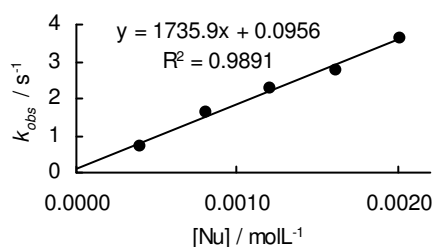


Table 34: Kinetics of the reaction of **1-K** (generated from **1-H** by addition of 1.05 equiv. KO $t$ Bu) with **5i** (20 °C, stopped-flow, at 521 nm).

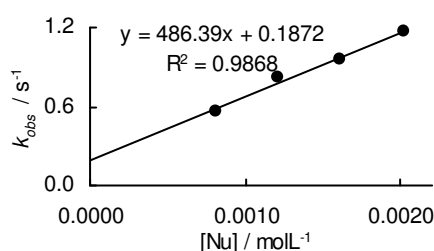
[ <b>5i</b> ] / mol L <sup>-1</sup>	[ <b>1-K</b> ] / mol L <sup>-1</sup>	[18-crown-6] / mol L <sup>-1</sup>	[ <b>1-K</b> ] / [ <b>5i</b> ]	$k_{\text{obs}}$ / s <sup>-1</sup>
$1.44 \times 10^{-5}$	$4.04 \times 10^{-4}$	$6.34 \times 10^{-4}$	28.1	0.697
$1.44 \times 10^{-5}$	$8.07 \times 10^{-4}$	$1.27 \times 10^{-3}$	56.2	1.64
$1.44 \times 10^{-5}$	$1.21 \times 10^{-3}$	$1.90 \times 10^{-3}$	84.2	2.25
$1.44 \times 10^{-5}$	$1.61 \times 10^{-3}$	$2.54 \times 10^{-3}$	112.3	2.76
$1.44 \times 10^{-5}$	$2.02 \times 10^{-3}$	$3.17 \times 10^{-3}$	140.4	3.64

$$k_2 = 1.74 \times 10^3 \text{ L mol}^{-1} \text{ s}^{-1}$$

Table 35: Kinetics of the reaction of **1-K** (generated from **1-H** by addition of 1.05 equiv. KO $t$ Bu) with **5i** (20 °C, stopped-flow, at 521 nm).

[ <b>5i</b> ] / mol L <sup>-1</sup>	[ <b>1-K</b> ] / mol L <sup>-1</sup>	[18-crown-6] / mol L <sup>-1</sup>	[ <b>1-K</b> ] / [ <b>5i</b> ]	$k_{\text{obs}}$ / s <sup>-1</sup>
$1.44 \times 10^{-5}$	$8.07 \times 10^{-4}$	0	56.2	1.64
$1.44 \times 10^{-5}$	$1.21 \times 10^{-3}$	0	84.2	2.25
$1.44 \times 10^{-5}$	$1.61 \times 10^{-3}$	0	112.3	2.76
$1.44 \times 10^{-5}$	$2.02 \times 10^{-3}$	0	140.4	3.64

$$k_2 = 4.86 \times 10^2 \text{ L mol}^{-1} \text{ s}^{-1}$$

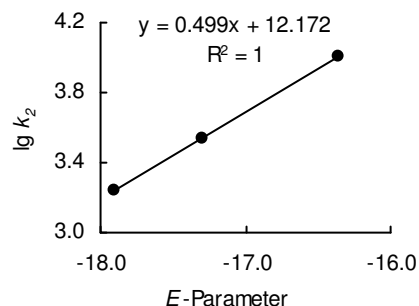


#### Determination of Reactivity Parameters $N$ and $s_N$ of Potassium 2-Oxo-1,2-diphenylethan-1-ide (**1-K**) in Acetone in Presence of 18-Crown-6

Table 36: Rate Constants for the reactions of **1-K** with different electrophiles (20 °C, in presence of 18-crown-6).

Electrophile	$E$	$k_2$ / L mol <sup>-1</sup> s <sup>-1</sup>	$\log k_2$
<b>5g</b>	-16.36	$1.02 \times 10^4$	4.01
<b>5h</b>	-17.29	$3.48 \times 10^3$	3.54
<b>5i</b>	-17.90	$1.74 \times 10^3$	3.24

$$N = 26.69, s_N = 0.39$$



#### 4.4.1.3. Reactions of **1-K** in THF

Table 37: Kinetics of the reaction of **1-K** (generated from **1-H** by addition of 1.05 equiv. KO $t$ Bu) with **5g** (20 °C, stopped-flow, at 490 nm).

[ <b>5g</b> ] / mol L <sup>-1</sup>	[ <b>1-K</b> ] / mol L <sup>-1</sup>	[18-crown-6] / mol L <sup>-1</sup>	[ <b>1-K</b> ] / [ <b>5g</b> ]	$k_{\text{obs}}$ / s <sup>-1</sup>
$1.09 \times 10^{-5}$	$2.45 \times 10^{-4}$	$3.80 \times 10^{-4}$	22.5	0.432
$1.09 \times 10^{-5}$	$4.90 \times 10^{-4}$	$9.50 \times 10^{-4}$	45.0	0.982
$1.09 \times 10^{-5}$	$7.35 \times 10^{-4}$	$1.14 \times 10^{-3}$	67.4	1.45
$1.09 \times 10^{-5}$	$9.80 \times 10^{-4}$	$2.66 \times 10^{-3}$	89.9	1.95
$1.09 \times 10^{-5}$	$1.23 \times 10^{-3}$	$1.90 \times 10^{-3}$	112	2.53

$$k_2 = 2.11 \times 10^3 \text{ L mol}^{-1} \text{ s}^{-1}$$

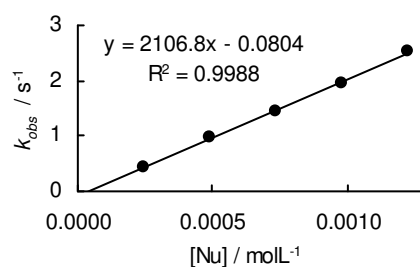
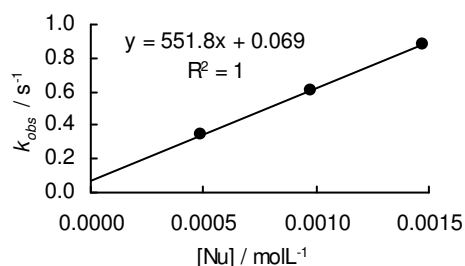




Table 38: Kinetics of the reaction of **1-K** (generated from **1-H** by addition of 1.05 equiv. KOtBu) with **5g** (20 °C, stopped-flow, at 490 nm).

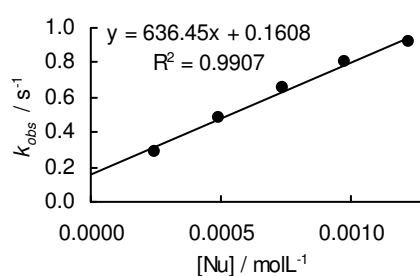
[ <b>5g</b> ] / mol L <sup>-1</sup>	[ <b>1-K</b> ] / mol L <sup>-1</sup>	[18-crown-6] / mol L <sup>-1</sup>	[ <b>1-K</b> ] /[ <b>5g</b> ]	$k_{\text{obs}}$ / s <sup>-1</sup>
$1.09 \times 10^{-5}$	$4.90 \times 10^{-4}$	0	45.0	0.340
$1.09 \times 10^{-5}$	$9.80 \times 10^{-4}$	0	89.9	0.609
$1.09 \times 10^{-5}$	$1.47 \times 10^{-3}$	0	135	0.881

$$k_2 = 5.52 \times 10^2 \text{ L mol}^{-1} \text{ s}^{-1}$$

Table 39: Kinetics of the reaction of **1-K** (generated from **1-H** by addition of 1.05 equiv. KOtBu) with **5h** (20 °C, stopped-flow, at 486 nm).

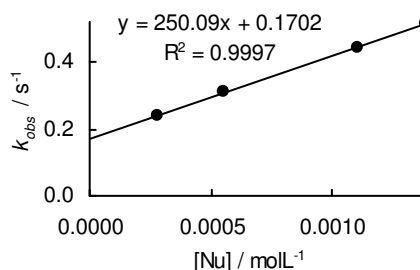
[ <b>5h</b> ] / mol L <sup>-1</sup>	[ <b>1-K</b> ] / mol L <sup>-1</sup>	[18-crown-6] / mol L <sup>-1</sup>	[ <b>1-K</b> ] /[ <b>5h</b> ]	$k_{\text{obs}}$ / s <sup>-1</sup>
$1.35 \times 10^{-5}$	$2.45 \times 10^{-4}$	$3.80 \times 10^{-4}$	18.2	0.291
$1.35 \times 10^{-5}$	$4.90 \times 10^{-4}$	$9.50 \times 10^{-4}$	36.4	0.487
$1.35 \times 10^{-5}$	$7.35 \times 10^{-4}$	$1.14 \times 10^{-3}$	54.5	0.652
$1.35 \times 10^{-5}$	$9.80 \times 10^{-4}$	$2.66 \times 10^{-3}$	72.7	0.799
$1.35 \times 10^{-5}$	$1.23 \times 10^{-3}$	$1.90 \times 10^{-3}$	90.9	0.915

$$k_2 = 6.36 \times 10^2 \text{ L mol}^{-1} \text{ s}^{-1}$$

Table 40: Kinetics of the reaction of **1-K** (generated from **1-H** by addition of 1.05 equiv. KOtBu) with **5i** (20 °C, stopped-flow, at 521 nm).

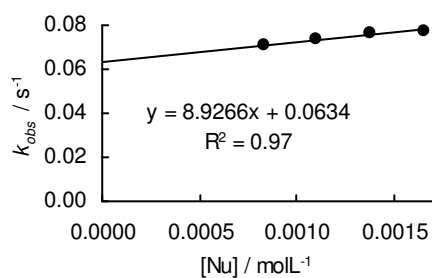
[ <b>5i</b> ] / mol L <sup>-1</sup>	[ <b>1-K</b> ] / mol L <sup>-1</sup>	[18-crown-6] / mol L <sup>-1</sup>	[ <b>1-K</b> ] /[ <b>5i</b> ]	$k_{\text{obs}}$ / s <sup>-1</sup>
$1.23 \times 10^{-5}$	$2.77 \times 10^{-4}$	$4.73 \times 10^{-4}$	22.5	0.238
$1.23 \times 10^{-5}$	$5.53 \times 10^{-4}$	$1.18 \times 10^{-3}$	44.9	0.311
$1.23 \times 10^{-5}$	$1.11 \times 10^{-3}$	$3.31 \times 10^{-3}$	89.8	0.445
$1.23 \times 10^{-5}$	$1.38 \times 10^{-3}$	$2.36 \times 10^{-3}$	112	0.517

$$k_2 = 2.50 \times 10^2 \text{ L mol}^{-1} \text{ s}^{-1}$$

Table 41: Kinetics of the reaction of **1-K** (generated from **1-H** by addition of 1.05 equiv. KOtBu) with **5i** (20 °C, stopped-flow, at 521 nm).

[ <b>5i</b> ] / mol L <sup>-1</sup>	[ <b>1-K</b> ] / mol L <sup>-1</sup>	[18-crown-6] / mol L <sup>-1</sup>	[ <b>1-K</b> ] /[ <b>5i</b> ]	$k_{\text{obs}}$ / s <sup>-1</sup>
$1.23 \times 10^{-5}$	$8.30 \times 10^{-4}$	0	67.4	$7.05 \times 10^{-2}$
$1.23 \times 10^{-5}$	$1.11 \times 10^{-3}$	0	89.8	$7.34 \times 10^{-2}$
$1.23 \times 10^{-5}$	$1.38 \times 10^{-3}$	0	112.3	$7.65 \times 10^{-2}$
$1.23 \times 10^{-5}$	$1.66 \times 10^{-3}$	0	134.8	$7.77 \times 10^{-2}$

$$k_2 = 8.93 \text{ L mol}^{-1} \text{ s}^{-1}$$

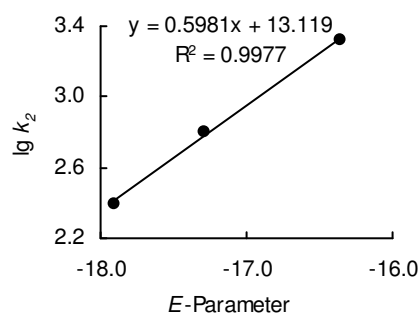


### Determination of Reactivity Parameters $N$ and $s_N$ of Potassium 2-Oxo-1,2-diphenylethan-1-ide (**1-K**) in THF in Presence of 18-Crown-6

Table 42: Rate Constants for the reactions of **1-K** with different electrophiles (20 °C, in presence of 18-crown-6).

Electrophile	$E$	$k_2 / \text{L mol}^{-1} \text{s}^{-1}$	$\log k_2$
<b>5g</b>	-16.36	$2.11 \times 10^3$	3.32
<b>5h</b>	-17.29	$6.36 \times 10^2$	2.80
<b>5i</b>	-17.90	$2.50 \times 10^2$	2.40

$$N = 21.93, s_N = 0.60$$



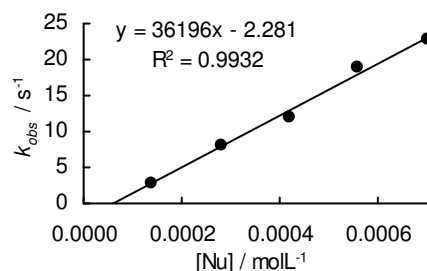
### 4.4.2. Reactions of the Potassium Salts of the Substituted Deoxybenzoins (**2-4**)-K in DMSO

#### 4.4.2.1. Reactions of **2-K**

Table 43: Kinetics of the reaction of **2-K** (generated from **2-H** by addition of 1.05 equiv. KO $t$ Bu) with **5g** (20 °C, stopped-flow, at 500 nm).

$[\mathbf{5g}] / \text{mol L}^{-1}$	$[\mathbf{2-K}] / \text{mol L}^{-1}$	$[\text{18-crown-6}] / \text{mol L}^{-1}$	$[\mathbf{2-K}] / [\mathbf{5g}]$	$k_{\text{obs}} / \text{s}^{-1}$
$1.24 \times 10^{-5}$	$1.40 \times 10^{-4}$		11.2	2.73
$1.24 \times 10^{-5}$	$2.79 \times 10^{-4}$	$4.40 \times 10^{-4}$	22.5	8.19
$1.24 \times 10^{-5}$	$4.19 \times 10^{-4}$		33.7	12.0
$1.24 \times 10^{-5}$	$5.59 \times 10^{-4}$	$8.79 \times 10^{-4}$	44.9	18.8
$1.24 \times 10^{-5}$	$6.98 \times 10^{-4}$		56.2	22.7

$$k_2 = 3.62 \times 10^4 \text{ L mol}^{-1} \text{s}^{-1}$$

Table 44: Kinetics of the reaction of **2-K** (generated from **2-H** by addition of 1.05 equiv. KO $t$ Bu) with **5h** (20 °C, stopped-flow, at 500 nm).

$[\mathbf{5h}] / \text{mol L}^{-1}$	$[\mathbf{2-K}] / \text{mol L}^{-1}$	$[\text{18-crown-6}] / \text{mol L}^{-1}$	$[\mathbf{2-K}] / [\mathbf{5h}]$	$k_{\text{obs}} / \text{s}^{-1}$
$1.62 \times 10^{-5}$	$1.84 \times 10^{-4}$		11.4	1.38
$1.62 \times 10^{-5}$	$3.69 \times 10^{-4}$	$4.40 \times 10^{-4}$	22.8	3.96
$1.62 \times 10^{-5}$	$5.53 \times 10^{-4}$		34.2	6.79
$1.62 \times 10^{-5}$	$7.37 \times 10^{-4}$	$8.79 \times 10^{-4}$	45.6	9.62
$1.62 \times 10^{-5}$	$9.21 \times 10^{-4}$		57.0	11.9

$$k_2 = 1.45 \times 10^4 \text{ L mol}^{-1} \text{s}^{-1}$$

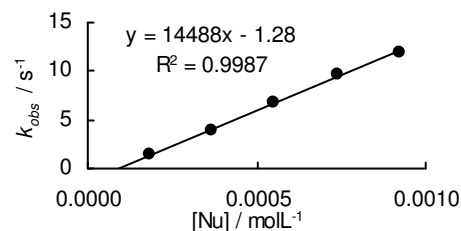
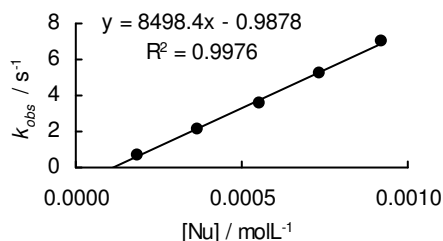


Table 45: Kinetics of the reaction of **2-K** (generated from **2-H** by addition of 1.05 equiv. KO<sup>t</sup>Bu) with **5i** (20 °C, stopped-flow, at 521 nm).

[ <b>5i</b> ] / mol L <sup>-1</sup>	[ <b>2-K</b> ] / mol L <sup>-1</sup>	[18-crown-6] / mol L <sup>-1</sup>	[ <b>2-K</b> ] / [ <b>5i</b> ]	$k_{\text{obs}}$ / s <sup>-1</sup>
$1.21 \times 10^{-5}$	$1.84 \times 10^{-4}$		15.3	0.704
$1.21 \times 10^{-5}$	$3.69 \times 10^{-4}$	$4.40 \times 10^{-4}$	30.6	2.09
$1.21 \times 10^{-5}$	$5.53 \times 10^{-4}$		45.8	3.57
$1.21 \times 10^{-5}$	$7.37 \times 10^{-4}$	$8.79 \times 10^{-4}$	61.1	5.22
$1.21 \times 10^{-5}$	$9.21 \times 10^{-4}$		76.4	6.97

$$k_2 = 8.50 \times 10^3 \text{ L mol}^{-1} \text{ s}^{-1}$$

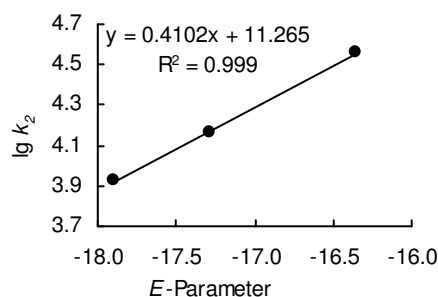


### Determination of Reactivity Parameters $N$ and $s_N$ of Potassium 1-(4-Methoxyphenyl)-2-oxo-2-phenylethan-1-ide (**2-K**) in DMSO

Table 46: Rate Constants for the reactions of **2-K** with different electrophiles (20 °C).

Electrophile	$E$	$k_2 / \text{L mol}^{-1} \text{ s}^{-1}$	$\log k_2$
<b>5g</b>	-16.36	$3.62 \times 10^4$	4.56
<b>5h</b>	-17.29	$1.45 \times 10^4$	4.16
<b>5i</b>	-17.90	$8.50 \times 10^3$	3.93

$$N = 27.46, s_N = 0.41$$

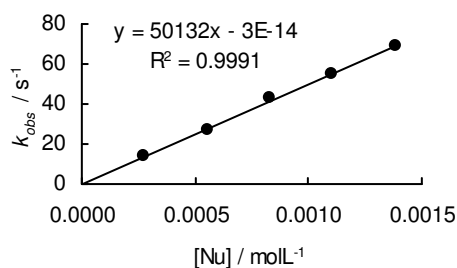


#### 4.4.2.2. Reactions of **3-K**

Table 47: Kinetics of the reaction of **3-K** with **5b** (20 °C, stopped-flow, at 533 nm).

[ <b>5b</b> ] / mol L <sup>-1</sup>	[ <b>3-K</b> ] / mol L <sup>-1</sup>	[18-crown-6] / mol L <sup>-1</sup>	[ <b>3-K</b> ] / [ <b>5b</b> ]	$k_{\text{obs}}$ / s <sup>-1</sup>
$1.34 \times 10^{-5}$	$2.76 \times 10^{-4}$		20.7	13.6
$1.34 \times 10^{-5}$	$5.53 \times 10^{-4}$	$7.05 \times 10^{-4}$	41.4	27.3
$1.34 \times 10^{-5}$	$8.29 \times 10^{-4}$		62.1	42.7
$1.34 \times 10^{-5}$	$1.11 \times 10^{-3}$	$1.41 \times 10^{-3}$	82.8	55.5
$1.34 \times 10^{-5}$	$1.38 \times 10^{-3}$		104	68.8

$$k_2 = 5.01 \times 10^4 \text{ L mol}^{-1} \text{ s}^{-1}$$

Table 48: Kinetics of the reaction of **3-K** with **5c** (20 °C, stopped-flow, at 360 nm).

[ <b>5c</b> ] / mol L <sup>-1</sup>	[ <b>3-K</b> ] / mol L <sup>-1</sup>	[18-crown-6] / mol L <sup>-1</sup>	[ <b>3-K</b> ] / [ <b>5c</b> ]	$k_{\text{obs}}$ / s <sup>-1</sup>
$1.21 \times 10^{-5}$	$3.26 \times 10^{-4}$		27.0	4.50
$1.21 \times 10^{-5}$	$6.52 \times 10^{-4}$	$7.05 \times 10^{-4}$	54.0	9.42
$1.21 \times 10^{-5}$	$9.79 \times 10^{-4}$		81.0	14.4
$1.21 \times 10^{-5}$	$1.30 \times 10^{-3}$	$1.41 \times 10^{-3}$	108	17.8

$$k_2 = 1.38 \times 10^4 \text{ L mol}^{-1} \text{ s}^{-1}$$

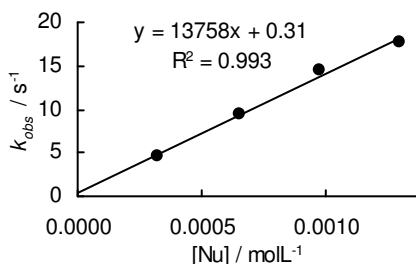
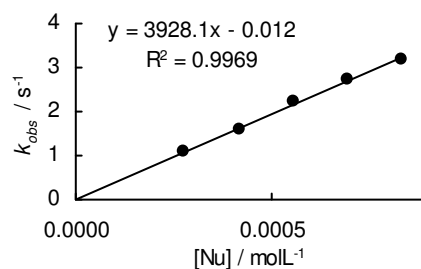


Table 49: Kinetics of the reaction of **3-K** with **5d** (20 °C, stopped-flow, at 354 nm).

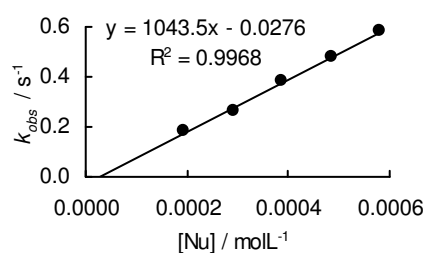
[ <b>5d</b> ] / mol L <sup>-1</sup>	[ <b>3-K</b> ] / mol L <sup>-1</sup>	[18-crown-6] / mol L <sup>-1</sup>	[ <b>3-K</b> ] / [ <b>5d</b> ]	$k_{\text{obs}}$ / s <sup>-1</sup>
$1.35 \times 10^{-5}$	$2.76 \times 10^{-4}$		20.4	1.07
$1.35 \times 10^{-5}$	$4.15 \times 10^{-4}$	$5.88 \times 10^{-4}$	30.6	1.57
$1.35 \times 10^{-5}$	$5.53 \times 10^{-4}$		40.8	2.22
$1.35 \times 10^{-5}$	$6.91 \times 10^{-4}$	$9.41 \times 10^{-4}$	51.0	2.74
$1.35 \times 10^{-5}$	$8.29 \times 10^{-4}$		61.3	3.20

$$k_2 = 3.93 \times 10^3 \text{ L mol}^{-1} \text{ s}^{-1}$$

Table 50: Kinetics of the reaction of **3-K** with **5d** (20 °C, stopped-flow, at 354 nm).

[ <b>5d</b> ] / mol L <sup>-1</sup>	[ <b>3-K</b> ] / mol L <sup>-1</sup>	[18-crown-6] / mol L <sup>-1</sup>	[ <b>3-K</b> ] / [ <b>5d</b> ]	$k_{\text{obs}}$ / s <sup>-1</sup>
$1.30 \times 10^{-5}$	$1.94 \times 10^{-4}$		15.0	0.184
$1.30 \times 10^{-5}$	$2.91 \times 10^{-4}$	$4.70 \times 10^{-4}$	22.4	0.261
$1.30 \times 10^{-5}$	$3.88 \times 10^{-4}$		29.9	0.381
$1.30 \times 10^{-5}$	$4.85 \times 10^{-4}$	$7.05 \times 10^{-4}$	37.4	0.479
$1.30 \times 10^{-5}$	$5.82 \times 10^{-4}$		44.9	0.581

$$k_2 = 1.04 \times 10^3 \text{ L mol}^{-1} \text{ s}^{-1}$$

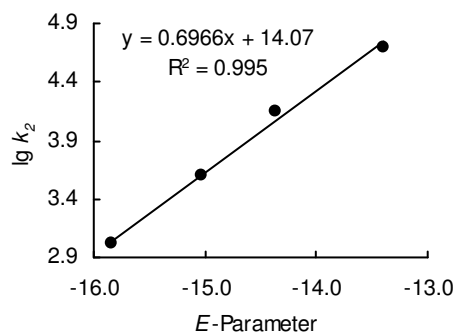


### Determination of Reactivity Parameters $N$ and $s_N$ of Potassium 1-(4-Cyanophenyl)-2-oxo-2-phenylethan-1-ide (**3-K**) in DMSO

Table 51: Rate Constants for the reactions of **3-K** with different electrophiles (20 °C).

Electrophile	$E$	$k_2$ / L mol <sup>-1</sup> s <sup>-1</sup>	$\log k_2$
<b>5b</b>	-13.39	$5.01 \times 10^4$	4.70
<b>5c</b>	-14.36	$1.38 \times 10^4$	4.14
<b>5d</b>	-15.03	$3.93 \times 10^3$	3.59
<b>5g</b>	-16.36	$1.04 \times 10^3$	3.02

$$N = 20.20, s_N = 0.70$$



#### 4.4.2.3. Reactions of **4-K**

Table 52: Kinetics of the reaction of **4-K** with **5a** (20 °C, stopped-flow, at 422 nm).

[ <b>5a</b> ] / mol L <sup>-1</sup>	[ <b>4-K</b> ] / mol L <sup>-1</sup>	[18-crown-6] / mol L <sup>-1</sup>	[ <b>4-K</b> ] / [ <b>5a</b> ]	$k_{\text{obs}}$ / s <sup>-1</sup>
$1.58 \times 10^{-5}$	$2.98 \times 10^{-4}$		18.9	5.99
$1.58 \times 10^{-5}$	$7.45 \times 10^{-4}$	$9.02 \times 10^{-4}$	47.1	22.9
$1.58 \times 10^{-5}$	$9.93 \times 10^{-4}$		62.9	29.3
$1.58 \times 10^{-5}$	$1.16 \times 10^{-3}$	$1.55 \times 10^{-3}$	73.3	33.1
$1.58 \times 10^{-5}$	$1.66 \times 10^{-3}$		105	48.4

$$k_2 = 3.07 \times 10^4 \text{ L mol}^{-1} \text{ s}^{-1}$$

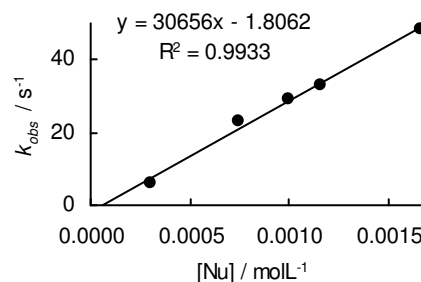
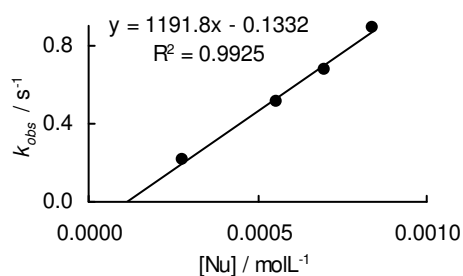


Table 53: Kinetics of the reaction of **4-K** with **5c** (20 °C, stopped-flow, at 374 nm).

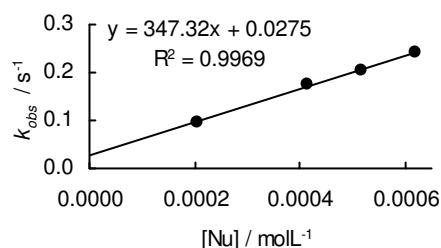
[ <b>5c</b> ] / mol L <sup>-1</sup>	[ <b>4-K</b> ] / mol L <sup>-1</sup>	[18-crown-6] / mol L <sup>-1</sup>	[ <b>3-K</b> ] / [ <b>5c</b> ]	$k_{\text{obs}}$ / s <sup>-1</sup>
$1.49 \times 10^{-5}$	$2.79 \times 10^{-4}$		18.8	0.216
$1.49 \times 10^{-5}$	$5.58 \times 10^{-4}$		37.6	0.509
$1.49 \times 10^{-5}$	$6.98 \times 10^{-4}$	$1.03 \times 10^{-3}$	47.0	0.680
$1.49 \times 10^{-5}$	$8.38 \times 10^{-4}$		56.4	0.891

$$k_2 = 1.19 \times 10^3 \text{ L mol}^{-1} \text{ s}^{-1}$$

Table 54: Kinetics of the reaction of **4-K** with **5d** (20 °C, stopped-flow, at 374 nm).

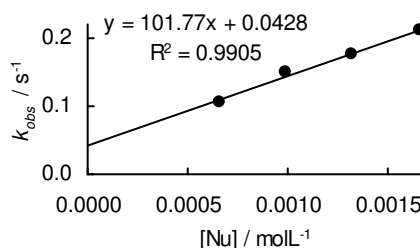
[ <b>5d</b> ] / mol L <sup>-1</sup>	[ <b>4-K</b> ] / mol L <sup>-1</sup>	[18-crown-6] / mol L <sup>-1</sup>	[ <b>3-K</b> ] / [ <b>5d</b> ]	$k_{\text{obs}}$ / s <sup>-1</sup>
$1.47 \times 10^{-5}$	$2.79 \times 10^{-4}$		14.1	0.0977
$1.47 \times 10^{-5}$	$4.14 \times 10^{-4}$		28.1	0.176
$1.47 \times 10^{-5}$	$5.17 \times 10^{-4}$	$6.45 \times 10^{-4}$	35.1	0.204
$1.47 \times 10^{-5}$	$6.21 \times 10^{-4}$		42.2	0.243

$$k_2 = 3.47 \times 10^2 \text{ L mol}^{-1} \text{ s}^{-1}$$

Table 55: Kinetics of the reaction of **4-K** with **5f** (20 °C, stopped-flow, at 405 nm).

[ <b>5f</b> ] / mol L <sup>-1</sup>	[ <b>4-K</b> ] / mol L <sup>-1</sup>	[18-crown-6] / mol L <sup>-1</sup>	[ <b>3-K</b> ] / [ <b>5f</b> ]	$k_{\text{obs}}$ / s <sup>-1</sup>
$1.68 \times 10^{-5}$	$6.62 \times 10^{-4}$	$7.73 \times 10^{-4}$	39.4	0.107
$1.68 \times 10^{-5}$	$9.93 \times 10^{-4}$		59.0	0.150
$1.68 \times 10^{-5}$	$1.32 \times 10^{-3}$	$1.55 \times 10^{-3}$	78.7	0.175
$1.68 \times 10^{-5}$	$1.66 \times 10^{-3}$		98.4	0.211

$$k_2 = 1.02 \times 10^2 \text{ L mol}^{-1} \text{ s}^{-1}$$

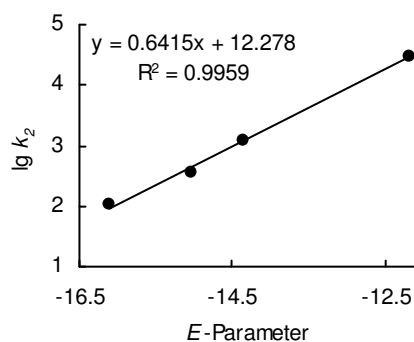


### Determination of Reactivity Parameters $N$ and $s_N$ of Potassium 1-(4-Nitrophenyl)-2-oxo-2-phenylethan-1-ide (**4-K**) in DMSO

Table 56: Rate Constants for the reactions of **4-K** with different electrophiles (20 °C).

Electrophile	$E$	$k_2 / \text{L mol}^{-1} \text{ s}^{-1}$	$\log k_2$
<b>5a</b>	-12.18	$3.07 \times 10^4$	4.49
<b>5c</b>	-14.36	$1.19 \times 10^3$	3.08
<b>5d</b>	-15.03	$3.47 \times 10^2$	2.54
<b>5f</b>	-16.11	$1.02 \times 10^2$	2.01

$$N = 19.14, s_N = 0.64$$



### 4.4.3. Reactions of the Potassium Salts of Deoxybenzoin with Butyl Iodide in Different Solvents

Table 57: Kinetics of the reaction of **1-K** (generated from **1-H** by addition of 1.02 equiv. KO<sup>t</sup>Bu) with BuI in DMSO (20 °C, diode array, at 398 nm).

[ <b>1-K</b> ] / mol L <sup>-1</sup>	[BuI] / mol L <sup>-1</sup>	[18-crown-6] / mol L <sup>-1</sup>	[BuI] / [ <b>1-K</b> ]	$k_{\text{obs}}$ / s <sup>-1</sup>
$1.32 \times 10^{-4}$	$2.19 \times 10^{-3}$		16.6	$2.48 \times 10^{-2}$
$1.32 \times 10^{-4}$	$3.28 \times 10^{-3}$		24.9	$3.34 \times 10^{-2}$
$1.32 \times 10^{-4}$	$4.39 \times 10^{-3}$		33.2	$5.30 \times 10^{-2}$
$1.31 \times 10^{-4}$	$5.44 \times 10^{-3}$		41.5	$6.06 \times 10^{-2}$
$1.31 \times 10^{-4}$	$6.53 \times 10^{-3}$		49.8	$7.35 \times 10^{-2}$

$$k_2 = 11.5 \text{ L mol}^{-1} \text{ s}^{-1}$$

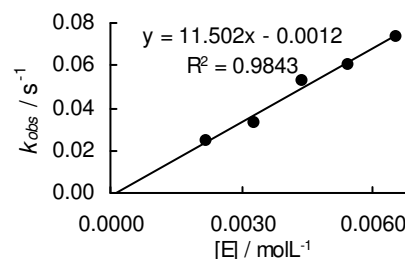


Table 58: Kinetics of the reaction of **1-K** (generated from **1-H** by addition of 1.03 equiv. KO<sup>t</sup>Bu) with BuI in DMF (20 °C, diode array, at 397 nm).

[ <b>1-K</b> ] / mol L <sup>-1</sup>	[BuI] / mol L <sup>-1</sup>	[18-crown-6] / mol L <sup>-1</sup>	[BuI] / [ <b>1-K</b> ]	$k_{\text{obs}}$ / s <sup>-1</sup>
$1.84 \times 10^{-4}$	$2.01 \times 10^{-3}$	$3.45 \times 10^{-4}$	10.9	$2.69 \times 10^{-2}$
$1.86 \times 10^{-4}$	$3.04 \times 10^{-3}$	$3.48 \times 10^{-4}$	16.4	$4.05 \times 10^{-2}$
$1.90 \times 10^{-4}$	$4.16 \times 10^{-3}$	$3.57 \times 10^{-4}$	21.8	$5.18 \times 10^{-2}$
$1.88 \times 10^{-4}$	$5.13 \times 10^{-3}$	$3.53 \times 10^{-4}$	27.3	$6.13 \times 10^{-2}$
$1.85 \times 10^{-4}$	$6.05 \times 10^{-3}$	$3.47 \times 10^{-4}$	32.7	$7.48 \times 10^{-2}$

$$k_2 = 11.4 \text{ L mol}^{-1} \text{ s}^{-1}$$

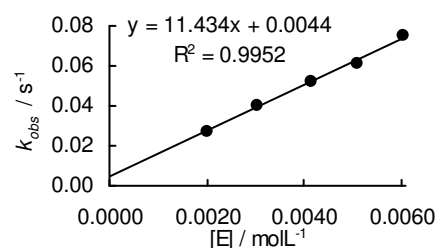


Table 59: Kinetics of the reaction of **1-K** (generated from **1-H** by addition of 1.04 equiv. KO<sup>t</sup>Bu) with BuI in acetone (20 °C, diode array, at 382 nm).

[ <b>1-K</b> ] / mol L <sup>-1</sup>	[BuI] / mol L <sup>-1</sup>	[18-crown-6] / mol L <sup>-1</sup>	[BuI] / [ <b>1-K</b> ]	$k_{\text{obs}}$ / s <sup>-1</sup>
$2.32 \times 10^{-4}$	$2.98 \times 10^{-3}$	$3.39 \times 10^{-4}$	17.1	$3.13 \times 10^{-2}$
$2.29 \times 10^{-4}$	$4.90 \times 10^{-3}$	$3.35 \times 10^{-4}$	21.4	$4.20 \times 10^{-2}$
$2.29 \times 10^{-4}$	$6.87 \times 10^{-3}$	$3.36 \times 10^{-4}$	30.0	$5.57 \times 10^{-2}$
$2.33 \times 10^{-4}$	$7.98 \times 10^{-3}$	$3.41 \times 10^{-4}$	34.3	$6.00 \times 10^{-2}$

$$k_2 = 5.92 \text{ L mol}^{-1} \text{ s}^{-1}$$

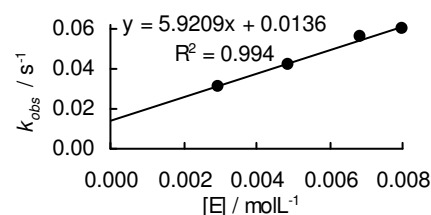
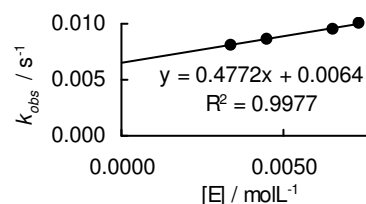


Table 60: Kinetics of the reaction of **1-K** (generated from **1-H** by addition of 1.04 equiv. KO<sup>t</sup>Bu) with BuI in THF (20 °C, diode array, at 382 nm).

[ <b>1-K</b> ] / mol L <sup>-1</sup>	[BuI] / mol L <sup>-1</sup>	[18-crown-6] / mol L <sup>-1</sup>	[BuI] / [ <b>1-K</b> ]	$k_{\text{obs}}$ / s <sup>-1</sup>
$2.00 \times 10^{-4}$	$3.38 \times 10^{-3}$	$5.64 \times 10^{-4}$	16.9	$8.04 \times 10^{-3}$
$2.01 \times 10^{-4}$	$4.52 \times 10^{-3}$	$5.65 \times 10^{-4}$	22.5	$8.58 \times 10^{-3}$
$1.95 \times 10^{-4}$	$6.60 \times 10^{-3}$	$5.50 \times 10^{-4}$	33.8	$9.51 \times 10^{-3}$
$1.88 \times 10^{-4}$	$7.39 \times 10^{-3}$	$5.28 \times 10^{-4}$	39.4	$9.99 \times 10^{-3}$

$$k_2 = 4.77 \times 10^{-1} \text{ L mol}^{-1} \text{ s}^{-1}$$



#### 4.4.4. Reactions of the Potassium Salts of Deoxybenzoin with Different Butyl Derivates in THF

Table 61: Kinetics of the reaction of **1-K** (generated from **1-H** by addition of 1.06 equiv. KO<sup>t</sup>Bu) with BuBr in THF (20 °C, diode array, at 382 nm).

[ <b>1-K</b> ] / mol L <sup>-1</sup>	[BuBr] / mol L <sup>-1</sup>	[18-crown-6] / mol L <sup>-1</sup>	[BuBr] / [ <b>1-K</b> ]	$k_{\text{obs}}$ / s <sup>-1</sup>
$1.17 \times 10^{-4}$	$5.33 \times 10^{-3}$	$3.37 \times 10^{-4}$	26.7	$1.97 \times 10^{-3}$
$2.05 \times 10^{-4}$	$8.21 \times 10^{-3}$	$3.47 \times 10^{-4}$	40.0	$2.61 \times 10^{-3}$
$2.02 \times 10^{-4}$	$1.34 \times 10^{-2}$	$3.41 \times 10^{-4}$	66.7	$4.21 \times 10^{-3}$
$1.99 \times 10^{-4}$	$1.59 \times 10^{-2}$	$3.36 \times 10^{-4}$	80.0	$4.71 \times 10^{-3}$

$$k_2 = 2.68 \times 10^{-1} \text{ L mol}^{-1} \text{ s}^{-1}$$

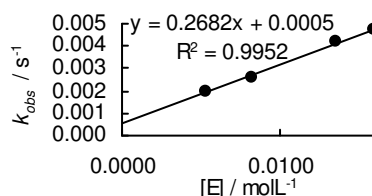


Table 62: Kinetics of the reaction of **1-K** (generated from **1-H** by addition of 1.04 equiv. KO<sup>t</sup>Bu) with BuCl in THF (20 °C, diode array, at 382 nm).

[ <b>1-K</b> ] / mol L <sup>-1</sup>	[BuCl] / mol L <sup>-1</sup>	[18-crown-6] / mol L <sup>-1</sup>	[BuCl] / [ <b>1-K</b> ]	$k_{\text{obs}}$ / s <sup>-1</sup>
$1.77 \times 10^{-4}$	$1.92 \times 10^{-2}$	$2.94 \times 10^{-4}$	109	$8.53 \times 10^{-4}$
$1.66 \times 10^{-4}$	$2.25 \times 10^{-2}$	$2.76 \times 10^{-4}$	136	$9.60 \times 10^{-4}$
$1.75 \times 10^{-4}$	$2.50 \times 10^{-2}$	$2.91 \times 10^{-4}$	143	$1.05 \times 10^{-3}$
$1.66 \times 10^{-4}$	$2.71 \times 10^{-2}$	$2.76 \times 10^{-4}$	163	$1.12 \times 10^{-3}$
$1.05 \times 10^{-4}$	$2.92 \times 10^{-2}$	$2.98 \times 10^{-4}$	163	$1.23 \times 10^{-3}$

$$k_2 = 3.72 \times 10^{-2} \text{ L mol}^{-1} \text{ s}^{-1}$$

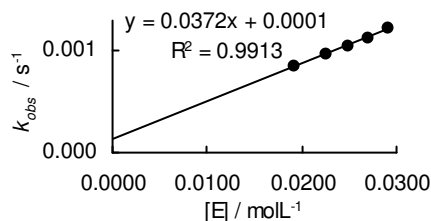


Table 63: Kinetics of the reaction of **1-K** (generated from **1-H** by addition of 1.04 equiv. KO<sup>t</sup>Bu) with BuOTs in THF (20 °C, stopped-flow, at 382 nm).

[ <b>1-K</b> ] / mol L <sup>-1</sup>	[BuOTs] / mol L <sup>-1</sup>	[18-crown-6] / mol L <sup>-1</sup>	[BuOTs] / [ <b>1-K</b> ]	$k_{\text{obs}}$ / s <sup>-1</sup>
$1.15 \times 10^{-4}$	$4.60 \times 10^{-3}$	$1.64 \times 10^{-4}$	41.5	10.2
$1.15 \times 10^{-4}$	$6.90 \times 10^{-3}$	$1.64 \times 10^{-4}$	62.3	14.9
$1.15 \times 10^{-4}$	$9.19 \times 10^{-3}$	$1.64 \times 10^{-4}$	83.1	19.5
$1.15 \times 10^{-4}$	$1.15 \times 10^{-2}$	$1.64 \times 10^{-4}$	104	24.8

$$k_2 = 2.11 \times 10^3 \text{ L mol}^{-1} \text{ s}^{-1}$$

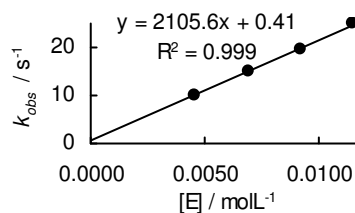
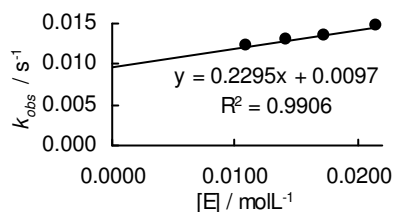


Table 64: Kinetics of the reaction of **1-K** (generated from **1-H** by addition of 1.08 equiv. KO<sup>t</sup>Bu) with BuOMes in THF (20 °C, diode array, at 382 nm).

[ <b>1-K</b> ] / mol L <sup>-1</sup>	[BuOMes] / mol L <sup>-1</sup>	[18-crown-6] / mol L <sup>-1</sup>	[BuOMes] / [ <b>1-K</b> ]	$k_{\text{obs}}$ / s <sup>-1</sup>
$1.50 \times 10^{-4}$	$1.09 \times 10^{-2}$	$2.34 \times 10^{-4}$	72.9	$1.22 \times 10^{-2}$
$1.46 \times 10^{-4}$	$1.30 \times 10^{-2}$	$2.29 \times 10^{-4}$	97.2	$1.30 \times 10^{-2}$
$1.42 \times 10^{-4}$	$1.35 \times 10^{-2}$	$2.23 \times 10^{-4}$	122	$1.35 \times 10^{-2}$
$1.48 \times 10^{-4}$	$1.47 \times 10^{-2}$	$2.32 \times 10^{-4}$	146	$1.47 \times 10^{-2}$

$$k_2 = 2.68 \times 10^{-1} \text{ L mol}^{-1} \text{ s}^{-1}$$



## 5. Appendix

### 5.1. Correlation

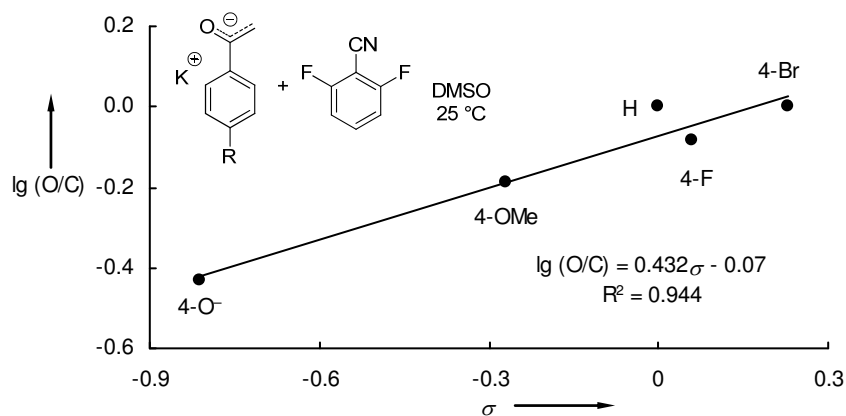


Figure 24: Correlation of O/C ratios for the reactions of the potassium salts of substituted acetophenones with 2,6-difluorobenzonitrile in DMSO at 25 °C.<sup>[21]</sup>

### 5.2. UV-Vis Spectra

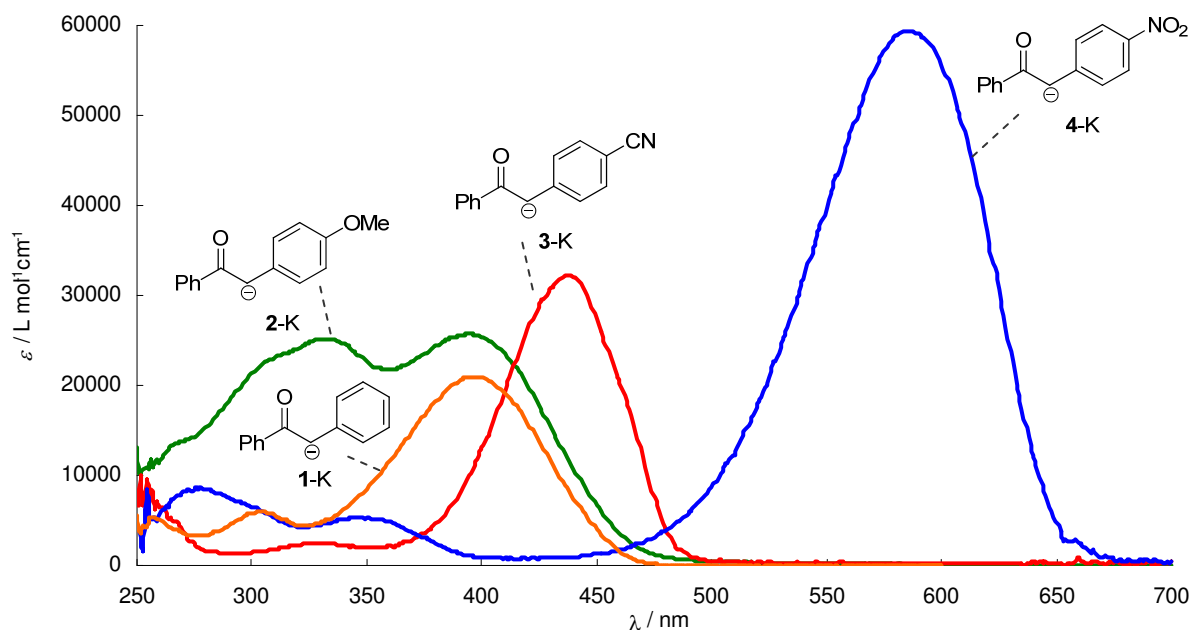


Figure 25: UV-Vis spectra of (1–4)-K in DMSO at 20 °C.

## 6. References

- [1] a) R. B. Bates, C. A. Ogle, *Carbanion Chemistry*, Springer, Berlin, **1983**; b) V. Snieckus, *Advances in Carbanion Chemistry Vol. 1*, JAI Press, Greenwich, CT, **1992**; c) E. Buncl, J. M. Dust, *Carbanion Chemistry*, Oxford, New York, **2003**.



- [2] a) R. G. Pearson, *J. Am. Chem. Soc.* **1963**, 85, 3533-3539; b) R. G. Pearson, *Science* **1966**, 151, 172-177; c) R. G. Pearson, J. Songstad, *J. Am. Chem. Soc.* **1967**, 89, 1827-1836; d) R. G. Pearson, *J. Chem. Educ.* **1968**, 45, 581-587; e) R. G. Pearson, *J. Chem. Educ.* **1968**, 45, 643-648; f) R. G. Pearson, *Chemical Hardness*, Wiley-VCH, Weinheim, **1997**.
- [3] H. E. Zimmerman, *Acc. Chem. Res.* **1987**, 20, 263-268.
- [4] a) R. Lucius, R. Loos, H. Mayr, *Angew. Chem.* **2002**, 114, 97-102; *Angew. Chem. Int. Ed.* **2002**, 41, 91-95; b) Compare results in Chapter 3 of this thesis.
- [5] E. Buncl, J. M. Dust, R. A. Manderville, *J. Am. Chem. Soc.* **1996**, 118, 6072-6073.
- [6] R. Gompper, H.-U. Wagner, *Angew. Chem.* **1976**, 88, 389-422; *Angew. Chem. Int. Ed. Engl.* **1976**, 15, 321-333.
- [7] A. Gobbi, D. Landini, A. Maia, S. Petrici, *J. Org. Chem.* **1998**, 63, 5356-5361.
- [8] W. J. Le Noble, H. F. Morris, *J. Org. Chem.* **1969**, 34, 1969-1973.
- [9] R. Gompper, H.-U. Wagner, *Chem. Ber.* **1981**, 114, 2866-2883.
- [10] C. Reichert, *Solvents and Solvents Effects in Organic Chemistry*, Wiley-VCH, Weinheim, **2003**.
- [11] a) N. Kornblum, R. Seltzer, P. Haberfeld, *J. Am. Chem. Soc.* **1963**, 85, 1148-1154; b) G. Brieger, W. M. Pelletier, *Tetrahedron Lett.* **1965**, 40, 3555-3558.
- [12] S. Shinkai, T. Fukunaga, O. Manabe, *J. Org. Chem.* **1979**, 44, 4990-4992.
- [13] When the regioselectivity of aromatic enolates, such as phenolates or naphthalenoates is discussed, it has to be considered, that it is contrary to that of aliphatic enolates. Phenolates are mainly oxygen-alkylated at conditions which lead to carbon-alkylation in reactions of enolates derived from aliphatic ketones.
- [14] N. Kornblum, A. P. Lurie, *J. Am. Chem. Soc.* **1959**, 81, 2705-2715.
- [15] M. Halpern, Y. Sasson, M. Rabinovitz, *Tetrahedron*, **1982**, 38, 3183-3187.
- [16] E. M. Arnett, V. M. de Palma, *J. Am. Chem. Soc.* **1977**, 99, 5828-5829.
- [17] P. Sarthou, G. Bram, F. Guibe, *Can. J. Chem.* **1980**, 58, 786-793.
- [18] a) H. E. Zaug, A. D. Schaefer, *J. Am. Chem. Soc.* **1965**, 87, 1857-1866; b) M. Raban, E. A. Noe, G. Yamamoto, *J. Am. Chem. Soc.* **1977**, 99, 6527-6531; c) M. Raban, D. P. Haritos, *J. Am. Chem. Soc.* **1979**, 101, 5178-5182; d) S. M. Esakov, A. A. Petrov, B.

- A. Ershov, *J. Org. Chem. USSR (Engl. Trans.)* **1975**, *11*, 679-688; e) A. A. Petrov, S. M. Esakov, B. A. Ershov, *J. Org. Chem. USSR (Engl. Trans.)* **1976**, *12*, 774-778.
- [19] C. Hansch, A. Leo, R. W. Taft, *Chem. Rev.* **1991**, *91*, 165-195.
- [20] T. Sakata, N. Seki, K. Yomogida, H. Yamagishi, A. Otsuki, C. Inoh, H. Yamataka, *J. Org. Chem.* **2012**, *77*, 10738-10744.
- [21] N.-E. Guedira, R. Beugelmans, *J. Org. Chem.* **1992**, *57*, 5577-5585.
- [22] R. Gompper, H.-H. Vogt, H.-U. Wagner, *Z. Naturforsch.* **1981**, *36b*, 1644-1652.
- [23] H. Mayr, M. Patz, *Angew. Chem.* **1994**, *106*, 990-1010; *Angew. Chem. Int. Ed. Engl.* **1994**, *33*, 938-957.
- [24] Selected Publications: a) H. Mayr, T. Bug, M. F. Gotta, N. Hering, B. Irrgang, B. Janker, B. Kempf, R. Loos, A. R. Ofial, G. Remennikov, H. Schimmel, *J. Am. Chem. Soc.* **2001**, *123*, 9500-9512; b) H. Mayr, B. Kempf, A. R. Ofial, *Acc. Chem. Res.* **2003**, *36*, 66-77; c) H. Mayr, A. R. Ofial, *Pure Appl. Chem.* **2005**, *77*, 1807-1821; d) D. Richter, N. Hampel, T. Singer, A. R. Ofial, H. Mayr, *Eur. J. Org. Chem.* **2009**, 3203-3211; e) H. Mayr, S. Lakhdar, B. Maji, A. R. Ofial, *Beilstein J. Org. Chem.* **2012**, *8*, 1458-1478; f) For a comprehensive listing of nucleophilicity parameters  $N$ ,  $s_N$  and electrophilicity parameters  $E$ , see <http://www.cup.uni-muenchen.de/oc/mayr/DBintro.html>.
- [25] S. T. A. Berger, F. H. Seeliger, F. Hofbauer, H. Mayr, *Org. Biomol. Chem.* **2007**, *5*, 3020-3026.
- [26]  $^1\text{H}$  NMR experiments of butyl iodide in  $[\text{D}_6]$ -DMSO show the formation of a new signal at 4.30 ppm after one hour. Similar results were found for dibutyl sulfate in DMSO. For experiments of dimethyl sulfate in DMSO compare V. M. de Palma, E. M. Arnett, *J. Am. Chem. Soc.* **1978**, *100*, 3514-3525.
- [27] A. L. Kurts, A. Macias, I. P. Beletskaya, O. A. Reutov, *Tetrahedron*, **1971**, *27*, 4759-4768.
- [28] H. E. Gottlieb, V. Kotlyar, A. Nudelman, *J. Org. Chem.* **1997**, *62*, 7512-7515.
- [29] I. Lantos, P. E. Bender, K. A. Razgaitis, B. M. Sutton, M. J. DiMartino, D. E. Griswold, D. T. Walz, *J. Med. Chem.* **1984**, *27*, 72-75.
- [30] E. Anders, T. Gaßner, *Chem. Ber.* **1984**, *117*, 1034-1038.
- [31] P. Wan, S. Muralidhara, *J. Am. Chem. Soc.* **1988**, *110*, 4336-4345.